Activités enzymatiques extracellulaires et composition des communautés bactériennes dans l'estuaire de l'Aulne et la rade de Brest : facteurs de régulation et rôle du quorum sensing

Marion Urvoy

Thèse de doctorat de

L'UNIVERSITE

DE BRETAGNE OCCIDENTALE

ECOLE DOCTORALE N° 598
Sciences de la Mer et du littoral
Spécialité : « *Biologie Marine* »

Par

Marion URVOY

Activités enzymatiques extracellulaires et composition des communautés bactériennes dans l'estuaire de l'Aulne et la rade de Brest : facteurs de régulation et rôle du quorum sensing

Thèse présentée et soutenue à Plouzané, le 20 Mai 2022
Unité de recherche : Laboratoire des Sciences de l'Environnement Marin (UMR 6539)

Rapporteurs avant soutenance :

Christian JEANTHON	Directeur de recherches CNRS, Station Biologique de Roscoff
Ingrid OBERNOSTERER	Directrice de recherches CNRS, Observatoire Océanologique de Banyuls-sur-Mer

Composition du Jury :

Ricardo RISO Président du jury	Professeur, Université de Bretagne Occidentale
Christian JEANTHON Rapporteur	Directeur de recherches CNRS, Station Biologique de Roscoff
Ingrid OBERNOSTERER Rapportrice	Directrice de recherches CNRS, Observatoire Océanologique de Banyuls-sur-Mer
Claudine BARAQUET Examinatrice	Maitre de conférence, Université de Toulon
Anne-Claire BAUDOUX Examinatrice	Chargée de recherches CNRS, Station Biologique de Roscoff
Stéphane L'HELGUEN Directeur de thèse	Chargé de recherches CNRS, Institut Universitaire Européen de la Mer
Claire LABRY Co-encadrante de thèse	Chercheuse, Ifremer Centre de Brest

Remerciements

Tout d'abord, j'aimerais remercier très sincèrement Christian Jeanthon, Ingrid Obernosterer, Claudine Baraquet, Anne-Claire Baudoux et Ricardo Riso d'avoir accepté de consacrer du temps à l'évaluation de ce travail de thèse.

Ensuite, je tiens à exprimer toute ma gratitude à toutes les personnes qui ont contribué de près ou de loin à ce projet de thèse. En premier lieu, Claire et Stéphane, merci infiniment de m'avoir accordé votre confiance pour entreprendre cette thèse, mais aussi tout au long de ces trois ans et demi. Merci de m'avoir laissée emmener ce projet là où j'en avais envie, je ne suis pas sûre que beaucoup d'encadrants m'auraient laissé cette chance ! Merci pour vos connaissances, votre soutien et vos relectures (intensives en cette fin de thèse !).

Daniel, derrière ta barbe se cache une belle rencontre. Merci de m'avoir transmis ta passion, tes envois de biblio intempestifs et tes relectures nocturnes ! Cette thèse n'aurait pas eu la même allure sans toi. Nos petits débriefs à la pause-café me manqueront. Merci surtout pour ta générosité à toute épreuve, au travail mais surtout en dehors : grâce à toi, j'ai découverts la plongée, le Banyuls et la feijoada (jamais deux sans trois ?) ! Patrick Poivron d'Armor et Fabrice Zucchini se souviendront de tes bons soins.

Raphaël, merci beaucoup pour ton accompagnement tout au long de cette thèse, ton enthousiasme et ta réactivité à toute heure du jour et de la nuit ! J'ai beaucoup appris à tes côtés et je t'en remercie sincèrement.

Je tiens à exprimer aussi tous mes remerciements à Catherine Dreanno, qui m'a accueillie sans réserve dans son laboratoire ; à David Daudé, pour son enthousiasme tout au long de notre collaboration ; à Mathieu Berchel, pour tout le temps que tu as passé au labo à plancher sur nos molécules, mais aussi pour ta réactivité ; à Gabriel Dulaquais, pour son investissement dans l'analyse des échantillons de l'Aulne ; et enfin, merci à Michèle Gourmelon pour ton aide au cours du projet CombactAulne.

J'aimerais aussi remercier Jean-Christophe Auguet et Anne-Claire Baudoux, de nouveau, pour leurs retours avisés pendant mon comité de thèse. Anne-Claire, tu as aussi largement contribué à mon envie de faire une thèse grâce à ton encadrement pendant mon stage de fin d'études.

Je tiens à remercier chaleureusement tout le laboratoire PELAGOS, j'ai passé trois super années grâce à vous ! Notamment et dans le désordre, merci Aurore, Cécile, Julien, Marie, Emilie, Raffaele, Mickaël, Anne, Erwan, Martin, Sophie, Joëlle, Marc, Véronique, Françoise, Florian, Erwan et ceux que j'oublie. Je garderai en mémoire votre bonne humeur, votre gentillesse et de vous entendre rire à

l'autre bout du couloir (oui Aurore, je parle de toi !). Un grand merci également au LEBCO pour ces pauses repas dans la bonne humeur, en particulier Mathieu, Gabin, Aurélien, Martin, Stanislas, Amélia et Touria.

Merci également aux membres du laboratoire LBBM qui m'ont accueillie pendant mon bref séjour à Banyuls. En particulier, merci Alice pour ta formation d'enfer à la spectrométrie de masse.

Je remercie aussi tous les membres du laboratoire LEMAR pour leur accueil, notamment à Christophe Lambert pour son aide en cytométrie.

Merci à tous les thésards, les vieux comme les nouveaux ! Lyndsay, Clément, Lou, Léa, Kevin, Mathisse, Laure, Alex (et Mathieu, je te recompte ici) ! Cet open-space aura vraiment été la meilleure chose de cette thèse ! Merci d'avoir fait chauffer la cafetière et d'avoir contribuer à notre diabète collectif avec tous ces petits déjs, merci pour les barres beaufs (Clément ?) et les bars à cocktails !

Merci à tous les membres d'Abysse pour ces journées plongées bien nécessaires pour s'aérer le neurone. Tristan, nos petites journées plongée, burgers, musique et tes conversations forts intéressantes me manqueront.

Merci à ma famille, mes parents, mon papi et ma mamie, ma sœur et mon frère, pour leur amour et leur soutien, à distance mais au quotidien. C'est grâce à vous si je suis arrivée jusque-là. Des gros bisous à la future génération qui s'annonce en force !

Enfin et par-dessus tout, Maéva, merci pour tout, merci pour ton amour chaque jour. Tu m'as portée à bout de bras jusqu'à la fin de cette thèse. Tout cela n'aurait pas eu de sens sans toi.

En écrivant ces mots, je me rends compte de la chance que j'ai eu de réaliser cette thèse dans de si bonnes conditions : merci à tous !

Sommaire

Liste des figures

Chapitre I

Chapitre II

Chapitre III

Chapitre IV

Chapitre V

Chapitre VI

Chapitre VII

Chapitre VIII

Liste des tableaux

Chapitre II

Chapitre III

Chapitre IV

Chapitre V

Liste des abréviations

Abréviations en français	
%Chla	Pourcentage de Chla dans les pigments totaux
%MOP	Pourcentage de MOP dans les MES
%POP	Pourcentage de POP dans le PPT
AACD	Acides aminés combinés dissous
AAD	Acides aminés dissous
AALD	Acides aminés libres dissous
AAP	Acides aminés particulaires
AB	Abondance bactérienne
ACP	Analyse en composantes principales
acyl-ACP	Protéine porteuse d'un groupement acyle
ADN	Acide désoxyribonucléique
AHL	N-Acyle homosérine lactone
AI	Auto-inducteur
AI-2	Auto-inducteur-2
ANOSIM	Analyse de similarité
ARN	Acide ribonucléique
ARNr	Acide ribonucléique ribosomique
ASV	Variant de séquence d'amplicon
CAI-1	*Vibrio cholerae* auto-inducteur-1
CAZymes	Enzymes actives sur les carbohydrates
Chla	Chlorophylle a
CHOD	Carbohydrates dissous
CHOP	Carbohydrates particulaires
CHOPI	Carbohydrates particulaires insolubles
CHOPS	Carbohydrates particulaires solubles
COD	Carbone organique dissous
COP	Carbone organique particulaire
dbRDA	Analyse de redondance sur matrice de distance
DMSO	Diméthylsulfoxyde
DMSP	Diméthylsulfoniopropionate
DO	Densité optique
EC	Enzyme commission
EtOAc	Acétate d'éthyle
GF/F	Filtre en fibre de verre
GFP	Protéine fluorescente verte
GLU	β-glucosidase
I/S	CHOPI sur CHOPS
K_m	Constance de Michaelis-Menten
LAM	Leucine aminopeptidase
LB	Milieu Luria Broth
LefSe	Analyse discriminante linéaire couplée à la taille d'effet
Leu-MCA	L-leucine 7-amido-4-methylcoumarine
MCA	4-methylcoumarinylamide
MCHOD	Monosaccharides dissous
MES	Matières en suspension
MIP	Matière inorganique particulaire
mLB	Milieu Luria Broth modifié
MOD	Matière organique dissoute
MOP	Matière organique particulaire

Abréviations en anglais	
%Chla	Percent of Chla in total pigments
%POM	Percent of POM in SPM
%POP	Percent of POP in TPP
AHL	*N*-acylhomoserine lactone
AI	Auto inducer
AI-2	Auto inducer-2
ANOSIM	Analysis of similarity
AP	Alkaline phosphatase
ASV	Amplicon sequence variant
BA	Bacterial abundance
BCC	Bacterial community composition
BP	Bacterial production
CAI-1	*Vibrio cholerae* autoinducer-1
Chla	Chlorophyll a
DAA	Dissolved amino acids
dbRDA	Distance-based redundancy analysis
DCAA	Dissolved combines amino acids
DCHO	Dissolved carbohydrates
DFAA	Dissolved free amino acids
DIN	Dissolved inorganic nitrogen
DMCHO	Dissolved monosaccharides
DOC	Dissolved organic carbon
DOM	Dissolved organic matter
DOP	Dissolved organic phosphorus
DPCHO	Dissolved polysaccharides
EC	Enzyme Commission
FL	Free-living
GLU	β-glucosidase
GOF	Goodness-of-fit
I/S	PICHO over PSCHO
LAM	Leucine aminopeptidase
LDA	Linear discriminant analysis
LefSe	Linear discriminant analysis effect size
log2FC	Log2 Fold change
MCA	4-methylcoumarinylamide
MTZ	Maximum turbidity zone
MUF	Methylumbelliferyl
NSTI	Weighted nearest sequenced taxon index
PA	Particle-attached
PAA	Particulate amino acids
PCA	Principal components analysis
PCoA	Principal coordinates analysis
PD	Phylogenetic diversity
PERMANOVA	Permutational multivariate analysis of variance
Pheo	Pheopigments
PICHO	Particulate insoluble carbohydrates
PIM	Particulate inorganic matter
PIP	Particulate inorganic phosphorus
PLS-PM	Partial least squares path modeling

MTZ	Zone de turbidité maximum (bouchon vaseux)
MUF	Methylumbelliferyl
MUF-P	4-methylumbelliferyl phosphate
NH_4^+	Ammonium
NOP	Azote organique particulaire
NSTI	Indice pondéré du taxon séquencé le plus proche (« weighted nearest sequenced taxon index")
PA	Phosphatase alcaline
PB	Production bactérienne
PBS	Tampon phosphate salin
PCHOD	Polysaccharides dissous
PCoA	Analyse en coordonnées principales
PCR	Réaction en chaine par polymérase
PERMANOVA	Analyse permutationnelle multivariée de la variance
Pheo	Pheopigments
PIP	Phosphore inorganique particulaire
PLS-PM	Modélisation structurelle des moindres carrés partiels
POD	Phosphore organique dissous
POP	Phosphore organique particulaire
PPT	Phosphore particulaire total
PQS	*Pseudomonas* quinolone signal
QQ	Quorum quenching
QS	Quorum sensing
RC_{Bray}	Score Raup-Crick basé sur Bray-Curtis
RDA	Analyse de redondance
SAM	S-adénosyl méthionine
SOMLIT	Service d'Observation en Milieu LITtoral
TCA	Acide trichloracétique
TDA	Acide tropodithietique
TSS	Transformation en abondance relative (normalisation par la somme totale)
UHPLC-HRMS/MS	Spectrométrie de masse couplée à de la chromatographie liquide ultra haute pression
VIF	Facteur d'inflation de variance
V_{max}	Vitesse maximale
βMNTD	Distance β moyenne au taxon le plus proche
βNTI	Indice β du taxon le plus proche ("β-nearest taxon index")

POC	Particulate organic carbon
POM	Particulate organic matter
PON	Particulate organic nitrogen
POP	Particulate organic phosphorus
PQS	*Pseudomonas* quinolone signal
PSCHO	Particulate soluble carbohydrates
QQ	Quorum quenching
QS	Quorum sensing
RC_{Bray}	Bray-Curtis-based Raup-Crick score
RDA	Redundance analysis
SOMLIT	Service d'Observation en Milieu LITtoral
SPM	Suspended particulate matter
TDA	Tropodithietic acid
TPP	Total particulate phosphorus
TSS	Total sum scaling
VIF	Variance inflation factor
βMNTD	B-mean nearest taxon distance
βNTI	β-nearest taxon index

Chapitre I.

Introduction générale

I. Les bactéries marines hétérotrophes, un rôle clef au sein des océans

I.A. Le rôle central des microorganismes marins

Les **microorganismes** dominent toute forme de vie sur terre. Ces entités microscopiques unicellulaires prospèrent notamment dans l'ensemble des habitats marins, qui recouvrent à eux seuls près de 71 % de la surface du globe. Les microorganismes englobent les protistes (c'est-à-dire les eucaryotes unicellulaires), les procaryotes (eux-mêmes constitués de bactéries et d'archées) ainsi que les virus. Les océans contiendraient jusqu'à 10^{29} cellules procaryotes (Whitman *et al.*, 1998), soit plus que les 10^{21} étoiles présentes dans notre univers (Pomeroy, 2007). Les procaryotes représentent ainsi 90 % de la biomasse des océans (Pomeroy, 2007; Suttle, 2007). Dans les eaux de surface, cela correspond à 5 x 10^5 bactéries par millilitre d'eau de mer en moyenne (Whitman *et al.*, 1998).

Au sein des écosystèmes marins, les microorganismes occupent différents rôles selon leur manière d'utiliser et de transformer le carbone, un élément essentiel constituant le vivant. Le **phytoplancton** inclue les organismes eucaryotes et procaryotes (cyanobactéries) photoautotrophes, majoritairement présents en suspension dans la couche euphotique des océans (**Figure I.1**). Ces organismes réalisent la photosynthèse, une étape cruciale où le dioxyde de carbone (CO_2) dissous d'origine atmosphérique est transformé en matière organique et en dioxygène (O_2) grâce à l'énergie lumineuse. Cette « production primaire » correspond au point d'entrée du carbone dans les océans et supporte l'ensemble des chaines trophiques marines. La production primaire marine représente environ la moitié de la production d'O_2 sur terre (Field *et al.*, 1976). Une partie de la biomasse phytoplanctonique résultant de la photosynthèse est ensuite transférée vers les niveaux trophiques supérieurs selon une chaine trophique dite « classique », commençant par le broutage du phytoplancton par le zooplancton, puis la prédation du zooplancton par les animaux de plus grande taille. Dans les océans profonds aphotiques, où la lumière ne pénètre pas, la production primaire peut être effectuée par des organismes chimiolithotrophes qui utilisent une source d'énergie d'origine chimique pour transformer le carbone inorganique en matière organique.

En contraste, les **procaryotes hétérotrophes** utilisent des molécules organiques comme source de carbone. Dans les eaux de surface des océans, les bactéries constituent l'essentiel des procaryotes hétérotrophes (Karner *et al.*, 2001). Celles-ci dégradent et utilisent la matière organique issue de la production primaire afin de supporter leur croissance et produire de la biomasse bactérienne : c'est la « production bactérienne » (**Figure I.1**). Ce faisant, elles relâchent dans le milieu des nutriments et minéraux essentiels (e.g., azote - N, phosphore - P) qui stimulent en retour la production primaire. De plus, les bactéries hétérotrophes alimentent une chaîne trophique d'organismes bactérivores de petite taille (e.g., flagellés hétérotrophes, ciliés) qui sont ensuite broutés par le zooplancton qui régénère

également les nutriments via ses activités d'excrétion. Cette « **boucle microbienne** » (Azam *et al.*, 1983) est essentielle car une partie de la matière organique qu'elle recycle resterait autrement inaccessible aux maillons supérieurs. On estime que jusqu'à 50 % de la production primaire marine est ainsi recyclée par la boucle microbienne (Ducklow et Carlson, 1992). Les bactéries hétérotrophes sont très diversifiées et effectuent de nombreuses fonctions en plus de leur rôle dans la dégradation de la matière organique. On peut citer à titre d'exemple la fixation du diazote d'origine atmosphérique, la méthanogenèse ou la catalyse des cycles du soufre.

Enfin, les **virus marins** forment le dernier maillon de ces communautés complexes. Ce sont les entités les plus abondantes des océans : bien qu'ils ne représentent que 5 % de la biomasse marine, ils constitueraient jusqu'à 94 % des organismes marins (Suttle, 2007). S'ils ne sont pas considérés comme des êtres vivants car ils ne possèdent pas leur propre métabolisme, les virus infectent l'ensemble des microorganismes marins pour se répliquer et jouent un rôle important d'architectes des communautés microbiennes. Les bactériophages, qui infectent les bactéries, lysent entre 20 et 40 % des bactéries présentes dans la couche de surface des océans par jour et participent largement aux flux de matière au sein des océans, un phénomène appelé « shunt viral » (Suttle, 2007).

En utilisant et en transformant les éléments essentiels à la vie (carbone, nutriments), les microorganismes jouent un rôle clef dans les océans. En particulier, les bactéries hétérotrophes influencent le devenir du carbone et des nutriments en catalysant les réactions de dégradation des composés organiques marins. Une des **préoccupations majeures des océanographes est de comprendre comment les bactéries utilisent et transforment cette matière organique et de déterminer l'impact de ces transformations sur les différents flux de carbone et de nutriments dans les océans**. L'utilisation de la matière organique par les bactéries marines dépend de sa composition, de la composition des communautés bactériennes et des différentes stratégies trophiques mises en place par celles-ci. L'étude de ces trois points et des processus les régulant est ainsi nécessaire pour mieux appréhender la complexité des interactions entre bactéries et matière organique.

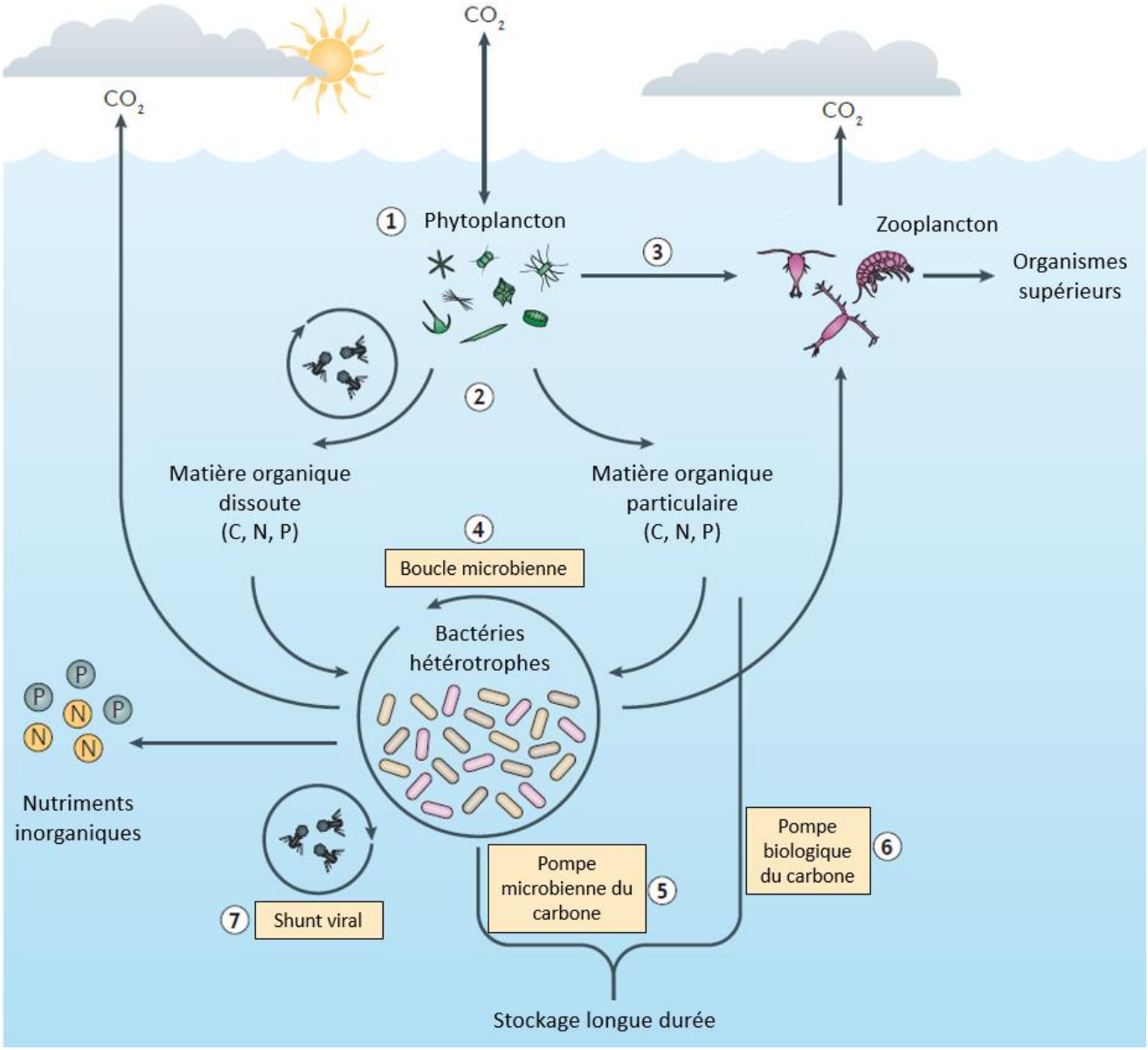

Figure I.1. Principaux processus affectant les cycles biogéochimiques au sein des océans. Le phytoplancton effectue la production primaire (1), c'est-à-dire la production de matière organique à partir de dioxyde de carbone et d'énergie lumineuse. Il participe à la production de matière organique particulaire, mais également dissoute (2), via des processus d'exsudation, de lyse ou de broutage (**cf I.B**). Une partie du phytoplancton est transférée vers les niveaux trophiques supérieurs suite à son broutage par le zooplancton (3) (chaine trophique classique). En parallèle, les bactéries hétérotrophes dégradent et utilisent la matière organique dissoute et particulaire, initiant la boucle microbienne via le broutage des protistes hétérotrophes (4). La matière dissoute et particulaire participe au stockage durable du carbone au sein des océans par l'intermédiaire de la pompe microbienne (5) et de la pompe biologique du carbone (6) (**cf I.B**). Le « shunt viral » (7) représente un flux important de matière organique dissoute. Modifié de Buchan *et al.* (2014).

I.B. La matière organique marine, support de l'activité bactérienne hétérotrophe

La matière organique marine est usuellement séparée en deux catégories : la matière organique dissoute (MOD) et la matière organique particulaire (MOP). Cette séparation opérationnelle est effectuée grâce à une étape de filtration à un seuil compris généralement entre 0.1 et 1 µm : la MOP est retenue par le filtre tandis que la MOD est comprise dans le filtrat (**Figure I.2**) (Harvey, 2006; Nagata, 2008). Cette distinction est essentielle car ces deux pools de matière supportent des fonctions différentes dans les cycles biogéochimiques, c'est-à-dire les processus de transport et de transformation que subissent tous les éléments comme le carbone, l'azote ou le phosphore.

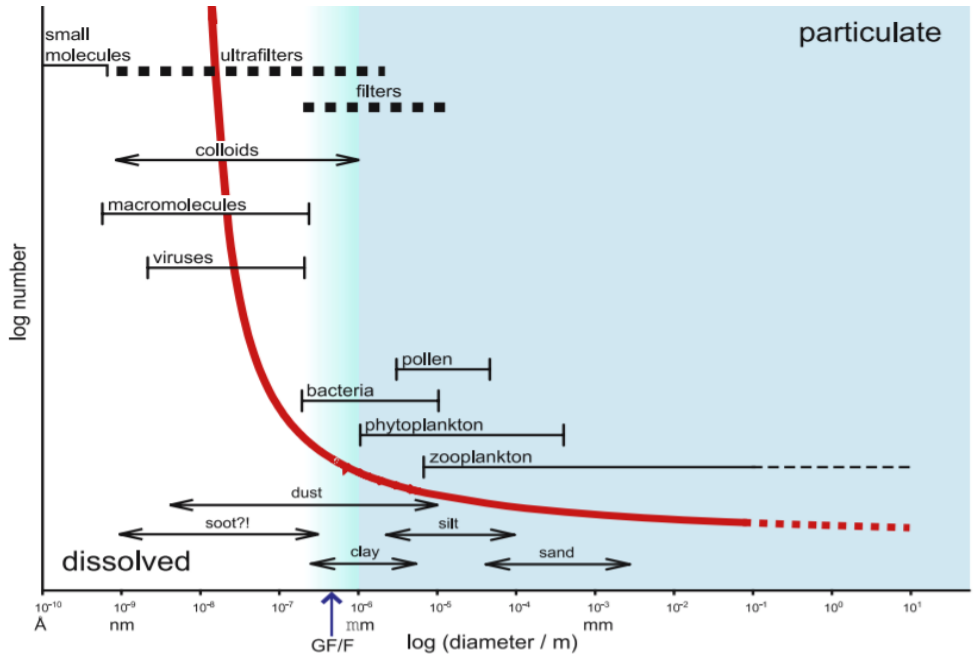

Figure I.2. Les différentes classes de taille des principaux composés présents dans la matière organique dissoute et particulaire. La courbe rouge représente le lien entre l'abondance et la taille des particules marines. Les lignes pointillées représentent la porosité des filtres et membrane d'ultrafiltration classiquement utilisés. La flèche bleue indique la porosité des filtres en fibre de verre (GF/F). Extrait de Harvey (2006).

I.B.1) *La matière organique dissoute*

La MOD est la forme de matière organique majoritaire dans les océans, représentant une masse de 662 GtC (Hansell, 2013). Etant définie par une porosité de filtre, elle inclue les composés réellement dissous (par exemple, les monosaccharides) mais aussi les virus, une partie des bactéries ou les colloïdes qui sont en réalité des composés non-dissous (**Figure I.2**) (Nagata, 2008).

En milieu côtier, la MOD provient de plusieurs sources, naturelles et anthropiques. Les sources naturelles incluent des apports autochtones et allochtones. La **MOD autochtone** correspond à une matière organique produite *in situ*. Elle est majoritairement d'origine phytoplanctonique, provenant par exemple de l'exsudation des cellules, de leur lyse virale ou de processus de « *sloppy feeding* » (relargage lors du broutage par les organismes supérieurs) (Nagata, 2008; Thornton, 2014). Chaque

année, 50 GtC de carbone organique dissous (COD) sont ainsi produits dans les océans (Harvey, 2006). A ces processus autochtones, se superposent les **apports allochtones**, comme par exemple, les dépôts atmosphériques (e.g., pluie, poussières sahariennes) ou les apports terrestres (e.g., apports des rivières, lessivage des sols) (Mopper et Zika, 1987; Harvey, 2006). Les apports des rivières sont particulièrement importants pour les zones côtières et représentent un flux d'environ 0.3 GtC par an de COD (Harvey, 2006). Les eaux fluviales sont chargées en composés d'origine terrestre, provenant par exemple de la dégradation des tissus de plantes supérieures. Enfin, les **sources anthropiques** correspondent, par exemple, aux eaux de ruissellement (e.g., lixiviat de décharges et chaussées), aux rejets urbains (e.g., stations d'épurations, industries) ou aux rejets agricoles (e.g., épandage d'engrais organiques). La contribution de chacune de ces sources peut fortement varier dans le temps et l'espace, notamment selon les changements de régime de précipitation (Harvey, 2006).

La **composition moléculaire** de la MOD reste un puzzle pour les océanographes du fait de sa complexité chimique : elle serait en grande partie (≈ 70 %) constituée de molécules de faible poids moléculaire (< 1000 Da) non caractérisables chimiquement (Hedges *et al.*, 2000; Dittmar et Kattner, 2003; Nagata, 2008). La partie caractérisable de la MOD correspond principalement à la **MOD produite de manière autochtone**, dérivant du phytoplancton. Celle-ci contient les mêmes molécules que celles constituant la biomasse phytoplanctonique, c'est-à-dire, des carbohydrates (mono- et polysaccharides), des acides aminés (libres et combinés sous forme de protéines) et des lipides (Dittmar et Kattner, 2003; Lee *et al.*, 2004). Ce sont des molécules hydrophiles, labiles et biodisponibles pour les microorganismes marins. Plus précisément, les cellules phytoplanctoniques contiendraient 5-50 % de carbohydrates, 25—50 % de protéines, 5-20 % de lipides, 3-20 % de pigments et jusqu'à 20 % d'acides nucléiques (Thornton, 2014). Les exsudats du phytoplancton contiendraient, eux, jusqu'à 90 % de carbohydrates (Myklestad, 1995). Les carbohydrates constituent en conséquence 15 à 50 % de la MOD océanique, principalement sous forme d'oligo- et polysaccharides (Arnosti *et al.*, 2021). Les acides aminés et monosaccharides sont très peu abondants et représenteraient ≈ 1 % de la MOD marine (Nagata, 2008).

La **MOD contenue dans les rivières** est principalement composée de substances humiques d'origine terrestre, qui peuvent représenter jusqu'à 80 % du COD dans les rivières et les estuaires (Dittmar et Kattner, 2003; Waeles *et al.*, 2013; Dulaquais, Breitenstein, *et al.*, 2018). Les substances humiques sont un mélange de molécules hydrophobes de composition et de poids moléculaire variables, qui dérivent de la dégradation de la matière terrestre (Dittmar et Kattner, 2003). Leur composition est à ce jour mal caractérisée. Elles contiendraient majoritairement des molécules de petite taille, éventuellement agrégées de manière non-covalente sous forme de macromolécules (Leenheer et Croué, 2003). Les substances humiques, hydrophobes et aliphatiques, sont généralement considérées comme résistantes à la dégradation microbienne même si elles peuvent être en partie

décomposées (Rosenstock et Simon, 2003; Rocker *et al.*, 2012). Elles peuvent cependant jouer un rôle important en tant que chélateur d'éléments essentiels (e.g., fer, cuivre) (Dulaquais, Waeles, *et al.*, 2018; Dulaquais *et al.*, 2020).

Comme la composition moléculaire de la MOD reste compliquée à établir, des approches non spécifiques peuvent être mise en place, notamment la détermination de sa **composition en éléments chimiques** (e.g., C, N, P, hydrogène - H, oxygène - O, soufre - S). L'analyse des rapports en éléments permet ensuite de traduire, par exemple, le caractère aromatique ou aliphatique de la matière (rapports O/C et H/C) ou encore son origine et son état de dégradation. Le rapport C/N est notamment souvent utilisé en milieu côtier pour différencier les matières terrigènes (C/N > 12) des matières nouvellement produites et faiblement dégradées (C/N < 10) (Savoye *et al.*, 2003; Liénart *et al.*, 2017).

I.B.2) *La matière organique particulaire*

La MOP correspond à la matière contenue dans diverses particules, allant des petites particules de l'ordre du micromètre (par exemple les particules d'exopolymères transparentes) aux larges agrégats macroscopiques qui composent la neige marine (> 500 µm) (Simon *et al.*, 2002). La MOP contenue dans les océans constitue un réservoir de 3 Gt de carbone, bien inférieur à celui constitué par la MOD (Harvey, 2006; Bianchi, 2011). De la même manière que pour la MOD, la MOP peut être d'origine autochtone ou allochtone et sa composition moléculaire reste peu définie (Lee *et al.*, 2004; Kharbush *et al.*, 2020). La **MOP autochtone**, majoritaire en milieu côtier (Liénart *et al.*, 2017), est constituée de matière vivante (e.g., cellules phytoplanctoniques, zooplancton, organismes supérieurs), mais aussi de matière détritique. Celle-ci comprend par exemple les cellules phytoplanctoniques sénescentes ou mortes, les débris de macro-algues et de zooplancton ou encore les pelotes fécales (Simon *et al.*, 2002). La fraction de biomasse vivante constituant la MOP est en général 10 fois moins importante que celle de biomasse détritique, bien que leurs proportions puissent varier dans le temps et l'espace (Volkman et Tanoue, 2002). La MOP autochtone serait composée de carbohydrates, acides aminés et lipides, molécules constituant les cellules vivantes (Simon *et al.*, 2002; Lee *et al.*, 2004). On estime que les carbohydrates et les acides aminés représenteraient respectivement 3 à 18 % et 40 à 50 % du carbone contenu dans la MOP exportée vers les océans profonds (Hedges *et al.*, 2001; Panagiotopoulos et Sempéré, 2005). La **MOP allochtone**, majoritairement de la matière terrestre charriée par les rivières, contiendrait aussi des composés dérivés de matières terrigènes (e.g., lignine) et du carbone « noir » (résultant de réactions de combustions incomplètes) (Bianchi et Bauer, 2012; Kharbush *et al.*, 2020).

Les agrégats jouent un rôle important pour les océans de par leur transport horizontal et vertical. Les agrégats charriés par les rivières et estuaires sont exportés horizontalement vers l'océan côtier, puis hauturier, et sont en partie minéralisés dans la colonne d'eau au cours de leur transport (Raymond et Bauer, 2001; Bianchi, 2011). En sédimentant sous l'action de la gravité, les agrégats

représentent aussi une voie d'export majeur du carbone des couches de surface vers les couches profondes des océans, un processus appelé la **pompe biologique du carbone** (**Figure I.1**).

I.B.3) *La labilité de la matière organique*

Si la composition de la MOP et de la MOD reste difficile à déterminer, on peut catégoriser les molécules qui les composent par leur **labilité**, c'est-à-dire leur biodisponibilité pour les microorganismes (Nagata, 2008). La labilité de la matière organique est usuellement déterminée par des expériences d'incubation avec des communautés bactériennes naturelles, permettant de déterminer la durée nécessaire pour son utilisation et le taux de matière consommée (Amon et Benner, 1996; Benner et Amon, 2015). On trouve ainsi : i) la matière labile, consommée sur une échelle de quelques heures à quelques jours (comprenant par exemples les composés issus du phytoplancton, comme les acides aminés et les protéines ou les carbohydrates) ; ii) la matière semi-labile, persistant de quelques mois à quelques années ; et iii) la matière réfractaire, persistant jusqu'à des milliers d'années (Nagata, 2008).

La labilité des molécules composant la matière organique peut être classifiée selon le « **continuum taille – réactivité »** proposé par Amon et Benner (1996) (**Figure I.3**). D'après ce modèle, les composés de haut poids moléculaire (> 1 kDa) sont plus biodisponibles que les composés de petit poids moléculaire (< 1 kDa). En effet, leur modèle est basé sur l'hypothèse que la matière de haut poids moléculaire issue du phytoplancton (i.e., polysaccharides, protéines) diminuerait en taille au cours de sa dégradation par les microorganismes, formant des composés de faible poids moléculaire très divers, peu concentrés et faiblement réactifs (i.e., avec de longs temps de demi-vie). Ces molécules réfractaires de faible poids moléculaire, très majoritaires, pourraient être inutilisables du fait de leur composition moléculaire ou de leur importante dilution (Nagata, 2008; Arrieta *et al.*, 2015; Shen et Benner, 2020). Il convient néanmoins de préciser qu'une faible partie des composés de bas poids moléculaire présent dans l'environnement marin correspond à de la matière très labile, comme par exemple les acides aminés et les monosaccharides (Nagata, 2008). Ces composés sont très rapidement utilisés par les microorganismes marins (de l'ordre de quelques minutes à quelques heures) et ne s'accumulent pas dans les océans, expliquant leurs faibles concentrations (Nagata, 2008).

La transformation de matière organique labile en matière réfractaire par les microorganismes est un processus important appelé la « **pompe microbienne du carbone** » et participe au stockage longue durée du carbone au sein des océans (Jiao *et al.*, 2010) (**Figure I.1**).

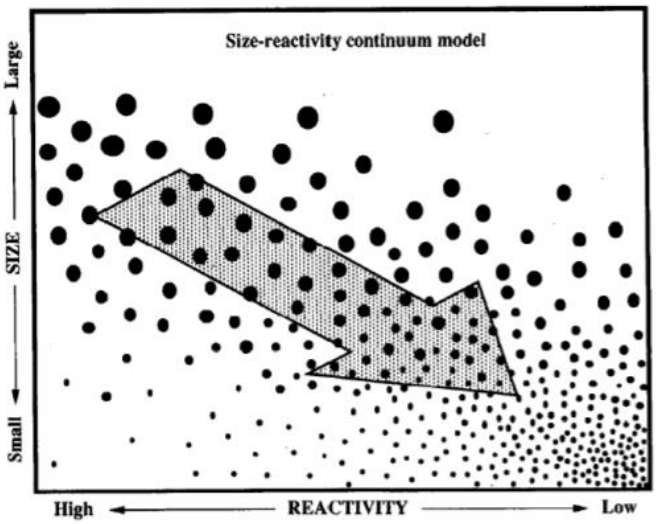

Figure I.3. Représentation conceptuelle du continuum taille – réactivité de la matière organique. La taille des points représente la taille de la matière organique. Extrait de Amon et Benner (1996).

I.C. Les communautés bactériennes marines

I.C.1) *Les techniques d'étude de la composition des communautés bactériennes*

Historiquement, l'abondance et la composition des communautés bactériennes étaient étudiées par des **méthodes d'isolement de bactéries**, permettant leur mise en culture. Cependant, les techniques de comptage par microscopie ont permis une découverte majeure : les bactéries marines sont bien plus abondantes que ne le laissaient présager les dénombrements effectués par mise en culture sur boite (« *Great plate count anomaly* ») (Staley et Konopka, 1985). Si l'isolement et la culture de bactéries restent essentiels à la microbiologie marine moderne, on sait désormais que moins de 1 % des bactéries marines sont cultivables (Staley et Konopka, 1985). C'est un biais important des techniques culture-dépendantes, qui ne permettent d'accéder qu'à une part restreinte de la biodiversité.

Depuis les années 1990, les nouvelles méthodes de séquençage de l'acide désoxyribonucléique (ADN) permettent de s'affranchir en partie de la nécessité de mise en culture des bactéries, ouvrant ainsi l'accès à la part non-cultivable des communautés. Ces méthodes sont aujourd'hui un élément essentiel de l'écologie marine. En particulier, le **développement du metabarcoding,** basé sur le séquençage d'un gène marqueur (« *barcode* »), permet d'évaluer la composition et la diversité des communautés bactériennes naturelles. Le principe consiste à extraire l'ADN présent dans des échantillons environnementaux et à amplifier le gène marqueur cible par réaction en chaine par polymérases (« *polymerase chain reaction* », PCR). Un gène marqueur est un gène dont la séquence varie entre différentes espèces mais qui est très conservée au sein d'une même espèce, lui conférant un fort pouvoir discriminant. On utilise en général une région du gène codant pour la petite sous-unité du ribosome des procaryotes (gène de l'ARNr 16S). Ensuite, l'ensemble des séquences amplifiées sont

séquencées et comparées à une base de données, de manière à les assigner à une espèce donnée. Cette méthode est très largement utilisée pour évaluer la diversité et la composition des communautés bactériennes marines dans le temps (e.g., série HOT à Hawaii – Bryant *et al.*, 2016, Observatoire microbien de St-Anne-du-Portzic - Lemonnier, 2019) et l'espace (e.g., les séries GOS - Kopf *et al.*, 2015, Malaspina - Duarte, 2015, ou Tara - Sunagawa *et al.*, 2015). Plus récemment, la démocratisation des **techniques de métagénomique** permet d'aller encore plus loin : au lieu de séquencer un seul gène marqueur, ces techniques donnent accès aux génomes des différentes espèces composant une communauté complexe. Dans cette dernière méthode, l'ADN est extrait, fragmenté et séquencé dans son ensemble. Les séquences ainsi obtenues sont ensuite assemblées *de novo* en séquences plus longues (contigs) et les gènes peuvent être prédits et annotés. Cela permet d'obtenir des indices quant à la physiologie et l'écologie des bactéries étudiées, par exemple concernant la présence de gènes liés au transport et à l'utilisation de certains composés de la matière organique (Simon *et al.*, 2014; Li *et al.*, 2018).

I.C.2) *La composition des communautés bactériennes marines*

L'avènement des techniques culture-indépendantes a rendu possible l'étude de la composition des communautés bactériennes marines à large échelle, révélant qu'elles sont i) très diverses, comprenant plus de 30 000 espèces réparties en 12 phyla (Sunagawa *et al.*, 2015; Yilmaz *et al.*, 2016) ; ii) très dynamiques dans le temps et l'espace (Zinger *et al.*, 2011; Fuhrman *et al.*, 2015; Sunagawa *et al.*, 2015). De manière plus spécifique, différentes études ont montré que les assemblages de bactéries marines sont généralement dominés par **quelques espèces abondantes**, le reste de la communauté étant composé d'une **large diversité d'espèces peu abondantes** (Sogin *et al.*, 2006; Galand *et al.*, 2009). Le rôle de cette biosphère rare est encore discuté à ce jour, mais il semblerait cependant qu'elle puisse présenter des patrons écologiques, être active et jouer un rôle dans les cycles biogéochimiques (Campbell *et al.*, 2011; Alonso-Sáez *et al.*, 2015; Hausmann *et al.*, 2019). Ces espèces rares peuvent aussi devenir abondantes sous l'influence de paramètres biotiques et abiotiques favorables (Gilbert *et al.*, 2012), participant alors à la dynamique de la composition des communautés.

Les bactéries marines sont principalement affiliées à quelques phyla majoritaires, notamment les **Protéobactéries** (principalement les Alpha- et Gammaproteobacteria), les **Bacteroidetes** (principalement les Flavobacteria), les **Actinobacteria** et les **Cyanobactéries** (bactéries autotrophes) (Pommier *et al.*, 2007; Zinger *et al.*, 2011; Sunagawa *et al.*, 2015) (**Figure I.4**). Les communautés bactériennes suivent à la fois de grands patrons biogéographiques et des variations saisonnières marquées. Par exemple, les SAR11 (Alphaproteobacteria) dominent largement dans les eaux de surface oligotrophes pauvres en nutriments (Morris *et al.*, 2002; Giovannoni, 2017) tandis que les milieux côtiers, riches en nutriments et en particules, sont comparativement enrichis en Flavobacteria (Bacteroidetes) et Rhodobacterales (Alphaproteobacteria) (Kirchman, 2002; Fortunato *et al.*, 2013;

Ortega-Retuerta *et al.*, 2013). On y trouve également la présence de Betaproteobacteria provenant probablement d'apports fluviatiles puisque cette classe est très abondante dans les eaux douces (Rappé *et al.*, 2000; Riemann *et al.*, 2008). Enfin, d'un point de vue temporel, les communautés tendent à s'enrichir en Flavobacteria, Gammaproteobacteria et Roseobacter (un groupe appartenant aux Rhodobacterales) lors de la croissance printanière du phytoplancton (Teeling *et al.*, 2012; Buchan *et al.*, 2014; Bunse *et al.*, 2016).

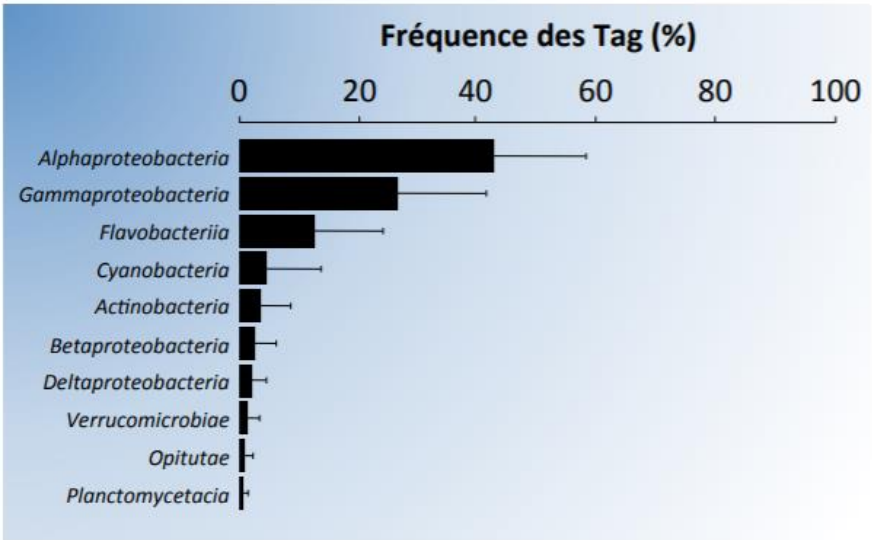

Figure I.4. Proportion moyenne des principaux groupes bactériens au sein des communautés bactériennes pélagiques marines issue d'une large gamme d'écosystèmes marins. Extrait de Zinger *et al.* (2011).

I.C.3) *Les facteurs contrôlant la composition des communautés bactériennes marines*

Un des grands challenges en écologie microbienne est de déterminer les facteurs et processus influençant la composition des communautés bactériennes marines (Hanson et al., 2012; Zhou et Ning, 2017). Deux grands types de processus influencent l'assemblage des communautés : les processus stochastiques, c'est-à-dire aléatoires, et les processus déterministes, correspondant à la sélection imposée par l'environnement biotique et abiotique des cellules.

i) Processus stochastiques et déterministes

L'écologie marine a été grandement construite sur le concept de « **niche écologique** », développé entre autre par Hutchinson (1957). L'hypothèse sous-jacente est que les organismes occupent tous des niches différentes. La niche d'un organisme correspond à un espace multidimensionnel regroupant ses capacités (traits fonctionnels) en terme d'interaction avec son environnement abiotique (e.g., conditions physicochimiques) et biotique (i.e., les espèces l'entourant) (Chase et Myers, 2011; Zhou et Ning, 2017). Elle correspond ainsi à l'ensemble des conditions au sein desquelles un organisme peut persister. La théorie des niches implique que les processus modulant l'assemblage des communautés bactériennes sont nécessairement **déterministes** (i.e., non-

aléatoires), puisqu'ils correspondent à une sélection découlant des conditions environnementales biotiques et abiotiques. Les processus déterministes incluent la sélection homogène (menant à des communautés similaires) et la sélection hétérogène (menant à des communautés dissimilaires) (Zhou et Ning, 2017).

Cependant, la **théorie neutre de la biodiversité,** plus récemment développée, remet ces fondements en question (Hubbell, 2001, 2005). Cette théorie se base sur l'hypothèse que toutes les espèces sont écologiquement équivalentes. Leur dynamique serait alors essentiellement contrôlée par des phénomènes **stochastiques** (i.e., aléatoires) et non par des différences dans leurs capacités à rivaliser avec leurs congénères. Les processus stochastiques incluent la dérive écologique (les fluctuations aléatoires dans l'abondance relative des organismes, liés aux évènements de reproduction et mort) et la dispersion (les mouvements spatiaux des espèces) (Hanson *et al.*, 2012; Zhou et Ning, 2017).

Ces deux théories ne sont pas exclusives mais plutôt complémentaires : les communautés bactériennes marines sont affectées par un mélange de processus déterministes et stochastiques, leur contribution pouvant varier dans le temps et l'espace (Gravel *et al.*, 2006; Stegen *et al.*, 2012). Un nombre encore restreint d'études s'est intéressé à l'impact relatif des facteurs stochastiques et déterministes au sein des environnements marins (J. Liu *et al.*, 2019).

ii) La sélection par l'environnement : influence des facteurs biotiques et abiotiques

La fameuse maxime de Baas-Becking cristallise un principe clef d'écologie microbienne : « ***everything is everywhere but the environment selects*** » (1934). Si la 1ère partie de cette phrase fait toujours débat (Martiny *et al.*, 2006; Fontaneto et Hortal, 2012), il a largement été démontré que l'environnement modulait la composition des communautés bactériennes marines, via l'influence de facteurs biotiques et abiotiques.

Les **facteurs abiotiques** connus pour influencer la composition des communautés sont, entre autres :

- La température, qui influence les métabolismes bactériens et qui est considérée comme un facteur clef influençant les successions saisonnières des communautés bactériennes (Pommier *et al.*, 2007; Sunagawa *et al.*, 2015) ;
- La salinité, qui structure largement les communautés bactériennes (Fortunato *et al.*, 2012; Ortega-Retuerta *et al.*, 2013) ;
- La quantité de nutriments, qui peut limiter la croissance des bactéries (Pinhassi *et al.*, 2006; Newton et McMahon, 2011) ;
- La qualité et la quantité de la matière organique, qui sert de source de nourriture : les communautés bactériennes réagissent par exemple très rapidement aux changements de

matière organique lors d'une efflorescence phytoplanctonique (Teeling *et al.*, 2012; Buchan *et al.*, 2014; Landa *et al.*, 2016) ;

- De nombreux autres facteurs, comme par exemple : la pression hydrostatique, les phénomènes affectant la structuration des masses d'eau (e.g., turbulence, vitesse du vent, advection verticale et horizontale), l'irradiation solaire, le pH, la concentration en dioxygène dissous.

Parallèlement, les **interactions biotiques** peuvent également moduler la composition des communautés bactériennes. En effet, les bactéries ne sont pas isolées dans l'environnement mais forment des réseaux d'interactions complexes. Celles-ci concernent les interactions bactéries-bactéries, mais aussi les interactions avec d'autres organismes, comme les virus (e.g., lyse bactérienne), les cellules phytoplanctoniques (e.g., échange de métabolites au sein de la phycosphère) ou le microzooplancton (e.g., prédation). Les interactions peuvent être positives (+, conférant un avantage), négatives (-, conférant un désavantage) ou neutre (ne conférant ni avantage, ni désavantage) pour l'un et l'autre des partenaires impliqués (Faust et Raes, 2012). Elles peuvent être ainsi classifiées sur un spectre allant du mutualisme (+, +) (e.g., quand deux espèces possédant des capacités différentes coopèrent pour l'utilisation d'un substrat) à la compétition (-, -) (e.g., quand deux espèces s'excluent entre elles en entrant en compétition pour le même substrat) (Faust et Raes, 2012).

Bien que participant probablement de manière importante à la structuration des communautés, les interactions entre microorganismes sont particulièrement difficiles à étudier. Classiquement, des méthodes de co-culture peuvent être utilisées pour déterminer leur existence et leur mode de fonctionnement (Faust et Raes, 2012; Cooper et Smith, 2015), mais elles sont forcément limitées dans leur mise en œuvre. Pour pallier ces problèmes, une manière d'inférer les interactions *in situ* est de s'intéresser à la **cooccurrence** entre les espèces. Cette méthode statistique, souvent présentée sous forme de réseaux de cooccurrence, permet de détecter les taxons présentant des cooccurrences positives (traduisant potentiellement des interactions mutualistes) et ceux présentant des cooccurrences négatives (traduisant potentiellement des interactions antagonistes, comme la compétition) (Barberán *et al.*, 2012; Carr *et al.*, 2019; J. Liu *et al.*, 2019). Cependant, les réseaux de cooccurrence peuvent être influencés par d'autres facteurs que les interactions biotiques et la validité des interactions inférées doit être vérifiée (Carr *et al.*, 2019).

I.D. Les bactéries hétérotrophes marines et l'utilisation de la matière organique

I.D.1) *Les bactéries libres et attachées aux particules*

Les communautés bactériennes présentes dans la colonne d'eau sont généralement séparées en deux catégories : les bactéries **libres** et celles **attachées aux particules**. Des traits fonctionnels comme la motilité ou le chimiotactisme permettent en effet à certaines bactéries de localiser et coloniser divers surfaces et agrégats (Kiørboe et Jackson, 2001; Pomeroy, 2007; Grossart, 2010). La

séparation entre ces deux types de communautés est effectuée de manière opérationnelle, le plus souvent avec un seuil de filtration entre 0.8 et 3 µm. Des fractions de taille différentes peuvent également être utilisées pour distinguer les bactéries associées aux petites et grosses particules (e.g., Mestre *et al.*, 2017). Il faut cependant noter qu'il existe un échange dynamique entre les deux compartiments, les bactéries pouvant à tout moment coloniser ou se détacher d'un agrégat ou d'une surface (Grossart, 2010).

Les bactéries attachées sont minoritaires dans les océans et représentent en moyenne moins de 10 % des communautés bactériennes pélagiques (Simon *et al.*, 2002). Cependant, elles peuvent ponctuellement atteindre 90 % de la communauté, en particulier dans les rivières, estuaires et zones côtières chargés en particules (Crump *et al.*, 1998; Simon *et al.*, 2002). Les communautés bactériennes attachées aux particules s'établissent souvent sous forme de biofilm, un amas structuré de cellules microbiennes encastrées au sein d'une matrice de polymères. Ces biofilms comportent une forte densité cellulaire (10^8-10^9 cellules mL^{-1}), souvent un à deux ordres de grandeur supérieur à celle de l'eau environnante (Azam et Long, 2001; Simon *et al.*, 2002).

La distinction entre ces deux modes de vie est importante puisque la colonisation permet aux bactéries d'accéder à de nouvelles ressources de matière organique. En effet, si la MOD est presque exclusivement assimilée par les bactéries hétérotrophes libres, les bactéries hétérotrophes attachées aux particules utilisent largement la MOP pour supporter leur croissance (Azam et Long, 2001). Les agrégats sont ainsi de véritables « *hotspots* » d'activité bactérienne. Comparées aux bactéries libres environnantes, les bactéries attachées aux particules sont souvent : i) plus grosses (Simon *et al.*, 2002) ; iii) avec des taux de production bactérienne plus élevés (Karner et Herndl, 1992; Middelboe *et al.*, 1995) ; iii) avec des voies métaboliques plus diversifiées (Lyons et Dobbs, 2012; Simon *et al.*, 2014) ; et iv) avec un niveau d'activités enzymatiques spécifiques plus important (Smith *et al.*, 1992; Grossart *et al.*, 2007; Rieck *et al.*, 2015). Le plus souvent, les communautés libres et attachées diffèrent également dans leur taxonomie (Bižic-Ionescu *et al.*, 2015; Rieck *et al.*, 2015; Mestre *et al.*, 2017) bien que l'inverse ait également été reporté (Hollibaugh *et al.*, 2000; Ortega-Retuerta *et al.*, 2013) et que les facteurs influençant ces différences taxonomiques ne soient pas bien compris. En général, les communautés attachées aux particules sont enrichies en bactéries appartenant aux groupes des Gammaproteobacteria, Bacteroidetes, Alphaproteobacteria, Verrucomicrobia et Planctomycetes (Rink *et al.*, 2008; Bižic-Ionescu *et al.*, 2015; Mestre *et al.*, 2017, 2020; Li *et al.*, 2021).

Les activités métaboliques importantes des bactéries fixées aux particules ont des conséquences fortes pour la biogéochimie marine. Leur intense production d'enzymes hydrolytiques dégrade et solubilise la MOP, et ce, de manière découplée avec leur taux assimilation (Smith *et al.*, 1992; Kirchman et White, 1999). Cela signifie que les bactéries hydrolysent plus de matière qu'elles n'en assimilent. Ce phénomène génère la formation d'une « trainée » enrichie en MOD et en

nutriments autour des agrégats de matière organique (Smith *et al.*, 1992; Azam et Long, 2001; Grossart, 2010). Bien que très localisée, il a été démontré que cette trainée est rapidement colonisée par les bactéries libres chimiotactiques et motiles, et qu'elle soutient une portion significative de la production bactérienne des bactéries libres (Kiørboe et Jackson, 2001; Grossart, 2010). En plus de libérer de la MOD, l'action des enzymes participe à la dégradation et la solubilisation des agrégats, modifiant leur taille et donc leur exportation.

I.D.2) *Des stratégies trophiques variées pour appréhender la complexité de la matière organique*

Les bactéries sont confrontées à des sources de MOD et de MOP d'une grande complexité chimique, dont la composition et la biodisponibilité évoluent dans le temps et l'espace. Elles doivent également faire face à des conditions de nutriments inorganiques fluctuantes, parfois limitantes. Les variations temporelles des sources de nourriture sont notamment marquées lors des efflorescences printanières du phytoplancton (« *bloom* »), menant à une diminution des nutriments inorganiques et un relargage de composés organiques labiles qui varient selon l'évolution du bloom. En effet, les cellules phytoplanctoniques libèrent préférentiellement de petits composés (acides aminés, acides organiques, monosaccharides, urée, diméthylsulfoniopropionate ou phosphonates) dans la phase initiale et le pic du bloom, puis des composés de haut poids moléculaire (polysaccharides, protéines, acides nucléiques et lipides) pendant le déclin du bloom (Buchan *et al.*, 2014; Francis *et al.*, 2021). La concentration et la qualité de la matière organique évoluent également spatialement. A l'échelle microscopique, la matière organique peut être localement très concentrée lorsqu'elle est associée à des particules estuariennes et marines ou aux environs des cellules phytoplanctoniques (phycosphère), alors qu'elle est très peu concentrée dans le milieu dissous environnant (Stocker, 2012). A une plus large échelle, il existe de larges variations de quantité et de qualité de la matière organique dans les zones côtières et estuariennes, influencées par différentes sources autochtones et allochtones de composition très distinctes (**cf I.B**).

Les bactéries marines hétérotrophes mettent en place **différentes stratégies** pour répondre à cette variabilité de ressources et exploiter au mieux les substrats disponibles. Ces stratégies trophiques sont variées, complexes et peuvent être classifiées selon différentes typologies opposant par exemple : i) les oligotrophes (se développant à des faibles concentrations de substrat) aux copiotrophes (nécessitant de plus fortes concentrations de substrat) ; ou bien ii) les généralistes (capables de croître en utilisant une large variété de composés) aux spécialistes (qui consomment un nombre de substrats plus restreint). Les bactéries hétérotrophes peuvent également se différencier selon leur capacité à utiliser des composés de bas poids ou de haut poids moléculaire. Ces différentes stratégies nutritives se traduisent nécessairement par des adaptions encodées génétiquement au sein des génomes bactériens.

Les **substrats organiques labiles de bas poids moléculaire** sont directement assimilables par les cellules bactériennes, qui sont essentiellement osmotrophes. En effet, les bactéries utilisent des perméases capables d'assimiler les substrats dissous même à faible concentration (Nagata, 2008). A titre d'exemple, on peut citer les roseobacters (Alphaproteobacteria) qui sont communément considérées comme des spécialistes de l'assimilation de petits composés (Teeling *et al.*, 2012; Landa *et al.*, 2016). Les roseobacters encodent typiquement plusieurs voies de transports dédiées, notamment des transporteurs ATP-dépendant et ATP-indépendant (Buchan *et al.*, 2014).

D'autres espèces peuvent se spécialiser dans l'assimilation de **substrats organiques complexes de haut poids moléculaire**. Cependant, ces substrats ne peuvent pas être métabolisés en l'état : ils doivent être préalablement hydrolysés en petits composés assimilables aux travers des membranes bactériennes (< 600-700 Da) (Payne, 1980; Arnosti, 2011). Cette étape d'hydrolyse est considérée comme cruciale et limitante dans l'utilisation de la matière organique marine par les bactéries (Arnosti, 2011). Jusqu'à récemment, on considérait que cette hydrolyse était uniquement réalisée par les enzymes extracellulaires bactériennes (**cf partie I.E**) qui clivent les composés organiques à l'extérieur des cellules, avant que les produits de dégradation ne soient assimilés (Chróst, 1990; Arnosti, 2011). Lorsque le couplage entre l'hydrolyse des polymères et l'assimilation de leurs produits de dégradation n'est pas parfait, une partie des produits de dégradation diffuse vers l'environnement extérieur (« *sharing bacteria* », **Figure I.5**) (Reintjes *et al.*, 2019). D'autres bactéries peuvent alors en profiter, sans participer à l'effort de production d'enzymes hydrolytiques (« *scavenging bacteria* », **Figure I.5**) (Enke *et al.*, 2019; Reintjes *et al.*, 2019). Cependant, une autre stratégie largement employée en milieu marin a récemment été mise en évidence : certaines bactéries peuvent lier les polysaccharides à la surface de leur cellule, les hydrolyser partiellement avec leurs enzymes membranaires et assimiler les produits d'hydrolyse de poids moléculaire intermédiaire à l'intérieur de leur espace périplasmique (Reintjes *et al.*, 2017, 2019). L'hydrolyse en petits composés se poursuit ensuite à l'intérieur des cellules, résultant en une perte diffusive minimale dans le milieu environnant (« *selfish bacteria* », **Figure I.5**) (Reintjes *et al.*, 2017, 2019). Jusqu'à 26 % de la communauté bactérienne, principalement des Bacteroidetes, des Planctomycetes et des Gammaproteobacteria, pourrait utiliser cette stratégie (Reintjes *et al.*, 2017, 2019).

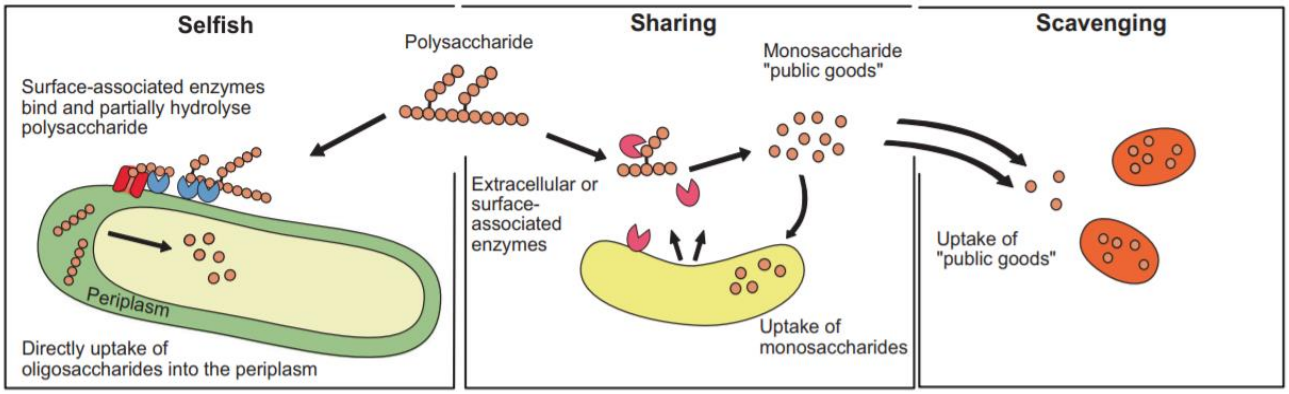

Figure I.5. Illustration des différentes stratégies trophiques utilisées par les bactéries marines pour assimiler la matière organique de haut poids moléculaire. Les « *sharing bacteria* » hydrolysent la matière organique polymérique à l'extérieur des cellules, permettant le développement des « *scavenging bacteria* » qui utilisent les produits d'hydrolyse non assimilés diffusant dans l'environnement. Au contraire, les « *selfish bacteria* » hydrolysent partiellement les polymères à l'extérieur des cellules, puis de manière plus complète dans leur espace périplasmique, limitant ainsi la perte de substrat. Extrait de Reintjes *et al*. (2019).

Les Flavobacteria (Bacteroidetes) sont par exemple largement considérées comme des spécialistes de la dégradation de polysaccharides et protéines complexes (Elifantz *et al.*, 2005; Fernàndez-Gómez *et al.*, 2013; Ferrer-González *et al.*, 2021). A ce titre, elles encodent de nombreuses enzymes hydrolytiques extracellulaires et membranaires comme des laminarinases ou des fucosidases (Buchan *et al.*, 2014). Elles possèdent également des récepteurs TonB-dependant, permettant la réquisition de larges molécules dans leur périplasme (Buchan *et al.*, 2014).

I.E. Les enzymes hydrolytiques, outils de la minéralisation bactérienne

En catalysant la conversion de molécules de haut poids moléculaire en petit composés assimilables, les enzymes extracellulaires jouent un rôle central et limitant dans l'utilisation de la matière organique par les bactéries. Il est crucial de connaitre les facteurs affectant la synthèse d'enzymes hydrolytiques ou leur niveau d'activité *in situ*, car ils affectent ainsi toute la cascade de minéralisation (Arnosti, 2011).

I.E.1) *Les enzymes hydrolytiques extracellulaires bactériennes*

Les enzymes hydrolytiques bactériennes peuvent être intracellulaires (agissant à l'intérieur des cellules) ou extracellulaires (agissant à l'extérieur des cellules), ces dernières impactant directement la transformation de la matière organique. Parmi les enzymes extracellulaires, on distingue : i) les « **ectoenzymes** », qui restent associées aux membranes des cellules ; et ii) les « **exoenzymes** », c'est-à-dire les enzymes sécrétées dans le milieu, qu'elles soient librement dissoutes ou adsorbées sur des surfaces inertes (e.g., particules) (Chróst, 1990; Nagata, 2008).

Les exoenzymes peuvent résulter de phénomènes actifs de sécrétion, mais aussi de processus passifs comme la lyse des cellules par les virus ou le broutage (Baltar, 2018). Elles ont des temps de demi-vie pouvant atteindre jusqu'à 20 jours dans l'océan (Steen et Arnosti, 2011; Baltar, 2018). On considérait initialement que les ectoenzymes étaient majoritaires dans l'environnement (Vives Rego *et al.*, 1985; Nagata, 2008). Cependant, plusieurs études ont depuis révélé que l'importance relative des ecto- et exoenzymes peut fortement varier, les exoenzymes pouvant représenter jusqu'à 100 % de l'activité enzymatique (Baltar, 2018; Baltar *et al.*, 2019; Thomson *et al.*, 2019). Les facteurs influençant ce ratio entre exo- et ectoenzymes restent cependant assez peu connus (Baltar *et al.*, 2017, 2019).

I.E.2) *Cinétique de Michaelis-Menten et méthodes de mesure des activités enzymatiques*

Le niveau d'activité des enzymes hydrolytiques est généralement relié à la concentration en substrat par le modèle de Michaelis-Menten. L'activité des enzymes est ainsi caractérisée par deux paramètres : leur vitesse maximale, quand tous les sites actifs sont saturés (V_{max}), ainsi que leur affinité pour le substrat (K_m, correspondant à la concentration de substrat pour laquelle l'enzyme fonctionne à la moitié de sa V_{max}) (**Figure I.6**).

Ces paramètres peuvent être mesurés grâce à l'utilisation de deux types de **substrats comportant des fluorophores**. Les substrats les plus utilisés actuellement correspondent à des petites molécules fluorogéniques, dont les propriétés de fluorescence sont significativement modifiées lorsqu'ils sont clivés. Ces molécules consistent en un petit groupement mimant le substrat naturel de l'enzyme cible (e.g., monosaccharides, acides aminés ou groupement phosphate) couplé à un fluorophore, le plus souvent un groupement methylumbelliferyl (MUF) ou 4-methylcoumarinylamide (MCA) (Chróst, 1990; Nagata, 2008; Arnosti, 2011). L'hydrolyse de ce substrat artificiel par l'enzyme libère le fluorophore et la vitesse de réaction peut être déterminée en suivant l'augmentation de la fluorescence dans le temps. Ces mesures sont faciles à mettre en place et peu chères mais posent des problèmes méthodologiques puisqu'elles ne miment pas la complexité des substrats naturels des activités mesurées (polymères de structure complexe) (Arnosti, 2011). Pour pallier ces limitations, des polymères marqués en fluorescence ont été développés. Ces polymères sont principalement des polysaccharides (Arnosti, 1995) ou des peptides (Pantoja *et al.*, 1997), représentant au mieux les substrats réels des enzymes bactériennes. Cette approche diffère de la première : ici, le fluorophore reste lié au polymère et c'est la diminution de taille de celui-ci qui est suivie dans le temps (par exemple par chromatographie sur gel perméable, Arnosti, 1995). Cette méthode possède d'autres limitations, notamment concernant la nécessité d'effectuer des incubations de longue durée (e.g., 2 à 8 jours dans D'Ambrosio *et al.*, 2014) peu compatibles avec les mesures d'activités enzymatiques de communautés bactériennes complexes, dont la dynamique évolue rapidement dans le temps.

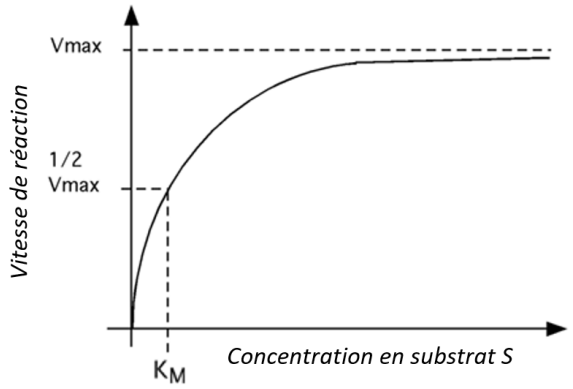

$$V = \frac{V_{max}[S]}{K_m + [S]}$$

Figure I.6. Equation de Michaelis-Menten et représentation de la courbe associée. La vitesse de l'enzyme est caractérisée par la concentration en substrat [S], la vitesse maximale de l'enzyme V_{max} et son affinité pour le substrat, K_m.

Un point important concerne les mesures habituellement réalisées en écologie microbienne marine. En effet, la détermination des activités enzymatiques correspond généralement à la détermination de la V_{max}, réalisée en utilisant de fortes concentrations en substrat, très supérieures au K_m. Cela ne traduit donc pas le niveau réel d'activité *in situ*, mais représente un indicateur de l'équipement enzymatique des cellules, la V_{max} étant proportionnelle à la concentration des enzymes présentes (Chróst, 1990; Nagata, 2008).

Une synthèse critique de la littérature sur les mesures des activités enzymatiques basées sur l'utilisation de substrats fluorogéniques a été menée dans le cadre d'un travail préliminaire. Ce travail a permis la rédaction d'un article de méthodologie démontrant trois écueils majeurs (**cf annexe I**, Urvoy *et al.*, 2020) :

- La présence éventuelle d'un artefact intrinsèque à la fluorimétrie, l'effet de filtre interne, entrainant une sous-estimation des V_{max} mesurées. Ce phénomène est bien connu mais n'a jamais été décrit dans les mesures d'activités enzymatiques en milieu marin ;
- L'utilisation de gammes de concentration en substrat insuffisantes lors de la réalisation de cinétique de Michaelis-Menten, qui peut mener à une estimation erronée des paramètres enzymatiques (V_{max} et K_m) ;
- La compétition entre les substrats naturellement présents dans l'eau de mer (e.g., polysaccharides, protéines, phosphomonoesters) et le substrat fluorogénique, qui peut réduire significativement la valeur de V_{max} mesurée lorsque les concentrations en substrat fluorogénique sont trop faibles.

I.E.3) *Les activités couramment mesurées en milieu marin*

Les enzymes impliquées dans la dégradation de la matière organique les plus couramment investiguées dans le milieu marin sont les aminopeptidases, les β-D-glucosidases et les phosphatases

alcalines (Chróst, 1990). On considère que ces enzymes hydrolytiques sont majoritairement produites par les bactéries hétérotrophes marines, exceptées les phosphatases alcalines qui sont également synthétisées par d'autres organismes comme les cellules phytoplanctoniques (Hoppe, 2003).

Les **activités aminopeptidases** sont mesurées avec la L-leucine 7-amido-4-methylcoumarine (leu-MCA). Ces enzymes hydrolysent les liaisons –CO–NH– présentes à l'extrémité N-terminale des protéines et peptides. Les acides aminés ainsi relargués constituent une matière très labile et sont directement assimilables pour les communautés bactériennes. La mesure avec la leu-MCA est parfois considérée comme représentative exclusive des L-Leucine aminopeptidases (EC 3.4.11.1) qui hydrolysent les résidus L-Leucine (Steen *et al.*, 2015). Cependant, l'hydrolyse de la leu-MCA représente en réalité l'action concertée de différentes enzymes, certaines hydrolysant préférentiellement d'autres composés que la leucine, comme des résidus arginines, méthionines ou tyrosines (Steen *et al.*, 2015). Cette activité est donc souvent considérée comme un proxy des activités peptidiques globales.

Le substrat 4-methylumbelliferyl β-D-glucopyranoside permet de mesurer les **activités β-D-glucosidases**. Elles hydrolysent les liaisons osidiques au sein desquelles un résidu glucose est relié par une liaison β, comprenant par exemple la cellulose (Chróst, 1990).

Enfin, le niveau d'activité des phosphatases des communautés microbiennes est déterminé en mesurant l'hydrolyse du 4-methylumbelliferyl phosphate. Les **phosphatases alcalines** fonctionnent sur une gamme de pH comprise entre 7.6 et 9.6 et sont donc les phosphatases majoritaires dans les océans (pH ≈ 8.2). Elles hydrolysent préférentiellement les liaisons phosphomonoesters (P–O–C), relâchant un groupement phosphate et une partie organique (Chróst, 1990). Les phosphatases alcalines sont considérées comme très spécifiques des liaisons phosphomonoesters mais elles ne sont pas spécifiques du radical organique, hydrolysant ainsi une large gamme de composés (Hoppe, 2003). La régénération du phosphate à partir de l'hydrolyse du phosphore organique dissous représente une source importante de ce nutriment, en particulier dans les eaux oligotrophes du large ou les zones côtières impactées par des apports terrestres déséquilibrés en ratio N/P (Hoppe, 2003; Vidal *et al.*, 2003). En relâchant à la fois un groupement phosphate et une partie organique contenant du carbone et de l'azote, l'activité des phosphatases alcalines pourrait régénérer ces trois composés à la fois, rendant son étude plus complexe (Hoppe, 2003). Les phosphatases alcalines dissoutes (exoenzymes) représentent souvent une fraction majeure des activités phosphatases alcalines totales et parfois plus de 70 % (Hoppe, 2003; Thomson *et al.*, 2019).

I.E.4) *Les facteurs contrôlant le niveau d'activité des enzymes hydrolytiques*

Le niveau d'activité des enzymes hydrolytiques *in situ* varie sous l'influence de nombreux facteurs. On peut distinguer les facteurs régulant la synthèse des enzymes (et donc, leur concentration dans le milieu) et ceux contrôlant le niveau d'activité des enzymes une fois synthétisées (Chróst, 1990).

i) Les facteurs impactant la synthèse des enzymes hydrolytiques

La synthèse des enzymes hydrolytiques extracellulaires peut-être affectée à deux niveaux : au niveau génomique (i.e., présence ou absence des gènes encodant les enzymes) et au niveau transcriptionnel (i.e., expression plus ou moins importante de ce potentiel génétique). En effet, certains groupes bactériens sont connus pour posséder plus de gènes codant pour des enzymes hydrolytiques que d'autres. Par exemple, plusieurs études de génomique comparative ont souligné la présence de nombreux gènes d'hydrolyse de polysaccharides et protéines chez les Flavobacteria, considérées comme des spécialistes de la dégradation (Thomas *et al.*, 2011; Fernàndez-Gómez *et al.*, 2013). En ce sens, il a aussi été observé que des différences dans le spectre d'hydrolyse de polysaccharides pouvaient corréler avec de grands patrons biogéographiques bactériens (Arnosti *et al.*, 2011; Arnosti, 2014; Kellogg et Deming, 2014; Balmonte *et al.*, 2019). Ces études soulignent ainsi l'importance des variations de composition des communautés bactériennes sur leur niveau d'activité enzymatique.

Certaines enzymes sont exprimées de manière **constitutive**, c'est-à-dire en continue, indépendamment de la concentration en substrat dans l'environnement (Chróst, 1990). Cependant, au vue du fort coût métabolique de cette synthèse (en énergie, carbone et azote), l'expression de la plupart des enzymes est fortement contrainte sur le plan transcriptionnel afin qu'elles ne s'expriment pas dans des conditions défavorables (Chróst, 1990; Nagata, 2008). Ces enzymes sont dites « **inductibles** » (Chróst, 1990; Nagata, 2008). La majorité des enzymes hydrolytiques extracellulaires produites par les bactéries hétérotrophes marines sont inductibles afin d'exploiter au mieux des substrats dont la quantité varie largement sur le plan spatial et temporel (Chróst, 1990; Nagata, 2008). Les enzymes inductibles sont synthétisées en très faible quantité en absence de leur substrat. Lorsque que celui-ci est détecté dans le milieu, les cellules expriment alors les enzymes permettant son hydrolyse (**induction par le substrat**). Ce phénomène perdure généralement jusqu'à la disparition du substrat ou l'accumulation de ses produits de dégradation (**répression par le produit final**) (Chróst, 1989, 1990; Nagata, 2008). La répression par le produit final permet d'éviter une hydrolyse excessive par rapport aux besoins de la cellule. Un exemple type de ces enzymes est la phosphatase alcaline, dont la synthèse est réprimée en présence de phosphate, le principal produit d'hydrolyse des phosphomonoesters (Chróst, 1990; Hoppe, 2003). Un autre système de régulation largement mis en

place par les bactéries hétérotrophes correspond à la **répression catabolique**, qui empêche la synthèse d'une enzyme quand une autre source de carbone plus labile est disponible (Chróst, 1990).

ii) Les facteurs impactant l'activité des enzymes hydrolytiques

Plusieurs facteurs peuvent inhiber l'activité des enzymes hydrolytiques une fois qu'elles sont synthétisées. On peut citer à titre d'exemple des facteurs biochimiques, comme l'accumulation du produit final de la réaction enzymatique, de trop fortes concentrations en substrat, ou la présence d'inhibiteurs compétitifs (augmentation du K_m) ou non compétitifs (diminution de la V_{max}) (Chróst, 1990). Le niveau d'activité des enzymes hydrolytiques peut également être impacté par des facteurs environnementaux comme la température ou le pH. Enfin, le niveau d'activité des enzymes dissoutes dépend de tous les facteurs déjà cités, mais également de ceux affectant leur temps de demi-vie (e.g., radiations UV, présence de protéases) (Baltar *et al.*, 2017; Baltar, 2018).

I.E.5) *Les enzymes hydrolytiques au sein des communautés fixées aux particules*

Si les bactéries fixées aux particules présentent des taux d'hydrolyse enzymatique plus élevés que les bactéries libres (**cf I.D.1**), les raisons derrière ce phénomène restent floues. Il pourrait résulter d'une régulation transcriptionnelle ou d'une différence de composition des communautés (**cf I.E.2**) mais l'importance relative de l'un par rapport à l'autre reste largement à déterminer (Arnosti, 2014).

Des études ont démontré que la simple fixation de souches isolées ou de communautés bactériennes naturelles sur des surfaces solides induisait une forte augmentation de leurs activités métaboliques (Taylor et Gulnick, 1996; Bonin *et al.*, 2001; Grossart *et al.*, 2007; Ziervogel *et al.*, 2010). Plus spécifiquement, Grossart *et al.* (2007) ont montré que la fixation à une surface induisait une forte augmentation (de 10 à 20 fois) des activités aminopeptidases spécifiques au sein de souches bactériennes isolées de particules de neige marine et ce, de manière presque immédiate. Ce résultat pointerait vers une régulation transcriptionnelle induisant l'augmentation du métabolisme des bactéries colonisant une surface. Cette surexpression des activités pourrait être due à une forte concentration en matière organique dans l'environnement local des bactéries fixées sur les particules. Ce type de comportement fait sens pour les bactéries marines vivant fixées aux agrégats : elles pourraient posséder un métabolisme faible lorsqu'elles vivent librement dans la colonne d'eau et augmenter celui-ci lors de la fixation sur un agrégat, exploitant au mieux les ressources environnantes (Grossart *et al.*, 2007). Cependant, ces phénomènes ont aussi été observés au sein de souches colonisant des substrats inertes, donc sans influence de la concentration en substrat (Taylor et Gulnick, 1996; Bonin *et al.*, 2001). Si les mécanismes en jeu restent à élucider, il a été suggéré que des phénomènes de signalisation cellulaire comme le quorum sensing (QS) (**cf II**) pourraient participer à l'augmentation du métabolisme des bactéries lors de leur attachement sur des particules (Gram *et al.*, 2002).

Les communautés colonisant les particules tendent à différer taxonomiquement des communautés libres les entourant (**cf I.D.1**), une particularité qui pourrait également expliquer les différences de métabolisme entre les deux types de communautés. En effet, il est connu que des variations de quantité et de qualité de la matière organique peuvent entrainer une modification de la composition communautés bactériennes, en sélectionnant des taxons capables d'utiliser les substrats présents (Teeling *et al.*, 2012; Landa *et al.*, 2016). La composition moléculaire des particules pourrait ainsi induire une sélection de taxons à fort potentiel dégradeur, au moins au début de la colonisation (Datta *et al.*, 2016; Enke *et al.*, 2018, 2019). Par exemple, Datta *et al.* (2016) ont utilisé des particules modèles formées de chitine pour étudier la dynamique des taxons les colonisant, ainsi que leurs traits phénotypiques. Ces auteurs ont montré que la colonisation bactérienne des particules s'effectuait en trois phases, avec une 1ère phase courte (< 20 h) où la composition des communautés attachées aux particules est gouvernée par la capacité d'attachement des bactéries, sans influence de leur capacité à utiliser la chitine. Une 2ème phase de sélection (20 - 44 h) entraine un déclin drastique de la diversité des communautés lié à une forte influence des conditions environnementales imposées par la composition de la particule. Cette phase correspond à la sélection de taxons spécialisés dans la dégradation et l'utilisation de la chitine, ce qui se traduit par une augmentation de la fréquence des gènes impliqués dans ce processus (e.g., chitinases extracellulaires). Ces contraintes sélectives sont ensuite relâchées dans la 3ème phase de colonisation (44 - 140 h), durant laquelle l'évolution des communautés est principalement modulée par les interactions trophiques. Cette phase correspond à l'arrivée de consommateurs secondaires, utilisant les substrats issus de l'activité des colonisateurs primaires (phénomènes de « *cross-feeding* » par exemple). Dans une étude similaire, Enke *et al.* (2019) ont démontré que la taxonomie des colonisateurs primaires est différente selon le polysaccharide composant les particules à coloniser, confirmant l'influence importante du substrat sur la sélection de taxon à fort potentiel dégradeur.

II. Le quorum sensing, un système de communication bactérienne

Les bactéries marines sont en compétition permanente pour les nutriments, le carbone et les niches écologiques à occuper. Cette compétition génère de **nombreuses interactions** qui contribuent à la structuration et au fonctionnement des communautés (Strom, 2008; Atkinson et Williams, 2009; Gralka *et al.*, 2020). Par exemple, les interactions trophiques, qui émergent suite à la dégradation de formes complexes de matière organique, sont centrales au sein de communautés microbiennes (Gralka *et al.*, 2020). Il existe également de nombreuses interactions non trophiques médiées par des métabolites secondaires bioactifs incluant, par exemple, les vitamines et autres cofacteurs, les antimicrobiens (e.g., antibiotiques, algicides, peptides antimicrobiens) ou encore les molécules de signalisation cellulaire (Gralka *et al.*, 2020). Le **quorum sensing** (QS) bactérien est un exemple de système de signalisation intercellulaire particulièrement bien caractérisé, permettant la coordination de l'expression de divers gènes au sein d'une communauté bactérienne (Miller et Bassler, 2001; Waters et Bassler, 2005).

II.A. La découverte du quorum sensing

La découverte du QS repose sur des expériences réalisées dans les années 1970, étudiant la **bioluminescence de la bactérie marine *Vibrio fischeri*** (Nealson *et al.*, 1970; Eberhard, 1972; Fuqua *et al.*, 1994). Lorsque celle-ci vit sous forme planctonique dans l'eau de mer, elle ne produit pas de bioluminescence. En revanche, lorsqu'elle vit en association avec la sépiole *Euprymna scolopes*, un petit céphalopode apparenté aux seiches, elle émet une bioluminescence qui permet à l'animal de se dissimuler en masquant son ombre. Les chercheurs montrent alors que ce phénotype est densité-dépendant : *V. fischeri* produit également cette bioluminescence lorsqu'elle atteint de fortes densités en culture (Nealson *et al.*, 1970). Les études suivantes ont permis d'élucider complètement le mécanisme de régulation de la bioluminescence chez cette bactérie, basé sur une molécule identifiée comme une *N*-acyle homosérine lactone (AHL) (Eberhard *et al.*, 1981). Le confinement de *V. fischeri* à l'intérieur de l'organe photophore de la sépiole permet d'atteindre une forte densité cellulaire et donc une forte concentration en AHLs. Les AHLs se lient alors à leur récepteur, appelé LuxR, et activent la transcription de l'opéron *lux* (Engebrecht et Silverman, 1984). Cela conduit à la production de l'enzyme luciférase qui catalyse la réaction permettant la bioluminescence. Si le système est initialement considéré comme spécifique à la régulation de la bioluminescence, de nombreux systèmes de régulation similaires ont ensuite été découverts chez une large variété d'isolats bactériens. Le terme de « quorum sensing » (littéralement, « détection du quorum ») a finalement été introduit par Fuqua et Winans (1994) et connait un succès immédiat.

Si le QS a été découvert grâce à la production de bioluminescence d'une bactérie marine, la plupart des études sur le sujet se sont ensuite concentrées sur des souches d'intérêt médical ou

agronomique (Lami, 2019). Ce n'est que depuis les années 2000 que l'on s'intéresse au rôle du QS dans les océans (McLean *et al.*, 1997; Gram *et al.*, 2002) où les implications de ce mécanisme complexe restent largement sous explorées à l'heure actuelle.

II.B. Les mécanismes du quorum sensing bactérien

Le QS est donc un mécanisme de communication intercellulaire permettant la coordination de l'expression d'un ensemble de gènes au sein d'une communauté bactérienne. Si les AHLs ont permis la découverte du QS, il existe de nombreuses autres molécules signal diffusibles, regroupées sous le terme d'**auto-inducteurs (AIs)** (**Figure I.7A**) (Waters et Bassler, 2005; Brameyer *et al.*, 2015). Ces molécules sont généralement considérées comme un reflet de la densité cellulaire. Lorsque la densité bactérienne augmente, les AIs s'accumulent dans le milieu jusqu'à atteindre une concentration seuil. Ils peuvent alors se lier à leur récepteur membranaire ou cytoplasmique, enclenchant la transduction du signal, qui permet finalement l'induction ou la répression de gènes cibles (**Figure I.7B**) (Miller et Bassler, 2001; Waters et Bassler, 2005). Les gènes régulés sont divers et concernent des processus importants, susceptibles de proférer des avantages écologiques à la population ciblée, comme par exemple : l'échange d'information génétique (conjugaison), la motilité, les facteurs de virulence, la production de biofilm, la luminescence ou la synthèse d'enzymes extracellulaires (Miller et Bassler, 2001; Waters et Bassler, 2005; Hmelo, 2017). On distingue plusieurs éléments clefs dans le mécanisme du QS bactérien : (i) la molécule signal, (ii) les gènes impliqués dans la synthèse et la réception du signal et (iii) les gènes régulés par le QS.

A)

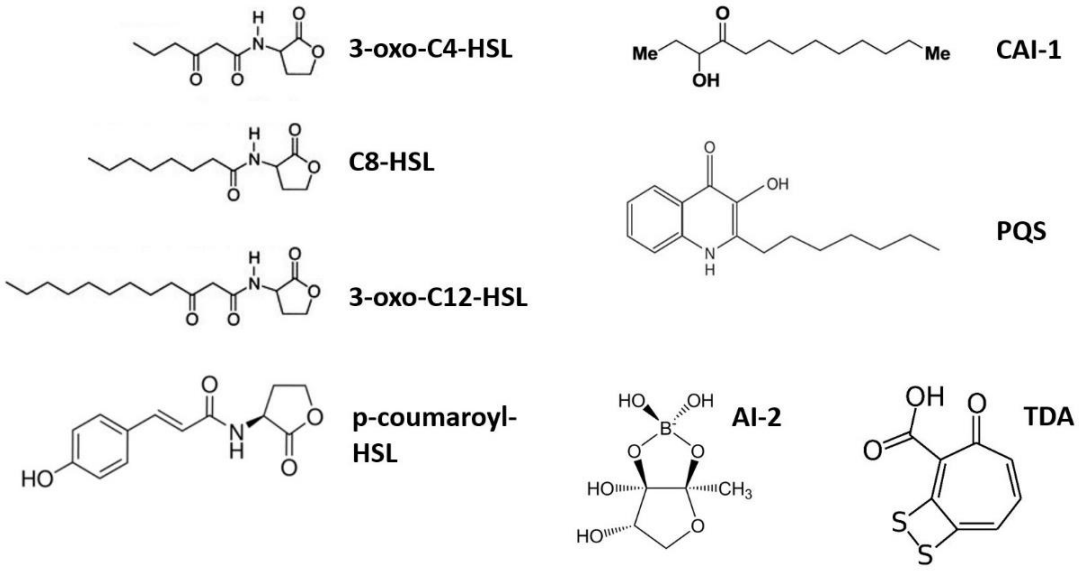

(cont.)

B)

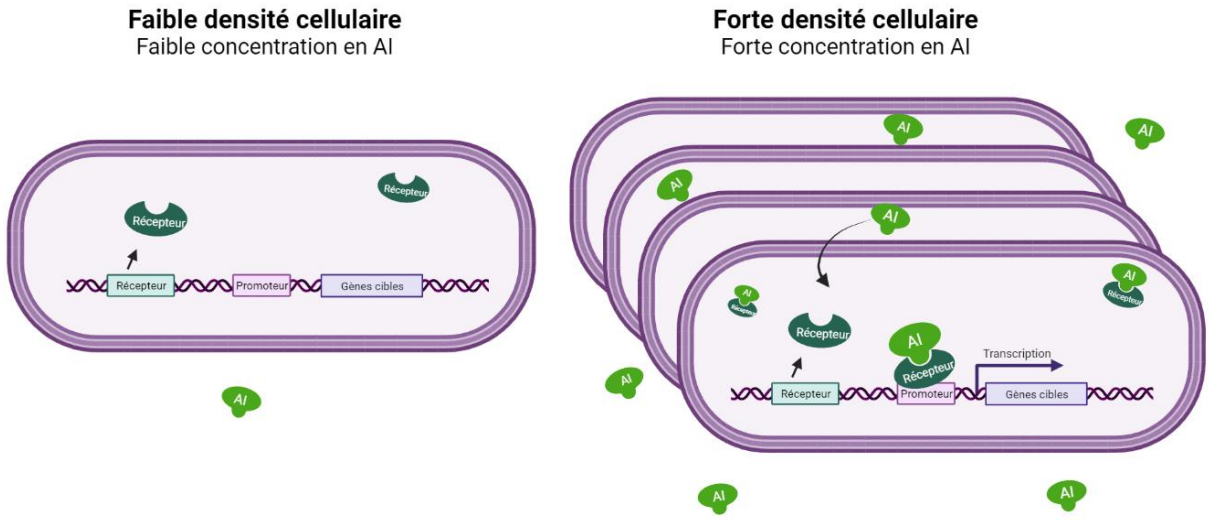

Figure I.7. (**A**) Exemples de formules chimiques de quelques AIs parmi les plus connus. 3-oxo-C4-HSL : *N*-(3-oxobutryryl)-DL-homoserine lactone ; C8-HSL : *N*-octanoyl-DL-homoserine lactone ; 3-oxo-C12-HSL : *N*-(3-oxododecanoyl)-DL-homoserine lactone ; p-coumaroyl-HSL : p-coumaroyl homoserine lactone ; CAI-1 : *Vibrio cholerae* auto-inducteur-1; PQS : *Pseudomonas* quinolone signal ; AI-2 : Auto-inducteur-2 ; TDA : Acide tropodithietique. (**B**) Représentation schématique du Quorum Sensing. A faible densité cellulaire, les molécules signal (AIs) ne peuvent pas s'accumuler dans le milieu. Lorsque la densité augmente, ces molécules s'accumulent et se fixent à leurs récepteurs permettant l'initiation de la régulation des gènes cibles. Parfois, l'AI-synthase est elle-même sous le contrôle du promoteur régulé par le complexe AI-récepteur, créant une boucle d'auto-induction. Créé avec https://biorender.com/.

II.B.1) *Les* N-*acyle homosérine lactones et la diversité des auto-inducteurs*

Parmi les diverses molécules signal existantes, les AHLs prennent une place particulière. Ce sont sans aucun doute les molécules du QS les plus étudiées, représentant le système de communication archétypique par lequel le QS fut découvert. Elles sont majoritairement utilisées par les bactéries Gram négatives, plus particulièrement chez les groupes Alpha-, Beta- et Gammaproteobactéries, abondants dans les écosystèmes océaniques et côtiers (Hmelo, 2017).

Les AHLs sont des molécules lipophiles dont la structure est relativement conservée : elles sont composées d'un cycle homosérine lactone de configuration L, uniquement substitué par un groupement *N*-acyle en position *a* (**Figure I.7A**). La chaine acyle contient généralement un nombre paire d'atomes de carbone compris 4 et 20 (Lami, 2019). Elle peut être insaturée (de configuration stéréochimique Z) ou encore substituée en 3ème position par un groupement cétone ou hydroxy. Quelques AHLs avec des chaines acyles ramifiées ont également été décrites, mais pas chez des souches marines jusqu'à présent (Lami, 2019). Ces modifications (substitutions, insaturation, ramification) permettraient une communication ciblée, car chaque espèce produirait une AHL ou une

combinaison d'AHLs spécifiques (Federle et Bassler, 2003). Il est toutefois compliqué d'établir un lien entre les AHLs produites et les phénotypes régulés.

Une notation allégée basée sur la structure de la chaine acyle a été adoptée par la communauté scientifique et est utilisée tout au long de ce manuscrit de thèse. Par exemple, une *N*-butyryl-L-homosérine lactone (avec une chaine acyle saturée à 4 atomes de carbone) est notée C4-HSL. La même AHL portant une insaturation est notée C4:1-HSL. Une *N*-(3-oxobutyryl-)-L-homosérine lactone (C4-HSL portant une substitution cétone en 3ème position de la chaine acyle) est notée 3-oxo-C4-HSL. Une *N*-(3-hydroxydecanoyl)-L-homosérine lactone (C4-HSL portant une substitution hydroxy en 3ème position de la chaine acyle) est notée 3-OH-C4-AHL.

Si les AHLs sont les AIs les plus étudiés en milieu marin à l'heure actuelle, il existe une multitude d'AIs associés à différentes machineries génétiques et moléculaires (**Figure I.7A**). Certains AIs sont intraspécifiques, d'autres interspécifiques (Atkinson et Williams, 2009). Les bactéries Gram négatives peuvent utiliser, à titre d'exemple, les hydroxy-quinolones (*Pseudomonas* Quinolone Signal - PQS) ou les *Vibrio cholerae* auto-inducteur-1 (CAI-1) (**Figure I.7A**), qui permettrait une communication intraspécifique (Atkinson et Williams, 2009; Brameyer *et al.*, 2015). Les auto-inducteurs de type 2 (AI-2), correspondant à des diesters de furanosyl borate, seraient communément produits par diverses bactéries Gram négatives et Gram positives. Ces molécules permettraient une communication inter-espèce (Federle et Bassler, 2003), bien que leur fonction de molécule signal soit l'objet de débats (Diggle *et al.*, 2007; Rezzonico et Duffy, 2008). Enfin, les bactéries Gram positives utiliseraient principalement des dérivés de peptides, détectés par un système de régulation à deux composants (Waters et Bassler, 2005).

Il n'est pas rare qu'une bactérie possède plusieurs circuits de QS interconnectés, reposant sur la production de différentes molécules signal. Par exemple, la bactérie *Pseudomonas aeruginosa* possède au moins quatre systèmes de QS organisés de manière hiérarchique, permettant de répondre à des signaux environnementaux variés (Hawver *et al.*, 2016). *Vibrio cholerae* en possèdent également quatre, participant tous à la colonisation de surfaces et à la production de biofilm, ce qui rendrait le système de régulation robuste aux perturbations et empêcherait une réponse prématurée du QS (Hawver *et al.*, 2016).

II.B.2) *Les gènes impliqués dans la synthèse et la réception des N-acylhomosérine lactones*

Les AHLs sont synthétisées par des protéines appelées **AHL synthases**, encodées par trois familles de gènes : *luxI*, *ainS* et *hdtS* (Fuqua et Greenberg, 2002). La 1ère famille est la plus connue et la plus étudiée : elle contient les homologues du gène utilisé par *V. fischeri* pour réguler sa production de bioluminescence. Les synthases de type LuxI (encodées par des gènes homologues de *luxI*) synthétisent les AHLs à partir de S-adénosyl méthionine (SAM) comme source d'homosérine lactone et d'une

protéine porteuse d'un groupement acyle (acyl-ACP) comme donneur de chaine acyle (**Figure I.8**) (Fuqua et Greenberg, 2002). Le donneur d'acide gras et la SAM sont impliqués dans des voies de biosynthèses essentielles aux bactéries (méthionine et acides gras) et sont en principe non limitants dans la cellule.

Si la structure des AHLs est relativement conservée, la séquence en acides aminés des homologues LuxI varie considérablement (seulement 28-35 % d'identité) et il est ainsi difficile de prédire la nature de l'AHL produite pour un gène *luxI* donné (Fuqua *et al.*, 1996; Fuqua et Greenberg, 2002). La conformation et la taille du site actif permettraient de sélectionner des acyl-ACP de structure définie (longueur de chaine et substitution), conduisant à la synthèse d'un certain type d'AHL (Fuqua et Greenberg, 2002; Gould *et al.*, 2006).

Une fois synthétisées, les AHLs sont transportées vers le milieu extérieur par diffusion passive pour les chaines courtes, plus hydrophiles (Kaplan et Greenberg, 1985; Pearson *et al.*, 1999). On suppose qu'un transport actif soit nécessaire pour les chaines longues, plus hydrophobes, bien que ces voies de transports soient encore globalement méconnues (Boyer et Wisniewski-Dyé, 2009). A l'heure actuelle, seules quelques pompes à efflux permettant la sécrétion des AHLs ont été caractérisées (Pearson *et al.*, 1999; Boyer et Wisniewski-Dyé, 2009).

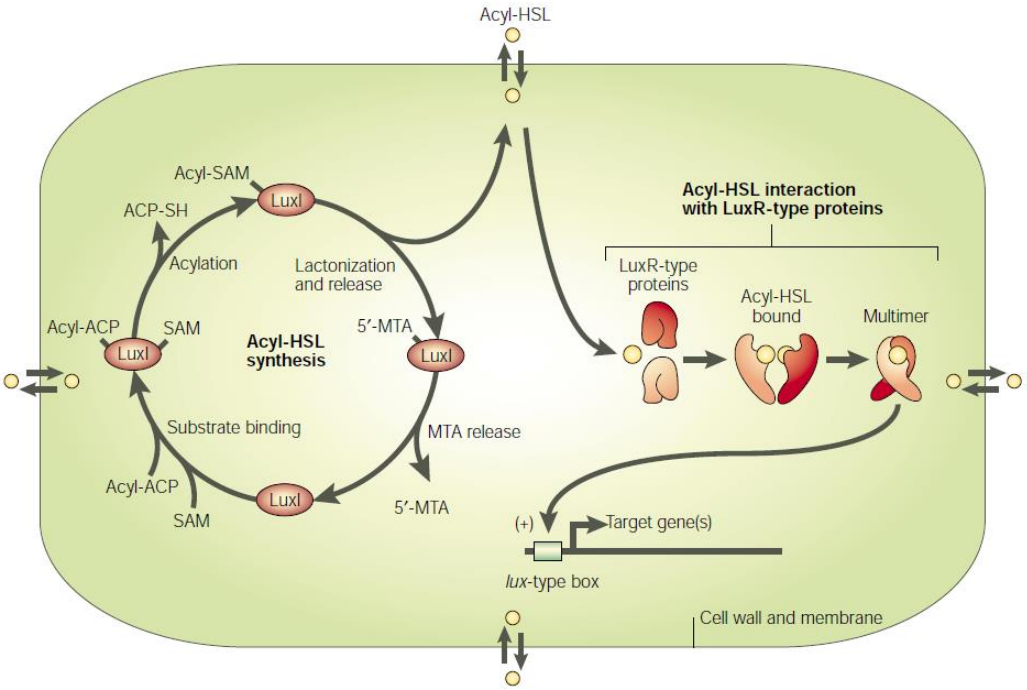

Figure I.8. Schéma modèle du fonctionnement du quorum sensing basé sur les AHLs. Les AHLs, produites par la synthase LuxI, diffusent librement entre les cellules et l'environnement extérieur. Lorsque les AHLs se fixent sur leur récepteur LuxR, elles induisent sa dimérisation. Le complexe AHL-LuxR ainsi stabilisé permet alors l'induction de la synthèse des gènes cibles en interagissant avec le promoteur de transcription (lux-box). Extrait de Fuqua et Greenberg (2002).

Lorsque la concentration seuil est atteinte, les AHLs sont détectées lors de leur liaison avec un **récepteur d'AHL** de type LuxR (encodées par des gènes homologues de *luxR*) ou LuxN (encodées par des gènes homologues de *luxN*). Les protéines LuxR sont cytoplasmiques et servent à la fois de récepteur et de régulateur de transcription. Celles-ci sont généralement mal repliées et insolubles en l'absence d'AHL. La liaison avec l'AHL induit des changements de conformation du récepteur (dimérisation) qui stabilise le complexe AHL-récepteur et permettent d'activer la synthèse des gènes cibles (Zhu et Winans, 1999; Fuqua et Greenberg, 2002). Les protéines LuxN, présentes notamment chez les *Vibrio*, sont des histidine-kinases à deux composantes. Les AHLs sont détectées à l'extérieur des cellules et induisent un changement dans la cascade de phosphorylation sous-jacente, modifiant l'activité de facteurs de transcription situés en aval (Fuqua *et al.*, 2001). Le complexe AHL-récepteur ou le facteur de transcription se fixe finalement sur une région spécifique au sein des promoteurs de transcription (palindrome appelé « lux-box ») et active (ou plus rarement réprime) l'expression des gènes cibles (Fuqua et Greenberg, 2002). Parfois, la production d'AHLs est elle-même sous l'influence du complexe AHL-récepteur, générant une production de molécules signal exponentielle grâce à une boucle de feedback positive (auto-induction).

La liaison entre l'AHL et le récepteur est effective lorsque la chaine acyle de l'AHL pénètre dans la poche hydrophobe de la protéine réceptrice. En général, le récepteur se lie à son AHL apparentée de manière très spécifique, selon la structure de la chaine acyle (longueur, substitution, insaturation) et la configuration du site actif. Cette spécificité AHL-récepteur permettrait aux bactéries de distinguer leurs propres molécules signal de celles des autres espèces (Federle et Bassler, 2003; Hawver *et al.*, 2016). Cependant, il existe aussi des récepteurs dit « *promiscuous* », capable de fixer une large gamme de ligands (Wellington et Greenberg, 2019). Là aussi, il est impossible de prédire l'AHL fixée par un récepteur à partir de sa séquence, les récepteurs ne partageant que 18-23% d'identité (Fuqua et Greenberg, 2002). La concentration minimale d'AHLs induisant une réponse du QS est compliquée à estimer, car la concentration locale peut être très différente de la concentration moyenne dans le milieu, notamment dans le cas de biofilm. Celle-ci semble être de l'ordre du nanomolaire (Kaplan et Greenberg, 1985; Fekete *et al.*, 2010).

Les gènes *luxI* et *luxR* fonctionnent en général en tandem et sont proches l'un de l'autre sur le chromosome. Il existe cependant **des gènes *luxI* (ou *luxR*) solos**, c'est-à-dire qu'on ne trouve pas de gènes *luxR* (ou *luxI*) associés dans le génome des bactéries en question (Venturi et Ahmer, 2015). La fonction et les implications écologiques de ces gènes solos sont encore peu étudiées. Les solos *luxR*, très répandus, pourraient correspondre à l'existence de souches « tricheuses » ne participant pas à l'effort de production d'AHLs mais capables de prendre l'information en répondant aux signaux exogènes (Venturi et Ahmer, 2015). Une autre hypothèse serait que ces solos *luxR* permettraient de répondre à des AHLs endogènes modifiées par les conditions environnementales, augmentant alors

les capacités des bactéries à sonder leur environnement (Venturi et Ahmer, 2015). Ils pourraient aussi répondre à des composés produits par des eucaryotes. Enfin, il est aussi possible que les synthases associées ne soient pas encore connues. Les solos *luxI* sont eux beaucoup moins fréquents et leur rôle reste à élucider, bien qu'ils pourraient fonctionner avec des récepteurs éloignés.

II.B.3) *Les gènes régulés par le quorum sensing*

Les gènes régulés par le QS sont divers et touchent des processus importants au sein des communautés bactériennes :

- La motilité bactérienne : le QS peut réguler certains mécanismes de motilité bactérienne, comme la nage ou l'essaimage, en modulant notamment la synthèse de flagelles. Par exemple, le QS régule la motilité chez les bactéries marines *V. fischeri* (Lupp et Ruby, 2005), *V. alginolyticus* (Tian *et al.*, 2008) ou *Pseudoalteromonas ulvae* (Ayé *et al.*, 2015). De plus, en créant un gradient de tension de surface, les AHLs à chaine longue pourraient agir comme bio-surfactant facilitant l'essaimage (Daniels *et al.*, 2006). En régulant la motilité, le QS pourrait faciliter l'accession des bactéries à une surface solide et donc leur colonisation.

- La formation de biofilm : Le QS peut réguler différentes étapes du développement du biofilm, comme sa formation, sa maturation et sa dispersion. Le lien entre QS et biofilm est beaucoup étudié dans le milieu médical car plusieurs pathogènes humains produisent des biofilms AHL-dépendant qui peuvent s'avérer particulièrement problématiques. Par exemple, chez la bactérie pathogène *Pseudomonas aeruginosa*, le QS est impliqué dans le relargage d'ADN extracellulaire et la production d'exopolysaccharides, permettant la mise en place du biofilm (Solano *et al.*, 2014). Le QS régule aussi la production de rhamnolipides, un biosurfactant impactant les dernières étapes du développement du biofilm (Solano *et al.*, 2014). La régulation de la production de biofilm par le QS a également été démontrée chez plusieurs souches marines, comme des *Vibrio* (Liu *et al.*, 2017), des Rhodobacterales (Su *et al.*, 2019; Fei *et al.*, 2020), des Pseudomonadales (Mangwani *et al.*, 2015) ou des *Pseudoalteromonas* (Ayé *et al.*, 2015).

- La production d'exoenzymes : Le QS semble également impliqué dans la régulation de la synthèse d'exoenzymes hydrolytiques extracellulaires comme des protéases ou des chitinases, comme démontré chez plusieurs souches cliniques et environnementales (Miller et Bassler, 2001; Waters et Bassler, 2005). Concernant les souches environnementales, quelques études ont mis en évidence des processus similaires pour diverses enzymes hydrolytiques, chez des Gammaproteobacteria (Jatt *et al.*, 2015; Mangwani *et al.*, 2015) et des Alphaproteoacteria (Su *et al.*, 2019; Yu *et al.*, 2020).

- La morphologie cellulaire et le mode de division : Patzelt *et al.* (2013) ont montré que le QS pouvait réguler des mécanismes essentiels au développement des cellules, notamment chez la

bactérie marine *Dinoroseobacter shibae*. Les AHLs produites par la bactérie induiraient une hétérogénéité de phénotype, avec la coexistence de petites cellules ovoïdes (se répliquant par fission binaire) et de bâtonnets de taille très variable (se répliquant par croissance polaire).

Beaucoup d'autres phénotypes sont sous l'influence du QS, par exemple : la bioluminescence, la nodulation, la production de facteurs de virulence, le transfert d'ADN (conjugaison et transformation), la production de divers produits extracellulaires (e.g., exopolysaccharides, toxines, antibiotiques, pigments, sidérophores) (Miller et Bassler, 2001; Waters et Bassler, 2005). La liste est encore longue : chez *P. aeruginosa* par exemple, ce sont plus de 200 gènes qui sont régulés par le QS (Schuster *et al.*, 2003).

II.C. Quorum quenching et dégradation abiotique

Les processus de communication bactérienne peuvent être perturbés par la dégradation des molécules signal, résultant de **mécanismes abiotiques ou biotiques**. La température et le pH sont les principaux facteurs abiotiques jouant sur le temps de demi-vie des AHLs. Des conditions de pH alcalin et de température élevée favorisent l'hydrolyse du cycle lactone des AHLs, produisant un composé *N*-acyle-homosérine, inactif en tant que molécule signal. Cette hydrolyse dépend de la longueur de la chaine carbonée et de ses substitutions : les AHLs à chaîne acyles longues y sont moins que les AHLs à chaînes acyles courtes (Yates *et al.*, 2002). Les AHLs substituées par un groupement cétone peuvent également réagir via une réaction spontanée appelée condensation de Claisen, réduisant encore plus leur temps de vie. Dans l'eau de mer artificielle, le temps de demi-vie d'une C6-AHL est ainsi de 15 heures environ (Hmelo et Van Mooy, 2009).

Les mécanismes de dégradation biotiques, regroupés sous le terme de ***quorum quenching*** (QQ) correspondent aux différentes stratégies de perturbation du QS employées par les microorganismes afin d'empêcher ou de réguler la mise en place de comportements communs. Deux phénomènes de QQ existent : la dégradation enzymatique et la production d'inhibiteurs du QS (Kalia, 2013; Grandclément *et al.*, 2015). Les AHL-acylases et les AHL-lactonases sont les deux enzymes principales dégradant les AHLs. La première hydrolyse la liaison amide des AHLs, libérant la molécule d'homosérine lactone et l'acide gras correspondant ; tandis que la deuxième hydrolyse la liaison ester du cycle lactone (Kalia, 2013; Grandclément *et al.*, 2015). Les inhibiteurs du QS peuvent interférer sur la production d'AHLs ou sur la réception du signal, par exemple en mimant la structure des AHLs. De nombreux organismes produisent des composés du QQ, tels que les bactéries, les plantes ou les champignons (Kalia, 2013).

II.D. Le quorum sensing : « uniquement » un senseur de la densité cellulaire ?

Le QS est historiquement considéré comme un mécanisme permettant aux bactéries de détecter la densité de population en utilisant la concentration d'AI comme proxy, d'où le nom de

« quorum » sensing. Cependant, ce système de régulation a été principalement étudié en laboratoire avec des cultures liquides monoclonales à forte densité, dans des conditions très éloignées des conditions environnementales. Or, les interactions bactériennes prennent tout leur sens dans un contexte environnemental, contenant des populations microbiennes complexes faisant face à des conditions fluctuantes. C'est pourquoi cette définition basée sur la seule densité cellulaire est de plus en plus remise en question : la concentration en AHLs ne serait pas seulement un proxy de la densité cellulaire, mais une résultante de nombreux facteurs, non pris en compte dans le model initial (Redfield, 2002; Hense *et al.*, 2007; Cornforth *et al.*, 2014).

Redfield (2002) propose d'abord le terme de « ***diffusion sensing*** », en partant du constat que l'accumulation d'AI dans un milieu est très influencée par les propriétés de transfert de masse dans le microenvironnement entourant la cellule. Par exemple, le nombre de cellules nécessaire pour atteindre un seuil de concentration d'AHLs induisant une réponse physiologique peut varier considérablement en fonction du taux de diffusion des AHLs dans le milieu ; ce taux pouvant lui-même varier fortement à l'échelle microscopique (nature de l'AHL, hydrophobicité, matrice d'exopolysaccharides). Les AIs pourraient alors jouer un rôle de senseur de transfert de masse, permettant d'induire la production de molécules impliqués dans des processus extracellulaires uniquement dans des conditions de diffusion favorables (exoenzymes, sidérophores, antibiotiques, facteur de virulence, *etc.*). Le concept de *diffusion sensing* n'est pas forcément à opposer au principe du QS mais remet plutôt en question son caractère social et coopératif : la détection d'AI ne servirait pas à jauger la densité de cellules appartenant à une même espèce, mais plutôt à identifier le retour sur investissement lié à la production d'exoproduits.

Hense *et al.* (2007) ont par la suite montré que la concentration de molécules signal dans l'environnement local de la cellule peut dépendre plus directement de la distribution spatiale des cellules que de leur densité. Comme les trois facteurs (densité, transfert de masse, distribution spatiale) affectant la concentration d'AI peuvent varier indépendamment, les bactéries ne seraient pas capables de distinguer lequel d'entre eux est à l'œuvre, mais peuvent seulement évaluer une combinaison des trois. Ils ont en conséquence introduit le concept d' « ***efficiency sensing*** », unifiant les deux théories précédentes (QS et diffusion sensing).

Plus récemment, Cornforth *et al.* (2014) ont proposé que la présence de plusieurs voies de QS au sein d'une bactérie pourrait lui permettre d'inférer à la fois la densité cellulaire et les propriétés de transfert de masse du milieu. Ils ont ainsi proposé le terme de « ***Combinatorial Sensing*** ».

Ces discussions mettent en lumière que, si l'on connait relativement bien les mécanismes du QS, peu d'hypothèses sur les fonctions de ce système sont réellement mises à l'épreuve. Il apparait maintenant essentiel de prendre en compte les conditions hétérogènes et fluctuantes rencontrées par les bactéries dans leur milieu naturel pour mieux appréhender le rôle du QS.

II.E. Les spécificités du quorum sensing en milieu marin

A l'heure actuelle, les mécanismes du QS restent largement sous explorés dans les océans alors qu'ils pourraient réguler des phénotypes clefs d'un point de vue écologique et biogéochimique. Les bactéries marines étant majoritairement des bactéries Gram négatives, les AHLs sont largement au centre des discussions sur le QS en milieu marin (Hmelo, 2017). La **prévalence du QS basé sur les AHLs** commence ainsi à être établie dans différents habitats marins, grâce à plusieurs études culture-dépendantes et indépendantes. Quelques études ont notamment pu quantifier la présence d'AHLs dans des environnements spécifiques, comme sur des échantillons de neige marine (Hmelo *et al.*, 2011; Jatt *et al.*, 2015), de phytoplancton (Van Mooy *et al.*, 2012), de biofilms (Huang *et al.*, 2009; Xu *et al.*, 2021) ou de tapis microbiens (Decho *et al.*, 2009). Il reste cependant difficile de doser les AHLs directement dans l'environnement, du fait de la faible concentration de ces molécules (Lami, 2019). A notre connaissance, aucune AHL n'a jusqu'à présent été détectée directement dans la colonne d'eau. De plus, la prévalence de gènes du QS et du QQ a été démontrée dans un nombre d'études encore relativement limité. Par exemple, Doberva *et al.* (2015) ont montré la prévalence de synthases d'AI-1 (familles *luxI*, *ainS* et *hdtS*) et d'AI-2 (famille *luxS*) dans la base de données GOS (Global Ocean Sampling) qui couvre trois océans. Muras *et al.* (2018) ont mis en évidence un nombre important de gènes impliqués dans la synthèse (familles *luxI*, *ainS* et *hdtS*), la réception (famille *luxR* et *ainR*) et la dégradation d'AHLS (lactonases, acylases) ou encore la synthèse d'AI-2 (famille *luxS*) sur des échantillons prélevés à différentes profondeurs de la mer Méditerranée. Enfin, plusieurs études ont démontré la production d'AHLs lors de la mise en culture de souches isolées de divers habitats marins (Gram *et al.*, 2002; Wagner-Döbler *et al.*, 2005; Muras *et al.*, 2018; Su *et al.*, 2019). Ces différentes études suggèrent que les mécanismes de communication bactérienne seraient répandus dans les environnements aquatiques. Cependant, les questions concernant l'établissement du QS, son rôle et ses conséquences biogéochimiques restent encore largement ouvertes.

Les discussions sur le QS dans les environnements marins sont intrinsèquement liées aux **biofilms**, établis sur diverses surfaces biotiques et abiotiques (e.g., particules marines ou estuariennes, tapis microbiens, phycosphere, macro-algues, coraux, microplastiques) (Lami, 2019). En effet, l'établissement des communications basées sur le QS repose sur la présence de conditions favorables à l'accumulation d'AIs dans le milieu. Il apparait ainsi peu probable que ce mécanisme prenne place chez les communautés bactériennes planctoniques, où les bactéries sont physiquement éloignées et où les AIs sont constamment dilués, empêchant une communication à l'échelle locale. Hmelo et Van Mooy (2009) ont calculé qu'une concentration minimale théorique de 1,2 x 10^9 cellules L^{-1} (monospécifiques) serait nécessaire pour que les taux de production d'AHLs soient supérieurs à leur taux de dégradation, induisant une accumulation dans la colonne d'eau. En plus d'abriter de fortes

densités cellulaires, la matrice de polymères constituant les biofilms permettrait de concentrer les AHLs en limitant leur diffusion, favorisant ainsi la mise en place du QS.

En conséquence, une des premières hypothèses avancées lors de l'étude du QS en milieu marin concerne **la surexpression des activités enzymatiques au sein des agrégats** : les bactéries fixées aux particules utiliseraient ce mécanisme de régulation pour synchroniser l'expression d'enzymes extracellulaires (Gram *et al.*, 2002; Kiørboe *et al.*, 2002). Gram *et al.* (2002) ont reporté la synthèse d'AHLs par des bactéries isolées de la neige marine, supportant cette hypothèse. Depuis, quelques études ont montré un lien direct entre le QS et l'expression d'enzyme au sein de communautés colonisant la neige marine (Hmelo *et al.*, 2011; Jatt *et al.*, 2015; Krupke *et al.*, 2016; Su *et al.*, 2019) ou la phycosphère (Van Mooy *et al.*, 2012). Cependant, les mécanismes derrière ces régulations sont loin d'être élucidés. Le QS pourrait tout d'abord influer directement la régulation de la synthèse d'enzymes hydrolytiques au niveau transcriptionnel, via la surexpression ou la sous-expression des gènes encodant des enzymes hydrolytiques. De plus, le QS pourrait influer indirectement sur ces phénotypes en modifiant la composition des communautés bactériennes. A l'heure actuelle, le lien entre QS et composition des communautés reste ténu et seules cinq études ont démontré une influence de molécule du QS sur la composition de communautés microbiennes marines (Dobretsov *et al.*, 2007; Huang *et al.*, 2019; Whalen *et al.*, 2019; R. Wang *et al.*, 2020) et limniques (Xu *et al.*, 2021).

Dans le cadre de cette thèse, le rôle du QS en milieu marin et ses impacts possibles sur les écosystèmes ont fait l'objet d'une synthèse bibliographique exhaustive publiée dans le journal *Frontiers in marine science* (Urvoy *et al.*, 2022, **chapitre VII**).

III. Les estuaires, des zones de transformation de la matière organique

III.A. L'importance des zones côtières

Les **régions côtières** comprennent des écosystèmes variés et interconnectés, de l'exutoire des rivières jusqu'au plateau continental. Les zones côtières constituent ainsi l'interface entre le continent et l'océan et sont influencées à la fois par les apports terrestres et les échanges avec l'océan hauturier. Ces zones impactent les cycles biogéochimiques globaux de manière considérable, de par leurs fortes activités de production primaire et secondaire, supportées en partie par la fertilisation des apports terrestres riches en nutriments (Bianchi, 2011; Bauer *et al.*, 2013; Cloern *et al.*, 2014). Bien qu'elles ne couvrent que 10 % des surfaces océaniques, les zones côtières supportent ainsi jusqu'à 30 % de la production primaire marine globale et contribuent pour 80 % au stockage de carbone organique dans les sédiments (Bianchi, 2011; Bauer *et al.*, 2013; Cloern *et al.*, 2014).

Les environnements côtiers sont cependant **fragiles et fortement dégradés** en raison d'une augmentation des pressions anthropiques au cours des dernières décennies (Cloern, 2001; Newton *et al.*, 2020). Les zones côtières sont impactées par divers polluants comme les nutriments, les hydrocarbones, les antibiotiques, les métaux ou les plastiques (Cloern, 2001; Newton *et al.*, 2020). La charge importante des rivières en **nutriments** constitue notamment une menace majeure d'eutrophisation pour les systèmes côtiers. En effet, leurs apports ont considérablement augmenté depuis plusieurs dizaines d'années en raison, d'une part, d'une intensification des pratiques agricoles et, d'autre part, d'une urbanisation et d'une industrialisation croissante des zones littorales (Grizzetti *et al.*, 2012; Peñuelas *et al.*, 2013). Si les apports en azote inorganique continuent d'augmenter, les teneurs en phosphate ont tendance à diminuer depuis les années 1980 suite à l'arrêt de l'utilisation de détergents phosphatés et un meilleur traitement des eaux usées (Grizzetti *et al.*, 2012; Peñuelas *et al.*, 2013). Cela provoque un fort déséquilibre N/P dans les apports de la majorité des fleuves de la façade Manche-Atlantique, qui se répercute sur les eaux côtières (Grizzetti *et al.*, 2012; Peñuelas *et al.*, 2013). Ces phénomènes perturbent le fonctionnement des systèmes côtiers : les forts apports en nutriments peuvent engendrer une augmentation de la production phytoplanctonique et conduire, dans certains cas, à la prolifération d'algues toxiques (Cloern, 2001; Anderson *et al.*, 2002). La matière organique issue de cette production primaire intense accroit les processus de dégradation et de minéralisation bactérienne dans la colonne d'eau (Cloern, 2001). Ces processus de régénération peuvent ensuite conduire à un déficit en oxygène dissous susceptible d'entraîner des changements importants tant au niveau de la flore (Duarte, 1995) que de la faune marine (Heip, 1995). Les déséquilibres N/P induisent, eux, une limitation de plus en plus précoce de la production primaire côtière par le phosphore. Cela entraine des phénomènes de dystrophie dont une restructuration des

réseaux trophiques favorisant les formes nano- et picoplanctoniques (Takamura et Nojiri, 1994; Labry *et al.*, 2002).

Dans ce contexte, il est essentiel de caractériser comment les nutriments et la matière organique sont transférés des écosystèmes fluviaux vers les zones côtières le long du continuum terre-mer. Au sein de ce continuum, les estuaires sont des milieux particulièrement intéressants d'un point de vue biogéochimique (Bianchi, 2011; Cai, 2011; Bauer *et al.*, 2013). Ces véritables « bioréacteurs » participent à la transformation, la rétention ou l'export de la matière organique et des nutriments fluviatiles, déterminant la quantité et la nature des apports aux zones côtières (Bauer *et al.*, 2013).

III.B. Les estuaires, au sein du continuum terre-mer

III.B.1) *Caractéristiques des estuaires*

Un **estuaire** correspond à la zone de mélange entre les eaux douces d'une rivière et les eaux marines dans lesquelles elle se jette. Les estuaires sont impactés par des **forçages hydrodynamiques forts**, principalement liés au débit du fleuve (qui résulte du régime de précipitations) et aux courants de marée, dont la force varie selon les cycles semi-diurne (pleine mer / basse mer) et semi-mensuel (vives eaux / mortes eaux) (Biggs et Cronin, 1981). L'influence relative de ces deux forçages dépend des caractéristiques de l'estuaire. Les estuaires de la façade Manche/Atlantique sont ainsi principalement dominés par la marée, à la différence des estuaires méditerranéens, essentiellement contraints par la dynamique des fleuves. Selon l'amplitude de la marée, il est possible de distinguer : les estuaires microtidaux (marnage < 1 m), mésotidaux (marnage de 1 à 5 m) ou macrotidaux (marnage > à 5 m) (Davies, 1964; Hayes, 1975). Les forçages hydrodynamiques impactent également la stratification haline des masses d'eau. La colonne d'eau des estuaires peut ainsi être verticalement homogène ou stratifiée, la stratification étant accentuée par de forts débits de fleuve et atténuée par les courants de marée (Biggs et Cronin, 1981). Dans le cas d'estuaires stratifiés, caractérisés par une faible amplitude de marée et des débits fluviaux forts, les eaux douces, moins denses, s'écoulent dans la couche de surface. Dans les estuaires homogènes, la turbulence qui résulte de forts courants de marée favorisent le mélange vertical des masses d'eaux (Biggs et Cronin, 1981).

Les caractéristiques hydrodynamiques modulent la morphologie de l'estuaire via des mécanismes de transport, de dépôt ou d'érosion. Dans les estuaires macrotidaux, ces mécanismes sont à l'origine de la formation d'une **zone de turbidité maximum appelée « bouchon vaseux »** où les sédiments fins en suspension sont fortement concentrés (Allen *et al.*, 1980; Herman et Heip, 1999). Les concentrations en **matières en suspension** (MES) au sein du bouchon vaseux peuvent être très importantes, de l'ordre du gramme par litre, soit plusieurs ordres de grandeur au-delà des concentrations trouvées dans les eaux marines (Herman et Heip, 1999; Uncles *et al.*, 2002). La formation du bouchon vaseux résulte de plusieurs mécanismes physiques et chimiques qui se

superposent. Le mélange des eaux douces et des eaux marines entraine des phénomènes de floculation et donc une augmentation des MES (Allen *et al.*, 1980; Herman et Heip, 1999). De plus, les concentrations en MES sont entretenues par l'action des courants de marée. De manière simplifiée, les courants de marée remobilisent les MES sédimentées lors des marées montantes (flot) et descendantes (jusant), tandis que les MES sédimentent à l'étale (Allen *et al.*, 1980; Herman et Heip, 1999). La fraction de MES déposée à l'interface eau-sédiment porte le nom de crème de vase. La quantité de MES dans le bouchon vaseux et la quantité de crème de vase sont ainsi fonction de l'intensité de la marée. La position du bouchon vaseux varie dans l'espace : celui-ci se déplace d'amont en aval de l'estuaire selon le débit du fleuve et les courants de marée. En période d'étiage, le bouchon vaseux se situe plutôt en amont, tandis que dans les périodes de crue, il se déplace vers l'aval et peut même être en partie expulsé vers l'océan côtier.

III.B.2) *Des processus intenses de transformation de la matière organique au sein des estuaires*

Les estuaires sont le siège de nombreuses transformations des nutriments et de la matière organique, générées par divers phénomènes biologiques ou physicochimiques, eux même contraints par la dynamique hydrosédimentaire de l'estuaire (**Figure I.9**).

Les fortes concentrations en MES engendrent une turbidité importante qui réduit la pénétration de la lumière et limite la production primaire (Middelburg et Herman, 2007; Cloern *et al.*, 2014). En revanche, les MES offrent un environnement favorable au **développement d'activités bactériennes hétérotrophes intenses**, à l'origine d'une transformation importante de la matière organique (Abril *et al.*, 1999; Servais et Garnier, 2006; Middelburg et Herman, 2007). Les activités bactériennes sont aussi très fortes dans la crème de vase, communément considérées comme un bioréacteur car les cycles fréquents de remise en suspension renouvèlent régulièrement les apports en oxygène (Abril *et al.*, 1999; Aller, 2004). Ainsi, les estuaires sont souvent considérés comme hétérotrophes dans les budgets globaux. Cela signifie que la respiration, qui découle des processus de minéralisation de la matière organique, dépasse la production d'O_2 par la production primaire. Ceci implique dont que les estuaires émettent du CO_2 vers l'atmosphère, leur conférant le statut de source de carbone (Cai, 2011; Bauer *et al.*, 2013).

Les fortes teneurs en MES dans les estuaires favorisent aussi **les interactions physicochimiques** entre les compartiments dissous et particulaires, notamment via des processus d'adsorption/désorption aux particules (e.g., de la MOD sur des surfaces minérales), d'agrégation/dissolution (e.g., des substances humiques ou des polysaccharides) ou encore photo-induits (e.g., photo-flocculation, photo-dissolution) (Bauer *et al.*, 2013; He *et al.*, 2016). En particulier, le phosphate est un élément très réactif vis-à-vis des particules. De plus, divers processus peuvent mener à des pertes significatives de matière organique, comme la photo-oxydation, la sédimentation ou la floculation induite par la salinité (**Figure I.9**) (Bauer *et al.*, 2013).

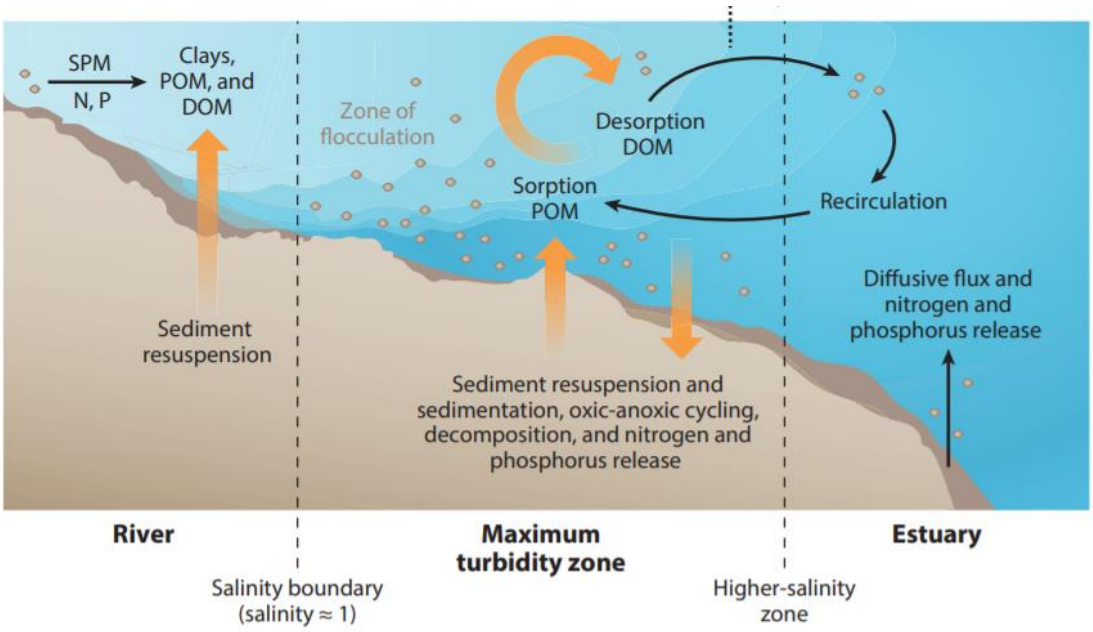

Figure I.9. Processus influençant le devenir de la matière organique au sein des maximums turbides estuariens. Les lignes verticales représentent la délimitation du bouchon vaseux. DOM : matière organique dissoute ; POM : matière organique particulaire ; SPM : matières en suspension. Extrait de Canuel et Hardison (2016).

Afin de caractériser si un estuaire comme puit ou source d'un composé, les **diagrammes de mélange** sont couramment utilisés. Ils représentent l'évolution de la concentration d'un composé le long du gradient salé (**Figure I.10**). La droite linéaire reliant les concentrations des eaux sources (marines et douces) correspond à la droite de dilution théorique. Un composé dont la concentration suit cette droite a un comportement « conservatif » : il résulte d'un simple mélange des masses d'eau et il ne subit pas de transformation au sein de l'estuaire. Alternativement, il est possible qu'il subisse des transformations, mais que la somme des sources et des puits se compensent. Si un composé présente une anomalie positive par rapport à la droite de dilution théorique, cela indique que l'estuaire est une source nette de ce composé (processus de production > processus de consommation). A l'inverse, l'estuaire est un puit pour les composés présentant une anomalie négative (processus de production < processus de consommation), qui sont alors retenus au sein de l'écosystème. On considère que ces comportements sont « non-conservatifs ». Par exemple, le phosphate et l'ammonium suivent souvent des comportements non-conservatifs (Lebo *et al.*, 1994; Morin et Morse, 1999).

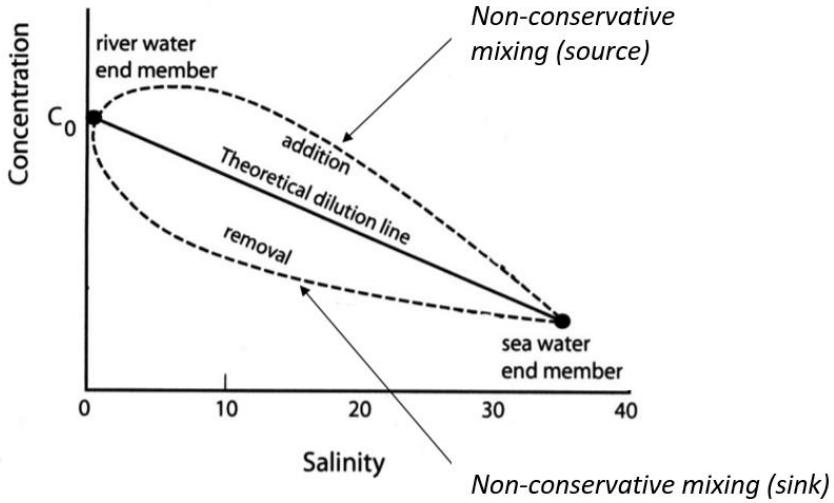

Figure I.10. Différents comportements possibles pour un composé transporté dans un estuaire. Le composé peut suivre un mélange conservatif (droite de dilution théorique) ou bien non-conservatif, en étant retenu (puit) ou produit (source) au sein de l'estuaire.

IV. Objectifs de la thèse

Les bactéries hétérotrophes jouent un rôle important dans les cycles biogéochimiques marins, en particulier par leur implication dans la dégradation de la MOD et de la MOP. Celles-ci sont en interactions constantes et forment des assemblages complexes, modulés par de nombreux facteurs stochastiques et déterministes (i.e., sélection biotique et abiotique). L'assimilation de composés de haut poids moléculaire nécessite la synthèse d'enzymes hydrolytiques, qui sont considérées comme limitantes dans l'utilisation de la matière organique marine. Les activités hydrolytiques sont particulièrement intenses chez les communautés bactériennes colonisant les particules, déterminant le devenir de la MOP. C'est le cas en particulier des estuaires, où elles impactent la qualité et quantité de matière exportée vers les zones côtières, des zones clefs pour les bilans globaux. L'augmentation du métabolisme des bactéries fixées sur les particules pourraient être liée à la mise en place du QS, un système de communication bactérienne permettant, entre autres, la régulation de la synthèse d'enzymes hydrolytiques et la structuration des communautés. Cependant, l'implication du QS dans ces processus est encore largement sous-explorée, notamment dans les estuaires (**Figure I.11**).

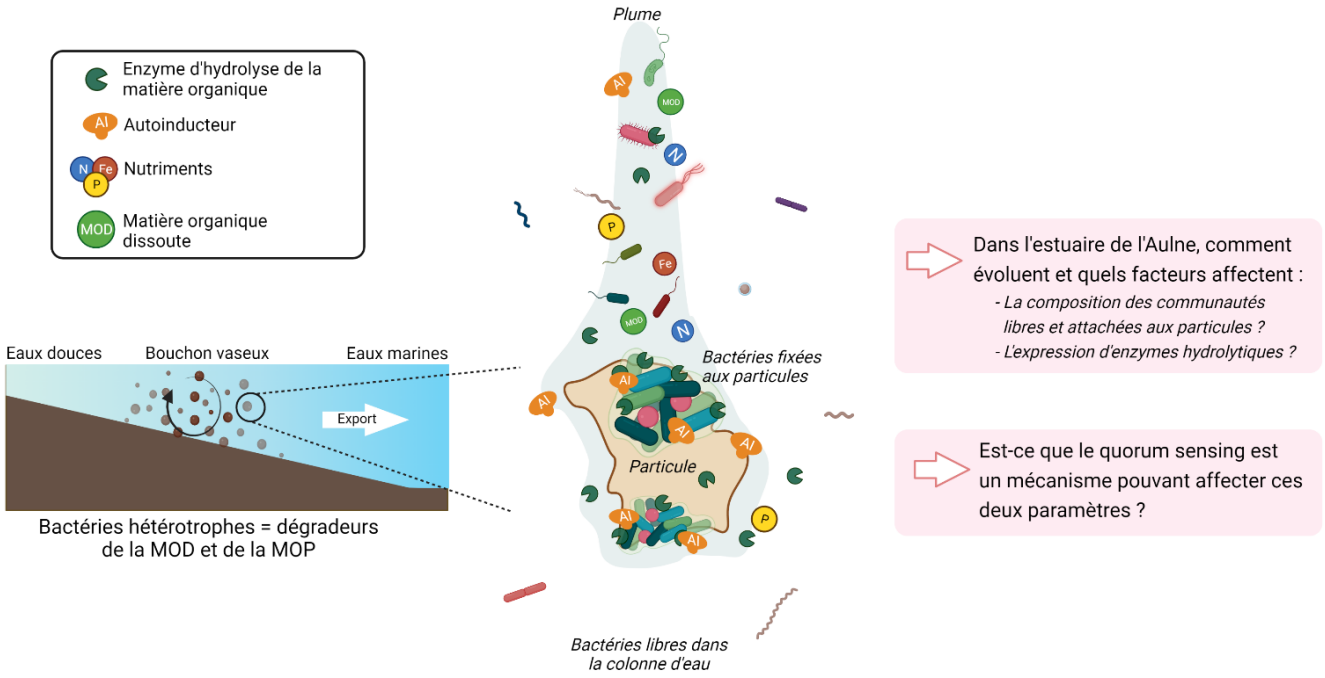

Figure I.11. Schéma conceptuel des problématiques développées au sein de cette thèse. Créé avec https://biorender.com/.

Cette thèse a pour but d'appréhender les facteurs de régulation des activités enzymatiques des bactéries ainsi que le rôle du QS dans leur expression au sein de deux écosystèmes français, l'estuaire de l'Aulne et les eaux côtières adjacentes de la rade de Brest. Il s'agit plus précisément de **répondre aux questions suivantes** :

- Quels sont les facteurs contrôlant les activités enzymatiques et la composition des communautés bactériennes libres et attachées aux particules dans l'estuaire de l'Aulne et les eaux côtières de la rade de Brest ?
- Quel est le rôle du QS dans la régulation des activités enzymatiques bactériennes d'hydrolyse de la matière organique, ainsi que dans la composition des communautés bactériennes estuariennes et marines ?

Cette thèse s'articule autour de huit parties. Après **l'introduction générale,** qui présente l'état de l'art du sujet étudié, un deuxième chapitre décrit l'ensemble des **matériels et méthodes** utilisés. Puis, deux chapitres constituent une étude réalisée au sein de l'estuaire de l'Aulne et des eaux côtières de la rade de Brest, visant à déterminer les variations spatiotemporelles de la composition des communautés bactériennes libres et attachées aux particules et de leurs activités enzymatiques. Les trois chapitres suivants sont consacrés au rôle du QS dans la régulation des activités enzymatiques bactériennes et de manière plus générale, dans les cycles biogéochimiques.

Plus précisément, le **chapitre III** s'intéresse aux variations spatiotemporelles de la composition des communautés bactériennes libres ou attachées aux particules de l'estuaire de l'Aulne et de la rade de Brest. Ce chapitre est présenté sous forme de publication pour une soumission envisagée au journal *Scientific Reports.*

Le **chapitre IV** étudie l'évolution saisonnière de trois activités enzymatiques d'hydrolyse de la matière organique (les aminopeptidases, les β-glucosidases et les phosphatases alcalines) le long du gradient de salinité de l'estuaire de l'Aulne, ainsi que les facteurs régulant l'expression de ces activités. Les résultats de cette étude sont présentés sous forme d'une publication qui sera soumise ultérieurement.

Le **chapitre V** correspond à une première étude sur le rôle du QS, menée sur des bactéries isolées de l'estuaire de l'Aulne. Celle-ci a permis de déterminer quelles bactéries produisent des AHLs et si, pour ces bactéries productrices, la disruption des voies de communication basées sur les AHLs entraine une modification de la synthèse d'enzymes hydrolytiques (aminopeptidases et β-glucosidases dissoutes et liées aux membranes) et de la production de biofilm. Les résultats de cette étude ont donné lieu à une publication dans le journal *Environmental microbiology*.

Le **chapitre VI** aborde des problématiques similaires au sein de communautés naturelles de la rade de Brest. Plus précisément, il s'agit de deux études menées en microcosme, examinant l'impact de l'ajout d'AHLs sur diverses activités enzymatiques et sur la composition des communautés bactériennes. Ces travaux ont été publiés dans le journal *Frontiers in microbiology.*

Le **chapitre VII** est une synthèse de la littérature étudiant l'implication du QS dans la régulation de processus bactériens impactant les cycles biogéochimiques marins. Celle-ci s'intéresse également aux contraintes actuelles limitant l'étude du rôle du QS et présente les futures perspectives envisagées sur le sujet. Cette synthèse bibliographique a été publiée dans le journal *Frontiers in marine science.*

Finalement, le **chapitre VIII** constitue une discussion générale de l'ensemble de ce travail de thèse, reprenant les principaux résultats et proposant différentes perspectives sur ces travaux.

Chapitre II. Matériels et méthodes

I. Sites d'étude : la rade de Brest et l'estuaire de l'Aulne

La **rade de Brest** est une baie semi-fermée de 180 km^2 localisée à la pointe ouest de la Bretagne (**Figure II.1**). Elle est reliée à la mer d'Iroise (océan Atlantique) par un goulet étroit d'environ 2 km de large pour 6 km de long. La rade est influencée d'un côté par les apports d'eau douce de différentes rivières, et de l'autre, par les apports de la mer d'Iroise. On estime qu'environ 40 % des eaux de la rade sont renouvelées chaque jour grâce aux forts courants de marée (Delmas et Tréguer, 1983). La rade de Brest est un environnement côtier particulièrement bien étudié, notamment de par sa biodiversité importante et la présence de nombreuses activités commerciales (présence du port de Brest), halieutiques (principalement la pêche de coquilles Saint-Jacques) ou encore récréatives (voile, plongée). On peut notamment citer l'existence de la Zone Atelier Brest Iroise (Zabri) ainsi que de nombreux réseaux de surveillance des zones de production de coquillages (REseau MIcrobiologique), du phytoplancton et des phycotoxines (REPHY) ou encore le Service d'Observation en Milieu LITtoral (SOMLIT). La période de développement du phytoplancton s'étend du début du printemps à la fin de l'automne (avril à octobre) et est caractérisée par une succession de blooms récurrents, généralement dominées par les diatomées (Ragueneau *et al.*, 1996). Des blooms d'espèces phytoplanctoniques toxiques sont également fréquemment observés, notamment des espèces *Alexandrium minutum* (Chapelle *et al.*, 2015) et *Pseudo-nitzschia* (Husson *et al.*, 2016).

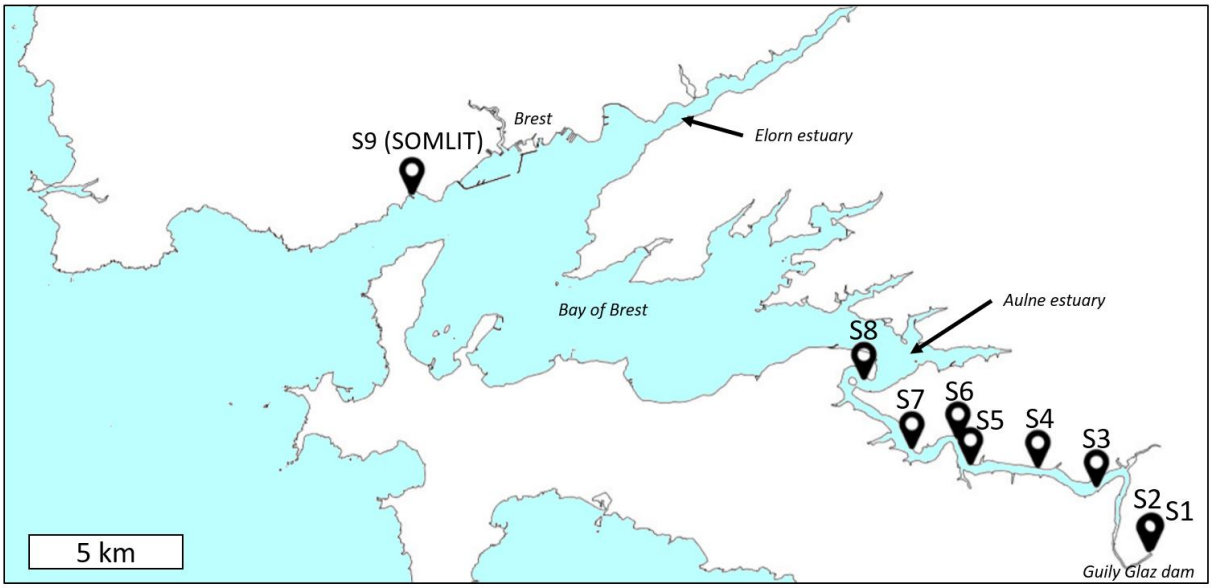

Figure II.1. Les sites d'étude : la rade de Brest et de l'estuaire de l'Aulne. Les stations d'eau douce (S1 et S2) et marines (S9) ont été prélevées à un endroit fixe tandis que la localisation des autres stations était dépendante de la salinité. Les stations de prélèvements de Mai 2019 sont indiquées en exemple.

L'Aulne est la rivière principale se jetant dans la rade de Brest et constitue 63 % de ses apports d'eau douce, contre 15 % pour l'Elorn (Auffret, 1983). Ce fleuve d'environ 140 km prend sa source dans les monts d'Arrée (Côtes-d'Armor). Son bassin versant d'environ 1900 km^2 est peu industrialisé mais

60 % des sols sont occupés par des activités agricoles intenses. **L'estuaire de l'Aulne** est typique des écosystèmes littoraux ouest-européens, fortement influencés par les marées. Cet estuaire macrotidal est caractérisé par des marnages importants, pouvant atteindre 8 m, qui favorisent la remise en suspension de particules. Son débit moyen est de 28 m^3 s^{-1}. Celui-ci varie entre 1 et plus de 250 m^3 s^{-1} et est contraint par un régime océanique qui génère de fortes précipitations entre novembre et février (période de crue) et de faibles temps de résidence des masses d'eaux (≈ 3 jours) (Bassoullet, 1979; Delmas et Tréguer, 1983). Pendant la période d'étiage estivale, les débits sont faibles et le temps de résidence des masses d'eaux peut atteindre plus de 30 jours (Bassoullet, 1979; Delmas et Tréguer, 1983). L'estuaire est relativement long puisque son gradient salé couvre en moyenne 40 km de long. L'intrusion de l'eau de mer est limitée en amont par la présence du barrage de Guily Glaz situé près de Port Launay. Son cours est sinueux, effectuant de nombreux méandres qui favorisent de longs temps de résidence des agrégats. Les eaux de l'estuaire sont caractérisées par un fort déséquilibre N/P en raison de concentrations en phosphate relativement faibles comparées aux rivières majeures de l'ouest de la Bretagne, couplées à de forts apports azotés liés à l'agriculture intensive (Abbott *et al.*, 2018). L'estuaire de l'Aulne est également caractérisé par d'intenses activités de minéralisation du phosphore organique dans le maximum turbide de l'estuaire, principalement liées aux bactéries fixées sur les particules (Labry *et al.*, 2016).

Toutes ces caractéristiques font de ces deux sites des milieux modèles pour l'étude des écosystèmes côtiers et du continuum terre-mer.

II. Prélèvements

II.A. Suivi mensuel

Les prélèvements dans l'Aulne et la rade de Brest (point SOMLIT) ont été effectués mensuellement en période de vives eaux, de Janvier à Décembre 2019, ainsi qu'en Juillet 2020 (**Tableau II.1**). Deux sorties supplémentaires ont également été effectuées en période de mortes eaux en Juillet et Juin 2019. Ces échantillonnages ont servi de support pour l'étude de la composition des communautés bactériennes dans l'estuaire de l'Aulne (**chapitre III**), des facteurs régulant leurs activités enzymatiques d'hydrolyse de la matière organique (**chapitre IV**) ainsi que pour l'isolement de bactéries afin d'étudier leurs capacités de QS et QQ (**chapitre V**).

Les eaux de surfaces ont été échantillonnées à neuf stations couvrant le gradient de salinité de l'estuaire. La station 1 (S1) correspond à une station d'eau douce située en amont du barrage de Guily Glaz et n'est ainsi pas soumise à l'influence des marées. La station 2 (S2) est également une station d'eau douce (salinité 0) collectée à un point fixe en aval du barrage, soumise à l'influence des marées. Les stations 3 à 8 (S3-S8) ont été échantillonnées le long du gradient de salinité (salinité moyenne de 5, 10, 15, 20, 25 et 30), leur position est donc variable et dépend du débit de l'Aulne et du coefficient

de marée. Enfin, la station 9 (S9) correspond à une référence marine, correspondant à la station SOMLIT de St Anne-du-Portzic (48°21'32.17'' N, 4°33'07.21'' O). La station S9 a été échantillonnée en premier à marée haute et les prélèvements ont été immédiatement amenés au laboratoire afin d'éviter un long temps de transport dans le bateau. Les autres prélèvements ont ensuite été réalisés de S1 à la S8, dans un délai de 4 h.

Tableau II.1. Dates de prélèvement, coefficient de marée, débit de l'Aulne et température moyenne des échantillons d'eau prélevés. (*) Échantillonnage metabarcoding. (†) Isolement de bactéries. n : nombre de stations échantillonnées. Les données de débit de l'Aulne ont été extraites de http://www.hydro.eaufrance.fr/ (station Châteaulin, identifiant J3821820).

Radiale	Date	Coefficient de marée	Débit ($m^3 s^{-1}$)	Température moyenne (°C)	n	Commentaires
R01	24 Janvier 2019	106	21.9	7.8	9	
R02	20 Février 2019	110	44.6	7.8	9	(*)
R03	25 Mars 2019	90	24.4	11.0	9	
R04	18 Avril 2019	97	18.1	12.4	8	(*†) La station S1 n'a pas été échantillonnée suite à des contraintes de navigation
R05	20 Mai 2019	93	10.0	16.0	9	
R06	18 Juin 2019	82	8.3	17.2	10	Une station additionnelle a été échantillonnée à la salinité 0.2 (appelée S2.5) vu sa forte turbidité
R07	25 Juin 2019	42	6.1	18.7	9	Mortes eaux
R08	11 Juillet 2019	58	1.2	23.2	9	Mortes eaux
R09	18 Juillet 2019	78	2.2	22.7	9	(*†) La station S2 n'a pas été échantillonnée (salinité > 4 au point d'échantillonnage fixe habituel). Une station additionnelle a été échantillonnée en compensation (salinité 7.7, appelée S3.5)
R10	3 Septembre 2019	102	2.2	18.8	9	
R11	30 Septembre 2019	116	5.1	17.0	9	
R12	14 Novembre 2019	87	90.0	10.4	9	(*)
R13	16 Décembre 2019	79	112.0	9.8	9	
R14	20 Juillet 2020	74	1.5	20.2	7	(*) Les stations S1 et S2 n'ont pas été échantillonnées suite à des contraintes de navigation

De nombreux paramètres physicochimiques (**Tableau II.2**) et bactériens (**Tableau II.3**) ont été mesurés à chaque station. Les échantillons pour les paramètres physicochimiques ont été filtrés immédiatement et conservés jusqu'à leur analyse ultérieure, comme décrit dans la partie **III.A**. Les échantillons pour les paramètres biologiques (abondance, production bactérienne, activités enzymatiques, diversité et isolement bactérien) ont été conservés à température *in situ* et traités immédiatement, comme décrit dans les parties **III.B** et **IV.A**.

Tableau II.2. Variables physicochimiques mesurées pendant le suivi mensuel dans l'estuaire de l'Aulne et la rade de Brest. Les variables composites, résultants de la combinaison de plusieurs variables, sont aussi indiquées. MOD : matière organique dissoute ; MOP : matière organique particulaire.

	Variable	Abréviation	Variable composite
	Température		
	Salinité		
Nutriments	Ammonium		
	Nitrite		
	Nitrate		
	Phosphate		
	Silicate		
MOD	Carbone organique dissous	COD	
	Phosphore organique dissous	POD	
	Monosaccharides dissous	MCHOD	PCHOD/MCHOD: Ratio des PCHOD sur MCHOD
	Polysaccharides dissous	PCHOD	CHOD/AAD: Somme des PCHOD et MCHOD sur la somme des AALD et des AACD
	Acides aminés libres dissous	AALD	AALD/AACD: Ratio des AALD sur AACD
	Acides aminés combinés dissous	AACD	
MOP	Matières particulaires en suspension	MES	
	Matière inorganique particulaire	MIP	
	Matière organique particulaire	MOP	%MOP: Pourcentage de MOP dans les MES
	Phosphore particulaire total	PPT	
	Phosphore inorganique particulaire	PIP	
	Phosphore organique particulaire	POP	COP/POP: Ratio de COP sur POP
	Carbone organique particulaire	COP	
	Azote organique particulaire	NOP	COP/NOP: Ratio de COP sur NOP
	Acides aminés particulaires	AAP	AAP/MES: Contenu des MES en AAP
			CHOP/AAP: Ratio des CHOP (CHOPI + CHOPS) sur AAP
	Carbohydrates particulaires solubles	CHOPS	I/S: Ratio de CHOPI sur CHOPo
	Carbohydrates particulaires insolubles	CHOPI	CHOP/MES: Contenu des MES en CHOP (CHOPS + CHOPI)
	Chlorophylle a	Chla	%Chla: Pourcentage de Chla sur les pigments totaux (Chla + Pheo)
	Pheopigments	Pheo	

Tableau II.3. Variables bactériennes mesurées pendant le suivi mensuel dans l'estuaire de l'Aulne et la rade de Brest.

	Paramètre	Abréviation
Fraction dissoute (<0.2 µm)	Activités des phosphatases alcalines	PA < 0.2 µm
Bactéries libres (< 3 µm)	Abondance bactérienne	AB < 3 µm
	Production bactérienne	PB < 3 µm
	Activités des aminopeptidases	LAM < 3 µm
	Activités des glucosidases	GLU < 3 µm
	Activités des phosphatases alcalines	PA 0.2-3 µm
	Composition des communautés bactériennes	BCC < 3 µm
Bactéries attachées (> 3 µm)	Abondance bactérienne	AB > 3 µm
	Production bactérienne	PB > 3 µm
	Activités des aminopeptidases	LAM > 3 µm
	Activités des glucosidases	GLU > 3 µm
	Activités des phosphatases alcalines	PA > 3 µm
	Composition des communautés bactériennes	BCC > 3 µm

II.B. Expérimentations en microcosme

Deux prélèvements de communautés bactériennes naturelles pour l'étude du QS en microcosme (**chapitre VI**) ont été réalisés à proximité de la station SOMLIT de St-Anne-du-Portzic (48° 21'33.5'' N, 4°33'0.27''). Ces prélèvements, effectués le 29 mars et le 3 mai 2021, correspondent à deux périodes contrastées du développement printanier du phytoplancton. Ils ont en effet été réalisés au début de la croissance phytoplanctonique (fortes teneurs en nutriments, faibles valeurs de chlorophylle *a*) et en période de forte croissance phytoplanctonique (faibles teneurs en nutriments, fortes valeurs de chlorophylle *a*). L'eau de mer a été prélevée à l'aide de bonbonnes de 10 L (Nalgene) préalablement lavées à l'acide chlorhydrique (10 %) et immédiatement filtrée sur une soie de 10 µm (Merck, Ref NY1004700) afin de retirer les agrégats et les cellules eucaryotes les plus larges. Les échantillons ont ensuite été stockés à température *in situ* (10.7 °C et 12.3 °C, respectivement) et traités dans l'heure (**cf IV.E**).

III. Protocoles d'analyses

III.A. Variables physicochimiques

III.A.1) *Echantillonnage*

La température et la salinité ont été mesurées *in situ* avec un thermosalinomètre WTW. Les échantillons pour l'ammonium, le nitrite, le nitrate, le COD, les mono- et polysaccharides dissous (MCHOD, PCHOD), les acides aminés libres et combinés dissous (AALD, AACD) et le phosphore organique dissous (POD) ont été filtrés par gravité sur des filtres en fibre de verre (Whatman GF/F, 47 mm) préalablement calcinés (2 h à 480 °C). Les filtrats ont été congelés à -20 °C, sauf pour le COD, conservé à 4 °C jusqu'à son analyse effectuée dans la même journée. Les filtrats pour la mesure des silicates ont été obtenus par filtration avec des filtres Minisart (0.45 µm, acétate de cellulose, Sartorius) et conservés à 4 °C. Les échantillons pour le phosphore particulaire total (PPT), phosphore particulaire inorganique (PIP), carbohydrates particulaires solubles (CHOPS), carbohydrates particulaires insolubles (CHOPI), acides aminés particulaires (AAP), MES, matière particulaire inorganique (MIP) carbone organique particulaire (COP), azote organique particulaire (NOP), chlorophylle *a* (Chl*a*) et pheopigments (Pheo) ont été filtrés sous vide sur des filtres Whatman GF/F (25 mm) avec une dépression inférieure à 50 mm Hg. Les filtres ont ensuite été conservés à -20 °C. Les volumes filtrés ont varié de 20 à 500 mL selon la turbidité.

III.A.2) *Nutriments*

Les **nutriments** (ammonium, nitrite, nitrate, silicate) ont été mesurés par analyse en flux segmenté selon la méthode d'Aminot *et al.* (2009). Les teneurs en phosphate ont été quantifiés

manuellement par le dosage colorimétrique au bleu de phosphomolybdate (Murphy et Riley, 1962) où l'absorbance a été lue avec une cuve de 5 cm et un spectrophotomètre Shimadzu UV 160.

III.A.3) *Matière organique dissoute*

Plusieurs méthodes, non-spécifiques et spécifiques, ont été utilisées afin de caractériser la MOD.

i) Méthodes non-spécifiques

Les teneurs en **COD** ont été estimées par leur spectre d'absorption dans les UV proches (250-500 m) avec un spectrophotomètre Shimadzu UV 160 (Pages et Gadel, 1990). Les teneurs en **POD** ont été analysées après transformation en phosphate par une méthode d'oxydation au persulfate alcalin (Koroleff, 1983) ; les teneurs en phosphate résultantes ont été dosées manuellement comme décrit précédemment.

ii) Méthodes spécifiques

Les **MCHOD** et les **PCHOD** ont été mesurés par le dosage au 2,4,6-tripyridyl-s-triazine selon la méthode de Myklestad *et al.* (1997). Pour cela, les MCHOD ont été directement dosés dans l'échantillon tandis que les monosaccharides totaux (incluant les monosaccharides compris dans les PCHOD et MCHOD) ont été dosés après une réaction d'hydrolyse des PCHOD de 20 h avec 0.1 M HCl à 100 °C et à pH neutre. Les PCHOD ont ainsi été déterminés comme la différence des deux mesures (**Figure II.2A**). Les mesures ont été réalisées en triplicats. Le D-glucose a été utilisé comme standard.

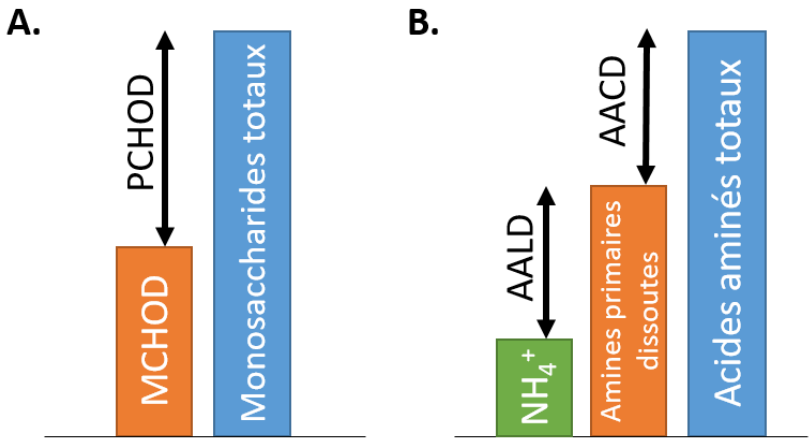

Figure II.2. Schéma conceptuel des différentes fractions constituant les carbohydrates (**A**) et les acides aminés (**B**) totaux. NH_4^+ : ammonium.

Les **AALD** et **AACD** ont été mesurés selon la méthode établie par Delmas *et al.* (1990). Pour cela, la concentration en amines primaires dissoutes a été quantifiée par mesure en flux de la fluorescence des acides aminés dérivés avec la o-phthaldialdehyde, en utilisant la glycine comme standard. La teneur en AALD a été déterminée en corrigeant la concentration d'amines primaires

dissoutes par la concentration en ammonium. Les acides aminés totaux ont été déterminés après une hydrolyse sous atmosphère azotée (5.8 N de HCl, 24 h à 105 °C) avec de l'acide ascorbique, suivie d'une neutralisation du pH réalisée avec 2.9 N de NaOH (Henrichs et Williams, 1985). L'acide ascorbique permet d'éviter la dégradation des AALD et AACD par les nitrates (Robertson *et al.*, 1987). Les AACD correspondent ainsi à la différence entre les acides aminés totaux et les amines primaires dissoutes (**Figure II.2B**). Pour les deux mesures, une correction pour la fluorescence naturelle a été réalisée en effectuant le protocole sans le réactif o-phthaldialdehyde. Toutes les mesures ont été réalisées en triplicats.

III.A.4) *Matière organique particulaire*

La matière particulaire a également été caractérisée par des mesures non-spécifiques et spécifiques.

i) Mesures non-spécifiques

Pour quantifier les **MES**, un volume déterminé d'échantillon a été filtré, rincé à l'eau milliQ afin de retirer les sels et séchés à 70 °C pendant 3 h. Les MES correspondent à l'augmentation de masse du filtre après séchage. LA **MIP** correspond au poids après une étape de calcination à 480 °C pendant 2 h, pendant laquelle les matières organiques sont carbonisées. La matière organique particulaire (**MOP**) correspond à la différence entre les MES et les MIP.

Les filtres utilisés pour quantifier le **COP** et le **NOP** ont été séchés 24 h à 60 °C. Les concentrations de COP et NOP ont été déterminés sur un spectromètre de masse à rapport isotopique (Delta plus, ThermoFisher Scientific, Bremen, Allemagne) couplé à un analyseur C/N (Flash EA, ThermoFisher Scientific). Les ratios molaires **COP/NOP** ont ensuite été calculés pour chaque échantillon.

Le **PPT** et le **PIP** ont été quantifiés comme décrit dans Labry *et al.* (2013) suivant les méthodes originelles de Solorzano et Sharp (1980) et Aspila *et al.* (1976), respectivement. Ces méthodes convertissent les différentes formes de phosphore en phosphate, qui est ensuite quantifié selon la méthode colorimétrique au bleu de phosphomolybdate (Murphy et Riley, 1962) par analyse en flux segmenté (Aminot *et al.*, 2009). Le phosphore organique particulaire (**POP**) correspond à la différence entre le PPT et le PIP.

ii) Mesures spécifiques

Les teneurs en **Chl*a*** et en **Pheo** ont été déterminées par fluorimétrie après extraction dans de l'acétone à 90 % (Holm-Hansen *et al.*, 1965). Le pourcentage de Chl*a* (**%Chl*a***) a été calculé pour évaluer la contribution de la Chl*a* aux pigments totaux (Chl*a* et Pheo).

Les **CHOPS** et **CHOPI** ont été extraits séquentiellement comme décrit dans Delmas (1983). Les CHOPS ont été extraits en incubant les filtres pendant 30 min à 100 °C avec 5 mL d'eau. Le surnageant

a été collecté après centrifugation et analysé par la méthode standard au phénol-acide sulfurique (Dubois *et al.*, 1956). Les CHOPI ont été ensuite extraits à partir des mêmes filtres avec 5 mL d'acide sulfurique 2 N, incubé 4 h à 100 °C et les surnageants ont été analysé comme précédemment.

Les **AAP** totaux ont été quantifiées comme décrit précédemment (**cf III.A.3.ii**), après une hydrolyse sur filtre et sous atmosphère azotée (5.8 N de HCl, 24 h à 105 °C), sans acide ascorbique.

III.B. Paramètres biologiques

III.B.1) *Abondance bactérienne*

Pour le suivi mensuel dans l'estuaire de l'Aulne (**chapitre IV**), l'abondance des bactéries libres et totales (incluant les bactéries libres et attachées) a été quantifiée par cytométrie en flux. Les bactéries libres ont été dénombrées après une étape de filtration à 3 µm (Whatman Nuclepore PC) tandis que le nombre total de bactéries a été quantifié sur des échantillons non filtrés, après une étape de désorption visant à détacher les bactéries attachées aux particules (adapté de Carreira *et al.*, 2015). Pour cela, tous les échantillons ont été fixés avec 0.25 % de glutaraldéhyde et 0.01 % de Poloxamer 188 pendant 10 min à l'obscurité et température ambiante (Marie *et al.*, 1999) et de l'EDTA à 0.5 M a été ajouté (concentration finale 0.125 M). Les échantillons pour les bactéries libres ont été immédiatement congelés à -20 °C tandis que les échantillons pour les bactéries totales ont été incubés pendant 1 h à l'obscurité et température ambiante (Carreira *et al.*, 2015). Les bactéries attachées ont été désorbées avec 3 cycles de sonication (10 s de sonication – 10 s de repos, sur glace) (Bioblock Scientific Vibracell 72442, 20 % d'amplitude) et congelés à – 20 °C. Lors des expérimentations en microcosme (**chapitre VI**), les échantillons non fractionnés ont été fixés comme décrit précédemment, puis congelés dans de l'azote liquide et conservés à -80 °C jusqu'à analyse.

L'analyse en cytométrie a été réalisée selon un protocole classique (Marie *et al.*, 1999) : les échantillons ont été décongelés, dilués avec de l'eau de mer stérile (autoclavée et filtrée à 0.2 µm) et marqués au SYBR Green I (1:10 000 de la dilution commerciale) pendant 10 min à température ambiante. L'acquisition des données a été réalisée avec un cytomètre FACS Verse (**chapitre IV**) ou Novocyte Advanteon (**chapitre VI**).

III.B.2) *Abondance phytoplanctonique*

L'**abondance du pico- et du nanophytoplancton** a été quantifiée par cytométrie en flux lors de l'étude en microcosme (**chapitre VI**) selon la méthode de Marie *et al.* (1999) basée sur leur autofluorescence naturelle. Pour cela, 250 µL d'échantillons non dilués, conservés comme décrit précédemment (**cf III.B.1**), ont été injectés dans le cytomètre Novocyte Advanteon. Le picophytoplancton, le nanophytoplancton, les cryptophytes et les cyanobactéries ont été discriminés selon leur fluorescence rouge et orange naturelle.

III.B.3) *Production bactérienne*

La **production bactérienne** a été mesurée lors du suivi mensuel dans l'estuaire de l'Aulne (**chapitre IV**) sur des échantillons non fractionnés ou filtrés à 3 µm, selon la méthode basée sur l'incorporation de ^{3}H-methyl-thymidine (Fuhrman et Azam, 1982). Les échantillons ont été incubés en triplicat avec 40 nM de ^{3}H-methyl-thymidine (20 Ci mmol^{-1}) à température *in situ* pendant 1 à 4 h. Des contrôles dans lesquels bactéries ont été préalablement tuées à l'acide trichloracétique (TCA) (5 % de concentration finale) ont été réalisés de la même manière. Le taux d'incorporation de ^{3}H-methyl-thymidine dans l'ADN a été converti en production de cellules bactériennes en considérant 2.18 x 10^{18} cellules par mole de ^{3}H-methyl-thymidine incorporée (Fuhrman et Azam, 1982). La production bactérienne en carbone a été estimée en considérant un contenu cellulaire de 16 fgC cellule^{-1}. La production des bactéries fixées aux particules (PB > 3 µm) a été déterminée comme la différence entre la production totale et la production dans la fraction < 3 µm.

III.B.4) *Activités enzymatiques*

Pour la mesure des activités enzymatiques, des substrats fluorogéniques dérivés de 7-amino-4-methylcoumarin (MCA) ou methylumbelliferone (MUF) ont été utilisés. Ces mesures ont consisté à suivre l'augmentation de la fluorescence liée à la libération de MCA ou de MUF au cours du temps, résultant de l'hydrolyse des substrats fluorogéniques par les enzymes hydrolytiques étudiées. Deux techniques de mesure de fluorescence ont été utilisées : **l'analyse en flux continu** (« *flux injection analysis* », FIA) et la **mesure en microplaque**.

i) Mesure en FIA

Principe. Pour la mesure en FIA, les échantillons sont incubés dans des conditions déterminées. Ensuite, une mesure de fluorescence est effectuée à la fin de la période d'incubation, permettant de déterminer la variation de fluorescence au cours du temps. La mesure en FIA correspond à une injection de l'échantillon dans un fluide de transport (ici, un tampon borate) via un système d'injection de chromatographie. L'échantillon est ainsi acheminé vers un spectrofluorimètre en flux.

Ce système a un avantage majeur : il permet de découpler les conditions d'incubation des conditions de mesure de fluorescence. En effet, pour être représentatives des conditions *in situ* et déterminer une valeur de V_{max} au plus proche de la réalité, les incubations doivent être effectuées au pH *in situ*. Par contre, comme la fluorescence des composés MUF et MCA est très pH-dépendante et varie fortement sur la gamme de pH 7-9 (Chrost et Krambeck, 1986), il est nécessaire de mesurer la fluorescence à un pH similaire pour tous les échantillons afin de ne pas induire de biais. C'est particulièrement important dans les estuaires où les eaux douces et les eaux marines présentent des pH différents (de pH 7.2 à 8.2 dans l'estuaire de l'Aulne, Riso *et al.*, 2021). De plus, de par son faible

trajet optique, le FIA permet de limiter les phénomènes de filtre interne (Urvoy *et al.*, 2020). La mesure en FIA a ainsi été adoptée pour le suivi mensuel dans l'estuaire de l'Aulne (**chapitre IV**).

Activités mesurées. Les activités phosphatases alcalines (PA) ont été mesurées avec le substrat 4-methylumbelliferyl phosphate (250 µM), les β-glucosidases (GLU) avec le substrat 4-methylumbelliferyl β-D-glucopyranoside (150 µM) et les aminopeptidases (LAM) avec le substrat L-leucine-7-amido-4-methylcoumarine (1000 µM). Ces mesures ont été effectuées sur les fractions totales (échantillon non filtré) et < 3 µm (Whatman Nuclepore PC). L'activité PA a également été mesurée dans la fraction dissoute (< 0.2 µm, Whatman Nuclepore PC). Les concentrations de substrat utilisées sont saturantes et permettent de mesurer l'activité potentielle des enzymes (V_{max}).

Incubations. Les échantillons (2 mL) ont été incubés 4 à 8 h dans le noir et à température *in situ* avec les différents substrats. A la fin de la période d'incubation, les réactions ont été inhibées avec les inhibiteurs suivant, et immédiatement congelées à -20 °C :

- PA : 450 µL de formol tamponné (0.05 M tétraborate, 18 % formol, pH 8.0) (Labry et Urvoy, 2020) ;
- GLU : 200 µL d'un tampon NH_4-glycine (0.2 M NH4, 0.05 M glycine, pH 10.5) (Chróst, 1989) ;
- LAM : 200 µL de SDS à 10 % (Delmas et Garet, 1995).

Contrôles. Des contrôles permettant d'évaluer la fluorescence naturelle des échantillons ont été réalisés en suivant le même protocole, mais les échantillons ont été immédiatement inhibés et congelés, sans étape d'incubation.

Détermination des activités. La mesure de fluorescence a été réalisée avec un tampon borate (0.1 M, pH 10.5) délivré à 1 mL min^{-1}. La fluorescence a été mesurée avec un spectrofluorimètre Kontron SFM25 dans une cellule comportant un trajet optique de 1 mm. Les longueurs d'onde d'excitation et d'émission étaient respectivement 364/460 nm pour le MUF et 380/440 nm pour la MCA. Le blanc de fluorescence correspondant au contrôle a été retiré de la valeur de fluorescence obtenue pour les échantillons et celle-ci a été convertie en activité potentielle avec des standards de MUF et MCA. Pour chaque duplicat biologique, la moyenne de la fluorescence a été calculée sur deux réplicats de mesure. L'activité enzymatique des bactéries fixées aux particules correspond à celle de la fraction totale moins celle de la fraction < 3 µm. Pour les PA, l'activité des bactéries libres correspond à celle de la fraction < 3 µm moins celle de la fraction < 0.2 µm.

ii) Mesure en microplaque

Principe. Pour les mesures d'activités en microplaque, l'échantillon est incubé directement dans le lecteur de plaque et la fluorescence est mesurée à intervalle de temps régulier (de l'ordre de quelques minutes). Cela permet de suivre l'évolution de la fluorescence de manière beaucoup plus fine et

augmente considérablement le nombre d'échantillons pouvant être traité en parallèle. Cependant, l'effet dû au confinement des échantillons est plus important : les volumes incubés sont plus petits et le rapport volume/surface plus élevé, favorisant les phénomènes d'adsorption. De plus, le lecteur de plaque utilisé ne permet pas de fixer la température d'incubation (incubation à température ambiante). Enfin, cette méthode ne permet pas de fixer le pH de la mesure indépendamment du pH d'incubation. En conséquence, il faut soit comparer des échantillons contenant des pH similaires, soit réaliser plusieurs gammes de calibration pour chaque pH testé. L'approche en microplaque a été utilisée pour les expériences effectuées sur des souches isolées (**chapitre V**) et lors de la réalisation de microcosmes avec des communautés naturelles (**chapitre VI**), car le but de ces expériences était plus de comparer différents traitements entre eux que d'obtenir une valeur de V_{max} absolue. De plus, le nombre d'échantillon dans ces expériences n'aurait pas permis d'utiliser la méthode FIA, beaucoup plus chronophage.

Mesure d'activités enzymatiques des souches de l'estuaire de l'Aulne. Les activités des LAM (L-Leucine-7-amido-4-methylcoumarine, 1000 µM) et des GLU (4-Methylumbelliferyl β-D-glucopyranoside, 150 µM) ont été mesurés dans la culture totale (activité dissoute et liée aux cellules) et dans le surnageant de culture (activité dissoute). Pour cela, 100 µL d'échantillon ont été répartis en microplaque (96 puits, noire, Corning No. 3631) avec les substrats et la fluorescence a été suivie pendant 3-4 h à l'aide d'un Spark Tecan Infinite M200PRO aux mêmes longueurs d'onde que précédemment (364/460 nm pour le MUF, 380/440 nm pour la MCA). Les activités ont été déterminées comme la pente de la partie linéaire de l'évolution de la fluorescence au cours du temps (AU min^{-1}). Les activités liées aux cellules ont été déterminées en soustrayant l'activité mesurée dans le surnageant de l'activité totale. Pour ces expériences, les PA n'ont pas pu être mesurée car les lactonases dégradent le substrat utilisé pour leur mesure.

Mesure d'activités enzymatiques des communautés naturelles en microcosme. Les activités des GLU (4-Methylumbelliferyl-b-D-glucopyranoside, 150 µM), β-glucuronidases (4-Methylumbelliferyl-b-D-glucuronide, 250 µM), *N*-acetyl-glucosaminidases (4-Methylumbelliferyl N-acetyl-b-D-glucosaminide 250 µM), lipases (4-Methylumbelliferyl butyrate, 800 µM), LAM (L-Leucine-7-amido-4-methylcoumarin, 1000 µM) et PA (4-Methylumbelliferyl phosphate, 250 µM) ont été mesurées. Pour cela, 80 µL d'échantillon ont été répartis en microplaque (384 puits, noire, « *low binding* », Greiner no. 781900). Les puits ont été complétés avec 20 µL de tampon Tris (10 mM, pH 8.2) contenant les différents substrats. Un contrôle pour la dégradation abiotique des substrats a été préparé en remplaçant les 80 µL d'échantillon par 80 µL de tampon Tris. La fluorescence a été suivie pendant 3-4 h à l'aide d'un Spark Tecan Infinite M200PRO aux mêmes longueurs d'onde que précédemment (364/460 nm pour le MUF, 380/440 nm pour la MCA). Les activités ont été déterminées comme la pente de la partie linéaire (AU min^{-1}), à laquelle la pente du contrôle de dégradation abiotique a été

retirée. Seul le 4-Methylumbelliferyl butyrate a présenté une dégradation abiotique. La fluorescence a été convertie en équivalent substrat à l'aide d'une gamme de standards réalisées dans 20 µL de tampon Tris et 80 µL d'eau de mer filtrée sur 0.2 µm et autoclavée. Les mesures ont été réalisées en duplicat (1ère expérience) ou quadruplicat (2ème expérience) techniques.

IV. Microbiologie

IV.A. Isolement et culture de souches bactériennes de l'estuaire de l'Aulne

Des bactéries ont été isolées des eaux de surface de l'Aulne en Avril et Juillet 2019 afin d'étudier leur capacité de QS et de QQ (**chapitre V**). Trois salinités ont été échantillonnées pour couvrir une large gamme de MES et augmenter la diversité des bactéries isolées : des eaux douces (salinité 0), des eaux du maximum turbide (salinité 5) et des eaux sous une influence marine plus importante (salinité 25). Toutes les étapes de culture ont ensuite été réalisées à température (12 °C en Avril, 22 °C en Juillet) et salinité *in situ*. Pour cela, trois milieux Luria Broth modifiés (mLB) ont été réalisés avec 1 % de peptone, 0.5 % d'extrait de levure et ajustés à la salinité *in situ* (0, 5 ou 25) avec de l'eau de mer artificielle (54 mM $MgCl_2$, 10 mM $CaCl_2$, 0.16 mM $SrCl_2$, 9 mM KCl, 2.4 mM $NaHCO_3$, 840 mM KBr, 440 mM H_3BO_3, 71 mM NaF, 0.40 M NaCl and 30 mM Na_2SO_4, pH 8.2). Pour le mLB à salinité 0, 1 % d'eau de mer artificielle a été ajouté pour assurer la présence d'ions essentiels.

Pour chaque échantillon, plusieurs méthodes ont été utilisées pour isoler des bactéries de la fraction totale, de la fraction attachée aux particules (> 3 µm) et de la fraction vivant librement dans la colonne d'eau (0.2 - 3 µm). Pour cela, des boites de mLB agar (mLB contenant 1.5 % d'agar) ont été inoculées en : i) étalant 100 µL d'eau estuarienne ; ii) étalant 100 µL d'eau estuarienne filtrée à 3 µm (Whatman Nuclepore polycarbonate - PC) ; iii) déposant un filtre de 3 µm, contenant les bactéries > 3 µm ; iv) déposant un filtre de 0.2 µm (Whatman Nuclepore PC), contenant les bactéries comprises entre 0.2 et 3 µm. Les colonies isolées résultant de ces incubations ont été purifiées, cultivées en mLB et conservées à – 80 °C avec 10 % de DMSO, résultant en une souchotèque de 299 bactéries.

IV.B. Capacités de quorum sensing et quorum quenching de souches estuariennes isolées

IV.B.1) *Les biosenseurs bactériens*

Des biosenseurs bactériens sont classiquement utilisés pour étudier les capacités de QS et QQ de bactéries isolées. Ce sont des bactéries génétiquement modifiées pour exprimer un gène rapporteur lorsqu'un AI exogène (e.g., AHL, AI-2, PQS) se lie au récepteur d'AI contenu dans le biosenseur (**Figure II.3**). Les gènes rapporteurs encodent des produits facilement quantifiables, comme par exemple des protéines fluorescentes (e.g., Green Fluorescente Protein - GFP, mCherry), une

protéine catalysant la réaction de bioluminescence (luciférase) ou des pigments (e.g., violacéine, progidiosine).

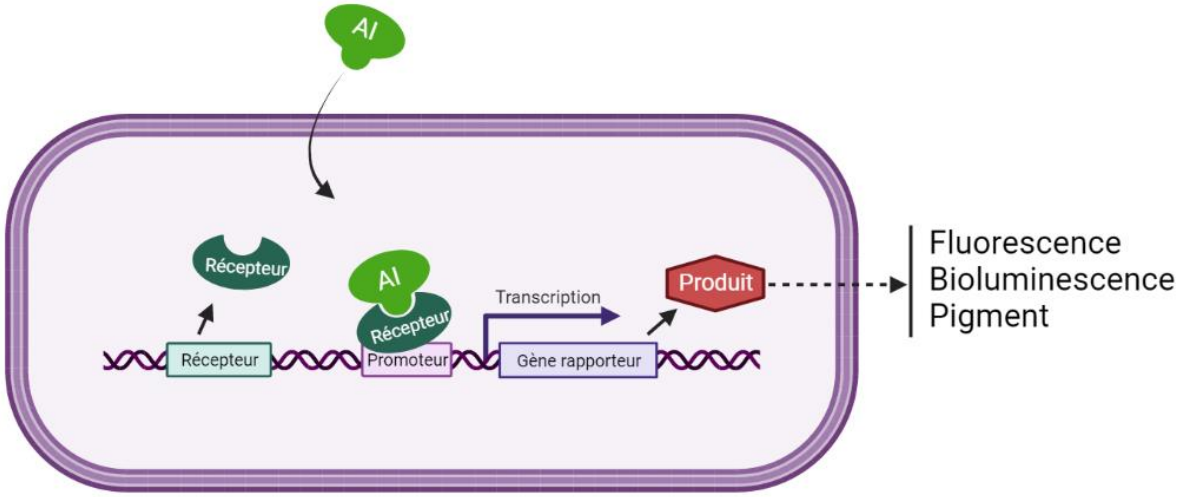

Figure II.3. Illustration du fonctionnement d'un biosenseur. L'AI exogène présent dans le surnageant de culture à tester se lie au récepteur d'AI présent chez le biosenseur (qui ne produit lui-même pas d'AI). Ce complexe se lie alors au promoteur, induisant la synthèse du gène rapporteur dont le produit est facilement quantifiable (fluorescence, bioluminescence, pigment). Créé avec https://biorender.com/

Dans le cadre de ce travail de thèse, nous avons utilisé les biosenseurs *Escherichia coli* MT102 (pJBA132) (Riedel *et al.*, 2001) et *Pseudomonas putida* F117 (pRK-C12) (Andersen *et al.*, 2001), qui produisent de la GFP en présence d'AHLs exogènes. Ils répondent préférentiellement aux AHLs à chaines courtes et longues, respectivement. *E. coli* MT102 et *P. putida* F117 ont été cultivés à 30°C en milieu LB (0.5 % d'extrait de levure, 1 % de peptone et 1 % de $NaCl_2$), en ajoutant 25 µg mL^{-1} de tetracycline ou 20 µg mL^{-1} de gentamicine, respectivement.

Ces biosenseurs peuvent être utilisés pour détecter les capacités de QS en les mettant au contact de surnageants de cultures bactériennes et en suivant la fluorescence de la GFP par rapport au témoin ne contenant pas d'AHL (donc sa production de fluorescence n'est pas induite). Les biosenseurs peuvent aussi être utilisés pour détecter les capacités de QQ des bactéries testées. Pour cela, le biosenseur est mis en contact du surnageant bactérien et d'une AHL commerciale. Une réduction de fluorescence en comparaison du témoin positif (contenant seulement l'AHL commerciale) indique un potentiel de QQ, c'est-à-dire une éventuelle dégradation de l'AHL ou un blocage de sa réception par le récepteur.

IV.B.2) *Capacités de quorum sensing*

La capacité de production d'AHLs par les souches bactériennes de l'estuaire de l'Aulne a dans un premier temps été évaluée grâce aux biosenseurs. Les deux biosenseurs ont été pré-cultivés à 30°C (150 rpm) en milieu LB toute une nuit. Ils ont ensuite été dilués à une densité optique à 600 nm (DO_{600})

de 0.02 (mesurée au NanoDrop 2000c avec une cuve de 1 cm, Thermo Scientific) et répartis en microplaque noire (96 puits, noire, Corning No. 3631, 150 µL par puit).

Les souches bactériennes à tester ont été cultivées dans leur milieu mLB respectif jusqu'à une DO_{600} comprise entre 0.6 et 1.2. Les cultures ont ensuite été centrifugées à 12 000 g pendant 10 min et filtrées à 0.2 µm (filtre à seringue Corning® PES) afin de retirer les cellules bactériennes. Les surnageants résultants ont été stockés à - 20 °C jusqu'à leur screening (1 semaine maximum). Après décongélation à température ambiante, les surnageants ont été ajoutés à la microplaque contenant les biosenseurs (50 µL par puit). La fluorescence de la GFP (excitation : 485 nm, émission : 535 nm) et la DO_{600} ont été lues (lecteur de microplaque Spark Tecan Infinite M200PRO, Tecan, Suisse) après une incubation sur la nuit (14-16 h) à 30 °C sous agitation faible (100 rpm). Les blancs de DO_{600} et de fluorescence ont été réalisés avec 150 µL de LB stérile et 50 µL de mLB à la salinité correspondante aux échantillons testés. Les contrôles négatifs ont été réalisés en ajoutant 50 µL de milieu mLB stériles aux 150 µL contenant le biosenseur. A chaque fois, le mLB utilisé pour les témoins correspondait au mLB utilisé pour les échantillons car les biosenseurs se sont révélés sensibles aux différentes concentrations en sels. Les contrôles positifs ont été réalisés en ajoutant 10 µM d'AHLs commerciales (C6-HSL pour *E. coli* MT102 et 3-oxo-C10-HSL pour *P. putida* F117) diluées dans du DMSO (concentration de DMSO finale de 1 %). En conséquence, un deuxième témoin négatif a été réalisé, contenant 1 % de DMSO.

L'induction spécifique de fluorescence par rapport au contrôle négatif a été calculée en divisant la fluorescence spécifique de l'échantillon testé ($FLUO_{GFP}^{ech} \ / \ DO_{GFP}^{ech}$) par celle dans le contrôle négatif ($FLUO_{GFP}^{ctr-} \ / \ DO_{GFP}^{ctr-}$). Cette induction spécifique a ensuite été arbitrairement classifiée dans les catégories suivantes : inhibition (< 0.8) ; pas de modification (0.8-1.2) ; induction questionnable (1.2-1.5) ; induction (1.5-3) ; et forte induction (> 3). Toutes les inductions spécifiques pas significativement différentes du contrôle négatif ont été comptées dans la catégorie « pas de modification ».

Cette première étape de screening a permis d'identifier 75 souches modulant l'activité des biosenseurs (induction spécifique < 0.8 ou > 1.2) et donc, susceptibles de produire des AHLs. Ces souches ont ensuite été analysées en spectrométrie de masse couplée à de la chromatographie liquide ultra haute pression (UHPLC-HRMS/MS) afin de valider la présence d'AHLs, de les identifier et de les quantifier. La chromatographie permet de fractionner l'échantillon et d'en réduire la complexité. La spectrométrie consiste en l'ionisation et le transfert vers une phase gazeuse des molécules contenues dans l'échantillon. L'analyse des ions ainsi formés permet d'obtenir leur rapport masse sur charge (*m/z*) ainsi que leur spectre de fragmentation. Pour réaliser cette analyse, 50 mL de surnageant de culture ont été préparés comme décrit précédemment. Les surnageants ont été extraits avec 50 mL d'acétate d'éthyle (EtOAc) pendant une nuit à température ambiante. Pendant cette incubation, les AHLs migrent dans la phase organique composée d'EtOAc du fait de leur hydrophobicité. Les phases

aqueuses et organiques ont ensuite été séparées et la phase aqueuse a de nouveau été extraite avec 50 mL d'EtOAc. Les deux fractions de 50 mL d'EtOAc ont ensuite été réunies et séchées avec un évaporateur rotatif. Les extraits séchés ont été repris dans 500 µL d'EtOAc, complètement séchés à l'aide d'un GeneVac HT-4X et stockés à - 20 °C jusqu'à analyse. L'analyse UHPLC-HRMS/MS a été réalisée avec un système Ultimate 3000^{TM} UHPLC (Thermo Fischer Scientific, Waltham, Massachusetts, USA). La colonne de chromatographie était une Phenomenex Luna Omega Polar C18 (150 x 2.1 mm, particules de 1.6 µm). La phase mobile était composée de 0.1 % d'acide formique dans de l'eau (A) et de 0.1 % d'acide formique dans l'acétonitrile (B). Le gradient d'élution a débuté avec 99 % de A, gardé constant pendant 4 min, puis la proportion de B a été linéairement augmentée jusqu'à 100 % pendant 10 min et laissée à 100 % pendant 5 min.

L'acquisition des données a consisté en un scan de masse de l'ensemble des ions parents formés par ionisation de l'échantillon dont le rapport *m/z* était compris entre 50 et 750 *m/z*. Ensuite, une acquisition dite « *data-dependent* » des ions secondaires produits par fragmentation (effectué à 15, 30 et 40 eV) des ions parents les plus abondants a été réalisée. Cette méthode permet d'acquérir des données haute-résolution de la masse des ions parents et de leurs produits de fragmentation en une seule analyse. Les spectres de fragmentation des AHLs sont caractérisés par la présence systématique d'un ion secondaire abondant (102.055 *m/z*) correspondant au cycle lactone, ainsi que par la présence habituelle de trois autres ions (56.050, 74.061 et 84.045 *m/z*). Les AHLs ainsi détectées ont été quantifiées grâce à l'utilisation de standards commercialement disponibles.

IV.B.3) *Capacités de quorum quenching*

Les souches bactériennes de l'estuaire de l'Aulne produisant des AHLs ont été testées pour leur capacité à perturber les voies de communication basées sur les AHLs. Les biosenseurs ont été cultivés comme décrit précédemment (**cf IV.B.2**), excepté que 1 µM d'AHL commerciale (C6-HSL pour *E. coli* MT102 et C14-HSL pour *P. putida* F117, 1 % de DMSO final) a été ajoutée au milieu LB avant sa répartition en microplaque (96-puits, noire). Les surnageants de culture bactériennes ont été produits comme précédemment (**cf IV.B.2**), sauf qu'ils ont été conservés à 4°C avant d'être testés (4 h maximum) afin d'éviter la dénaturation éventuelle des composés QQ potentiellement présents. Les contrôles positifs contenaient 1 µM de l'AHL commerciale utilisée et les contrôles négatifs contenaient 1 % de DMSO. La réduction spécifique de fluorescence par rapport au contrôle positif a été calculée comme précédemment ($\frac{FLUO_{GFP}^{ech} / DO_{GFP}^{ech}}{FLUO_{GFP}^{ctr+} / DO_{GFP}^{ctr+}}$).

Afin de vérifier si la diminution de fluorescence éventuellement observée ne provient pas d'une réduction de la viabilité du biosenseur, une mesure à la résazurine a été effectuée. La résazurine est un composé bleu faiblement fluorescent qui est réduit en résorufine par le métabolisme aérobie des cellules vivantes. La résorufine est un composé rose fluorescent facilement quantifiable qui reflète

ainsi l'activité métabolique des cellules. Pour réaliser cette mesure, 100 µL de chaque puit de la microplaque de screening contenant les biosenseurs sont amendés avec 30 µL de résazurine à 0.01 % et incubé 4 h à 30°C. La fluorescence de la résorufine résultante est mesurée à une longueur d'onde d'excitation et d'émission respective de 530 et 590 nm.

IV.C. Capacités de production de biofilm de souches estuariennes isolées

La production de biofilm des souches bactériennes a été quantifiée par un dosage au cristal violet. Pour cela, les souches ont été cultivées dans leur milieu mLB respectifs en microplaque 96 puits (Greiner Bio-One, Cat-No 655160) pendant 24 h (à 22 °C, pour les souches isolées en Juillet) ou 48 h (à 12 °C, pour les souches isolées en Avril) à une agitation de 100 rpm, permettant le développement d'un biofilm au fond des puits de la microplaque. Le biofilm a ensuite été quantifié selon les étapes suivantes, réalisées délicatement afin de préserver son intégrité. Le surnageant de culture a d'abord été retiré et les cellules non-adhérées ont été lavées avec 200 µL de tampon PBS (pH 7.4). Les microplaques ont été séchées à 60 °C pendant 1 h. Le biofilm a ensuite été marqué avec 100 µL de cristal violet (0.2 % w/v, 15 min) qui se lie aux molécules négativement chargées (membrane cellulaire, exopolysaccharides du biofilm). Le cristal violet non lié à la biomasse bactérienne a été retiré et les puits de la microplaque ont été rincés 3 fois avec 200 µL d'eau MilliQ stérile. Ensuite, le cristal violet contenu dans le biofilm a été solubilisé avec 200 µL d'une solution de décoloration (50 % éthanol, 10 % acide acétique dans de l'eau MilliQ). Finalement, la DO résultante a été quantifiée à 540 nm (Nanodrop 2000c avec une cuvette de 1 cm, Thermo Scientific).

IV.D. Impact de la disruption du QS sur des souches estuariennes isolées

Une approche basée sur l'utilisation de lactonases a été utilisée pour étudier l'implication du QS dans la régulation de la synthèse d'enzymes hydrolytiques et la production de biofilm au sein des souches bactériennes de l'Aulne identifiées comme productrices d'AHLs. Les lactonases sont des enzymes qui hydrolysent le cycle lactone des AHLs, les rendant inactives en tant que molécule signal. Les cultures « témoin », sans lactonase, contiennent ainsi les AHLs naturellement produites par les souches lors de leur croissance. Les cultures traitées avec lactonases ne contiennent pas (ou peu) d'AHLs car celles-ci ont été dégradées par les lactonases, empêchant la mise en place du QS basé sur les AHLs.

Une préparation commerciale de lactonases dérivées de l'enzyme SsoPox, encodée par l'archée *Saccharolobus solfataricus*, a été obtenue de l'entreprise Gene&GreenTK (Marseille, France), spécialisée dans le développement d'enzymes. Cette préparation de lactonases a été produite de manière hétérologue chez *Escherichia coli*, purifiée par chromatographie d'exclusion de taille et éluée dans un tampon HEPES (50 mM HEPES, 150 mM NaCl, pH 8.0) (Hiblot *et al.*, 2013; Guendouze *et al.*, 2017; Rémy *et al.*, 2020).

Les bactéries de l'Aulne produisant des AHLs ont été pré-cultivées sur la nuit dans leurs milieux mLB respectifs à 12 °C ou 22 °C. Les précultures ont ensuite été diluées à une DO_{600} de 0.001 et la préparation de lactonase (concentration finale de 0.5 mg L^{-1}) ou la quantité équivalente de tampon HEPES a été ajoutée (condition contrôle). Les cultures ont été réalisées en triplicat, à partir de la même pré-culture. Ensuite, 200 µL ont immédiatement été transférés en microplaque pour quantification de la production de biofilm (**cf IV.C**). Les cultures ont été incubées 24 h (à 22 °C pour les souches isolées en Juillet) ou 48 h (à 12 °C pour les souches isolées en Avril) avec une agitation douce (100 rpm). A la fin de la période d'incubation, la DO_{600}, les activités des LAM et des GLU dissoutes et totales ont été mesurées (**cf III.B.4**). Les surnageants de culture ont également été testés avec les biosenseurs *P. putida* F117 et *E. coli* MT102 (**cf IV.B.2**) afin de vérifier l'efficacité des lactonases. Pour chaque paramètre mesuré (production de biofilm, activités enzymatiques, induction des biosenseurs), l'effet du traitement avec les lactonases a été évalué en calculant le ratio entre les valeurs obtenues dans le traitement avec lactonase et celles obtenues dans le contrôle sans lactonase ($ratio_{lac/ctr}$).

IV.E. Impact de l'ajout de molécule du QS sur des communautés naturelles

L'implication des AHLs dans la synthèse d'enzymes hydrolytiques et la composition des communautés bactériennes naturelles a été évaluée par une approche en microcosme (**Figure II.4**). Des échantillons d'eau de mer, contenant des communautés naturelles de bactéries, ont été prélevés en rade de Brest à deux saisons différentes (29 mars et 3 mai 2021, **cf II.B**) et répartis dans des flacons de culture (150 mL par flasque T-175, cat. No. 83.3912, Sarsted). Cinq AHLs différentes (C4-, C6-, 3-oxo-C8-, C12- et C16-HSL) ont été diluées en DMSO et ajoutées séparément à une concentration de 50 nM (150 µL, soit une concentration finale de 0.1 % de DMSO). En parallèle, un contrôle contenant le volume équivalent de DMSO a été réalisé. Les différentes AHLs ont été choisies pour couvrir une large gamme de longueur de chaine acyle. La concentration choisie a été optimisée dans une expérience préalable afin de maximiser la réponse des activités enzymatiques et minimiser la concentration en AHLs, de manière à limiter leur utilisation éventuelle comme source nutritionnelle. Les microcosmes ont été incubés à température *in situ*, dans le noir et en triplicat (1ère expérience) ou quintuplicat (2ème expérience).

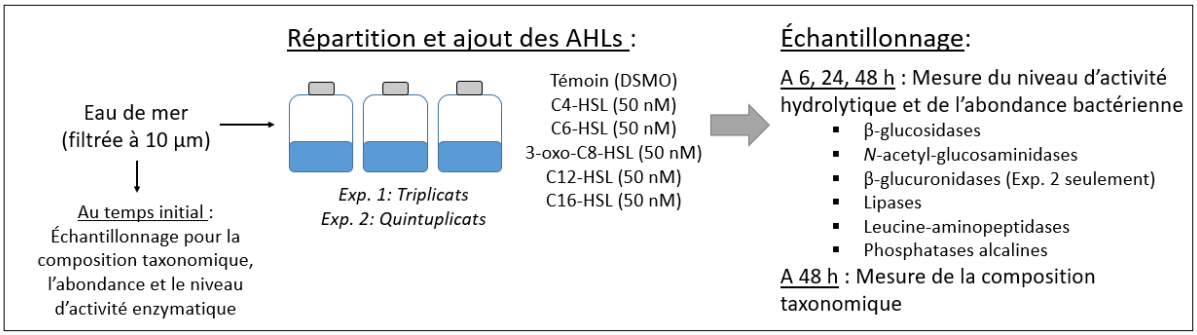

Figure II.4. Schéma de l'expérience d'ajout d'AHLs réalisée avec des communautés bactériennes naturelles en microcosme.

Les échantillons pour la détermination des activités enzymatiques (LAM, GLU, PA, *N*-acetyl-glucosaminidases, β-glucosidases, lipases) et de l'abondance bactérienne ont été collectés dans des tubes stériles (Falcon, Ref 352070) au temps initial (avant répartition en microcosme) ainsi qu'à 6, 24 et 48 h d'incubation. La composition des communautés bactériennes (BCC) initiale a été échantillonnée en triplicat en filtrant 3 x 200 mL d'eau de mer (< 10 µm) sur des filtres 0.2 µm (Whatman Nuclepore PC membrane). La BCC finale a été échantillonnée en filtrant l'eau restante dans chaque microcosme (≈ 100 mL).

V. Biologie moléculaire

V.A. Identification taxonomiques des souches estuariennes isolées

Les souches bactériennes isolées de l'estuaire de l'Aulne présentant des caractéristiques intéressantes ont été **identifiées par séquençage du gène de l'ARNr 16S** (**chapitre V**). Pour chaque souche, une colonie isolée a été resuspendue dans 50 µL d'eau MilliQ et incubée à 95 °C pendant 15 min afin de lyser les cellules. Le gène d'intérêt a été amplifié par PCR avec une solution contenant 1 µL de lysat, 21 µL de GoTaq Green Master Mix (Promega) et 1.5 µL des amorces universelles 27F (10 µM, 5'-AGAGTTTGATCMTGGCTCAG-3') et 1492R (10 µM, 5'-ACGGYTACCTTGTTACGACTT-3'). Le programme PCR consistait en un cycle de dénaturation (95 °C, 5 min), 35 cycles d'amplification (95 °C, 30 s – 56 °C, 30 s – 72 °C, 30 s) puis d'une extension finale de 5 min à 72 °C. Les produits PCR ont été purifiés avec le kit « NucleoSpin Gel and PCR Clean-up » (Macherey-Nagel). Ils ont ensuite été séquencés par l'entreprise Eurofins Genomics (Köln, Allemagne) à l'aide de la technique de séquençage Sanger (amorces 27F/1492R).

La qualité des séquences obtenues a été vérifiée manuellement à l'aide du logiciel Bioedit. Les séquences ont été identifiées avec la base de données EzTaxon-e (https://www.ezbiocloud.net, Kim *et al.*, 2012) depuis laquelle les séquences 16S et le pourcentage de similarité de séquence des bactéries les plus proches ont été récupérées. L'ensemble des séquences obtenu a été aligné avec l'algorithme MUSCLE, implémenté dans MEGA 7.0 et un arbre phylogénétique a été construit (modèle « maximum likelihood Tamura Nei »). Les séquences de *Geobacter sulfurreducens* (NR 132673.1) et *Geobacter soli* (NR 134039.1) ont été utilisées comme groupe externe (« *outgroup* »). La fiabilité de chaque nœud de l'arbre été déterminée par « *bootstrap* » (500 répétitions) et les nœuds avec une valeur inférieure à 50 ont été réduits. L'arbre résultant a été visualisé dans R avec le package ggtree (v2.2.4).

V.B. Séquençage de génome bactérien

Quatre souches bactériennes (*Pseudomonas* sp. AF3-9, *Pseudomonas* sp. B20, *Acinetobacter* sp. DF3-8 et *Vibrio* sp. E14) isolées de l'estuaire de l'Aulne ont été **séquencées afin d'identifier les gènes impliqués dans le QS, le QQ, la production d'enzymes hydrolytiques et la formation de biofilm** (**chapitre V**). Pour cela, les souches ont été cultivées en mLB à 12 °C ou 22 °C (à la température et salinité d'isolement) jusqu'à la phase stationnaire de croissance. Les cellules ont été culottées par centrifugation et leur ADN a été extrait avec le kit GenElute Bacteial Genomic DNA (Sigma-Aldrich). L'ADN a été séquencé avec un séquenceur Illumina MiSeq. La qualité des données a été évaluée avec FastQC (http://www.bioinformatics.babraham.ac.uk/projects/) et les séquences répondants aux critères suivant ont été conservées : i) longueur de séquence ≥ 50 pb et ii) score de qualité phred ≥ 30 pour chaque base. Les adaptateurs de séquençage ont été retirés et l'assemblage *de novo* des génomes a été réalisé avec Unicycler (v0.4.8) avec une longueur de contig minimale de 500 pb (Wick *et al.*, 2017). Ces contigs ont ensuite été comparés à la base de données UniVec (datée du 20 mars 2017) à l'aide de l'outil BLASTN (Altschul *et al.*, 1990) afin de retirer les contaminants éventuels. La couverture de séquençage a été estimée en alignant les séquences au génome obtenus avec Bowtie2 (v2.3.5) (Langmead et Salzberg, 2012) en mode « sensitive » puis en calculant la couverture de séquençage avec Mosdepth (v0.2.7) (Pedersen et Quinlan, 2018). La complétude des assemblages a été évaluée avec BUSCO (v4.0.0) (Simão *et al.*, 2015) en mode « genome » et en spécifiant le profile approprié (i.e., *Pseudomonadales* or *Vibrionales*, parution des profils : Avril 2019). Le nombre de contigs, le pourcentage de bases guanines et cytosines (%GC), la taille de l'assemblage, la valeur N50 et le pourcentage de couverture ont été calculés sur chaque génome obtenus. La prédiction automatique de gènes a été effectuée grâce au pipeline Prokka (v1.14.5) (Seemann, 2014) avec les paramètres par défaut, en spécifiant le genre correspondant.

Les analyses suivantes ont été effectuées sur les séquences de protéines prédites par Prokka :

- Pour rechercher **les gènes du QS et du QQ** (synthases d'AHL, les récepteurs d'AHL, les AHL-acylases et les AHL-lactonase), une base de données de référence de ces gènes a d'abord été compilée. Cela a été réalisé à partir de la base de référence UniProt/Swiss-Prot, inspectée à l'aide de différents mots-clefs ('acyl-homoserine-lactone synthase', 'IPR036693', 'AHL acylase' et 'AHL lactonases') et manuellement revue. De plus, trois séquences de la base de données UniProt/TrEMBL ont été manuellement ajoutées pour représenter les synthases des familles HdtS et AinS et le récepteur AinR. Les protéines contenues dans les génomes séquencés ont ensuite été comparées aux bases de gènes QS et QQ établies (BLASTP, E-value seuil 10^{-15}). Les séquences retenues ont été blastées contre la base UniProt/Swiss-Prot et celles avec une meilleure annotation dans cette base ont été retirées de la sélection. Enfin, les domaines des

protéines sélectionnées ont été annotés avec InterProScan (v.36.75). Les protéines contenant tous les domaines appropriés (**Tableau II.4**) ont été considérées comme des gènes QS putatifs. Ils ont été alignés à leur base de données de références respectives à l'aide de MUSCLE (implémenté dans Geneious Prime, v2021.0.3) et les arbres phylogénétiques consensus ont été construits (méthode 'Neighbour joining', 500 bootstraps).

Tableau II.4. Liste des domaines INTERPRO utilisés pour sélectionner les gènes QS et QQ.

LuxI-type AHL-synthase	
IPR001690	Autoinducer synthase
IPR016181	Acyl-CoA N-acyltransferase
HdtS-type AHL-synthase	
IPR002123	Phospholipid/glycerol acyltransferase
LuxM-type and AinS-type AHL-synthase	
IPR035304	AHL synthase
LuxR-type AHL receptor	
IPR005143	Transcription factor LuxR-like, autoinducer-binding domain
IPR000792	Transcription regulator LuxR, C-terminal
IPR016032	Signal transduction response regulator, C-terminal effector
IPR036388	Winged helix-like DNA-binding domain
LuxN-type and AinR-type AHL receptor	
IPR011006	CheY-like superfamily
IPR003594	Histidine kinase/HSP90-like ATPase
IPR036890	Histidine kinase/HSP90-like ATPase superfamily
IPR005467	Histidine kinase domain
IPR003661	Signal transduction histidine kinase, dimerisation/phosphoacceptor domain
IPR036097	Signal transduction histidine kinase, dimerisation/phosphoacceptor domain superfamily
IPR004358	Signal transduction histidine kinase-related protein, C-terminal
IPR001789	Signal transduction response regulator, receiver domain
AHL-lactonase	
IPR001279	Metallo-beta-lactamase
IPR036866	Ribonuclease Z/Hydroxyacylglutathione hydrolase-like
AHL-acylase	
IPR002692	Penicillin/GL-7-ACA/AHL/aculeacin-A acylase
IPR014395	Penicillin/GL-7-ACA/AHL acylase

- Les **gènes impliqués dans la motilité et l'adhérence** (flagelle, pili, fimbriae, chimiotactisme)**,** susceptibles d'être impliqués dans la formation de biofilm, ont été prédits à l'aide de VFanalyzer (B. Liu *et al.*, 2019) en spécifiant le genre correspondant au génome étudié.

- Les gènes codant pour des **protéases ou des inhibiteurs de protéases** ont été prédits par BLASTN avec la base de données de protéases MEROPS (v12.1) (Rawlings *et al.*, 2018) avec une E-value seuil de 10^{-50} et 70 % d'identité.

- Les enzymes actives sur les carbohydrates (**CAZymes**) ont été prédites avec la base de données CAZy (Lombard *et al.*, 2014) à l'aide de dbCAN2 (HMMdb v9.0) (Zhang *et al.*, 2018). Seules les CAZymes détectées par les trois méthodes implémentées dans dbCAN2 (i.e., HMMER, Diamond et Hotpep) ont été sélectionnées.

V.C. Metabarcoding d'échantillons environnementaux

La technique de **metabarcoding de la région V3/V4 du gène de l'ARNr 16S** a été utilisée pour étudier la composition des communautés bactériennes dans l'estuaire de l'Aulne (**chapitre III**) et lors des expériences en microcosme sur le rôle du QS (**chapitre VI**). Pour cela, les échantillons ont été filtrés (filtres 0.2 µm ou 3 µm selon la fraction étudiée, Whatman Nuclepore PC) et immédiatement congelés dans de l'azote liquide puis conservés à -80 °C. Des filtres secs ont également été traités de la même façon afin de servir de contrôle de contamination. Les filtres ont été découpés en morceaux en conditions stériles. L'ADN a été extrait avec le kit NucleoSpin Plant II Mini Kit (Macherey Nagel Ref. 740770.50) selon les instructions du fournisseur, avec une étape de lyse additionnelle réalisée pendant 2 h à 56 °C avec 25 µL de protéinase K (20 mg mL^{-1}, Macherey Nagel Ref. 740506) et 100 µL de lysozyme (20 mg mL^{-1}, Sigma ref 4403-5g). Les librairies ont été préparées et séquencées par l'entreprise Génome Québec (Montréal, Canada) à l'aide des amorces 341F/785R (Klindworth *et al.*, 2013). Les échantillons ont été séquencés sur un Illumina MiSeq (2 x 300 pb, chimie V3). Les données ont été pré-traitées avec le pipeline d'analyse SAMBA (v3.0.1) développé par l'équipe bio-informatique de l'Ifremer (SeBiMER). Brièvement, le pipeline utilise des outils standards (QIIME2, Dada2) pour inférer des variants de séquence d'amplicon (ASVs) et les clusteriser à l'aide de dbOTU3 (implémenté dans QIIME2). Les ASVs ont ensuite été assignées avec la base de données Silva v138, formatée pour les amorces 341F/805R utilisées (Quast *et al.*, 2013). Les tables d'ASVs ainsi générées ont ensuite été traitées selon les étapes décrites ci-dessous (**cf VI.A**).

VI. Traitement des données

Toutes les données ont été traitées avec le langage R (v4.1.0, 2021-05-18) implémenté dans Rstudio (v2021.09.0) et représentées grâce au package ggplot2 (v3.3.5), sauf si précisé autrement.

VI.A. Etude de la composition des communautés bactériennes

VI.A.1) *Traitement général des données de metabarcoding*

Une fois les tables d'ASVs générées (**cf V.C**), les données de metabarcoding des communautés de l'estuaire de l'Aulne (**chapitre III**) et des expériences en microcosme (**chapitre VI**) ont été principalement traitées avec les packages phyloseq (v1.32.0), vegan (v2.5.7) et microeco (v0.6.0).

i) Composition des communautés, courbes de raréfaction et correction de la profondeur de séquençage

Tout d'abord, les ASVs correspondant aux éventuelles séquences d'eucaryotes, d'archées, de mitochondries ou de chloroplastes ont été retirées des jeux de données pour toutes les analyses réalisées. La composition des communautés a ensuite été visualisée à l'aide de **diagrammes en barre** représentant les abondances relatives des ASVs les plus abondantes, regroupées au niveau de l'ordre ou de la classe.

Les **courbes de raréfaction** ont été tracées avec la fonction ggrare (package ranacapa, v0.1.0). Elles représentent le nombre d'espèces en fonction de la profondeur de séquençage (i.e., le nombre de séquences) et permettent d'estimer si celle-ci est suffisante pour correctement évaluer le nombre d'espèces présentes. Pour cela, les courbes de raréfaction doivent atteindre un plateau, signifiant qu'un effort de séquençage supérieur ne permettrait pas (ou peu) de détecter d'espèces supplémentaires.

Pour certaines analyses statistiques, il est nécessaire d'avoir la même profondeur de séquençage, i.e., le même nombre de séquence dans chaque échantillon. Pour cela, les communautés ont été soit raréfiées, soit transformées en abondance relative (« *total sum scaling* », TSS) selon les propriétés des jeux de données et l'analyse réalisée. La table d'ASVs raréfiée a été obtenue par un sous-échantillonnage aléatoire des ASVs à une profondeur de séquençage donnée (fonction rarefy_even_depth, rngseed = 999).

ii) Diversité α

Plusieurs indices de **diversité α**, représentant la diversité au sein d'un échantillon, ont été calculés sur la table d'ASVs raréfiée. La richesse spécifique (package phyloseq) correspond au nombre d'espèces contenues dans l'échantillon. L'indice de Shannon (package phyloseq) est un indice de diversité qui prend en compte la richesse spécifique (i.e., le nombre d'espèce) et l'abondance relative des espèces (i.e., leur équitabilité). Ainsi, à nombre d'espèces égal, une communauté dominée par quelques espèces majoritaires aura un indice de Shannon plus faible qu'une communauté dont les espèces sont équitablement dominantes. L'indice de Shannon est sensible aux variations d'abondance des espèces les plus rares. L'indice de diversité phylogénétique de Faith (Faith PD, calculé avec le package PhyloMeasures, v2.1) prend en compte, comme son nom l'indique, la diversité

phylogénétique des espèces. Cet indice est défini comme la somme de la longueur des branches de l'arbre phylogénétique connectant toutes les espèces d'un assemblage (Faith, 1992). Ainsi, l'indice de Faith sera plus élevé dans le cas d'une communauté comprenant des espèces phylogénétiquement éloignées entre elles. La significativité des différences de diversité α entre plusieurs groupes d'échantillons a été testée avec le test non-paramétrique de Wilcoxon (stat_compare_means, package ggpubr, v0.4.0).

iii) Diversité β

La **diversité β**, calculée sur la table d'ASVs en abondance relative (TSS, **chapitre III**) ou raréfiée (**chapitre VI**), permet de comparer la diversité entre plusieurs échantillons. Elle représente le taux de remplacement des espèces dans un gradient environnemental. Deux indices de diversité β ont été utilisés : l'indice de dissimilarité de Bray-Curtis (diversité taxonomique) et la distance β moyenne au taxon le plus proche (« *β mean nearest taxon distance* » ou βMNTD, diversité phylogénétique). La dissimilarité de Bray-Curtis (calculée avec le package phyloseq) représente la dissemblance entre deux échantillons et varie entre 0 (pas de dissimilarité) et 1 (dissimilarité totale, aucune espèce en commun). Elle prend en compte l'abondance relative des espèces et donne ainsi plus de poids aux espèces abondantes. La βMNTD (calculée avec le package microeco) prend en compte la distance phylogénétique moyenne entre les ASVs présentes dans un échantillon X et les ASVs les plus proches phylogénétiquement dans l'échantillon Y. Nous avons utilisé la βMNTD pondérée par l'abondance relative, qui donne ainsi plus de poids aux espèces abondantes. Les matrices de dissimilarité résultantes ont été visualisées par une **analyse en coordonnées principales** (PCoA, package ape v5.5), en appliquant la correction de Cailliez lors de l'obtention de valeurs propres négatives (**chapitre III**).

L'**analyse permutationnelle multivariée de la variance** (PERMANOVA) et l'**analyse de similarité** (ANOSIM) ont permis de tester de manière non-paramétrique si des groupes d'échantillons étaient significativement différents (e.g., communautés à des saisons différentes, **chapitre III** ; communautés traitées avec des AHLs différentes, **chapitre VI**). La PERMANOVA (fonction adonis2, package vegan) compare la variance intra-groupe à la variance intergroupe et permet de tester l'hypothèse que le centroïde (point au centre du groupe dans l'espace multivarié) et la dispersion sont équivalents pour l'ensemble des groupes testés. Ce test est complété par une analyse betadisper (package vegan), qui teste uniquement l'homogénéité de dispersion des groupes. L'ANOSIM (fonction anosim, package vegan) compare la moyenne des dissimilarités au sein d'un groupe à la moyenne des dissimiliarités au sein d'un autre groupe. L'ANOSIM permet d'obtenir une valeur appelée R. Proche de 0, cette valeur indique une faible dissimilarité intergroupe tandis qu'une valeur proche de 1 indique une forte dissimilarité.

VI.A.2) *Spécificités du traitement des données de l'estuaire de l'Aulne*

i) Analyse discriminante linéaire couplée à la taille d'effet

Une analyse discriminante linéaire couplée à la taille d'effet (« *linear discriminant analysis effect size* », LefSe) a été réalisée pour déterminer les ordres bactériens les plus à mêmes d'expliquer les différences entre divers groupes (e.g., communautés à des saisons différentes). Les LefSe ont été implémentées avec le package microbiomeMarker (v1.1.1) sur les tables d'abondances raréfiées.

ii) Processus d'assemblage

La **prédominance de processus d'assemblage stochastiques et déterministes** a été évaluée dans le cadre de travail développé par Stegen *et al.* (2012, 2015) basé sur de la modélisation phylogénétique. Pour cela, la βMNTD pondérée par l'abondance a été calculée pour tous les échantillons. La distribution nulle de βMNTD a été déterminée en échangeant aléatoirement les noms et abondance des ASVs au bout des branches de l'arbre phylogénétique correspondant (999 permutations, package microeco). Cela a permis la détermination du βNTI ("*β-nearest taxon index*", package microeco), qui représente le nombre de déviation standard dont la βMNTD s'écarte de la moyenne de la distribution nulle. Ainsi, un βNTI > 2 ou < -2 indique que l'assemblage des communautés est gouverné par des processus déterministes (respectivement, la sélection variable et la sélection homogène). Un βNTI compris entre -2 et 2 indique une prédominance des processus stochastiques. Dans ce cas, le score Raup-Crick basé sur Bray-Curtis (RC_{Bray}) a été estimé (999 permutations, package microeco). Un $RC_{Bray} < -0.95$ indique une prédominance des processus de dispersion homogène, un $RC_{Bray} > 0.95$ suggère des processus de limite de dispersion et un RC_{Bray} entre -0.95 et 0.95 peut être interprété comme de la dérive ou des processus indéterminés (Stegen *et al.*, 2015).

iii) Cohésion des communautés

La **cohésion** est une mesure du degré de connectivité des communautés. Elle est décomposée en deux métriques : la cohésion positive et la cohésion négative, calculées d'après Herren et McMahon (2017) (**Figure II.5**). Pour cela, les corrélations deux à deux ont été calculées pour chaque espèce (coefficient de Pearson) et corrigées par une valeur obtenue par randomisation (Herren et McMahon, 2017). Les moyennes des corrélations corrigées positives et négatives ont été respectivement calculées pour chaque ASV, donnant la « *connectedness* » positive et négative. Enfin, les cohésions positives et négatives ont été calculées pour chaque échantillon en sommant les valeurs de *connectedness* positives et négatives, pondérées par l'abondance relative de chaque ASV. Ainsi, la valeur absolue de la cohésion augmente quand l'abondance d'espèces très connectées augmente. D'après les conseils des auteurs (https://github.com/cherren8/Cohesion), les ASVs de faibles prévalences (représentant moins de 150 séquences sur l'ensemble des échantillons) ont d'abord été retirées, puis la table d'ASVs

a été transformée en abondance relative (TSS). Ce filtre retire la plupart des ASVs (12.3 % d'ASVs restantes, soit 1959 ASVs), mais conserve la plupart des séquences (92.1 % de séquences restantes). La cohésion a ensuite été calculée selon le script proposé par Herren et McMahon (2017) (https://github.com/cherren8/Cohesion), avec les paramètres suivants : persistence cutoff = 0.1 ; number of iteration = 200 ; shuffle algorithm = taxa shuffle.

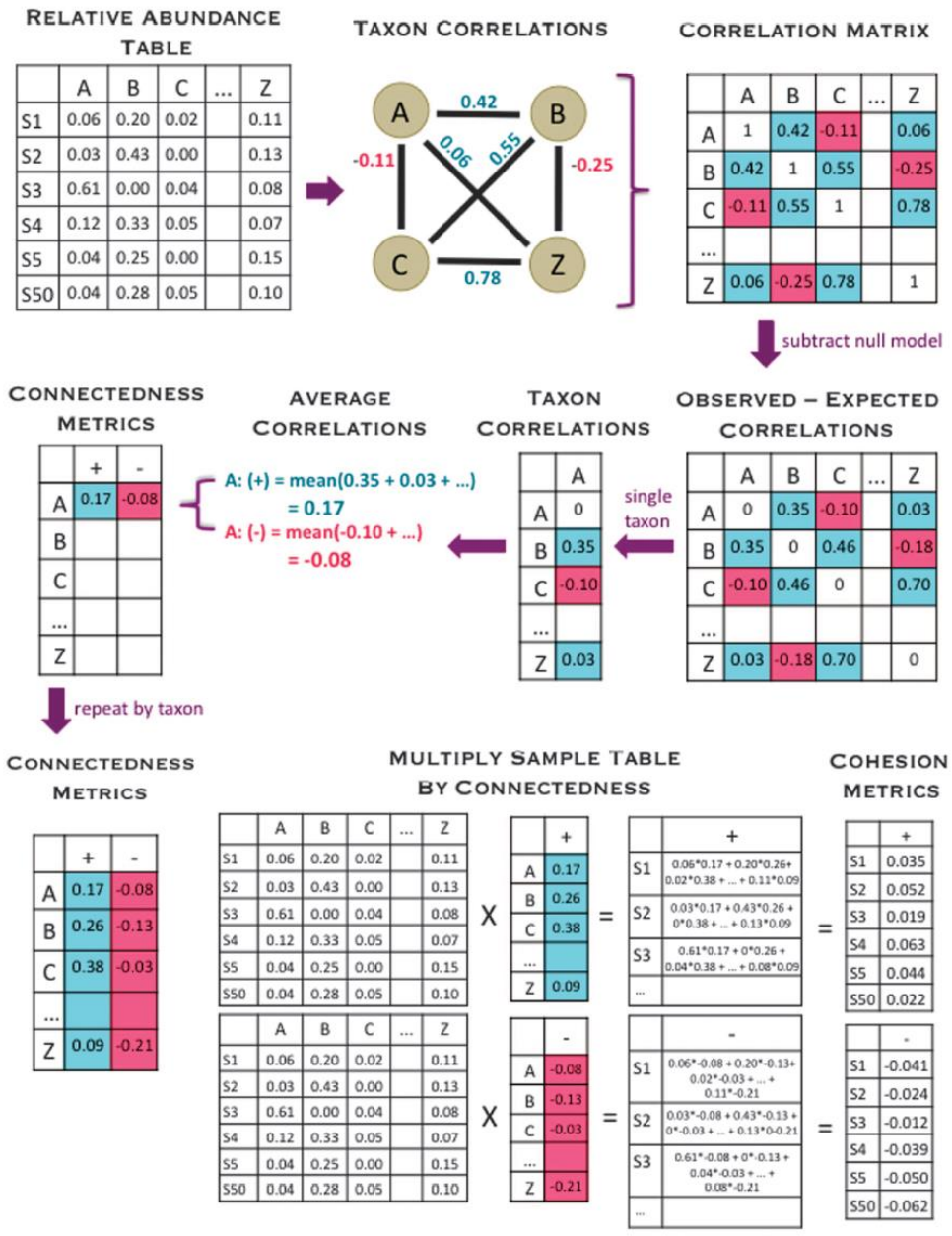

Figure II.5. Etapes de détermination de la métrique de cohésion. La table d'abondance relative (ligne : échantillon, colonne : espèce) est utilisée pour calculer toutes les corrélations deux à deux entre les espèces. Les corrélations résultant de randomisation sont retirées afin de corriger les biais liés à la structure des données. Pour chaque espèce, les corrélations positives (« *positive connectedness* ») et négatives (« *negative connectedness* ») sont sommées. Enfin, la cohésion positive est calculée comme la somme de la « *positive connectedness* » de chaque espèce contenue dans l'échantillon, pondérée par l'abondance de l'espèce en question. La cohésion négative est calculée de la même manière en utilisant la *connectedness* négative. Extrait de Herren et McMahon (2017).

iv) Lien entre paramètres environnementaux et composition des communautés (dbRDA)

Le lien entre la composition des communautés bactériennes, la cohésion et les paramètres environnementaux a été étudié par analyse de redondance basée sur la distance de Bray Curtis (dbRDA, package vegan) avec la correction de Cailliez pour les valeurs propres négatives. La valeur absolue de la cohésion négative a été utilisée afin que le nombre de corrélations négatives augmente avec la valeur de la cohésion négative, de manière plus intuitive. Toutes les variables prédictives ont été centrées-réduites. La présence éventuelle de variable multicolinéaire a été vérifiée avec le facteur d'inflation de la variance (VIF, package usdm v1.1.18). En conséquence, certaines variables multicolinéaires n'ont pas été utilisées dans l'analyse (azote inorganique dissous, silicate, %POP) afin d'obtenir des VIF finaux < 10. Les R^2 des dbRDAs et la variance expliquée par chaque axe ont été ajustés. La significativité des dbRDAs et de leurs axes ont été testés par un test non-paramétrique (anova.cca dans vegan, 999 permutations). La variance expliquée par différents groupes a été décomposée grâce à une analyse de partition de variance (varpart, package vegan, avec correction de Cailliez). Les groupes utilisés étaient : la salinité, la température, la matière organique et les nutriments (MES, %MOP, Chla, DOP, phosphate) et la cohésion (négative et positive).

v) Lien entre paramètres environnementaux et dissimilarité des communautés libres et attachées

Le lien entre la dissimilarité des communautés bactériennes libres et attachées (calculée avec les indices Bray-Curtis et βMNTD), la cohésion et les paramètres environnementaux a été étudié par analyse de redondance (RDA, fonction rda, package vegan). La méthode est la même que celle décrite pour la dbRDA (cf **VI.A.2.iv**). Les variables azote inorganique dissous, silicate, %POP et cohésion négative des communautés fixées aux particules ont été retirées en raison de problèmes de multicolinéarité.

vi) Inférence de métagénome

Les **métagénomes des communautés ont été inférés grâce à l'outil PICRUSt2** (« Phylogenetic Investigation of Communities by Reconstruction of Unobserved States », v2.4.1). Cet outil infère le contenu fonctionnel d'un d'échantillon pour lequel un seul gène marqueur a été séquencé (e.g., une région du gène de l'ARNr 16S). Pour cela, l'outil utilise les bases de données de génomes séquencés disponibles. Sa performance dépend donc de la qualité et de la quantité des données bancarisées. Lorsque le génome exact d'une ASV n'est pas disponible, PICRUSt2 utilise le génome de microorganismes apparentés. L'indice « *weighted nearest sequenced taxon index*" (NSTI) permet d'évaluer la mesure dans laquelle une ASV présente dans un échantillon est proche du génome de référence auquel elle est affiliée. Des NSTI < 0.06 indique la disponibilité de génome fortement affiliés aux ASVs environnementales, tandis qu'un NSTI > 0.15 indique que peu de génomes fortement affiliés

sont disponibles et donc, que les prédictions sont de faible qualité (https://picrust.github.io/picrust/tutorials/quality_control.html).

L'analyse PICRUSt2 a été réalisée avec le script « picrust2_pipeline.py » (paramètres par défaut) sur la table d'ASVs filtrée (sans séquence d'eucaryotes, d'archées, de mitochondries et de chloroplastes). Les numéros de « l'*Enzyme Commission* » (EC) prédits ont été alignés contre les voies métaboliques MetaCyc. La table de voies métaboliques ainsi définies a été raréfiée à la profondeur minimum (fonction rrarefy du package vegan) et visualisée à l'aide d'une PCoA basée sur la dissimilarité de Bray-Curtis. La significativité des différences entre les communautés libres et attachées a été déterminée avec les analyses PERMANOVA et betadisper, comme décrit précédemment. Les voies métaboliques caractérisant les communautés libres et attachées ont été déterminées grâce à une LefSe, comme décrit précédemment.

VI.A.3) *Spécificités du traitement des données de l'étude en microcosme*

i) Abondance différentielle

La package DESeq2 (v1.28.1) a été utilisé afin d'étudier les **ASVs dont l'abondance varie différentiellement et significativement entre les microcosmes contrôles** (contenant du DMSO) **et ceux traités avec les différentes AHLs** (C4-, C6-, 3-oxo-C8-, C12- et C16-HSL). Pour réaliser cette analyse, les ASVs rares (5 séquences ou moins sur une expérience) ont été retirées de la table d'ASVs brute. Les ASVs détectées ont été considérées comme différentiellement abondante lorsque la p-value (ajustée par la méthode de Benjamini-Hochberg) était inférieure à 0.05 et la valeur absolue du log2 du changement d'abondance était supérieure à 0.5 ($|log2FC| > 0.5$).

ii) Corrélation entre composition des communautés et activités enzymatiques (Procrustes)

L'**association entre les activités enzymatiques spécifiques et la composition des communautés** à la fin des microcosmes a été étudiée par une analyse de Procrustes symétrique. Cette analyse permet de comparer les formes de nuages de point générées par deux ordinations (e.g., ACP, PCoA) en essayant de les superposer. Pour réaliser cette analyse, une ACP (fonction rda du package vegan) a été réalisée sur la table d'ASVs raréfiées et transformée avec la méthode d'Hellinger (fonction decostand). Une ACP a également été réalisée sur les données d'activités spécifiques (à 48 h d'incubation), réduites à une variance de 1. L'analyse de Procruste a été réalisée sur les deux ordinations résultantes avec la fonction procrustes (package vegan) et sa significativité a été quantifiée avec la fonction protest (package vegan, 999 permutations)

VI.B. Etude des activités bactériennes dans l'estuaire de l'Aulne

VI.B.1) *Visualisation des données*

Toutes les données (bactériennes et physicochimiques) ont été visualisées en les représentant le long du gradient de salinité. De plus, leurs corrélations ont été évaluées par des analyses en composantes principales (ACP) et par le calcul de leur coefficient de corrélation de Spearman. Pour cela, toutes les variables ont été log2 + 1 transformées, centrées et réduites. Les **ACPs** ont été réalisées avec le package FactoMineR (v2.4) où la salinité et la température ont été utilisées comme variables supplémentaires afin de faciliter l'interprétation. Cela signifie que ces variables sont projetées sur l'ordination sans participer à sa construction. Les **coefficients de Spearman** (fonction cor, package stat, v4.1.0) et les p-values associées (cor.mtest, package corrplot, v0.9.0) ont été visualisées avec le package corrplot et une classification par clustering Ward D2.

VI.B.2) *Liens entre activités bactériennes et facteurs environnementaux*

i) Phosphatase alcalines dans la fraction dissoute (< 0.2 µm)

Le lien entre l'activité PA dissoute et les paramètres physicochimiques a été étudié à l'aide d'une régression linéaire multiple. Pour cela, toutes les variables ont été log2 + 1 transformées et centrées-réduites. Les problèmes éventuels de multicolinéarité ont été étudiés avec le VIF et les variables avec un VIF > 10 ont été retirées. La régression a été réalisée avec la fonction lm (package stats).

ii) Activités des bactéries libres (0.2-3 µm ou < 3 µm)

La corrélation entre les activités bactériennes (production bactérienne et activités enzymatiques), l'abondance bactérienne et les variables physicochimiques (nutriments et MOD) a été évaluée par un **test de Mantel** (package vegan, 999 permutations, Spearman). Un test de Mantel partiel a aussi permis d'évaluer ces corrélations en contrôlant l'effet de la température et de la salinité. Pour cela, les distances euclidiennes (fonction dist, package stats) ont été calculées pour les différents jeux de donnée, contenant toutes les variables listées dans les **Tableaux II.2** et **II.3**, log2 + 1 et centrées-réduites.

Le lien entre les activités bactériennes (production bactérienne et activités enzymatiques) et leurs variables explicatives (abondance bactérienne et paramètres physicochimiques) a ensuite été plus finement étudié à l'aide d'une **RDA**. Pour cela, toutes les variables ont été log2 + 1 transformées, centrées-réduites et les variables colinéaires retirées (VIF < 10). Les variables explicatives finales incluaient : la salinité, la température, le phosphate, l'ammonium, le nitrite, le POD, les PCHOD, le ratio PCHOD/MCHOD, les AALD, les AACD et le ratio AALD/AADC. La variance expliquée par la RDA et ses axes a été ajustée (R^2_{ajd}). La significativité de la RDA et de ses axes a été déterminée par permutations

(1000 permutations, anova.cca fonction dans vegan). L'effet de différent groupes sur la variance expliquée a été déterminé avec une **analyse de partition variance** (varpart, vegan). Les groupes étaient constitués comme ceci : la salinité, la température, les nutriments et la MOD (phosphate, ammonium, nitrite, POD, PCHOD, PCHOD/MCHOD, AALD, AACD et AALD/AADC) et l'abondance bactérienne (AB < 3 µm).

Enfin, les relations complexes entre ces différentes variables ont été modélisées avec une **modélisation structurelle des moindres carrés partiels** (« *partial least squares path modeling* », PLS-PM) afin de démêler leurs liens directs et indirects. La PSL-PM est une approche permettant d'unir des variables dépendantes et indépendantes dans un réseau de relations causales linéaires. Elle repose sur l'utilisation de variables observées (i.e., directement mesurée, comme la salinité) et de variables latentes, formées à partir de plusieurs variables observées pour représenter un construit plus large. Cette approche permet de déterminer les coefficients de régression standardisés, quantifiant l'impact d'une variable sur une autre (effet direct). La PSL-PM a été réalisée avec le package pslpm (v.0.4.9). Toutes les variables sauf la salinité et la température ont été log2 + 1 transformée, toutes les variables ont été centrées-réduites. Parfois, la valeur négative de certaines variables a été utilisée pour mieux représenter la variable latente modélisée et satisfaire les conditions d'unidimensionnalité des variables latentes (Sanchez, 2013). Par exemple, la valeur négative des ratios I/S et COP/NOP, qui représentent la dégradation de la MOP et son caractère réfractaire, a été utilisée pour représenter la qualité de la MOP. Toutes les variables listées dans le **Tableau II.2** ont été initialement inclues, puis celles avec des coefficients inférieurs à 0.2 ont été retirées. La significativité des coefficients de régression et les R^2 des variables ont été testés par boostrap (1000 boostraps). La capacité de prédiction du modèle a été déterminée avec l'indice GOF (« *goodness-of-fit* »). Les résultats ont été tracés avec le package DiagrammeR (v1.0.6.1).

iii) Activités des bactéries attachées (> 3 µm)

Les activités résultant des communautés fixées aux particules ont été étudiées de la même manière que pour les bactéries libres. Les variables explicatives finales inclues dans la RDA étaient : la salinité, la température, les MES, le %MOP, le %Chl*a*, le COP/NOP, les AAP/MES, les CHOP/AAP et le I/S. Les groupes inclus dans l'analyse de partition de variance étaient : la salinité, la température, la matière organique (MES, %MOP, %Chl*a*, COP/NOP, AAP/MES, CHOP/AAP et I/S) et l'abondance bactérienne (AB > 3 µm).

VI.B.3) *Liens entre activités bactériennes, composition bactérienne et facteurs environnementaux*

Des approches similaires ont été mises en place pour évaluer les liens entre les activités bactériennes, la composition des communautés et les variables physicochimiques pour les communautés libres et attachées aux particules. Les tests de Mantel ont été réalisés comme

précédemment, en utilisant la dissimilarité de Bray-Curtis sur la table d'ASVs raréfiée. Ensuite, les ASVs ont été regroupées au niveau de la classe, en ne retenant que les plus abondantes (représentant au moins 0.001% de l'abondance totale). L'abondance des classes majoritaires a été transformée avec la méthode d'Hellinger, centrée-réduite et utilisée dans les analyses suivantes (ACP et PLS-PM). Nous n'avons pas effectué de RDA en raison de la forte multicolinéarité des prédicteurs (variables physicochimiques et composition des communautés). A la place, des ACPs ont été réalisées pour visualiser la corrélation entre les différentes variables. Les activités bactériennes (production, PA, GLU et LAM) ont été utilisées comme variables actives, tandis que l'abondance, les variables physicochimiques et les variables de composition des communautés ont été utilisées comme variables supplémentaires. A ce titre, elles sont projetées sur l'ordination mais ne participent pas à sa construction. L'analyse PLS-PM a été réalisée comme décrit précédemment, en ajoutant une variable latente représentant la composition des communautés.

Chapitre III. *Evolutions spatiotemporelles des communautés bactériennes de l'estuaire de l'Aulne*

I. Introduction

Une des préoccupations majeures de la microbiologie marine est de comprendre comment les communautés bactériennes se structurent dans le temps et dans l'espace, en particulier en différenciant les communautés libres et attachées. L'estuaire de l'Aulne offre une zone d'étude intéressante pour se pencher sur ces problématiques grâce à ses forts gradients physicochimiques et la présence d'un bouchon vaseux riche en particules. Les communautés bactériennes de cet estuaire n'ont jusqu'à présent jamais été caractérisées alors que l'Aulne constitue la source d'eau douce principale pour la rade de Brest. La composition des communautés bactériennes planctoniques et fixées sur les particules a été étudiée le long de cet estuaire, avec comme objectifs de :

- Caractériser les variations spatiales et temporelles de la composition des communautés bactériennes libres et attachées aux particules ;
- Déterminer les processus d'assemblage (i.e., déterministes ou stochastiques) impactant chaque fraction le long du gradient de salinité de l'estuaire ;
- Déterminer quels facteurs biotiques et abiotiques corrèlent avec les changements de composition des communautés libres et attachées, ainsi qu'avec la dissimilarité entre les deux types de communautés ;
- Déterminer si des différences de composition taxonomique se traduisent par des différences fonctionnelles.

Pour répondre à ces problématiques, cinq séries de prélèvements ont été réalisées le long du gradient de salinité de l'estuaire de l'Aulne, à des périodes contrastées du cycle saisonnier (Février 2019, Avril 2019, Juillet 2019, Novembre 2019 et Juillet 2020). La composition des communautés bactériennes libres et fixées aux particules a été étudiée par une approche de metabarcoding du gène de l'ARNr 16S. Cette étude a montré que les communautés bactériennes de l'estuaire de l'Aulne sont très largement structurées par des processus déterministes et qu'elles suivent des variations temporelles et spatiales marquées. Les communautés sont ainsi fortement impactées par la salinité (correspondant au mélange des masses d'eaux) et par des facteurs temporels (e.g., température, chlorophylle *a*). La cohésion, une variable biotique représentant le degré de cooccurrence des communautés (proportion de taxons à fort potentiel d'interaction), explique également une part importante de la variation de communautés. De manière intéressante, la dissimilarité entre les communautés libres et attachées varie dans l'espace et le temps : elle est plus importante dans les eaux douces et marines et diminue en été. Elle semble impactée par la qualité de la matière organique, la cohésion de communautés et des facteurs saisonniers.

Ce chapitre est présenté sous forme d'une publication pour une future soumission envisagée à *Scientific Reports*.

II. Article 1 : Free-living and particle-attached bacterial community composition, assembly processes and determinants across spatiotemporal scales in a macrotidal temperate estuary

Marion Urvoy[1,2,*], Michèle Gourmelon[1], Joëlle Serghine[1], Stéphane L'Helguen[2], Claire Labry[1,*]

[1]Ifremer, DYNECO, F-29280 Plouzané, France

[2]Université de Bretagne Occidentale, CNRS, IRD, Ifremer, UMR 6539, Laboratoire des Sciences de l'Environnement Marin (LEMAR), F-29280 Plouzané, France

[*]Correspondence: marion.urvoy@outlook.fr, claire.labry@ifremer.fr

Running title:

Bacterial community composition in the Aulne estuary

Keywords:

Bacteria, free-living, particle-attached, bacterial community composition, bacterial community composition, assembly processes, Aulne estuary, Bay of Brest

Abstract

Bacteria transform and remineralize organic matter, playing an important role in the ocean biogeochemistry. Particles are notable hotspots of bacterial activity, hosting particle-attached (PA) communities that can largely differ from their free-living (FL) counterparts in diversity, composition and functions. However, long-standing questions remain concerning bacterial community assembly processes (deterministic vs. stochastic) and driving factors (biotic and abiotic) across spatiotemporal scales, especially concerning the FL and PA communities' dissimilarity. Land-sea transition zones such as estuaries are interesting ecosystems to investigate these questions since they possess high loads of particles and foster highly active communities. This study investigated the FL and PA community diversity, composition and determinants in the Aulne estuary (Bay of Brest, France) using 16S metabarcoding. Our results revealed that the FL and PA community composition greatly varied with salinity and seasons, which explained a larger part of the variance than the sampling fraction. Both FL and PA communities were largely driven by deterministic assembly processes and impacted by similar factors. The FL-PA dissimilarity varied across space and time: it decreased in the inner estuarine stations compared to the end members and in summer compared to other seasons. Interestingly, cohesion, a measure of the communities' interconnectedness, explained a significant proportion of the FL and PA communities' β-diversity and dissimilarity, suggesting the importance of co-occurrence patterns in their structuration. Finally, inferred metagenomics suggested that FL and PA communities possessed different metabolic pathways. Altogether, our results shed light on the factors influencing the bacterial communities within the Aulne estuary and are a first step toward understanding their biogeochemical impacts.

Introduction

Bacterial communities are of critical importance in the oceans. Through their transformation of dissolved (DOM) and particulate organic matter (POM), they carry out functions that profoundly impact global biogeochemical cycles (Azam and Malfatti, 2007). Consequently, one of the long-standing questions in microbial biogeography is to understand how bacterial communities are shaped across spatiotemporal scales (Martiny *et al.*, 2006; Hanson *et al.*, 2012). Bacterial communities are usually operationally separated into free-living (FL) or particle-attached (PA) bacteria via size fractionation, although there are dynamic exchanges between the two communities (Grossart, 2010). Particles are considered hotspots of bacterial activities (Smith *et al.*, 1992; Simon *et al.*, 2002). Indeed, PA communities are usually more active (Smith *et al.*, 1992; Grossart *et al.*, 2007; Rieck *et al.*, 2015) and with different metabolic capacities (Lyons and Dobbs, 2012; Simon *et al.*, 2014) than FL bacteria. These differences in functional capacities can be paralleled by differences in bacterial community composition (BCC): PA bacteria are often more diverse and taxonomically different from their FL counterparts (Bižic-Ionescu *et al.*, 2015; Rieck *et al.*, 2015; Mestre *et al.*, 2017). However, several studies have reported that PA communities were not significantly different from FL bacteria (Noble *et al.*, 1997; Hollibaugh *et al.*, 2000; Ortega-Retuerta *et al.*, 2013). Since few studies have addressed the seasonal variations of PA and FL communities, the factors driving their dissimilarities are not well characterized.

Bacterial community assembly is influenced by both deterministic and stochastic processes, governing their spatiotemporal patterns. Deterministic processes correspond to the ecological selection of species, driven by biotic (i.e., interactions among microorganisms) and abiotic factors (e.g., temperature). Deterministic processes include homogeneous and heterogeneous selection that respectively lead to more or less similar communities (Zhou and Ning, 2017). Stochastic processes are random events and include ecological drift, homogenizing dispersal and dispersal limitation (Hanson *et al.*, 2012; Zhou and Ning, 2017). PA and FL marine BCC and functions may be affected by stochastic and deterministic processes in different proportions, which has not been well characterized in marine ecosystems and land-sea transition zones, especially across spatiotemporal scales (Yao *et al.*, 2019; Jain *et al.*, 2021; Wang *et al.*, 2021).

Several studies have matched patterns in BCC to abiotic factors such as temperature, salinity, organic matter quantity and composition or nutrient concentrations (e.g., Fortunato *et al.*, 2012; Ortega-Retuerta *et al.*, 2013; Balmonte *et al.*, 2019; Jain *et al.*, 2021). In addition, the quality and quantity of particles and nutrient concentrations have been suggested to drive FL-PA community dissimilarities (Noble *et al.*, 1997; Hollibaugh *et al.*, 2000; Hu *et al.*, 2020; Yawata *et al.*, 2020). However, fewer have investigated the impact of biotic interactions among bacterial communities despite their increasingly recognized importance (Lima-Mendez *et al.*, 2015; Milici *et al.*, 2016; Herren

and McMahon, 2017). Due to their inner complexity, these interactions must be statistically inferred by correlating species' relative abundances (Herren and McMahon, 2017). To this extent, different tools have been developed, such as co-occurrence networks or, more recently, the cohesion metrics (Herren and McMahon, 2017).

Estuaries are interesting study zones to examine BCC structuration and FL-PA dissimilarities. These highly dynamic ecosystems exhibit strong gradients that shape biological processes, and their high particle loads favor the establishment of highly productive PA bacterial communities (Labry *et al.*, 2016; Crump *et al.*, 2017). Consequently, estuaries are vital components of the land-sea continuum, modulating the quality and quantity of organic matter exported to coastal areas (Bianchi, 2011). In particular, the Aulne estuary (Brittany, France) hosts high bacterial production and hydrolytic activity levels resulting from particle-attached bacterial communities (Labry *et al.*, 2016). However, the bacterial communities in this estuary have never been characterized. Understanding BCC dynamics and its determinants along the Aulne estuary salinity gradient could help identify the microbial transformation of organic matter in this area.

The objectives of this study were to determine: (i) the spatiotemporal variation of the FL and PA BCC in the Aulne estuary; (ii) the assembly processes (stochastic vs. deterministic) driving the structuration of FL and PA communities along the salinity gradient; (iii) the factors (biotic and abiotic) driving the FL and PA BCC as well as the FL-PA dissimilarity; and (iv) the FL and PA communities' inferred functional capacities. To answer these questions, we examine the FL and PA BCC in the Aulne estuary using 16S rRNA gene metabarcoding sequencing from fresh- to marine waters, covering contrasting seasons. Our initial hypotheses were that: i) the BCC would be largely driven by the salinity; ii) the FL-PA dissimilarity would be controlled by POM quality.

Materials and methods

1. Study site

Located in the North-West of France, the Aulne river is 130 km long, drains an area of approximately 1800 km^2 and supplies 63% of the freshwater inputs to the semi-enclosed Bay of Brest (Auffret, 1983). The Aulne estuary is a temperate macrotidal estuary, approximately 30 km long from the Guily-Glaz dam (that limits the tidal influence upstream) to the river mouth. Its catchment is characterized by the presence of agricultural areas and meadows. The river flow regime range from 1 to over 250 $m^3\ s^{-1}$ (mean of 28 $m^3\ s^{-1}$) and is constrained by a temperate oceanic climate, which generates markedly higher precipitations in winter (Roger Delmas and Tréguer, 1983). As a result, 60% of the annual flow occurs between December and March. The important semi-diurnal tidal amplitude (between 1.2 m and 7.5 m) results in intense water depth variations in the estuary, affecting particulate matter

resuspension and deposition. The residence time of water is dependent on river flow and tidal range and varies between 3 and 30 days (Bassoullet, 1979).

2. Sampling strategy

The samplings were carried out at spring tide in February 20 (R02), April 18 (R04), July 18 (R09) and November 14 (R12), 2019 as well as July 20, 2020 (R14) (**Table 1**). Surface waters were collected at nine stations spread over the salinity gradient (**Figure 1**). Station 1 (S1) was a freshwater reference upstream of the dam and was not subjected to the tidal influence. Station 2 (S2) corresponded to a freshwater station (salinity 0) under tidal influence and was collected at a fixed location in front of the dam. Stations 3 to 8 (S3-S8) were sampled every 5 of salinity (5 to 30), monitored using a WTW thermosalinometer. Their location consequently varied depending on tides and river discharges. Finally, station 9 (S9) was a marine reference sampled at the SOMLIT (Service d'Observation en Milieu Littoral, https://www.somlit.fr/) station of Saint Anne-du-Portzic (48°21'32.17'' N, 4°33'07.21'' O, salinity ranged from 33.3 to 34.7). Sampling was carried out from high tide to mid-tide. The marine station was first sampled and processed immediately to limit the tidal influence and avoid long trip duration. Sampling was then carried out from the Aulne river (S1) to the downstream estuary (S8). All stations were sampled within four hours and immediately processed in the lab.

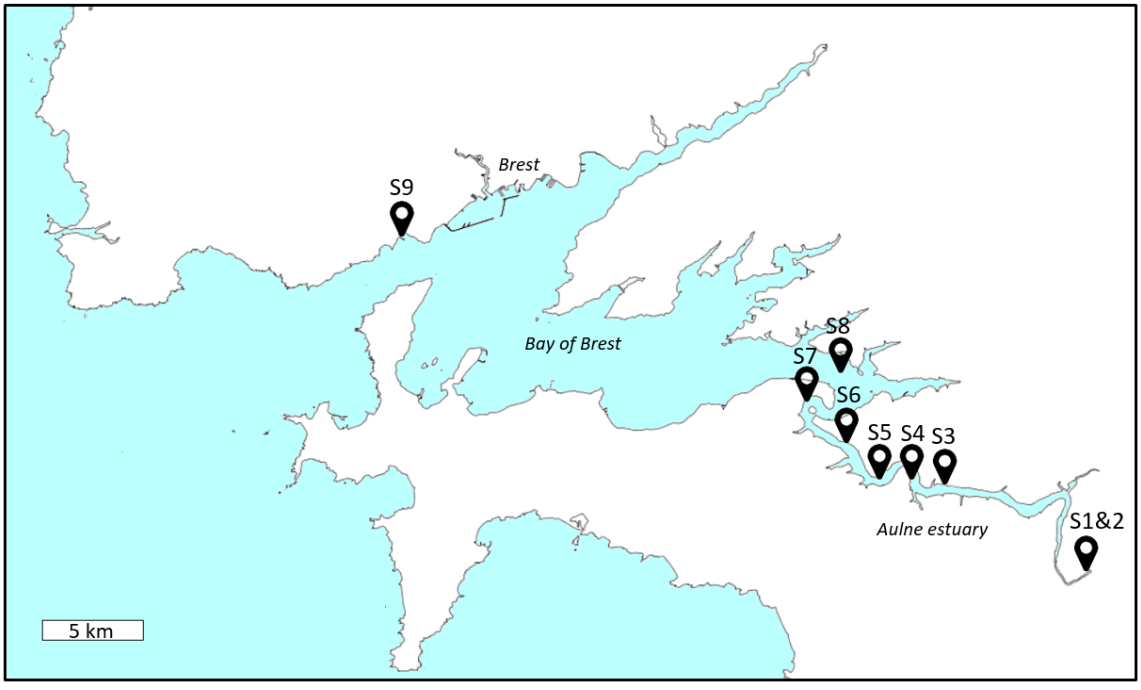

Figure 1. Map of the Bay of Brest and the Aulne estuary. Freshwater (S1, S2) and marine water (S9) stations were collected at fixed locations while the other stations were variable depending on the salinity. The locations of the April sampling (R04) stations are indicated as an example.

Table 1. Sampling dates and their associated tidal coefficient, river flow and mean water temperature. n: number of sampled stations. Flow data were retrieved from http://www.hydro.eaufrance.fr/ at the Châteaulin station (J3821820).

Name	Sampling Date	Season	Tidal coefficient	Flow ($m^3 s^{-1}$)	Mean Temperature (°C)	n	Comments
R02	February 20, 2019	Winter	110	44.6	7.8	9	
R04	April 18, 2019	Spring	97	18.1	12.4	6	S1 was not sampled due to navigation constraints, S3 and S7 extraction failed
R09	July 18, 2019	Summer	78	2.2	22.7	7	S2 and S7 extraction failed
R12	November 14, 2019	Autumn	87	90.0	10.4	8	S1 was not sampled due to technical constraints
R14	July 20, 2020	Summer	74	1.5	20.2	7	S1 and S2 were not sampled due to navigation constraints

3. Physicochemical variables

Temperature and salinity were measured *in situ* using a WTW thermosalinometer. Ammonium, nitrite, nitrate, phosphate, silicate, dissolved organic phosphorus (DOP), suspended particulate matters (SPM), total particulate phosphorus (TPP), particulate inorganic phosphorus (PIP), chlorophyll *a* (Chl*a*) and pheopigments (Pheo) were measured as described in the supplementary methods. Particulate organic phosphorus (POP) was determined as the difference between TPP and PIP and expressed in percentage of TPP (%POP). Dissolved inorganic nitrogen (DIN) was calculated as the sum of ammonium, nitrite and nitrate. Percentage of Chl*a* (%Chl*a*) was determined as Chl*a* over Chl*a* and Pheo.

4. DNA sequencing and bioinformatics

The BCC was determined using metabarcoding of the V3-V4 region of the 16S rRNA gene. To recover PA communities, 200 mL of water were filtered through 3-µm filters (Whatman Nuclepore PC membrane) for each station. Several filters were used per station depending on the turbidity to avoid filter clogging, which would retain smaller bacteria. The 3-µm filtrates were filtrated through 0.2-µm filters (Whatman Nuclepore PC membrane) to recover FL communities. Filters were flash-frozen in liquid nitrogen and stored at - 80°C until processing. Blank dry filters were sampled simultaneously and used as contamination controls. DNA was extracted using the NucleoSpin Plant II Kit (Macherey-Nagel Ref. 740770.50) as advised by the supplier with an additional lysis step performed for 2 h at 56°C with 25 mL of proteinase K (20 mg mL^{-1}, Macherey Nagel Ref. 740506) and 100 mL of lysozyme (20 mg mL^{-1}, Sigma ref 4403-5g). If several filters were used for one station, the extracted DNA was pooled. The libraries were prepared using the 341F (5'-CCTACGGGNGGCWGCAG-3') and 785R (5'-GACTACHVGGGTATCTAATCC-3') primers (Klindworth *et al.*, 2013) at the GénomeQuebec platform that performed the sequencing. Libraries were sequenced using an Illumina MiSeq with 2x300 pb and V3

chemistry, resulting in 13,387,145 reads over 73 samples (37 PA community samples, 36 FL community samples).

Data were pre-processed using the SAMBA pipeline (v3.0.1) (https://github.com/ifremer-bioinformatics/samba) developed by the IFREMER bioinformatics team (SeBiMER), implementing QIIME2 (Bolyen, 2019, 2019.10.0). Briefly, reads were quality-trimmed and joined. Amplicon sequence variants (ASVs) were inferred and denoised using q2-dada2 (Callahan *et al.*, 2016). This resulted in 25,949 ASVs that were clustered using q2-dbOTU (Olesen *et al.*, 2017) yielding 16,906 ASVs (35% clustering). The final ASVs were assigned against the Silva v138 database (Quast *et al.*, 2013) formatted for the 341F/805R primers, and a phylogenetic tree was built using fasttree in q2-phylogeny.

5. Statistical analysis

All data were analysed in R (v4.1.0) implemented in Rstudio (v2021.09.0) and displayed using ggplot2 (v3.3.5) unless specified otherwise.

5.1. Environmental variables

The overall pattern of environmental variable evolution was visualized using a principal component analysis (PCA) on z-score standardized variables, as implemented in FactoMineR (v2.4). Environmental variable correlations were quantified using the Spearman rank coefficient (stats package, v4.1.10) on raw data and displayed using the corrplot package (v0.90).

5.2. Metabarcoding data analysis

Metabarcoding data were analysed using phyloseq (v1.36.0), vegan (v2.5-7), and microeco (v0.6.0) packages. First, ASVs corresponding to eukaryotes, archaea, mitochondria and chloroplasts were removed (22% of total reads, 21% being chloroplasts), leaving 15,911 remaining ASVs. The rarefaction curves were visualized using the ranacapa package (v0.1.0), revealing that all samples reached proper saturation with 49,765 reads per sample on average (range: 11,922-82,219 reads) (**Figure S1**). All subsequent analyses were performed as described below from this filtered read counts table.

Community composition

The community composition was visualized using barplots. To this extent, the filtered read counts table was transformed to relative abundance and the ASVs were pooled to the phylum or order taxonomic level. Linear discriminant analysis effect size (LefSe) was used to determine which orders most likely explained the differences between various groups (e.g., FL vs. PA, summer vs. other seasons). LefSe was implemented with the microbiomeMarker package (v1.1.1) on the rarefied table, using a linear discriminant analysis (LDA) score cut-off of 1.5 and a p-value cut-off of 0.05.

α-diversity

All α-diversity indices were computed on rarefied counts to correct for uneven sampling depth. Counts were rarefied using the *rarefy_even_depth* function (phyloseq, rarefaction depth = 26,700 reads per sample, rngseed = 999), resulting in the removal of two samples (PA communities in S9 of April 2019 and S9 of July 2020) (**Figure S1**). Specie richness and Shannon index were computed using the phyloseq package. The Faith's phylogenetic diversity (PD) was computed using the PhyloMeasures (v2.1) package. The α-diversity indices were regressed against the temperature (lm function, stats package) to assess seasonal trends. The mean α-diversity in different groups was compared using the Wilcoxon test (stat_compare_means, ggpubr function).

β-diversity

The β-diversity indices were computed on the filtered read count table transformed to relative abundances (total sum scaling) according to McKnight *et al.* (2019). Two β-diversity indices were calculated: i) The Bray-Curtis dissimilarity (computed using the phyloseq package), that takes into account the ASV abundance and range from 0 (no dissimilarity) and 1 (complete dissimilarity); ii) The abundance-weighted β-mean nearest taxon distance (βMNTD) (computed using the microeco package), that takes into account the mean pairwise phylogenetic distance between each ASV in one community and its closest relative in the second community, weighted by the ASV abundance. The β-diversity was visualized using Principal Coordinate Analysis (PCoA, as implemented in the ape package, v5.5), applying the Cailliez correction for negative eigenvalues (Legendre and Legendre, 2012). Permutational multivariate analysis of variance (PERMANOVA) was performed using the *adonis2* function (with the Cailliez correction) and variance homogeneity was checked for using the *betadisper* test (vegan package).

Community assembly processes

The community assembly processes were assessed in the framework developed by Stegen *et al.* (2012, 2015) and based on phylogenetic null modeling. Briefly, the abundance-weighted βMNTD was calculated for all pairwise-comparison of samples. The null βMNTD distribution was quantified by randomly shuffling the ASVs name and abundance across the tips of the phylogenetic tree (999 permutations, microeco package). This allowed the calculation of the β-nearest taxon index (βNTI, microeco package), which represents the number of standard deviations that βMNTD departs from the null distribution mean. A βNTI > 2 or < -2 indicates that the community assembly is governed by deterministic processes (respectively, variable and homogeneous selection). A βNTI comprised between -2 and 2 indicates the predominance of stochastic processes. For this range of βNTI, the Bray-Curtis-based Raup-Crick score (RC_{Bray}) was estimated (999 permutations, microeco package). An RC_{Bray} < -0.95 suggests the predominance of homogenizing dispersal, an RC_{Bray} > 0.95 suggests dispersal

limitation and an RC_{Bray} between -0.95 and 0.95 can be interpreted as drift or undominated mechanism (Stegen *et al.*, 2015).

Bacterial community cohesion

Cohesion, a measure of the degree of connectivity of a community, was calculated for all samples as proposed by Herren and McMahon (2017). Briefly, the pairwise Pearson correlation of all ASVs was computed and corrected by the "expected" correlation generated from null modeling. The average positive and negative corrected correlations were respectively calculated for each ASVs, giving rise to the connectedness metrics. The cohesion metrics (comprising positive and negative cohesion) was then computed for each sample by summing the abundance-weighted positive and negative connectedness metrics. Negative and positive cohesion thus range from −1 to 0 and 0 to 1, respectively. The absolute value of cohesion increases when the abundance of highly connected taxa increases, reflecting the degree of correlation or interconnectedness within a community (Herren and McMahon, 2017). The cohesion metrics was computed using the authors' script (https://github.com/cherren8/Cohesion) with the following parameters: persistence cutoff = 0.1; number of iteration = 200; shuffle algorithm = taxa shuffle. As per author guidelines, low prevalence ASVs (comprising less than 150 reads across all samples) were removed beforehand. This filter removed most ASVs (1,959 or 12.3% remaining ASVs) but retained most reads (92.1% remaining reads).

5.3. Factors driving FL and PA community composition

The effect of biotic (cohesion variables) and abiotic variables on the composition of FL and PA communities was assessed using distance-based redundancy analysis (dbRDA, dbrda function in the vegan package) on the Bray-Curtis dissimilarity (with the Cailliez correction). It should be noted that the absolute value of negative cohesion was used, so that the amount of negative correlations increases with the absolute value of negative cohesion. All predictors were z-score standardized and multicollinearity was checked using the variance inflation factor (VIF, usdm package). In consequence, DIN, silicate and %Chl*a* were removed (final VIF < 10) as they correlated with salinity (for DIN and silicate) or temperature and DOP (for %Chl*a*). The R^2 of the dbRDA was adjusted using RsquareAdj (vegan package) and the variance explained by each axis was proportionally corrected. The overall model and dbRDA axes significance were tested using an analysis of variance (ANOVA)-like permutation test (anova.cca in vegan package, 1000 permutations). The effects of different groups of variables included in the dbRDAs (i.e., salinity and temperature, organic matter and nutrients and cohesion) were investigated using variance partitioning (varpart function in vegan, with the Cailliez correction).

5.4. Factors driving the FL-PA pairwise dissimilarity

The effects of biotic (cohesion variables) and abiotic variables on the FL-PA pairwise dissimilarity were estimated using redundancy analysis (RDA, rda function in vegan) on Bray-Curtis dissimilarity and βMNTD. The methodology was the same as described for dbRDA. DIN, silicate, %Chl*a* and PA negative cohesion were removed due to multicolinearity with salinity (for DIN and silicate), temperature and DOP (for %Chl*a*) and PA positive cohesion (for PA negative cohesion).

5.5. Inferred functional profiles

The community metagenomes was inferred using the PICRUSt2 pipeline (v2.4.1) ("picrust2_pipeline.py" script with default parameters), generating Enzyme Commission (EC) numbers. To evaluate the quality of the predicted metagenome, we used the weighted nearest sequenced taxon index (NSTI) that summarizes the extent to which the ASVs in a sample are related to the available reference genomes. The mean NSTI on predicted EC numbers was 0.15 (range: 0.06-0.28), which is similar to other environmental studies (Langille *et al.*, 2013; Roth Rosenberg *et al.*, 2021) but suggested that the results should be analyzed with caution. The predicted EC were then collapsed into Metacyc pathways. The resulting table was rarefied to the minimum depth (rrarefy function in vegan) and visualized using a PCoA on Bray-Curtis dissimilarity. The significant separation between groups was assessed by PERMANOVA and Betadisper as described above. The Metacyc pathways most likely to explain differences between the FL and PA fraction were assessed using linear discriminant analysis effect size (LEfSe) as described above, with a LDA and p-value threshold of 3 and 0.01, respectively.

Results

1. Physicochemical characteristics

Physicochemical variable values are shown in **Table S1** and plotted in **Figure S2**. The temperature varied from 6.3 to 23.4°C throughout the samplings. In February and November, the river end (S1) was colder than the marine end (S9), while the opposite trend was observed for the other sampling dates. DIN and silicate followed the theoretical dilution curve along the salinity gradient (respective Spearman correlation of -0.93 and -0.97 with the salinity, **Figures S2, S3**) and both decreased during summer. In contrast, phosphate did not follow the theoretical dilution curve but increased in the S3-S8 compared to the end members. Overall, the phosphate concentration was higher in July 2019 compared to the other sampling dates (**Figure S2**). DOP did not follow a clear pattern along the salinity gradient and increased in summer (July 2019, 2020) compared to the other seasons. Concerning the particulate fraction, SPM increased in the 5-10 salinity range (S3-S4) which corresponds to the maximum turbidity zone (MTZ). SPM were especially important in February and April 2019, where they reached 197 and 112 mg L^{-1}, respectively. The MTZ and estuarine stations (S3-S8) were characterized by a lower %POM content and %POP, consistent with the presence of less labile POM. Chl*a* and %Chl*a*

increased in summer (**Figure 2, Figure S2**), concomitantly with the increase in temperature and decrease in turbidity that favored light penetration and phytoplankton growth. Consequently, the sampling dates were largely differentiated based on their season sampling, with the summer samplings (July 2019 and 2020) differing from the other seasons (February, April and November 2019) (**Figure 2**).

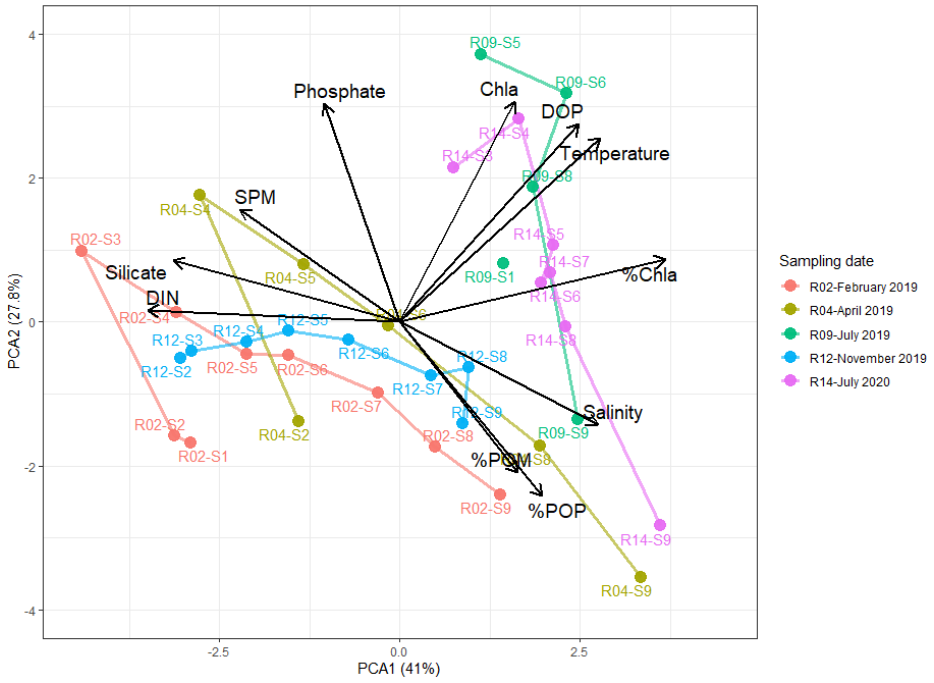

Figure 2. Principal component analysis (PCA) representing the physicochemical characteristics of all samples. Samples are labeled as "sampling date-sampling station". The lines link the different stations within one sampling time in their spatial order (S1 to S9). R02: February 2019; R04: April 2019; R09: July 2019; R12: November 2019; R14: July 2020.

2. Spatiotemporal variations of the FL and PA bacterial communities

2.1. Bacterial community composition

Overall, the bacterial communities were dominated by Proteobacteria (mean relative abundance and standard deviation of 50 ± 11% across all samples), Bacteroidia (22 ± 7%), Actinobacteriota (9 ± 8%), Planctomycetota (5 ± 5%) and Verrucomicrobia (4 ± 3%) (**Figure 3A**). The BCC presented a continuous shift along the salinity gradient (**Figure 3**). The most abundant groups enriched in the freshwater stations (S1-S2) were the Burkholderiales (23 ± 8%, Betaproteobacteria) and the Cytophagales (11 ± 11 %, Bacteroidota) (**Figure S4**). In contrast, the most abundant group enriched in the MTZ (S3-4) was the Frankiales (7 ± 7%, Actinobacteriota). In the downstream estuarine stations (S5-S8), the Rhodobacterales (24 ± 7%, Alphaproteobacteria), the Flavobacteriales (18 ± 5%, Bacteroidota) and the Puniceispirillales (5 ± 2%, Alphaproteobacteria) were enriched. Finally, the marine stations (S9) stations were enriched in various Gammaproteobacteria such as the Oceanospirillales (6 ± 8%), Cellvibrionales (6 ± 3%) and Alteromonadales (5 ± 5%) (**Figure 3B**).

A)

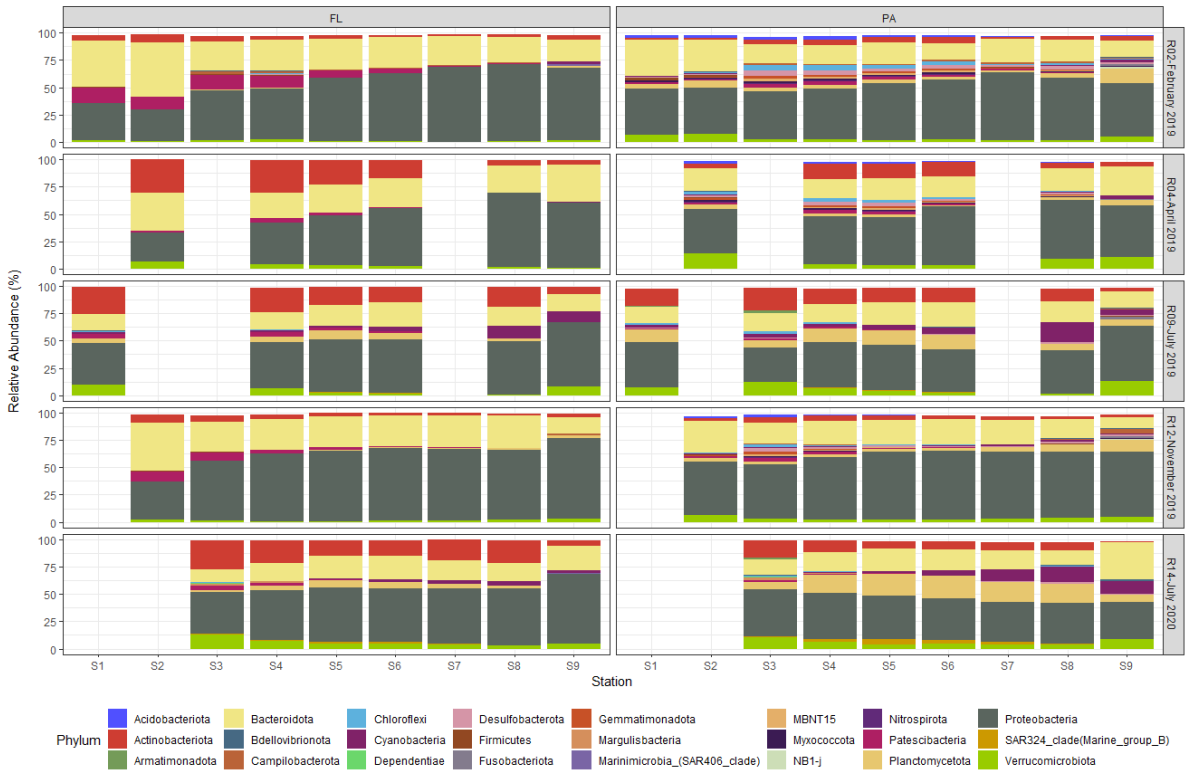

B)

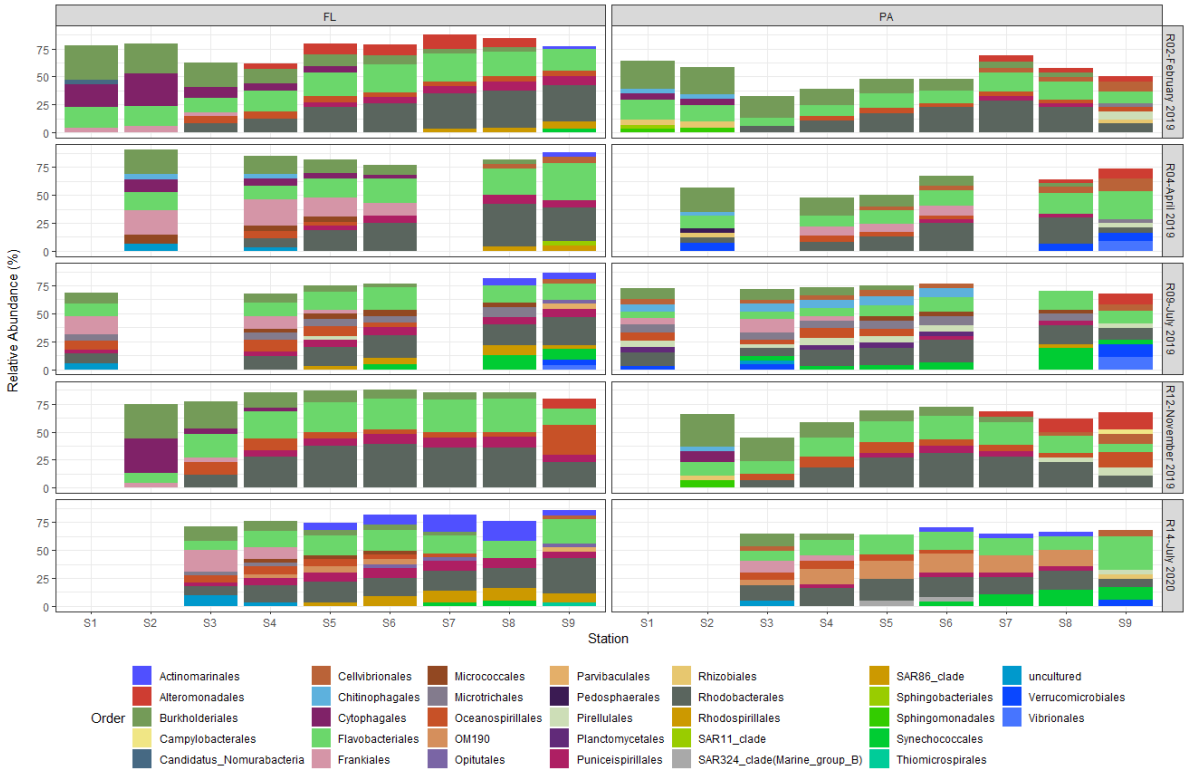

Figure 3. Barplots showing the taxonomic composition of the FL and PA bacterial communities, aggregated at the phylum (**A**) or order (**B**) rank. Only the groups representing more than 0.5% (phylum) or 3% (order) within a sample are represented for readability.

We then looked at the orders enriched in the PA and FL fractions in summer (July 2019, 2020) and in the others seasons (February, April and November 2019) (**Figure S5**). The FL communities in

summer were enriched in Puniceispirillales (7 ± 2%, Alphaproteobacteria) and Actinomarinales (6 ± 6%, Actinobacteriota). The PA communities in summer were enriched in OM190 (7 ± 7%, Planctomycetota) and Synechococcales (6 ± 6%, Cyanobacteria), but also less abundant orders usually involved in carbohydrates degradation (e.g., Chitinophagales, Verrucomicrobiales, Planctomycetales). In the other seasons, the FL communities were mainly enriched in Burkholderiales (12 ± 9%, Betaproteobacteria), Flavobacteriales (21 ± 6%, Bacteroidota) and Cytophagales (6 ± 9%, Bacteroidota). In contrast, the PA communities were mainly enriched in Alteromonadales (3 ± 4%, Gammaproteobacteria) and Rhizobiales (2 ± 1%, Alphaproteobacteria), but also in orders containing anaerobic bacteria present in marine sediments (Anaerolineales, Desulfobulbales, Desulfobacteriales), to a lesser extent.

2.2. α-diversity

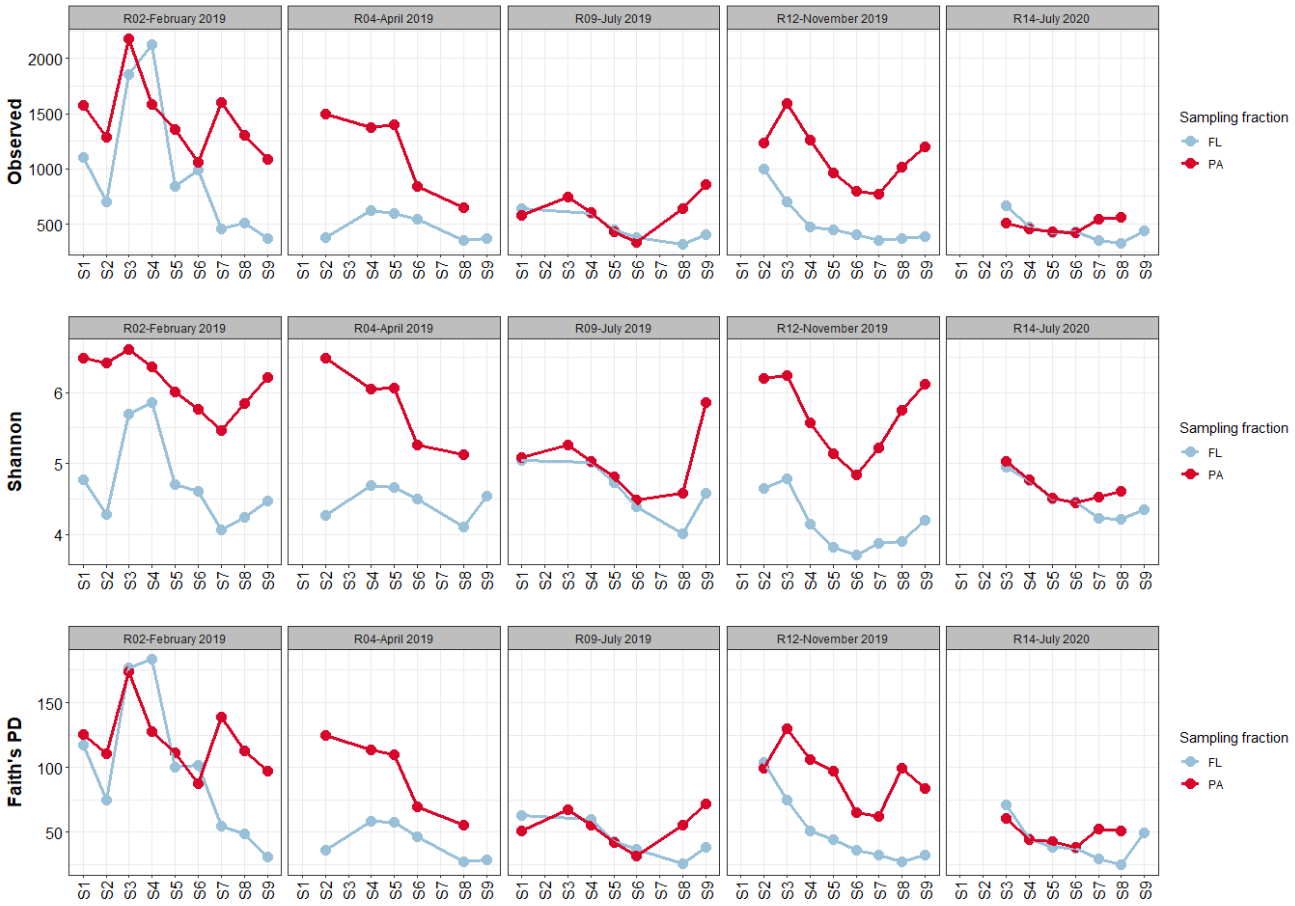

Figure 4. Alpha diversity indices (Observed number of ASVs, Shannon index and Faith's PD) characterizing the PA and FL communities along the Aulne estuary salinity gradient at the five sampling dates. Two samples were removed in the rarefication process (PA community in S9 of April 2019 and S9 of July 2020).

All three α-diversity indices exhibited similar patterns overall (**Figure 4**). In February, April and November 2019, there was a higher α-diversity in the PA fraction (mean Observed: 1256; Shannon: 5.9; Faith's PD: 104) compared to the FL fraction (mean Observed: 694; Shannon: 4.5; Faith's PD: 67) (Wilcoxon, $p < 0.001$ for all diversity indices). In contrast, both fractions exhibited similar α-diversity

levels in summer (July 2019, 2020) (Wilcoxon, not significant except for the Shannon index: mean PA Shannon = 4.8, mean FL Shannon = 4.6, $p < 0.05$). PA community α-diversity decreased in summer (July 2019, 2020) as highlighted by a significant negative correlation between all α-diversity indices and temperature (Observed: R^2_{adj} = 66%, Shannon: R^2_{adj} = 58%, Faith's PD: R^2_{adj} = 65%; $p < 0.001$ for all indices) (**Figure 4**). Along the salinity gradient, the α-diversity of the PA communities was higher upstream (S1-S4) and in marine waters (S9) than in the intermediate stations S5-S8 (Wilcoxon, Observed: not significant; Shannon and Faith's PD: $p < 0.05$). In contrast, the α-diversity of the FL communities was relatively stable over time (**Figure 4**). Temperature thus explained less variance than for PA communities (Observed: R^2_{adj} = 17%, $p < 0.001$; Shannon: not significant; Faith's PD: R^2_{adj} = 20%, $p < 0.001$). The α-diversity of the FL communities followed a similar spatial pattern than the PA communities with a significant decrease in the intermediate stations (S5-S8) (Wilcoxon, $p < 0.05$ for all diversity indices), although these variations were less pronounced.

2.3. β-diversity

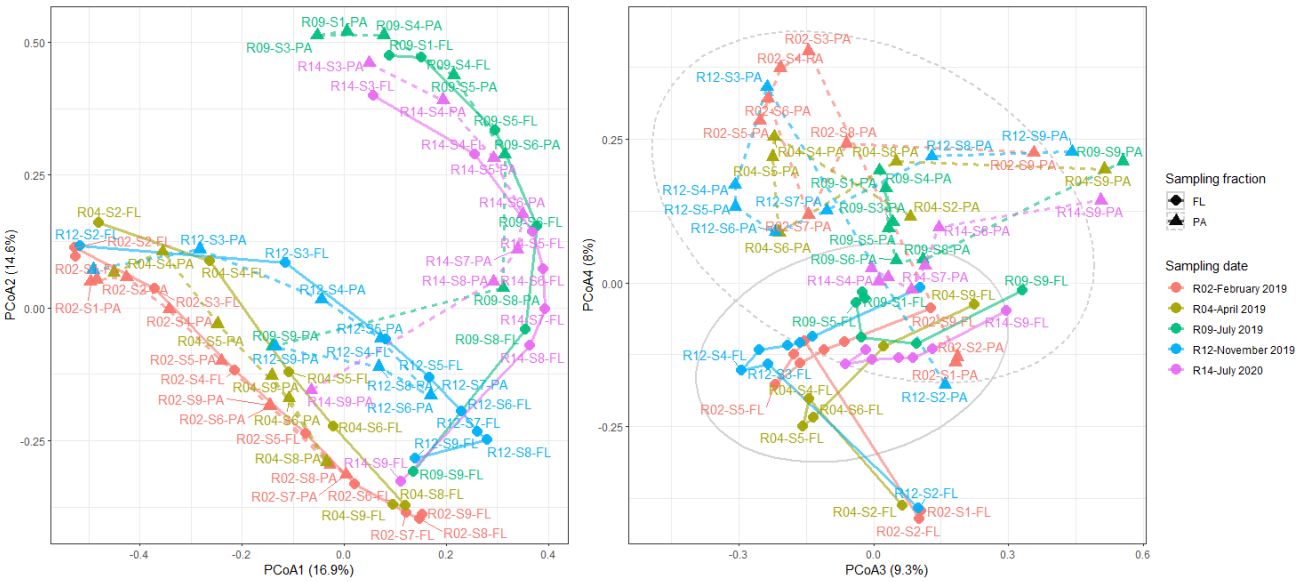

Figure 5. PCoA ordination of all samples based on the Bray-Curtis dissimilarity (left: axes 1-2; right: axes 3-4). The lines link the different stations within one sampling time in their spatial order (S1 to S9) (full line: FL communities, dashed line: PA communities). Samples are labeled as "sampling date-sampling station-fraction". R02: February 2019; R04: April 2019; R09: July 2019; R12: November 2019; R14: July 2020.

Variation in bacterial community structure was visualized using PCoA on the Bray-Curtis dissimilarity (taxonomic composition, **Figure 5**) and βMNTD (phylogenetic composition, **Figure S6**). The Bray-Curtis-based PCoA showed a marked spatial pattern with a separation between the freshwater (S1) and the marine samples (S9) along the 1st axis (16.9% of variance) (**Figure 5, left**). There was also a clear seasonal pattern with the 2nd axis (14.6% of variance) separating the summer samples (July 2019, 2020) from the other seasons. The 3rd axis (9.3% of variance) opposed the end members (freshwater – S1-S2 – and marine stations – S9) to the intermediate estuarine stations (S3-S8) (**Figure 5, right**). The

communities also differed according to the sampling fraction (4th axis, 8.0% of variance). Coherently, most of the variance was explained by the sampling station (PERMANOVA, 27%, F = 4.7, p < 0.001), the sampling time (PERMANOVA, 25%, F = 8.8, p < 0.001) and the sampling fraction (PERMANOVA, 7%, F = 9.5, p < 0.001). The Betadisper test showed no difference in dispersion for the sampling time and sampling fraction, supporting that the PERMANOVA results came from a difference in location. Significant heterogeneity in dispersion was found for the sampling stations; however, the PCoA plot clearly supports a difference in both location and dispersion between the stations.

The first two axes of the PCoA based on abundance-weighted βMNTD showed a similar pattern overall but explained less variance, highlighting complex variations of the phylogenetic β-diversity (**Figure S6**). Part of the variance was explained by the sampling station (PERMANOVA, 16%, F = 1.8, p<0.001), the sampling date (PERMANOVA, 11%, F = 2.3, p<0.001) and the sampling fraction (PERMANOVA, 4%, F = 3.5, p<0.001). The test for heterogeneity in dispersion showed no difference, supporting that the PERMANOVA results are due to differences in location.

2.4. FL-PA communities pairwise dissimilarity

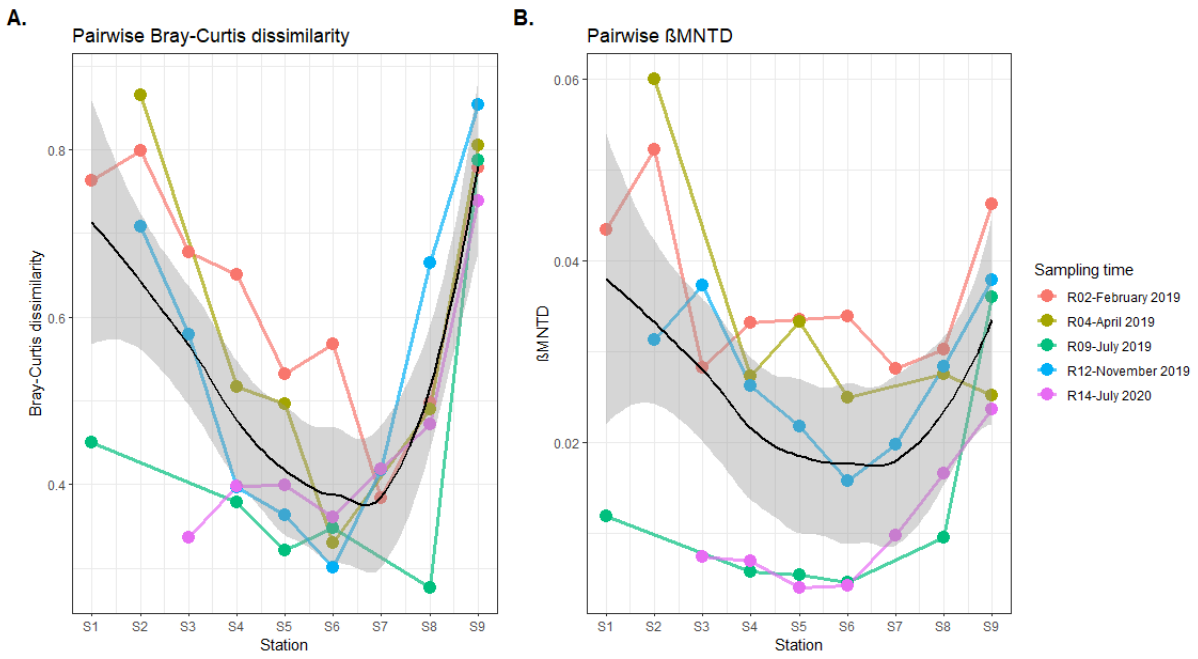

Figure 6. Pairwise Bray-Curtis (**A**) and abundance-weighted βMNTD (**B**) dissimilarity between the FL and PA fraction for each sample. The black line represents the loess regression curve and the dark area its confidence interval.

We computed the pairwise dissimilarity between the FL and PA fraction for each sample, based on Bray-Curtis dissimilarity and abundance-weighted βMNTD (**Figure 6**). The PA and FL communities were always dissimilar, as highlighted by the Bray-Curtis dissimilarity values (mean of 0.53, range: 0.28-0.86). However, the FL-PA dissimilarity decreased in the mid-salinity range (S4-S8) compared to both the marine and freshwater end members (Wilcoxon, p < 0.01 for Bray-Curtis and βMNTD). Interestingly, when taking into account the phylogeny (βMNTD), the FL-PA pairwise dissimilarity also decreased in

summer (July 2019, 2020) compared to the other seasons (February, April, November 2019) (mean summer = 0.011; mean other seasons = 0.032; Wilcoxon, $p < 0.001$) which was especially pronounced at the S1-S8 stations. This pattern was present but less clear with the taxonomic dissimilarity (mean summer = 0.44; mean other seasons = 0.58; Wilcoxon, $p < 0.05$).

3. Bacterial community cohesion

In order to determine the overall community connectivity, we computed the positive and negative cohesion reflecting the degree of positive and negative correlations, respectively (**Figure 7**). Overall, the positive cohesion was higher in the PA communities than in the FL communities (Wilcoxon, $p < 0.05$), especially in the intermediate stations (S3-S8) in February, April and November. The FL positive cohesion decreased from S1 to S9 (range: 0.19-0.29). The PA positive cohesion was more variable (range: 0.13-0.34). It first increased in the MTZ (S3) (especially in R02, R04 and R12) then decreased from S3 to S9, with a sharper decrease at the marine station (S9). Both FL and PA positive cohesion increased in the summer samplings although it was not significant for the PA communities (Wilcoxon, FL: $p < 0.001$; PA: $p = 0.22$). The absolute value of negative cohesion was more important in the FL fraction than in the PA fraction (Wilcoxon, $p < 0.001$). For both FL and PA communities, the absolute negative cohesion increased at the intermediate stations (S4-S8) compared to the end members (Wilcoxon, $p < 0.001$). Both FL and PA absolute negative cohesion tended to increase in the summer samplings although it was not significant for the FL communities (Wilcoxon, FL: $p = 0.16$; PA: $p < 0.05$).

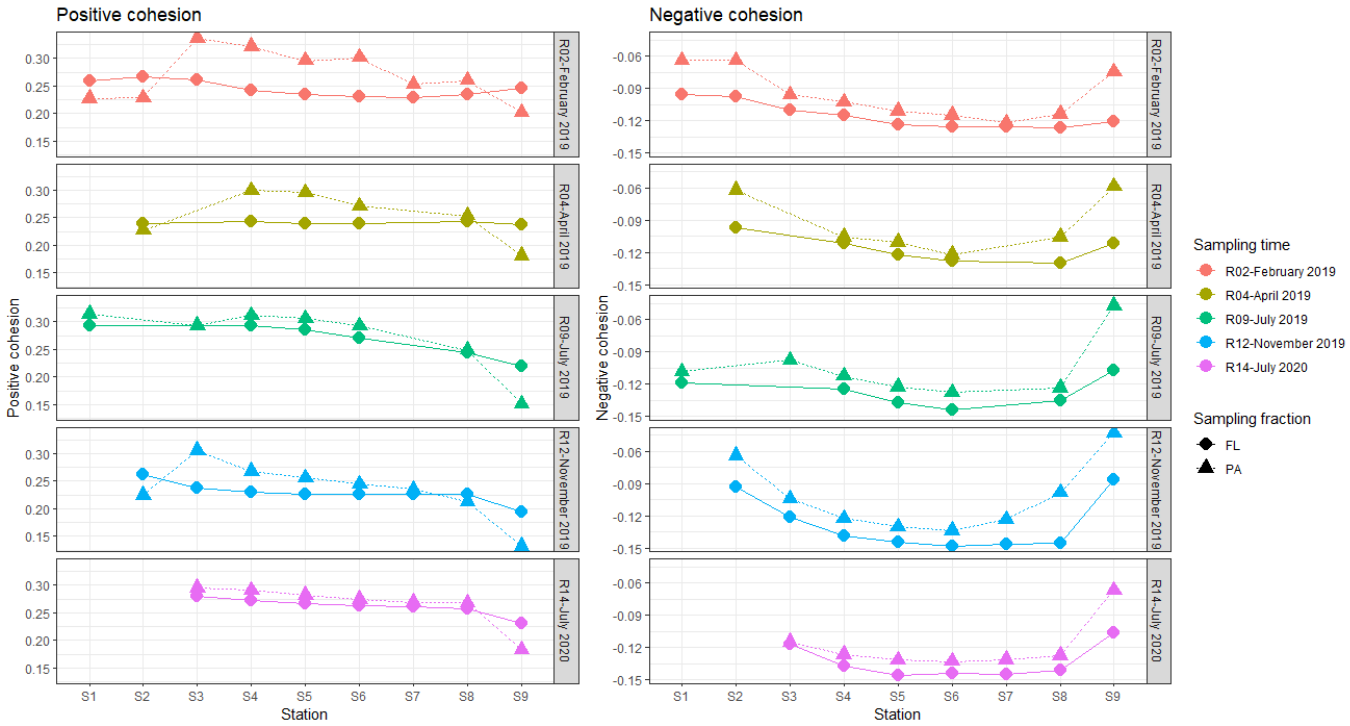

Figure 7. Positive and negative cohesion of FL and PA communities along the salinity gradient of the Aulne estuary.

4. Community assembly processes

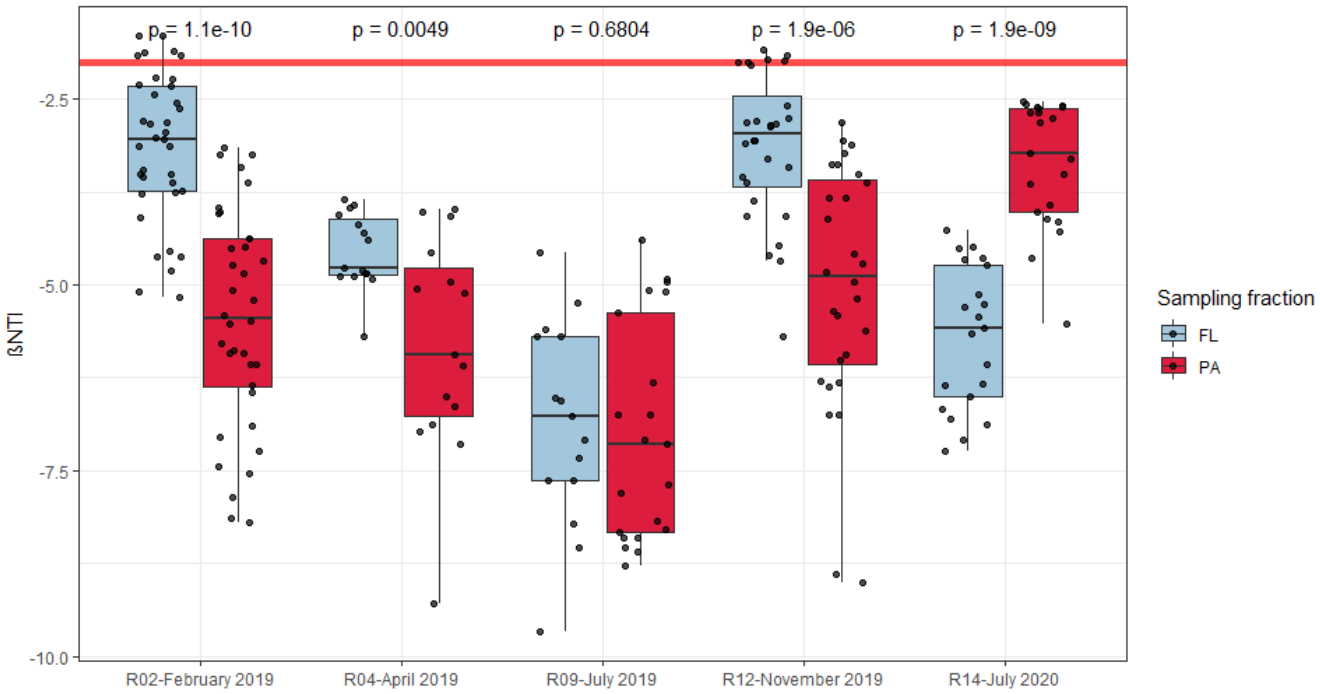

Figure 8. βNTI values for the FL and PA fraction across the five sampling dates. The βNTI < -2 threshold (red line) indicates the predominance of deterministic homogeneous selection. The p-values compare the mean βNTI of the FL and PA fractions for each sampling date (Wilcoxon test).

Ecological null modeling based on the βNTI value was performed to determine whether the community assembly was driven by stochastic or deterministic processes. All FL and PA community assemblies were largely dominated by deterministic homogeneous selection (βNTI < -2, **Figure 8**) with a mean contribution of 96% to assembly processes. In February, April and November 2019, PA communities were more significantly impacted by homogeneous selection than the FL communities as the mean βNTIs were significantly lower ($p < 0.005$, Wilcoxon test). In contrast, in the summer group, the mean PA community's βNTI were either not significantly different (July 2019) or higher (July 2020) than the mean FL-βNTIs. Stochastic processes also contributed to the FL communities assembly by 16.7% (2.8% dispersal limitation and 13.9% undominated) and 14.3% (8.3% homogenizing dispersal and 2.8% undominated) in February 2019 and November 2019, respectively.

5. Biotic and abiotic factors driving the FL and PA community composition

The influence of biotic and abiotic variables on the FL and PA BCC was assessed using dbRDA and variance partitioning on the Bray-Curtis dissimilarity (**Figure 9**). The dbRDAs based on Bray-Curtis dissimilarity showed that the FL and PA communities similarly correlated with biotic and abiotic factors, explaining most of the variance (FL: $R^2_{ajd} = 63\%$, $p < 0.001$; PA: $R^2_{ajd} = 57\%$, $p < 0.001$). For both communities, the first two axes clearly separated the sampling stations along the salinity gradient

(free-living community: 1st axis, 23.1% of variance; particle-attached community: 2nd axis, 12.3% of variance), logically correlating with salinity (**Figure 9A, 9B**). They also separated the summer samplings (July 2019, 2020) from the other sampling dates (February, April, November 2019) (free-living community: 2nd axis, 16.3% of variance; particle-attached community: 1st axis, 17.2% of variance). The summer samplings correlated with seasonal factors such as temperature, DOP or Chl*a*, but also with positive and negative cohesion. Variance partitioning showed that salinity, nutrients and organic matter and cohesion explained similar amounts of variance on their own (FL: 11%, 9% and 11%, respectively; PA: 6%, 7% and 10%, respectively) (**Figure 9C, 9D**). Temperature alone explained low amounts of variance (FL: 2%; PA: 1%) but an important part was shared with cohesion and/or organic matter and nutrients, reflecting their complex relationships.

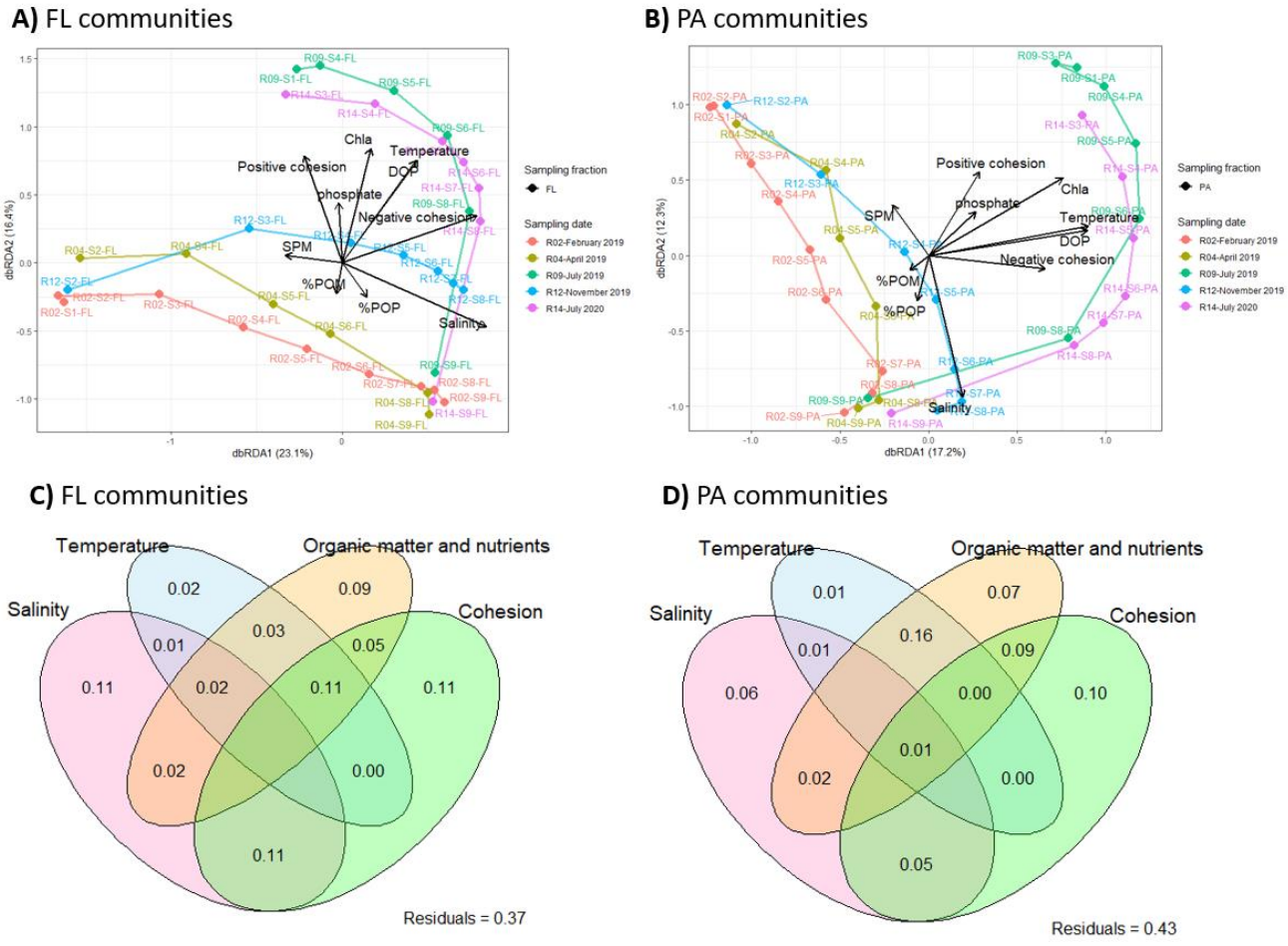

Figure 9. Bray-Curtis-based dbRDA (**A-B**) and variance partitioning (**C- D**) on the Bray-Curtis dissimilarity for FL (**A-C**) and PA (**B-D**) communities. (**A-B**) The lines link the different stations within one sampling time in their spatial order (S1 to S9) (full line: FL communities, dashed line: PA communities). It should be noted that the absolute value of negative cohesion was used, so that the degree of negative correlation increases with the absolute value of negative cohesion. Samples are labeled as "sampling date-sampling station-fraction". R02: February 2019; R04: April 2019; R09: July 2019; R14: July 2020. (**C-D**) Organic matter and nutrients regroup the variables SPM, %POM, Chl*a*, DOP and phosphate while the cohesion comprises both positive and negative cohesion. Negative R^2 values are not shown.

6. Biotic and abiotic factors driving the FL-PA dissimilarity

We performed a RDA on the pairwise FL-PA Bray-Curtis dissimilarity and βMNTD to better constrain their determinants (**Figure 10**). The RDA (R^2_{ajd} = 76%, p < 0.001) showed that the increased dissimilarity in the end members correlated with markers of POM lability (%POM, %POP) while the decreased dissimilarity in the estuarine stations correlated with phosphate, PA positive cohesion and FL negative cohesion. The decreased phylogenetic pairwise βMNTD in summer correlated with seasonal variables (e.g., temperature, DOP, Chl*a*) but also with FL positive cohesion.

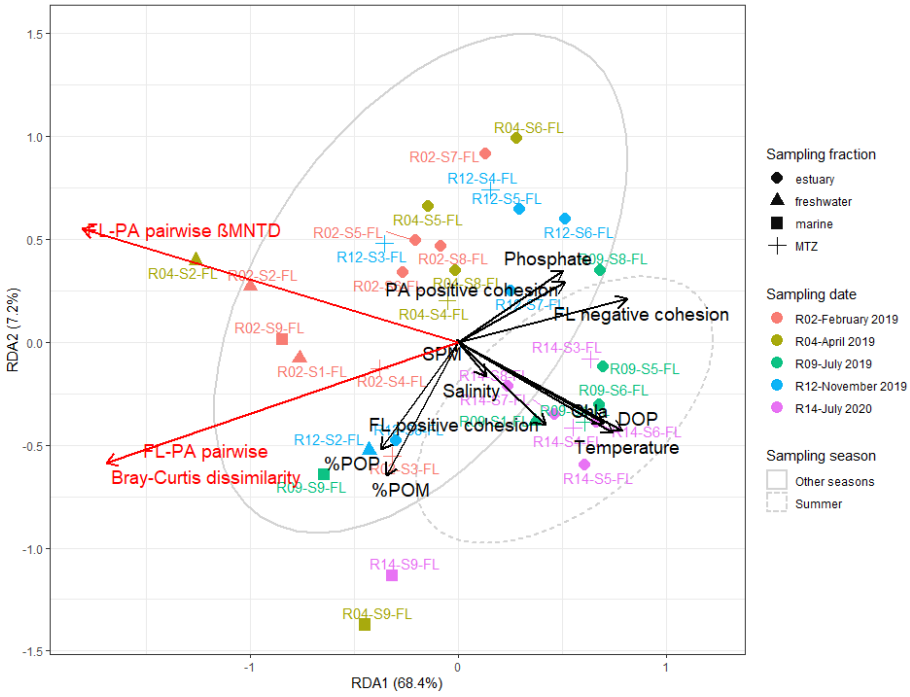

Figure 10. Redundancy analysis (RDA) of the pairwise FL-PA dissimilarity based on Bray-Curtis dissimilarity and βMNTD. The ellipses represent the sampling season (dashed line: summer, solid line: other seasons). It should be noted that the absolute value of negative cohesion was used, so that the degree of negative correlation increases with the absolute value of negative cohesion. Samples are labeled as "sampling date-sampling station-fraction". Red arrow: response variable; Black arrow: explanatory variable; R02: February 2019; R04: April 2019; R09: July 2019; R14: July 2020.

7. FL and PA inferred functional capacities

We used the PICRUSt2 pipeline to infer the communities' metabolic pathways. The PCoA and PERMANOVA revealed that there was a significant difference between the FL and PA community (PERMANOVA, R^2 = 15%, *F* = 28.7, p < 0.001). The betadisper test was significant for the fraction size (p < 0.05) but the PCoA plot supports a difference in both location and dispersion (**Figure S7**). The same FL-PA dissimilarity pattern as before was observed with a decrease in the estuarine stations and summer (**Figure S8**), suggesting that differences in composition result in differences in functional

capacities. We then looked at the features that were significantly different between the two fractions (**Figure 11**). The FL fraction was enriched in pathways related to amino acids and proteins anabolism (e.g., VALSYN-PWY, ILEUSYN-PWY, PWY-5101, 5103 and 5104) and catabolism (PWY-1541). In contrast, the PA fraction was enriched in pathways related to carbohydrate metabolism (e.g., GLYCOCAT-PWY, PWY-6737, GLYCOGENSYNTH-PWY), lipids metabolism (PWY-5971, FAO-PWY), autotrophic processes (e.g., P23-PWY, SUCSYN-PWY) and anaerobic metabolism (e.g., P164-PWY, PWY-5100), among others.

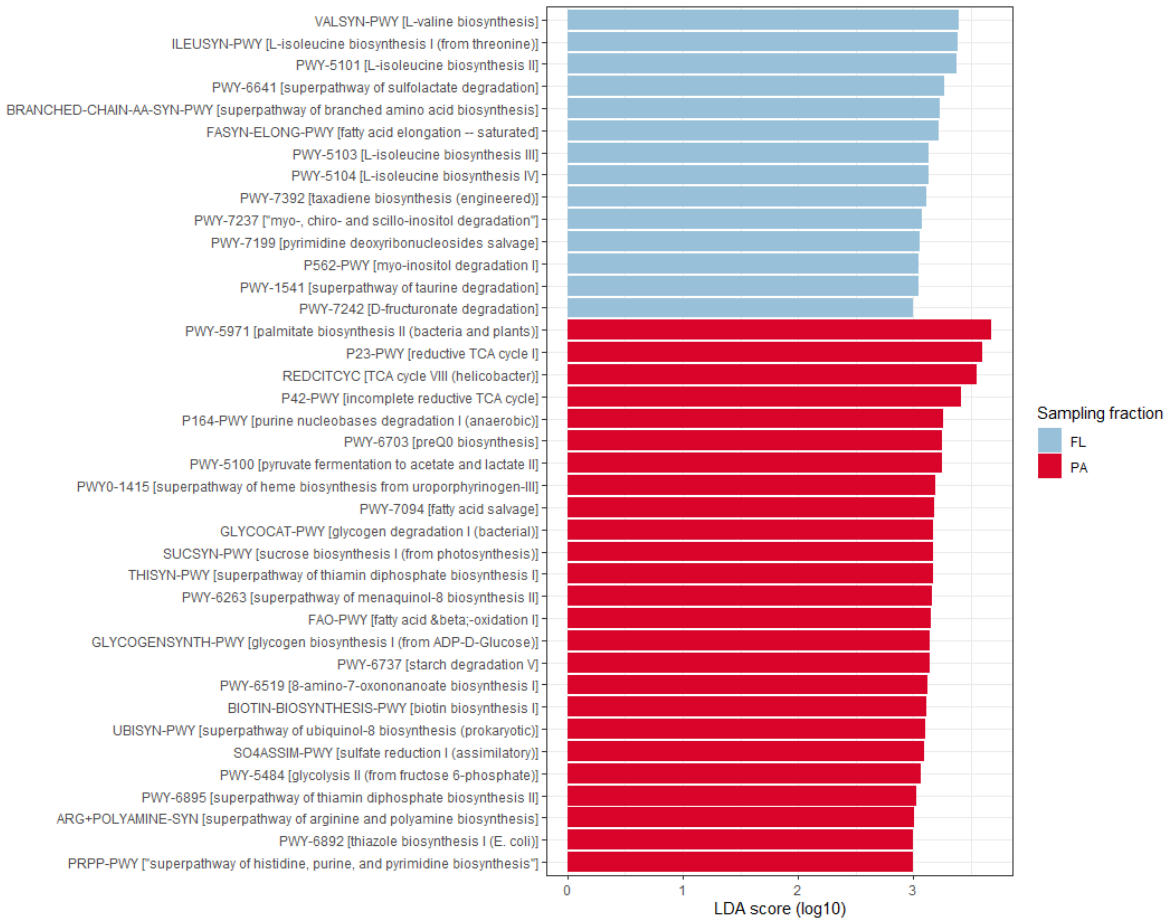

Figure 11. LEfSe analysis of the Metacyc pathways predicted by PICRUSt2. The linear discriminant analysis (LDA) threshold score was set to 3 and the threshold p-value to 0.01. Blue pathways are enriched in the FL fraction while red pathways are enriched in the PA fraction.

Discussion

Characterizing FL and PA bacterial communities and their determinants in estuaries is a first step towards understanding their biogeochemical impact on the organic matter and nutrients exported to coastal ecosystems. Understanding the differences between FL and PA communities is especially interesting since they contribute differently to the ecosystem's functioning. This study consequently depicts for the first time the diversity, composition and driving factors of the FL and PA bacterial communities within the Aulne estuary and the adjacent Bay of Brest coastal waters.

1. FL and PA assembly processes are dominated by homogeneous selection

Ecological null modeling showed that FL and PA bacterial community assemblies were largely driven by homogeneous selection, meaning that the biotic and abiotic environmental conditions led to bacterial communities that were more similar than what would be expected by random changes. Few studies have quantified assembly processes for FL and PA communities in coastal ecosystems thus far; however, homogeneous selection was an important driver in other land-sea transition areas (Wu *et al.*, 2020; Y. Wang *et al.*, 2020). The predominance of deterministic processes has been suggested to lead to communities well adapted to their environment, thus potentially having a stronger biogeochemical impact than communities assembling through stochastic processes (Graham and Stegen, 2017). This is consistent with the idea of estuaries as natural bioreactors where organic matter is heavily transformed by estuarine bacteria (Crump *et al.*, 2017).

2. FL and PA communities followed pronounced spatiotemporal patterns and were driven by similar factors

The β-diversity of the FL and PA communities largely differed across space and time and were driven by similar variables, with comparable relative importance. Since the sampling stations and sampling time explained most of the variance of the FL and PA communities' β-diversity (**Figure 5** and associated PERMANOVA), salinity and seasonal variables (e.g., temperature, Chl*a*, DOP) explained a large part of the variation in bacterial communities' variation (**Figure 9**). Salinity is logically an important driver of bacterial communities along fresh to marine water gradients such as fjords, estuaries and coastal margins (Fortunato *et al.*, 2012; Campbell and Kirchman, 2013; Ortega-Retuerta *et al.*, 2013; Balmonte *et al.*, 2019; Jain *et al.*, 2021). Salinity reflects the mixing of fresh- and marine water masses and directly impacts the BCC by selecting taxa capable of growing at a specific saline concentration. Similar to other studies (e.g., Campbell and Kirchman, 2013; Ortega-Retuerta *et al.*, 2013; Balmonte *et al.*, 2019), the freshwater communities shifted from a predominance of Actinobacteriota (e.g., Frankiales) and Betaproteobacteria (e.g., Burkholderiales) to a majority of Alphaproteobacteria (e.g., Rhodobacterales, SAR11), Gammaproteobacteria (e.g., Alteromonadales, Oceanospirillales,

Vibrionales) and Bacteroidetes (e.g., Flavobacteriales) in the estuarine and marine samples. However, the BCC in the estuarine stations (S3-S8) did not only result from the mixing of water masses: these stations hosted native FL and PA bacterial communities that differed from both the freshwater (S1-S2) and marine (S9) stations (**Figure 5**, right panels). A native estuarine community can only occur if the doubling time of the bacteria within the estuary is inferior to the flushing time of the water. This is the case in the Aulne estuary where the bacterial generation times estimated from bacterial production were extremely fast for all sampling times (11-55 h and 1-12 h for the FL and PA communities for S3-S8; Urvoy *et al.*, in prep., **chapitre IV**) compared to the residence time of the water masses (3-30 days, Bassoullet, 1979). This reinforces the idea that the Aulne estuary is a biogeochemical bioreactor hosting adapted and active specific communities.

Among seasonal variables, water temperature is an important driver of microbial communities (Fuhrman *et al.*, 2015; Sunagawa *et al.*, 2015). However, temperature on its own explained low amounts of variance as it was correlated with other variables such as phytoplankton development (Chl*a* and %Chl*a*), DOP and phosphate (**Figure 9**), which can select specific bacterial taxa. For instance, Flavobacteria (Bacteroidota), members of the roseobacters (Rhodobacterales, Alphaproteobacteria) and Gammaprotobacteria (e.g., Alteromonadaceae) have been consistently linked with algal bloom occurrences (Buchan *et al.*, 2014). In our study, the communities in summer largely differed from the communities in the other seasons. They were overall less diverse, enriched in autotrophic Synechoccocales; but also in groups usually involved in carbohydrates degradation such as Chitinophagales, Verrucomicrobiales or Planctomycetales which can be linked to phytoplankton development in this season.

In addition to variables related to space and time, cohesion explained an important fraction of the variance on its own and shared with organic matter, temperature or salinity (**Figure 9**); suggesting both its importance in explaining BCC patterns and its link with environmental variables. Negative cohesion reflects the importance of negative co-occurrences, which arise when the presence of one taxon prevents the presence of others. Negative co-occurrence can result from differences in niches or antagonist interactions such as competition (i.e., the taxa compete for the same resource) (J. Liu *et al.*, 2019; Gralka *et al.*, 2020). In contrast, positive cohesion reflects the magnitude of positive co-occurrences, which can result from beneficial interactions (e.g., division of labor to exploit the same resource) or niche partitioning (J. Liu *et al.*, 2019; Gralka *et al.*, 2020). As such, even though they are not appropriate to imply accurate interactions (J. Liu *et al.*, 2019), co-occurrence patterns can drive community evolution by creating feedback loops that can stabilize or differentiate the communities (J. Liu *et al.*, 2019; Gralka *et al.*, 2020). Consequently, cohesion was found to be an important factor explaining BCC in other studies (Herren and McMahon, 2017; 2018; Hernandez *et al.*, 2021). In our study, the summer samples contained higher positive and negative cohesion levels than the other

sampling dates, possibly reflecting their importance in structuring the community from winter to summer.

3. FL-PA dissimilarity differed across space and time and was driven by various factors

Even though the sampling fraction explained less variance than the sampling station and date, the FL and PA communities were largely dissimilar (**Figure 5** and associated PERMANOVA, **Figure 6**). The pairwise FL-PA Bray-Curtis dissimilarity (taxonomic composition) and βMNTD (phylogenetic composition) varied spatially and temporally. Most strikingly, both FL-PA taxonomic and phylogenetic dissimilarities decreased in the intermediate estuarine stations compared to the end members for all sampling dates. The pairwise βMNTD also showed that FL-PA dissimilarity significantly decreased in summer (July 2019, 2020) compared to the other seasons, which was concomitant with a decrease in PA α-diversity. These patterns can be explained by the superposition of several factors (**Figure 10**). The higher FL-PA dissimilarity in the freshwater and marine end members (S1-S2, S9) correlated with the presence of a more labile POM compared to the inner estuarine stations. The colonization of labile POM was suggested to provide a larger advantage than the colonization of refractory terrestrial POM commonly found in estuaries, thus increasing FL-PA dissimilarity (Hollibaugh *et al.*, 2000; Ortega-Retuerta *et al.*, 2013). Conversely, the estuarine stations contained less labile POM, possibly explaining the lower FL-PA dissimilarity. In addition, these stations were characterized by higher PA positive cohesion and FL negative cohesion levels. The increased PA positive cohesion could suggest that the colonizing bacteria cooperated to degrade complex, refractory estuarine POM. Interestingly, SPM did not seem to explain the FL-PA dissimilarity (**Figure 10**). However, they may contribute to some extent to the FL-PA dissimilarity in February, April and November 2019, where strong hydrodynamic forcings may resuspend benthic communities. This would be coherent with the enrichment of anaerobic bacterial groups usually found in marine sediments in these sampling dates (**Figure S5**).

The decrease in phylogenetic FL-PA dissimilarity in summer logically correlated with seasonal variables (temperature, Chl*a*, DOP) and FL positive cohesion. POM and DOM are expected to be more labile in summer, with an increased proportion of autochthonous processes (i.e., increase in primary production) compared to allochthonous inputs (e.g., refractory terrestrial matter run-off). As such, these results seem conflicting: on the one hand, more labile POM was linked to a higher taxonomic and phylogenetic dissimilarity in the end members; on the other hand, FL-PA phylogenetic dissimilarity decreased in summer, which most likely contains more labile organic matter. A possible explanation is that the autochthonous labile DOM and POM produced during the summer have similar molecular compositions (e.g., phytoplankton components such as polysaccharides or proteins). This may lead to the selection of closely related taxon (decrease in α-diversity), able to assimilate similar substrates in both fractions and thereby increase the communities' positive cohesion (e.g., increase in positive co-occurrence driven by similar niches). Simultaneously, PA communities are known to solubilize POM

into DOM (Smith *et al.*, 1992; Grossart, 2010). It is possible that these DOM releases increase in summer due to a higher bacterial metabolism, especially within the estuary (Urvoy *et al.*, in prep, **chapitre IV**). This would likely participate in the homogenization of substrate pools and reduce the FL-PA dissimilarity. The decreased river flow in summer also likely favors the exchange of bacteria and organic matter between both fractions by increasing particles and water residence time.

4. FL and PA differed in their inferred functional capacities

The PICRUsT2 analysis showed that differences in FL and PA communities' composition translated into functional differences. First, the PA communities were enriched in pathways associated with autotrophic and anaerobic processes. The former is most likely linked to the enrichment of Synecchococcales in PA communities in summer, while the latter could be due to the resuspension of benthic bacteria in February, April and November 2019, as discussed above. In addition, FL inferred metagenomes were enriched in pathways involved in amino acid metabolism, while PA communities were enriched in pathways contributing to carbohydrates and lipids metabolisms. This dichotomy was already noted in similar studies (Borrego *et al.*, 2020; Hu *et al.*, 2020). It could signify that FL and PA are adapted to consume different substrates, partly explaining their taxonomic dissimilarity. This could indicate different transformation processes and carbon and nitrogen mineralization rates in the dissolved and particulate phase, consequently impacting the exports to the Bay of Brest. However, inferred metabolic capacities must be inspected cautiously in marine environments because of the limited availability of sequenced genomes compared to other environments (Langille *et al.*, 2013). Further studies using conventional metagenomics are necessary to confirm this.

Conclusion

This study depicts the FL and PA bacterial communities within the Aulne estuary for the first time, which is a step towards understanding their biogeochemical impact. It showed the importance of deterministic processes in structuring both FL and PA communities. Their evolution was driven by salinity and seasonal variables, but also by organic matter composition, nutrients and cohesion, highlighting the need to integrate co-occurrence patterns in such studies. Interestingly, our study showed that FL-PA dissimilarity varied across space and time and that taxonomic and phylogenetic dissimilarity painted complementary pictures. Finally, FL and PA communities seemed to differ in their metabolic capacities, suggesting that they could differently affect the inputs to the Bay of Brest.

Acknowledgement

This work was supported by a grant from the INSU-CNRS EC2CO (Ecosphère Continentale et Côtière) program (project "Friezbee") and Ifremer funds (project "CombactAulne"). We are thankful to the Hesione crew, Isabelle Bihannic, Erwan Amice and Thierry Le Bec for their help during sampling. We would like to thank Daniel Delmas for his insightful comments and support during this study.

Author contribution

All authors contributed to the experiments. MU analyzed the data and wrote the first draft. All authors edited, proofread and approved the final manuscript.

Data availability statement

The sequencing data generated during this study are available on online repositories under the accession number [*data to be deposed*].

Competing interests

The authors declare no competing interests.

References

Auffret, G.A. (1983) Dynamique sédimentaire de la marge continentale celtique-Evolution Cénozoïque-Spécificité du Pleistocène supérieur et de l'Holocène.

Azam, F. and Malfatti, F. (2007) Microbial structuring of marine ecosystems. Nat Rev Microbiol 5: 782–791.

Balmonte, J.P., Hasler-sheetal, H., Glud, R.N., Andersen, T.J., Sejr, M.K., Middelboe, M., et al. (2019) Sharp contrasts between freshwater and marine microbial enzymatic capabilities, community composition, and DOM pools in a NE Greenland fjord. Limnol Oceanogr 65: 77–95.

Bassoullet, P. (1979) Etude de la dynamique des sédiments en suspension dans l'estuaire de l'Aulne (rade de Brest).

Bianchi, T.S. (2011) The role of terrestrially derived organic carbon in the coastal ocean: A changing paradigm and the priming effect. Proc Natl Acad Sci U S A 108: 19473–19481.

Bižic-Ionescu, M., Zeder, M., Ionescu, D., Orlic, S., Fuchs, B.M., Grossart, H., and Amann, R. (2015) Comparison of bacterial communities on limnic versus coastal marine particles reveals profound differences in colonization. Environ Microbiol 17: 3500–3514.

Bolyen, E. (2019) Reproducible, interactive, scalable and extensible microbiome data science using QIIME 2. Nat Biotechnol 37: 852–857.

Borrego, C., Sabater, S., and Proia, L. (2020) Lifestyle preferences drive the structure and diversity of bacterial and archaeal communities in a small riverine reservoir. Sci Rep 10: 11288.

Buchan, A., Lecleir, G.R., Gulvik, C.A., and González, J.M. (2014) Master recyclers: features and functions of bacteria associated with phytoplankton blooms. Nat Rev Microbiol 12: 686–698.

Callahan, B.J., McMurdie, P.J., Rosen, M.J., Han, A.W., Johnson, A.J.A., and Holmes, S.P. (2016) DADA2: High-resolution sample inference from Illumina amplicon data. Nat Methods 13: 581–583.

639 Campbell, B.J. and Kirchman, D.L. (2013) Bacterial diversity, community structure and potential growth rates
640 along an estuarine salinity gradient. ISME J 7: 210–220.

641 Crump, B.C., Fine, L.M., Fortunato, C.S., Herfort, L., Needoba, J.A., Murdock, S., and Prahl, F.G. (2017) Quantity
642 and quality of particulate organic matter controls bacterial production in the Columbia River estuary.
643 Limnol Oceanogr 62: 2713–2731.

644 Dang, H. and Lovell, C.R. (2016) Microbial Surface Colonization and Biofilm Development in Marine
645 Environments. Microbiol Mol Biol Rev 80: 91–138.

646 Delmas, R. and Tréguer, P. (1983) Évolution saisonnière des nutriments dans un écosystème eutrophe d'Europe
647 occidentale (la rade de Brest). Interactions marines et terrestres. Oceanol Acta 6: 345–356.

648 Fortunato, C.S., Herfort, L., Zuber, P., Baptista, A.M., and Crump, B.C. (2012) Spatial variability overwhelms
649 seasonal patterns in bacterioplankton communities across a river to ocean gradient. ISME J 6: 554–563.

650 Fuhrman, J.A., Cram, J.A., and Needham, D.M. (2015) Marine microbial community dynamics and their ecological
651 interpretation. Nat Rev Microbiol 13: 133–146.

652 Graham, E.B. and Stegen, J.C. (2017) Dispersal-based microbial community assembly decreases biogeochemical
653 function. Processes 5: 65.

654 Gralka, M., Szabo, R., Stocker, R., and Cordero, O.X. (2020) Trophic Interactions and the Drivers of Microbial
655 Community Assembly. Curr Biol 30: R1176–R1188.

656 Grossart, H.P. (2010) Ecological consequences of bacterioplankton lifestyles: Changes in concepts are needed.
657 Environ Microbiol Rep 2: 706–714.

658 Grossart, H.P. and Tang, K.W. (2010) Communicative & Integrative Biology. Commun Integr Biol 3: 491–494.

659 Grossart, H.P., Tang, K.W., Kiørboe, T., and Ploug, H. (2007) Comparison of cell-specific activity between free-
660 living and attached bacteria using isolates and natural assemblages. FEMS Microbiol Lett 266: 194–200.

661 Hanson, C.A., Fuhrman, J.A., Horner-Devine, M.C., and Martiny, J.B.H. (2012) Beyond biogeographic patterns:
662 Processes shaping the microbial landscape. Nat Rev Microbiol 10: 497–506.

663 Hernandez, D.J., David, A.S., Menges, E.S., Searcy, C.A., and Afkhami, M.E. (2021) Environmental stress
664 destabilizes microbial networks. ISME J 15: 1722–1734.

665 Herren, C.M. and McMahon, K.D. (2017) Cohesion: A method for quantifying the connectivity of microbial
666 communities. ISME J 11: 2426–2438.

667 Herren, C.M. and McMahon, K.D. (2018) Keystone taxa predict compositional change in microbial communities.
668 Environ Microbiol 20: 2207–2217.

669 Hollibaugh, J.T., Wong, P.S., and Murrell, M.C. (2000) Similarity of particle-associated and free-living bacterial
670 communities in northern San Francisco Bay, California. Aquat Microb Ecol 21: 103–114.

671 Hu, Y., Xie, G., Jiang, X., Shao, K., Tang, X., and Gao, G. (2020) The Relationships Between the Free-Living and
672 Particle-Attached Bacterial Communities in Response to Elevated Eutrophication. Front Microbiol 11:
673 423.

674 Jain, A., Balmonte, J.P., Singh, R., Bhaskar, P.V., and Krishnan, K.P. (2021) Spatially resolved assembly,
675 connectivity and structure of particle-associated and free-living bacterial communities in a high Arctic
676 fjord. FEMS Microbiol Ecol 97: 1–12.

677 Klindworth, A., Pruesse, E., Schweer, T., Peplies, J., Quast, C., Horn, M., and Glöckner, F.O. (2013) Evaluation of
678 general 16S ribosomal RNA gene PCR primers for classical and next-generation sequencing-based
679 diversity studies. Nucleic Acids Res 41: e1.

680 Labry, C., Delmas, D., Youenou, A., Quere, J., Leynaert, A., Fraisse, S., et al. (2016) High alkaline phosphatase
681 activity in phosphate replete waters: The case of two macrotidal estuaries. Limnol Oceanogr 61: 1513–
682 1529.

683 Langille, M.G.I., Zaneveld, J., Caporaso, J.G., McDonald, D., Knights, D., Reyes, J.A., et al. (2013) Predictive
684 functional profiling of microbial communities using 16S rRNA marker gene sequences. Nat Biotechnol
685 31: 814–821.

686 Legendre, P. and Legendre, L. (2012) Numerical Ecology (3rd english edition), Amsterdam: Elsevier.

687 Lima-Mendez, G., Faust, K., Henry, N., Decelle, J., Colin, S., Carcillo, F., et al. (2015) Determinants of community
688 structure in the grobal plankton interactome. Science (80-) 348: 1262073-1–10.

689 Liu, J., Meng, Z., Liu, X., and Zhang, X.-H. (2019) Microbial assembly, interaction, functioning, activity and
690 diversification: a review derived from community compositional data. Mar Life Sci Technol 1: 112–128.

691 Lyons, M.M. and Dobbs, F.C. (2012) Differential utilization of carbon substrates by aggregate-associated and
692 water-associated heterotrophic bacterial communities. Hydrobiologia 686: 181–193.

693 Martiny, J.B.H., Bohannan, B.J.M., Brown, J.H., Colwell, R.K., Fuhrman, J.A., Green, J.L., et al. (2006) Microbial
694 biogeography: Putting microorganisms on the map. Nat Rev Microbiol 4: 102–112.

695 McKnight, D.T., Huerlimann, R., Bower, D.S., Schwarzkopf, L., Alford, R.A., and Zenger, K.R. (2019) Methods for
696 normalizing microbiome data: An ecological perspective. Methods Ecol Evol 10: 389–400.

697 Mestre, M., Ferrera, I., Borrull, E., Ortega-Retuerta, E., Mbedi, S., Grossart, H.P., et al. (2017) Spatial variability of
698 marine bacterial and archaeal communities along the particulate matter continuum. Mol Ecol 26: 6827–
699 6840.

700 Milici, M., Deng, Z.L., Tomasch, J., Decelle, J., Wos-Oxley, M.L., Wang, H., et al. (2016) Co-occurrence analysis of
701 microbial taxa in the Atlantic ocean reveals high connectivity in the free-living bacterioplankton. Front
702 Microbiol 7: 649.

703 Noble, P.A., Bidle, K.D., and Fletcher, M. (1997) Natural microbial community compositions compared by a back-
704 propagating neural network and cluster analysis of 5S rRNA. Appl Environ Microbiol 63: 1762–1770.

705 Olesen, S.W., Duvallet, C., and Alm, E.J. (2017) dbOTU3: A new implementation of distribution-based OTU calling.
706 PLoS One 12: 1–13.

707 Ortega-Retuerta, E., Joux, F., Jeffrey, W.H., and Ghiglione, J.F. (2013) Spatial variability of particle-attached and
708 free-living bacterial diversity in surface waters from the Mackenzie River to the Beaufort Sea (Canadian
709 Arctic). Biogeosciences 10: 2747–2759.

710 Quast, C., Pruesse, E., Yilmaz, P., Gerken, J., Schweer, T., Yarza, P., et al. (2013) The SILVA ribosomal RNA gene
711 database project: Improved data processing and web-based tools. Nucleic Acids Res 41: 590–596.

712 Rieck, A., Herlemann, D.P.R., Jürgens, K., and Grossart, H. (2015) Particle-Associated Differ from Free-Living
713 Bacteria in Surface Waters of the Baltic Sea. Front Microbiol 6: 1297.

714 Roth Rosenberg, D., Haber, M., Goldford, J., Lalzar, M., Aharonovich, D., Al-Ashhab, A., et al. (2021) Particle-
715 associated and free-living bacterial communities in an oligotrophic sea are affected by different
716 environmental factors. Environ Microbiol 23: 4295–4308.

717 Simon, H.M., Smith, M.W., and Herfort, L. (2014) Metagenomic insights into particles and their associated
718 microbiota in a coastal margin ecosystem. Front Microbiol 5: 466.

719 Simon, M., Grossart, H.P., Schweitzer, B., and Ploug, H. (2002) Microbial ecology of organic aggregates in aquatic
720 ecosystems. Aquat Microb Ecol 28: 175–211.

721 Smith, D.C., Simon, M., Alldredge, A.L., and Azam, F. (1992) Intense hydrolytic enzyme activity on marine
722 aggregates and implications for rapid particle dissolution. Nature 359: 139–142.

723 Stegen, J.C., Lin, X., Fredrickson, J.K., and Konopka, A.E. (2015) Estimating and mapping ecological processes
724 influencing microbial community assembly. Front Microbiol 6: 370.

725 Stegen, J.C., Lin, X., Konopka, A.E., and Fredrickson, J.K. (2012) Stochastic and deterministic assembly processes
726 in subsurface microbial communities. ISME J 6: 1653–1664.

727 Sunagawa, S., Coelho, L.P., Chaffron, S., Kultima, J.R., Labadie, K., Salazar, G., et al. (2015) Structure and function
728 of the global ocean microbiome. Science (80-) 348: 1261359-1–10.

729 Wang, Jianing, Wang, L., Hu, W., Pan, Z., Zhang, P., Wang, C., et al. (2021) Assembly processes and source tracking
730 of planktonic and benthic bacterial communities in the Yellow River estuary. Environ Microbiol 23: 2578–
731 2591.

732 Wang, Y., Pan, J., Yang, J., Zhou, Z., Pan, Y., and Li, M. (2020) Patterns and processes of free-living and particle-
733 associated bacterioplankton and archaeaplankton communities in a subtropical river-bay system in
734 South China. Limnol Oceanogr 65: 161–179.

735 Wu, W., Xu, Z., Dai, M., Gan, J., and Liu, H. (2020) Homogeneous selection shapes free-living and particle-
736 associated bacterial communities in subtropical coastal waters. Divers Distrib 00: 1–14.

737 Yao, Z., Du, S., Liang, C., Zhao, Y., Dini-andreote, F., Wang, K., and Zhang, D. (2019) Bacterial Community Assembly
738 in a Typical Estuarine Marsh. Appl Environ Microbiol 85: e02602-18.

739 Yawata, Y., Carrara, F., Menolascina, F., and Stocker, R. (2020) Constrained optimal foraging by marine
740 bacterioplankton on particulate organic matter. Proc Natl Acad Sci U S A 117: 25571–25579.

741 Zhou, J. and Ning, D. (2017) Stochastic Community Assembly: Does It Matter in Microbial Ecology? Microbiol Mol
742 Biol Rev 81: e00002-17.

743

III. Données supplémentaires

I. Supplementary methods

Temperature (T) and salinity (S) were measured *in situ* using a WTW thermosalinometer. Samples for ammonium, nitrite, nitrate, phosphate and dissolved organic phosphorus (DOP) were filtered by gravity using pre-combusted (4 h, 480°C) Whatman 25 mm GF/F glass-fiber filters. Filtrates were frozen at -20 °C until measurement. Samples for silicate were filtered (0.45 µm, cellulose acetate, Sartorius Minisart) and kept at 4°C. Samples for total particulate phosphorus (TPP) and particulate inorganic phosphorus (PIP), suspended particulate matters (SPM), chlorophyll *a* (Chl*a*) and pheopigments (Pheo) were filtered under low pressure (< 50 mm Hg) on pre-combusted Whatman GF/F filters and filters were stored at -20°C. Filtered volumes varied from 20 to 500 mL depending on turbidity.

The nutrient concentrations (ammonium, nitrite, nitrate and silicate) were measured using segmented flow analysis according to Aminot et al. (2009). TPP and PIP were determined as described in Labry *et al.* (2013) following the methods of Solorzano and Sharp (1980) and Aspila *et al.* (1976), respectively. DOP was analysed according to the alkaline persulfate oxidation procedure (Koroleff, 1983). These methods consist in converting the different phosphorus forms into phosphate, which was quantified with the phosphomolybdate-blue colorimetric reaction (Murphy and Riley, 1962) using either 5 cm cuve and Shimadzu UV 160 spectrophotometer (DOP and phosphate) or segmented flow analysis (TPP and PIP). Particulate organic phosphorus (POP) was determined as the difference between TPP and PIP and expressed in percentage of TPP (%POP). Dissolved inorganic nitrogen (DIN) was calculated as the sum of ammonium, nitrite and nitrate. SPM were measured using pre-weighted combusted GF/F filters. The filters were rinsed with Milli-Q water to remove salts. SPM corresponded to the increase in weight after drying at 70°C for 3 h. Particulate inorganic matter (PIM) corresponded to the weight after 2 h at 480°C. The particulate organic matter (POM) was determined as the difference between the two measurements and expressed in percentage of SPM (%POM). Chl*a* and Pheo were determined by acidification fluorometric procedure in 90% acetone extracts (Holm-Hansen *et al.*, 1965) and the percent of Chla (%Chla) was determined as Chla over Chla and Pheo.

References:

Aminot, A., Kérouel, R., and Coverly, S. (2009) Nutrients in seawater using segmented flow analysis. In Practical Guidelines for the Analysis of Seawater. Wurl, O. (ed). Boca Raton: CRC Press, pp. 143–178.

Aspila, K.I., Agemian, H., and Chau, A.S.Y. (1976) A semi-automated method for the determination of inorganic, organic and total phosphate in sediments. Analyst 101: 187–197.

Holm-Hansen, O., Lorenzen, C.J., Holmes, R.W., and Strickland, J.D.H. (1965) Fluorometric determination of chlorophyll. ICES J Mar Sci 30: 3–15.

Koroleff, F. (1983) Determination of phosphorus. In Methods of Seawater analysis. Grasshoff, K., Ehrhardt, M., and Kremling, K. (eds). Weinheim: Verlag Chemie, pp. 125–139.

Labry, C., Youenou, A., Delmas, D., and Michelon, P. (2013) Addressing the measurement of particulate organic and inorganic phosphorus in estuarine and coastal waters. Cont Shelf Res 60: 28–37.

Murphy, J. and Riley, J.P. (1962) A modified single solution method for the determination of phosphate in natural waters. Anal Chim Acta 27: 31–36.

Solorzano, L. and Sharp, J.H. (1980) Determination of total dissolved phosphorus and particulate phosphorus in natural waters. Limnol Oceanogr 25: 758–760.

II. Supplementary data

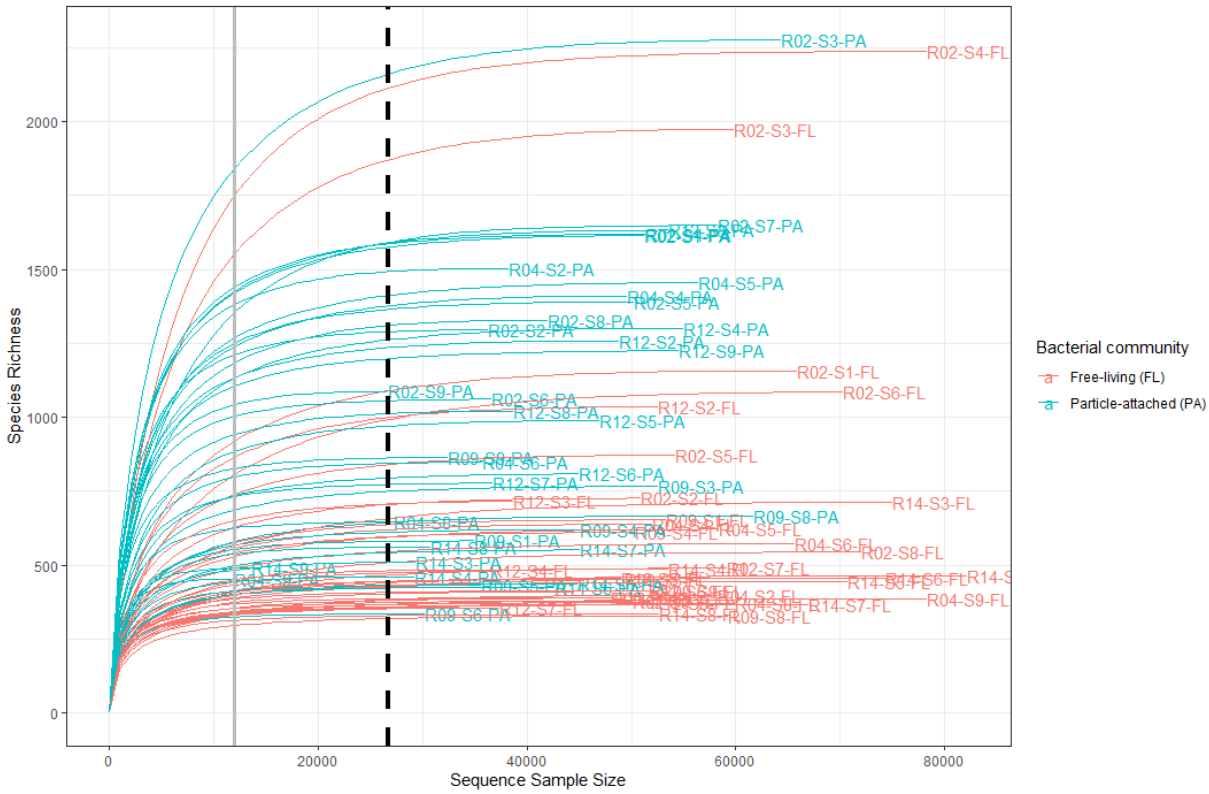

Figure S1. Rarefaction curves of all samples. The grey line represents the minimum sequencing depth while the black dashed line represents the rarefaction depth used, which resulted in two samples loss (R04-S9-PA and R14-S9-PA). Samples are named as "sampling date-sampling station-fraction". R02: February 2019; R04: April 2019; R09: July 2019; R12: November 2019; R14: July 2020; PA: Particle-attached; FL: Free-living.

	Station	Salinity	Temperature (°C)	DIN (µM)	Phosphate (µM)	Silicate (µM)	DOP (µM)	SPM (mg/L)	%POM (%)	Chla (µg/L)	%Chla (%)	%POP (%)
R02 - February 2019	S1	0	6.3	456	0.55	155	0.16	5	42.9	0.29	19	55.5
	S2	0	6.3	454	0.53	155	0.12	4.9	39.8	0.30	19	50.8
	S3	5	6.9	366	0.72	121	0.18	197	15.2	2.12	14	37.8
	S4	10.8	7.4	303	0.74	99	0.17	102.9	16	1.59	17	41.2
	S5	14.7	7.7	258	0.76	84	0.15	40	20.1	1.09	23	41.0
	S6	20.2	8.1	181	0.77	62	0.19	44.6	20.6	0.96	21	40.8
	S7	26	8.4	111	0.64	39	0.2	19.5	24.1	0.76	34	41.9
	S8	29.5	9.0	67	0.57	25	0.13	9.1	29.8	0.68	42	48.9
	S9	33.6	10.0	18	0.48	9	0.13	12.4	26.1	0.75	45	67.4
R04 - April 2019	S2	0	12.7	352	0.28	120	0.25	3.3	37.3	0.76	28	58.2
	S4	9.8	12.7	237	0.75	86	0.24	112.3	14.6	2.97	25	16.0
	S5	15.6	12.6	181	0.92	68	0.25	58.6	15.3	2.13	32	37.8
	S6	20.3	12.5	132	0.64	47	0.29	25.8	18.3	1.75	39	41.8
	S8	30.0	12.3	40	0.24	14	0.28	10.8	28.9	1.70	59	58.5
	S9	34.1	11.6	4	0.08	2	0.25	1.7	73	2.76	63	66.9
R09 - July 2019	S1	0	23.4	207	0.22	120	0.39	6.9	39.7	16.1	69	58.9
	S3	4.4	23.8	198	0.46	104	0.46	42	25.2	26.1	65	40.0
	S4	9.9	23.4	136	1.27	83	0.53	74	18.3	16.7	49	39.4
	S5	15.3	23.4	108	1.33	63	0.45	40	20.5	18.6	61	35.9
	S6	19.6	23.3	72	1.14	47	0.56	24.3	25.7	18.9	65	44.7
	S8	29.5	22.5	25	1.19	17	0.49	17.7	21.6	3.22	52	38.4
	S9	34.7	18.1	0.5	0.16	2	0.32	13.9	26	1.49	54	55.7
R12 - November 2019	S2	0	8.9	420	0.67	158	0.22	9.7	27.1	0.44	18	48.9
	S3	5.5	9.5	330	0.57	122	0.18	55.5	16.3	0.74	15	49.0
	S4	9.8	10.0	281	0.64	106	0.2	24.4	17.3	0.71	23	43.2
	S5	14.6	10.4	221	0.7	87	0.26	23.4	18.9	0.54	23	40.7
	S6	21.1	11.0	147	0.7	61	0.26	19.2	17.2	0.57	30	41.5
	S7	24.7	11.3	105	0.64	45	0.24	11.8	19.1	1.00	49	50.9
	S8	28.8	10.9	62	0.7	29	0.25	7.4	21.1	0.93	57	46.2
	S9	33.3	12.5	18	0.54	10	0.23	4.7	26.3	0.40	28	
R14 - July 2020	S3	4.8	21.4	208	0.66	105	0.39	24.7	25.5	20.7	57	51.9
	S4	9.8	20.8	170	0.69	83	0.67	27.8	24.1	19.0	60	49.3
	S5	15.6	21.0	121	0.52	58	0.48	13.2	34.3	14.2	62	54.1
	S6	20.6	20.5	99	0.52	41	0.48	12.4	31.3	7.78	54	51.9
	S7	25.1	20.6	50	0.46	26	0.52	12.6	19.9	5.65	51	48.7
	S8	29.5	20.1	25	0.32	11	0.43	8.6	23.8	3.87	53	46.5
	S9	34.4	16.7	0.3	0.05	2	0.33	1.8	54.7	2.01	62	72.5

Table S1. Physicochemical variables for all samples. DIN: Dissolved inorganic nitrogen; DOP: Dissolved organic phosphorus; SPM: Suspended particulate matter; %POM: Particulate organic matter (in percent of SPM); Chl*a*: Chlorophyll *a*; %Chl*a*: Chl*a* in percent of total pigments (Chl*a* and Pheopigments); %POP: Particulate organic phosphorus (in percent of total particulate phosphorus).

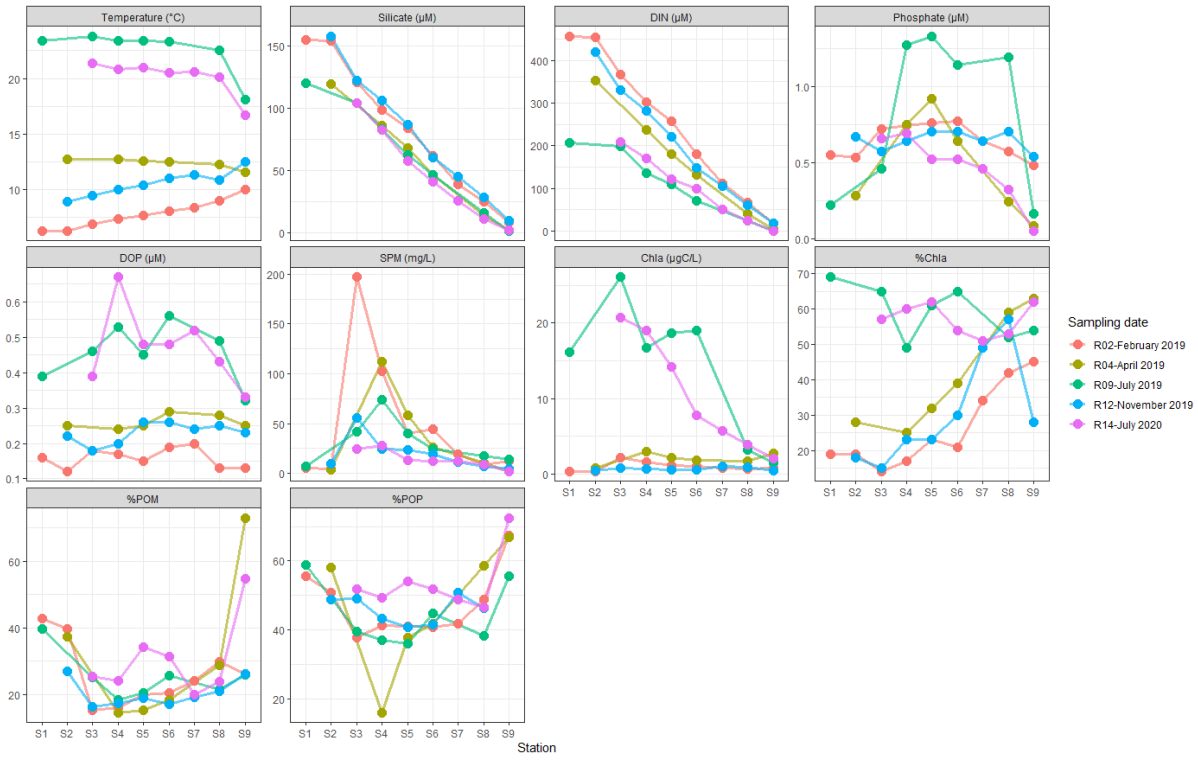

Figure S2. Evolution of the physicochemical variables along the Aulne salinity gradient for all sampling dates.

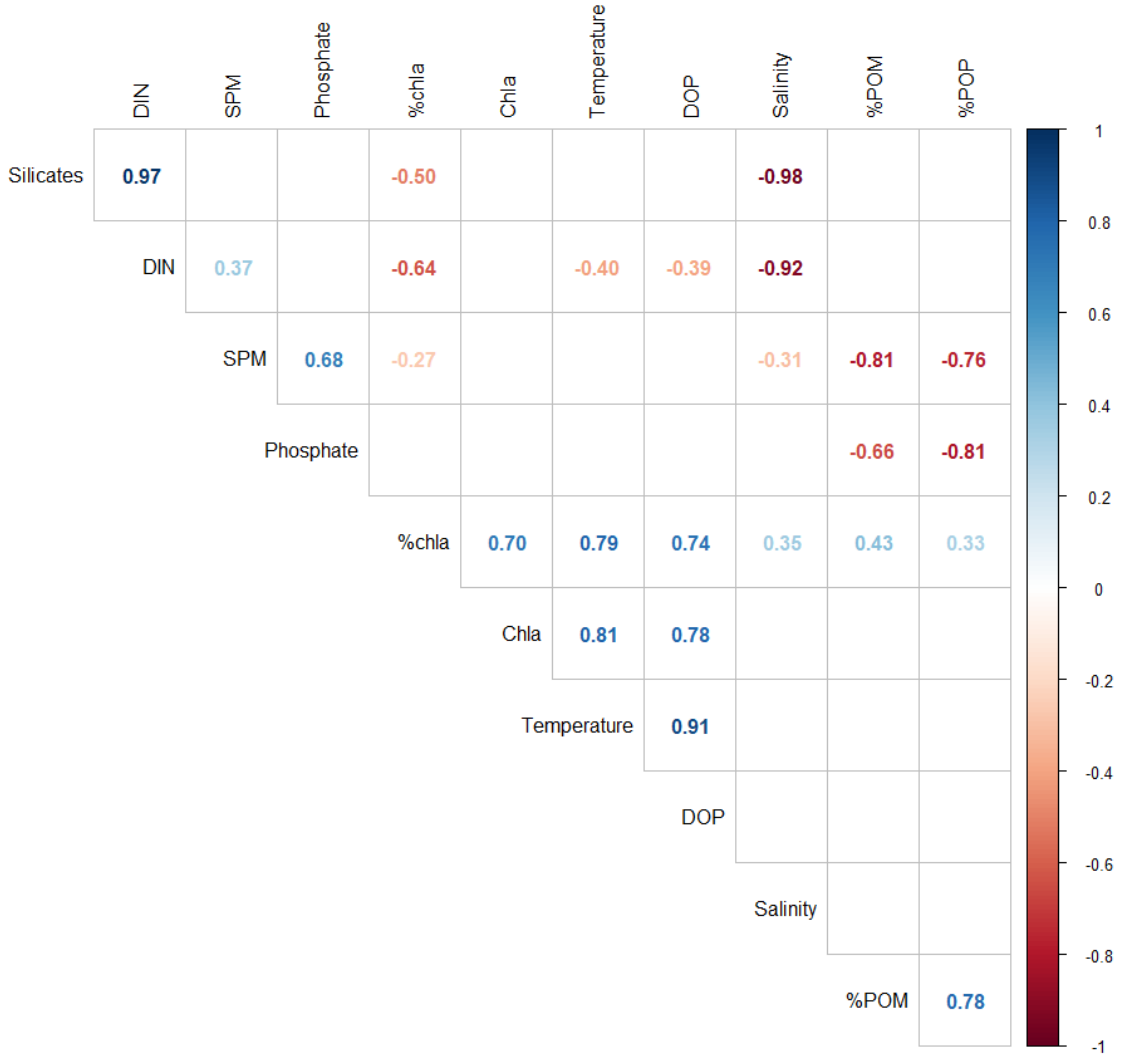

Figure S3. Spearman correlation coefficients of the environmental variables. The variables are grouped according to an "hclust" clustering. Only significant correlations ($p < 0.05$) are displayed.

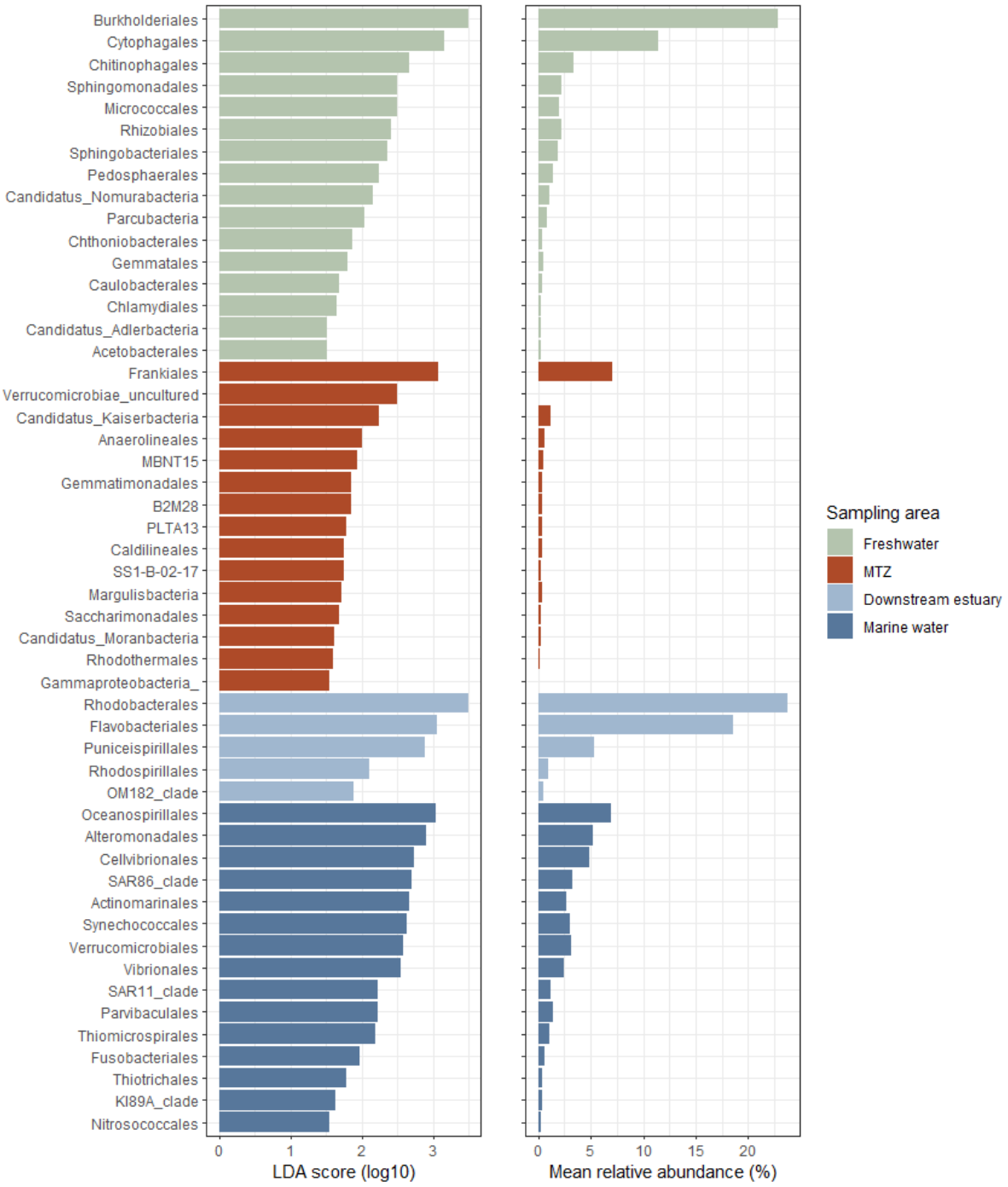

Figure S4. Orders identified by the linear discriminant analysis effect size (LefSe) as most likely to explain the differences between the different areas of the estuary (freshwater, MTZ, downstream estuary, marine water). Left: linear discriminant analysis (LDA) scores; Right: mean abundance in the enriched area.

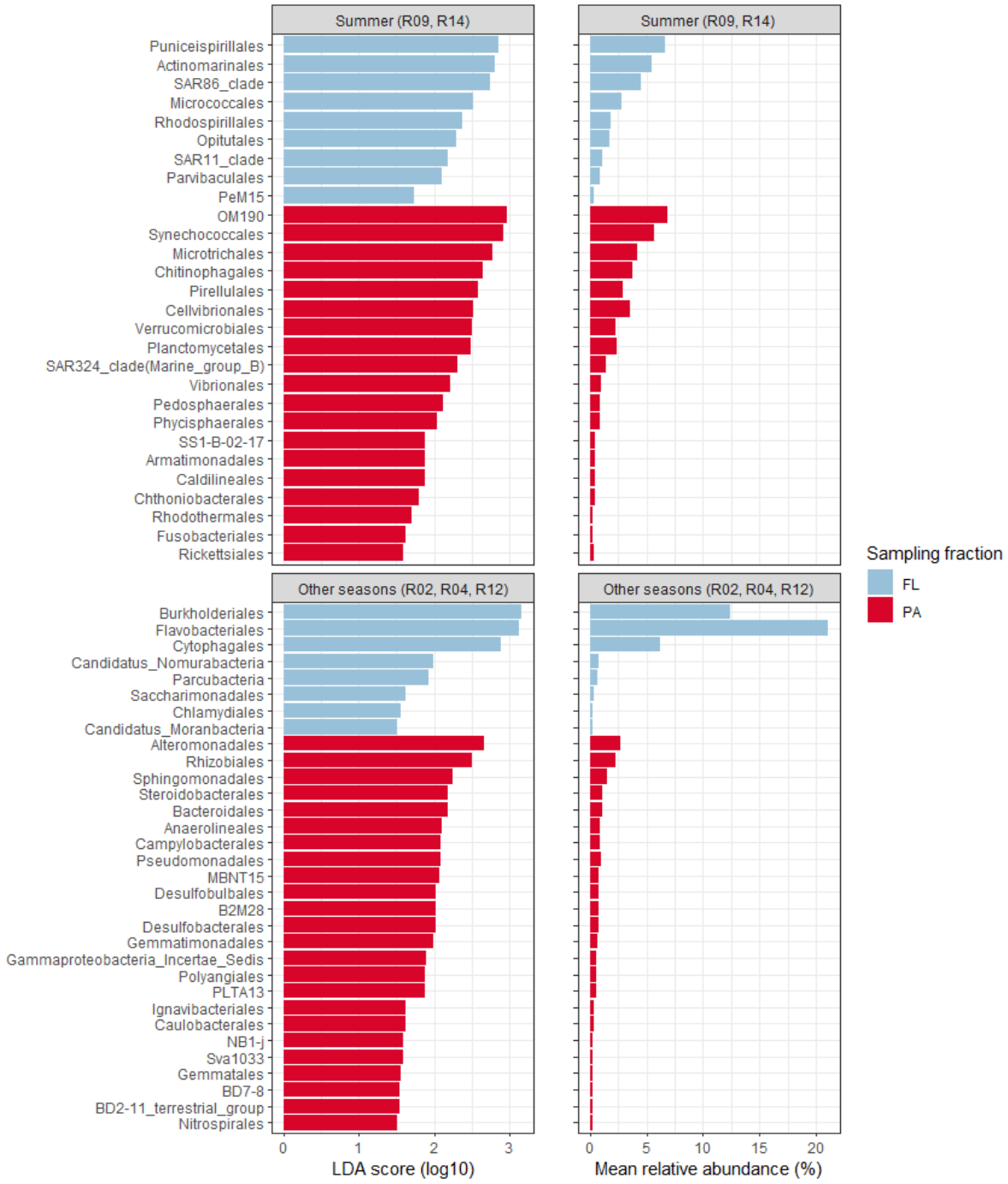

Figure S5. Orders identified by the linear discriminant analysis effect size (LefSe) as most likely to explain the differences between four groups: PA communities in summer, FL communities in summer, PA communities in the other seasons and FL communities in the other seasons. Left: linear discriminant analysis (LDA) scores; Right: mean abundance in the enriched area. Cut-off LDA score: 1.5; cut-off p-value: 0.05.

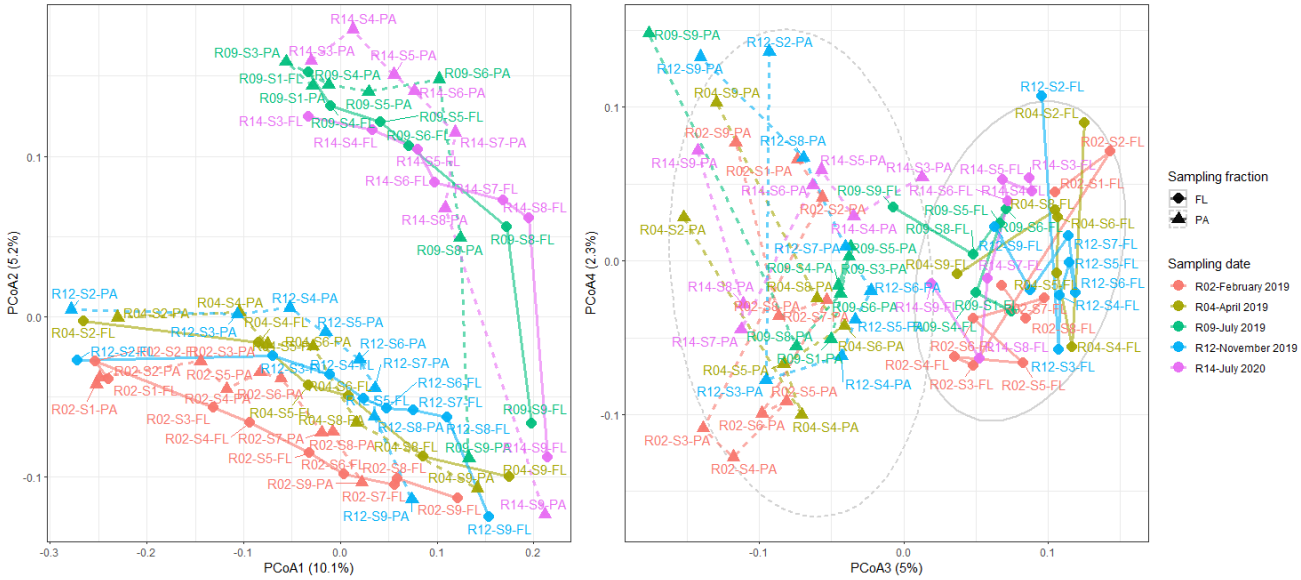

Figure S6. PCoA ordination of all samples based on the abundance-weighted βMNTD (left: axes 1-2; right: axes 3-4). The lines link the different stations within one sampling time in their spatial order (S1 to S9) (full line: FL communities, dashed line: PA communities). Samples are labeled as "sampling date-sampling station-fraction". R02: February 2019; R04: April 2019; R09: July 2019; R12: November 2019; R14: July 2020.

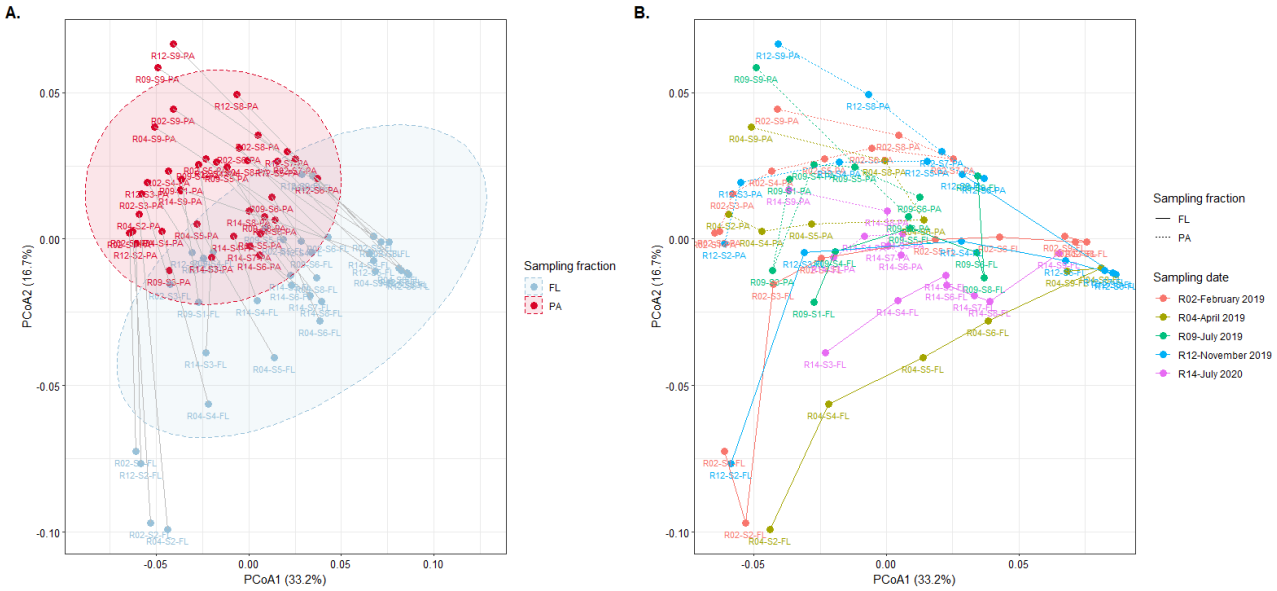

Figure S7. Bray-Curtis-based PCoA on FL and PA communities' inferred metagenomics pathways. The two plots represent the same ordination. (**A**) the two bacterial fractions (FL and PA) are highlighted and the grey lines link the FL and PA communities among one sample. The ellipses on the left panels represent the 95% confidence interval for the PA and FL fractions. (**B**) The five sampling dates are highlighted and the lines represent the path between the different stations within one sampling time (full line: FL communities, dashed line: PA communities). Samples are labeled as "sampling date-sampling station-fraction". R02: February 2019; R04: April 2019; R09: July 2019; R12: November 2019; R14: July 2020; PA: Particle-attached; FL: Free-living.

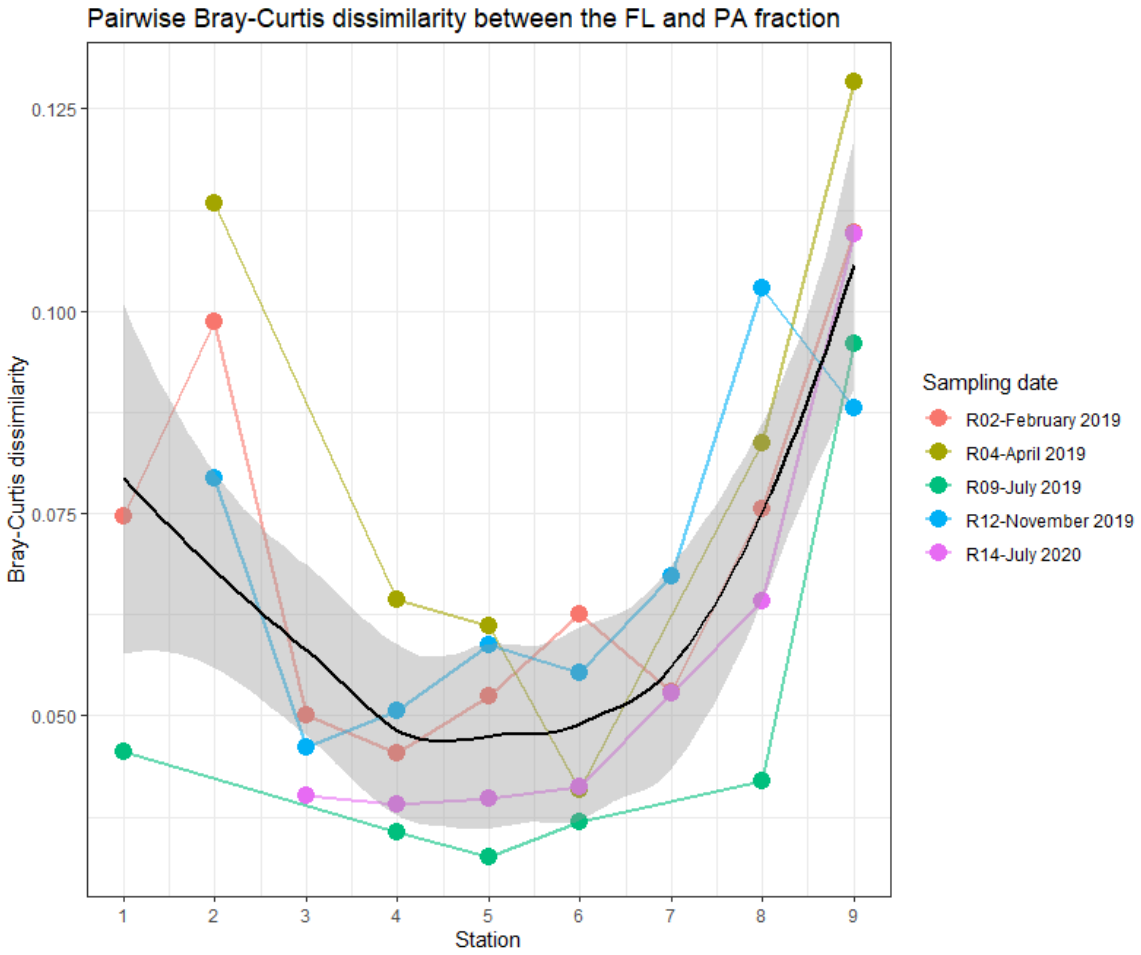

Figure S8. Pairwise Bray-Curtis dissimilarity between the FL and PA inferred metagenome pathways for each sample. The black line represents the loess regression curve and the dark area its confidence interval. R02: February 2019; R04: April 2019; R09: July 2019; R12: November 2019; R14: July 2020.

Chapitre IV*. Evolutions spatiotemporelles des activités enzymatiques dans l'estuaire de l'Aulne et facteurs de régulation*

I. Introduction

L'estuaire de l'Aulne présente des niveaux d'activités des phosphatases alcalines importants qui résultent principalement des bactéries fixées sur les particules estuariennes. Ces activités intenses sont surprenantes compte tenu de la présence de teneurs élevées en phosphate. Cela soulève une question : **quels sont les facteurs et mécanismes régulant les activités phosphatasiques dans l'estuaire et qu'en est-il des autres activités enzymatiques, liées notamment aux cycles du carbone et de l'azote** ?

Nous nous sommes intéressés aux variations spatiotemporelles et aux facteurs régulant les phosphatases alcalines (PA), les leucine-aminopeptidases (LAM) et les β-glucosidases (GLU) des bactéries libres et attachées de l'estuaire de l'Aulne et des eaux côtières adjacentes. Un suivi mensuel a été réalisé le long du gradient de salinité pendant un an, durant lequel plusieurs paramètres biologiques (abondance bactérienne, production bactérienne et activités enzymatiques dans les fractions libre et attachée) et physicochimiques (e.g., matières en suspension, phosphore dissous et particulaire, sucres dissous et particulaires, protéines dissoutes et particulaires, nutriments, chlorophylle *a*) ont été mesurés.

Les résultats montrent que l'estuaire est partagé en trois zones distinctes : i) la zone d'eau douce, caractérisée par une dominance des bactéries libres et un niveau d'activité des PA et des GLU relativement important ; ii) la zone du bouchon vaseux contenant une majorité de bactéries attachées avec de forts niveaux d'activité liés aux LAM, GLU et PA, dont la proportion varie selon la saison ; et iii) les stations en aval de l'estuaire, avec une dominance des bactéries libres et de l'activité des LAM. Ces différences de patrons spatiaux et temporels entre les activités hydrolytiques s'expliquent par l'implication de différents facteurs dans leur régulation. Par exemple, les PA et GLU des communautés attachées sont plus influencées par la quantité de matière particulaire et la composition des communautés bactériennes que les LAM, qui suivent principalement une évolution saisonnière. En contraste, les activités hydrolytiques des communautés libres semblent principalement régulées par des facteurs saisonniers ainsi que par la composition de la matière organique pour les GLU et les PA.

Ce chapitre est présenté sous forme d'une publication pour une future soumission à un journal scientifique.

II. Article 2 : Spatiotemporal dynamics and determinants of hydrolytic enzyme activities and bacterial production in the free-living and particle-attached bacterial communities of a temperate macrotidal estuary

Marion Urvoy[1,2,*], Daniel Delmas[1], Christophe Lambert[2], Emilie Rabiller[1], Stéphane L'Helguen[2], Claire Labry[1,*]

[1]Ifremer, DYNECO, F-29280 Plouzané, France

[2]Université de Bretagne Occidentale, CNRS, IRD, Ifremer, UMR 6539, Laboratoire des Sciences de l'Environnement Marin (LEMAR), F-29280 Plouzané, France

[*]Correspondence: marion.urvoy@outlook.fr, claire.labry@ifremer.fr

Running title

Factors regulating hydrolytic enzymes in a macrotidal estuary

Keywords

Hydrolytic enzymes, bacterial production, free-living, particle-attached, bacterial community composition, Aulne estuary, partial least squares modeling

Abstract

Extracellular hydrolytic enzymes play a major role in the oceans. They allow heterotrophic bacteria to assimilate high molecular weight organic matter, thus supporting overall bacterial metabolism. However, the factors driving their synthesis are not fully characterized, especially regarding the relative influence of abiotic factors and bacterial community composition (BCC). This study aimed to describe the bacterial production and hydrolytic enzymatic activities spatiotemporal variations within the Aulne estuary (Bay of Brest, France) and determine their controlling factors. To this end, various physicochemical variables related to nutrients, dissolved and particulate organic matter were measured monthly for a year. Bacterial abundance (BA), bacteria production (BP), alkaline phosphatase (AP), β-glucosidase (GLU) and leucine aminopeptidase (LAM) activities were monitored in the dissolved (for AP), free-living and particle-attached fraction. The BCC was determined in four contrasting periods. Our results showed that the Aulne estuary acted like a natural bioreactor hosting high bacterial rates, especially in the particulate fraction. The estuary was divided into three distinct areas: i) the freshwater stations, dominated by free-living bacteria with a relatively high proportion of AP and GLU activities; ii) the maximum turbidity zone, characterized by intense particle-attached activities whose enzyme synthesis varied depending on the season; and iii) the downstream stations, dominated by free-living bacteria and LAM activities. These different patterns resulted from different controlling factors. LAM activities were mostly impacted by seasonal factors, either directly or indirectly, and seemed functionally redundant. AP and GLU activities resulting from free-living bacteria were more related to dissolved organic matter concentration, while the BCC strongly controlled AP and GLU activities in the particulate fraction. Overall, our results shed light on the factors regulating bacterial metabolism within the Aulne estuary, highlighting that bacterial communities heavily impact the organic matter and nutrients exported to the adjacent bay of Brest.

Introduction

Heterotrophic bacteria play a central role in biogeochemical carbon and nutrient cycling in the oceans (Azam and Malfatti, 2007; Arnosti, 2011). They produce various extracellular hydrolytic enzymes to cleave polymeric organic matter into low molecular weight compounds that can be transported into the cells and metabolized (Chróst, 1990; Arnosti, 2011). This hydrolysis step is considered limiting in the utilization of organic matter by bacterial communities (Arnosti, 2011). Thus, any factor affecting hydrolytic activities ultimately affects bacterial community functioning and the entire mineralization pathway (Chróst, 1990; Arnosti, 2011).

Extracellular hydrolytic enzymes exist as cell-bound enzymes, associated with the cell wall or the periplasmic space of the cells, or as cell-free enzymes dissolved in the surrounding water (Chróst, 1990). Cell-bound enzymes hydrolyze polymeric substrates that cannot penetrate the cytoplasm, yielding readily utilizable monomers nearby the enzyme-producing cell. In contrast, dissolved enzymes can hydrolyze organic matter away from the cell. They are actively secreted by bacteria or passively released due to viral lysis, grazing or starvation, among others (Baltar, 2018). Dissolved enzymes can make up a substantial proportion of total enzymatic activity, potentially leading to an uncoupling of hydrolysis and bacterial uptake (Baltar, 2018; Baltar *et al.*, 2019; Thomson *et al.*, 2019).

Hydrolytic enzyme activity levels result from a combination of genetic potential, determined by the bacterial community composition (BCC), and the differential expression of this potential. Different bacterial communities may have different hydrolytic capacities depending on the presence of taxonomic groups well-equipped to assimilate specific compounds (Fernández-Gómez *et al.*, 2013; Zimmerman *et al.*, 2013; Ferrer-González *et al.*, 2021). In return, changes in substrate composition, thus in hydrolytic demands, can shape the BCC (Teeling *et al.*, 2012; Landa *et al.*, 2016; Logue *et al.*, 2016). Hydrolytic enzyme production is also tightly regulated at the transcriptional level. Most enzymes synthesized by aquatic microorganisms are inducible enzymes whose synthesis is upregulated in the presence of their substrate, until this substrate disappears or the end-product accumulates (Chróst, 1990). Consequently, nutrient levels and organic matter concentration and composition are key variables driving hydrolytic enzyme synthesis. Dissolved enzymes activity levels are further affected by factors impacting their distribution (such as physical advection processes) or lifetime (e.g., protease levels or UV irradiations, which can degrade them) (Chróst, 1990; Baltar, 2018).

Despite their broad biogeochemical implications, we still lack knowledge about the factors controlling bacterial extracellular enzyme activities in marine environments (Arnosti, 2011, 2014). For instance, the relative influence of BCC versus differential expression on extracellular hydrolytic levels remains to be determined. Indeed, some studies have reported a low impact of BCC on bacterial communities' functions (e.g., hydrolytic enzymes synthesis, bacterial production) (Langenheder *et al.*, 2005; Comte and Del Giorgio, 2010; Lindström *et al.*, 2010), while others have shown a close

relationship between them (Bertilsson *et al.*, 2007; Boucher and Debroas, 2009; Delgado-Baquerizo *et al.*, 2016; Logue *et al.*, 2016). These conflicting results can be explained by the existence of functional redundancy, i.e., different species performing the same function (Allison and Martiny, 2008; Louca *et al.*, 2018). In this context, integrated studies of organic matter composition, bacterial hydrolytic activities and BCC may give valuable insights into microbial organic matter transformations.

Estuaries are crucial land-sea transition zones and are among the most biologically active areas of the biosphere. They contain important organic matter concentrations resulting from both allochthonous (e.g., terrestrial run-offs, marine inputs) and autochthonous processes (e.g., inner estuarine microbial dynamics) (Bianchi, 2011; Bauer *et al.*, 2013). The mixing between fresh and marine waters and strong hydrodynamic forcings result in pronounced environmental gradients that affect the estuarine BCC, function and lifestyle (i.e., free-living or particle-attached). These forcings can notably generate maximum turbidity zones (MTZ), hosting highly active particle-attached bacterial communities (Servais and Garnier, 2006; Middelburg and Herman, 2007; Crump *et al.*, 2017). The extensive organic matter transformation within estuaries has important biogeochemical repercussions for the entire coastal ecosystem (Middelburg and Herman, 2007; Bianchi, 2011). In particular, the Aulne estuary (Bay of Brest, France) was shown to possess intense alkaline phosphatases (AP) and bacterial production (BP) rates (Labry *et al.*, 2016). Such AP activity levels are surprising in this phosphate-replete estuary (Roger Delmas and Tréguer, 1983; Labry *et al.*, 2016) given that AP synthesis is usually induced under limiting phosphate concentration (< 0.1 µM) (Nausch, 1998; Hoppe, 2003; Labry *et al.*, 2005). The spatiotemporal dynamics and determinants of AP and other hydrolytic enzymes related to different biogeochemical cycles have not been characterized thus far.

This study aims to: (1) Characterize the spatial and temporal variations in the free-living and particle-attached heterotrophic bacterial communities within the Aulne estuary water column in terms of bacterial abundance, bacterial production and hydrolytic activity levels; (2) Determine the environmental factors controlling bacterial production and enzymatic activities in the free-living and particle-attached fractions; (3) Determine the relative contribution of environmental factors and BCC in regulating bacterial production and enzymatic activities. To this end, the Aulne estuary was monitored every month for a year along its salinity gradient. AP, β-glucosidases (GLU) and leucine-aminopeptidases (LAM) activities, related to phosphorus, carbon and nitrogen cycles, were assayed. The free-living and particle-attached BCC was examined during four contrasted periods (Urvoy *et al.*, in prep., **Chapitre III**). The relationships between bacterial dynamics, BCC and physicochemical variables were analyzed with the hypothesis that free-living bacteria would be mainly impacted by nutrients and dissolved organic matter (DOM), while particle-attached bacteria would be mainly impacted by particulate organic matter (POM). In addition, we hypothesized that salinity (as a

reflection of water masses mixing) and temperature (as a reflection of seasonality) would be the main drivers of both bacterial and physicochemical variables.

Materials and methods

Study site

The Aulne river drains an area of approximately 1800 km^2 characterized by intense agricultural activities and supplies 63% of the semi-enclosed Bay of Brest freshwater inputs (Auffret, 1983). The Aulne estuary is a temperate macrotidal estuary approximately 30 km long from the Guily Glaz Dam to the river mouth, limiting the tidal influence upstream. The river flow regime (**Table 1**) is constrained by a temperate oceanic climate, generating markedly higher precipitations in winter (Roger Delmas and Tréguer, 1983). As a result, 60% of the annual flow occurs between December and March. The important semi-diurnal tidal amplitude (between 1.2 m and 7.5 m) results in intense water depth variations within the estuary, affecting particulate matter resuspension and deposition. The water residence time within the estuary is dependent on river flow and tidal range and varies between 3 and 30 days (Bassoullet, 1979).

Table 1. Sampling dates and their associated tidal coefficient, river flow and mean water temperature. (*) Dates when diversity was sampled. Flow data were retrieved from http://www.hydro.eaufrance.fr/ at the Châteaulin station (J3821820).

Name	Sampling Date	Season	Tidal coefficient	Flow ($m^3 s^{-1}$)	Mean Temperature (°C)	Comments
R01	January 24	Winter	106	21.9	7.8	
R02	February 20	Winter	110	44.6	7.8	(*)
R03	March 25	Spring	90	24.4	11.0	
R04	April 18	Spring	97	18.1	12.4	(*) S1 was not sampled due to navigation constraints
R05	May 20	Spring	93	10.0	16.0	
R06	June 18	Summer	82	8.3	17.2	An additional station was sampled at salinity 0.2 (named S2.5)
R07	June 25	Summer	42	6.1	18.7	Neap tide
R08	July 11	Summer	58	1.2	23.2	Neap tide
R09	July 18	Summer	78	2.2	22.7	(*) S2 was not sampled du to a high salinity at the usual sampling point (> 4). An additional station was sampled in remplacement (7.7 of salinity, named S3.5)
R10	September 3	Summer	102	2.2	18.8	
R11	September 30	Autumn	116	5.1	17.0	
R12	November 14	Autumn	87	90.0	10.4	(*)
R13	December 16	Winter	79	112.0	9.8	

Sampling strategy

The samplings were carried out monthly from January to December 2019 during spring tide, and two additional samplings were performed at neap tide in June and July (**Table 1**). The surface water was collected in nine stations spread over the salinity gradient (**Figure 1**). Station 1 (S1) was a freshwater reference upstream from the Guily Glaz dam and was not subjected to tidal influence. Station 2 (S2) corresponded to a freshwater station (salinity of 0) under tidal influence collected at a fixed location in front of the dam. Station 3 to 8 (S3-S8) were collected every 5 salinity units (from salinity 5 to 30), monitored using a WTW thermosalinometer. Consequently, their location was variable and depended on tide and water discharges. Finally, station 9 (S9) was a marine reference sampled at the SOMLIT (Service d'Observation en Milieu Littoral, https://www.somlit.fr/) station of St Anne-du-Portzic (48°21'32.17'' N, 4°33'07.21'' O, salinity 33.3 to 34.8). S9 was first sampled at high tide and processed immediately to avoid prolonged boat time. Sampling was then carried out from S1 to S8, within two hours. Samples were collected with a bucket and stored in 5-L carboys (Nalgene) in the dark until return to the lab, where they were processed immediately.

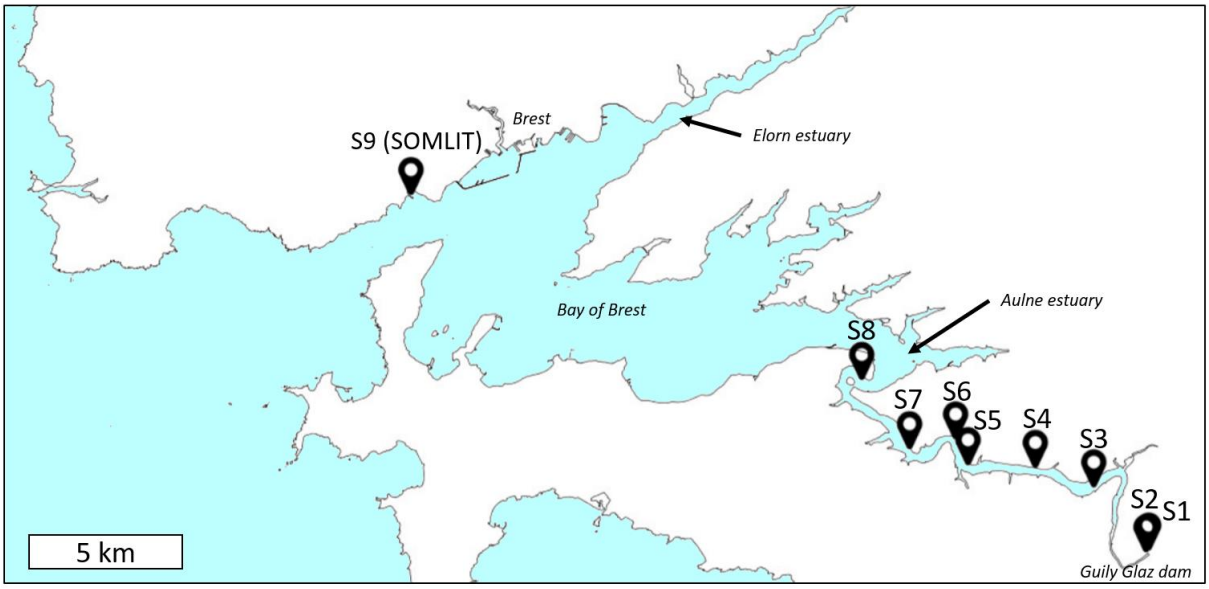

Figure 1. Map of the Bay of Brest and the Aulne estuary. Freshwater (S1, S2) and marine water (S9) stations were collected at fixed locations while the other stations depended on the salinity. The May (R05) sampling locations are indicated as an example.

Physicochemical variables

Temperature and salinity were measured *in situ* using a WTW thermosalinometer. Samples for dissolved inorganic nutrients (ammonium, nitrite, nitrate, phosphate) and dissolved organic compounds [dissolved organic carbon (DOC), dissolved monosaccharides (DMCHO), dissolved polysaccharides (DPCHO), dissolved free amino acid (DFAA), dissolved combined amino acids (DCAA)

and dissolved organic phosphorus (DOP)] were filtered by gravity using pre-combusted (4 h, 480°C) filters (Whatman GF/F, 47 mm). Filtrates were frozen at -20 °C, except for DOC samples that were kept at 4°C until measurement, which was done the same day. Silicate samples were filtered (0.45 µm, cellulose acetate, Sartorius Minisart) and kept at 4°C. Samples for particulate matter variables [total particulate phosphorus (TPP), particulate inorganic phosphorus (PIP), particulate proteins, particulate organic carbon (POC), particulate organic nitrogen (PON), particulate soluble carbohydrates (PSCHO), particulate insoluble carbohydrates (PICHO), suspended particulate matters (SPM), particulate inorganic matter (PIM), chlorophyll *a* (Chl*a*) and pheopigments (Pheo)] were filtered under low pressure (< 50 mm Hg) and the filters (pre-combusted, Whatman GF/F, 25 mm) were stored at -20°C. Filtered volumes varied from 20 to 500 mL depending on turbidity. All measured physicochemical variables are listed in **Table 2** with their corresponding abbreviation. All analysis protocols are described in the supplementary material and methods.

Table 2. Physicochemical variables measured during the study, and their abbreviations. Composite variables (resulting from a combination of several parameters) are also indicated.

	Variable	Abbreviation	Composite variable
	Temperature		
	Salinity		
Nutrients	Ammonium		
	Nitrite		
	Nitrate		
	Phosphate		
	Silicate		
DOM	Dissolved organic carbon	DOC	
	Dissolved organic phosphorus	DOP	
	Dissolved monosaccharides	DMCHO	DPCHO/DMCHO: Dissolved poly- to monosaccharides ratio, DCHO/DAA: Ratio of the sum of DPCHO and DMCHO to the sum of DFAA and DCAA
	Dissolved polysaccharides	DPCHO	
	Dissolved free amino acid	DFAA	DCAA/DFAA: Dissolved combined to free amino acids ratio
	Dissolved combined amino acids	DCAA	
POM	Suspended particulate matter	SPM	
	Particulate inorganic matter	PIM	
	Particulate organic matter	POM	%POM: Percent of POM in SMP, as a marker of POM organic content and lability
	Total particulate phosphorus	TPP	
	Particulate inorganic phosphorus	PIP	
	Particulate organic phosphorus	POP	POC/POP: POC to POP ratio, as a marker of POM degradation
	Particulate organic carbon	POC	
	Particulate organic nitrogen	PON	POC/PON: POC to PON ratio, as a marker of POM origin and degradation
	Particulate amino acids	PAA	PAA/SPM: ratio of PAA to SPM
			PCHO/PAA: sum of PSCHO and PICHO to PAA ratio
	Particulate soluble carbohydrates	PSCHO	I/S: Ratio of PICHO to PSCHO, as a marker of POM degradation
	Particulate insoluble carbohydrates	PICHO	PCHO/SPM: sum of PSCHO and PICHO to SPM ratio
	Chlorophyll *a*	Chl*a*	%Chl*a*: Percent of Chl*a* in Chl*a* and Pheo as a marker of phytoplankton development and POM lability
	Pheopigments	Pheo	

Several additional composite variables were derived from these measurements, described in **Table 2**. In the dissolved fraction, DPCHO/DMCHO and DCAA/DFAA were used to assess the relative importance of high to low molecular weight dissolved carbohydrates and amino acids, respectively. DCHO/DAA

was used to assess the relative importance of carbohydrates and amino acids. In the particulate fraction, %POM was used as a marker of SPM organic content and by extension, lability. POC/POP and POC/PON were considered markers of POM origin and degradation. %Chl*a* was used to assess the physiological state of phytoplankton communities and was thus also considered an indirect marker of POM lability. I/S is a marker of POM degradation (Delmas, 1983). I/S decreases during phytoplankton growth due to the relative increase of PSCHO, which are glucose-containing reserve polysaccharides that accumulate inside phytoplankton cells. I/S increases during POM degradation with the relative increase of PICHO, corresponding to structural carbohydrates associated with the phytoplankton cell wall (Delmas, 1983; Labry *et al.*, 2020). PAA/SPM and PCHO/SPM represented particulate matter content in amino acids and carbohydrates, respectively. Finally, PCHO/PAA represented the relative importance of carbohydrates to amino acids in POM.

Bacterial variables

All bacterial variables (abundance, production and enzymatic activity, listed in **Table 3**) were quantified from the same total or size fractioned (< 3 µm) samples to avoid sampling bias.

Table 3. Bacterial variables measured during the study and their abbreviations.

Fraction	Variable	Abbreviation
Dissolved (< 0.2 µm)	Alkaline phosphatase	AP < 0.2 µm
Free-living (0.2-3 µm or < 3 µm)	Bacterial abundance	BA < 3 µm
	Bacterial production	BP < 3 µm
	Leucine aminopeptidase	LAM < 3 µm
	Glucosidases	GLU < 3 µm
	Alkaline phosphatase	AP 0.2-3 µm
	Bacterial community composition	BCC < 3 µm
Particle-attached (> 3 µm)	Bacterial abundance	BA > 3 µm
	Bacterial production	BP > 3 µm
	Leucine aminopeptidase	LAM > 3 µm
	Glucosidases	GLU > 3 µm
	Alkaline phosphatase	AP > 3 µm
	Bacterial community composition	BCC > 3 µm

Bacterial abundance

Free-living and total bacteria (including free-living and particle-attached bacteria) were quantified using flow cytometry. Free-living bacteria were measured after 3-µm filtration (Whatman Nuclepore polycarbonate). Total bacteria were quantified on whole water samples after a desorption step to release particle-attached bacteria (adapted from Carreira *et al.*, 2015). Samples were fixated using 0.25% of glutaraldehyde and 0.01% of Poloxamer 188 for 15 min at ambient temperature in the dark (Marie *et al.*, 1999). All samples were amended with 0.5 M ethylenediaminetetraacetic acid at a final concentration of 0.1 M to destroy cation links between EPS polymers and particles (Carreira *et al.*,

2015). Samples for free-living bacteria were then directly frozen at - 20°C. Samples for total bacteria were incubated for 1 h in the dark at ambient temperature and subsequently desorbed from particles using 3 cycles of sonication (10 s on, 10 s off) on ice (Bioblock Scientific Vibracell 72442 probe, 20 % amplitude) and frozen at – 20 °C until analysis (adapted from Carreira *et al.*, 2015). For flow cytometry, samples were thawed, appropriately diluted in autoclaved 0.2 µm filtrated seawater and labeled with SYBR Green I (1:10,000 dilution of stock solution) for 10 min in the dark (Marie *et al.*, 1999). The acquisition was performed in triplicate on a FACS Verse cytometer with a threshold on SYBR Green I fluorescence. Particle-attached bacterial abundance was determined as the difference between total and free-living bacterial abundance (BA < 3 µm). For ease of reading, particle-attached bacterial abundance was abbreviated "BA > 3 µm" even though it does not strictly correspond to the abundance in the > 3 µm fraction.

Bacterial production

Bacterial production (BP) was measured on total and size fractioned samples (< 3 µm) using the ^{3}H-methyl-thymidine incorporation method (Fuhrman and Azam, 1982). Triplicate samples and trifluoroacetic acid (TCA)-killed controls (5% final concentration) were incubated with 40 nmol L^{-1} of ^{3}H-methyl-thymidine (20 Ci $mmol^{-1}$, Perkin Elmer) at *in situ* temperature for 1 h to 4 h (depending on the season). The rate of ^{3}H-methyl-thymidine incorporation into DNA was converted into cell production using 2.18 x 10^{18} cells per mole of thymidine incorporated (Fuhrman and Azam, 1982). Bacterial carbon production was estimated assuming a carbon cell content of 16 fgC. Particle-attached bacterial production (BP > 3 µm) was determined as the difference between total and free-living bacterial production (BP < 3 µm).

Extracellular enzymatic activities

AP, GLU and LAM potential activities were determined using the commonly used model fluorogenic substrates 4-methylumbelliferyl phosphate, 4-methylumbelliferyl β-D-glucopyranoside and L-leucine-7-amino-4-methylcoumarin. Briefly, 2 mL of total or size fractioned (< 3 µm) samples were incubated in the dark at *in situ* temperature for 4 to 8 h (depending on the season) with saturating substrate concentration (respectively, 250, 150 and 1000 µM). Since saturating substrate concentrations were used, the measured activities correspond to potential maximum activity rates and reflect enzyme concentrations (Chróst, 1990). At the end of the incubations, the different reactions were stopped by adding 200 µL of NH_4-glycine buffer (0.2 M NH_4, 0.05 M glycine, pH 10.5) for GLU (Chróst, 1989); 450 µL of buffered formalin (0.05 M tetraborate, 18 % formalin, pH 8.0) for AP (Labry and Urvoy, 2020); or 200 µL of 10% sodium dodecyl sulfate for LAM (Delmas and Garet, 1995) and immediately frozen until analysis. In addition, dissolved AP activities were determined using 0.2-µm filtrated samples (Whatman Nuclepore polycarbonate) as they were found to represent a significant proportion of total AP activity (Labry *et al.*, 2016). Dissolved LAM and GLU were not measured as they were found to represent a

minor proportion of total activity (Delmas D., pers. com.). Incubations were performed in duplicates. In addition, one blank for each station was prepared as described above, skipping the incubation step.

Fluorescence was measured using flow injection analysis, a liquid chromatography injection system connected to a Kontron SFM25 fluorescence spectrometer with a 1 mm optic path (Delmas *et al.*, 1994). The carrier fluid was 0.1 M buffered borate solution (pH 10.5) delivered at 1 mL min^{-1}. Excitation and emission wavelength were respectively 364 and 460 nm for methylumbelliferone (MUF)-derived substrates and 380 and 440 nm for 7-amino-4-methylcoumarin (MCA)-derived substrate. The presence of an inner filter effect was checked as described in Urvoy *et al.* (2020) and found negligible with this system. Fluorescence was converted to potential degradation rates using MUF and MCA standards. For each biological replicate, activities were averaged over duplicated readings. The activity of free-living bacteria corresponds to the 3-µm filtrated fraction, minus the dissolved fraction (< 0.2 µm) for AP. The activity of particle-attached bacteria corresponds to the total minus the 3-µm filtrated fraction.

Bacterial community composition

The BCC in the Aulne estuary was examined in four contrasting periods (R02-February, R04-April, R09-July, R12-November, **Table 1**) by sequencing the V3/V4 region of the 16S rRNA gene of particle-attached (> 3 µm) and free-living (0.2-3 µm) communities (Urvoy et al., in prep., **Chapitre III**). All processing steps and bioinformatics analyses were performed as described in Urvoy et al. (in prep., **Chapitre III**). The table of amplicon sequence variants (ASVs) rarefied to minimum sampling depth was used in this study for all subsequent analyses (12 996 ASVs, 11 922 reads per sample).

Statistical analyses

All data were analyzed using the R language (v4.1.0) implemented in Rstudio (v2021.09.0) and displayed with ggplot2 (v3.3.5) unless specified otherwise.

Missing values

The abundance of particle-attached bacteria was determined by subtraction between total bacteria (after a desorption step involving sonication) and < 3 µm bacteria. This process sometimes generated negatives values of particle-attached bacterial abundances downstream of the estuary (S7-S9). This was likely due to the low prevalence of particle-attached bacteria in these stations and a possible cell disruption caused by sonication. These negative values were removed from the dataset (27 missing values out of 117). In addition, GLU values are missing for June samplings (R06 and R07) due to a technical error. Finally, 10 values (out of 117) of DCAA and DFAA are missing due to contaminations during sampling.

Data visualization

All bacterial-, nutrients-, DOM- and POM-related variables were plotted against the salinity gradient. Wilcoxon tests were performed using the stats_compare_means function (ggpubr package, v0.4.0). Principal component analysis (PCA) and Spearman rank coefficients were computed to examine the correlations between the different variables. To this extent, the samples containing missing values were removed, the remaining data were log2 + 1 and z-score (i.e., scaled to unit variance and centered on their mean) transformed. PCAs were performed in FactoMineR (v2.4). Salinity and temperature were included as supplementary variables to facilitate the PCA interpretation. As such, they are projected onto the ordination but do not participate in its construction. In addition, PCAs were performed with and without BA > 3 µm, GLU > 3 µm and < 3 µm, DCAA and DFAA to evaluate the effect of missing samples on the ordinations. Spearman rank coefficients (r_S) (cor function in stats package, v4.1.0) and their associated p-values were computed (cor.mtest function in corrplot package, v0.90) and displayed with Ward D2 hierarchical clustering using the corrplot package.

Link between bacterial activities and environmental factors

The correlation between bacterial activities (BP, GLU, AP and LAM) (respectively, free-living or particle-attached), bacterial abundance (respectively, free-living or particle-attached) and physicochemical variables (respectively, nutrients and DOM or POM) was assessed using the Mantel test based on Spearman correlations (vegan package, 999 permutations). A partial Mantel test was performed to control for the effect of temperature and salinity. To this extent, Euclidean distances (dist function, stats package) were computed for the different datasets containing all variables listed in **Table 2** and **Table 3** (log2 + 1 and z-score transformed).

The link between environmental variables, bacterial abundance and bacterial activities (BP, GLU, AP and LAM) was further investigated using multiple linear regression (MLR, for AP < 0.2 µm) and redundancy analysis (RDA, for free-living and particle-attached bacterial variables). Samples containing missing values were removed and data were log2 + 1 and z-score transformed. Multicollinearity issues were investigated using variance inflation factor (VIF), and the variables with VIF > 10 were removed. MLR was performed using the lm function (stats package). RDA was performed using the rda function in vegan (v2.5.7). The variance explained by the RDA and RDA axes was adjusted (R^2_{adj}). The significance of the overall model and RDA axes were assessed by permutations (1000 permutations, anova.cca function in vegan). For the bacterial variables in the free-living fraction (< 3 µm or 0.2-3 µm for AP), the final explanatory variables included were salinity, temperature, BA < 3 µm, phosphate, ammonium, nitrite, DOP, DPCHO, DPCHO/DMCHO, DFAA and DCAA. The RDA was also run without GLU < 3 µm to test the influence of missing samples. For the bacterial variables in the particulate fraction (> 3 µm), the final explanatory variables were salinity, temperature, BA > 3 µm, SPM, %POM, %Chl*a*, COP/NOP, PAA/SPM, PCHO/PAA, and I/S. Similar, the RDA was also run without i) GLU > 3 µm and ii) GLU > 3 µm

and BA > 3 µm to test the influence of missing values in these variables. The amount of variance in explained by different groups of variables (i.e., salinity, temperature, nutrients, DOM, POM quality, POM quantity) was assessed using variance partitioning (varpart function in vegan).

Finally, partial least squares path modeling (PSL-PM) was used to model the complex relationships between the variables and disentangle their direct and indirect relationships. PSL-PM is a type of structural equation modeling that unites dependent and independent variables into a single network and examines their linear causal relationships. It relies on observed (i.e., directly measured) and latent variables, inferred from several observed variables to represent a wider construct. This approach allows the determination of standardized path coefficients, which quantifies the effect of one variable on another variable (i.e., direct effect). Indirect effects are the product of the multiple paths coefficients present between a predictor and a response variable. PSL-PM was implemented with the pslpm package (v0.4.9). Samples containing missing data were removed. All variables except salinity and temperature were log2 + 1 transformed; all variables were z-score transformed. The negative value of some standardized variables was used to better represent the underlying latent variable and satisfy latent variable unidimensionality (Sanchez, 2013), as annotated on the PLS-PM figures. For instance, the negative value of COP/NOP and I/S, which represent POM degradation, was used to represent POM lability. All variables listed in **Table 2** were initially included, then observed variables with loadings < 0.2 were removed since they poorly contributed to the latent variable construction. Path coefficient, endogenous variable R^2 and loading estimates and significance were computed over 1000 bootstraps. The overall model was assessed using the goodness-of-fit statistic (GOF). The resulting models were plotted using DiagrammeR (v1.0.6.1).

Link between bacterial activities, bacterial community composition and environmental factors

To assess the correlation between bacterial activities (i.e., BP, GLU, AP and LAM), BCC and physicochemical variables, Mantel tests were performed as before, using the Bray-Curtis dissimilarity computed on the ASVs table (vegdist function in vegan). The ASVs were pooled at the class level, retaining only ASVs contributing to more than 0.001% of total abundance. The most abundant bacterial classes were retained, Hellinger (decostand function in vegan) and z-score transformed and used in subsequent analyses. RDA was not performed because the high multicollinearity between the predictors (physicochemical and BCC variables) would bias the analysis. Instead, PCA was used to visualize the correlation between the different datasets by using bacterial variables (BP, GLU, AP and LAM) as active variables and bacterial abundance, BCC and physicochemical variables as supplementary variables (thus, they are projected onto the ordination but do not participate in its construction). PLS-PM was performed as described above with the same variables, except that a latent variable representing BCC was added.

Results

Physicochemical variables

Dissolved fraction

Silicate, nitrate, DOC, DMCHO and DCAA overall followed a conservative mixing behavior throughout the estuary. In contrast, ammonium, nitrite and phosphate deviated from the theoretical dilution curve and mostly showed a net production within the estuary (**Figure S1, S2**). The DPCHO/DMCHO ratio increased in the marine stations (S7-S9), compared to upstream stations, while the DCAA/DFAA ratio followed an opposite trend (**Figure S2**). Consequently, the 1st PCA axis (explaining 44.1% of variance, **Figure 2A**) opposed the most marine stations (S8-S9), characterized by high DPCHO/DMCHO ratio, to freshwater stations (S1-S2), characterized by a high silicate, nitrate, DOC, DMCHO, DCAA and DCAA/DFAA content.

Silicate and nitrate decreased in the summer samplings (R06-R10) while nitrite increased. Phosphate and ammonium also increased in summer, although their temporal pattern was less clear. DOC, DOP, DMCHO, DPCHO, DFAA and DCHO/DAA increased in summer compared to the other seasons while DCAA and DCAA/DFAA decreased. The DPCHO/DMCHO was relatively stable over time. The 2nd PCA axis (21.3% of variance) thus opposed the summer samplings (R06-R10), characterized by higher ammonium, nitrite, phosphate, DOP and DPCHO content, to the other sampling dates.

Particulate fraction

The MTZ, containing high loads of particulate matter, was located in the S3-S4 stations (corresponding to 5-10 salinity) (**Figure S3**). Consequently, variables that represent particulate matter quantity showed a maximum in this area (e.g., SPM, POM, PIM, POC, PON, POP, PIP, PSCHO, PICHO, PAA). Particulate matter was more labile in the end members, as indicated by lower values of I/S and higher values of %POM, PCHO/SPM and PAA/SPM. This is coherent with the retention of processed particulate matter within the MTZ and the resuspension of refractory POM. Accordingly, the 1st PCA axis (explaining 56.3% of variance) opposed the estuarine stations (S3-S6), characterized by high loads of SPM and associated variables (e.g., POC, PON), to the end members (S1-S2, S9) that contained more labile POM (increase of %POM, decrease of I/S, POC/PON) (**Figure 2B**).

The SPM (thus, variables related to POM quantity) decreased during summer (R06-R10) due to less intense hydrodynamic forcings; as well as in R12-R13, most likely due to heavy precipitations that exported SPM to the coastal area (**Table 1**). Summer samplings (R06-R10) were characterized by high Chl*a* and %Chl*a* values, suggesting the presence of phytoplankton cells. However, it remains unclear if it corresponded to living phytoplankton cells given the important turbidity of the estuary that likely limits phytoplankton activity. Compared to other seasons, the summer samplings also contained less degraded POM, with a decrease in I/S and POC/PON. In addition, PCHO/PAA decreased while PAA/SPM

366 increased, suggesting a higher proteinaceous content in summer. Consequently, the 2nd axis (19.3% of
367 variance) opposed the summer samples (R06-R10), characterized by elevated values of markers of
368 phytoplankton development and POM lability (%Chl*a*, Chl*a*, PAA/SPM, %POM), to winter samples
369 (R01-R03, R13), characterized by elevated values of POM degradation markers (I/S, POC/POP,
370 POC/PON).

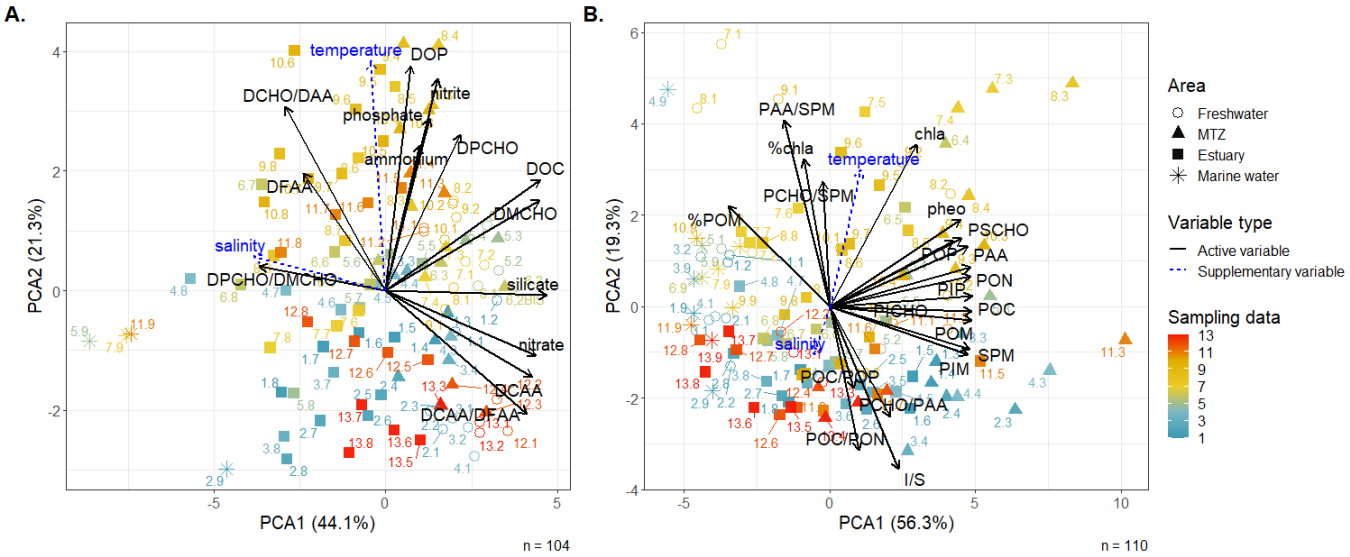

371

372 **Figure 2.** Principal component analysis (PCA) ordination of variable characterizing the dissolved (nutrients and
373 DOM) (**A**) and particulate (**B**) fraction. Blue arrows (temperature and salinity) are supplementary variables added
374 to facilitate PCA interpretation but did not participate in its construction. PCAs were also performed without DCAA,
375 DFAA and DCAA/DFAA due to missing values in these variables, which did not impact their interpretation (**Figure**
376 **S4**). Samples are labeled as "sampling month.sampling station" (e.g., S9 of R02 was labeled "2.9"). n: number of
377 samples.

378 ***Bacterial variables***

379 <u>Spatiotemporal patterns</u>

380 Bacterial variables followed various spatiotemporal patterns, which differed depending on the
381 sampling fraction (**Figure 3, 4**).

382 *i) Dissolved fraction (< 0.2 µm)*

383 Dissolved AP activities were maximum in the freshwater stations (S1-S2) and decreased along the
384 estuarine salinity gradient (correlation with salinity: r_S = - 0.84) (**Figure 3**). This decrease was overall
385 linear, except at the transition between freshwater (S1-S2) and MTZ (S3-S4), where AP < 0.2 µm were
386 removed compared to the theoretical dilution curve (**Figure 3**). AP < 0.2 µm did not exhibit a clear
387 seasonal pattern (r_S with temperature not significant).

388

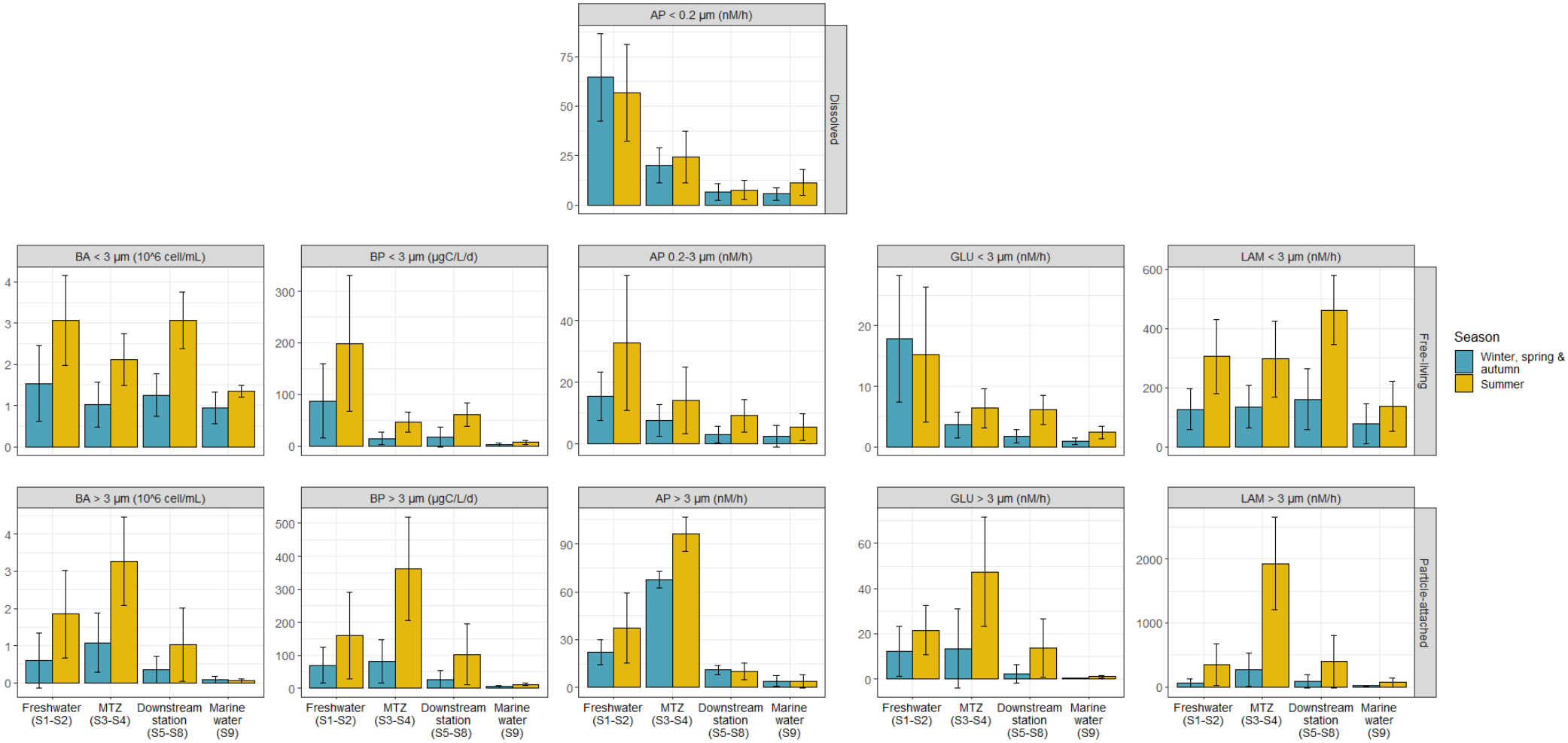

Figure 3. Evolution of bacterial parameters (abundance, bacterial production and enzymatic activities) along the Aulne salinity gradient for winter, spring and autumn (R01-R05, R11-R13) and summer (R06-R10) samplings in the dissolved (< 0.2 µm, top), free-living (0.2-3 µm or < 3 µm, middle) and particle-attached fraction (> 3 µm, bottom). Error bars represent standard deviation.

393 *ii) Free-living bacterial fraction (0.2-3 µm or < 3 µm)*

394 Two types of spatial patterns were visible for the variables related to free-living bacteria (**Figure 3, 4A**,
395 **Figure S6**). BA < 3 µm and LAM < 3 µm decreased in the MTZ (S3-S4) compared to upstream stations
396 (S1-S2); increased in the downstream estuarine stations (S5-S8) to a comparable or higher level than
397 in S1-S2; and decreased at the marine station (S9). This spatial pattern ("*И*" shape) was especially
398 pronounced during summer (R06-R10) (**Figure 3**). In contrast, BP < 3 µm, AP 0.2-3 µm and GLU < 3 µm
399 activities were maximal in the freshwater stations (S1-S2) and decreased along the salinity gradient.
400 All bacterial variables related to the free-living communities followed the same temporal pattern with
401 an increase in summer (R06-R10) compared to the other seasons. However, the temporal variations of
402 BA < 3 µm and LAM < 3 µm were more pronounced than for the other bacterial variables (**Figure 3**),
403 which was traduced by a higher correlation with temperature (**Figure 4A, Figure S9**).

404 Consequently, all activities correlated with the 1st PCA axis (71.1% of variance) opposing the
405 winter and summer samplings (**Figure 4A**). BA- and LAM < 3 µm were separated from AP 0.2-3 µm and
406 GLU < 3 µm along the 2nd PCA axis (17.5% of variance) (**Figure 4A**), the former being driven by high
407 values in summer downstream of the estuary and the latter by elevated values in the freshwater
408 stations in others seasons. BP < 3 µm had an intermediate behavior since it showed both higher values
409 in summer and elevated values in the freshwater stations (**Figure 4A**).

410 *iii) Particle-attached bacterial fraction (> 3 µm)*

411 Bacterial abundance, bacterial production and enzymatic activities related to the particle-attached
412 communities exhibited the same spatial pattern with a maximum in the MTZ (S3-S4) (**Figure 3**). All
413 particle-attached bacterial variables thus correlated positively with the 1st PCA axis that opposed the
414 MTZ stations (S3-S4) to the end-members (S1-S2, S9) and explained most of the variance (81.7%)
415 (**Figure 4B**).

416 Two groups of bacterial variables could be distinguished based on their temporal patterns. BA-
417 , BP- and LAM > 3 µm followed a clear, pronounced seasonal pattern. Coherently, they correlated with
418 temperature (r_S = 0.50, 0.58 and 0.66, respectively, $p < 0.001$). In contrast, AP- and GLU > 3 µm
419 temporal pattern was less pronounced (r_S = 0.46 and 0.22, respectively, $p < 0.001$). For instance, in the
420 MTZ, AP > 3 µm were similar or higher in R02, R04 and R11 (119, 101 and 291 nM/h, respectively) than
421 in R05 or R10 (116 and 87 nM/h, respectively) (not shown). Consequently, these variables were
422 separated along the 2nd PCA axis (7.7% of variance, **Figure 4B**), AP- and GLU > 3 µm being driven by
423 high values in the MTZ (S3-S4) in winter and BA-, BP- and LAM > 3 µm by high values in downstream
424 stations (S6-S7) during summer.

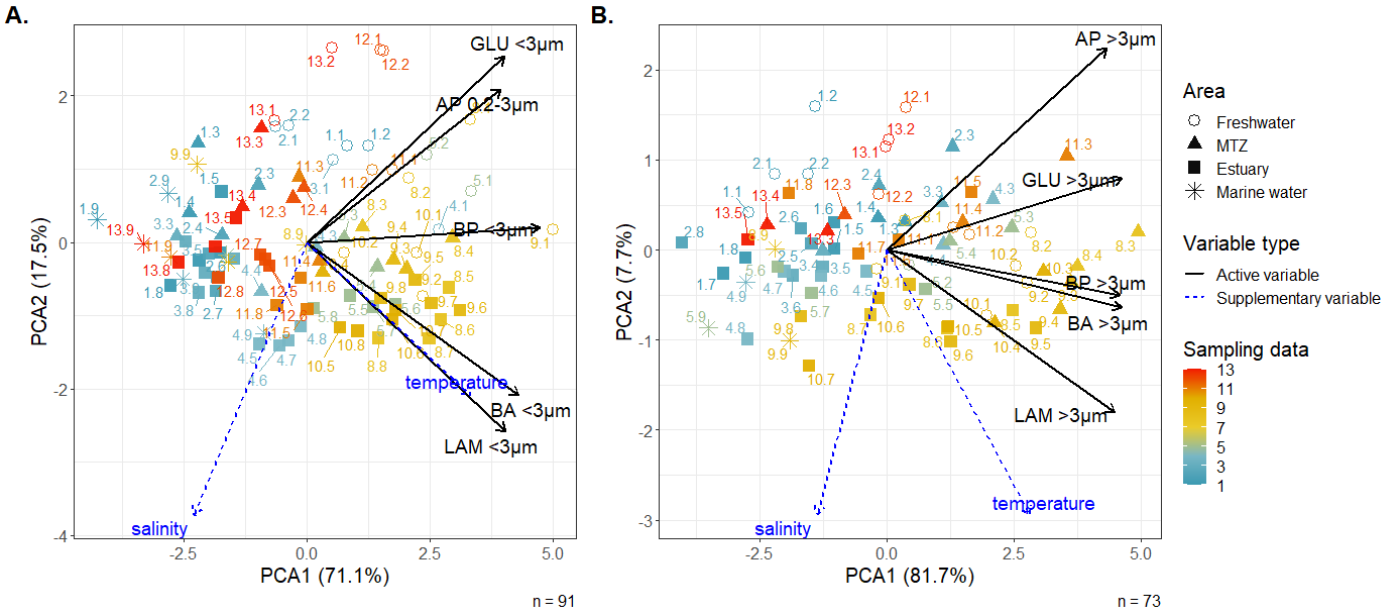

Figure 4. PCA ordination for the bacterial abundance, production and hydrolytic activities in the free-living (**A**) and particle-attached fraction (**B**). Blue dashed arrows (temperature and salinity) are supplementary variables added to facilitate interpretations but did not participate in PCA construction. PCAs were also performed without BA > 3 µm, GLU < 3 µm and GLU > 3 µm due to missing values, which did not impact their interpretation (**Figure S5**). Samples are labeled as "sampling month.sampling station" (e.g., S9 of R02 was labeled "2.9"). n: number of samples.

<u>Activity levels within the estuary</u>

The estuary hosted elevated bacterial production rates (mean: 143 µgC L^{-1} d^{-1}, range: 2-720 µgC L^{-1} d^{-1}). In terms of hydrolytic activities, total LAM activities were dominant with a mean of 769 nM h^{-1} (range: 32-3419 nM h^{-1}). Then, total AP represented most of the hydrolysis potential of the communities (mean: 60 nM h^{-1}, range: 4-365 nM h^{-1}), followed by GLU (mean: 17 nM h^{-1}, range: 0.5-82 nM h^{-1}). Differences in activity relative contributions could be observed along the estuary: the freshwater stations (S1-S2) were characterized by a significantly higher percentage of AP and GLU activities to total activity compared to the downstream stations, for both the free-living (mean in S1-S2: 40%; mean in S3-S9: 12%; Wilcoxon, $p < 0.001$) and particle-attached communities (mean in S1-S2: 43%; mean in S3-S9: 17%; Wilcoxon, $p < 0.001$) (**Table 4**). In addition, the relative contribution of AP and GLU to total activity decreased in summer compared to the other seasons for the particle-attached communities (mean in summer: 9%; mean in other seasons: 28%; Wilcoxon, $p < 0.001$). The free-living community exhibited a similar trend, although it was not significant (**Table 4**).

Table 4. Mean and standard deviation of AP and GLU contribution to the total hydrolytic activity for the < 3 µm fraction (dissolved and free-living) and > 3 µm fraction (particle-attached). The remaining percentages correspond to LAM activities. Left: comparison between freshwater (S1-S2) and downstream (S3-S9) stations for all sampling dates (except R06 and R07). Right: comparison between winter, spring and autumn (R01-R05, R11-R13) and summer (R08-R10) samples for all sampling stations. R06 and R07 were not included because of missing values in GLU. Significance was tested with the Wilcoxon test. ***: $p < 0.001$. ns: not significant.

	S1-S2	S3-S9		Winter, spring, autumn	Summer	
< 3 µm	40 ± 15%	12 ± 9 %	***	20 ± 17%	13 ± 12%	ns.
> 3 µm	43 ± 28%	17 ± 18%	***	28 ± 24%	9 ± 5%	***

Proportions of dissolved, free-living and particle-attached bacterial variables

Free-living bacteria outnumbered particle-attached bacteria throughout the estuary (overall mean and standard deviation of 76 ± 24%). However, particle-attached bacteria usually comprised more than 50% of the cell abundances in the MTZ (S3-S4) (mean of 50 ± 20%) (**Figure 5, left**). Although particle-attached bacteria were generally less abundant than free-living bacteria, their production often constituted more than half of the total BP throughout the estuary (mean: 61 ± 23%) (**Figure 5, middle**). Enzymatic activities (AP, GLU and LAM) followed a pattern similar to bacterial abundance: particle-attached bacterial activities dominated in the MTZ (S3-S4), while dissolved and free-living bacterial activities dominated elsewhere (**Figure 5, right**). A large part of AP activity was found in the dissolved fraction (AP < 0.2 µm), especially at the freshwater stations (S1-S2, up to 80%, **Figure 3**).

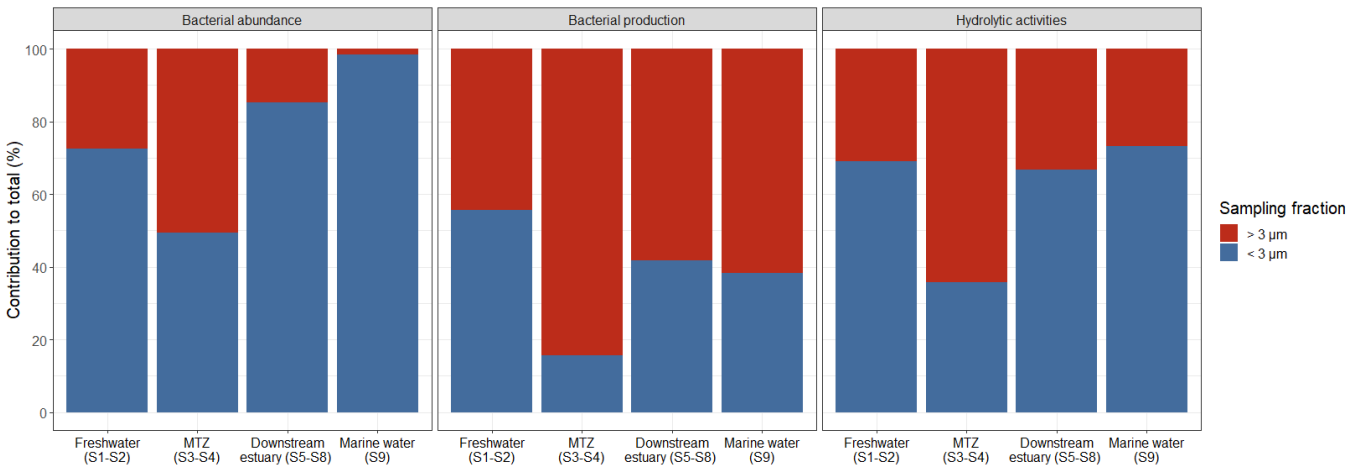

Figure 5. Mean contribution of the < 3 µm and > 3 µm fraction to the bacterial abundance, bacterial production and summed hydrolytic enzymes (AP, GLU and LAM) in the different areas of the estuary (freshwater, MTZ, downstream stations and marine water).

Generation time and specific hydrolytic activities

The high contribution of particle-attached activities despite their lower overall bacterial abundance resulted from higher specific activities (i.e., per cell) in particle-attached than in free-living communities (**Table 5**). Specific BP was expressed as generation time, reflecting the average time for

a doubling of the population. Generation times were fast for both free-living and particle-attached communities throughout the year and were as low as a few hours for the MTZ particle-attached communities (**Table 5**). On average, the particle-attached communities had a 3.4-fold faster growth rate than the free-living communities (Wilcoxon, $p < 0.001$). Mean particle-attached specific AP, GLU and LAM activities were 2.9-6.5-fold higher than mean free-living specific hydrolytic activities (Wilcoxon, $p < 0.001$).

Table 5. Mean and standard deviation of generation time and specific hydrolytic activities in the different areas of the estuary (freshwater, MTZ, downstream stations, marine water) depending on the season. Winter, spring and autumn samplings include R01-R05 and R11-R13. Summer samplings include R06-R10. For the particle-attached bacterial specific activities, only the samples containing more than 0.1×10^6 cells mL^{-1} were used in the calculations as low abundances yielded impossibly high specific rates, likely due to important errors on these measures. Consequently, all samples in the marine station (S9) were removed. GT: generation time.

		GT < 3 µm	GT > 3 µm	AP 0.2-3 µm	GLU < 3 µm	LAM < 3 µm	AP > 3 µm	GLU > 3 µm	LAM > 3 µm
		h		amol cell^{-1} h^{-}					
Winter, spring & autumn	S1-S2	9 ± 4	16 ± 32	11 ± 6	16 ± 14	85 ± 19	76 ± 92	51 ± 64	111 ± 70
	S3-S4	35 ± 14	6 ± 4	9 ± 9	4 ± 2	136 ± 27	54 ± 22	11 ± 6	229 ± 111
	S5-S8	41 ± 21	28 ± 80	3 ± 3	1 ± 1	122 ± 33	36 ± 15	8 ± 4	295 ± 146
	S9	187 ± 71		3 ± 4	1 ± 1	79 ± 66			
Summer	S1-S2	10 ± 8	13 ± 25	11 ± 7	6 ± 5	100 ± 21	22 ± 16	9 ± 5	167 ± 125
	S3-S4	19 ± 5	4 ± 1	6 ± 4	3 ± 1	136 ± 36	26 ± 15	12 ± 5	664 ±343
	S5-S8	21 ± 6	3 ± 1	3 ± 2	2 ± 1	154 ± 37	14 ± 8	18 ± 8	582 ± 196
	S9	92 ± 37		4 ± 3	2 ± 1	105 ± 66			

Environmental factors driving the bacterial activities

Dissolved alkaline phosphatase activity (< 0.2 µm)

As outlined above, AP < 0.2 µm did not exhibit clear temporal variations and its spatial pattern within the estuary was most likely constrained by salinity (conservative mixing). It is possible that AP < 0.2 µm removal in the MTZ resulted from adsorption to SPM (Tietjen and Wetzel, 2003). MLR was performed to estimate the relative influence of salinity and SPM on AP < 0.2 µm ($R^2_{adj} = 74.9\%$, $p < 0.001$), showing that salinity had the largest impact (coefficient = -0.88, $p < 0.001$) compared to SPM (coefficient = 0.11, $p = 0.08$).

Free-living bacterial activities (0.2-3 µm or < 3 µm)

We hypothesized that bacterial activities resulting from free-living bacteria (BP < 3 µm, LAM < 3 µm, GLU < 3 µm and AP 0.2-3 µm) were impacted by free-living bacterial abundance (BA < 3 µm), temperature, nutrients and DOM. In support of this hypothesis, free-living bacterial activities were correlated to bacterial abundance (Mantel, $r = 0.53$, $p < 0.001$) and nutrient- and DOM-related variables (Mantel, $r = 0.36$, $p < 0.001$), even when controlling for the influence of salinity and temperature (partial Mantel, $r = 0.39$ and 0.14, respectively, $p < 0.001$).

RDA was performed to identify which factors explained the variations in bacterial production and hydrolytic enzymes of the free-living communities. The RDA explained 78.1% of the variance ($p < 0.001$) (**Figure 6A**). All bacterial variables negatively correlated with the first RDA axis (59.9% of variance), opposing winter and autumn samples (R01-R03, R11-R13) to spring and summer samples (R05-R10). The second RDA axis (16.0% of variance) opposed LAM < 3 µm to AP 0.2-3 µm, GLU < 3 µm and BP < 3 µm. LAM < 3 µm correlated most with variables that varied seasonally, such as BA < 3 µm, temperature or DOP. Interestingly, LAM < 3 µm was not correlated with its substrate, DCAA, but correlated positively with DFAA and ammonium, that could result from its hydrolytic activity. AP 0.2-3 µm, GLU < 3 µm and BP < 3 µm correlated most with DPCHO, DCAA and DOP, and negatively with salinity. AP 0.2-3 µm levels also positively correlated with phosphate, its degradation product. Missing values in GLU < 3 µm did not impact the overall RDA interpretation, but removing GLU < 3 µm increased the separation between BP < 3 µm and AP 0.2-3 µm on the one hand, and LAM < 3 µm on the other hand (**Figure S6A**).

Variation partitioning was then used to estimate the fraction of variation in the bacterial activities explained by salinity, temperature, nutrients and DOM and BA < 3 µm (**Figure 6B**). BA < 3 µm and salinity alone explained the most variance (7% each). However, a large part of the explained variance was shared between nutrients and DOM, BA < 3 µm and temperature (28%), as well as nutrients and DOM and salinity (23%). This indicated an important covariation in the different datasets and a complex entanglement between bacterial dynamics, nutrients and DOM composition and spatiotemporal variables.

PSL-PM was thus performed to better constrain the direct and indirect effects of the different variables, disentangle their shared variance, and validate if the hypothesized causal relationships fitted the data. PLS-PM was performed on the two groups of bacterial activities identified in the RDA (LAM < 3 µm vs. AP < 0.2-3 µm, GLU- and BP < 3 µm). We first hypothesized that salinity (as a proxy of water masses mixing) and temperature (as a proxy of season, but also as a direct influence on bacterial metabolism) impacted nutrients, DOM and BA < 3 µm. Second, we hypothesized that bacterial activities were impacted by temperature, nutrients, DOM and BA < 3 µm. Although both groups of activities were well modeled ($R^2 > 0.81$), GOF values < 0.65 indicated a limited prediction performance of the model, especially for LAM < 3 µm (**Figure 6C, 6D**). LAM < 3 µm were mostly directly impacted by BA < 3 µm (path coefficient = 0.76) and to a lesser extent DOM (path coefficient = -0.13) while the effect of other variables was not significant. In contrast, GLU < 3 µm, AP 0.2-3 µm and BP < 3 µm were directly affected by DOM (path coefficient = 0.79), BA < 3 µm (path coefficient = 0.47) and nutrients (path coefficient = -0.27), in this order of importance. Temperature and salinity affected both groups of activities indirectly, by modulating BA < 3 µm and DOM.

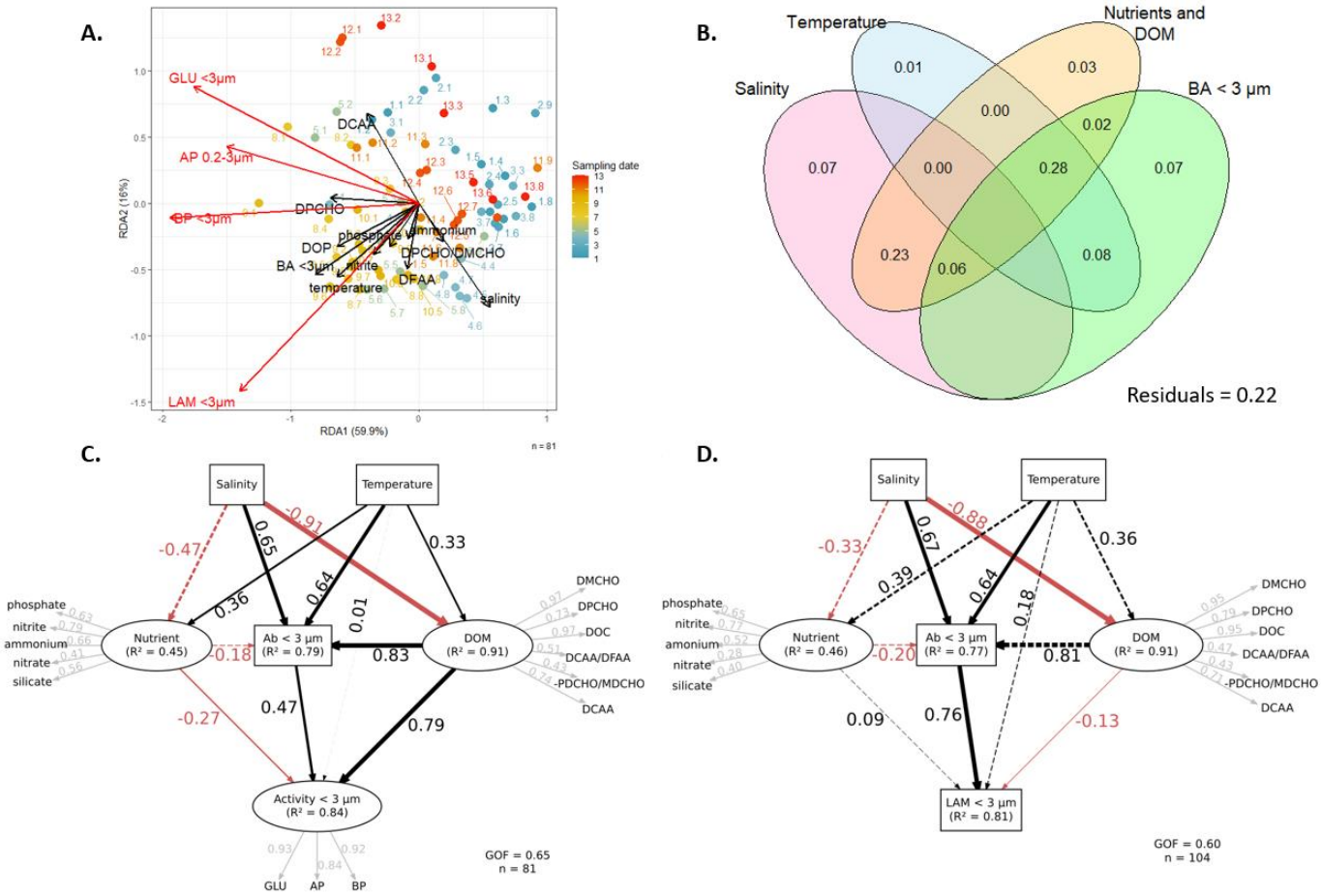

Figure 6. Redundancy analysis (RDA), variance partitioning and partial least squares path modeling (PLS-PM) of the bacterial variables related to the free-living activities. (**A**) RDA. Black arrow: explanatory variable; red arrow: response variable. Samples are labeled as "sampling month.sampling station" (e.g., S9 of R02 was labeled "2.9"). (**B**) Variance partitioning. The same variables as in RDA were used and regrouped under the terms salinity, temperature, nutrients and DOM (nitrite, ammonium, phosphate, DPCHO, DPCHO/DMCHO, DFAA, DCAA and DOP) and bacterial abundance (BA < 3 µm). (**C-D**) PSL-PM of the two groups of activities identified in the RDA: GLU, AP and BP (**C**) or LAM (**D**). Ellipses are latent variables while rectangles are observed variables. Black and red solid arrows represent significant positive and negative relationships, respectively. Dashed arrows represent insignificant relationships. The thicknesses of the arrows reflect the magnitude of the standardized path coefficients given alongside. Grey arrows and prints represent the loadings associated to latent variables. The R^2 value for each dependent variable is indicated inside the boxes. All parameters (path coefficient, R^2 and loadings) are mean values obtained after bootstrapping. n: number of samples.

Particle-attached bacterial activities (> 3 µm)

We hypothesised that bacterial activities resulting from particle-attached bacteria (BP-, AP-, GLU- and LAM > 3 µm) were impacted by particle-attached bacterial abundance (BA > 3 µm), POM-related variables, salinity and temperature. In support of this hypothesis, particle-attached bacterial activities were correlated with bacterial abundance (Mantel, $r = 0.65$, $p < 0.001$) and POM-related variables (Mantel, $r = 0.54$, $p < 0.001$), even when controlling for the influence of salinity and temperature (partial Mantel, $r = 0.63$ and 0.47, respectively, $p < 0.001$).

The RDA explained 80.2% of the variance ($p < 0.001$) (**Figure 7A**). All bacterial-related variables correlated with SPM and BA > 3 µm along the first RDA axis (70.4%). This is coherent with the maximum of activity observed in the MTZ, hosting the highest SPM loads and particle-attached bacterial abundance. The second RDA axis (7.0%) opposed AP- and GLU > 3 µm to BP- and LAM > 3 µm. AP > 3 µm correlated with marker of POM degradation (COP/NOP, I/S) and with a higher PCHO/PAA ratio. On the other hand, BP- and LAM > 3 µm correlated with temperature and %Chl*a*, but not with the particulate matter protein content (PAA/SPM). Missing values in GLU > 3 µm and BA > 3 µm did not impact RDA interpretation (**Figure S7B**), although removing these variables increased the correlation between AP > 3 µm and COP/NOP, I/S and PCHO/PAA.

As previously, variation partitioning was used to estimate the fraction of variation in bacterial activities that was related to salinity, temperature, bacterial abundance and particulate matter (**Figure 7B**). Particulate matter alone explained the most variance (9%) and the other groups explained less than 4% of variance. However, most of the explained variance was shared between temperature, BA > 3 µm and temperature (30%) and POM and BA > 3 µm (27%), indicating an important covariation among the different datasets.

PLS-PM was performed on two groups of bacterial activities (LAM- and BP > 3 µm vs. GLU- and AP > 3 µm) identified in the RDA. As before, we first hypothesized that salinity and temperature impacted POM quantity, POM quality and BA < 3 µm. We also hypothesized that activities were impacted by BA > 3 µm, POM quantity, POM quality and temperature. Both groups of activities were well modeled ($R^2 > 0.83$) and GOF values were acceptable (GOF = 0.70) (**Figure 7C, 7D**). LAM- and BP > 3 µm were directly and positively impacted by POM quantity, temperature and abundance, in this order of importance (path coefficient = 0.49, 0.41 and 0.22, respectively). POM quality did not directly affect these activities (path coefficient = 0.01, not significant). GLU- and AP > 3 µm were also impacted by POM quantity and BA > 3 µm, in similar magnitude (path coefficient = 0.42, and 0.47, respectively). However, GLU- and AP > 3 µm were not significantly affected by temperature and the effect of POM quality was negative and more important than for LAM- and BP > 3 µm (path coefficient = -0.18), although not significant.

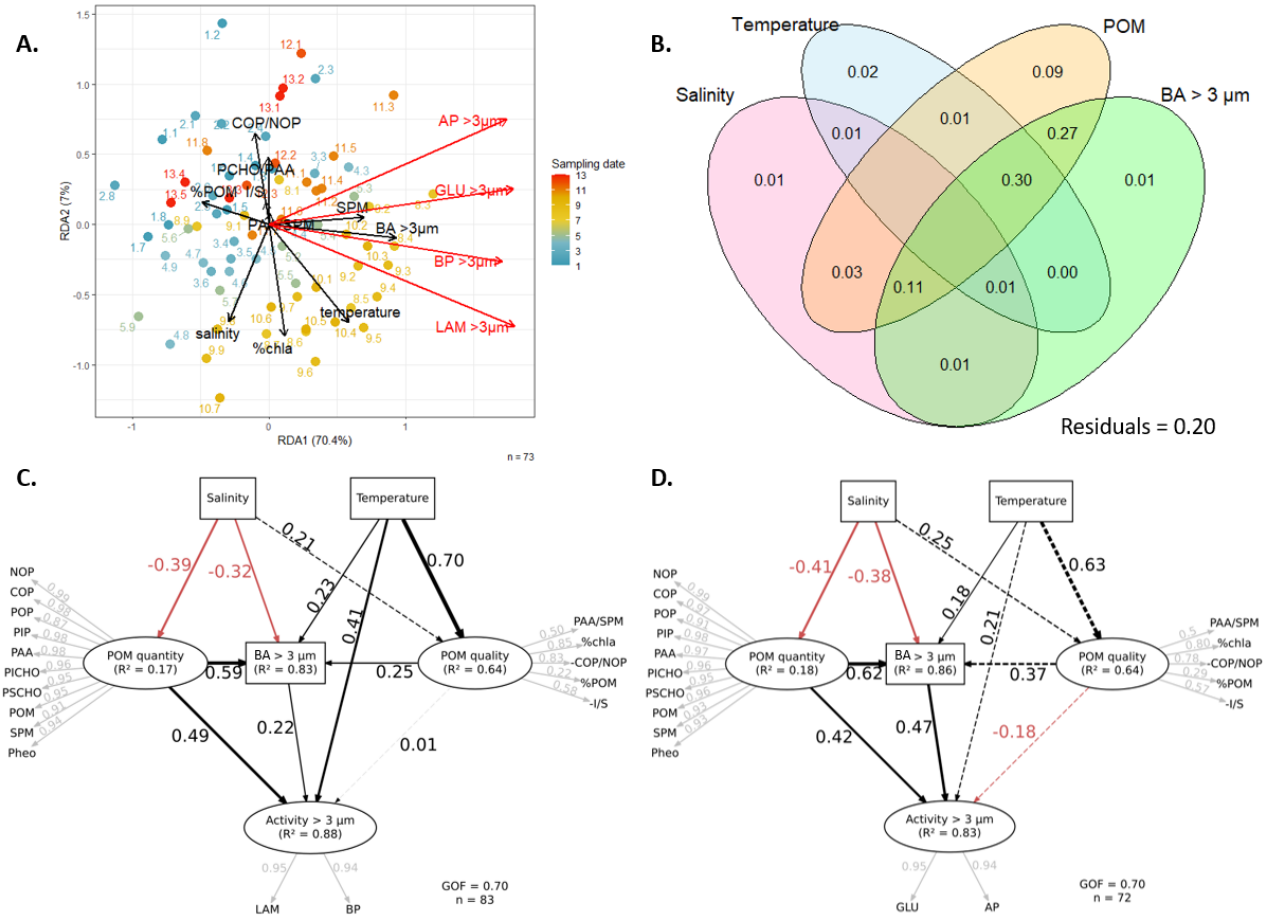

Figure 7. Redundancy analysis (RDA), variance partitioning and partial least squares path modeling (PLS-PM) of the bacterial variables related to particle-attached activities. (**A**) RDA. Black arrow: explanatory variable; red arrow: response variable. Samples are labeled as "sampling month.sampling station" (e.g., S9 of R02 was labeled "2.9"). (**B**) Variance partitioning. The same variables as in RDA were used and regrouped under the terms salinity, temperature, POM (SPM, %Chla, %POM, COP/NOP, PAA/MES, PCHO/PAA and I/S) and bacterial abundance (BA > 3 µm). (**C-D**) PSL-PM of the two groups of activities identified in the RDA: LAM- and BP > 3 µm (**C**) vs. GLU- and AP > 3 µm (**D**). Ellipses are latent variables while rectangles are observed variables. Black and red solid arrows represent significant positive and negative relationships, respectively. Dashed arrows represent insignificant relationships. The thicknesses of the arrows reflect the magnitude of the path regression coefficients given alongside. Grey arrows and prints represent the loadings associated to latent variables. The R^2 value for each dependent variable is indicated inside the boxes. All parameters (path coefficient, R^2 and loadings) are mean values obtained after bootstrapping. n: number of samples.

Relative influence of organic matter and bacterial community composition on bacterial activities

The BCC, determined in four sampling times (R02, R04, R09 and R12), exhibited large spatiotemporal variations. The upstream stations (S1-S4) were notably enriched in Betaproteobacteria (e.g., Burkholderiales), Bacteroidota (e.g., Cytophagales) and Actinobacteriota (e.g., Frankiales) while the downstream stations (S5-S9) were enriched in Alphaproteobacteria (e.g., Rhodobacterales,

599 Puniceispirillales), Bacteroidota (e.g., Flavobacteriales) and Gammaproteobacteria (e.g.,
600 Oceanospirillales, Cellvibrionales, Alteromonadales) (Urvoy *et al.*, in prep., **Chapitre III**). In addition,
601 particle-attached communities were more diverse and differed taxonomically and phylogenetically
602 from free-living communities (Urvoy *et al.*, in prep., **Chapitre III**). Those four sampling times were used
603 to assess the relative influence of BCC and physicochemical factors on hydrolytic enzyme activities
604 levels.

605 Activities resulting from free-living bacteria (0.2-3 µm or < 3 µm)

606 The BCC of free-living communities correlated with both free-living bacterial activities (Mantel, $r = 0.58$,
607 $p < 0.001$) and nutrients and DOM-related variables (Mantel, $r = 0.51$, $p < 0.001$), highlighting the high
608 inter-correlation and intricate relationships between the three datasets. PCA showed that, as with the
609 full dataset, AP-, GLU and BP < 3 µm were opposed to LAM and BA < 3 µm along the second PCA axis
610 (18.7% of variance), although BP < 3 µm had a more intermediate behavior than before. As previous,
611 AP 0.2-3 µm, GLU < 3 µm and BP < 3 µm correlated positively with physicochemical variables such as
612 DOC, DMCHO or DCAA and negatively with salinity, while LAM correlated with BA < 3 µm, temperature,
613 nitrite or DOP. These groups of activities also correlated with different bacterial classes. AP 0.2-3 µm
614 and GLU < 3 µm correlated positively with bacterial classes such as the Parcubacteria,
615 Gammaproteobacteria, Saccharimonadia, Planctomycetes or Verrucomicrobia, and negatively with
616 the Alphaproteobacteria. In contrast, LAM correlated positively with the Actinobacteria,
617 Verrucomicrobia, Planctomycetes and negatively with the Campylobacteria.

618 The same model PLS-PM model as before was used, with the addition of a latent variable
619 representing BCC < 3 µm. The hypotheses were that BCC < 3 µm was influenced by salinity,
620 temperature, nutrients and DOM. In addition, we hypothesized that BCC directly influenced bacterial
621 activities: The two groups of activities previously defined (BP-, GLU- and AP < 3 µm vs. LAM < 3 µm)
622 were well modeled ($R^2 > 0.86$) with a satisfying fit (GOF > 0.68) (**Figure 8B, 8C**). For both groups of
623 activity, the influence of BCC on the activities was minor compared to the influence of DOM and BA <
624 3 µm, although none of the path coefficients affecting activities were significant. Interestingly, the two
625 groups of activity seemed differently affected by the BCC (path coefficient = -0.16 and 0.13 for the
626 GLU, AP and BP < 3 µm vs. LAM < 3 µm, respectively). BCC was largely driven by salinity and
627 temperature. It should be noted that the small sample size (n = 25 or 26) probably limits the path
628 coefficient significance and, as such, those models should be interpreted cautiously.

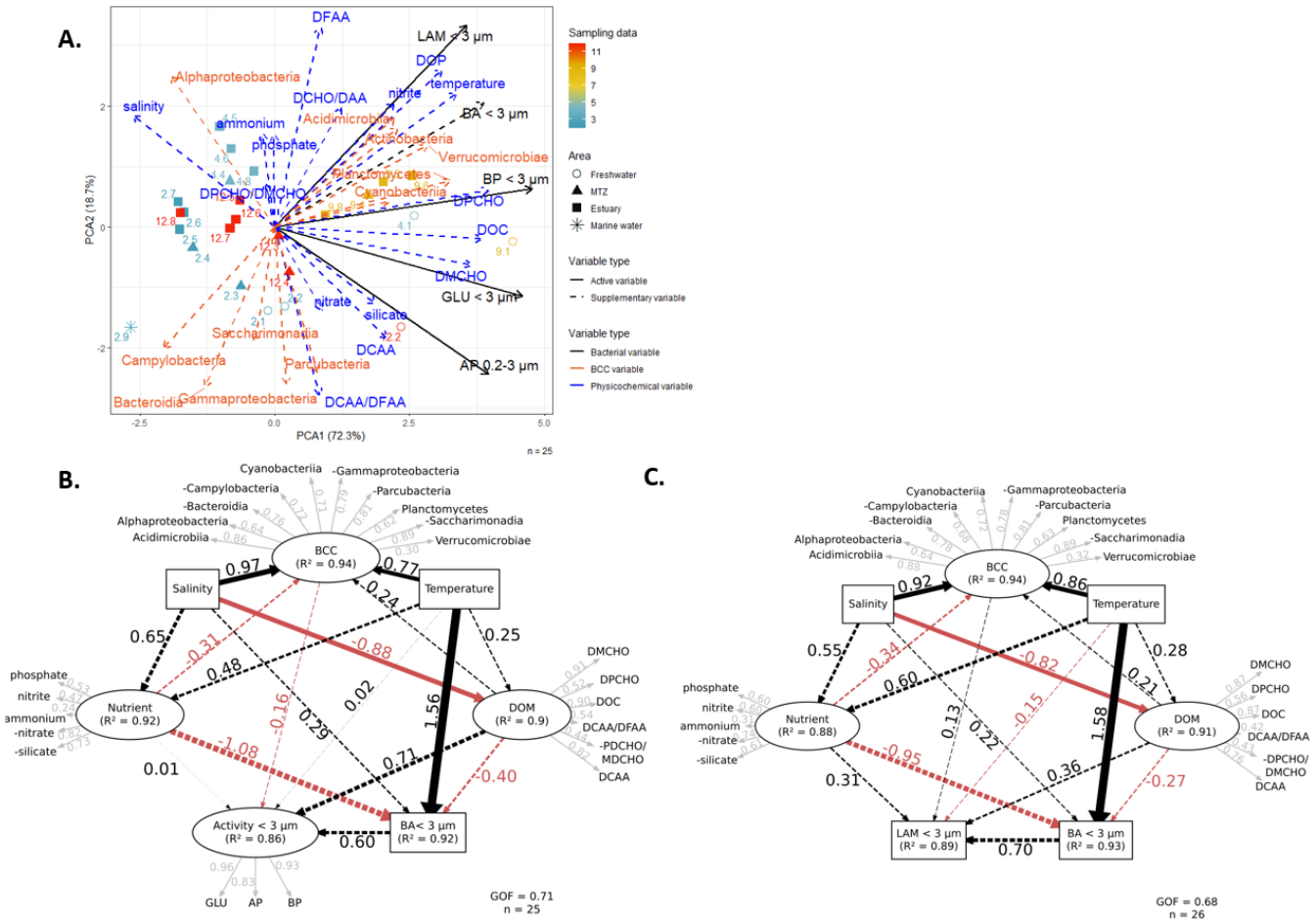

Figure 8. Principal component analysis (PCA) and partial least squares path modeling (PLS-PM) of the bacterial activities resulting from free-living bacteria, taking into account the bacterial community composition (BCC). (**A**) PCA performed on the bacterial activities. The physicochemical, bacterial abundance and BCC-related variables are supplementary variables projected onto the ordination to investigate their correlation to bacterial variables and did not participate in the PCA construction. Black solid arrow: active bacterial variable; black dashed arrow: supplementary bacterial variable; blue dashed arrow: supplementary physicochemical variable; orange dashed arrow: supplementary BCC variable. Samples are labeled as "sampling month.sampling station" (e.g., S9 of R02 was labeled "2.9"). (**B-C**) PSL-PM of the two groups of activities identified previously: BP < 3 µm, GLU < 3 µm and AP 0.2-3 µm (**B**) vs. LAM < 3 µm (**C**). Ellipses are latent variables while rectangles are observed variables. Black and red solid arrows represent significant positive and negative relationships, respectively. Dashed arrows represent insignificant relationships. The thicknesses of the arrows reflect the magnitude of the standardized path coefficients given alongside. Grey arrows and prints represent the loadings associated to latent variables. The R^2 value for each dependent variable is indicated inside the boxes. All parameters (path coefficient, R^2 and loadings) are mean values obtained after bootstrapping. n: number of samples.

Activities resulting from particle-attached bacteria (> 3 µm)

The BCC of particle-attached communities was correlated to particle-attached bacterial activities (Mantel, r = 0.57, p < 0.01) and POM-related variables (Mantel, r = 0.51, p < 0.001), highlighting the inter-correlation between the three datasets. As previous, all bacterial activities correlated with variables related to POM quantity (e.g., SPM, COP) (**Figure 9A**). AP > 3 µm correlated most with markers of POM degradation (COP/NOP, I/S) and PCHO/PAA while LAM- and BP > 3 µm were more related to BA > 3 µm, temperature and markers of phytoplankton development and POM quality (e.g., Chla, %Chla, PAA/SPM). GLU > 3 µm had a more intermediate behavior than in previous analyses. The different groups of activities also correlated with different bacterial classes. AP > 3 µm correlated positively with the Parcubacteria, Anaerolineae or Gemmatimonadetes and negatively with the Alphaproteobacteria, among others. In contrast, BP- and LAM > 3 µm correlated most with the Actinobacteria and Planctomycetes but also negatively with the Campylobacterales (**Figure 9A**).

As before, PLS-PM was used with the hypothesis that BCC > 3 µm was influenced by salinity, temperature, POM quantity and quality while directly impacting bacterial activities. Activities were well modeled in both cases (R^2 > 0.87) and GOF indicated a satisfying fit to the data (GOF > 0.66) (**Figure 9B, 9C**). GLU- and AP > 3 µm were significantly and directly affected by POM quantity (path coefficient = 1.18) and BCC > 3 µm (path coefficient = 0.82). They were also indirectly affected by salinity (which impacted POM quantity) and by temperature and POM quantity (which affected BCC > 3 µm). In contrast, LAM > 3 µm were directly affected by BA > 3 µm (path coefficient = 0.70) and, to a lesser extent, POM quantity (path coefficient = 0.22) and but not by BCC > 3 µm (path coefficient = 0.01, not significant). In addition, LAM > 3 µm were also indirectly affected by temperature and POM quantity (which affected BA > 3 µm) and salinity (which affected POM quantity). BCC > 3 µm was mostly driven by POM quantity and temperature. As previous, those models should be interpreted cautiously given the small sample size (n = 25).

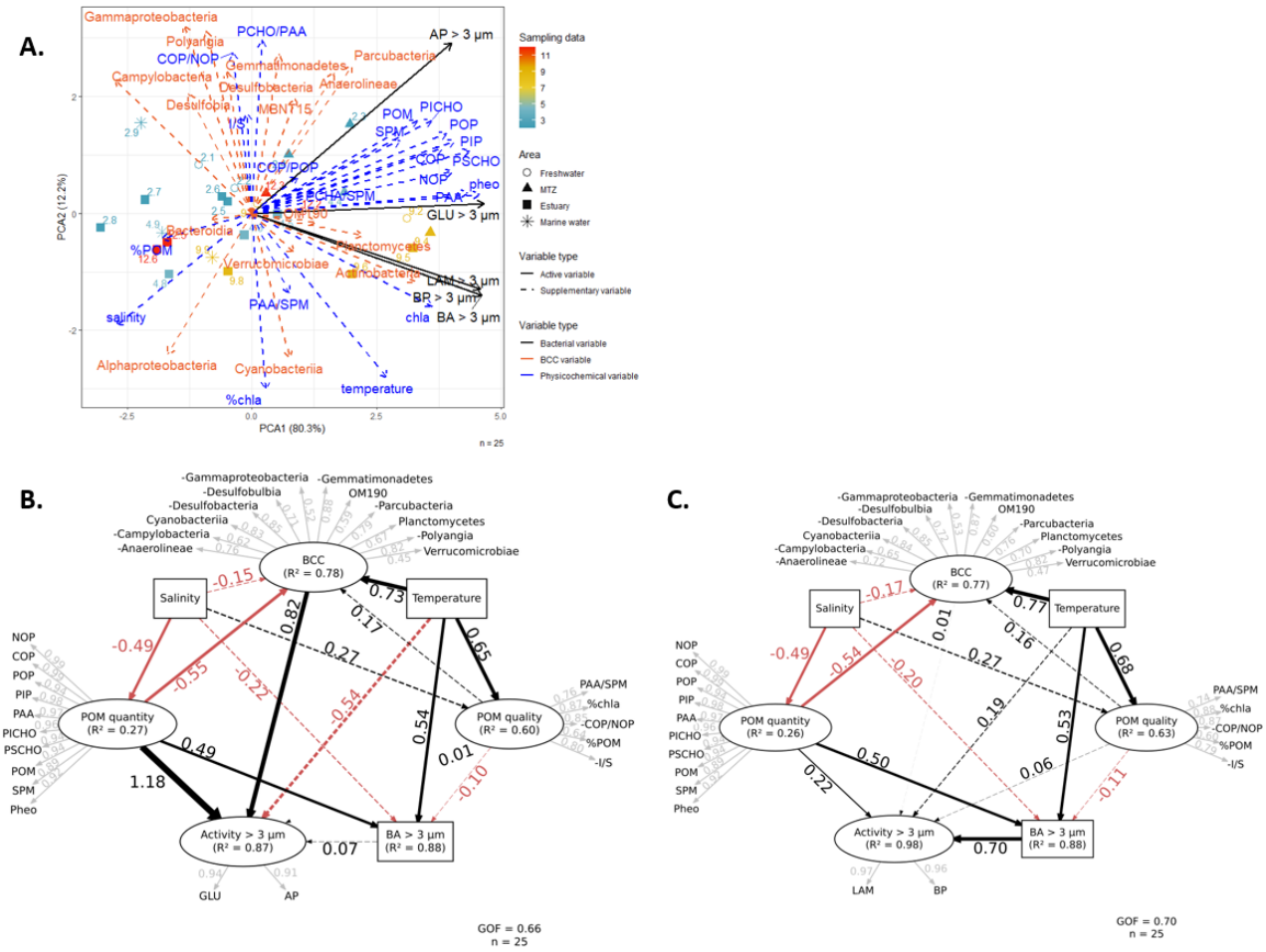

Figure 9. Principal component analysis (PCA) and partial least squares path modeling (PLS-PM) of the bacterial activities resulting from particle-attached bacteria, taking into account the bacterial community composition (BCC). (**A**) PCA performed on the bacterial activities. The physicochemical, bacterial abundance and BCC-related variables are supplementary variables projected onto the ordination to investigate their correlation to bacterial variables and did not participate in the PCA construction. Black solid arrow: active bacterial variable; black dashed arrow: supplementary bacterial variable; blue dashed arrow: supplementary physicochemical variable; orange dashed arrow: supplementary BCC variable. Samples are labeled as "sampling month.sampling station" (e.g., S9 of R02 was labeled "2.9"). (**B-C**) PSL-PM of the two groups of activities identified in the PCA: GLU- and AP > 3 µm (**B**) vs. LAM- and BP > 3 µm (**C**). Ellipses are latent variables while rectangles are observed variables. Black and red solid arrows represent significant positive and negative relationships, respectively. Dashed arrows represent insignificant relationships. The thicknesses of the arrows reflect the magnitude of the standardized path coefficients given alongside. Grey arrows and prints represent the loadings associated to latent variables. The R^2 value for each dependent variable is indicated inside the boxes. All parameters (path coefficient, R^2 and loadings) are mean values obtained after bootstrapping. n: number of samples.

Discussion

Heterotrophic bacteria play an important role in marine biogeochemistry as they alter the fate of organic matter through the synthesis of hydrolytic enzymes. Bacterial metabolisms are particularly intense in estuaries, where they impact the exports of nutrients and organic matter to coastal areas and ultimately, their functioning. Estuaries are under strong hydrodynamic forcings that shape the water masses mixing, particulate matter resuspension and biological processes. In particular, the Aulne estuary possesses intense alkaline phosphatase rates resulting from particle-attached bacteria, whose drivers remained unexplained. Our objectives were thus to describe the spatiotemporal patterns and determinants of free-living and particle-attached bacterial production and enzymatic activities (AP, GLU and LAM) related to different elemental cycles (phosphorus, carbon and nitrogen) in this estuary.

The Aulne estuary as a natural bioreactor hosting high bacterial metabolisms

The Aulne estuary hosted elevated BP that translated into fast generation time for both free-living and particle-attached communities, beneath the flushing time of estuarine waters (3-30 days, Bassoullet, 1979). This suggests that bacterial communities significantly impact the organic matter within the estuary. These results are similar to the BP rates measured in other estuaries (Ducklow and Carlson, 1992; Schultz *et al.*, 2003; Servais and Garnier, 2006; Pollard and Ducklow, 2011), which are among the fastest measured in natural aquatic ecosystems (Pollard and Ducklow, 2011) (**Table 6**). This is consistent with the belief that estuaries act as natural "bioreactors" of heterotrophic activities, heavily processing organic matter and nutrients before their export to coastal areas. These transformations are likely fueled by particle-attached bacterial communities that exhibited 3.4-times faster growth rates than free-living bacteria and generation times as low as a few hours in the MTZ.

These important BP rates were likely supported by similarly high potential hydrolytic activities. Hydrolytic enzymes are crucial tools that hydrolyze high molecular weight organic matter and supply assimilable carbon and nutrients (Arnosti, 2011). If GLU and LAM are considered to be mainly produced by heterotrophic bacteria, AP can result from other microorganisms, especially phytoplankton (Hoppe, 2003). However, in this study, we considered that AP mainly originated from bacteria. Indeed, phytoplankton AP are usually induced by low phosphate levels (< 0.1 µM) (Nausch, 1998; Hoppe, 2003; Labry *et al.*, 2005). This induction threshold is well below the phosphate levels within the Aulne estuary (mean of 0.7 µM). In contrast, bacterial production of AP in phosphate-replete environments was demonstrated in a few studies (Koike and Nagata, 1997; Hoppe and Ullrich, 1999; Labry *et al.*, 2016; Davis and Mahaffey, 2017; Thomson *et al.*, 2019; see discussion below). Finally, AP 0.2-3 µm and AP > 3 µm greatly correlated with other bacterial variables (abundance, production and activities) but not with %Chl*a* (**Figure 7A, Figure S6**), confirming that they mainly originated from bacteria.

718 Table 6. Comparison of bacterial activities (BP, AP, GLU and LAM) across a range of environments. Values are given as mean and range when possible. *Estimated from specific
719 bacterial production using 16 fgC cell^{-1}.

720

	Location	Fraction	BP µgC L^{-1} d^{-1}	AP	GLU nM h^{-1}	LAM	GT h	Specific AP	Specific GLU amol cell^{-1} h^{-1}	Specific LAM
This study	Aulne estuary and Bay of Brest (France)	Free-living	50 (1-428)	10 (0-67)	6 (0-39)	222 (13-734)	40 (3-278)	6 (0-30)	4 (0-42)	120 (9-232)
		Particle-attached	92 (1-682)	29 (0-331)	11 (0-76)	356 (1-3228)	12 (1-307)	38 (5-303)	18 (2-202)	343 (26-1257)
Karner and Herndl (1992)	Gulf of Trieste (Italy) Northern Adriatic Sea	Free-living	1.66-19.3	-	0.15-1.92	150-694	3-69	-	0-2.4	102-723
		Marine-snow associated	9.9-22.3	-	1.46-26.32	550-9306		-	0.7-14	277-4996
Rath *et al.* (1993)	Caribbean Sea (Belize) Trophic gradient from the outer reef to a mangrove island	Total bacteria	11.5 (9.2-15.5)	50 (31-60)	1.1 (0.3-1.8)	282 (247-306)	22 (16-30)	-	1.3 (0.6-1.8)	562 (316-766)
Martinez *et al.* (1996)	Isolated bacteria in culture		-	-	-	-	-	96.4 (0.7-410)	2.3 (0.0-35)	191 (4-3810)
	Natural assemblages	Total bacteria	-	-	-	-	-	5-30	0-5	40-160
	Microcosms of natural assemblage with phytoplankton aggregates amendments	Free-living	-	-	-	-	-	4-18	1-4	250-2700
		Phytoplankton aggregates	-	-	-	-	-	22-68	5-25	1700-24000
Cunha *et al.* (2000)	Ria de Aveiro (Portugal) Shallow tidal estuary	Total bacteria	-	-	4.3-181	490-5374	-	-	10 (5-25)	384 (189-626)
Labry *et al.* (2005)	Phosphorus-limited Gironde plume waters in the Bay of Biscay (France)	Total bacteria	-	1-477	-	-	-	1-99	-	-
Williams and Jochem (2015)	Florida Bay Shallow estuary	Total bacteria	-	61-1022	2.3-26.2	70-1650	-	44-1029	0.7-23.6	52-1572
Lamy *et al.* 2009)	Costal station in the Eastern English Channel during a Phaeocystis globosa bloom	Total bacteria	0.008-0.179	-	-	-	-	-	0-37.3	50-240
Pollard and Ducklow (2011)	Bremer River (Australia) Eutrophic subtropical river	Total bacteria	77.5 (23.5-137.8)	-	-	-	1.7 (0.6-4.5)	-	-	-
Piontek *et al.* (2014)	Fram Strait (Arctic Ocean)	Total bacteria	0.10-2	-	0.2-1.6	1-43	59-480 *	-	0.8-6.0	10-160
Labry *et al.* (2016)	Aulne and Elorn estuary (Bay of Brest, France)	Total bacteria	7-343	50-506	-	-	-	4-113	-	-
David *et al.* (2021)	Can Gio estuary (Vietnam) Human impacted, mangrove dominated tropical estuary	Total bacteria	-	-		24-505	-	-	-	5-180

Potential hydrolytic activities within the estuary were largely dominated by LAM, followed by AP and GLU. Potential activities do not reflect the actual *in situ* hydrolysis rates, complex to estimate, but represent the enzymatic equipment of the cells (Chróst, 1990). Large ratio of LAM to GLU activities, especially in downstream stations and marine waters (S5-S9), suggests a dominant use of proteins over carbohydrates (Christian and Karl, 1995; Fukuda *et al.*, 2000) which may explain the high ratio of carbohydrates to amino acids within the estuary (DCHO/DAA and PCHO/PAA > 1). Low AP to LAM ratio suggests that the communities were not P-limited (Sala *et al.*, 2001). Enzymatic activity rates were in the upper range of the values reported by other studies across various environments (**Table 6**). This was true for both absolute and specific rates, indicating that high activity levels do not only result from high bacterial densities. Specific AP activities were notably in the range of severely phosphate-limited bacteria AP levels (1-99 amol $cell^{-1}$ h^{-1}, Labry *et al.*, 2005). Specific particle-attached bacterial activities were higher than free-living specific activities, similar to what was reported in other aggregates such as marine snow (**Table 6**).

Hydrolytic activities were regulated by different factors

The Aulne estuary could be differentiated in three distinct areas: (i) the freshwater stations (S1-S2), dominated by free-living bacteria with a relatively high contribution of GLU and AP to total activity; (ii) the MTZ (S3-S4), dominated by particle-attached bacteria with variable ratio of LAM to AP and GLU depending on the season; and (iii) the downstream stations (S5-S9), dominated by free-living bacteria and LAM activity (**Figure 10**). These different zones arose from differences in the factors controlling the hydrolytic enzyme activities.

Dissolved alkaline phosphatases dynamics and determinants

In this study, dissolved AP activities were high in the freshwater stations (S1-S2), low in the marine station (S9) and their spatial pattern was mostly constrained by the mixing of water masses. AP < 0.2 µm exhibited low temporal variations. The factors controlling dissolved hydrolytic activities are poorly understood so far (Baltar, 2018; Baltar *et al.*, 2019). They are complex to study because they originate from various active and passive processes (e.g., active secretion, viral lysis) and can reflect water masses past conditions due to their long half-life time (up to 20 days, Baltar, 2018; Thomson *et al.*, 2019). Some studies hypothesized that dissolved activities result from particle-attached bacteria (Ziervogel and Arnosti, 2008; Baltar *et al.*, 2010). However, in our study, dissolved AP were more important in freshwater stations (S1-S2), containing a lower number of attached cells than other stations (such as in the MTZ) (**Figure 10**), suggesting a different release mechanism. High dissolved AP levels in freshwater stations could be linked to higher DOM concentration in these stations, as suggested by modeling studies (Traving *et al.*, 2015).

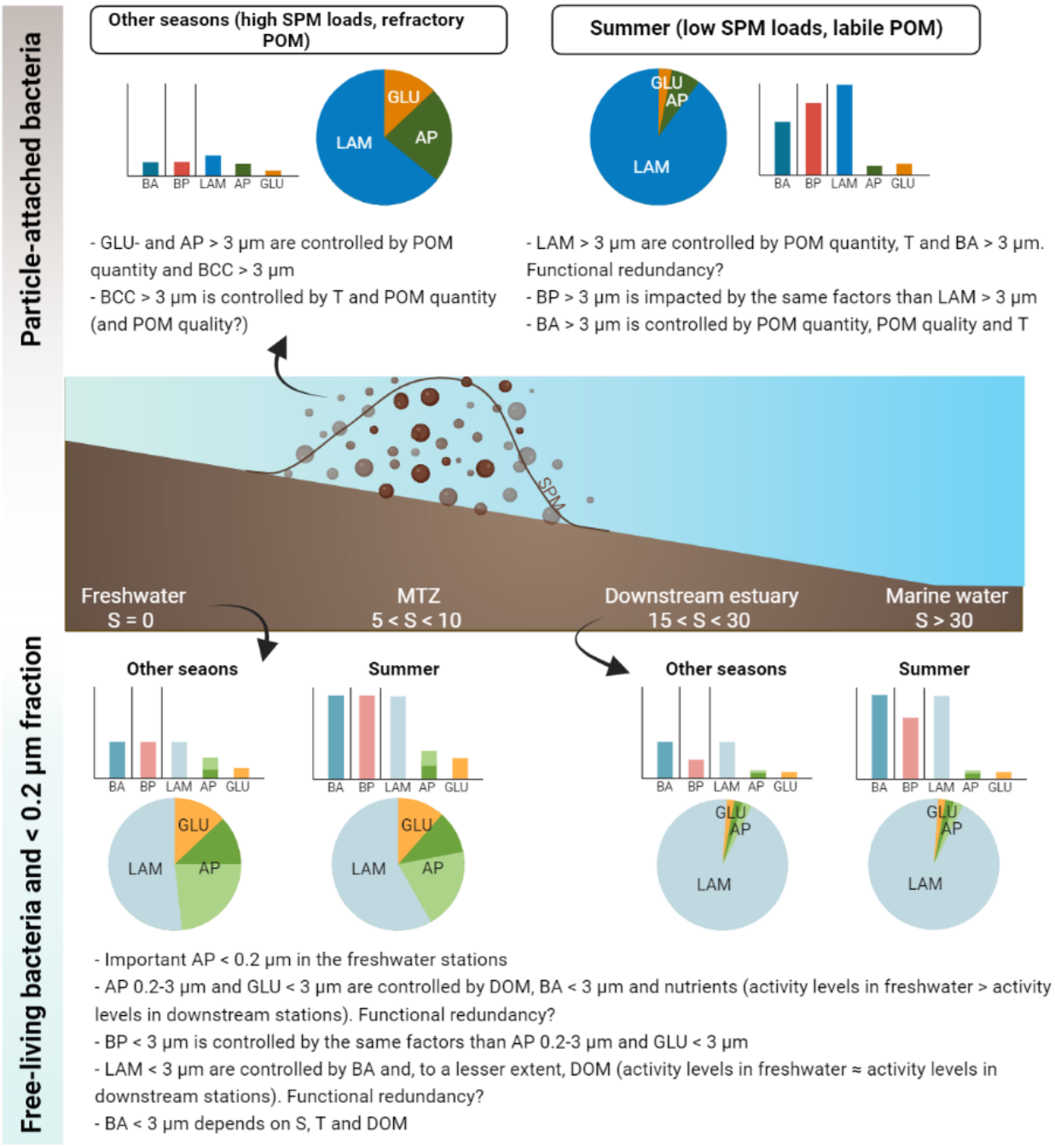

Figure 10. Conceptual diagram of the free-living and particle-attached bacterial dynamics within the Aulne estuary, in terms of bacterial abundance (BA), bacterial production (BP) and enzymatic activities. The estuary could be divided in three distinct zones depending on the contribution of free-living and particle-attached communities and LAM, GLU and AP proportions: i) the freshwater stations were characterized by high activities of free-living bacteria and a relatively important contribution of AP and GLU to total activity; ii) the MTZ, with intense activities of particle-attached bacteria whose relative contribution varied depending on season and SPM loads; iii) downstream estuarine stations, dominated by LAM resulting from free-living bacteria. The bar charts represent the absolute values of bacterial variables while the pie charts represent the relative contribution of the different hydrolytic enzymes. SPM: suspended particulate matters; POM: particulate organic matter; GLU: AP: alkaline phosphatase; LAM: leucine aminopeptidases; MTZ: maximum turbidity zone; T: temperature; DOM: dissolved organic matter; S: Salinity.

Free-living bacterial hydrolytic activity dynamics and determinants

Free-living bacteria overall dominated in freshwater (S1-S2) and downstream estuarine stations (S5-S9). Their hydrolytic activities followed the same overall temporal pattern, with an increase in summer. However, LAM < 3 µm followed a different spatial pattern than GLU < 3 µm and AP 0.2-3 µm. LAM < 3 µm activity was most largely controlled by free-living bacterial abundance and not correlated to its substrate, DCAA. Free-living bacterial abundance was mainly controlled by season (temperature) and mixing of water masses (salinity), which are consequently important indirect drivers of LAM. This is in agreement with other studies that showed that temperature was one of the main driver of LAM activity (Patel *et al.*, 2000; Boucher and Debroas, 2009). In contrast, AP 0.2-3 µm and GLU < 3 µm were mostly driven by DOM concentration (DOC, DOP, DPCHO and DCAA, **Figure 7**), and to a lesser extent, by free-living bacterial abundance and nutrients. AP 0.2-3 µm synthesis did not seem induced by phosphate depletion, as phosphate levels were high. In addition, AP 0.2-3 µm activities and phosphate were positively correlated. Interestingly, the BCC did not seem to impact the two groups of activity (LAM vs. AP and GLU activities), suggesting some functional redundancy within free-living bacterial communities.

These different patterns led to different proportions of activity the up- and downstream stations (**Figure 10**): GLU < 3 µm and AP 0.2-3 µm represented an important part of the total hydrolytic activity in the freshwater stations (S1-S2). In contrast, LAM activities closely followed the bacterial abundance levels and thus increased downstream (S5-S9), where they represented 88% of the total hydrolytic activity on average. This pattern is coherent with past literature in the fact that freshwater communities seem to rely more on carbohydrates than marine communities, which primarily consume proteins (Murrell *et al.*, 1999; Cunha *et al.*, 2000; Balmonte *et al.*, 2019). This pattern did not seem to arise from differences in taxonomic composition between freshwater and marine communities but was driven by DOM and nutrient concentrations, suggesting a transcriptional regulation. However, it should be noted that this analysis was limited by a low sample size and that we measured one polysaccharidase activity, giving only a glimpse into bacterial polysaccharide degradation capacities. It is possible that the measurement of different, more specific enzymes (e.g., *N*-acetyl glucosaminidases, fucoidanases, alginate lyases, carrageenases) would highlight different regulation patterns, similar to the study by Balmonte *et al.* (2019).

Particle-attached bacterial hydrolytic activity dynamics and determinants

The spatial pattern of particle-attached bacterial community was closely linked to SPM dynamics and was consequently similar for all bacterial variables: a marked maximum in activities was observed in the MTZ, generated by high SPM loads (direct substrate induction) and/or higher particle-attached abundance. However, particle-attached bacterial activities followed different temporal patterns, leading to a large dominance of LAM activities in summer and a more equal contribution of LAM vs.

GLU and APA in other seasons (**Figure 10**). Indeed, LAM > 3 µm were controlled by seasonal factors (i.e., temperature, both as a direct and indirect influence), POM quantity (substrate induction), and bacterial abundance, to a lesser extent. POM quality and protein content (PAA/SPM) did not directly influence LAM expression. However, we assessed POM quality through global measurements (COP/NOP, I/S), which may not represent the fine variations in POM quality. BCC > 3 µm did not control LAM > 3 µm activity levels, suggesting functional redundancy within the particle-attached communities for this activity.

In contrast, AP- and GLU > 3 µm were largely controlled by POM quantity and BCC > 3 µm, in similar magnitude. Groups such as Parcubacteria, Anaerolineae, Gemmatimodates correlated positively with AP- and GLU > 3 µm. BCC > 3 µm was itself influenced by temperature, which is one of the main driver of BCC in the environment (Crump *et al.*, 2004; Sunagawa *et al.*, 2015), and by POM quantity. POM quantity effect on BCC may partly results from the resuspension of sediments, comprising different bacterial communities. As previous, POM quality did not significantly influence BCC and activity, but this analysis is likely limited by the low sample size. AP activities were not significantly correlated to COP/POP, suggesting the low importance of POP content in their regulation (**Figure S6**). However, AP and GLU correlated with PCHO/PAA and markers of POM degradation (COP/NOP, I/S) (**Figure 8**), suggesting a possible role in refractory carbon and phosphorus-containing substrates such as structural polysaccharides. Particle-attached bacterial communities may be enriched in taxa capable of hydrolyzing such substrates through GLU and AP synthesis. This is coherent with Boucher and Debroas (2009) that noted that BCC contributed differently to AEE regulation. These authors showed that α-glucosidases and AP expression was more controlled by diversity-related parameters than LAM expression, which depended more on environmental variables.

Links between free-living and particle-attached bacterial dynamics

We chose to study the free-living and particle-attached bacterial dynamics separately; and hypothesized that free-living bacteria were impacted by DOM and nutrients variables while particle-attached bacteria were impacted by POM variables. In reality, both compartments are dynamically linked as bacteria alternate between free-living and particle-attached lifestyles (Grossart, 2010). In addition, it is well established that there is an uncoupling between hydrolysis and uptake among particle-attached bacteria in marine snow and lake particles, meaning that particle-attached bacteria hydrolyze more POM than they assimilate (Smith *et al.*, 1992; Grossart, 2010). As such, the intense activities in the MTZ likely lead to DOM and nutrients release for the free-living bacteria (Smith *et al.*, 1992; Grossart, 2010). In support of this hypothesis, ammonium and DFAA correlated with LAM > 3 µm and AP > 3 µm with phosphate, suggesting that they could be solubilized from particles by particle-attached bacteria. POM to DOM releases resulting from particle-attached bacterial activities are a

possible explanation of the increased bacterial abundance and activities downstream of the MTZ (S5-S7).

The paradox of strong alkaline phosphatase activities in phosphate-replete environments

Thomson *et al*. (2019) reported that the important contribution of dissolved AP to total activity, associated with a long lifetime of cell-free enzymes, may explain the paradoxical presence of important AP rates in phosphate-replete waters. Although this is likely to be an explanation in some regions, for instance containing low particle concentrations, our study illustrated that high AP in phosphate-replete conditions can result from particle-attached bacteria, and free-living bacteria to a lesser extent. For both fraction, AP activities did not seem related with POP or DOP dynamics and positively correlated with phosphate; but they were correlated with GLU activities and organic matter quantity. This suggested that AP could be a means to access the organic part of the hydrolyzed substrate, as hypothesized in studies in the deep ocean (Hoppe and Ullrich, 1999; Nicholson *et al.*, 2006; Davis and Mahaffey, 2017). More studies are necessary to better understand the occurrence of high AP in phosphate-replete environments as well as their effect on phosphorus speciation in estuarine ecosystems.

Conclusion

To conclude, our study shed light on the spatiotemporal variation of bacterial abundance, production and hydrolytic activities within the Aulne estuary, and their determinants. The Aulne estuary hosted intense bacterial production supported by high hydrolytic activities, especially within the particle-attached communities. These activities were regulated by different factors, resulting in different proportions of LAM, PA and GLU depending on the area or the season. LAM activities were mostly impacted by seasonal factors, while AP and GLU activities were more related to organic matter concentration. Interestingly, BCC in the particle-attached fraction was related to GLU and AP synthesis, illustrating that the link between BCC and function may differ depending on the size fraction and the enzymatic activity considered. Finally, our results suggested that intense particle-attached PA activities in this phosphate-replete estuary may be linked to the hydrolysis of refractory POM. More studies are needed to assess the effect of potentially high AP on phosphorus speciation within estuaries.

Acknowledgement

This work was supported by a grant from the INSU-CNRS EC2CO (Ecosphère Continentale et Côtière) program (project "Friezbee"). We are thankful to the Hesione crew, Isabelle Bihannic, Erwan Amice and Thierry Le Bec, for their help during sampling. We thank Florian Caradec for his help with filtrations. We also thank Aurélien Boyer for its advice on statistics.

Author contributions

CL and DD designed the study. All authors contributed to the experiments. MU analyzed the data and wrote the first draft. All authors edited, proofread and approved the final manuscript.

References

Allison, S.D. and Martiny, J.B.H. (2008) Resistance, resilience, and redundancy in microbial communities. Proc Natl Acad Sci U S A 105: 11512–11519.

Arnosti, C. (2011) Microbial Extracellular Enzymes and the Marine Carbon Cycle. Annu Rev ofMarine Sci 3: 401–425.

Arnosti, C. (2014) Patterns of Microbially Driven Carbon Cycling in the Ocean: Links between Extracellular Enzymes and Microbial Communities. Adv Oceanogr 2014: 1–12.

Auffret, G.A. (1983) Dynamique sédimentaire de la marge continentale celtique-Evolution Cénozoïque-Spécificité du Pleistocène supérieur et de l'Holocène.

Azam, F. and Malfatti, F. (2007) Microbial structuring of marine ecosystems. Nat Rev Microbiol 5: 782–791.

Balmonte, J.P., Hasler-sheetal, H., Glud, R.N., Andersen, T.J., Sejr, M.K., Middelboe, M., et al. (2019) Sharp contrasts between freshwater and marine microbial enzymatic capabilities, community composition, and DOM pools in a NE Greenland fjord. Limnol Oceanogr 65: 77–95.

Baltar, F. (2018) Watch out for the "living dead": Cell-free enzymes and their fate. Front Microbiol 8: 2438.

Baltar, F., Arístegui, J., Gasol, J.M., Sintes, E., Van Aken, H.M., and Herndl, G.J. (2010) High dissolved extracellular enzymatic activity in the deep central Atlantic ocean. Aquat Microb Ecol 58: 287–302.

Baltar, F., De Corte, D., Thomson, B., and Yokokawa, T. (2019) Teasing apart the different size pools of extracellular enzymatic activity in the ocean. Sci Total Environ 660: 690–696.

Bassoullet, P. (1979) Etude de la dynamique des sédiments en suspension dans l'estuaire de l'Aulne (rade de Brest).

Bauer, J.E., Cai, W.J., Raymond, P.A., Bianchi, T.S., Hopkinson, C.S., and Regnier, P.A.G. (2013) The changing carbon cycle of the coastal ocean. Nature 504: 61–70.

Bertilsson, S., Eiler, A., Nordqvist, A., and Jørgensen, N.O.G. (2007) Links between bacterial production, amino-acid utilization and community composition in productive lakes. ISME J 1: 532–544.

Bianchi, T.S. (2011) The role of terrestrially derived organic carbon in the coastal ocean: A changing paradigm and the priming effect. Proc Natl Acad Sci U S A 108: 19473–19481.

Boucher, D. and Debroas, D. (2009) Impact of environmental factors on couplings between bacterial community composition and ectoenzymatic activities in a lacustrine ecosystem. FEMS Microbiol Ecol 70: 66–78.

Carreira, C., Staal, M., Middelboe, M., and Brussaard, P.D. (2015) Counting Viruses and Bacteria in Photosynthetic Microbial Mats. Appl Environ Microbiol 81: 2149–2155.

Christian, J.R. and Karl, D.M. (1995) Bacterial ectoenzymes in marine waters: Activity ratios and temperature responses in three oceanographic provinces. Limnol Oceanogr 40: 1042–1049.

Chróst, R.J. (1989) Characterization and significance of β-glucosidase activity in lake water. Limnol Oceanogr 34: 660–672.

Chróst, R.J. (1990) Microbial Ectoenzymes in Aquatic Environments. In Aquatic Microbial Ecology: Biochemical and molecular approaches. Overbeck, J. and Chróst, R.J. (eds). New York, pp. 47–77.

Comte, J. and Del Giorgio, P.A. (2010) Linking the patterns of change in composition and function in bacterioplankton successions along environmental gradients. Ecology 91: 1466–1476.

Crump, B.C., Fine, L.M., Fortunato, C.S., Herfort, L., Needoba, J.A., Murdock, S., and Prahl, F.G. (2017) Quantity and quality of particulate organic matter controls bacterial production in the Columbia River estuary. Limnol Oceanogr 62: 2713–2731.

Crump, B.C., Hopkinson, C.S., Sogin, M.L., and Hobbie, J.E. (2004) Microbial Biogeography along an Estuarine Salinity Gradient: Combined Influences of Bacterial Growth and Residence Time. Appl Environ Microbiol 70: 1494–1505.

Cunha, M.A., Almeida, M.A., and Alcantara, F. (2000) Patterns of ectoenzymatic and heterotrophic bacterial activities along a salinity gradient in a shallow tidal estuary. Mar Ecol Prog Ser 204: 1–12.

David, F., Meziane, T., Marchand, C., Rolland, G., Thanh-nho, N., and Lamy, D. (2021) Estuarine, Coastal and Shelf Science Prokaryotic abundance, cell size and extracellular enzymatic activity in a human impacted and mangrove dominated tropical estuary (Can Gio, Vietnam). Estuar Coast Shelf Sci 251: 107253.

Davis, C.E. and Mahaffey, C. (2017) Elevated alkaline phosphatase activity in a phosphate-replete environment: Influence of sinking particles. Limnol Oceanogr 62: 2389–2403.

Delgado-Baquerizo, M., Giaramida, L., Reich, P.B., Khachane, A.N., Hamonts, K., Edwards, C., et al. (2016) Lack of functional redundancy in the relationship between microbial diversity and ecosystem functioning. J Ecol 104: 936–946.

Delmas, D. (1983) Les glucides et l'évolution de la matière organique dans les sédiments marins. Oceanol Acta 6: 157–165.

Delmas, D. and Garet, M.J. (1995) SDS-preservation for deferred measurement of exoproteolytic kinetics in marine samples. J Microbiol Methods 22: 243–248.

Delmas, D., Legrand, C., Bechemin, C., Collinot, C., Legrand, C., Bechemin, C., and Collinot Aquat, C. (1994) Exoproteolytic activity deterrnined by flow injection analysis: its potential importance for bacterial growth in coastal marine ponds.

Delmas, R. and Tréguer, P. (1983) Évolution saisonnière des nutriments dans un écosystème eutrophe d'Europe occidentale (la rade de Brest). Interactions marines et terrestres. Oceanol Acta 6: 345–356.

Ducklow, H.W. and Carlson, C.A. (1992) Oceanic Bacterial Production. In Advances in Microbial Ecology. Marshall, K.C. (ed). New York: Plenum Press, pp. 113–181.

Fernández-Gómez, B., Richter, M., Schüler, M., Pinhassi, J., Acinas, S.G., González, J.M., and Pedrós-Alió, C. (2013) Ecology of marine bacteroidetes: A comparative genomics approach. ISME J 7: 1026–1037.

Ferrer-González, F.X., Widner, B., Holderman, N.R., Glushka, J., Edison, A.S., Kujawinski, E.B., and Moran, M.A. (2021) Resource partitioning of phytoplankton metabolites that support bacterial heterotrophy. ISME J 15: 762–773.

Fuhrman, J.A. and Azam, F. (1982) Thymidine incorporation as a measure of heterotrophic bacterioplankton production in marine surface waters: Evaluation and field results. Mar Biol 66: 109–120.

Fukuda, R., Sohrin, Y., Saotome, N., Fukuda, H., Nagata, T., and Koike, I. (2000) East-west gradient in ectoenzyme activities in the subarctic Pacific: Possible regulation by zinc. Limnol Oceanogr 45: 930–939.

Grossart, H.P. (2010) Ecological consequences of bacterioplankton lifestyles: Changes in concepts are needed. Environ Microbiol Rep 2: 706–714.

Hoppe, H.G. (2003) Phosphatase activity in the sea. Hydrobiologia 493: 187–200.

Hoppe, H.G. and Ullrich, S. (1999) Profiles of ectoenzymes in the Indian Ocean: Phenomena of phosphatase activity in the mesopelagic zone. Aquat Microb Ecol 19: 139–148.

Karner, M. and Herndl, G.J. (1992) Marine Biology in free-living and marine-snow-associated bacteria. Mar Biol 347: 341–347.

Koike, I. and Nagata, T. (1997) High potential activity of extracellular alkaline phosphatase in deep waters of the central Pacific. Deep Res Part II Top Stud Oceanogr 44: 2283–2294.

Labry, C., Delmas, D., and Herbland, A. (2005) Phytoplankton and bacterial alkaline phosphatase activities in relation to phosphate and DOP availability within the Gironde plume waters (Bay of Biscay). J Exp Mar Bio Ecol 318: 213–225.

Labry, C., Delmas, D., Moriceau, B., Gallinari, M., Quere, J., and Youenou, A. (2020) Effect of P depletion on the functional pools of diatom carbohydrates, and their utilization by bacterial communities. Mar Ecol Prog Ser 641: 49–62.

Labry, C., Delmas, D., Youenou, A., Quere, J., Leynaert, A., Fraisse, S., et al. (2016) High alkaline phosphatase activity in phosphate replete waters: The case of two macrotidal estuaries. Limnol Oceanogr 61: 1513–1529.

Labry, C. and Urvoy, M. (2020) Formaldehyde preservation for deferred measurements of alkaline phosphatase activities in marine samples. Heliyon 6: e05333.

Lamy, D., Obernosterer, I., Laghdass, M., Artigas, L.F., Breton, E., Grattepanche, J.D., et al. (2009) Temporal changes of major bacterial groups and bacterial heterotrophic activity during a Phaeocystis globosa bloom in the eastern English Channel. Aquat Microb Ecol 58: 95–107.

Landa, M., Blain, S., Christaki, U., Monchy, S., and Obernosterer, I. (2016) Shifts in bacterial community composition associated with increased carbon cycling in a mosaic of phytoplankton blooms. ISME J 10: 39–50.

Langenheder, S., Lindström, E.S., and Tranvik, L.J. (2005) Weak coupling between community composition and functioning of aquatic bacteria. Limnol Oceanogr 50: 957–967.

Lindström, E.S., Feng, X.M., Granéli, W., and Kritzberg, E.S. (2010) The interplay between bacterial community composition and the environment determining function of inland water bacteria. Limnol Oceanogr 55: 2052–2060.

Logue, J.B., Stedmon, C.A., Kellerman, A.M., Nielsen, N.J., Andersson, A.F., Laudon, H., et al. (2016) Experimental insights into the importance of aquatic bacterial community composition to the degradation of dissolved organic matter. ISME J 10: 533–545.

978 Louca, S., Polz, M.F., Mazel, F., Albright, M.B.N., Huber, J.A., O'Connor, M.I., et al. (2018) Function and functional
979 redundancy in microbial systems. Nat Ecol Evol 2: 936–943.

980 Marie, D., Partensky, F., Vaulot, D., and Brussaard, C. (1999) Enumeration of Phytoplankton, Bacteria, and Viruses
981 in Marine Samples. Curr Protoc Cytom 11.11.1-11.11.15.

982 Martinez, J., Smith, D.C., Steward, G.F., and Azam, F. (1996) Variability in ectohydrolytic enzyme activities of
983 pelagic marine bacteria and its significance for substrate processing in the sea. Aquat Microb Ecol 10:
984 223–230.

985 Middelburg, J.J. and Herman, P.M.J. (2007) Organic matter processing in tidal estuaries. Mar Chem 106: 127–
986 147.

987 Murrell, M.C., Hollibaugh, J.T., Silver, M.W., and Wong, P.S. (1999) Bacterioplankton dynamics in northern San
988 Francisco Bay: Role of particle association and seasonal freshwater flow. Limnol Oceanogr 44: 295–308.

989 Nausch, M. (1998) Alkaline phosphatase activities and the relationship to inorganic phosphate in the Pomeranian
990 Bight (southern Baltic Sea). Aquat Microb Ecol 16: 87–94.

991 Nicholson, D., Dyhrman, S., Chavez, F., and Paytan, A. (2006) Alkaline phosphatase activity in the phytoplankton
992 communities of Monterey Bay and San Francisco Bay. Limnol Oceanogr 51: 874–883.

993 Patel, A.B., Fukami, K., and Nishijima, T. (2000) Regulation of seasonal variability of aminopeptidase activities in
994 surface and bottom waters of Uranouchi Inlet, Japan. Aquat Microb Ecol 21: 139–149.

995 Piontek, J., Sperling, M., Nöthig, E., and Engel, A. (2014) Regulation of bacterioplankton activity in Fram Strait
996 (Arctic Ocean) during early summer: The role of organic matter supply and temperature. J Mar Syst 132:
997 83–94.

998 Pollard, P.C. and Ducklow, H. (2011) Ultrahigh bacterial production in a eutrophic subtropical Australian river:
999 Does viral lysis short-circuit the microbial loop? Limnol Oceanogr 56: 1115–1129.

1000 Rath, J., Schiller, C., and Herndl, G.J. (1993) Ectoenzymatic activity and bacterial dynamics along a trophic gradient
1001 in the Caribbean Sea. Mar Ecol Prog Ser 102: 89–96.

1002 Sala, M.M., Karner, M., Arin, L., and Marrasé, C. (2001) Measurement of ectoenzyme activities as an indication
1003 of inorganic nutrient imbalance in microbial communities. Aquat Microb Ecol 23: 301–311.

1004 Sanchez, G. (2013) PLS Path Modeling with R. Berkeley Trowchez Ed 235.

1005 Schultz, G.E., White, E.D., and Ducklow, H.W. (2003) Bacterioplankton dynamics in the York River estuary: Primary
1006 influence of temperature and freshwater inputs. Aquat Microb Ecol 30: 135–148.

1007 Servais, P. and Garnier, J. (2006) Organic carbon and bacterial heterotrophic activity in the maximum turbidity
1008 zone of the Seine estuary (France). Aquat Sci 68: 78–85.

1009 Smith, D.C., Simon, M., Alldredge, A.L., and Azam, F. (1992) Intense hydrolytic enzyme activity on marine
1010 aggregates and implication for rapid particle dissolution. Nature 359: 139–141.

1011 Sunagawa, S., Coelho, L.P., Chaffron, S., Kultima, J.R., Labadie, K., Salazar, G., et al. (2015) Structure and function
1012 of the global ocean microbiome. Science (80-) 348: 1261359.

1013 Teeling, H., Fuchs, B.M., Becher, D., Klockow, C., Gardebrecht, A., Bennke, C.M., et al. (2012) Substrate-controlled
1014 succession of marine bacterioplankton populations induced by a phytoplankton bloom. Science (80-)
1015 336: 608–611.

1016 Thomson, B., Wenley, J., Currie, K., Hepburn, C., Herndl, G.J., and Baltar, F. (2019) Resolving the paradox:
1017 Continuous cell-free alkaline phosphatase activity despite high phosphate concentrations. Mar Chem
1018 214: 103671.

1019 Tietjen, T. and Wetzel, R.G. (2003) Extracellular enzyme-clay mineral complexes: Enzyme adsorption, alteration
1020 of enzyme activity, and protection from photodegradation. Aquat Ecol 37: 331–339.

1021 Traving, S.J., Thygesen, U.H., Riemann, L., and Stedmon, C.A. (2015) A Model of Extracellular Enzymes in Free-
1022 Living Microbes: Which Strategy Pays Off ? Appl Environ Microbiol 81: 7385–7393.

1023 Urvoy, M., Labry, C., Delmas, D., Creac'h, L., and L'Helguen, S. (2020) Microbial enzymatic assays in environmental
1024 water samples: Impact of inner filter effect and substrate concentrations. Limnol Oceanogr Methods 18:
1025 725–738.

1026 Williams, C.J. and Jochem, F.J. (2015) Ectoenzyme kinetics in Florida Bay: Implications for bacterial carbon source
1027 and nutrient status. Hydrobiologia 569: 113–127.

1028 Ziervogel, K. and Arnosti, C. (2008) Polysaccharide hydrolysis in aggregates and free enzyme activity in aggregate-
1029 free seawater from the north-eastern Gulf of Mexico. Environ Microbiol 10: 289–299.

1030 Zimmerman, A.E., Martiny, A.C., and Allison, S.D. (2013) Microdiversity of extracellular enzyme genes among
1031 sequenced prokaryotic genomes. ISME J 7: 1187–1199.

III. Données supplémentaires

I. Supplementary material and methods

Nutrients

Nutrients (ammonium, nitrite, nitrate, silicate) were measured using segmented flow analysis according to Aminot et al. (2009). Phosphate was manually measured by the phosphomolybdate-blue colorimetric reaction (Murphy and Riley, 1962) using a 5 cm cuvette and Shimadzu UV 160 spectrophotometer.

Dissolved organic matter characterization

Several non-specific and specific parameters were measured to assess the different components of the global pool of dissolved organic matter (DOM). Dissolved organic carbon (DOC) concentration was estimated from absorption spectra in the near-UV (250-30 nm) using a Shimadzu UV 160 spectrophotometer (Pages and Gadel, 1990). Dissolved organic phosphorus (DOP) was analyzed according to the alkaline persulfate oxidation procedure (Koroleff, 1983), which converts DOP into phosphate. The subsequent quantification of phosphate was achieved by the phosphomolybdate-blue colorimetric reaction (Murphy and Riley, 1962) using a 5 cm cuvette and Shimadzu UV 160 spectrophotometer, as described above.

Dissolved monosaccharides (DMCHO) and dissolved polysaccharides (DPCHO) were quantified as described in Labry *et al.* (2005) using the 2,4,6-tripyridyl-S-triazine method of (Myklestad *et al.*, 1997). Briefly, DMCHO were determined by direct reaction without hydrolysis, while total monosaccharides were analyzed after a 20 h hydrolysis with 0.1 M HCl at 100°C (under nitrogen atmosphere) and pH neutralization. DPCHO was determined as the difference between the two measurements. All measurements were conducted in triplicates.

Dissolved free amino acids (DFAA) and dissolved combined amino acids (DCAA) were determined according to Delmas *et al.* (1990). Briefly, dissolved primary amine concentration was determined by Flow Injection Analysis based on the fluorescence of o-phthaldialdehyde amino acids derivatives using glycine as standard. DFAA was determined by correcting dissolved primary amine concentration with ammonium concentrations. Total amino acids were determined after a hydrolysis step (Henrichs and Williams, 1985) under nitrogen atmosphere (5.8 N hydrochloric acid final concentration, 24 h at 105°C) with ascorbic acid and neutralization with 2.9 N sodium hydroxide. Ascorbic acid was used to prevent the DFAA and DCAA degradation in the presence of nitrate during the hydrolysis (Robertson *et al.*, 1987). DCAA was determined as the difference between total amino acids and DFAA. For both fractions, correction for the natural fluorescence was done using the same protocol without the o-phthaldialdehyde reagent. All measurements were conducted in triplicates.

Particulate organic matter characterization

Particulate matter composition was characterized by measuring non-specific global parameters as well as specific compounds (carbohydrates, amino acids). SPM were measured using pre-weighted pre-combusted (4 h, 480°C) glass-fiber filters (GF/F) filters, as described in Labry *et al.* (2016). The filters were rinsed with Milli-Q water to remove salts. SPM corresponded to the increase in weight after drying at 70°C for 3 h. Particulate inorganic matter (PIM) corresponded to the weight after 2 h at 480 °C. The organic proportion of SPM (particulate organic matter, POM) was determined as the difference between the SPM and PIM. Chlorophyll *a* (Chl*a*) and Pheopigments (Pheo) were determined by acidification fluorometric procedure in 90% acetone extracts (Holm-Hansen *et al.*, 1965). The percentage of Chl*a* (%Chl*a*) was calculated as Chl*a* over Chl*a* and Pheo.

Filters for particulate organic carbon (POC) and particulate organic nitrogen (PON) were dried at 60 °C for 24 h. POC and PON concentrations were determined on an isotope ratio mass spectrometer (IRMS, Delta plus, ThermoFisher Scientific, Bremen, Germany) coupled with a C/N analyzer (Flash EA, ThermoFisher Scientific) via a type III interface. The particulate COP/NOP molar ratios were calculated from those measurements.

Total particulate phosphorus (TPP) and particulate inorganic phosphorus (PIP) were determined as described in Labry *et al.* (2013) following the original method of Solorzano and Sharp (1980) and Aspila *et al.* (1976), respectively. Since all methods consist in converting the different forms of phosphorus into phosphate, the subsequent quantification of phosphate was achieved by the phosphomolybdate-blue colorimetric reaction (Murphy and Riley, 1962) using segmented flow analysis. Particulate organic phosphorus (POP) was determined as the difference between TPP and PIP.

Filters for particulate soluble (PSCHO) and insoluble (PICHO) carbohydrates were sequentially extracted (Delmas, 1983). PSCHO were extracted using 5 mL of water and 30 min incubation at 100°C. PICHO were extracted using the same filter with 5 mL of 2 N sulfuric acid and 4 h incubation at 100°C. Each time, the supernatant was collected after centrifugation and analyzed using the standard phenol-sulfuric acid method (Dubois *et al.*, 1956).

Particulate amino acids (PAA) were determined as described for DAA, after a hydrolysis step directly on the filter (nitrogen atmosphere, 5.8 N hydrochloric acid, 24 h at 105°C) and without ascorbic acid.

References

Aspila, K.I., Agemian, H., and Chau, A.S.Y. (1976) A semi-automated method for the determination of inorganic, organic and total phosphate in sediments. Analyst 101: 187–197.

Delmas, D. (1983) Les glucides et l'évolution de la matière organique dans les sédiments marins. Oceanol Acta 6: 157–165.

Delmas, D., Frikha, M.G., and Linley, E.A.S. (1990) Dissolved primary amine measurement by flow injection analysis with o-phthaldialdehyde: Comparison with high-performance liquid chromatography. Mar Chem 29: 145–154.

Dubois, M., Gilles, K.A., Hamilton, J.K., Rebers, P.A., and Smith, F. (1956) Colorimetric Method for Determination of Sugars and Related Substances. Anal Chem 28: 350–356.

Henrichs, S.M. and Williams, P.M. (1985) Dissolved and particulate amino acids and carbohydrates in the sea surface microlayer. Mar Chem 17: 141–163.

Holm-Hansen, O., Lorenzen, C.J., Holmes, R.W., and Strickland, J.D.H. (1965) Fluorometric determination of chlorophyll. ICES J Mar Sci 30: 3–15.

Koroleff, F. (1983) Determination of phosphorus. In Methods of Seawater analysis. Grasshoff, K., Ehrhardt, M., and Kremling, K. (eds). Weinheim: Verlag Chemie, pp. 125–139.

Labry, C., Delmas, D., and Herbland, A. (2005) Phytoplankton and bacterial alkaline phosphatase activities in relation to phosphate and DOP availability within the Gironde plume waters (Bay of Biscay). J Exp Mar Bio Ecol 318: 213–225.

Labry, C., Delmas, D., Youenou, A., Quere, J., Leynaert, A., Fraisse, S., et al. (2016) High alkaline phosphatase activity in phosphate replete waters: The case of two macrotidal estuaries. Limnol Oceanogr 61: 1513–1529.

Labry, C., Youenou, A., Delmas, D., and Michelon, P. (2013) Addressing the measurement of particulate organic and inorganic phosphorus in estuarine and coastal waters. Cont Shelf Res 60: 28–37.

Murphy, J. and Riley, J.P. (1962) A modified single solution method for the determination of phosphate in natural waters. Anal Chim Acta 27: 31–36.

Myklestad, S.M., Skånøy, E., and Hestmann, S. (1997) A sensitive and rapid method for analysis of dissolved mono- and polysaccharides in seawater. Mar Chem 56: 279–286.

Pages, J. and Gadel, F. (1990) Dissolved organic matter and UV absorption in a tropical hyperhaline estuary. Sci Total Environ 99: 173–204.

Robertson, K.J., Williams, P.M., and Bada, J.L. (1987) Acid hydrolysis of dissolved combined amino acids in seawater: A precautionary note. Limnol Oceanogr 32: 996–997.

Solorzano, L. and Sharp, J.H. (1980) Determination of total dissolved phosphorus and particulate phosphorus in natural waters. Limnol Oceanogr 25: 758–760.

II. Supplementary data

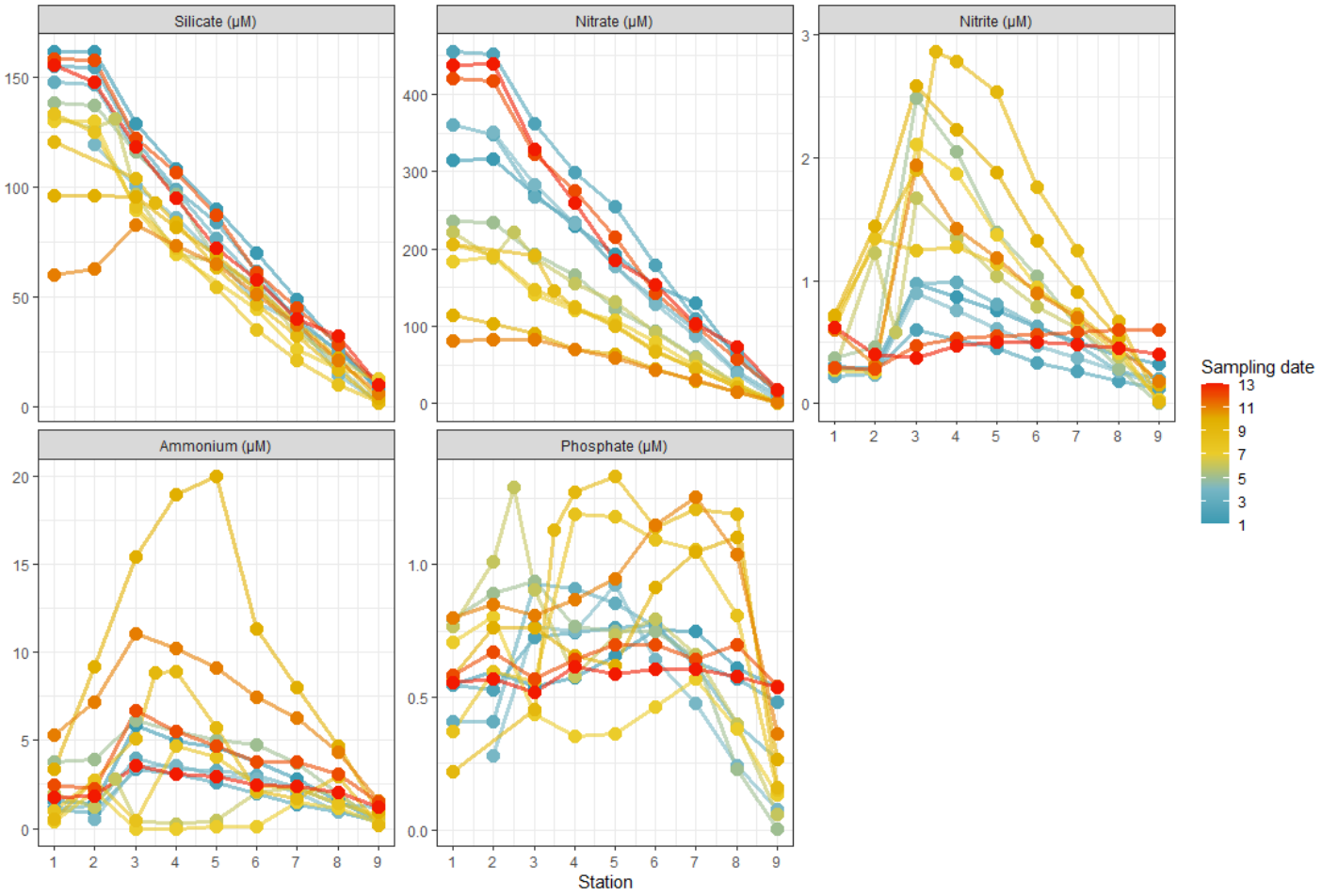

Figure S1. Evolution of the nutrient concentration along the Aulne salinity gradient for each sampling date.

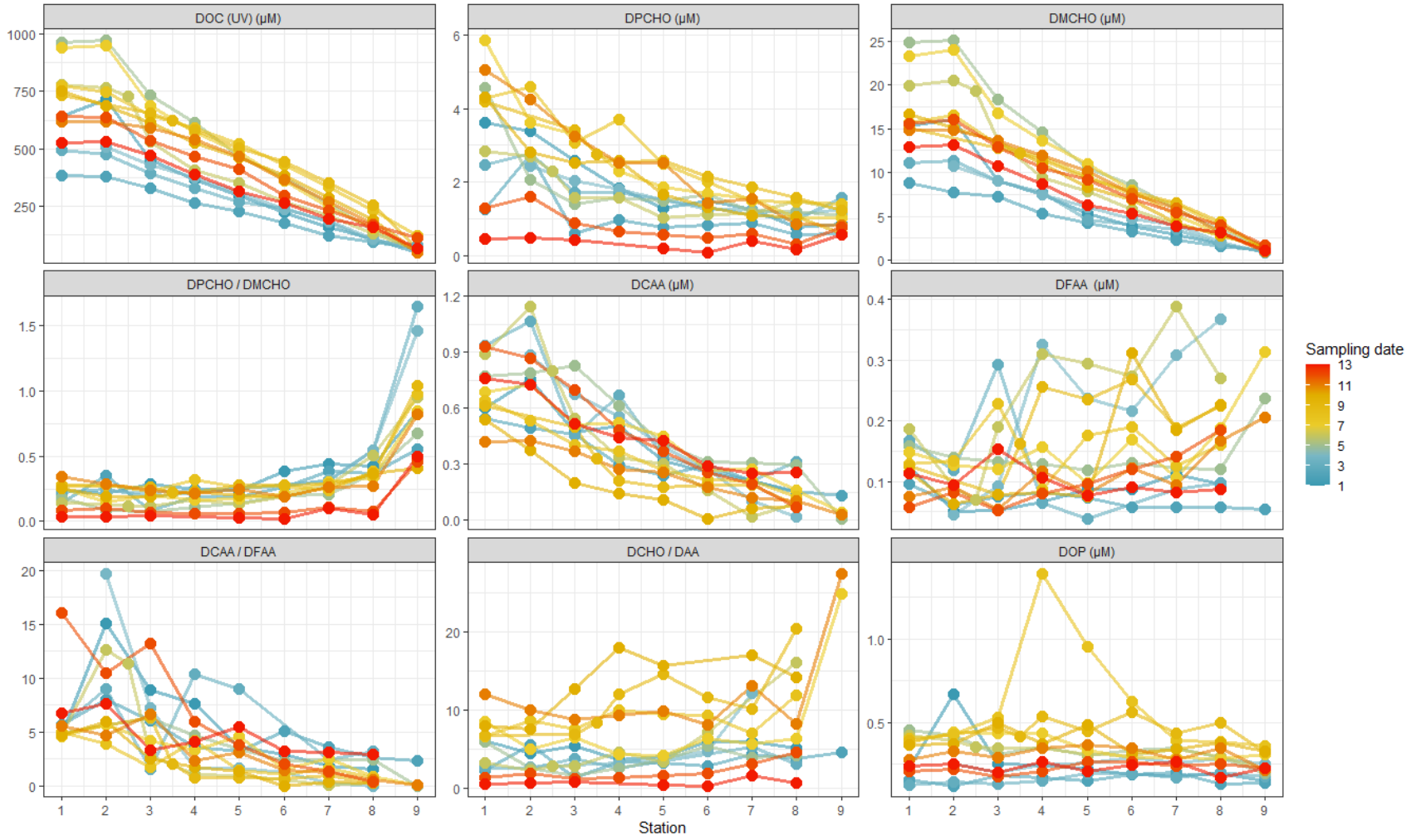

Figure S2. Evolution of the dissolved organic matter-related parameter concentration along the Aulne salinity gradient for each sampling date. DOC: dissolved organic carbon; DPCHO: dissolved polysaccharides: DMCHO: dissolved monosaccharides; DCHO: dissolved carbohydrates (DPCHO + DMCHO); DCAA: dissolved combined amino acids; DFAA: dissolved free amino acids; DAA: dissolved amino acids (DFAA + DCAA); DOP: dissolved organic phosphorus.

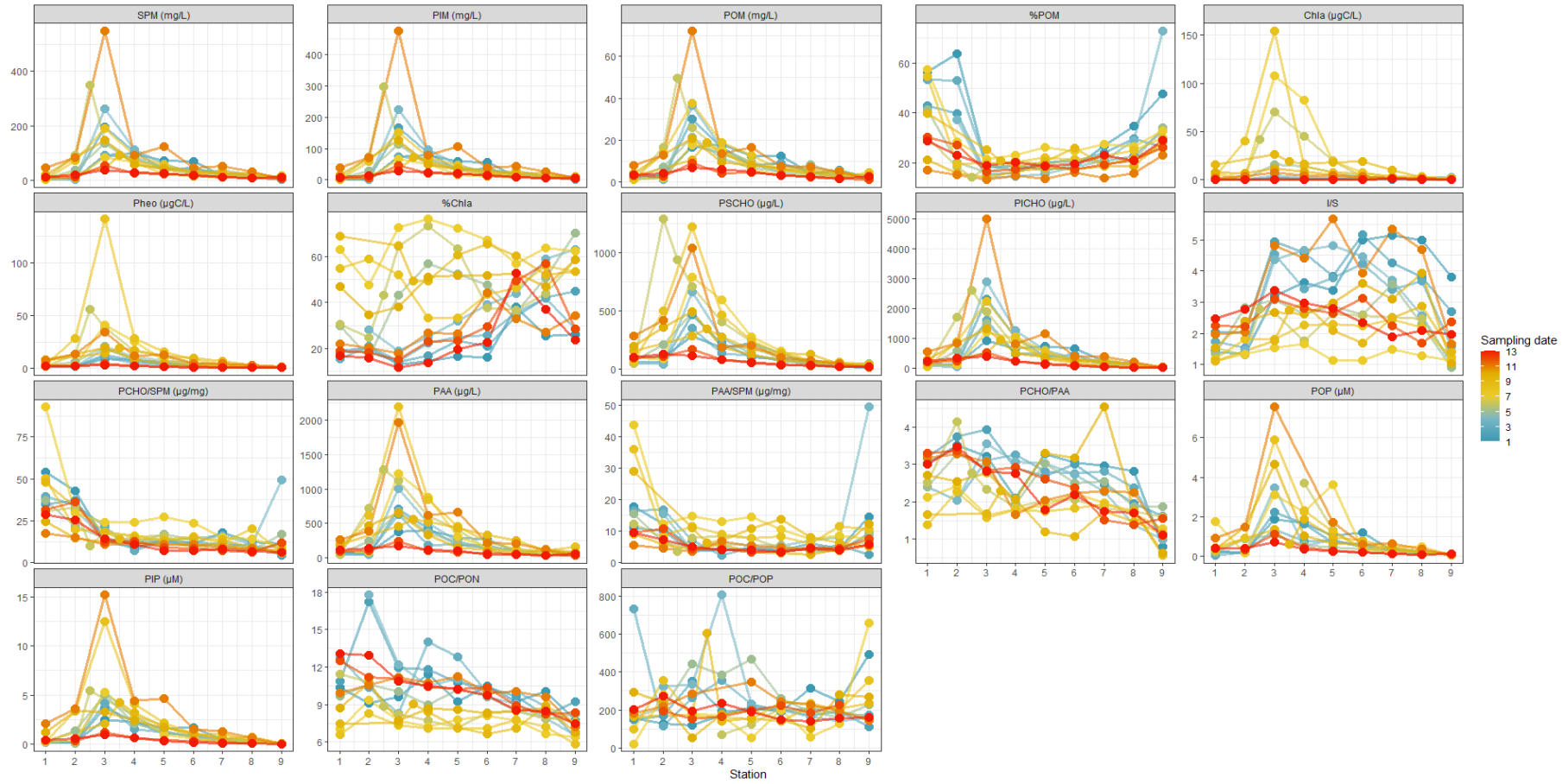

Figure S3. Evolution of the particulate organic matter-related parameter concentration along the Aulne salinity gradient for each sampling date. SPM: suspended particulate matter; PIM: particulate inorganic matter; POM: particulate organic matter; %POM: percent of POM; Chl*a*: Chlorophyll *a*; Pheo: Pheopigments; %Chl*a*: percent Chl*a*, PSCHO: particulate soluble carbohydrates; PICHO: particulate insoluble carbohydrates; I/S: PICHO over PSCHO; PCHO: particulate carbohydrate (PICHO + PSCHO); PAA: particulate amino acids; POP: particulate organic phosphorus; PIP: particulate inorganic phosphorus; POC: particulate organic carbon; PON: particulate organic nitrogen.

A. All DOM- and nutrients-related variables

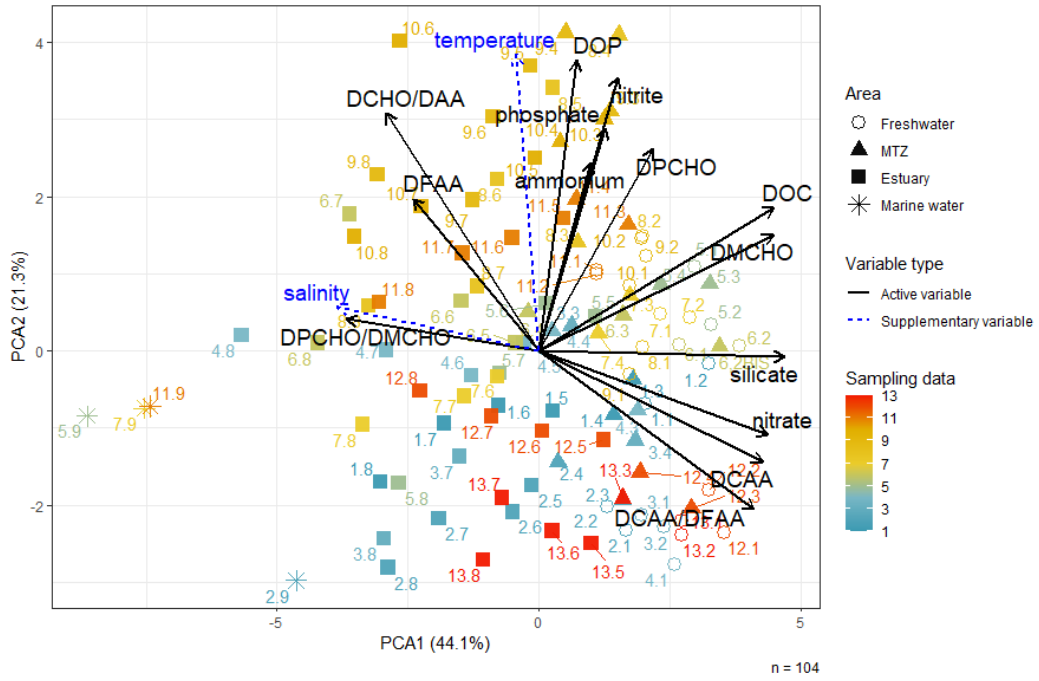

B. Without DCAA, DFAA, DFAA/DCAA and DCHO/DAA

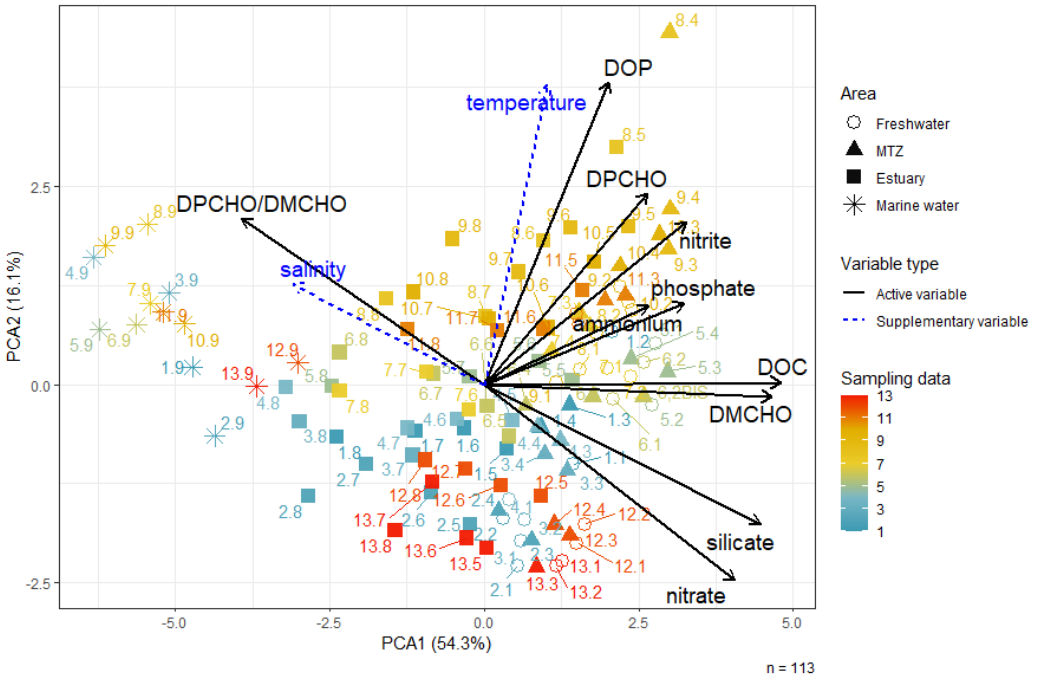

Figure S4. Impact of missing values on the PCA ordination performed on variables characterizing the dissolved fraction. (**A**) All nutrient and DOM-related variables were used (n = 104). (**B**) DCAA, DFAA and DCAA/DFAA were removed because of missing values at the station S9 (n = 113). Blue arrows (temperature and salinity) are supplementary variables added to facilitate interpretation but did not participate in the PCA construction. n: number of samples used in the PCA. Samples are labeled as "sampling month.sampling station".

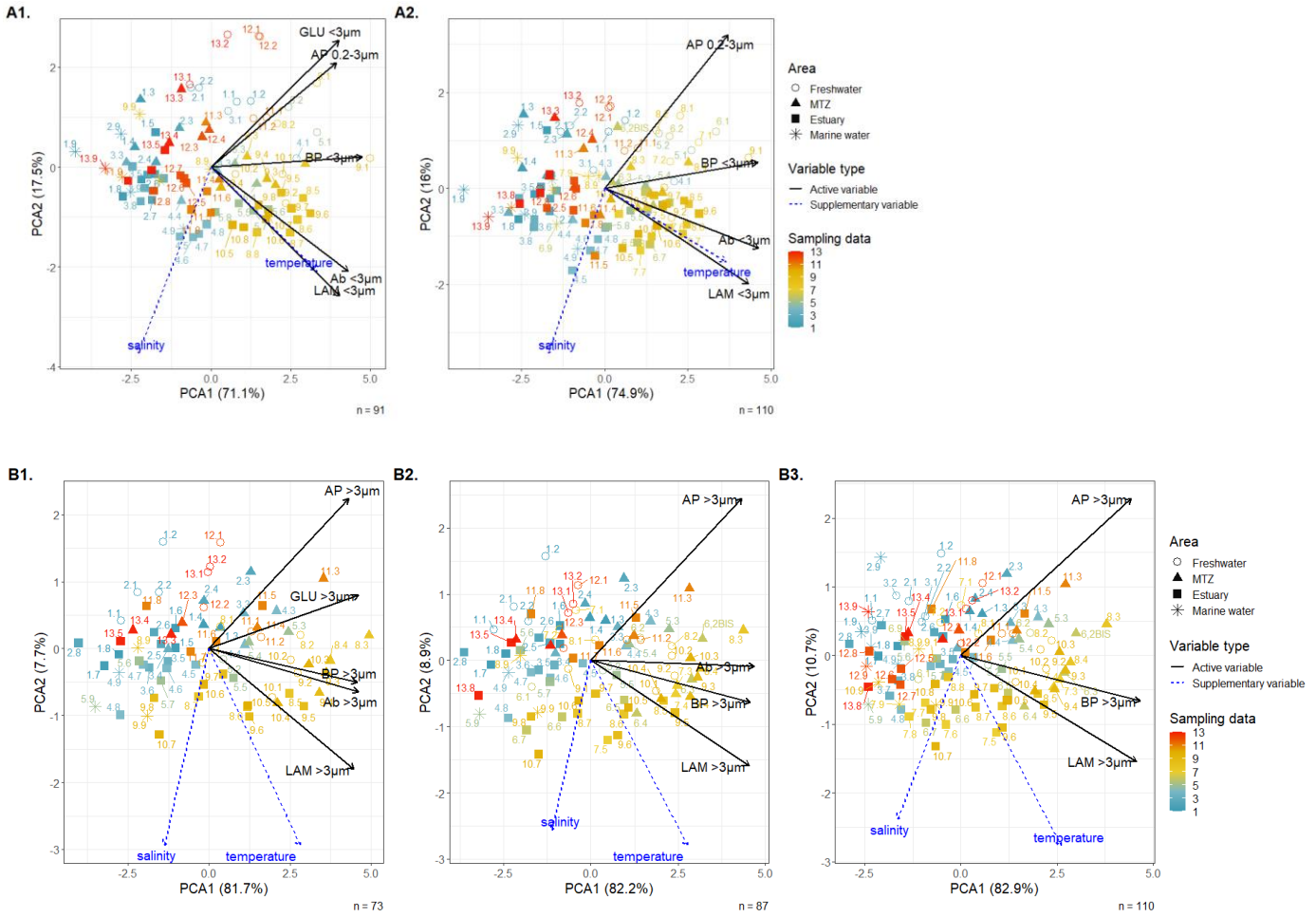

Figure S5. Impact of missing values on the PCA ordinations performed on the bacterial parameters (enzymatic activities, bacterial production and bacterial abundance) for the < 3 µm (**A1-2**) and > 3 µm fraction (**B1-3**). (**A1**) All parameters were used. (**A2**) GLU < 3 µm was removed. (**B1**) All parameters were used. (**B2**) GLU > 3 µm was removed. (**B3**) GLU- and Ab > 3 µm were remove. Missing values did not impact PCA interpretation. Blue arrows (temperature and salinity) are supplementary variables added to facilitate interpretation but did not participate in the PCA construction. n: number of samples used in the PCA. Samples are labeled as "sampling month.sampling station".

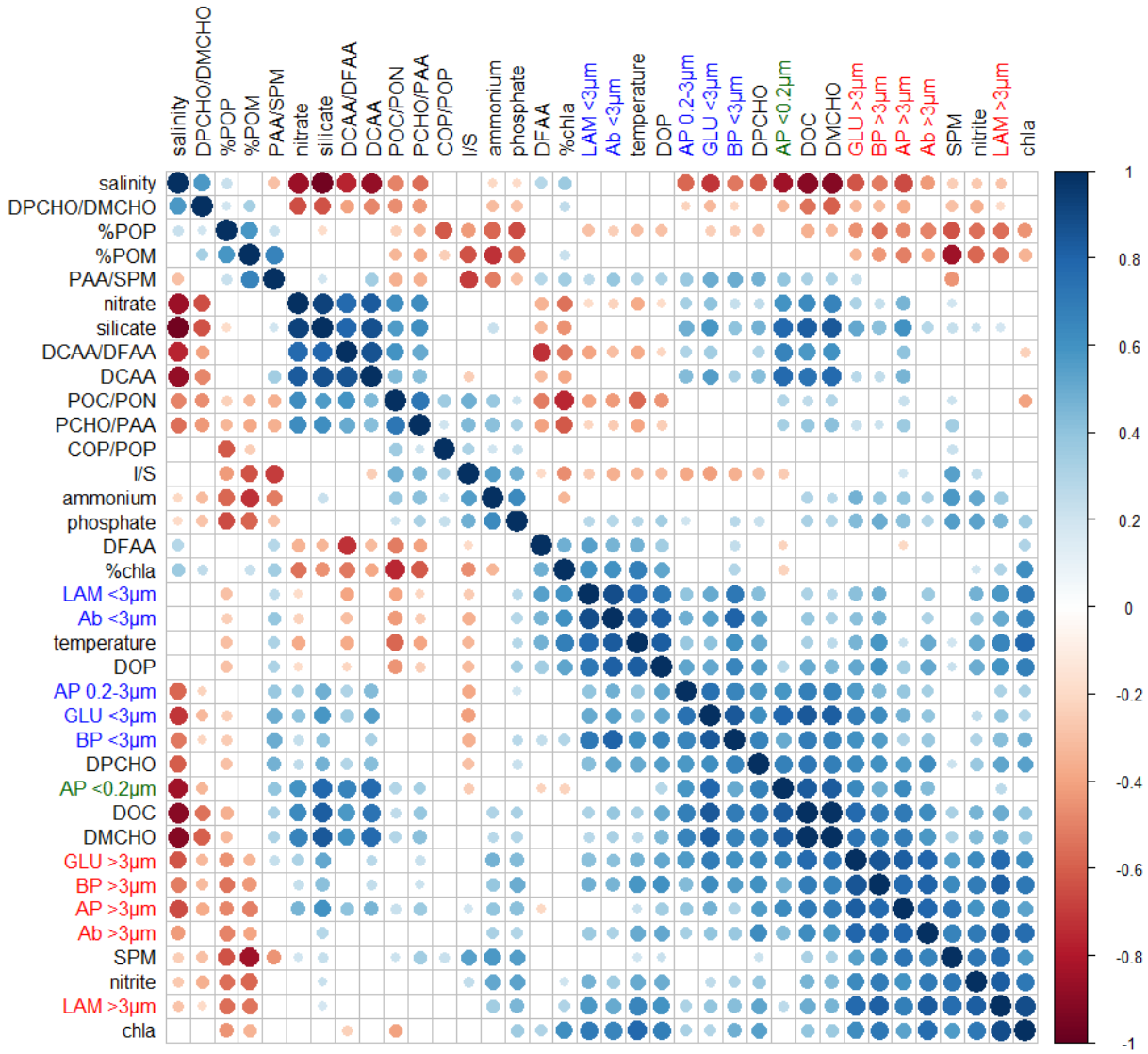

Figure S6. Spearman correlation coefficient for the physicochemical parameters (black font), the particle-attached-related bacterial parameters (red font), the free-living-related bacterial parameters (blue font) and the dissolved AP (green font). Only significant coefficients are shown ($p < 0.05$) and the parameters are ordered according to ward clustering.

A.

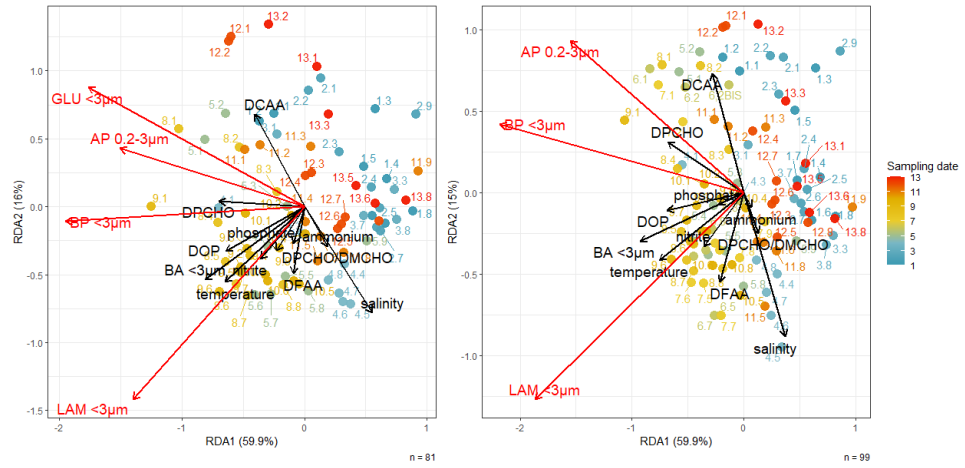

B.

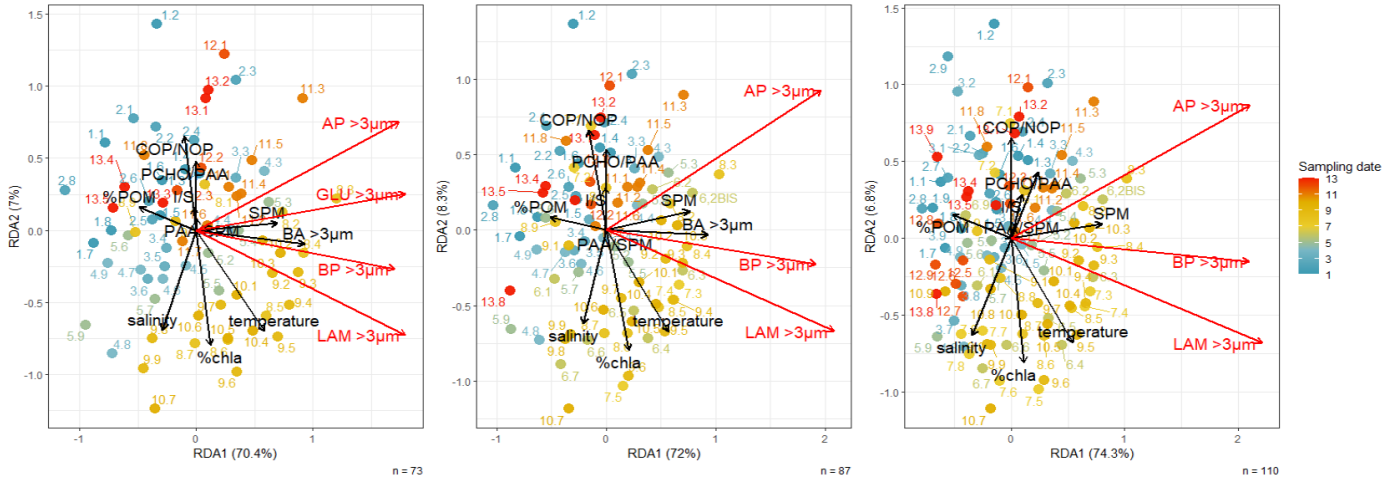

Figure S7. Impact of missing values on the RDA performed on < 3 µm (**A**) and > 3 µm (**B**) activities. (**A**) RDAs were performed with all variables (left, n = 81) and without GLU < 3 µm (middle, n = 99). (**B**) RDAs were performed with all variables (left, n = 73); without GLU > 3 µm (middle, n = 87); and without GLU > 3 µm and Ab > 3 µm (right, n = 110). n: number of samples used in the RDA; Samples are labeled as "sampling month.sampling station".

Chapitre V*. Le quorum sensing régule la synthèse d'enzymes hydrolytiques et la production de biofilm au sein de bactéries de l'estuaire de l'Aulne*

I. Introduction

Les bactéries hétérotrophes jouent un rôle important dans la transformation de la matière organique. Leur métabolisme semble particulièrement intense lorsqu'elles colonisent des particules, formant des biofilms densément peuplés. Cependant, les raisons et mécanismes derrière cette observation sont encore peu élucidés, bien qu'une possible régulation par le quorum sensing (QS) ait été avancée. Dans ce chapitre, nous avons cherché à étudier le lien entre le QS et les activités enzymatiques hydrolytiques au sein de souches bactériennes estuariennes. Les deux objectifs principaux étaient de :

- Déterminer si des souches isolées de l'Aulne produisent des *N*-acyle homosérine lactones (AHLs), molécules du QS, lors de leur mise en culture ;
- Déterminer si les AHLs produites par les souches influencent leur production de biofilm et d'enzymes hydrolytiques.

Dans ce but, près de 300 souches bactériennes ont été isolées à différentes salinités de l'estuaire de l'Aulne et leurs capacités de QS et quorum quenching (QQ) ont été étudiées en combinant l'utilisation de biosenseurs et la spectrométrie de masse (UHPLC-HRMS/MS). Nous avons ainsi démontré la production de diverses AHLs chez 28 souches de l'estuaire. Nous avons aussi montré que 10 de ces 28 souches possédaient également des capacités de QQ, suggérant que les mécanismes de QS et QQ coexistent fréquemment chez les bactéries

Nous avons ensuite étudié l'implication du QS dans la régulation de la production de biofilm et des activités aminopeptidases et β-glucosidases dissoutes et liées aux cellules chez les 28 souches isolées produisant des AHLs. Pour cela, nous avons inhibé la communication bactérienne grâce à l'ajout de lactonases, des enzymes qui dégradent les AHLs, puis quantifié l'effet sur la croissance, la production de biofilm et les activités enzymatiques. Cette étude a mis en évidence une large implication du QS dans la régulation de ces phénotypes puisque 23 souches ont vu au moins un phénotype significativement modifié par le traitement. Nos résultats ont également mis en lumière la complexité des interactions basées sur le QS puisque l'effet des lactonases semble très contrasté, même au sein de souches proches d'un point de vue phylogénétique.

Ces résultats ont fait l'objet d'une publication dans le journal *Environmental microbiology* en 2021.

environmental microbiology

Environmental Microbiology (2021) **00**(00), 00–00 doi:10.1111/1462-2920.15775

Quorum sensing disruption regulates hydrolytic enzyme and biofilm production in estuarine bacteria

Marion Urvoy,[1,2*] **Raphaël Lami**,[3] **Catherine Dreanno**,[4] **David Daudé**,[5] **Alice M. S. Rodrigues**,[3] **Michèle Gourmelon**,[1] **Stéphane L'Helguen**[2] **and Claire Labry**[1]

[1]*Ifremer, DYNECO, Plouzané, F-29280, France.*

[2]*Université de Bretagne Occidentale, CNRS, IRD, Ifremer, UMR 6539, Laboratoire des Sciences de l'Environnement Marin (LEMAR), Plouzané, F-29280, France.*

[3]*Sorbonne Université, CNRS, Laboratoire de Biodiversité et Biotechnologies Microbiennes (LBBM), 66650 Banyuls-sur-Mer, France.*

[4]*Ifremer, RDT, Plouzané, F-29280, France.*

[5]*Gene&GreenTK, 19-21 Boulevard Jean Moulin, Marseille, 13005, France.*

Summary

Biofilms of heterotrophic bacteria cover organic matter aggregates and constitute hotspots of mineralization, primarily acting through extracellular hydrolytic enzyme production. Nevertheless, regulation of both biofilm and hydrolytic enzyme synthesis remains poorly investigated, especially in estuarine ecosystems. In this study, various bioassays, mass spectrometry and genomics approaches were combined to test the possible involvement of quorum sensing (QS) in these mechanisms. QS is a bacterial cell–cell communication system that relies notably on the emission of *N*-acylhomoserine lactones (AHLs). In our estuarine bacterial collection, we found that 28 strains (9%), mainly *Vibrio*, *Pseudomonas* and *Acinetobacter* isolates, produced at least 14 different types of AHLs encoded by various *luxI* genes. We then inhibited the AHL QS circuits of those 28 strains using a broad-spectrum lactonase preparation and tested whether biofilm production as well as β-glucosidase and leucine-aminopeptidase activities were impacted. Interestingly, we recorded contrasted responses, as biofilm production, dissolved and cell-bound β-glucosidase and leucine-aminopeptidase activities significantly increased in 4%–68% of strains but decreased in 0%–21% of strains. These findings highlight the key role of AHL-based QS in estuarine bacterial physiology and ultimately on biogeochemical cycles. They also point out the complexity of QS regulations within natural microbial assemblages.

Introduction

Heterotrophic microbial communities play a central role in biogeochemical carbon (C) and nutrients cycling in the oceans (Azam and Malfatti, 2007). As organic matter mostly consists of unavailable polymeric substrates, heterotrophic prokaryotes need to cleave them into smaller molecules that can be transported across their cell membranes (Arnosti, 2011). These activities rely on the expression of a diverse array of dissolved (cell-free) and cell-bound extracellular hydrolytic enzymes. Those enzymes initiate organic matter mineralization through the 'microbial loop' (Pomeroy, 1974; Azam *et al*., 1983), ultimately affecting C export, nutrient cycling and energy flow through the food web (Chróst, 1990; Azam and Malfatti, 2007).

Estuaries are important transition zones where organic matter is heavily transformed before reaching coastal areas. Those mineralization processes are particularly intense in the maximum turbidity zone, where aggregate concentrations may reach several grams per litre. Marine bacteria living on such aggregates frequently reside in complex multi-layered environments called biofilms, where they are embedded in a matrix of extracellular polymers (Dang and Lovell, 2016; Flemming *et al*., 2016). Those particle-attached microorganisms are often more active than their free-living counterparts in terms of bacterial production and enzymatic activity (Crump *et al*., 1999; Millar *et al*., 2015). These enzymes actively solubilize particulate organic matter into dissolved compounds, impacting both local organic matter composition and C export to coastal waters (Azam and Malfatti, 2007; Dang and Lovell, 2016). Dissolved enzymes, which may be actively secreted or result from viral lysis and grazing (Baltar, 2018), are also involved in the mineralization of organic matter. They often account

Received 28 June, 2021; revised 2 September, 2021; accepted 10 September, 2021. *For correspondence. E-mail marion.urvoy@outlook.fr; Tel. (+33)2 29 00 85 76.

for a large proportion of total enzymatic activities (Baltar, 2018; Thomson *et al*., 2019).

Despite their important ecological implications, the mechanisms that regulate bacterial colonization, cell-bound and dissolved hydrolytic enzyme expression among these microbial consortia have been poorly characterized, especially in estuarine environments. *In situ* enzymatic activity of bacterial communities likely results from the communities' genetic potential (determined by the bacterial community composition), as well as the differential expression of those genes, driven by environmental factors (Arnosti, 2011). Indeed, distinct microbial communities with specific taxonomic and functional compositions may colonize organic matter particles and express various hydrolytic enzymes (Delong *et al*., 1993; Middelboe *et al*., 1995; Rieck *et al*., 2015). Hydrolytic enzyme production is also tightly regulated at the transcriptional level (Chróst, 1990; Arnosti, 2011). In particular, the concentration and composition of organic matter are key factors driving hydrolytic enzyme production through substrate induction, end-product repression or catabolic repression (Chróst and Siuda, 2002; Arnosti, 2011).

Quorum sensing (QS) is a widespread communication system allowing bacterial assemblages to synchronize their gene expression at the population level (Miller and Bassler, 2001; Waters and Bassler, 2005). This mechanism relies on the production, diffusion and sensing of small diffusible molecules called autoinducers (AIs). When the concentration of AIs increases under favourable conditions (i.e. high cellular density, low mass-transfer properties), they bind their cognate receptors and regulate the transcription of their target genes (Waters and Bassler, 2005; Papenfort and Bassler, 2016). These target genes are involved in diverse functions such as bioluminescence, motility, biofilm formation, virulence and hydrolytic enzyme production (Miller and Bassler, 2001; Hmelo, 2017). In Gram-negative bacteria, the most well-characterized QS system is based on the synthesis of *N*-acylhomoserine lactones (AHLs) (Papenfort and Bassler, 2016; Hmelo, 2017). These cell–cell QS-based interactions can be disrupted by quorum quenching (QQ) mechanisms (Kalia, 2013; Grandclément *et al*., 2015). They rely on the enzymatic degradation of signal molecules or on the production of QS inhibitors that block the signal production or reception, among other mechanisms (Kalia, 2013; Grandclément *et al*., 2015).

QS and QQ are widespread mechanisms among aquatic microbial communities. A large diversity of QS and QQ genes have been identified in metagenomics datasets (Doberva *et al*., 2015; Muras *et al*., 2018). AHLs have been detected in various types of aquatic environments such as marine aggregates (Hmelo *et al*., 2011; Jatt *et al*., 2015, corals and sponges (Tait *et al*., 2010) and bacterial mats (Decho *et al*., 2009). Similarly, numerous bacteria isolated from aquatic environments exhibit AI production or quenching capacities in culture (Gram *et al*., 2002; Romero *et al*., 2011; Tourneroche *et al*., 2019). To the best of our knowledge, no QS study has been conducted in estuarine ecosystems.

In aquatic environments, biofilm production, emission of QS compounds and hydrolytic activities are inherently linked. Densely packed biofilms favour both high enzymatic activities and the accumulation of QS compounds (Dang and Lovell, 2016; Flemming *et al*., 2016; Hmelo, 2017). QS mechanisms are also known to regulate the biofilm formation, maturation and dispersion (Lami, 2019). In this vein, it was shown that the addition of QS compounds to both natural bacterial communities and bacterial cultures modified the activity of extracellular hydrolytic enzymes (Hmelo *et al*., 2011; Jatt *et al*., 2015; Krupke *et al*., 2016; Su *et al*., 2019), as well as their biofilm production (Liu *et al*., 2017; Su *et al*., 2019). Nevertheless, the role of QS as a regulatory mechanism of those bacterial functions involved in crucial biogeochemical processes remains underexplored, especially in estuaries.

In this study, we investigated the prevalence of AHL-based QS and QQ circuits among bacterial strains isolated in the Aulne estuary (Bay of Brest, France), combining bioassays, liquid chromatography coupled to mass spectrometry (UHPLC-HRMS/MS) and genomics approaches. We then explored whether AHL-based QS regulates biofilm production as well as dissolved and cell-bound leucine aminopeptidase (LAM) and β-glucosidase (β-glc) synthesis among the identified AHL-producing bacteria. An original approach of our work is the use of enzyme-driven QQ to disrupt the expression of QS circuits in several strains. Taken together, our results revealed that the studied estuarine bacteria synthesize a diverse array of AHLs. The inhibition of AHL signals led to contrasted effects on biofilm production and hydrolytic enzyme activities in several of the targeted strains, highlighting the importance of QS in the regulation of estuarine bacteria physiology and ultimately in biogeochemical cycles.

Results

Production of QS metabolites among estuarine bacteria

A total of 299 bacterial strains were isolated from the Aulne estuary (Supporting Information Table S1) and screened for their ability to produce AHLs, using the *Pseudomonas putida* F117 and *Escherichia coli* MT102 biosensors. Among them, only a few strains (19 strains, 6%) clearly induced at least one biosensor compared with the negative control (ratio > 1.5, $P < 0.05$; Supporting Information Table S2). In addition, 56 strains

(19%) induced either a questionable induction ($1.2 < \text{ratio} < 1.5$, $P < 0.05$) or an inhibition (ratio < 0.8, $P < 0.05$) of the green fluorescent protein (GFP) production. To increase the probability of finding AHL-producing bacteria, we selected all 75 strains (25% of total isolated strains) for the analytical assessment of AHL production. Among those 75 bacteria, AHLs were detected in the supernatant of 28 strains using a UHPLC-HRMS/MS approach. Among those 28 strains, 26 (9% of total isolated strains) showed an AHL production that was quantifiable using commercially available standards (Table 1, see the Experimental procedures for the full AHL names). The two additional strains (*Pseudomonas* sp. AF02-5 and *Sphingobacterium* sp. AF02-2) seemed to produce an unsaturated C16-HSL (C16:1-HSL) given its mass, molecular formula and the presence of its characteristic fragments. Unfortunately, this AHL could not be confirmed nor quantified because the corresponding standard is not commercially available. Such AHLs are qualified as 'putative' in this study (Table 1).

Overall, the AHLs produced by the isolated estuarine strains were diverse. A total of 14 different AHLs (Table 1) were identified, with a side-chain length ranging from 4 to 14 C atoms. Both hydroxyl and carbonyl substitutions were found at the C3 position among the identified AHLs. We also found several other putative AHLs (C6:1-HSL, C12:1-HSL, C16:1- and 3-OH-C7-HSL), which also could not be confirmed nor quantified. It is worth noting that the χ^2 test and Fischer's exact test showed no significant impact of the salinity or the sampling fraction (i.e. attached or free-living) on the number of isolated AHL-producing strains (data not shown).

Taxonomic identification of AHL-producing isolates

The 28 AHL-producing bacteria were either Gammaproteobacteria (27 strains) or Bacteroidetes (1 strain). More precisely, they belonged to the genera *Vibrio* (10 strains), *Pseudomonas* (10 strains), *Acinetobacter* (5 strains), *Obesumbacterium* (1 strain), *Morganella* (1 strain) and *Sphingobacterium* (1 strain, Fig. 1, Table 1; Supporting Information Table S3). For samples at salinity 0, only *Pseudomonas*-affiliated strains (6 strains) were detected as AHL producers, except one strain affiliated with *Sphingobacterium faecium*. There was a greater diversity of AHL-producing isolates retrieved at salinity 5, corresponding to the maximum turbidity zone. Those strains were affiliated with the *Pseudomonas*, *Acinetobacter*, *Morganella* and *Obesumbacterium* genera. At salinity 25, all AHL-producing strains were affiliated with *Vibrio* species (two strains affiliated with *V. echinoideorum* in April and eight strains affiliated with *V. alginolyticus* in July). Interestingly, all the *Vibrio* strains were found to produce 3-OH-C6-HSL, while none of the other strains produced this type of AHL. The AHL production among the other *Pseudomonas* and *Acinetobacter* species was much more diverse as they produce both long- and short-chain AHLs.

Identification of strains capable of QQ

AHL-producing strains were further assessed for their capacities to produce anti-AHL compounds (Fig. 1; Supporting Information Fig. S1), a common feature in environmental bacteria (Romero *et al*., 2012). None of the 28 tested strains showed significant quenching of C6-HSL. Indeed, only *Vibrio* sp. CFL-9 and *Vibrio* sp. CFL-25 significantly inhibited the biosensor-specific GFP production (by 13% and 12%, respectively, $P < 0.05$). However, they also presented a cytotoxic effect as the biosensor viability was reduced by 18% and 12%, respectively, compared with the control ($P < 0.01$, data not shown). As viability reduction accounted for the GFP reduction, those strains were not counted as AHL quenchers.

A total of 10 strains (36% of the tested strains) significantly quenched C14-HSL ($P < 0.05$). They were affiliated with the *Pseudomonas* genus (seven strains), with the addition of *Acinetobacter* sp. DF3-8, *Vibrio* sp. EF02-7 and *Morganella* sp. DF3-16. All these strains exhibited low quenching abilities, with a reduction of GFP production between 6% and 20%, except for *Pseudomonas* sp. AF3-2 and AF3-9, which decreased GFP production by 46% and 29%, respectively. In addition, *Vibrio* sp. CFL-9 and *Vibrio* sp. CFL-25 reduced the biosensor-specific GFP production, but with a similar reduction in the biosensor viability (data not shown), so those strains were not counted as AHL quenchers.

Effects of lactonase on AHL production

We then tested whether QS circuits regulated biofilm production and hydrolytic enzyme synthesis. To this end, QS mechanisms were inhibited using a lactonase preparation active over a broad range of AHLs, including among others C4-HSL, C6-HSL, C8-HSL, C9-HSL, C10-HSL, C11-HSL, 3-oxo-C6-HSL, 3-oxo-C10-HSL, 3-oxo-C12-HSL, 3-OH-C10-HSL and 3-OH-C11-HSL (Hiblot *et al*., 2013; Rémy *et al*., 2020; Mion *et al*., 2021). We first evaluated whether the AHL production of the 28 AHL-producing strains was affected by the lactonase treatment (Table 2). Among those 28 strains, 14 were found to significantly induce at least one of the biosensors (specific fold induction > 1.5, $P < 0.05$) at the end of the lactonase assay, allowing the assessment of the lactonase efficiency. Interestingly, the AHL production of 11 of them was

Table 1. AHLs quantified in the supernatants of the bacterial strains isolated from the Aulne estuary.

Strain	Salinity	Month	Isolation fraction	C4	C6	3-OH-C6	3-oxo-C6	C8	3-OH-C8	3-oxo-C8	C10	3-OH-C10	3-oxo-C10	3-OH-C12	C12	3-oxo-C12	C14	Putative AHLs
Pseudomonas sp. A14	0	April	Total	–	–	–	–	6	–	–	71	1	–	–	21	–	–	C12:1
Pseudomonas sp. A20	0	April	Total	–	30	–	73	–	–	–	–	–	–	–	–	–	–	–
Pseudomonas sp. AF3-2	0	April	Attached	–	37	–	229	–	–	4	12	–	–	–	1	–	0.1	–
Pseudomonas sp. AF3-9	0	April	Attached	–	–	–	–	5	–	–	66	6	–	–	8	–	–	C12:1
Sphingobacterium sp. AF02-2	0	April	Free	–	–	–	–	–	–	–	–	–	–	–	–	–	–	C16:1
Pseudomonas sp. AF02-5	0	April	Free	–	–	–	–	–	–	–	–	–	–	–	–	–	–	C16:1
Pseudomonas sp. AF02-15	0	April	Free	–	–	–	–	–	–	–	–	–	108	–	–	24	–	–
Pseudomonas sp. B20	5	April	Total	–	11	–	23	–	–	–	–	–	–	–	–	–	–	–
Acinetobacter sp. BF3-12	5	April	Attached	–	–	–	–	–	–	–	16	–	–	–	4	–	–	C12:1
Pseudomonas sp. BF02-28	5	April	Free	–	–	–	–	–	–	–	1	–	–	–	–	–	–	–
Vibrio sp. CFL-9	25	April	Free	–	–	19	–	–	–	–	–	–	–	–	–	–	–	–
Vibrio sp. CFL-25	25	April	Free	–	–	18	–	–	–	–	–	–	–	–	–	–	–	–
Obesumbacterium sp. DF3-3	5	July	Attached	–	–	–	172	–	–	1	–	–	–	–	–	–	–	3-oxo-C7
Acinetobacter sp. DF3-8	5	July	Attached	–	–	–	22	–	–	0.2	–	–	–	–	–	–	–	–
Acinetobacter sp. DF3-12	5	July	Attached	–	–	–	–	–	–	–	–	–	1	–	–	–	–	–
Acinetobacter sp. DF3-15	5	July	Attached	311	–	–	–	–	–	–	–	–	–	–	–	–	–	–
Morganella sp. DF3-16	5	July	Attached	356	–	–	–	–	–	–	–	–	–	–	–	–	–	–
Acinetobacter sp. DF02-2	5	July	Free	84	–	–	–	–	–	–	–	–	–	–	–	–	–	–
Pseudomonas sp. DF02-8	5	July	Free	116	–	–	–	–	–	–	–	–	–	–	–	–	–	–
Pseudomonas sp. DF02-13	5	July	Free	–	–	–	–	–	–	–	–	–	–	14	–	–	–	
Vibrio sp. E14	25	July	Total	–	–	234	–	–	44	–	–	–	–	–	–	–	–	C6:1
Vibrio sp. E15	25	July	Total	–	–	233	–	–	40	–	–	–	–	–	–	–	–	C6:1
Vibrio sp. EFL-3	25	July	Free	–	–	179	–	–	40	–	–	–	–	–	–	–	–	C6:1
Vibrio sp. EFL-16	25	July	Free	–	–	16	–	–	–	–	–	–	–	–	–	–	–	–
Vibrio sp. EF3-1	25	July	Attached	–	–	194	–	–	38	–	–	–	–	–	–	–	–	C6:1, 3-OH-C7
Vibrio sp. EF02-14	25	July	Free	–	–	75	–	–	17	–	–	–	–	–	–	–	–	–
Vibrio sp. EF02-15	25	July	Free	–	–	57	–	–	13	–	–	–	–	–	–	–	–	C6:1
Vibrio sp. EF02-7	25	July	Free	–	–	53	–	–	7	–	–	–	–	–	–	–	–	–

AHL concentrations are in nM. Putative AHLs are molecules that possess the characteristic fragmentation spectrum of AHLs but for which we do not have commercial standards.

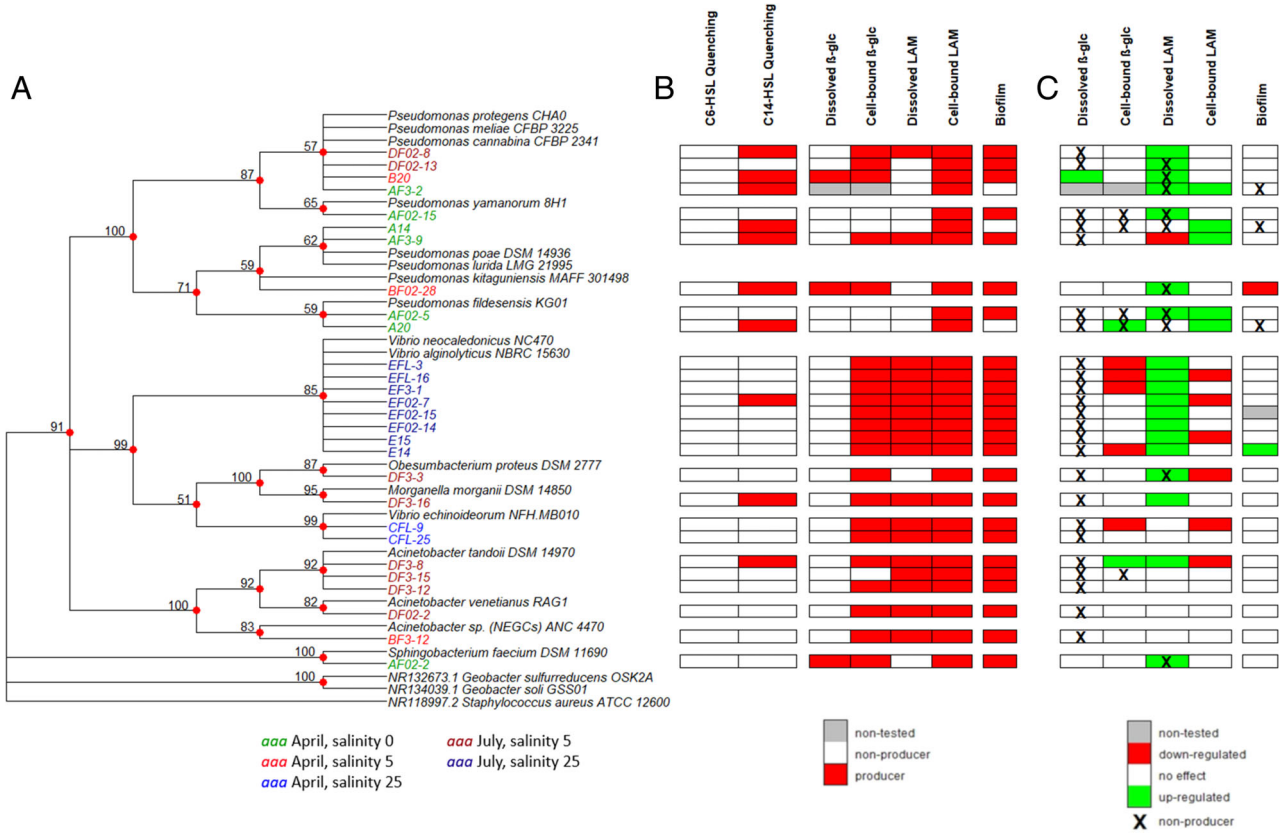

Fig. 1. A. The phylogenetic tree of the strains for which AHLs were detected using MS. The tree was constructed by maximum likelihood using the Tamura-Nei model as implemented in MEGA 7.0. Nodes with bootstrap value inferior to 50 were collapsed.
B. The ability of each strain to: quench C6-HSL and C14-HSL, produce hydrolytic enzymes (dissolved β-glucosidases, cell-bound β-glucosidases, dissolved leucine aminopeptidase and cell-bound leucine aminopeptidase) and produce biofilm. Red: producer, white: non-producer, grey: not tested, LAM: leucine aminopeptidase, β-glc: β-glucosidase.
C. The impact of lactonase treatment on the production of hydrolytic enzymes and biofilm for each strain. White: non-significant effect of lactonase treatment, red: significant downregulation, green: significant upregulation, grey: not tested, black cross: no production in control treatment (without lactonase), LAM: leucine aminopeptidase, β-glc: β-glucosidase. Significance threshold = 0.05. [Color figure can be viewed at wileyonlinelibrary.com]

significantly reduced by the lactonase treatment ($ratio_{lac/ctr}$ ranged from 0.0 to 0.6, $P < 0.05$), confirming the broad spectrum of the lactonase treatment. Three strains (*Pseudomonas* sp. AF02-5 and *Vibrio* sp. CFL-9 and E14) activated one biosensor in the control condition but were not significantly impacted by the lactonase treatment.

The 14 other strains did not sufficiently induce the biosensors in the control condition at the end of the assay, preventing the assessment of the lactonase efficiency. Indeed, five *Vibrio strains* (CFL-25, EF3-1, EFL-3, EFL-16 and EF02-15) induced a questionable GFP fold induction between 1.21 and 1.33, which is too low to demonstrate a significant effect of the lactonases. The remaining nine strains did not induce the biosensors (ratio < 1.2). Among them, five strains were in the 'questionable induction' during the initial screening. The difference in the growth stage at which the screening was performed could explain the absence of induction since the AHL production and degradation is growth phase-dependent.

Effects of lactonase treatment on biofilm production

Among the 28 tested strains, 25 were found to produce biofilm in the tested set-up. Two of those strains had their biofilm production significantly impacted by the lactonase treatment (Fig. 1, Table 3): a decrease in biofilm production was seen in *Pseudomonas* sp. BF02-28 ($ratio_{lac/ctr} = 0.48$, $P < 0.05$) while an increase was observed in *Vibrio* sp. E14 ($ratio_{lac/ctr} = 2.29$, $P < 0.01$). Interestingly, among the eight other *Vibrio* strains tested, biofilm production seemed reduced in five strains (*Vibrio* sp. CFL-9, CFL-25, EFL-3, EFL-16 and EF3-1) but increased in three strains (*Vibrio* sp. E15, EF02-7 and EF02-14),

Table 2. Mean value of specific GFP fold induction of the biosensors in the control condition (no lactonase) and the specific GFP ratio of lactonase treatment to control at the end of the lactonase assay, averaged over triplicate measurements.

	Specific fold induction of *E. coli* MT102 biosensor in control treatment	$Ratio_{lac/ctr}$ of *E. coli* MT102 specific GFP production	Specific fold induction of *P. putida* F117 biosensor in control treatment	$Ratio_{lac/ctr}$ of *P. putida* F117 specific GFP production
Lactonase-treatment decreases the biosensors GFP production				
Pseudomonas sp. AF3-9	4.8***	0.0***		
Pseudomonas sp. AF02-15	50**	0.0**		
Sphingobacterium sp. AF02-2	2.1**	0.0**		
Pseudomonas sp. B20	126***	0.0***		
Acinetobacter sp. BF3-12	98***	0.0***	1.7**	0.7
Pseudomonas sp. BF02-28	7.7**	0.1**	2.7***	0.3**
Acinetobacter sp. DF3-8	2.0*	0.0***		
Pseudomonas sp. DF02-13	1.7**	0.5*	2.5***	0.1***
Vibrio sp. EF02-7	1.5**	0.5*		
Vibrio sp. EF02-14	1.6**	0.6**		
Vibrio sp. E15	1.6**	1.1	2.4***	0.4*
Lactonase-treatment does not decrease the biosensors GFP production				
Pseudomonas sp. AF02-5			2.1***	0.9
Vibrio sp. CFL-9			1.8*	1.5
Vibrio sp. E14			1.6*	0.6

Only strains that were considered to activate the biosensors in the control condition at the end of the lactonase assay are reported for readability, that is to say strains with a specific fold induction > 1.5 that is significantly different from negative control ($P < 0.05$). *$P < 0.05$, **$P < 0.01$, ***$P < 0.001$. Lac: lactonase treatment. Ctr: control (buffer amendment).

although not significantly (Table 3). In addition, biofilm production seemed to decrease in *Acinetobacter* sp. DF3-15 and DF02-2 ($ratio_{lac/ctr} = 0.6$ and 0.8, respectively, $P < 0.1$).

Effect of lactonase treatment on LAM activity

Dissolved LAM production was found in 61% of the strains, especially in *Vibrio* and *Acinetobacter* species. However, they were mostly negligible compared with cell-bound LAM, except for *Vibrio* sp. CFL-9 and CFL-25, for which dissolved LAM represented most of the total activity (Table 3). Upon lactonase addition, dissolved LAM production was affected in 19 out of 28 strains ($P < 0.05$; Fig. 1, Table 3, Supporting Information Fig. S2). Dissolved LAM production increased ($ratio_{lac/ctr}$ between 1.25 and 7.47, $P < 0.05$) in 18 strains (seven *Pseudomonas*-, one *Sphingobacterium*-, one *Acinetobacter*-, one *Obesumbacterium*-, one *Morganella*- and seven *Vibrio*-affiliated strains). In contrast, LAM production decreased in *Pseudomonas* sp. AF3-9 ($ratio_{lac/ctr} = 0.19$, $P < 0.01$). Interestingly, among the 12 tested strains that did not produce dissolved LAM in the absence of AHLs, eight strains showed a detectable production with the lactonase treatment.

The lactonase treatment affected cell-bound LAM production in 11 out of 28 strains ($P < 0.05$; Fig. 1, Table 3, Supporting Information Fig. S2). Among them, five *Pseudomonas*-affiliated strains (A14, A20, AF3-2, AF3-9, AF02-5) had their cell-bound LAM production increased ($ratio_{lac/ctr}$ between 1.30 and 2.44, $P < 0.05$). In contrast, six strains (*Vibrio* sp. CFL-9, E15, EFL-16, EF02-7; *Obesumbacterium* sp. DF3-3; and *Acinetobacter* sp. DF3-8) exhibited a decreased cell-bound LAM ($ratio_{lac/ctr}$ between 0.59 and 0.89, $P < 0.05$).

Effect of lactonase treatment on β-glc activity

Production of dissolved β-glc was not frequent, with only three strains exhibiting a detectable hydrolysis of MUF-glc in the absence of lactonase (*Sphingobacterium* sp. AF02-2, *Pseudomonas* sp. B20 and *Pseudomonas* sp. BF02-28, Table 3). Among them, dissolved β-glc represented an important fraction of total β-glc in *Pseudomonas* sp. B20 and BF02-28 (respectively, 57% and 72%, Table 3). *Pseudomonas* sp. B20 was significantly impacted by the lactonase treatment ($ratio_{lac/ctr} = 1.33$, $P < 0.01$; Fig. 1, Table 3). The strains that did not exhibit a detectable amount of dissolved β-glc in the absence of lactonase also did not produce a detectable amount of dissolved β-glc upon lactonase treatment.

Overall, 22 strains out of 28 produced cell-bound β-glc and most of them exhibited low activity, with the exception of *Sphingobacterium* sp. AF02-2, *Obesumbacterium* sp. DF3-3 and *Vibrio* sp. CFL-9 and CFL-25. Among the 28 strains, seven strains had their cell-bound β-glc significantly impacted by the lactonase treatment ($P < 0.05$; Fig. 1, Table 3, Supporting Information Fig. S2). *Acinetobacter* sp. DF3-8 ($ratio_{lac/ctr} = 1.32$, $P < 0.05$) and *Pseudomonas* sp. A20 (production not detected in control treatment, $P < 0.01$) exhibited an increase in cell-bound β-glc with the lactonase treatment while five *Vibrio*

Table 3. Mean values of biofilm production, dissolved LAM, cell-bound LAM, dissolved β-glc and cell-bound β-glc measured at the end of the lactonase assays for control (ctr) and lactonase treatment (lac) conditions with lactonases (lac) averaged over triplicated measurements.

		Biofilm (OD_{540})	Dissolved LAM (AU min^{-1} $OD_{600}{}^{-1}$)	Cell-bound LAM (AU min^{-1} $OD_{600}{}^{-1}$)	Dissolved β-glc (AU min^{-1} $OD_{600}{}^{-1}$)	Cell-bound β-glc (AU min^{-1} $OD_{600}{}^{-1}$)
Pseudomonas sp. A14	ctr	0.1	nd.	256	nd.	nd.
	lac	0.1	nd.	626	nd.	nd.
	ratio	1.0	**–****	**2,4****	–	–
Pseudomonas sp. A20	ctr	0.1	nd.	371	nd.	nd.
	lac	0.1	nd.	724	nd.	0.04
	ratio	1.0	**–***	**2.0***	–	**–****
Pseudomonas sp. AF3-2	ctr	0.1	nd.	5	*nt.*	*nt.*
	lac	0.1	1.7	10	*nt.*	*nt.*
	ratio	1.0	**–***	**2.08***	–	–
Pseudomonas sp. AF3-9	ctr	2.6	10.3	304	nd.	0.9
	lac	2.0	2.0	397	nd.	0.6
	ratio	0.8	**0,2****	**1.3****	–	0.7
Sphingobacterium sp. AF02-2	ctr	1.9	nd.	1029	6	183
	lac	1.6	0.9	907	7	168
	ratio	0.8	**–***	*0.9*°	1.1	0.9
Pseudomonas sp. AF02-5	ctr	1.2	nd.	378	nd.	nd.
	lac	2.0	0.8	536	nd.	1.6
	ratio	1.7	**–*****	**1.4****	–	–
Pseudomonas sp. AF02-15	ctr	2.5	nd.	686	nd.	0.1
	lac	2.0	2.0	644	nd.	0.1
	ratio	0.8	**–*****	0.9	–	1.1
Pseudomonas sp. B20	ctr	0.5	nd.	601	4.9	3.5
	lac	0.4	6.9	584	7.4	3.8
	ratio	0.9	**–*****	1.0	**1,5****	1.1
Acinetobacter sp. BF3-12	ctr	2.6	2.1	263	nd.	0.3
	lac	2.1	9.9	247	nd.	1.0
	ratio	0.8	*4,8*°	0.9	–	3.1
Pseudomonas sp. BF02-28	ctr	2.8	nd.	454	1.8	0.7
	lac	1.3	5.4	431	1.8	0.8
	ratio	**0.5***	**–*****	1.0	1.1	1.2
Vibrio sp. CFL-9	ctr	2.1	313	166	nd.	35
	lac	1.4	392	101	nd.	30
	ratio	*0.6*°	*1.2*°	**0.6***	–	**0.9*****
Vibrio sp. CFL-25	ctr	2.3	377	262	nd.	37
	lac	1.6	436	270	nd.	38
	ratio	*0,7*°	1.2	1.0	–	1.0
Obesumbacterium sp. DF3-3	ctr	1.9	nd.	2424	nd.	49
	lac	1.7	20.4	2146	nd.	46
	ratio	0.9	**–***	**0.9***	–	0.9
Acinetobacter sp. DF3-8	ctr	1.4	13	533	nd.	4
	lac	1.8	42	430	nd.	5
	ratio	1.2	**3,2****	**0.8****	–	**1.3***
Acinetobacter sp. DF3-12	ctr	3.6	nd.	303	nd.	1.1
	lac	2.6	nd.	277	nd.	1.2
	ratio	0.7	–	*0.9*°	–	1.0
Acinetobacter sp. DF3-15	ctr	5.0	33	756	nd.	nd.
	lac	3.2	30	763	nd.	0.3
	ratio	*0.6*°	0.9	1.0	–	–
Morganella sp. DF3-16	ctr	7.7	1.0	526	nd.	0.5
	lac	8.3	3.3	536	nd.	0.4
	ratio	1.1	**3.5*****	1.0	–	0.9
Acinetobacter sp. DF02-2	ctr	2.9	1.2	597	nd.	0.1
	lac	2.5	1.8	661	nd.	0.3
	ratio	*0.8*°	*1.5*°	1.1	–	4.0
Pseudomonas sp. DF02-8	ctr	4.9	2.3	492	nd.	0.4
	lac	4.0	8.2	469	nd.	0.5
	ratio	0.8	**3.6***	1.0	–	1.1
Pseudomonas sp. DF02-13	ctr	4.1	nd.	275	nd.	1
	lac	5.5	2.4	287	nd.	1
	ratio	1.4	**–****	1.0	–	1.0
Vibrio sp. E14	ctr	2.4	0.6	260	nd.	10
	lac	5.4	2.9	297	nd.	8
	ratio	**2.3****	**4.6****	1.2	–	**0.8***

(Continues)

Table 3. Continued

		Biofilm (OD_{540})	Dissolved LAM (AU min^{-1} OD_{600}^{-1})	Cell-bound LAM (AU min^{-1} OD_{600}^{-1})	Dissolved β-glc (AU min^{-1} OD_{600}^{-1})	Cell-bound β-glc (AU min^{-1} OD_{600}^{-1})
Vibrio sp. E15	ctr	1.5	0.4	340	nd.	6
	lac	2.3	2.7	303	nd.	6
	ratio	1.5	**7.4****	**0.9***	–	*0.9°*
Vibrio sp. EFL-3	ctr	2.6	0.5	328	nd.	9
	lac	2.1	4.1	277	nd.	7
	ratio	*0.8°*	**7.4****	*0.8°*	–	**0.8****
Vibrio sp. EFL-16	ctr	2.5	1.3	465	nd.	12
	lac	1.8	5.4	276	nd.	9
	ratio	0.7	**4.0 ****	0.6	–	**0.7***
Vibrio sp. EF3-1	ctr	4.7	0.5	387	nd.	19
	lac	2.4	2.2	309	nd.	12
	ratio	0.5	**4.3*****	0.8	–	**0.6***
Vibrio sp. EF02-7	ctr	1.6	1.0	321	nd.	12
	lac	2.9	5.0	266	nd.	11
	ratio	1.8	**5.0****	**0.8****	–	1.0
Vibrio sp. EF02-14	ctr	2.0	1.2	305	nd.	8
	lac	3.0	5.3	289	nd.	9
	ratio	1.5	**4.4****	1.0	–	1.2
Vibrio sp. EF02-15	ctr	*nt*.	1.5	501	nd.	16
	lac	*nt*.	8.8	524	nd.	17
	ratio	–	**5.9***	1.1	–	1.0

The ratio corresponds to the control over test condition. Significance was assessed using the t-test ($^{\circ}P < 0.1$, $^{*}P < 0.05$, $^{**}P < 0.01$, $^{***}P < 0.001$). Significant results are highlighted in bold when $P < 0.05$ and in italic when $P < 0.1$. nd, not detected; nt, not tested; -, ratio not calculable.

sp. (CFL-9, E14, EFL-3, EFL-16 and EF3-1) exhibited decreased activity ($ratio_{lac/ctr}$ between 0.83 and 0.63, $P < 0.05$).

Identification of QS, QQ, hydrolase and biofilm-related genes in estuarine bacteria genomes

The genomes of four strains of *Pseudomonas* sp. (AF3-9 and B20), *Vibrio* sp. E14 and *Acinetobacter* sp. DF3-8 were sequenced to find AHL-related QS and QQ genes, carbohydrate-active enzymes (CAZymes), proteases and biofilm-related genes (pili, flagella, fimbriae and chemotaxis) (Table 4). Those strains were chosen because they covered the taxonomic diversity of the AHL-producing strains and exhibited marked responses to lactonase addition. The genome assembly metrics are given in the Supporting Information Table S5. *Pseudomonas* sp. AF3-9 and B20 possessed complex AHL-based QS circuits, with each having two putative AHL synthases (*luxI*-type and *hdtS*-type), several AHL receptors and three AHL acylases. Interestingly, the AHL receptors included several *luxR* solos, that is to say, without an accompanying synthase (Fuqua, 2006). The *hdtS* synthases were not located near an AHL receptor. *Acinetobacter* sp. DF3-8 and *Vibrio* sp. E14 encoded, respectively, one *luxI*/*luxR* and one *luxM*/*luxN* tandem and no QQ enzymes. The phylogenetic trees of the QS and QQ genes are presented in the Supporting Information Fig. S3.

All the strains contained numerous genes coding for hydrolases, including metallopeptidases (which include LAM) and glycoside hydrolases (which include β-glc). Interestingly, one of the *Pseudomonas* sp. AF3-9 solo *luxR* genes was located directly next to two serine peptidases (Supporting Information Fig. S4). They also all possessed numerous genes involved in motility and adhesion (pili, flagella, fimbriae and chemotaxis), which are linked to biofilm development (Wolska *et al*., 2016; Berne *et al*., 2018; Rossi *et al*., 2018).

Discussion

Although QS-dependent phenotypes have been extensively studied in strains of medical interest, much less work has been conducted on environmental strains. In particular, the question of a possible implication of QS mechanisms in the regulation of bacterial phenotypes involved in key biogeochemical processes remains open (Hmelo, 2017). In this study, several strains were isolated from the Aulne estuary (Bay of Brest, France), which is known to host high hydrolytic activities (Labry *et al*., 2016). We then inhibited their AHL-based QS communication to test whether this mechanism regulated biofilm and extracellular hydrolytic enzyme production (β-glc and LAM), which are known to play a major role in organic matter biodegradation (Chróst and Siuda, 2002; Arnosti, 2011). One limitation to this approach is that it is restricted to the cultivable bacterial fraction.

Table 4. Number of functionally annotated genes related to QS, QQ, hydrolases and biofilm production in each draft genome.

	Gene	*Pseudomonas* sp. AF3-9	*Pseudomonas* sp. B20	*Acinetobacter* sp. DF3-8	*Vibrio* sp. E14
QS and QQ	*LuxI-type AHL-synthase*	1	1	1	0
	LuxR-type AHL-receptor	3	4	1	0
	LuxM-type AHL-synthase	0	0	0	1
	LuxN-type AHL-receptor	0	0	0	1
	HdtS-type AHL synthase	1	1	0	0
	AinS-type AHL synthase	0	0	0	0
	AinR-type AHL receptor	0	0	0	0
	AHL-acylase	3	3	0	0
	AHL-lactonase	0	0	0	0
Protease	*Aspartic peptidase*	7	6	7	4
	Cysteine peptidase	40	32	42	28
	Glutamic peptidase	0	0	0	0
	Metallo peptidase	65	68	66	70
	Asparagine peptidase	9	10	4	5
	Mixed peptidase	1	0	0	0
	Serine peptidase	83	90	55	67
	Threonine peptidase	6	6	5	5
	Unknown peptidase	4	1	4	4
	Peptidase inhibitor	12	10	5	13
CAZyme	*Glycoside hydrolase*	27	31	35	43
	Glycosyl transferase	28	34	28	14
	Polysaccharide lyase	2	6	0	1
	Carbohydrate esterase	4	2	3	2
	Auxiliary activity	1	2	0	3
Motility and adherence	*Flagella*	45	46	48	48
	Pili	24	32	2	16
	Fimbriae	1	0	9	0
	Chemotaxis	2	2	6	7

Estuarine bacteria produce diverse QS signals

Several estuarine bacterial strains were found to produce AHLs quantifiable by UHPLC-HRMS/MS. They were affiliated with the genera *Vibrio*, *Pseudomonas*, *Acinetobacter*, *Obesumbacterium*, *Morganella* and *Sphingobacterium* based on 16S rRNA gene sequencing. *Pseudomonas*, *Vibrio* and *Acinetobacter* species are frequently isolated in coastal and marine environments (Elliot and Colwell, 1985; Baffone *et al*., 2006; Abd-Elnaby *et al*., 2019) and have been well studied for their QS properties (Eberl, 1999; Miller and Bassler, 2001). The production of AHLs has also previously been reported in *Obesumbacterium* (Priha *et al*., 2014) and *Morganella morganii* (Guzman *et al*., 2020). To the best of our knowledge, AHL production has not previously been reported in *Sphingobacterium* isolates, although AHL synthase sequences matching the *Sphingomonadaceae* family have been reported in environmental metagenomics databases (Doberva *et al*., 2015). The AHL-producing isolates were phylogenetically different depending on the salinity at which they were isolated, suggesting that the bacterial community members engaged in QS communication may vary along the estuary.

The identified bacterial estuarine strains involved in QS communication produced a diverse array of QS molecules, with 14 AHLs detected and quantified in total. This finding is consistent with previous studies showing that a single marine strain can produce a large, diverse array of QS signals (Doberva *et al*., 2017). This broad spectrum of emitted AHLs suggests that estuarine bacterial communities produce and respond to multiple AHL signals emitted in the environment. Most strains produced short- and medium-length AHLs (C6-HSL to C12-HSL), and a majority of them were substituted at the C3 position, two structural properties that could increase AHL solubility in brackish water and seawater (Hmelo *et al*., 2011). Interestingly, all the *Vibrio* strains were found to produce 3-OH-C6-HSL, while none of the other type of strains produced this type of AHL, suggesting a particular signal specificity within those strains. This is in contrast with previous studies that reported no clear pattern of QS activity in *Vibrionaceae* strains, including *Vibrio* sp. (Tait *et al*., 2010; Freckelton *et al*., 2018). The AHL production among *Pseudomonas* and *Acinetobacter* was much more diverse, with no clear production pattern. Interestingly, the sequencing data showed that the two *Pseudomonas*-affiliated strains had

complex QS circuits, with several AHL synthases and receptors, including *luxR* solos. As QS compounds have been less studied in *Obesumbacterium*, *Morganella* and *Sphingobacterium*, our study contributes to describe their QS circuits, revealing the production of 3-oxo-C6-HSL and 3-oxo-C8-HSL in *Obesumbacterium*, C4-HSL in *Morganella* and the possible production of C16:1-HSL in *Sphingobacterium*.

QS and QQ circuits co-occur in estuarine bacteria

Interestingly, based on our bioassays, 10 out of 28 AHL-producing strains (36%) also showed the QQ ability to interfere with long-chain AHLs, while none of them interfered with short-chain AHLs. The sequencing data suggested that *Pseudomonas* sp. AF3-9 and B20 quenching abilities result from the degradation of AHLs based on the emission of acylases, a QQ enzyme that cleaves the acyl side chain of AHLs. No QQ enzymes (i.e. acylase or lactonase) were found in *Acinetobacter* sp. DF3-8 and *Vibrio* sp. E14 genomes, although *Acinetobacter* sp. DF3-8 presented a QQ activity during the bioassay. Such an observation concerning *Acinetobacter* suggests that estuarine bacteria could be a source of new QQ enzymes for biotechnological applications. The observation of bacteria that simultaneously emit pro- and anti-QS compounds has been evidenced in a few strains, for example, in *Agrobacterium tumefaciens* (Zhang *et al*., 2004), a marine *Shewanella* sp. (Tait *et al*., 2009), in two isolates related to *Endozoicomonas* (Freckelton *et al*., 2018) or *Acinetobacter* and *Burkholderia* strains isolated from the rhizosphere (Chan *et al*., 2011). Such co-occurrence of QS and QQ features in our collection of estuarine strains raises the question of the co-expression of these two phenotypes, especially within the natural environment. In any case, our data highlight the complexity of QS regulation within the natural estuarine communities. They also point out the importance of QS-based cell–cell cooperation and QQ-based competition within these communities.

QS regulates biofilm formation and hydrolytic enzyme production in estuarine bacteria

We then investigated the role of QS in biofilm formation and hydrolytic enzyme synthesis in the 28 AHL-producing estuarine strains, two important physiological features when considering the role of bacteria in the marine C cycle (Arnosti, 2011; Dang and Lovell, 2016). To this extent, we used a lactonase-based QS disruption approach. Lactonases have been shown to catalyse the opening of the lactone ring of AHLs, thus preventing their use as a signal molecule. *Sso*Pox lactonase has been shown to inhibit a range of behaviours under QS control, including biofilm and protease production, in *P. aeruginosa* (Hraiech *et al*., 2014; Guendouze *et al*., 2017; Mion *et al*., 2019; Rémy *et al*., 2020) and *Chromobacterium violaceum* (Mion *et al*., 2021). They also modulated *in vitro* (Schwab *et al*., 2019) and *in situ* (Huang *et al*., 2019) bacterial community composition. Contrary to some other well-known QS inhibitors, such as 5-fluoro-uracil or the brominated furanone C-30, lactonases do not induce cytotoxic effects that may bias the experiments (Mahan *et al*., 2020).

Most of the AHL-producing strains (89%) were also biofilm producers. The lactonase treatment significantly impacted the biofilm production in two of them, with contrasting effects: *Pseudomonas* sp. BF02-28 exhibited a significant biofilm decrease (−52%), while *Vibrio* sp. E14 biofilm production was increased (+128%). In contrast, the lactonase treatment did not significantly modify biofilm production in other *Vibrio* strains. Previous studies have mostly reported the inhibition of biofilm production in the presence of lactonases (Muras *et al*., 2020; Paluch *et al*., 2020; Rémy *et al*., 2020), although biofilm upregulation has also been described in such conditions (Su *et al*., 2019; Mahan *et al*., 2020). Those contrasting effects probably result from the fact that biofilm production is under complex and interconnected regulatory mechanisms, including AHL-based QS, furanosyl diester borate (AI-2)-based QS and c-diGMP production, among others (Wolska *et al*., 2016; Hmelo, 2017; Lami, 2019). In another report, Liu *et al*. (2017) noticed that the addition of 3-oxo-C10-HSL differentially affected the biofilm formation of *V. alginolyticus* isolates with apparent strain specificity and a dose-dependent response. Clearly, our results revealed that biofilm production is under the control of QS in some estuarine microbial communities, but they also suggest the complexity of QS-dependent regulations of biofilm production in such ecosystems. Biofilm formation among estuarine bacteria may drive their capacities to colonize particulate organic matter (Simon *et al*., 2002; Dang and Lovell, 2016; Sivadon *et al*., 2019). Thus, QS involvement in biofilm formation possibly shapes the diversity of particle-attached communities. However, we evaluated QS involvement in monospecific cultures while biofilm formation is a complex multi-species phenomenon in natural environments. As such, it will be necessary to evaluate QS involvement on complex community assemblages in the future to obtain a better picture of the QS-based interactions at play, as has been done in a few studies (Huang *et al*., 2019; Schwab *et al*., 2019).

We then assessed whether the expression of AHL-based QS regulates the activity of hydrolytic enzymes. Most studies to date that have examined the possible regulation of hydrolytic enzyme activity by QS in isolated

strains have focused on dissolved extracellular enzymes (Gram *et al*., 2002; Jatt *et al*., 2015; Guendouze *et al*., 2017; Li *et al*., 2019; Su *et al*., 2019; Mahan *et al*., 2020). In contrast, most studies have been carried out on natural communities focused on cell-bound (Hmelo *et al*., 2011) or total activities (Krupke *et al*., 2016). Thus, in this study we decided to bridge this gap by assaying both dissolved and cell-bound activities of two hydrolytic enzymes: LAM, which are involved in N cycling and considered to be a broader proxy for proteases activity (Steen *et al*., 2015), and β-glc, which are broad-specificity enzymes involved in C cycling and carbohydrate dynamics (Chróst, 1989). Interestingly, the lactonase treatment significantly impacted the activity of dissolved and cell-bound LAM in, respectively, 71% and 39% of the tested strains, suggesting that QS might regulate LAM production in numerous estuarine bacteria. The influence of QS on β-glc production appeared less pronounced, with dissolved and cell-bound activities being significantly modified by the lactonase treatment in 4% and 26% of the tested strain, respectively. However, β-glc production was not as widespread as LAM production: only 3 and 17 strains produced dissolved and cell-bound β-glc, respectively, versus 18 and 28 for LAM, respectively. Clearly, our study evidenced that hydrolytic enzyme activities are under QS regulation in many strains. To the best of our knowledge, only Jatt *et al*. (2015) and Su *et al*. (2019) have described such an effect after QS inhibition in *Pantoea* and *Ruegeria* strains isolated from marine snow, respectively. Our study demonstrated a broader effect because more phylogenetically diversified strains were tested. This clearly points out the need to investigate at a much larger scale this question in aquatic environments, as QS communication may represent an underestimated mechanism of N and C recycling by marine bacteria.

The effect of AHL-based QS inhibition on the activity of hydrolytic enzymes was contrasted as both increase and decrease in dissolved and cell-bound activities were observed. Indeed, the cell-bound LAM activity of several *Pseudomonas* strains increased, while those of other genera (*Acinetobacter*, *Obesumbacterium*, *Sphingobacterium* and *Vibrio*) decreased. Similar results were observed for β-glc activity, which decreased in some *Vibrio* strains but increased in one *Pseudomonas* strain and one *Acinetobacter* strain. Such complex effects have been reported after AHL addition to marine snow: Krupke *et al*. (2016) found that 3-oxo-C8-HSL induced phosphatase activity but decreased aminopeptidase and lipase activities after 6 h of incubation with communities from the Atlantic Ocean. Su *et al*. (2019) also highlighted that 3-oxo-C8-HSL increased galactosaminidase and β-xylosidase activities but decreased β-glucosidase and mannosidase activities in marine particles collected in the Yellow Sea of China. A few strains exhibited interesting behaviour, where dissolved and cell-bound activities were differentially affected by the lactonase treatment. For example, the inhibition of QS circuits induced a decrease in *Pseudomonas* sp. AF3-9 dissolved LAM, but an increase in cell-bound LAM. The opposite phenomenon was observed for *Acinetobacter* sp. DF3-8 and *Vibrio* sp. CFL-9. This overall variability is probably linked to the complexity of hydrolase regulation, which are under tight transcriptional control given their metabolic cost (Chróst and Siuda, 2002).

Collectively, our findings revealed that estuarine bacteria can synthesize a large array of AHLs and present a wide range of quenching activities. Our results also clearly demonstrated the importance of AHL-based QS regulation on a range of phylogenetically different estuarine strains, suggesting an underestimated role of QS in microbial N and C cycling in aquatic environments. In the particular case of the Aulne estuary, for which high enzymatic activities have been reported (Labry *et al*., 2016), QS involvement in hydrolase synthesis may have important consequences on biogeochemical fluxes of nutrients to coastal waters. The effects of QS inhibition were contrasted, illustrating the complexity of those cell–cell regulations. Thus, our study paves the way for future studies, highlighting the need to introduce concepts and tools of chemical ecology in marine microbial ecology to address broader questions relative to ecosystem functioning.

Experimental procedures

Standard N-*acylhomoserine lactones*

All AHLs used in this study were purchased from Sigma-Aldrich (Darmstadt, Germany). The following abbreviations are used: *N*-butyryl-DL-homoserine lactone (C4-HSL), *N*-hexanoyl-DL-homoserine lactone (C6-HSL), *N*-(3-hydroxyhexanoyl)-DL-homoserine lactone (3-OH-C6-HSL), *N*-(3-oxohexanoyl)-DL-homoserine lactone (3-oxo-C6-HSL), *N*-octanoyl-DL-homoserine lactone (C8-HSL), *N*-(3-hydroxyoctanoyl)-DL-homoserine lactone (3-OH-C8-HSL), *N*-(3-oxooctanoyl)-DL-homoserine lactone (3-oxo-C8-HSL), *N*-decanoyl-DL-homoserine lactone (C10-HSL), *N*-(3-hydroxydecanoyl)-DL-homoserine lactone (3-OH-C10-HSL), *N*-(3-oxodecanoyl)-DL-homoserine lactone (3-oxo-C10-HSL), *N*-dodecanoyl-DL-homoserine lactone (C12-HSL), *N*-(3-hydroxydodecanoyl)-DL-homoserine lactone (3-OH-C12-HSL), *N*-(3-oxododecanoyl)-DL-homoserine lactone (3-oxo-C12-HSL) and *N*-tetradecanoyl-DL-homoserine lactone (C14-HSL). All AHLs were dissolved in dimethyl sulfoxide (DMSO).

Isolation of estuarine bacterial strains

Bacteria were isolated from the surface water of the Aulne estuary (Bay of Brest) in April and July 2019. Three type of waters were sampled along the salinity gradient in order to cover a large range of suspended matter concentrations: riverine waters (salinity 0), brackish waters in the maximum turbidity zone (salinity 5) and brackish waters under greater marine influence (salinity 25, Supporting Information Table S1).The salinity was measured *in situ* with a thermosalinometer (WTW Cond 330i) using the practical salinity scale and as such, is reported with no unit (UNESCO, 1985). All culturing steps were performed at the *in situ* water temperature (i.e. 12 and 22°C for April and July, respectively) using modified Luria Broth medium (mLB) containing 1% (w/v) peptone and 0.5% (w/v) yeast extract and adjusted to the salinity at which the strains were isolated (0, 5 or 25) with artificial seawater (54 mM $MgCl_2$, 10 mM $CaCl_2$, 0.16 mM $SrCl_2$, 9 mM KCl, 2.4 mM $NaHCO_3$, 840 mM KBr, 440 mM H_3BO_3, 71 mM NaF, 0.40 M NaCl and 30 mM Na_2SO_4, pH 8.2). For the 0 salinity mLB, 1% (v/v) of artificial seawater was added to ensure the presence of essential ions.

For each sample, four different isolation strategies were conducted to isolate bacteria from the total, particle-attached (>3 μm) and free-living (0.2–3 μm) fractions of sampled water. Thus, mLB agar plates (mLB amended with 1.5% w/v agar) were inoculated by (i) spreading 100 μl of total water; (ii) spreading 100 μl of <3 μm-filtered water (Whatman Nuclepore™ PC membrane, GE Healthcare Life Sciences, Little Chalfont, UK); (iii) depositing >3 μm filters; or (iv) depositing 0.2 μm filters (Whatman Nuclepore™ PC membrane) used with 3 μm-filtered water. Single colonies were isolated, purified, grown in mLB and stored at −80°C using 10% (v/v) DMSO.

Identification of AHL-producing strains

We then determined whether the isolated bacterial strains could produce AHLs, following previously published protocols. Briefly, bacterial supernatants were screened with bacterial biosensors, *P. putida* F117 (pRK-C12) (Andersen *et al*., 2001) and *E. coli* MT102 (pJBA132) (Riedel *et al*., 2001). Those biosensors produce GFP in the presence of AHLs. *P. putida* F117 allows a good detection of long-chain AHLs while *E. coli* MT102 preferentially detects short-chain AHLs (Andersen *et al*., 2001; Riedel *et al*., 2001).

Both biosensors were grown at 30°C (150 rpm) in LB (0.5% w/v yeast extract, 1% w/v peptone, 1% w/v sodium chloride) using, respectively, 20 μg ml^{-1} of gentamicin or 25 μg ml^{-1} of tetracycline. An overnight culture of each biosensor was inoculated at a 600 nm optical density (OD_{600}, measured using a NanoDrop 2000c with a 1 cm cuvette, Thermo Scientific) of 0.02 into fresh LB medium and dispensed into a 96-well black microplate (150 μl per well). Bacterial strains to be tested for AHL production were grown in mLB (in the salinity at which they were isolated) until an OD_{600} of 0.6–1.2 was reached (typically 12–48 h). Cultures were centrifuged at 12 000 *g* for 10 min and filtered through a 0.2 μm filter (Corning® PES syringe filter). The resulting supernatants were stored at −20°C until screening (1 week maximum) and then were added to the biosensors microplate in triplicate (50 μl $well^{-1}$) after thawing at ambient temperature.

Blanks consisted of sterile LB medium amended with mLB at the corresponding salinity. Negative controls for the test samples consisted of biosensor strains with sterile mLB amendments, as the mLB was found to modify growth and fluorescence production of the biosensors depending on the salt concentration. Positive controls consisted of biosensor strains amended with 10 μM commercial AHL (C6-HSL for *E. coli* MT102 and 3-oxo-C10-HSL for *P. putida* F117) with a final DMSO concentration of 1% (v/v). In consequence, a second negative control was prepared with DMSO (1% v/v). GFP fluorescence (excitation: 485 nm, emission: 535 nm) and OD_{600} were read on a Spark Tecan Infinite M200PRO microplate reader (Tecan, Switzerland) after an overnight incubation (14–16 h) at 30°C under low agitation (100 rpm).

Specific fold induction of fluorescence was calculated by dividing the specific GFP fluorescence ($FLUO_{GFP}$/OD_{600}) of the test sample by the specific GFP fluorescence of the negative control (each containing mLB with the same salinity). Specific fold inductions were arbitrarily classified into inhibition (<0.8), no modification (0.8–1.2), questionable induction (1.2–1.5), induction (1.5–3) and strong induction (>3; see Supporting Information Table S1). All fold inductions that were not significantly different from the control were also counted in the 0.8–1.2 category.

Quantification of AHLs produced by isolated strains

Bacterial strains that induced a response with AHL biosensors were further investigated to confirm AHL production using non-targeted UHPLC-HRMS/MS (MS). For each strain, 50 ml of supernatant was obtained as described above. Supernatants were extracted with 50 ml of ethyl acetate (EtOAc, overnight incubation at room temperature). Aqueous and organic phases were separated, and the aqueous phase was extracted again with 50 ml of EtOAc. The 2 × 50 ml EtOAc extracts were pooled and evaporated using a rotary evaporator. Crude extracts were dissolved in 500 μl of EtOAc, evaporated to dryness using a GeneVac HT-4X and stored at −20°C

until analysis. Extracts were then dissolved in 500 μl of methanol for UHPLC-HRMS/MS analysis, which was performed using a Q Exactive Focus Orbitrap System coupled to an Ultimate 3000™ UHPLC system (Thermo Fisher Scientific, Waltham, Massachusetts, USA). The column was a Phenomenex Luna Omega Polar C18 (150 × 2.1 mm, 1.6 μm particle size). The mobile phase was composed of 0.1% (v/v) formic acid in water (A) and 0.1% (v/v) formic acid in acetonitrile (B). The elution gradient started with 99% (v/v) of A, keeping this composition constant for 4 min. The proportion of B was linearly increased to 100% (v/v) over 10 min and left at 100% (v/v) for 5 min.

The analytical method includes full-scan MS (50–750 *m/z*) with successive data-dependent MS/MS (dd-MS^2) scan, allowing the acquisition of high-resolution data of the parent ion and daughter ion masses in a single chromatographic run. The selected parent ions were fragmented using 15, 30 and 40 eV. AHL fragmentation spectra are characterized by the systematic presence of one abundant daughter ion (102.055 *m/z*), which corresponds to the lactone ring. Three other fragments are usually observed (56.050, 74.061 and 84.045 *m/z*). AHLs were confirmed and quantified using commercially available standards.

Identification of strains capable of QQ

AHL-producing strains were tested for both long- and short-chain AHL quenching. QQ identification relied on the use of the biosensors *E. coli* MT102 and *P. putida* F117 and followed previously published protocols (Blanchet *et al*., 2017). Briefly, biosensors were grown as described above, except that 1 μM of a commercial AHL was added to the LB medium before dispatching into a 96-well plate (C6-HSL for *E. coli* MT102 and C14-HSL for *P. putida* F117). Supernatants exhibiting QQ capacities reduced GFP production compared with the control. Supernatants were produced as described above but were stored at 4°C until screening (4 h maximum) because QQ enzymes may be denatured upon freezing. Controls were realized as described previously for the screening of AHL-producing strains, except that positive controls contained 1 μM of AHLs and negative controls contained the equivalent quantity of DMSO (1% v/v). The fold reduction of fluorescence was calculated as described previously. To check that loss of fluorescence was not caused by cytotoxicity, 100 μl of each well of the biosensor assay was reacted with 30 μl of 0.01% (w/v) resazurin and incubated for 4 h at 30°C under low agitation (Tourneroche *et al*., 2019). The resulting fluorescence (excitation: 530 nm, emission: 590 nm) corresponds to the reduction of resazurin to resorufin by viable cells with active metabolism.

Finally, the pH was checked at the end of separate cultures as it can affect AHLs degradation. The two biosensors and three representative strains (*Pseudomonas* sp. AF3-9, *Acinetobacter* sp. DF3-8 and *Vibrio* sp. E14) were grown in the same conditions as during the QQ assays, in 4 ml. The mean pH at the end of the incubation was 7.1 (range 6.5–7.9), which is near neutral pH.

Taxonomic identification of AHL-producing strains

AHL-producing bacteria were identified using partial 16S rRNA gene sequencing. For each bacterial strain, a single colony grown on an mLB agar plate was resuspended in 50 μl of MilliQ water and incubated at 95°C for 15 min. The polymerase chain reaction (PCR) mix contained 1 μl of this lysate, 21 μl of GoTaq Green Master Mix (Promega) and 1.5 μl of each universal primer 27F (10 μM, 5′-AGAGTTTGATCMTGGCTCAG-3′) and 1492R (10 μM, 5′-ACGGYTACCTTGTTACGACTT-3′). One cycle of denaturation (95°C for 5 min) was followed by 35 cycles at 95°C for 30 s, 56°C for 30 s and 72°C for 30 s. The final extension was realized at 72°C for 5 min. The PCR products were purified using the NucleoSpin Gel and PCR Clean-up Kit (Macherey-Nagel). The final products were sequenced using the Sanger technique by Eurofins Genomics (Köln, Germany) using the same primers. Each sequence was manually checked using Bioedit and blasted against the EzTaxon-e database (https://www.ezbiocloud.net/; Kim *et al*., 2012), from which reference sequences were retrieved. The pairwise sequence similarity between the isolates and their closest relatives was also calculated using the EzTaxon-e server (Supporting Information Table S3). All sequences were aligned in Muscle (MEGA 7.0), and a phylogenetic tree was constructed by maximum likelihood using the Tamura-Nei model. *Geobacter sulfurreducens* (NR 132673.1) and *Geobacter soli* (NR 134039.1) sequences were used as an outgroup. The reliability of each node in the tree was assessed by bootstrapping over 500 replicates and nodes with boostrap values inferior to 50 were collapsed. The resulting tree was displayed using the ggtree package (v2.2.4) in R.

Biofilm production in isolated strains

Biofilm production was quantified using a crystal violet (CV) assay as described previously (Blanchet *et al*., 2017) with slight modifications. Briefly, 200 μl of culture was grown in mLB medium (at the isolation salinity) in a 96-well microplate (Greiner Bio-One, Cat.-No 655160) for 24 h (at 22°C) or 48 h (at 12°C) under low agitation (100 rpm). Each subsequent step was performed gently to preserve the biofilm. The supernatant of each culture was removed and non-adherent cells were

washed with 200 μl of phosphate-buffered saline (PBS, pH 7.4, VWR). Microplates were dried at 60°C for 1 h. Biofilms were stained with 0.2% (w/v) CV for 15 min. Unbound CV was then removed and the wells were washed 3 times with sterile water. CV in biofilm was dissolved with 200 μl of a destaining solution (50% ethanol, 10% acetic acid in MilliQ water, v/v) and the resulting OD was measured at 540 nm (OD_{540}). Strains with $OD_{540} < 0.1$ were considered non-adherent to the plate surface.

Enzymatic activity assay on isolated strains

The potential LAM and β-glc activities were quantified using model fluorogenic substrates: L-leucine-7-amido-4-methylcoumarin (LLMCA) and 4-methylumbelliferyl-β-D-glucopyranoside (MUF-glc), respectively. Those substrates release a fluorescent moiety upon hydrolysis, 7-amido-4-methylcoumarin (MCA) and 4-methylumbelliferone (MUF), respectively (Chróst, 1990). LAM and β-glc were assayed in the supernatant (which corresponds to dissolved cell-free enzymes) and in total culture (which includes dissolved and cell-bound extracellular enzymes). To perform the assay, 100 μl of either supernatant or total culture was transferred into a 96-well microplate and amended with 1000 μM of LLMCA or 150 μM of MUF-glc, which were saturating concentrations (not shown). Fluorescence was monitored for 3–4 h using a Spark Tecan Infinite M200PRO with excitation/emission wavelengths of 364/460 nm for MUF and 380/440 nm for MCA. Activities were determined as the slope of the linear part of the curve (AU min^{-1}). Cell-bound activity was determined by subtracting the mean dissolved fraction activity from total fraction activity. All reported activities are specific (normalized using OD_{600}).

Effect of lactonases on enzymatic activities and biofilm production

QS involvement in biofilm formation and expression of β-glc and LAM was assessed by comparing their production with and without lactonase, which degrade AHLs and thus inhibit QS circuits (Grandclément *et al*., 2015). A broad-spectrum lactonase preparation based on *Sso*Pox lactonase from the archaeon *Saccharolobus solfataricus* was obtained from Gene&GreenTK (Marseille, France), which is specialized in the development of enzymes, including quorum quenching lactonases. The commercial preparation obtained from Gene&GreenTK was produced heterogeneously in *E. coli*, purified to homogeneity by size-exclusion chromatography (Hiblot *et al*., 2013; Guendouze *et al*., 2017; Rémy *et al*., 2020) and eluted in HEPES buffer (50 mM HEPES, 150 mM NaCl and pH 8.0).

Bacterial isolates that were shown to produce AHLs were pre-cultured overnight in mLB (in the salinity at which they were isolated) at the appropriate temperature (12 or 22°C). The pre-cultures OD_{600} was measured using a NanoDrop 2000c with 1 cm cuvette. They were diluted to a theoretical initial OD_{600} of 0.001 and amended with the lactonase preparation (at a final concentration of 0.5 mg l^{1}) or the equivalent amount of HEPES buffer. All cultures were done in triplicate, starting from the same pre-culture. Two hundred microliters of each culture were immediately transferred into a microplate for biofilm production assay (see above procedure). Cultures were then incubated for 24 h (at 22°C) or 48 h (at 12°C) under low agitation (100 rpm). At the end of the incubation, OD_{600} and enzymatic activities (see above procedure) were quantified (one assay per replicate). The resulting supernatants were also tested with *P. putida* F117 and *E. coli* MT102 as described above to ensure the proper AHL reduction upon lactonase treatment. For each parameter (biofilm production, specific enzymatic activity and specific GFP fold induction), the effect of the lactonase treatment was assessed by calculating the ratio of control to test sample value ($ratio_{lac/ctr}$).

Whole-genome sequencing of representative strains

The genome of four strains (*Pseudomonas* sp. AF3-9, *Pseudomonas* sp. B20, *Acinetobacter* sp. DF3-8 and *Vibrio* sp. E14) was sequenced to identify the genes involved in QS, QQ, hydrolytic enzymes and biofilm production. Those strains were chosen because they covered the taxonomic diversity of the AHL-producing strains and exhibited marked responses to lactonases addition. The four selected strains were grown to stationary phase in mLB (at the salinity at which they were isolated) at 12°C (*Pseudomonas* sp. AF3-9 and *Pseudomonas* sp. B20) or 22°C (*Acinetobacter* sp. DF3-8 and *Vibrio* sp. E14). Cells were harvested by centrifugation and genomic DNA was extracted using the GenElute Bacterial Genomic DNA Kit (Sigma-Aldrich) according to the manufacturer's instructions. DNA was sequenced using an Illumina MiSeq. Data quality was assessed using FastQC (http://www.bioinformatics.babraham.ac.uk/projects/fastqc) and reads that met the following criteria were kept: (i) read length ≥ 50 base pairs (bp) and (ii) phred score per base ≥30x. Adapters were filtered away based on an internal Illumina adapter database. *De novo* assembly of genomes from raw reads was performed using Unicycler (v0.4.8) with a minimal contig length of 500 bp (Wick *et al*., 2017). Contigs were then searched for similarities against the UniVec database (20 March 2017) using BLASTN (Altschul *et al*., 1990) to remove potential contaminants from the genome assemblies. Sequencing coverage was estimated by first mapping

paired reads to the genome with Bowtie2 (v2.3.5) (Langmead and Salzberg, 2012) in 'sensitive' mode and then computing the coverage with Mosdepth (v0.2.7) (Pedersen and Quinlan, 2018). The completeness of the genome assembly was assessed using BUSCO (v4.0.0) (Simão *et al*., 2015) in 'genome' mode specifying the profile as appropriate (i.e., *Pseudomonadales* or *Vibrionales*, release April 2019, Supporting Information Table S5). The obtained drafts were checked for the number of contigs, %GC content, total assembly size, N50 values and percentage of coverage. Automatic gene prediction was done with the Prokka pipeline (v1.14.5) (Seemann, 2014) using default parameters, specifying the corresponding genus.

The following analyses were done using the predicted protein sequence output from Prokka. To search for AHL synthases, AHL receptors, AHL acylases and AHL lactonases, reference databases were built using the reviewed UniProt/Swiss-Prot database (with the respective keywords: 'acyl-homoserine-lactone synthase', 'IPR036693', 'AHL acylase' and 'AHL lactonases') and manually inspected. In addition, three sequences from UniProt/TrEMBL were added to represent the HdtS and AinS AHL synthase families and the AinR AHL receptors. Predicted proteins were blasted against the custom reference databases using a cut-off E-value of 10^{-15}. Shortlisted proteins were then blasted against the complete UniProt/Swiss-Prot database and proteins with a better match in the UniProt/Swiss-Prot database were removed from the hit list. Finally, the protein domains of those hits were annotated using InterProScan (v5.36.75) (Jones *et al*., 2014). Hits containing the appropriate domains were considered putative QS genes (see Supporting Information Table S4 for domain list). They were aligned to their custom reference databases using MUSCLE as implemented in Geneious Prime (v2021.0.3) and consensus neighbour-joining trees were built using 500 bootstraps.

Genes related to motility and adherence likely to be involved in biofilm production (flagella, pili, fimbriae, chemotaxis) were predicted using VFanalyzer (Liu *et al*., 2019), specifying the appropriate genus. Proteases and protease inhibitors were predicted using BLASTN against the MEROPS protease database (v12.1) (Rawlings *et al*., 2018) with a cut-off E-value of 1e-50 and 70% of identity. CAZymes were predicted against the CAZy database (Lombard *et al*., 2014) using dbCAN2 (HMMdb release v9.0) (Zhang *et al*., 2018). Only CAZymes that were predicted by HMMER, Diamond and Hotpep tools were selected.

Statistical analysis

All statistical analyses were implemented in R software (R Studio v1.1.463). T-tests (package ggpubr, v0.4.0) were used to determine the statistical significance of the means between control and test samples (fold induction or inhibition of biosensors, hydrolytic enzymes and biofilm production), with a significance level of 0.05. Plots display the mean and associated standard error of triplicate values, unless specified otherwise. Statistical analysis for the effect of the origin of the sample (salinity, fraction and month of isolation) on the abundance of AHL-producing strains was carried out using the χ^2 square test and Fisher's exact test (chisq.test and fischer.test functions, stats package v4.1.0) with a significance level of 0.05.

Data availability

The genome assemblies of *Pseudomonas* sp. AF3-9, *Pseudomonas* sp. B20, *Acinetobacter* sp. DF3-8 and *Vibrio* sp. E14 are available under the DDBJ/ENA/GenBank accession numbers JAHPJF000000000, JAHPJG000000000, JAHPJH000000000 and JAHPJI 000000000, respectively. The AHL-related genes databases are available upon request.

Acknowledgements

This work was supported by the French National programme EC2CO (Ecosphère Continentale et Côtière) and by an ISblue (Interdisciplinary graduate school for the blue planet) project (ANR-17-EURE-0015), co-funded by a grant from the French government under the programme 'Investissements d'Avenir'. This work was also carried out in conjunction with the European Marine Biological Resource Centre (EMBRC-ERIC), EMBRC-France and BIO2MAR platform (https://www.obs-banyuls.fr/fr/rechercher/plateformes/bio2mar.html). French state funds are managed by the ANR within the Investments of the Future programme under the grant number ANR-10-INSB-02. The authors would like to thank the crew of the Hésione – Isabelle Bihannic, Thierry Le Bec and Erwan Amice – for their help during sampling. We would also like to thank the BIO2MAR platform (https://www.obs-banyuls.fr/fr/rechercher/plateformes/bio2mar.html) for providing technical support and access to instrumentation. In addition, the authors are deeply grateful to Amine Boukerb (University of Rouen) for performing the whole-genome sequencing, Alexandre Cormier (SeBiMer, IFREMER) for assembling the genomes and Cyril Noël (SeBiMer, IFREMER) for his constructive advice on bioinformatics. Finally, the authors would like to thank Daniel Delmas for his perspicacious comments and support throughout this research project.

D.D. has filled the patent FR3093894. D.D. is CEO and shareholder of Gene&GreenTK and received personal fees during the conduct of the study. The other authors declare that the research was conducted in the absence of any commercial or financial relationships that could be construed as a potential conflict of interest.

References

Abd-Elnaby, H.M., Abou-Elela, G.M., Hussein, H., Ghozlan, H.A., and Sabry, S.A. (2019) Characterization and bioremediation potential of marine psychrotolerant Pseudomonas spp. isolated from the Mediterranean Sea, Egypt. *Egypt J Aquat Biol Fish* **23**: 669–683.

Altschul, S.F., Gish, W., Miller, W., Myers, E.W., and Lipman, D.J. (1990) Basic local alignment search tool. *J Mol Biol* **215**: 403–410.

Andersen, J.B., Heydorn, A., Hentzer, M., Eberl, L., Geisenberger, O., Christensen, B.B., *et al*. (2001) gfp-based N-acyl homoserine-lactone sensor systems for detection of bacterial communication. *Appl Environ Microbiol* **67**: 575–585.

Arnosti, C. (2011) Microbial extracellular enzymes and the marine carbon cycle. *Annu Rev Marine Sci* **3**: 401–425.

Azam, F., Fenchel, T., Field, J., Gray, J., Meyer-Reil, L., and Thingstad, F. (1983) The ecological role of water-column microbes in the sea. *Mar Ecol Prog Ser* **10**: 257–263.

Azam, F., and Malfatti, F. (2007) Microbial structuring of marine ecosystems. *Nat Rev Microbiol* **5**: 782–791.

Baffone, W., Tarsi, R., Pane, L., Campana, R., Repetto, B., Mariottini, G.L., and Pruzzo, C. (2006) Detection of free-living and plankton-bound vibrios in coastal waters of the Adriatic Sea (Italy) and study of their pathogenicity-associated properties. *Environ Microbiol* **8**: 1299–1305.

Baltar, F. (2018) Watch out for the "living dead": cell-free enzymes and their fate. *Front Microbiol* **8**: 2438.

Berne, C., Ellison, C.K., Ducret, A., and Brun, Y.V. (2018) Bacterial adhesion at the single-cell level. *Nat Rev Microbiol* **16**: 616–627.

Blanchet, E., Prado, S., Stien, D., da Silva, J.O., Ferandin, Y., Batailler, N., *et al*. (2017) Quorum sensing and quorum quenching in the Mediterranean seagrass *Posidonia Oceanica* microbiota. *Front Mar Sci* **4**: 218.

Chan, K., Atkinson, S., Mathee, K., Sam, C., Chhabra, S.R., and Cámara, M. (2011) (11AD) characterization of N-acylhomoserine lactone- degrading bacteria associated with the *Zingiber officinale* (ginger) rhizosphere: co-existence of quorum quenching and quorum sensing in Acinetobacter and Burkholderia characterization of N -acylhomoserine la. *BMC Microbiol* **11**: 1–13.

Chróst, R.J. (1989) Characterization and significance of β-glucosidase activity in lake water. *Limnol Oceanogr* **34**: 660–672.

Chróst, R.J. (1990) Microbial Ectoenzymes in aquatic environments. In *Aquatic Microbial Ecology: Biochemical and Molecular Approaches*, Overbeck, J., and Chróst, R.J. (eds). New York, NY: Springer-Verlag, pp. 47–77.

Chróst, R.J., and Siuda, W. (2002) Ecology of microbial enzymes in Lake ecosystems. In *Enzymes in the Environment: Activity, Ecology and Applications*, Burns, R.G., and Dick, R.P. (eds). New York, NY: CRC Press, pp. 35–72.

Crump, B.C., Armbrust, E.V., and Baross, J.A. (1999) Phylogenetic analysis of particle-attached and free-living bacterial communities in the Columbia River, its estuary, and the adjacent coastal ocean. *Appl Environ Microbiol* **65**: 3192–3204.

Dang, H., and Lovell, C.R. (2016) Microbial surface colonization and biofilm development in marine environments. *Microbiol Mol Biol Rev* **80**: 91–138.

Decho, A.W., Visscher, P.T., Ferry, J., Kawaguchi, T., He, L., Przekop, K.M., *et al*. (2009) Autoinducers extracted from microbial mats reveal a surprising diversity of N-acylhomoserine lactones (AHLs) and abundance changes that may relate to diel pH. *Environ Microbiol* **11**: 409–420.

Delong, E.F., Franks, D.G., and Alldredge, A.L. (1993) Phylogenetic diversity of aggregate-attached vs free-living marine bacterial assemblages. *Limnol Oceanogr* **38**: 924–934.

Doberva, M., Sanchez-Ferandin, S., Toulza, E., Lebaron, P., and Lami, R. (2015) Diversity of quorum sensing autoinducer synthases in the Global Ocean sampling metagenomic database. *Aquat Microb Ecol* **74**: 107–119.

Doberva, M., Stien, D., Sorres, J., Hue, N., Sanchez-Ferandin, S., Eparvier, V., *et al*. (2017) Large diversity and original structures of acyl-homoserine lactones in strain MOLA 401, a marine Rhodobacteraceae bacterium. *Front Microbiol* **8**: 1152.

Eberl, L. (1999) N-acyl Homoserinelactone-mediated gene regulation in Gram-negative bacteria. *Syst Appl Microbiol* **22**: 493–506.

Elliot, E.L., and Colwell, R.R. (1985) Indicator organisms for estuarine and marine waters. *FEMS Microbiol Lett* **32**: 61–79.

Flemming, H.C., Wingender, J., Szewzyk, U., Steinberg, P., Rice, S.A., and Kjelleberg, S. (2016) Biofilms: an emergent form of bacterial life. *Nat Rev Microbiol* **14**: 563–574.

Freckelton, M.L., Høj, L., and Bowden, B.F. (2018) Quorum sensing interference and structural variation of quorum sensing mimics in Australian soft coral. *Front Mar Sci* **5**: 198.

Fuqua, C. (2006) The QscR quorum-sensing regulon of *Pseudomonas aeruginosa*: an orphan claims its identity. *J Bacteriol* **188**: 3161–3171.

Gram, L., Grossart, H.P., Schlingloff, A., and Kiørboe, T. (2002) Possible quorum sensing in marine snow bacteria: production of acylated homoserine lactones by Roseobacter strains isolated from marine snow. *Appl Environ Microbiol* **68**: 4111–4116.

Grandclément, C., Tannières, M., Moréra, S., Dessaux, Y., and Faure, D. (2015) Quorum quenching: role in nature and applied developments. *FEMS Microbiol Rev* **40**: 86–116.

Guendouze, A., Plener, L., Bzdrenga, J., Jacquet, P., Rémy, B., Elias, M., *et al*. (2017) Effect of quorum quenching lactonase in clinical isolates of Pseudomonas aeruginosa and comparison with quorum sensing inhibitors. *Front Microbiol* **8**: 227.

Guzman, J.P.M.D., De las Alas, T.P., Lucban, M.C., and Sevilla, C.E.C. (2020) Green tea (*Camellia sinensis*) extract inhibits biofilm formation in acyl homoserine lactone-producing, antibiotic-resistant *Morganella morganii* isolated from Pasig River, Philippines. *Heliyon* **6**: e05284.

Hiblot, J., Gotthard, G., Elias, M., and Chabriere, E. (2013) Differential active site loop conformations mediate promiscuous activities in the lactonase SsoPox. *PLoS One* **8**: e75272.

Hmelo, L.R. (2017) Quorum sensing in marine microbial environments. *Annu Rev Mar Sci* **9**: 257–281.

Hmelo, L.R., Mincer, T.J., and Van Mooy, B.A.S. (2011) Possible influence of bacterial quorum sensing on the

hydrolysis of sinking particulate organic carbon in marine environments. *Environ Microbiol Rep* **3**: 682–688.

Hraiech, S., Hiblot, J., Lafleur, J., Lepidi, H., Papazian, L., Rolain, J.M., *et al*. (2014) Inhaled lactonase reduces *pseudomonas aeruginosa* quorum sensing and mortality in rat pneumonia. *PLoS One* **9**: e107125.

Huang, S., Bergonzi, C., Schwab, M., Elias, M., and Hicks, R.E. (2019) Evaluation of biological and enzymatic quorum quencher coating additives to reduce biocorrosion of steel. *PLoS One* **14**: e0217059.

Jatt, A.N., Tang, K., Liu, J., Zhang, Z., and Zhang, X.H. (2015) Quorum sensing in marine snow and its possible influence on production of extracellular hydrolytic enzymes in marine snow bacterium *Pantoea ananatis* B9. *FEMS Microbiol Ecol* **91**: 1–13.

Jones, P., Binns, D., Chang, H.Y., Fraser, M., Li, W., McAnulla, C., *et al*. (2014) InterProScan 5: genome-scale protein function classification. *Bioinformatics* **30**: 1236–1240.

Kalia, V.C. (2013) Quorum sensing inhibitors: an overview. *Biotechnol Adv* **31**: 224–245.

Kim, O.S., Cho, Y.J., Lee, K., Yoon, S.H., Kim, M., Na, H., *et al*. (2012) Introducing EzTaxon-e: a prokaryotic 16s rRNA gene sequence database with phylotypes that represent uncultured species. *Int J Syst Evol Microbiol* **62**: 716–721.

Krupke, A., Hmelo, L.R., Ossolinski, J.E., Mincer, T.J., and Van Mooy, B.A.S. (2016) Quorum sensing plays a complex role in regulating the enzyme hydrolysis activity of microbes associated with sinking particles in the ocean. *Front Mar Sci* **3**: 55.

Labry, C., Delmas, D., Youenou, A., Quere, J., Leynaert, A., Fraisse, S., *et al*. (2016) High alkaline phosphatase activity in phosphate replete waters: the case of two macrotidal estuaries. *Limnol Oceanogr* **61**: 1513–1529.

Lami, R. (2019) Quorum sensing in marine biofilms and environments. In *Quorum Sensing: Molecular Mechanism and Biotechnological Application*. Amsterdam: Elsevier.

Langmead, B., and Salzberg, S.L. (2012) Fast gapped-read alignment with bowtie 2. *Nat Methods* **9**: 357–359.

Li, T., Wang, D., Ren, L., Mei, Y., Ding, T., Li, Q., *et al*. (2019) Involvement of exogenous N-acyl-Homoserine lactones in spoilage potential of *Pseudomonas fluorescens* isolated from refrigerated turbot. *Front Microbiol* **10**: 2716.

Liu, B., Zheng, D., Jin, Q., Chen, L., and Yang, J. (2019) VFDB 2019: a comparative pathogenomic platform with an interactive web interface. *Nucleic Acids Res* **47**: D687–D692.

Liu, J., Fu, K., Wang, Y., Wu, C., Li, F., Shi, L., and Ge, Y. (2017) Detection of diverse N-acyl-Homoserine lactones in vibrio alginolyticus and regulation of biofilm formation by lactone in vitro. *Front Microbiol* **8**: 1097.

Lombard, V., Golaconda Ramulu, H., Drula, E., Coutinho, P. M., and Henrissat, B. (2014) The carbohydrate-active enzymes database (CAZy) in 2013. *Nucleic Acids Res* **42**: 490–495.

Mahan, K., Martinmaki, R., Larus, I., Sikdar, R., Dunitz, J., and Elias, M. (2020) Effects of signal disruption depends on the substrate preference of the lactonase. *Front Microbiol* **10**: 3003.

Middelboe, M., Sondergaard, M., Letarte, Y., and Borch, N. H. (1995) Attached and free-living bacteria: production and polymer hydrolysis during a diatom bloom. *Microb Ecol* **29**: 231–248.

Millar, J.J., Payne, J.T., Ochs, C.A., and Jackson, C.R. (2015) Particle-associated and cell-free extracellular enzyme activity in relation to nutrient status of large tributaries of the lower Mississippi River. *Biogeochemistry* **124**: 255–271.

Miller, M.B., and Bassler, B.L. (2001) Quorum sensing in bacteria. *Annu Rev Microbiol* **55**: 165–199.

Mion, S., Carriot, N., Lopez, J., Plener, L., Ortalo-Magné, A., Chabrière, E., *et al*. (2021) Disrupting quorum sensing alters social interactions in *Chromobacterium violaceum*. *NPJ Biofilms Microbiomes* **7**: 40.

Mion, S., Rémy, B., Plener, L., Brégeon, F., Chabrière, E., and Daudé, D. (2019) Quorum quenching lactonase strengthens bacteriophage and antibiotic arsenal against *Pseudomonas aeruginosa* clinical isolates. *Front Microbiol* **10**: 2049.

Muras, A., López-Pérez, M., Mayer, C., Parga, A., Amaro-Blanco, J., and Otero, A. (2018) High prevalence of quorum-sensing and quorum-quenching activity among cultivable bacteria and metagenomic sequences in the mediterranean sea. *Genes (Basel)* **9**: 100.

Muras, A., Otero-Casal, P., Blanc, V., and Otero, A. (2020) Acyl homoserine lactone-mediated quorum sensing in the oral cavity: a paradigm revisited. *Sci Rep* **10**: 9800.

Paluch, E., Rewak-Soroczyńska, J., Jędrusik, I., Mazurkiewicz, E., and Jermakow, K. (2020) Prevention of biofilm formation by quorum quenching. *Appl Microbiol Biotechnol* **104**: 1871–1881.

Papenfort, K., and Bassler, B.L. (2016) Quorum sensing signal-response systems in Gram-negative bacteria. *Nat Rev Microbiol* **14**: 576–588.

Pedersen, B.S., and Quinlan, A.R. (2018) Mosdepth: quick coverage calculation for genomes and exomes. *Bioinformatics* **34**: 867–868.

Pomeroy, L.R. (1974) The Ocean's food web, a changing paradigm. *Bioscience* **24**: 499–504.

Priha, O., Virkajärvi, V., Juvonen, R., Puupponen-Pimiä, R., Nohynek, L., Alakurtti, S., *et al*. (2014) Quorum sensing Signalling and biofilm formation of brewery-derived bacteria, and inhibition of Signalling by natural compounds. *Curr Microbiol* **69**: 617–627.

Rawlings, N.D., Barrett, A.J., Thomas, P.D., Huang, X., Bateman, A., and Finn, R.D. (2018) The MEROPS database of proteolytic enzymes, their substrates and inhibitors in 2017 and a comparison with peptidases in the PANTHER database. *Nucleic Acids Res* **46**: D624–D632.

Rémy, B., Plener, L., Decloquement, P., Armstrong, N., Elias, M., Daudé, D., and Chabrière, É. (2020) Lactonase specificity is key to quorum quenching in *Pseudomonas aeruginosa*. *Front Microbiol* **11**: 762.

Rieck, A., Herlemann, D.P.R., Jürgens, K., and Grossart, H. P. (2015) Particle-associated differ from free-living bacteria in surface waters of the Baltic Sea. *Front Microbiol* **6**: 1297.

Riedel, K., Hentzer, M., Geisenberger, O., Huber, B., Steidle, A., Wu, H., *et al*. (2001) N-acylhomoserine-lactone-mediated communication between Pseudomonas aeruginosa and *Burkholderia cepacia* in mixed biofilms. *Microbiology* **147**: 3249–3262.

Romero, M., Martin-Cuadrado, A.B., and Otero, A. (2012) Determination of whether quorum quenching is a common activity in marine bacteria by analysis of cultivable bacteria and metagenomic sequences. *Appl Environ Microbiol* **78**: 6345–6348.

Romero, M., Martin-Cuadrado, A.B., Roca-Rivada, A., Cabello, A.M., and Otero, A. (2011) Quorum quenching in cultivable bacteria from dense marine coastal microbial communities. *FEMS Microbiol Ecol* **75**: 205–217.

Rossi, E., Paroni, M., and Landini, P. (2018) Biofilm and motility in response to environmental and host-related signals in Gram negative opportunistic pathogens. *J Appl Microbiol* **125**: 1587–1602.

Schwab, M., Bergonzi, C., Sakkos, J., Staley, C., Zhang, Q., Sadowsky, M.J., *et al*. (2019) Signal disruption leads to changes in bacterial community population. *Front Microbiol* **10**: 611.

Seemann, T. (2014) Prokka: rapid prokaryotic genome annotation. *Bioinformatics* **30**: 2068–2069.

Simão, F.A., Waterhouse, R.M., Ioannidis, P., Kriventseva, E.V., and Zdobnov, E.M. (2015) BUSCO: assessing genome assembly and annotation completeness with single-copy orthologs. *Bioinformatics* **31**: 3210–3212.

Simon, M., Grossart, H.P., Schweitzer, B., and Ploug, H. (2002) Microbial ecology of organic aggregates in aquatic ecosystems. *Aquat Microb Ecol* **28**: 175–211.

Sivadon, P., Barnier, C., and Urios, L. (2019) Biofilm formation as a microbial strategy to assimilate particulate substrates. *Environ Microbiol Rep* **11**: 749–764.

Steen, A.D., Vazin, J.P., Hagen, S.M., Mulligan, K.H., and Wilhelm, S.W. (2015) Substrate specificity of aquatic extracellular peptidases assessed by competitive inhibition assays using synthetic substrates. *Aquat Microb Ecol* **75**: 271–281.

Su, Y., Tang, K., Liu, J., Wang, Y., Zheng, Y., and Zhang, X. H. (2019) Quorum sensing system of *Ruegeria mobilis* Rm01 controls lipase and biofilm formation. *Front Microbiol* **10**: 3304.

Tait, K., Hutchison, Z., Thompson, F.L., and Munn, C.B. (2010) Quorum sensing signal production and inhibition by coral-associated vibrios. *Environ Microbiol Rep* **2**: 145–150.

Tait, K., Williamson, H., Atkinson, S., Williams, P., Cámara, M., and Joint, I. (2009) Turnover of quorum sensing signal molecules modulates cross-kingdom signalling. *Environ Microbiol* **11**: 1792–1802.

Thomson, B., Wenley, J., Currie, K., Hepburn, C., Herndl, G. J., and Baltar, F. (2019) Resolving the paradox: continuous cell-free alkaline phosphatase activity despite high phosphate concentrations. *Mar Chem* **214**: 103671.

Tourneroche, A., Lami, R., Hubas, C., Blanchet, E., Vallet, M., Escoubeyrou, K., *et al*. (2019) Bacterial-fungal interactions in the kelp endomicrobiota drive autoinducer-2 quorum sensing. *Front Microbiol* **10**: 1693.

UNESCO (1985) The international system of units (SI) in oceanography. UNESCO Tech Pap Mar Sci 45. 131p.

Waters, C.M., and Bassler, B.L. (2005) Quorum sensing: cell-to-cell communication in bacteria. *Annu Rev Cell Dev Biol* **21**: 319–346.

Wick, R.R., Judd, L.M., Gorrie, C.L., and Holt, K.E. (2017) Unicycler: resolving bacterial genome assemblies from short and long sequencing reads. *PLoS Comput Biol* **13**: e1005595.

Wolska, K.I., Grudniak, A.M., Rudnicka, Z., and Markowska, K. (2016) Genetic control of bacterial biofilms. *J Appl Genet* **57**: 225–238.

Zhang, H., Wang, C., and Zhang, L. (2004) The quormone degradation system of *agrobacterium tumefaciens* is regulated by starvation signal and stress alarmone (p) ppGpp. *Mol Microbiol* **52**: 1389–1401.

Zhang, H., Yohe, T., Huang, L., Entwistle, S., Wu, P., Yang, Z., *et al*. (2018) DbCAN2: a meta server for automated carbohydrate-active enzyme annotation. *Nucleic Acids Res* **46**: W95–W101.

Supporting Information

Additional Supporting Information may be found in the online version of this article at the publisher's web-site:

Appendix S1: Supplementary Information

III. Données supplémentaires

Table S1: Number of isolated bacteria per sample and per isolation methods. Isolations were performed by: (i) spreading 100 µL of total water, (ii) spreading 100 µL of < 3 µm water, (iii) depositing > 3 µm filters or (iv) depositing 0.2 µm filters used with 3 µm filtrated water. MTZ: Maximum Turbidity Zone.

Date	GPS coordinates	Salinity	Suspended matter (mg L^{-1})	Total number of isolates	Number of isolates (per method of isolation)			
					i	ii	iii	iv
April 18, 2019	48° 12.653 N 4° 5.841 W	0	3.3	64	25	7	17	15
April 18, 2019	48° 14.962 N 4° 11.457 W	5	261.7	59	29	2	19	9
April 18, 2019	48° 17,165 N 4° 16,997 W	25	14.6	63	24	27	7	5
July 18, 2019	48° 13,501 N 4° 6,893 W	5	90.8	62	22	12	15	13
July 18, 2019	48° 14,926 N 4° 12,523 W	25	31.3	51	10	12	15	14

Table S2: Specific fold induction of the 299 isolates screened to assess AHLs production, for each sampling site

	Fold induction	< 0.8	0.8-1.2	1.2-1.5	1.5-3	> 3	Significantly different from control
Salinity 0, April	*E. coli* MT102	0	61	1	1	1	3 (5%)
	P. putida F117	1	52	8	2	1	12 (19%)
Salinity 5, April	*E. coli* MT102	3	53	0	0	3	6 (11%)
	P. putida F117	2	51	5	1	0	8 (15%)
Salinity 25, April	*E. coli* MT102	1	58	4	0	0	5 (8%)
	P. putida F117	8	52	3	0	0	11 (17%)
Salinity 5, July	*E. coli* MT102	6	44	6	2	4	18 (29%)
	P. putida F117	4	46	7	5	0	16 (26%)
Salinity 25, July	*E. coli* MT102	2	44	3	2	0	7 (14%)
	P. putida F117	1	44	5	1	0	7 (14%)

Table S3: Taxonomic identification of the 28 AHL-producing strains, including the name of the closest affiliated strain, the sequence length, the pairwise similarity between the two sequences and the corresponding affiliated order.

Isolate	Top hit taxon (top hit strain)	Sequence length (pb)	Similarity (%)	Order
Pseudomonas sp. A14	*Pseudomonas poae* (DSM 14936)	1410	99.93	*Pseudomonadales*
Pseudomonas sp. A20	*Pseudomonas fildesensis* (KG01)	1407	99.86	*Pseudomonadales*
Pseudomonas sp. AF3-2	*Pseudomonas meliae* (CFBP 3225)	1329	99.55	*Pseudomonadales*
Pseudomonas sp. AF3-9	*Pseudomonas lurida* (LMG 21995)	1385	99.71	*Pseudomonadales*
Sphingobacterium sp. AF02-2	*Sphingobacterium faecium* (DSM 11690)	1336	99.25	*Sphingobacteriales*
Pseudomonas sp. AF02-5	*Pseudomonas fildesensis* (KG01)	1411	99.93	*Pseudomonadales*
Pseudomonas sp. AF02-15	*Pseudomonas yamanorum* (8H1)	1402	99.79	*Pseudomonadales*
Pseudomonas sp. B20	*Pseudomonas cannabina* (CFBP 2341)	1408	99.86	*Pseudomonadales*
Acinetobacter sp. BF3-12	*Acinetobacter* sp. (NEGC_s, ANC 4470)	947	99.89	*Pseudomonadales*
Pseudomonas sp. BF02-28	*Pseudomonas kitaguniensis* (MAFF 301498)	1411	99.93	*Pseudomonadales*
Vibrio sp. CFL-9	*Vibrio echinoideorum* (NFH.MB010)	1123	100.00	*Vibrionales*
Vibrio sp. CFL-25	*Vibrio echinoideorum* (NFH.MB010)	1427	99.79	*Vibrionales*
Obesumbacterium sp. DF3-3	*Obesumbacterium proteus* (DSM 2777)	1411	99.72	*Enterobacteriales*
Acinetobacter sp. DF3-8	*Acinetobacter tandoii* (DSM 14970)	1385	98.92	*Pseudomonadales*
Acinetobacter sp. DF3-12	*Acinetobacter tandoii* (DSM 14970)	780	99.74	*Pseudomonadales*
Acinetobacter sp. DF3-15	*Morganella morganii* subsp. *sibonii* (DSM 14850)	1401	99.70	*Pseudomonadales*
Morganella sp. DF3-16	*Acinetobacter tandoii* (DSM 14970)	1357	99.00	*Enterobacterales*
Acinetobacter sp. DF02-2	*Acinetobacter venetianus* (RAG-1)	857	100.00	*Pseudomonadales*
Pseudomonas sp. DF02-8	*Pseudomonas protegens* (CHA0)	1404	99.79	*Pseudomonadales*
Pseudomonas sp. DF02-13	*Pseudomonas protegens* (CHA0)	1400	99.79	*Pseudomonadales*
Vibrio sp. E14	*Vibrio alginolyticus* (NBRC 15630)	1407	99.50	*Vibrionales*
Vibrio sp. E15	*Vibrio alginolyticus* (NBRC 15630)	1167	99.40	*Vibrionales*
Vibrio sp. EFL-3	*Vibrio alginolyticus* (NBRC 15630)	1409	99.57	*Vibrionales*
Vibrio sp. EFL-16	*Vibrio neocaledonicus* (NC470)	1396	99.56	*Vibrionales*
Vibrio sp. EF3-1	*Vibrio alginolyticus* (NBRC 15630)	1408	99.50	*Vibrionales*
Vibrio sp. EF02-7	*Vibrio alginolyticus* (NBRC 15630)	1369	99.51	*Vibrionales*
Vibrio sp. EF02-14	*Vibrio alginolyticus* (NBRC 15630)	1201	99.42	*Vibrionales*
Vibrio sp. EF02-15	*Vibrio alginolyticus* (NBRC 15630)	1425	99.58	*Vibrionales*

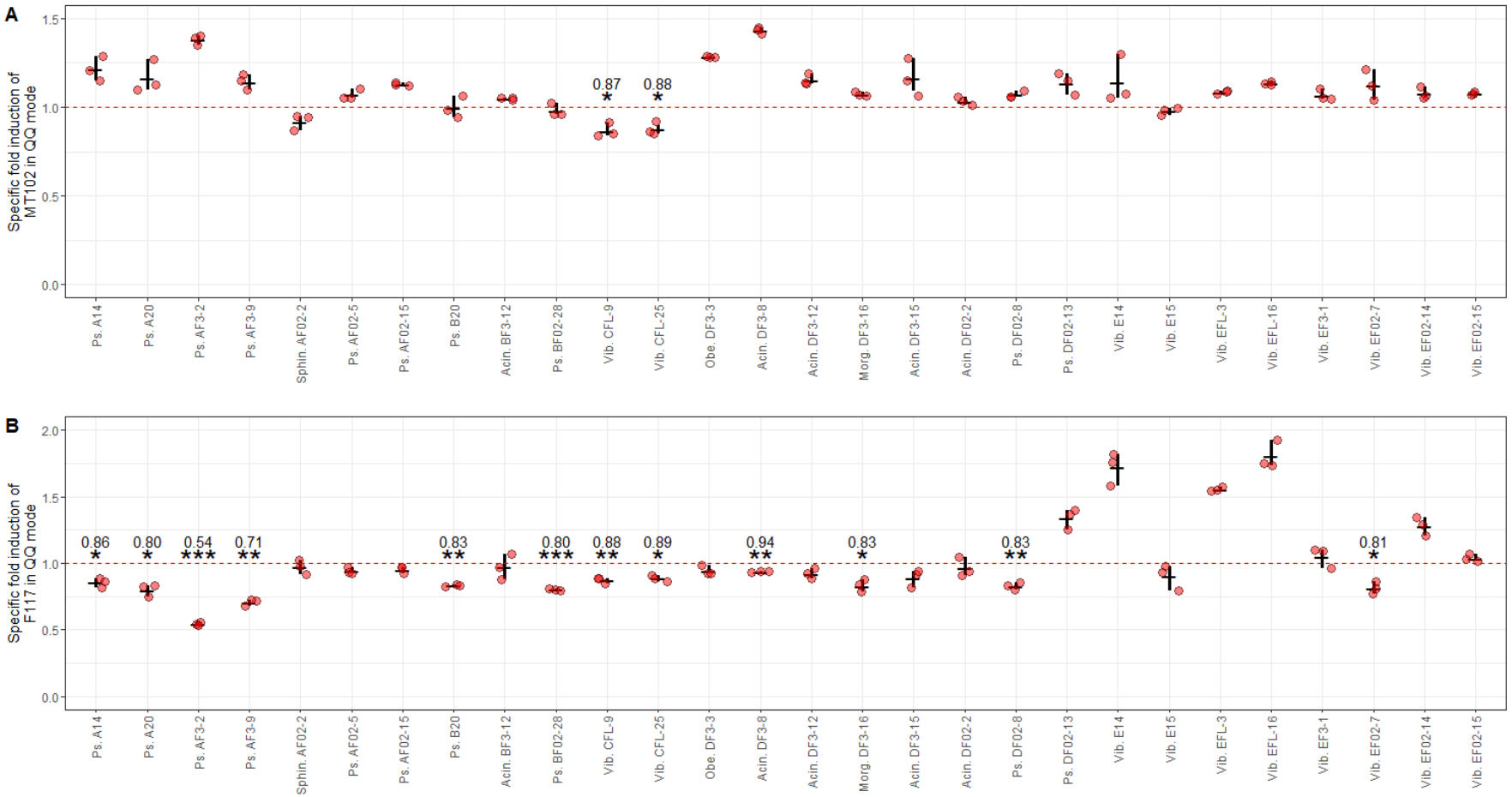

Figure S1: Specific fold induction of biosensors used to screen for QQ abilities of the AHLs-producing strains. Detection of C6- and C14HSL quenching using MT102 (A) and F117 (B), respectively. The specific fold induction is specified for results significantly inferior to 1, which means that there is a disruption of AHL sensing. Red dots represent each triplicate while black cross represent mean and 95% confidence interval. *: $p < 0.05$, **: $p < 0.01$, ***: $p < 0.001$.

Figure S2: Dissolved LAM (**A**), cell-bound LAM (**B**) and cell-bound β-glc (**C**) production for the strains that were significantly impacted by the lactonase treatment. Note the broken y-axis in A. Red: control (buffer amendment), blue: lactonase amendment. The lactonase over control ratio is annotated when calculable (lac/ctr), along with the p-value (°: $p < 0.1$,*: $p < 0.05$, **: $p < 0.01$, ***: $p < 0.001$). Error bar represents standard error. Acin.: *Acinetobacter* sp., Morg.: *Morganella* sp., Obe.: *Obesumbacterium* sp., Ps.: *Pseudomonas* sp., Vib.: *Vibrio* sp., Sphin.: *Sphingobacterium* sp.

Table S4: List of InterPro domains used to select QS and QQ gene

LuxI-type AHL-synthase	
IPR001690	Autoinducer synthase
IPR016181	Acyl-CoA N-acyltransferase
HdtS-type AHL-synthase	
IPR002123	Phospholipid/glycerol acyltransferase
LuxM-type and AinS-type AHL-synthase	
IPR035304	AHL synthase
LuxR-type AHL receptor	
IPR005143	Transcription factor LuxR-like, autoinducer-binding domain
IPR000792	Transcription regulator LuxR, C-terminal
IPR016032	Signal transduction response regulator, C-terminal effector
IPR036388	Winged helix-like DNA-binding domain
LuxN-type and AinR-type AHL receptor	
IPR011006	CheY-like superfamily
IPR003594	Histidine kinase/HSP90-like ATPase
IPR036890	Histidine kinase/HSP90-like ATPase superfamily
IPR005467	Histidine kinase domain
IPR003661	Signal transduction histidine kinase, dimerisation/phosphoacceptor domain
IPR036097	Signal transduction histidine kinase, dimerisation/phosphoacceptor domain superfamily
IPR004358	Signal transduction histidine kinase-related protein, C-terminal
IPR001789	Signal transduction response regulator, receiver domain
AHL-lactonase	
IPR001279	Metallo-beta-lactamase
IPR036866	Ribonuclease Z/Hydroxyacylglutathione hydrolase-like
AHL-acylase	
IPR002692	Penicillin/GL-7-ACA/AHL/aculeacin-A acylase
IPR014395	Penicillin/GL-7-ACA/AHL acylase

Table S5: Assembly metrics for the four draft genomes. BUSCO output notation: Complete (C), Single-copy (S), Duplicated (D), Fragmented (F) or Missing (M) genes (n: number of genes used).

	Genome size (bp)	Contigs number	Maximum length (bp)	Minimum length (bp)	N50 (bp)	%GC	%Mapped	Coverage	BUSCO profile	BUSCO results	Number of predicted proteins (Prokka)
***Pseudomonas* sp. AF3-9**	6 012 247	63	784 999	661	263 518	61.15	98.21	55.99	pseudomonadales_odb10	C:99.4%[S:99.4%,D:0.0%], F:0.1%,M:0.5%, n:782	5407
***Pseudomonas* sp. B20**	5 843 918	57	622 712	700	204 117	59.43	97.98	50.78	pseudomonadales_odb10	C:99.4%[S:99.4%,D:0.0%], F:0.3%,M:0.3%,n:782	5016
***Acinetobacter* sp. DF3-9**	4 622 955	77	477 336	506	136 924	48.61	89.19	70.31	pseudomonadales_odb10	C:99.9%[S:99.4%,D:0.5%], F:0.1%,M:-0.0%,n:782	4129
***Vibrio* sp. E14**	5 164 120	48	1 224 714	517	596 858	44.72	98.81	64.64	vibrionales_odb10	C:80.2%[S:79.4%,D:0.8%], F:1.2%,M:18.6%,n:782	4597

A)

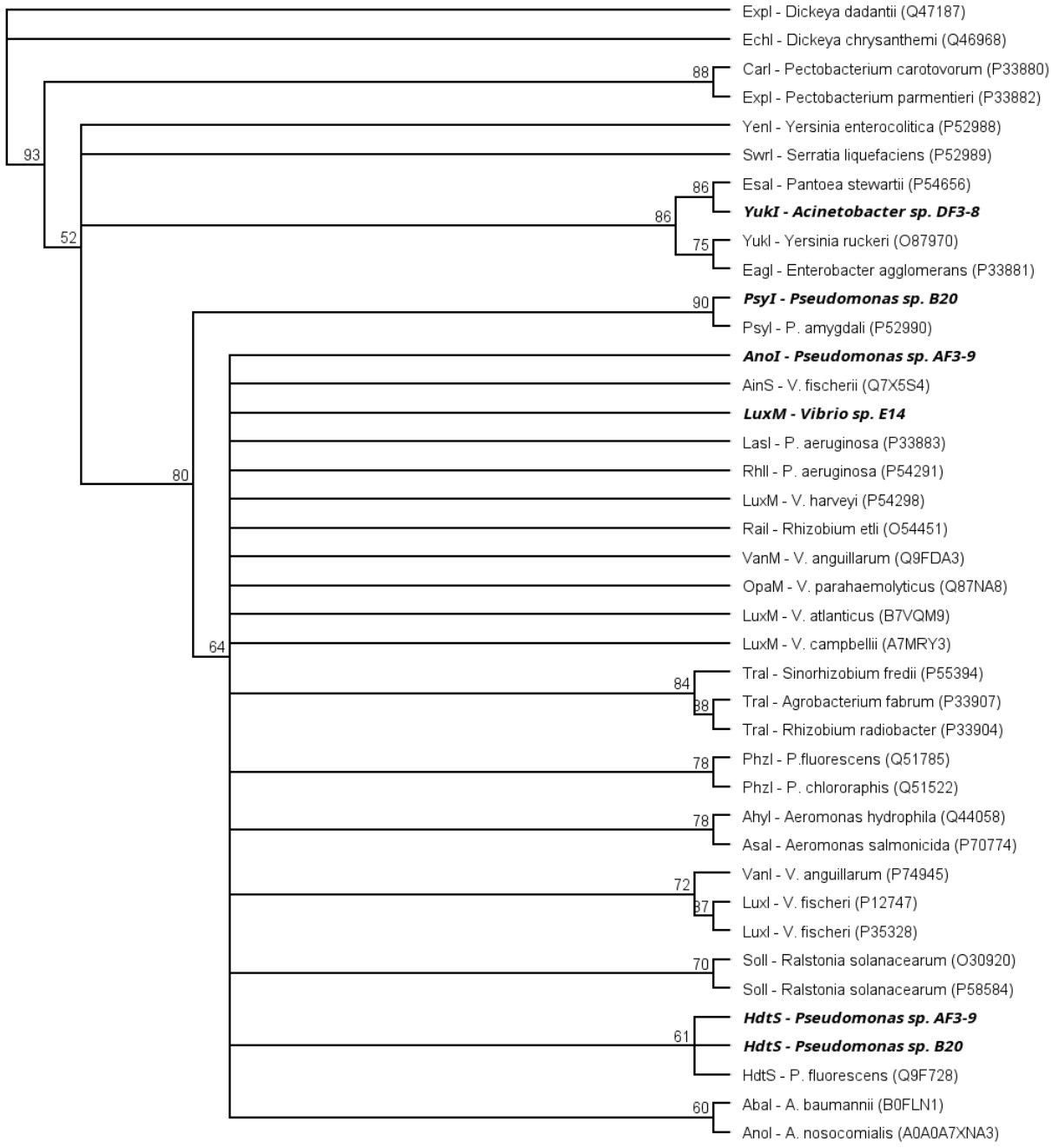
ExpI - Dickeya dadantii (Q47187)
EchI - Dickeya chrysanthemi (Q46968)
CarI - Pectobacterium carotovorum (P33880)
ExpI - Pectobacterium parmentieri (P33882)
YenI - Yersinia enterocolitica (P52988)
SwrI - Serratia liquefaciens (P52989)
EsaI - Pantoea stewartii (P54656)
YukI - Acinetobacter sp. DF3-8
YukI - Yersinia ruckeri (O87970)
EagI - Enterobacter agglomerans (P33881)
PsyI - Pseudomonas sp. B20
PsyI - P. amygdali (P52990)
AnoI - Pseudomonas sp. AF3-9
AinS - V. fischerii (Q7X5S4)
LuxM - Vibrio sp. E14
LasI - P. aeruginosa (P33883)
RhlI - P. aeruginosa (P54291)
LuxM - V. harveyi (P54298)
RaiI - Rhizobium etli (O54451)
VanM - V. anguillarum (Q9FDA3)
OpaM - V. parahaemolyticus (Q87NA8)
LuxM - V. atlanticus (B7VQM9)
LuxM - V. campbellii (A7MRY3)
TraI - Sinorhizobium fredii (P55394)
TraI - Agrobacterium fabrum (P33907)
TraI - Rhizobium radiobacter (P33904)
PhzI - P.fluorescens (Q51785)
PhzI - P. chlororaphis (Q51522)
AhyI - Aeromonas hydrophila (Q44058)
AsaI - Aeromonas salmonicida (P70774)
VanI - V. anguillarum (P74945)
LuxI - V. fischeri (P12747)
LuxI - V. fischeri (P35328)
SolI - Ralstonia solanacearum (O30920)
SolI - Ralstonia solanacearum (P58584)
HdtS - Pseudomonas sp. AF3-9
HdtS - Pseudomonas sp. B20
HdtS - P. fluorescens (Q9F728)
AbaI - A. baumannii (B0FLN1)
AnoI - A. nosocomialis (A0A0A7XNA3)
93
88
86
86
52
75
90
80
64
84
38
78
78
72
37
70
61
60

B)

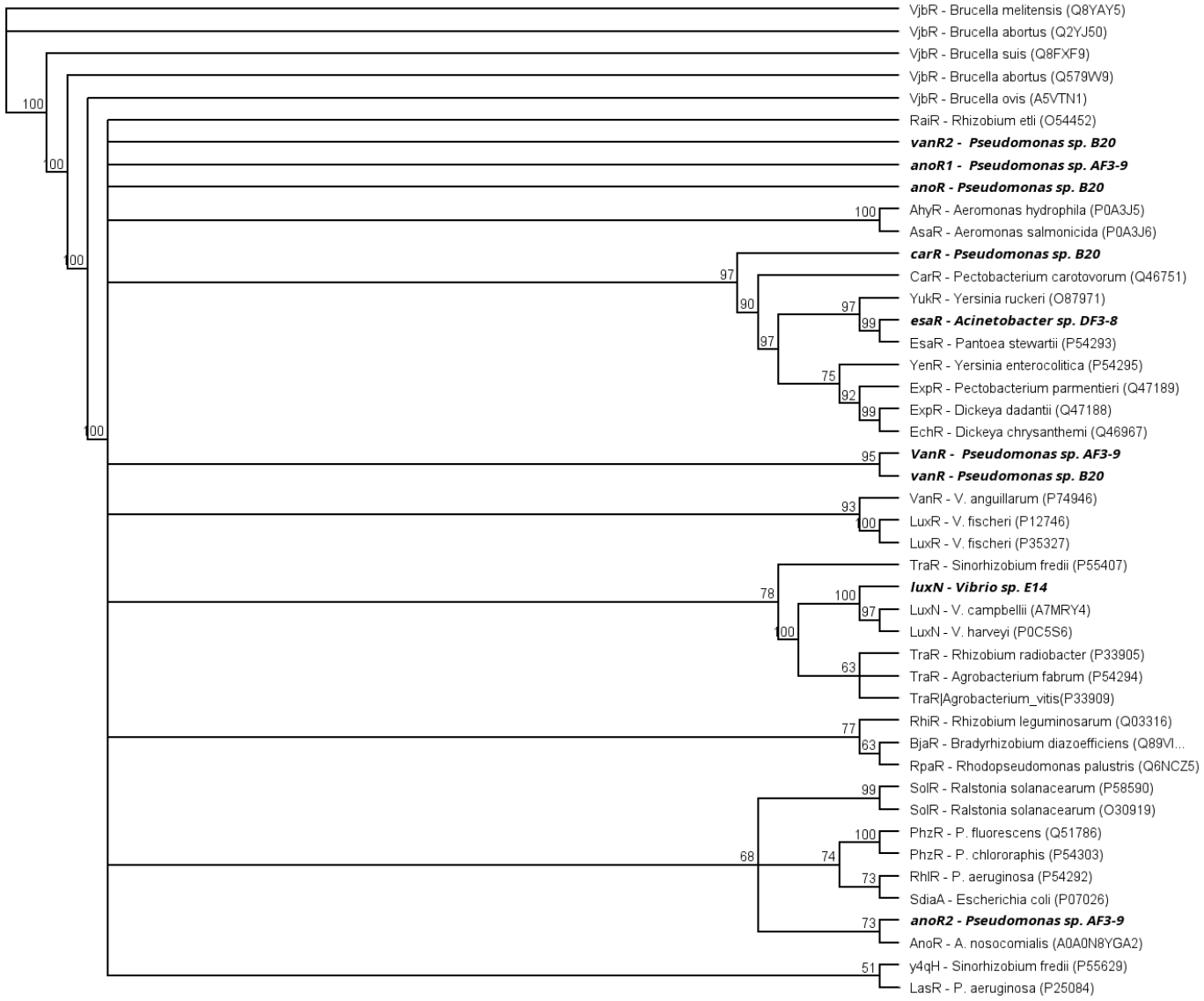
VjbR - Brucella melitensis (Q8YAY5)
VjbR - Brucella abortus (Q2YJ50)
VjbR - Brucella suis (Q8FXF9)
VjbR - Brucella abortus (Q579W9)
VjbR - Brucella ovis (A5VTN1)
RaiR - Rhizobium etli (O54452)
vanR2 - Pseudomonas sp. B20
anoR1 - Pseudomonas sp. AF3-9
anoR - Pseudomonas sp. B20
AhyR - Aeromonas hydrophila (P0A3J5)
AsaR - Aeromonas salmonicida (P0A3J6)
carR - Pseudomonas sp. B20
CarR - Pectobacterium carotovorum (Q46751)
YukR - Yersinia ruckeri (O87971)
esaR - Acinetobacter sp. DF3-8
EsaR - Pantoea stewartii (P54293)
YenR - Yersinia enterocolitica (P54295)
ExpR - Pectobacterium parmentieri (Q47189)
ExpR - Dickeya dadantii (Q47188)
EchR - Dickeya chrysanthemi (Q46967)
VanR - Pseudomonas sp. AF3-9
vanR - Pseudomonas sp. B20
VanR - V. anguillarum (P74946)
LuxR - V. fischeri (P12746)
LuxR - V. fischeri (P35327)
TraR - Sinorhizobium fredii (P55407)
luxN - Vibrio sp. E14
LuxN - V. campbellii (A7MRY4)
LuxN - V. harveyi (P0C5S6)
TraR - Rhizobium radiobacter (P33905)
TraR - Agrobacterium fabrum (P54294)
TraR|Agrobacterium_vitis(P33909)
RhiR - Rhizobium leguminosarum (Q03316)
BjaR - Bradyrhizobium diazoefficiens (Q89VI...
RpaR - Rhodopseudomonas palustris (Q6NCZ5)
SolR - Ralstonia solanacearum (P58590)
SolR - Ralstonia solanacearum (O30919)
PhzR - P. fluorescens (Q51786)
PhzR - P. chlororaphis (P54303)
RhlR - P. aeruginosa (P54292)
SdiaA - Escherichia coli (P07026)
anoR2 - Pseudomonas sp. AF3-9
AnoR - A. nosocomialis (A0A0N8YGA2)
y4qH - Sinorhizobium fredii (P55629)
LasR - P. aeruginosa (P25084)

C)

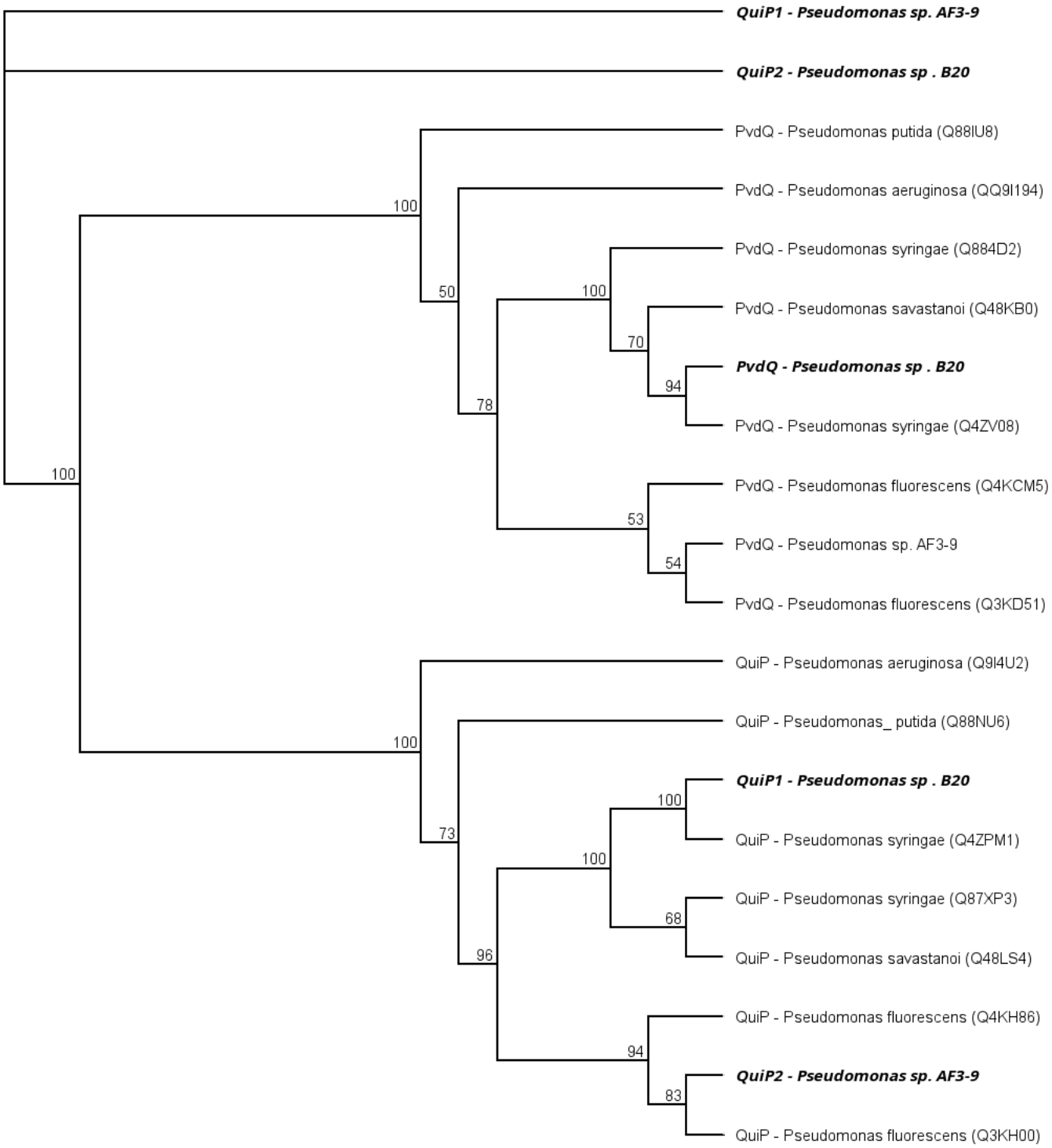

Figure S3: Phylogenetic tree of the AHL-synthases (**A**), AHL-receptors (**B**) and AHL-acylases (**C**) found in the draft genomes of the four sequenced strains. Branch labels indicated the bootstrap value.

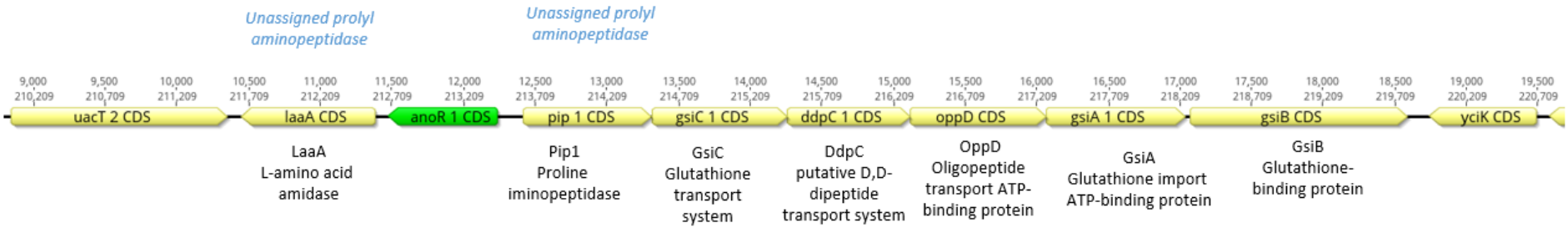

Figure S4: Predicted CDS located next to one of *Pseudomonas* sp. AF3-9 solo luxR (annotated anoR1). Prokka and MEROPS annotations are reported in black and blue, respectively.

Chapitre VI. *Le quorum sensing régule la production d'enzymes hydrolytiques et la composition de communautés bactériennes de la rade de Brest*

I. Introduction

Dans le chapitre précédant, nous avons démontré que la disruption de la communication basée sur les AHLs au sein de souches bactériennes isolées pouvait influencer la production d'enzymes hydrolytiques et la formation de biofilm, mettant en évidence l'implication du quorum sensing (QS) dans la régulation de ces phénotypes. Peut-on démontrer l'implication du QS dans la synthèse d'enzymes hydrolytiques de communautés bactériennes naturelles ? Et est-ce que cette communication peut influencer la composition de ces communautés ?

Pour tenter de répondre à ces questions, nous avons utilisé une approche en microcosme, consistant à ajouter cinq AHLs différentes à des communautés bactériennes prélevées dans la rade de Brest à deux moments distincts du développement printanier du phytoplancton. Dans chaque microcosme, six activités enzymatiques (aminopeptidases, phosphatases alcalines, β-glucosidases, *N*-acetyl glucosaminidases, β-glucuronidases, lipases) et la composition des communautés (metabarcoding du gène de l'ARNr 16S) ont été suivies pendant 48 h. Ces deux expériences ont mis en lumière un effet rapide des molécules du QS sur les activités enzymatiques, dès 6 h d'incubation. Cet effet s'est avéré extrêmement variable d'une expérience à l'autre, démontrant là aussi la complexité des régulations liées au QS. De plus, les deux expériences ont démontré que l'ajout d'AHLs entrainait une modification significative de la composition des communautés bactériennes. De manière intéressante, ces variations de composition des communautés sont corrélées avec les variations du niveau d'activité hydrolytique, suggérant que les changements du niveau d'activité induits par les AHLs peuvent générer des changements dans la composition des communautés bactériennes.

Ces travaux ont été publiés en 2021 dans le journal *Frontiers in microbiology* (section "*Aquatic microbiology*").

frontiers in Microbiology

ORIGINAL RESEARCH
published: 10 December 2021
doi: 10.3389/fmicb.2021.780759

Quorum Sensing Regulates the Hydrolytic Enzyme Production and Community Composition of Heterotrophic Bacteria in Coastal Waters

Marion Urvoy[1,2], Raphaël Lami[3], Catherine Dreanno[4], Daniel Delmas[1], Stéphane L'Helguen[2] and Claire Labry[1]**

[1] Ifremer, DYNECO, Plouzané, France, [2] Université de Bretagne Occidentale, CNRS, IRD, Ifremer, UMR 6539, Laboratoire des Sciences de l'Environnement Marin (LEMAR), Plouzané, France, [3] Sorbonne Université, CNRS, Laboratoire de Biodiversité et Biotechnologies Microbiennes (LBBM, USR 3579), Observatoire Océanologique de Banyuls, Banyuls-sur-Mer, France, [4] Ifremer, RDT, Plouzané, France

OPEN ACCESS

Edited by:
Catarina Magalhães, University of Porto, Portugal

Reviewed by:
Ashley Isaac, New York University Abu Dhabi, United Arab Emirates
Jin Zhou, Tsinghua University, China

***Correspondence:**
Marion Urvoy
marion.urvoy@outlook.fr
Claire Labry
Claire.Labry@ifremer.fr

Specialty section:
This article was submitted to Aquatic Microbiology, a section of the journal Frontiers in Microbiology

Received: *21 September 2021*
Accepted: *17 November 2021*
Published: *10 December 2021*

Citation:
Urvoy M, Lami R, Dreanno C, Delmas D, L'Helguen S and Labry C (2021) Quorum Sensing Regulates the Hydrolytic Enzyme Production and Community Composition of Heterotrophic Bacteria in Coastal Waters. Front. Microbiol. 12:780759. doi: 10.3389/fmicb.2021.780759

Heterotrophic microbial communities play a central role in biogeochemical cycles in the ocean by degrading organic matter through the synthesis of extracellular hydrolytic enzymes. Their hydrolysis rates result from the community's genomic potential and the differential expression of this genomic potential. Cell-cell communication pathways such as quorum sensing (QS) could impact both aspects and, consequently, structure marine ecosystem functioning. However, the role of QS communications in complex natural assemblages remains largely unknown. In this study, we investigated whether *N*-acylhomoserine lactones (AHLs), a type of QS signal, could regulate both hydrolytic activities and the bacterial community composition (BCC) of marine planktonic assemblages. To this extent, we carried out two microcosm experiments, adding five different AHLs to bacterial communities sampled in coastal waters (during early and peak bloom) and monitoring their impact on enzymatic activities and diversity over 48 h. Several specific enzymatic activities were impacted during both experiments, as early as 6 h after the AHL amendments. The BCC was also significantly impacted by the treatments after 48 h, and correlated with the expression of the hydrolytic activities, suggesting that changes in hydrolytic intensities may drive changes in BCC. Overall, our results suggest that QS communication could participate in structuring both the function and diversity of marine bacterial communities.

Keywords: hydrolytic enzymes, bacterial community composition, quorum sensing, *N*-acylhomoserine lactone, coastal waters

INTRODUCTION

Heterotrophic bacterial communities play a central role in carbon (C) and nutrient cycling in the oceans (Azam and Malfatti, 2007; Falkowski et al., 2008). They rely on the expression of a large diversity of dissolved and cell-bound extracellular enzymes to hydrolyze polymeric organic matter into smaller molecules that can be transported into the cells and metabolized (Payne, 1980;

Arnosti, 2011). Hydrolytic enzymes initiate the mineralization of organic matter, ultimately affecting key biogeochemical processes such as C export or nutrient cycling (Chróst, 1990; Azam and Malfatti, 2007). As such, it is essential to understand the mechanisms driving hydrolase expression in marine bacterial communities.

Hydrolytic activity levels result from a combination of genomic potential, determined by the bacterial community composition (BCC), and the differential expression of this genetic potential (Arnosti, 2011). Indeed, bacterial communities may possess different degradation pathways, depending on the presence of specific taxonomic groups (Zimmerman et al., 2013; Arnosti, 2014), resulting in different hydrolytic enzyme capacities (Arnosti, 2011). At the transcriptional level, several factors may drive enzyme synthesis, such as the composition and concentration of organic matter or the nutrient levels (Chróst, 1990; Arnosti, 2011). However, despite their broad biogeochemical implications, we still lack knowledge about the factors and mechanisms driving bacterial extracellular enzyme production (Arnosti, 2011, 2014) and BCC (Konopka et al., 2015) in marine environments, especially concerning the role of biotic interactions (Arnosti, 2014; Cosetta and Wolfe, 2019).

Quorum sensing (QS) is a bacterial signaling system allowing the synchronized expression of numerous genes among a bacterial population (Miller and Bassler, 2001; Waters and Bassler, 2005). QS communications are based on the production, diffusion, and sensing of diffusible molecules called autoinducers (AIs). When the AI concentration reaches a certain threshold, they bind their cognate receptors and initiate the transcriptional regulation of their target genes (Fuqua et al., 1994; Papenfort and Bassler, 2016), including genes involved in bioluminescence, motility, biofilm formation, virulence, or hydrolytic enzyme production (Miller and Bassler, 2001; Hmelo, 2017). Quorum quenching (QQ) encompasses mechanisms that either degrade AI molecules or impede their production or reception (Grandclément et al., 2015). In gram-negative bacteria, the most studied QS system is based on the expression of *N*-acylhomoserine lactones (AHLs), consisting of a homoserine lactone and a fatty acid side-chain (Papenfort and Bassler, 2016; Hmelo, 2017). AHL-based QS is widespread among marine bacteria: diverse QS genes have been found during metagenomic surveys (Doberva et al., 2015; Muras et al., 2018; Su et al., 2021), and AHLs have been detected in a few environments such as marine aggregates (Hmelo et al., 2011; Jatt et al., 2015), subtidal biofilms (Huang et al., 2009), or intertidal sediment (Stock et al., 2021). In addition, numerous strains isolated from marine environments produced AHLs during cultivation (Gram et al., 2002; Blanchet et al., 2017; Su et al., 2019; Urvoy et al., 2021).

However, the implication of QS expression on key biogeochemical functions is largely unknown and mostly stems from cultivation-dependent methods (Lami, 2019), which lack the inherent complexity of natural bacterial assemblages. QS expression could substantially impact functional phenotypes through direct transcriptional regulation of hydrolytic enzymes and through the modification of BCC. Indeed, QS regulation of hydrolytic enzymes at the transcriptional level has been demonstrated in several environmental strains (Jatt et al., 2015; Su et al., 2019; Urvoy et al., 2021). A limited number of studies have investigated the link between QS and hydrolytic activities in natural communities (Hmelo et al., 2011; Van Mooy et al., 2012; Krupke et al., 2016; Su et al., 2019). Hmelo et al. (2011) were the first to suggest that the expression of QS promoted the degradation of particulate organic matter, demonstrating that the addition of AHL to bacterial communities colonizing marine snow increased the activity of several hydrolases. This finding was later supported by Krupke et al. (2016) and Su et al. (2019), who performed similar experiments on marine snow, extending the impact of QS-regulation to other enzymatic activities and locations. Krupke et al. (2016) highlighted the complexity of those cell-cell mechanisms, as the responses varied depending on the sampling location, AHL concentration, and time scale. Additionally, Van Mooy et al. (2012) broadened those observations to the epibiont of *Trichodesmium* colonies, where QS seemed to regulate phosphorus acquisition through alkaline phosphatases regulation.

Even fewer studies have looked into the interplay between QS and BCC in marine communities so far. Huang et al. (2019) demonstrated that AHL-based QS disruption modified the composition of marine communities colonizing steel coupons. Whalen et al. (2019) showed that alkylquinolone signals, another type of AIs, contributed to the structuration of both free-living and particle-attached bacterial communities during a simulated coastal phytoplankton bloom. In other environments, Schwab et al. (2019) demonstrated that AHL signal disruption affected the BCC in both biofilm-forming and suspended soil bacterial communities. Studies performed on sludge (Gao et al., 2018; Lv et al., 2018; Ma et al., 2018) or a bio-membrane reactor (Jo et al., 2016) also pointed out that AHL amendment or AHL disruption modulated both BCC and bacterial metabolism rates. However, to the best of our knowledge, no studies have shown the direct influence of AHL-based QS on the BCC in the marine environment, and the ecological role of QS remains understudied.

In this study, we investigated the influence of QS on hydrolytic enzyme production and taxonomic diversity of marine heterotrophic prokaryotic communities. To this extent, two independent microcosm-based experiments were performed, where five different AHLs were separately amended to natural assemblages from the Bay of Brest (France). Both hydrolytic potential and BCC were monitored over 48 h. Altogether, our results suggest that QS is involved in the regulation of several hydrolytic enzymes and may influence the composition of marine bacterial communities.

MATERIALS AND METHODS

Chemical Reagents and *N*-Acylhomoserine Lactone Preparation

The AHLs used were purchased from Sigma-Aldrich (Darmstadt, Germany) or Cayman Chemical (Ann Arbor, MI, United States): *N*-butanoyl-DL-homoserine lactone (C4-HSL), *N*-hexanoyl-DL-homoserine lactone (C6-HSL), *N*-(3-Oxooctanoyl)-DL-homoserine lactone (3-oxo-C8-HSL),

N-dodecanoyl-DL-homoserine lactone (C12-HSL), *N*-tetra decanoyl-DL-homoserine lactone (C14-HSL), *N*-hexadecanoyl-DL-homoserine lactone (C16-HSL). All AHLs were dissolved in dimethyl sulfoxide (DMSO) at 50 μM, stored at −20°C, and thawed at the beginning of the experiment. All other chemicals were purchased from Sigma-Aldrich, Darmstadt, Germany (biochemical grade).

Effect of *N*-Acylhomoserine Lactone Amendment on Functional and Taxonomic Diversity

Two independent microcosm experiments were performed to assess the variability in response to AHL amendments. To this extent, seawater was sampled near the Service d'Observation en Milieu LITtoral (SOMLIT)[1] station of Sainte-Anne-du-Portzic (48°21′33.5″ N, 4°33′02.7″ W, Bay of Brest, France) on March 29 (10.7°C *in situ*, salinity 32.4) and May 3, 2021 (12.3°C, salinity 33.7), using acid-washed 10-L carboys (Nalgene). The two sampling dates correspond to two contrasting periods, namely the beginning (high nutrient, low chlorophyll *a* levels) and the peak (low nutrient, high chlorophyll *a* levels) of the annual phytoplankton spring growth (**Supplementary Figure 1**). Additional details concerning the bloom's characteristics are given in **Supplementary Figure 1**. The sampled seawater was immediately 10-μm-filtered (Merck, Ref NY1004700) to remove aggregates and larger eukaryotic cells, stored at *in situ* temperature, and processed within 1 h. The bacterial community is later referred to as planktonic because of the removal of bacteria attached to those aggregates.

To assess the effect of AHLs on hydrolytic enzymes and taxonomic diversity, 150 mL of the 10-μm filtered seawater was dispatched into T-175 flasks (Sarstedt cat. no. 83.3912), and five different AHLs (C4-, C6-, 3-oxo- C8-, C12-, and C16-HSL) were separately amended at a final concentration of 50 nM (0.1% v/v of DMSO final concentration). The different AHLs were chosen to cover a large spectrum of AHL side-chain lengths. The AHL concentration (50 nM) was chosen based on previous results (**Supplementary Figure 2**), aiming to maximize the enzymatic activity response and minimize the AHL concentration to limit their use as a nutritional source. In addition, a control condition was prepared with 0.1% (v/v) DMSO. The incubations were performed at *in situ* temperature in the dark, in triplicates (First experiment) or in quintuplicates (Second experiment). Samples for hydrolytic enzyme activities and bacterial abundance were collected in sterile tubes (Falcon, Ref 352070) at 0 (on initial water before dispatching), 6, 24, and 48 h. The initial BCC was determined in triplicate by filtering 200 mL of 10-μm filtered seawater (before dispatching) through 0.2-μm filters (Whatman Nuclepore PC membrane). The final diversity was sampled by filtering the leftover seawater in each microcosm (approximately 100 mL) through 0.2-μm filters. The experimental design is schematized in **Figure 1**.

[1]http://somlit.fr

Bacterial and Phytoplankton Abundance Measurement

Bacterial and phytoplankton abundances were quantified according to standard flow cytometry protocols (Marie et al., 1999). Bacterial samples were fixed with 0.25% glutaraldehyde and 0.01% Poloxamer 188 for 10 min at ambient temperature in the dark. Samples were then flash-frozen in liquid nitrogen and stored at −80°C until flow cytometry analysis. Samples were thawed, appropriately diluted in 0.2-μm-filtered autoclaved seawater, and labeled with SYBR Green I (1:10,000 dilution of stock solution) for 10 min at ambient temperature in the dark. The acquisition was performed on a Novocyte Advanteon Cytometer with a threshold on FITC, recording less than 1,000 events per second. Bacteria were discriminated using the green and orange fluorescence of SYBR Green I and forward and side scatter criteria. For each microcosm, abundance was averaged over triplicated samples.

In addition, the initial phytoplankton cell counts were measured using the same samples, at the initial time (10-μm filtered seawater before dispatching) and in the DMSO-treated microcosms at the final time (48 h). To this extent, the cytometry acquisition was performed using 250 μL of undiluted, unlabeled samples. The picophytoplankton, nanophytoplankton, cryptophytes and cyanobacteria cells were discriminated using the orange and red fluorescence. This measurement suggested that phytoplankton cells were correctly removed from the microcosms (**Supplementary Figure 3**).

Hydrolytic Enzyme Assay

Several hydrolytic enzymes involved in different biogeochemical cycles were assayed: β-glucosidases (β-glc), β-glucuronidases (β-glucu), and *N*-acetyl-glucosaminidases (N-ac) degrade polysaccharides (C and N cycles), lipases (Lip) degrade lipids (C cycle), leucine aminopeptidases (LAM) degrade peptides (N and C cycles), and alkaline phosphatases (AP) are used to acquire phosphorus (P). Activities were determined using model fluorogenic substrates which release either 7-amido-4-methylcoumarin (MCA) or 4-Methylumbelliferone (MUF) upon hydrolysis. Those substrates were, respectively: 4-Methylumbelliferyl-β-D-glucopyranoside (MUF-β-glc), 4-Methylumbelliferyl-β-D-glucuronide (MUF-β-glucu), 4-Methylumbelliferyl N-acetyl-β-D-glucosaminide (MUF-N-Ac), 4-Methylumbelliferyl butyrate (MUF-but), L-Leucine-7-amido-4-methylcoumarin (LLMCA), and 4-Methylumbelliferyl phosphate (MUF-P). Substrates and standards for enzymatic assays were dissolved in 2-methoxyethanol using sonication if necessary, and stored at −20°C.

Total potential activities were assayed, which include dissolved and cell-bound enzymes. To this extent, 80 μL of sample was dispatched in a 384-well low-binding black microplate (Greiner Item no. 781900) and amended with 20 μL of Tris buffer (10 mM, pH 8.2) containing the fluorogenic substrate at saturating concentration. Saturating concentrations were previously determined as follows: 150 μM MUF-β-glc, 250 μM MUF-β-glucu, 250 μM MUF-N-ac, 800 μM MUF-but, 1,000 μM LLMCA, and 250 μM MUF-P (data not shown). Tris buffer was

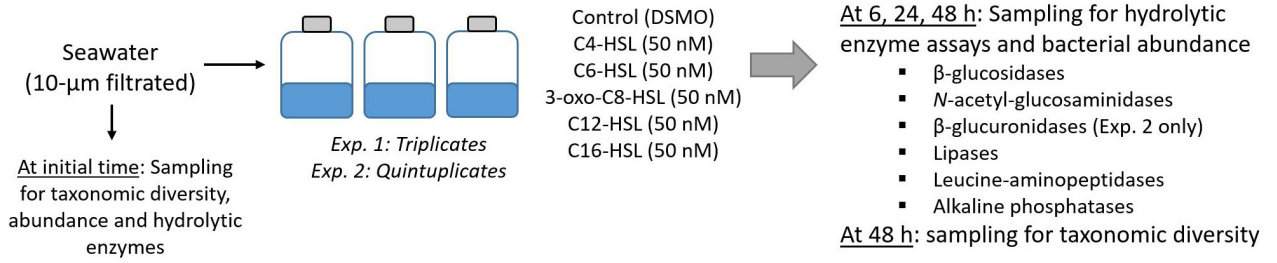

FIGURE 1 | Design of the study. Seawater was sampled on two separated occasions (early and peak bloom) and 10-µm-filtrated to remove aggregates and larger eukaryotes. The seawater was then dispatched, and 50 nM of AHLs or DMSO were amended. The hydrolytic enzyme activities were assayed at 0, 6, 24, and 48 h. Initial and final diversity were assessed using partial 16S rDNA gene metabarcoding. Exp., experiment.

used to avoid bias induced by pH changes over time as MUF and MCA fluorescence yields are highly pH-dependent. Additionally, a control for substrate abiotic degradation was prepared with 80 µL of Tris buffer instead of seawater sample. Given the number of samples in the Second experiment, the activities were measured in two separate microplates: LAM, AP, and Lip were measured first, followed by β-glc, β-glucu, and N-ac. To avoid any bias, fresh samples were collected in new tubes before the second incubation.

Fluorescence was monitored every 11 min for 3–4 h using a Spark Tecan Infinite M200PRO with excitation/emission wavelengths of 364/460 nm for MUF and 380/440 nm for MCA. Activities were then determined as the slope of the linear part of the curve (AU min^{-1}). Blanks corresponding to abiotic degradation were subtracted from the samples. Only MUF-but presented a substantial abiotic degradation. Fluorescence units were converted into substrate equivalents using a standard curve of MCA and MUF dissolved in 20 µL of Tris buffer and 80 µL of 0.2-µm-filtered and autoclaved seawater. Enzymatic activities were determined as the average of technical duplicates (First experiment) or quadruplicates (Second experiment). Specific activities were obtained by normalizing activities with bacterial abundance and expressed as $amol_{MUF\ or\ MCA}\ h^{-1}\ 10^6\ cells^{-1}$.

Bacterial Taxonomic Diversity

The BCC was determined by metabarcoding of the V3/V4 region of the 16S rRNA gene. Filters dedicated to bacterial diversity were immediately flash-frozen in liquid nitrogen and stored at −80°C until processing. Blank dry filters were sampled simultaneously and used as a contamination control. The two experiments were processed simultaneously. Filters were cut into pieces and DNA was extracted using the NucleoSpin Plant II Mini Kit (Macherey Nagel Ref. 740770.50) according to the manufacturer's instructions, with an additional lysis step performed for 2 h at 56°C with 25 µL of proteinase K (20 mg mL^{-1}, Macherey Nagel Ref. 740506) and 100 µL of lysozyme (20 mg mL^{-1}, Sigma ref 4403-5g). Libraries were prepared and sequenced by Génome Québec using the 341F/785R primers (Klindworth et al., 2013). Samples were sequenced on an Illumina MySeq using 2 × 300 pb and V3 chemistry. Data were processed using the SAMBA pipeline (v3.0.1)[2] developed by the IFREMER bioinformatics team (SeBiMER). This resulted in 2,120 amplicon sequence variants (ASVs), which were then clustered using dbOTU3 (Olesen et al., 2017), resulting in 1,502 ASVs (29% clustering) that were assigned against the Silva v138 database (Quast et al., 2013).

Statistical Analysis

All data were analyzed in R (v4.0.3, 2020-10-10) and displayed using ggplot2 (v3.3.2). Plots representing abundance and specific enzymatic activity display biological replicates as dots and means and standards errors as crossbars. Statistical comparison of the specific enzymatic activity in the different treatments was performed using the *t*-test (function *compare_means*, ggpubr package v0.4.0) with the Benjamini-Hochberg correction for *p*-values (p_{BH}). Results were plotted using compact letter display as implemented in the rcompanion package (v2.3.26), applying a significance threshold of 0.1.

Metabarcoding data were analyzed in R using the Phyloseq (v1.32.0) and Vegan (v2.5.7) packages. The ASVs corresponding to eukaryotes, mitochondria, and chloroplasts were removed (6.4% of reads). The barplots representing the relative abundances of the ASVs were plotted based on the raw count table transformed to relative abundance. The rarefaction curves (**Supplementary Figure 4**) were visualized using the *ggrare* function from the ranacapa package (v0.1.0). Data were then rarefied to the minimum sampling depth (32,196 sequences per samples) (*rarefy_even_depth* function, rngseed = 999). Principal Coordinates Analysis (PCoA) was performed on the rarefied table, based on the Bray-Curtis dissimilarity. Permutational multivariate analysis of variance (PERMANOVA) was done on the rarefied table using the *adonis* function (999 permutations) based on the Bray-Curtis dissimilarity, using the treatment as a grouping variable (DMSO, C4-, C6-, 3-oxo- C8-, C12-, and C16-HSL). Homogeneity of variance was checked using the *betadisper* function. Analysis of similarities (ANOSIM) was performed on the rarefied table using the *anosim* function (999 permutations) based on Bray-Curtis dissimilarity, using the same groups. The DESeq2 package (v1.28.1) was used on the raw count table to detect ASVs that were differentially abundant between the AHL treatments (C4-, C6-, 3-oxo- C8-, C12-, and C16-HSL) and the DMSO control in each experiment. Low-prevalence ASVs (five reads or less across one experiment) were removed

[2]https://github.com/ifremer-bioinformatics/samba

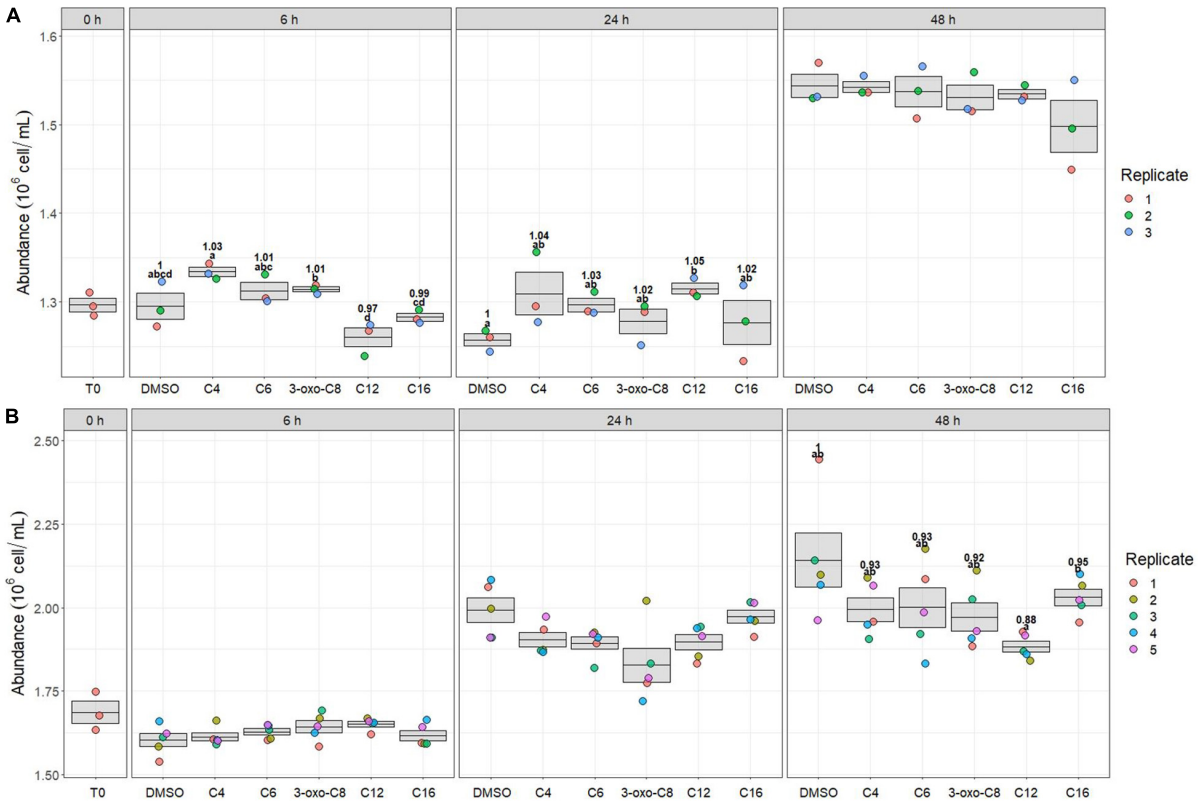

FIGURE 2 | Bacterial abundances at 0, 6, 24, and 48 h for the first **(A)** and second **(B)** experiment, corresponding to early and peak bloom conditions, respectively. Significance of the mean abundance comparison between treatments is indicated using compact letter display (*t*-test, $p_{BH} < 0.1$). Ratio of the mean abundance compared to DMSO treatment is annotated for each time with significantly different results.

beforehand. The cut-offs used to consider the DESeq2 results significant were as follows: $p_{BH} < 0.05$ and log2 fold change (log2FC) > 0.5 or < -0.5.

The association between the specific enzymatic activities and the BCC at the end of the incubation was assessed using a symmetric Procrustes analysis. This analysis aimed to test if the distance matrix of the community shows superposition with the distance matrix of the activities. To this extent, the rarefied community matrix was Hellinger-transformed (function *decostand*) and ordinated using a Principal Components Analysis (PCA, as implemented in the *rda* function in the Vegan package). The specific activities (at 48 h) were scaled to unit variance and ordinated using a PCA (*rda* function). Symmetric Procrustes analysis was performed on the two resulting ordinations (function *procrustes* in the Vegan package) and its significance was assessed (function *protest* in the Vegan package) using 999 permutations.

RESULTS

Effect of *N*-Acylhomoserine Lactone Amendment on Bacterial Abundance

During the First experiment (early bloom), bacterial growth was slow and mainly occurred between 24 and 48 h (**Figure 2A**). Mean bacterial abundance increased from 1.30 to 1.53 $\times$ 10^6 cells mL^{-1} (+18%) between 0 and 48 h. Overall, bacterial growth was not significantly different between the DMSO and the AHL-treated microcosms, except at 24 h, where the abundance was increased in the C12-HSL microcosms (+5%, $p_{BH} = 0.06$). Significant differences were also observed between the AHL-treated microcosms at 6 h, as the C4-HSL-treated microcosms contained more bacteria than the microcosms treated with 3-oxo-C8-, C12-, and C16-HSL (largest increase of +6% between C4- and C12-HSL, $p_{BH} = 0.05$).

During the Second experiment (peak bloom), bacterial growth was also slow and started between 6 and 24 h (**Figure 2B**). Mean bacterial abundance increased from 1.69 to 2.00 $\times$ 10^6 cells mL^{-1} (+18%) between 0 and 48 h. Bacterial growth was not significantly different between the DMSO control and the AHL-treated microcosms, although bacteria were significantly less abundant in the C12-HSL-treated microcosms than in the C16-HSL-treated microcosms at 48 h (−7%, $p_{BH} = 0.02$).

Effect of *N*-Acylhomoserine Lactone Amendment on Hydrolytic Enzyme Activities

During the First experiment (early bloom), AHL amendment affected specific LAM, N-ac, and Lip activities (**Figure 3**). Although no AHL-treated microcosms were significantly different from the control condition, specific LAM activities were affected by the treatment at 48 h: LAM activities in the

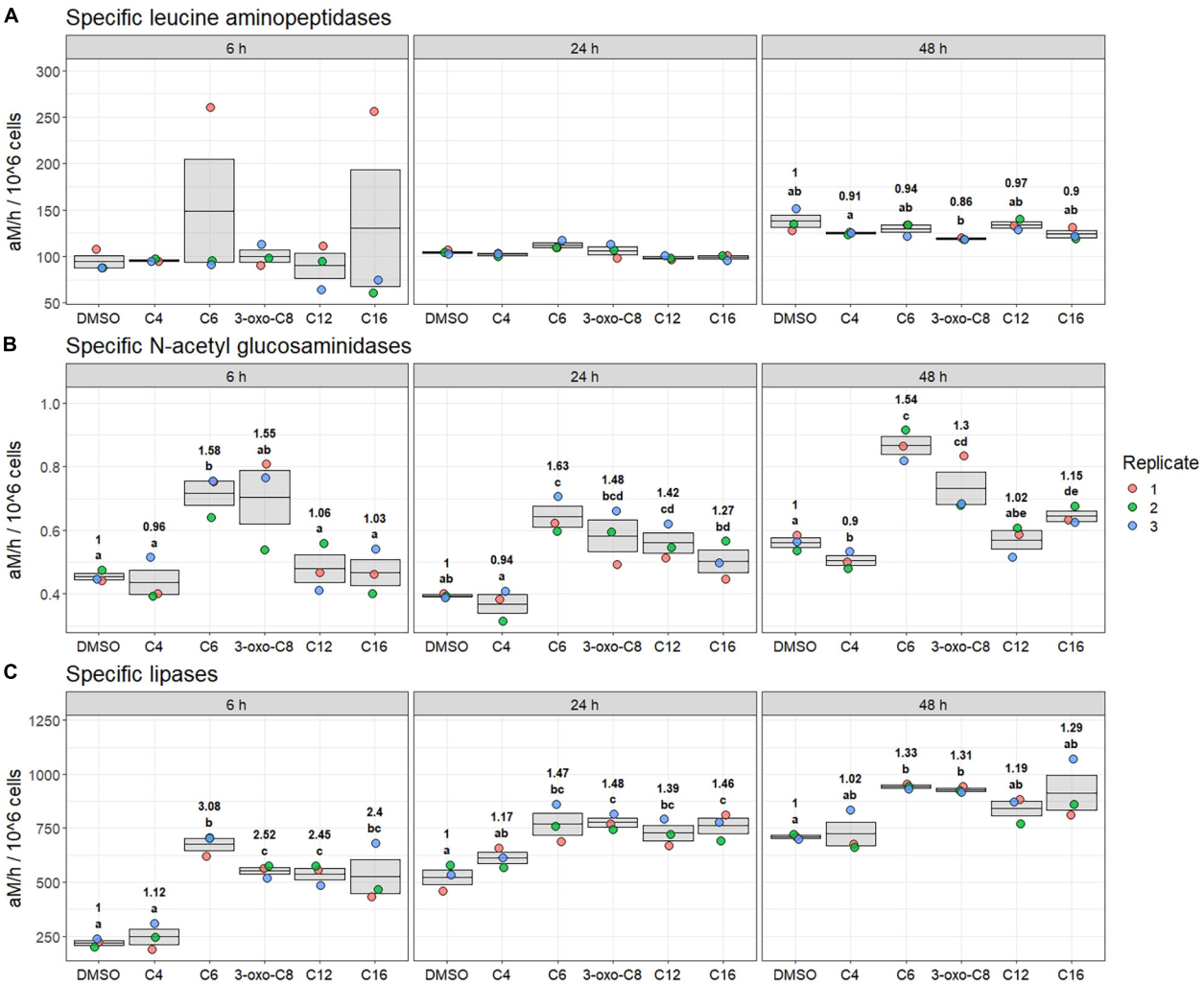

FIGURE 3 | Specific leucine-aminopeptidase **(A)**, N-acetyl-glucosaminidases **(B)**, and lipase **(C)** activities at 6, 24, and 48 h during the first experiment (early bloom). Significance of the mean specific activity comparison between treatments is indicated using compact letter display (*t*-test, $p_{BH} < 0.1$). Ratio of the mean specific activity compared to DMSO treatment is annotated for each time with significantly different results.

3-oxo-C8-HSL-treated microcosm were significantly reduced compared with those in the C4-HSL-treated microcosm (−5%, $p_{BH} = 0.10$, **Figure 3A**).

The AHL effect on specific N-ac activity was visible at all sampling times (**Figure 3B**). Overall, the microcosms containing the C6-HSL were the most affected ones: the treatment induced an average +58% increase in activity compared with DMSO treatment across all sampling times ($p_{BH} < 0.08$). The microcosms containing 3-oxo-C8-HSL followed a similar pattern, although the induction was only significant at 48 h (+30%, $p_{BH} = 0.10$). The AHLs with longer side-chains (C12- and C16-HSL) also increased the specific N-ac activity, albeit to a lesser extent: C12-HSL significantly induced the activity at 24 h (+42%, $p_{BH} = 0.09$), whereas C16-HSL significantly induced the activity at 48 h (+15%, $p_{BH} = 0.05$). On the contrary, C4-HSL-amended microcosms exhibited a decrease in activity at 48 h (−10% compared with the DMSO control, $p_{BH} = 0.10$).

The AHL amendment also affected specific Lip activities at all sampling times (**Figure 3C**). At 6 and 24 h, Lip activities were induced in all AHL-containing microcosms compared with the DMSO treatment, except for the C4-HSL treatment which did not differ from the control. At 6 h, C6-HSL had the most effect (+208%, $p_{BH} = 0.01$). The 3-oxo- C8-, C12-, and C16-HSL had a similar effect at this sampling time, with an average +146% increase in specific activity ($p_{BH} < 0.08$). For those four AHLs (C6-, 3-oxo- C8-, C12-, and C16-HSL), the treatment effect then lessened with time: at 24 h, the activity was significantly increased by an average of +39% ($p_{BH} < 0.06$). At 48 h, the induction was only significant for the C6- and 3-oxo-C8-HSL (+33 and +31%, respectively, $p_{BH} < 0.001$).

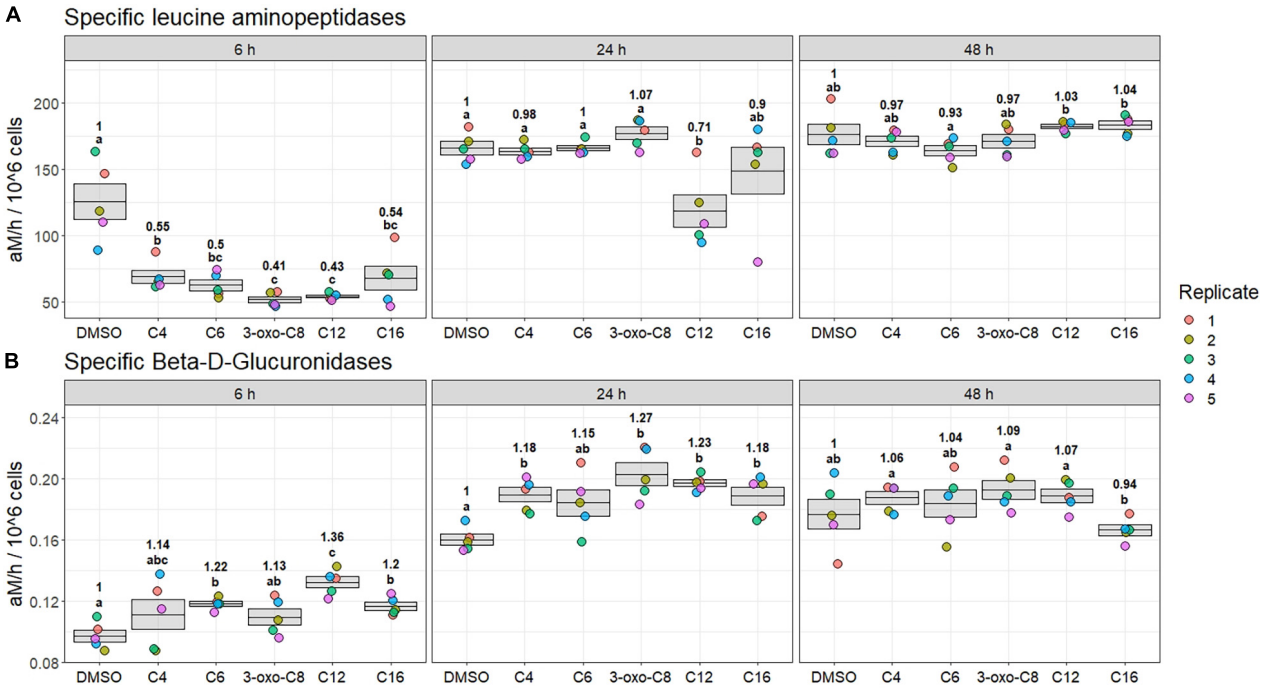

FIGURE 4 | Specific leucine-aminopeptidase **(A)** and β-glucuronidase **(B)** activities at 6, 24, and 48 h during the second experiment (peak bloom). Significance of the mean specific activity comparison between treatments is indicated using compact letter display (*t*-test, $p_{BH} < 0.1$). Ratio of the mean specific activity compared to DMSO treatment is annotated for each time with significantly different results.

Finally, no significant effect of AHL amendment was observed on β-glc, AP were too low to be detected, and β-glucu were not measured during the First experiment (data not shown).

During the Second experiment (peak bloom), there was an effect of AHL addition on specific LAM and β-glucu activities (**Figure 4**). At 6 h, all AHL amendments had led to a reduction of LAM activity, with a decrease ranging from −45 to −59% (p_{BH} = 0.03, **Figure 4A**). Those effects were especially pronounced for 3-oxo-C8- and C12-HSL amendments (−59 and −57%, respectively, p_{BH} = 0.03). The AHL impact then lessened over time: at 24 h, all microcosms had reverted to the control level, except for C12-HSL-amended microcosms (−29%, p_{BH} = 0.07). At 48 h, no microcosm was significantly different from the control, although in C12- and C16-HSL microcosms, activity levels were significantly higher than in C6-HSL microcosms (+11% on average, p_{BH} = 0.05).

Significant effects were also observed on specific β-glucu activity (**Figure 4B**). At 6 h, β-glucu activity in the C6-, C12-, and C16-HSL-amended microcosms was significantly induced compared with the control condition (+14 to +36%, $p_{BH} < 0.02$), with the most pronounced effect resulting from C12-HSL treatment (+36%, p_{BH} = 0.003). At 24 h, there was a +18 to +27% activity increase in the C4-, 3-oxo-C8, C12-, and C16-HSL-amended microcosms compared with the control ($p_{BH} < 0.01$). The activity in the C6-HSL-amended communities also seemed induced, although not significantly. At 48 h, all microcosms were similar to the control condition, but the activity in the C16-HSL microcosms was significantly lower than in the C4-, 3-oxo- C8-, and C12-HSL-treated microcosms ($p_{BH} < 0.04$).

In addition, no significant effect was observed on β-glc, AP, and N-ac (data not shown). Finally, the Lip measurements were discarded as the abiotic blank had a similar activity level than the samples, resulting in negative values. In any case, AHL-amendment had a limited effect on this activity: none of the AHL-treated microcosms differed from the DMSO control, although C12- and C16-HSL were significantly higher than C4-, C6-, and 3-oxo-C8-HSL at 24 h ($p_{BH} < 0.08$, data not shown).

Effect of *N*-Acylhomoserine Lactone Amendment on Taxonomic Diversity

The effect of the AHL treatment on the BCC at the end of the First experiment (early bloom) was visualized using PCoA (**Figure 5A**), explaining 68% of the variability. This analysis separated the AHL-treated communities from the DMSO control communities. The C6-HSL-treated communities were the furthest from the control communities, followed by the 3-oxo-C8- and C12-HSL-treated communities. The PERMANOVA and ANOSIM tests both supported a significant effect of the AHL-treatment (PERMANOVA: $p = 0.002$, $R^2 = 0.52$, F-statistic = 2.60; ANOSIM: p = 0.001, R-statistic = 0.45), although both F- and R-statistics suggested a limited size-effect. The test for the homogeneity of variance did not show a significant difference in variance among the treatments (p = 0.46), supporting the PERMANOVA results.

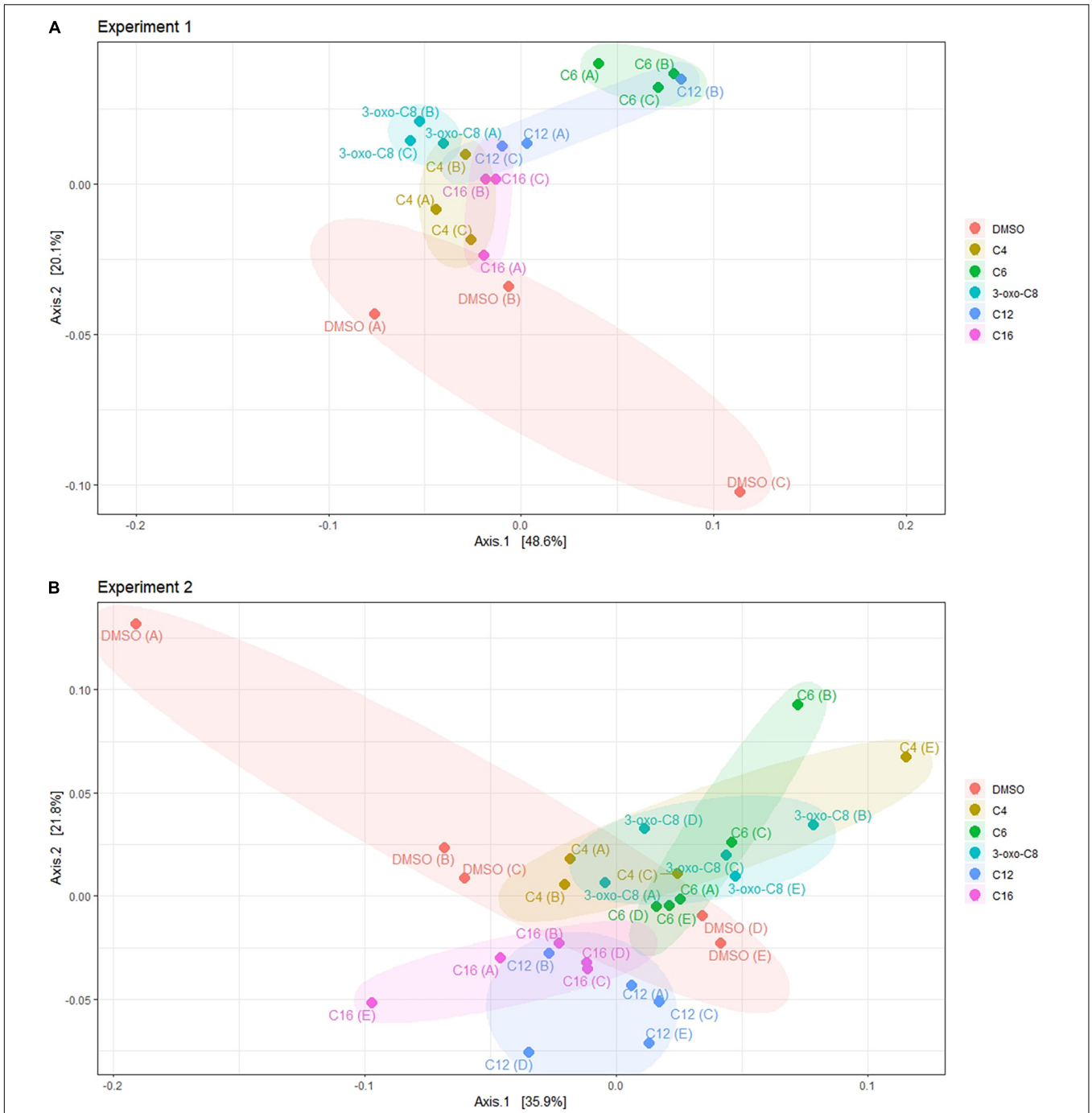

FIGURE 5 | PCoA ordination based on the Bray-Curtis dissimilarity, at the end of the incubation for the First **(A)** and Second **(B)** experiment, corresponding to early and peak bloom conditions, respectively. Ellipses were drawn to facilitate visualization but do not hold a statistical meaning.

Differential abundance analysis for the First experiment highlighted 29 ASVs (out of 497 ASVs, i.e., 5.8%) that were significantly different in at least one AHL treatment compared to the DMSO control (**Figure 6A**). Coherently with the PCoA, C6-HSL treatment had the most effect on the BCC with 21 impacted ASVs, including 9 ASVs affiliated with Bacteroidia (all belonging to the Flavobacteriales order), 9 affiliated with Gammaproteobacteria (3 Alteromonadales, 2 Vibrionales, 2 Oceanospirillales, 1 Cellvibrionales, and 1 Thiomicrospirales), 2 affiliated with Alphaproteobacteria (2 Rhodobacterales), and 1 affiliated with Campylobacteria (Campylobacterales). Exposure to C6-HSL increased the relative abundance of Rhodobacterales, Oceanospirillales, Vibrionales, and Campylobacterales but decreased those of Thiomicrospirales (Gammaproteobacteria)

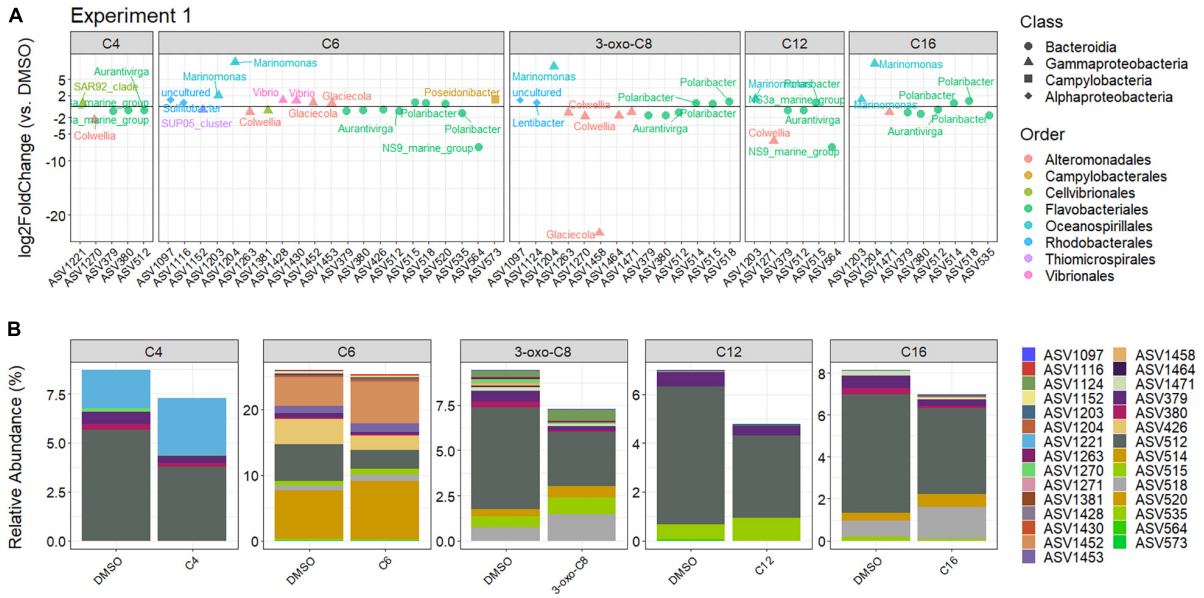

FIGURE 6 | (A) Log2 fold change of the differentially abundant ASVs for each AHL-treatment compared to the DMSO control during the First experiment, corresponding to the beginning of the bloom (cut-off p_{BH} = 0.05, cut-off log2FC = 0.5 or –0.5). **(B)** Relative abundances of the differentially abundant ASVs for each treatment compared to the DMSO control during the First experiment.

and Cellvibrionales. The effect on Flavobacteriales and Alteromonadales was more contrasted with both increase and decrease in relative abundances. The 3-oxo-C8-HSL was the second-most potent AHL, affecting 14 ASVs (6 Bacteroidia, 2 Alphaproteobacteria, and 6 Gammaproteobacteria). The 3-oxo-C8-HSL increased the abundance of the Rhodobacterales, Oceanospirillales, and three Flavobacteriales (*Polaribacter* and *Aurantivirga* ASVs) but decreased the relative abundance of Alteromonadales and two Flavobacteriales (*NS3a marine group*). The C4-, C12-, and C16-HSL treatment affected five ASVs (3 Bacteroidia and 2 Gammaproteobacteria), six ASVs (4 Bacteroidia and 2 Gammaproteobacteria), and nine ASVs (6 Bacteroidia and 3 Gammaproteobacteria), respectively, with both increase and decrease in relative abundances. Interestingly, 14 of those 29 differentially abundant ASVs were affected by at least two AHLs (ASVs 379, 380, 512, 514, 515, 518, 535, 564, 1,097, 1,203, 1,204, 1,263, 1,270, and 1,471, **Supplementary Figure 5**, top), mostly belonging to the Flavobacteriales order. Among them, ASVs 379 and 512, two abundant Flavobacteriales (**Figure 6B** and **Supplementary Table 1**), were affected by all AHLs with a similar impact (respective mean log2FC of −1.00 and −0.73).

Although few ASVs were differentially abundant across the AHL treatments (29 out of 497 ASVs), 13 (45%) of them (ASV 379, 380, 426, 512, 514, 515, 518, 520, 1,124, 1,152, 1,221, 1,452, and 1,453) were in the 50 most abundant ASVs present in the DMSO control at the end of the incubation (**Figure 6B** and **Supplementary Table 1**), representing 27.7% of the control community.

At the end of Second experiment (peak bloom), PCoA (**Figure 5B**, 55% of variance explained) indicated a separation between the communities amended with short-chain AHLs (C4-, C6-, and 3-oxo-C8-HSL) and those amended with long-chain AHLs (C12- and C16-HSL). Similar to the First experiment, the PERMANOVA and ANOSIM results both supported a significant effect of the treatment, with a small size-effect (PERMANOVA: p = 0.001, R^2 = 0.35, F-statistic = 2.60; ANOSIM: p = 0.001, R-statistic = 0.29) and the test for homogeneity of variance did not show a significant difference in variance (p = 0.36).

Differential abundance analysis highlighted a total of 22 ASVs (out of 450 ASVs i.e., 4.9%) that were significantly different in at least one AHL treatment (**Figure 7A**) at the end of the Second experiment. Coherently with the PCoA results, the effect of the AHL treatment on the differential abundance of ASVs seemed to differ according to the side-chain length of the AHL (**Figures 7A,B**). The C4-, C6-, and 3-oxo-8-HSL affected four ASVs (2 Bacteroidia and 2 Gammaproteobacteria), five ASVs (3 Bacteroidia and 2 Gammaproteobacteria), and three ASVs (3 Bacteroidia), respectively. The ASV 379 and 512 (2 Flavobacteriales) were commonly affected by the three AHLs, which induced similar effects (**Figure 7** and **Supplementary Figure 5**). Interestingly, those three AHLs reduced the relative abundances of the Flavobacterial-affiliated ASVs (log2FC between −2.77 and −0.50) but increased the relative abundance of the *Pseudoalteromonas*-affiliated ASVs (log2FC > 19). The C12-HSL treatment had the most impact, with 14 affected ASVs, 6 being affiliated with Bacteroidia (all Flavobacteriales, including the ASV 379 and 512, also affected by the shorter-chain AHLs) and 8 with Gammaproteobacteria (3 Cellvibrionales, 2 Alteromonadales, 2 Oceanospirillales, and 1 KI89A clade). The C12-HSL reduced the relative abundances of all Flavobacterial–affiliated ASVs. The effect on Gammaproteobacteria was more contrasted, with

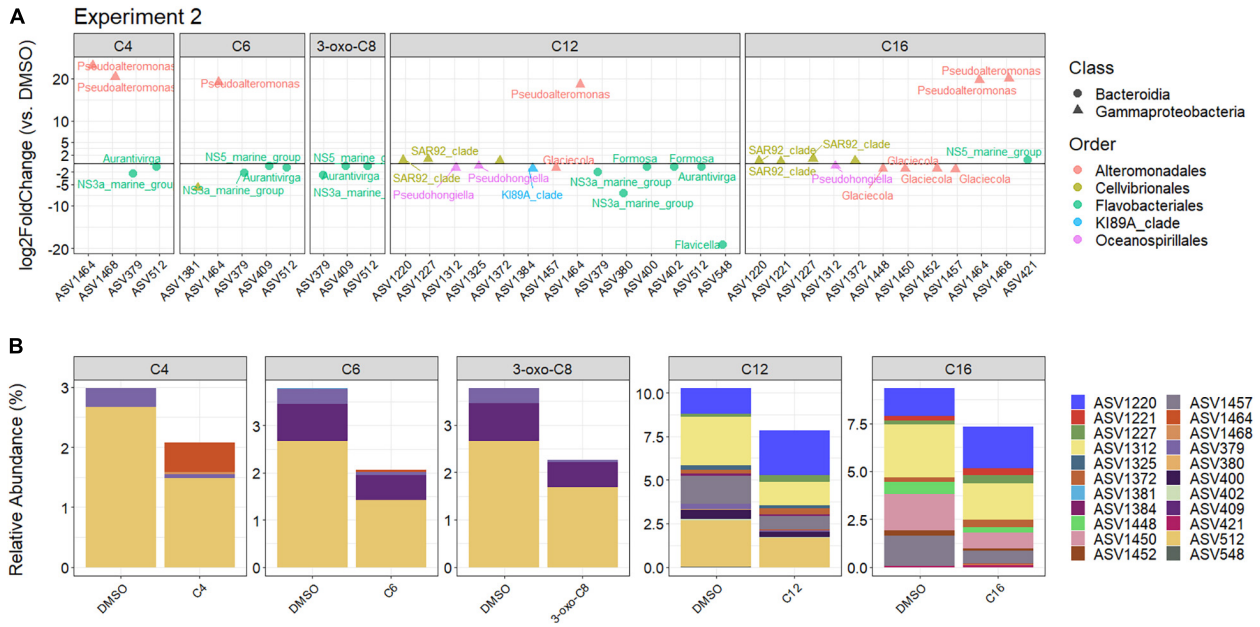

FIGURE 7 | (A) Log2 fold change of the differentially abundant ASVs for each AHL-treatment compared to the DMSO control during the Second experiment, corresponding to the peak of the bloom (cut-off p_{BH} = 0.05, cut-off log2FC = 0.5 or –0.5). **(B)** Relative abundances of the differentially abundant ASVs for each treatment compared to the DMSO control during the Second experiment.

a relative increase in Cellvibrionales and *Pseudoalteromonas* (Alteromonadales) but a decrease in Oceanospirillales, KI89A clade and *Glaciecola* (Alteromonadales). The C16-HSL affected 1 Bacteroidia (Flavobacteriales) and 11 Gammaproteobacteria ASVs (6 Alteromonadales, 4 Cellvibrionales, and 1 Oceanospirillales), with six ASVs being in common with the C12-HSL treatment. The C16-HSL effect was similar to the C12-HSL since it increased the relative abundances of Cellvibrionales and *Pseudoalteromonas* but decreased those of Oceanospirillales and *Glaciecola*. Interestingly, 10 of those 22 differentially abundant ASVs were affected by at least two AHLs (ASVs 379, 409, 512, 1,220, 1,227, 1,312, 1,372, 1,457, 1,464, and 1,468, **Supplementary Figure 5**, bottom). The ASVs 379 and 512 (Flavobacteriales), the most abundant ones, were affected by all molecules except C16-HSL, and the four AHLs induced a similar response (mean log2FC = −0.70 and –2.60, respectively).

Similar to the First experiment, only a few ASVs were differentially abundant with the AHL treatment (22 out of 450 ASVs), but 12 of them (54%) (ASV 379, 400, 409, 512, 1,220, 1,221, 1,312, 1,325, 1,448, 1,450, 1,452, and 1,457) belonged to the 50 most abundant ASVs present in the DMSO control at the end of the incubation (**Supplementary Table 1**), representing 13.4% of the control community.

Associations Between Specific Enzymatic Activities and Diversity

For both experiments, Procrustes analysis revealed significant associations between the specific enzymatic activities assayed at 48 h and the final diversity (First experiment: m^2 = 0.54, r = 0.68, p = 0.001; Second experiment: m^2 = 0.59, r = 0.64, p = 0.001) (**Supplementary Figure 6**).

DISCUSSION

Marine microorganisms, especially heterotrophic prokaryotes, play a major role in marine biogeochemical cycles by consuming and recycling organic matter and nutrients. Their recycling capacities depend, among others, on the community composition and the differential expression of this genomic potential, which could be impacted by cell-cell communication systems such as AHL-based QS. Our current knowledge of QS mechanisms mostly stems from isolated bacteria cultivated *in vitro*, which established the basic molecular foundation of QS communication (Lami, 2019). However, natural bacterial communities consist of complex assemblages facing fluctuating environmental conditions. As such, it is crucial to understand the role of QS communications in these communities (Hmelo, 2017; Mukherjee and Bassler, 2019). A few studies have examined the impact of AHL amendment on hydrolytic enzyme activities from marine snow-attached bacteria (Hmelo et al., 2011; Van Mooy et al., 2012; Jatt et al., 2015; Krupke et al., 2016; Su et al., 2019). However, to the best of our knowledge, none were conducted on planktonic bacterial communities. In addition, the effect of AHL amendments on the composition of marine bacterial assemblages is currently unknown. To bridge this gap, this study examined the variability in the effect of AHL amendments on several hydrolases and the BCC of planktonic bacterial communities sampled in coastal waters (Bay of Brest, France).

N-Acylhomoserine Lactones as a Nutritional Source

As first suggested by Hmelo et al. (2011), the impact of the AHL amendments could result from their use as a C and/or N source, instead of a QS-based regulation. However, similar to previous studies (Hmelo et al., 2011; Krupke et al., 2016), we discarded this hypothesis for several reasons. First, the microcosms were amended with 50 nM of AHL, equaling between 0.4 and 1 μM of C (depending on the AHL side-chain length), which is well beneath the usual dissolved organic C concentration in the studied waters (around 70 μM at this time of the year) (Dulaquais et al., 2018). Furthermore, the amendments did not affect the bacterial abundance compared to the control condition, suggesting that AHLs are not an additional nutritional source. In addition, different AHLs elicited both increase and decrease in specific hydrolytic activities and acted on a limited number of activities (which differed between each experiment). Those two points suggest a specific regulation of particular phenotypes as opposed to a global increase in bacterial metabolism. Finally, in the preliminary studies used to determine the AHL concentration (**Supplementary Figure 2**), the impact of AHL seemed to lessen with increased molecule concentration, which is counterintuitive with their use as a nutritional source. As such, it is likely that the observed changes in specific activities and BCC do not result from the use of AHL as C and/or N source.

Quorum Sensing Modulates the Hydrolytic Activity of Marine Bacterial Communities

To investigate the involvement of QS in hydrolases production, we monitored several enzymatic activities involved in the degradation of different types of molecules (polysaccharides, peptides, and lipids) and elements (C, N, and P) throughout the microcosm duration: β-glc, N-ac, and β-glucu activities are related to polysaccharides cycling; Lip and LAM activities, respectively, degrade lipids and peptides while AP activities are involved in P cycling. Overall, our results highlighted the involvement of QS in hydrolytic enzyme regulation among natural marine bacterial communities. During the First experiment (early bloom), AHL addition mostly increased the specific N-ac and Lip activities, with C6-HSL being the most potent AHL. In contrast, at the beginning of the Second experiment (peak bloom), the specific LAM activity decreased and the specific β-glucu activities increased with all added AHLs, especially C12- and 3-oxo-C8-HSL. Enzymatic activities were most largely impacted after 6 h of incubation, suggesting that their synthesis was driven by a transcriptional QS-based mechanism. Indeed, a modification of activities driven by changes in BCC is more likely to occur over a longer timescale (>24 h).

Within the same experiment, the different AHLs mostly induced similar responses, which is in contrast with the results reported by Krupke et al. (2016), where two AHLs rarely elicited the same response. However, the effect of AHL was highly variable from the First to Second experiment: none of the tested activities responded similarly between the two experiments. This variability in the response to AHL amendment is not surprising given the complexity of the mechanisms at play. The response of the bacterial community to AHL amendment may depend, for instance, on the initial BCC (presence/absence of QS and QQ genes), which differed between the two experiments (**Supplementary Figures 7**, **8**). Different AHL degradation capacities, mediated for instance by AHL-lactonases or AHL-acylases, could especially influence the fate of the amended AHLs. In addition, global gene regulation results from the assimilation of different signals (Nickzad and Déziel, 2016; Rolland et al., 2016; Whiteley et al., 2017; Mukherjee and Bassler, 2019). In particular, AHL-based QS regulations are modulated by signaling molecules (including AHLs and other AI types) (Long et al., 2009), C sources (Medina-Martínez et al., 2006; Shrout et al., 2006), nutrient levels (McIntosh et al., 2009; Boyle et al., 2015), or algal compounds (Rolland et al., 2016; Dow, 2021 and ref. therein), among others. The initial bacterial communities were sampled at the beginning and the peak of the spring phytoplankton growth (**Supplementary Figure 1**), which is likely to have a major impact on those parameters. The variability of responses between the two experiments is in concordance with previously reported results. For instance, Krupke et al. (2016) noted that the effect of AHL amendment on hydrolytic activity was "remarkably inconsistent" when comparing several sampling locations.

Taken together, the AHL amendment experiments from this study and from previous ones demonstrate the involvement of QS-based communication in hydrolytic activity regulation. They also highlight the complexity of such regulation as no pattern seems to emerge from the different AHL amendment experiments.

Quorum Sensing Modulates the Composition of Marine Bacterial Communities

We then investigated whether AHL amendment modulated the BCC by monitoring the diversity, using metabarcoding of the V3/V4 region of the 16S rRNA gene. Both the PCoA ordination (and subsequent PERMANOVA and ANOSIM tests) and the differential abundance analyses revealed a significant effect of the AHL treatment on the BCC compared to the DMSO control. In addition, although few ASVs were affected, they were amongst the most abundant ASVs in the control community for both experiments. During the First experiment, C6-HSL and 3-oxo-C8-HSL affected the largest number of ASVs, including Bacteroidia and Gammaproteobacteria. The other AHLs mainly affected Bacteroidia. During the Second experiment, the effect of the AHL treatment seemed to differ according to the side-chain length of the AHL: the short-chain AHLs (C4-, C6-, and 3-oxo-C8-HSL) reduced the abundance of a core of two Flavobacteriales ASVs. The C12-HSL affected the largest number of ASVs, including the same two Flavobacteriales ASVs as well as several Gammaproteobacteria. In contrast, the C16-HSL mostly affected Gammaproteobacteria.

Overall, the affected ASVs were affiliated to Bacteroidia (only Flavobacteriales and mostly Flavobacteriaceae), Gammaproteobacteria (mainly Vibrionales, Alteromonadales,

and Oceanospirillales) and Alphaproteobacteria (only Rhodobacterales), which is in agreement with the literature. Indeed, the members of Gamma- and Alphaproteobacteria are broadly involved in QS communications. Several environmental Vibrionales, Alteromodales, and Rhodobacterales strains use AHL-based QS (Gram et al., 2002; Cuadrado-silva et al., 2013; Su et al., 2019). In addition, several marine metagenomic datasets have shown the important contribution of Rhodobacterales, Vibrionales, Alteromonadales, Cellvibrionales, and Oceanospirillales to the number of sequences coding for AHL synthases (Doberva et al., 2015; Huang et al., 2018; Su et al., 2021), AHLs receptors (Su et al., 2021) or AHL QQ genes (Huang et al., 2018; Su et al., 2021). Similarly, several cultivated Flavobacteriaceae species can produce or degrade AHLs during cultivation (Romero et al., 2010; Su et al., 2019). In addition, Flavobacteriales have been found to code for AHL receptors and AHL QQ genes (Su et al., 2021) in marine metagenomic datasets.

To our knowledge, no study has previously demonstrated the direct effect of AHL amendment on marine planktonic bacterial community structuration. However, a few studies have suggested that QS-based cell-cell communications may be an overlooked mechanism structuring marine bacterial communities. For instance, Whalen et al. (2019) showed that 2-heptyl-4-quinolone (HHQ, another type of QS signal belonging to the alkylquinolone) amendment to microbial communities sampled along a simulated bloom differently modulated the BCC depending on the bloom stage. The authors found, among others, that HHQ amendment increased the relative abundances of Gammaproteobacteria but decreased those of Bacteroidetes. This seems to be in agreement with our study, where two distinct communities sampled at different stages of the spring phytoplankton growth responded differently to AHL amendment. In addition, Huang et al. (2019) demonstrated that QS disruption through lactonase-based degradation of AHLs impacted the diversity of colonized immerged steel coupons, reducing the abundances of Burkholderiales, Pseudomonadales, and Rhodospirillales, among others.

It is mostly unclear how QS affected BCC, which probably resulted from the combined action of several mechanisms. First, QS can regulate the production of "public goods" (Whiteley et al., 2017; Mukherjee and Bassler, 2019), which are common-pool compounds or functions providing a collective benefit (Smith and Schuster, 2019). They include, among others, extracellular hydrolases, siderophores, or biosurfactants. The upregulation or downregulation of those common goods would likely drive changes in BCC. For instance, the evidenced modification in hydrolytic activities could allow non-degrading "cheater" cells to grow. Interestingly, in our study, the effect of AHL treatment on the BCC seemed to mirror the effect on specific enzymatic activities, as suggested by the Procrustes analysis, which supports this hypothesis. Second, QS-regulated mechanisms could impact microbial communities through the production of antimicrobial compounds that kill or inhibit the growth of microorganisms (including antibiotics or algaecides), which has previously been documented in aquatic strains (Rolland et al., 2016; Mion et al., 2021). Finally, it is possible that AHL-driven changes in BCC resulted from the additional functions of AHLs (or their degradation products), which include antibacterial activity and iron chelation properties (Kaufmann et al., 2005; Schertzer et al., 2009).

Relevance of Quorum Sensing Communications *in situ*

In marine and aquatic environments, QS is believed to occur in biofilm-associated communities, covering biotic (such as phytoplankton or coral) or abiotic surfaces (such as marine snow) (Hmelo and Van Mooy, 2009; Hmelo, 2017). Those densely populated would allow the AHL induction threshold to be reached, whereas this seems unrealistic in free-living, open-ocean communities. However, the quick phenotypic response observed in our experiments (between 0 and 6 h) suggests that QS has implications beyond those biofilm environments. Indeed, the diffusion of AHLs in the vicinity of biofilms, for example in marine snow plume or in the phycosphere (Stocker, 2012), can potentially impact the surrounding free-living communities on such a short time-scale. The modulation of the free-living community genes' expression may then drive changes in its composition and functions. Such interpretation has been proposed by Schwab et al. (2019), who demonstrated that AHL disruption in soil communities affected not only the biofilm formation, but also the suspended communities, suggesting that AHL signaling extends beyond biofilms.

CONCLUSION

Overall, this study demonstrates that AHL-based QS is involved in regulating hydrolytic enzyme production and BCC structuration in marine bacterial communities, which drive mineralization pathways. If initial experiments carried out on marine snow suggested that particulate organic matter degradation is coordinated by QS, this study extended those results to free-living bacterial coastal communities for the first time. In addition, to the best of our knowledge, this study is the first to demonstrate the direct impact of AHL amendment on the composition of marine planktonic bacterial communities. As such, QS communication pathways could be an unaccounted mechanism with profound ecological and biogeochemical implications for the oceans. The variability of response following AHL amendment points out the complexity of cell-cell communication mechanisms. In the future, more research will be needed to better characterize the function and the mechanisms of action of bacterial cell-cell communications in free-living and surface-attached communities, using both isolated strains, synthetic microbial communities, and natural assemblages.

DATA AVAILABILITY STATEMENT

The datasets presented in this study can be found in online repositories. The names of the repository/repositories and accession number(s) can be found below: https://www.ncbi.nlm.nih.gov/search/all/?term=PRJNA759568.

AUTHOR CONTRIBUTIONS

MU, CL, and DD performed the experiments. MU analyzed the data and wrote the first draft of the manuscript. All authors contributed to the conception and design of the study, manuscript revision, read, and approved the submitted version.

FUNDING

This work was supported by the French National Program Ecosphère Continentale et Côtière (EC2CO) and ISblue (Interdisciplinary Graduate School for the Blue Planet) project (ANR-17-EURE-0015), co-funded by a grant from the French Government under the program "Investissements d'Avenir".

ACKNOWLEDGMENTS

We are deeply thankful to Cyril Noël (SeBiMER, IFREMER) for his help with bioinformatic analyses. We would also like to thank the SOMLIT network for providing nutrient and chlorophyll *a* data, as well as the PHYTOBS network for providing information on the phytoplankton community at the SOMLIT station.

SUPPLEMENTARY MATERIAL

The Supplementary Material for this article can be found online at: https://www.frontiersin.org/articles/10.3389/fmicb.2021.780759/full#supplementary-material

REFERENCES

Arnosti, C. (2011). Microbial extracellular enzymes and the marine carbon cycle. *Annu. Rev. Mar. Sci.* 3, 401–425.

Arnosti, C. (2014). Patterns of microbially driven carbon cycling in the ocean: links between extracellular enzymes and microbial communities. *Adv. Oceanogr.* 2014:706082.

Azam, F., and Malfatti, F. (2007). Microbial structuring of marine ecosystems. *Nat. Rev. Microbiol.* 5, 782–791. doi: 10.1038/nrmicro1747

Blanchet, E., Prado, S., Stien, D., da Silva, J. O., Ferandin, Y., Batailler, N., et al. (2017). Quorum sensing and quorum quenching in the Mediterranean Seagrass Posidonia Oceanica microbiota. *Front. Mar. Sci.* 4:218. doi: 10.3389/fmars.2017.00218

Boyle, K. E., Monaco, H., van Ditmarsch, D., Deforet, M., and Xavier, J. B. (2015). Integration of metabolic and quorum sensing signals governing the decision to cooperate in a bacterial social trait. *PLoS Comput. Biol.* 11:e1004279. doi: 10.1371/journal.pcbi.1004279

Chróst, R. J. (1990). "Microbial ectoenzymes in aquatic environments," in *Aquatic Microbial Ecology: Biochemical and Molecular Approaches*, eds J. Overbeck and R. J. Chróst (New York, NY: Springer), 47–77. doi: 10.1007/978-1-4612-3382-4_3

Cosetta, C. M., and Wolfe, B. E. (2019). Causes and consequences of biotic interactions within microbiomes. *Curr. Opin. Microbiol.* 50, 35–41.

Cuadrado-silva, C. T., Castellanos, L., Arévalo-ferro, C., and Osorno, O. E. (2013). Detection of quorum sensing systems of bacteria isolated from fouled marine organisms. *Biochem. Syst. Ecol.* 46, 101–107. doi: 10.1016/j.bse.2012.09.010

Doberva, M., Sanchez-Ferandin, S., Toulza, E., Lebaron, P., and Lami, R. (2015). Diversity of quorum sensing autoinducer synthases in the global ocean sampling metagenomic database. *Aquat. Microb. Ecol.* 74, 107–119. doi: 10.3354/ame01734

Dow, L. (2021). How do quorum-sensing signals mediate algae–bacteria interactions? *Microorganisms* 9:1391. doi: 10.3390/microorganisms9071391

Dulaquais, G., Breitenstein, J., Waeles, M., Marsac, R., and Riso, R. (2018). Measuring dissolved organic matter in estuarine and marine waters: size-exclusion chromatography with various detection methods. *Environ. Chem.* 15, 436–449. doi: 10.1071/en18108

Falkowski, P. G., Fenchel, T., and Delong, E. F. (2008). The microbial engines that drive Earth's biogeochemical cycles. *Science* 320, 1034–1039.

Fuqua, W. C., Winans, S. C., and Greenberg, E. P. (1994). Quorum sensing in bacteria: the LuxR-LuxI family of cell density- responsive transcriptional regulators. *J. Bacteriol.* 176, 269–275. doi: 10.1128/jb.176.2.269-275.1994

Gao, J., Duan, Y., Liu, Y., Zhuang, X., Liu, Y., Bai, Z., et al. (2018). Long- and short-chain AHLs affect AOA and AOB microbial community composition and ammonia oxidation rate in activated sludge. *J. Environ. Sci.* 78, 53–62. doi: 10.1016/j.jes.2018.06.022

Gram, L., Grossart, H. P., Schlingloff, A., and Kiørboe, T. (2002). Possible quorum sensing in marine snow bacteria: production of acylated homoserine lactones by *Roseobacter* strains isolated from marine snow. *Appl. Environ. Microbiol.* 68, 4111–4116. doi: 10.1128/AEM.68.8.4111-4116.2002

Grandclément, C., Tannières, M., Moréra, S., Dessaux, Y., and Faure, D. (2015). Quorum quenching: role in nature and applied developments. *FEMS Microbiol. Rev.* 40, 86–116.

Hmelo, L. R. (2017). Quorum sensing in marine microbial environments. *Annu. Rev. Mar. Sci.* 9, 257–281. doi: 10.1146/annurev-marine-010816-060656

Hmelo, L. R., Mincer, T. J., and Van Mooy, B. A. S. (2011). Possible influence of bacterial quorum sensing on the hydrolysis of sinking particulate organic carbon in marine environments. *Environ. Microbiol. Rep.* 3, 682–688. doi: 10.1111/j.1758-2229.2011.00281.x

Hmelo, L., and Van Mooy, B. A. S. (2009). Kinetic constraints on acylated homoserine lactone-based quorum sensing in marine environments. *Aquat. Microb. Ecol.* 54, 127–133.

Huang, S., Bergonzi, C., Schwab, M., Elias, M., and Hicks, R. E. (2019). Evaluation of biological and enzymatic quorum quencher coating additives to reduce biocorrosion of steel. *PLoS One* 14:e0217059. doi: 10.1371/journal.pone.0217059

Huang, X., Zhu, J., Cai, Z., Lao, Y., Jin, H., Yu, K., et al. (2018). Profiles of quorum sensing (QS)-related sequences in phycospheric microorganisms during a marine dinoflagellate bloom, as determined by a metagenomic approach. *Microbiol. Res.* 217, 1–13. doi: 10.1016/j.micres.2018.08.015

Huang, Y., Ki, J., Lee, O. O., and Qian, P. (2009). Evidence for the dynamics of Acyl homoserine lactone and AHL-producing bacteria during subtidal biofilm formation. *ISME J.* 3, 296–304. doi: 10.1038/ismej.2008.105

Jatt, A. N., Tang, K., Liu, J., Zhang, Z., and Zhang, X. H. (2015). Quorum sensing in marine snow and its possible influence on production of extracellular hydrolytic enzymes in marine snow bacterium *Pantoea ananatis* B9. *FEMS Microbiol. Ecol.* 91, 1–13. doi: 10.1093/femsec/fiu030

Jo, S. J., Kwon, H., Jeong, S. Y., Lee, S. H., Oh, H. S., Yi, T., et al. (2016). Effects of quorum quenching on the microbial community of biofilm in an anoxic/oxic MBR for wastewater treatment. *J. Microbiol. Biotechnol.* 26, 1593–1604. doi: 10.4014/jmb.1604.04070

Kaufmann, G. F., Sartorio, R., Lee, S. H., Rogers, C. J., Meijler, M. M., Moss, J. A., et al. (2005). Revisiting quorum sensing: discovery of additional chemical and biological functions for 3-oxo-N-acylhomoserine lactones. *Proc. Natl. Acad. Sci. U.S.A.* 102, 309–314. doi: 10.1073/pnas.0408639102

Klindworth, A., Pruesse, E., Schweer, T., Peplies, J., Quast, C., Horn, M., et al. (2013). Evaluation of general 16S ribosomal RNA gene PCR primers for classical and next-generation sequencing-based diversity studies. *Nucleic Acids Res.* 41:e1. doi: 10.1093/nar/gks808

Konopka, A., Lindemann, S., and Fredrickson, J. (2015). Dynamics in microbial communities: unraveling mechanisms to identify principles. *ISME J.* 9, 1488–1495. doi: 10.1038/ismej.2014.251

Krupke, A., Hmelo, L. R., Ossolinski, J. E., Mincer, T. J., and Van Mooy, B. A. S. (2016). Quorum Sensing plays a complex role in regulating the enzyme hydrolysis activity of microbes associated with sinking particles in the ocean. *Front. Mar. Sci.* 3:55. doi: 10.3389/fmars.2016.00055

Lami, R. (2019). "Quorum sensing in marine biofilms and environments," in *Quorum Sensing: Molecular Mechanism and Biotechnological Application*, ed. G. Tommonaro (Cambridge, MA: Academic Press), 55–96. doi: 10.1016/b978-0-12-814905-8.00003-4

Long, T., Tu, K. C., Wang, Y., Mehta, P., Ong, N. P., Bassler, B. L., et al. (2009). Quantifying the integration of quorum-sensing signals with single-cell resolution. *PLoS Biol.* 7:e1000068. doi: 10.1371/journal.pbio.1000068

Lv, L., Li, W., Zheng, Z., Li, D., and Zhang, N. (2018). Exogenous acyl-homoserine lactones adjust community structures of bacteria and methanogens to ameliorate the performance of anaerobic granular sludge. *J. Hazard. Mater.* 354, 72–80. doi: 10.1016/j.jhazmat.2018.04.075

Ma, H., Ma, S., Hu, H., Ding, L., and Ren, H. (2018). The biological role of N-acyl-homoserine lactone-based quorum sensing (QS) in EPS production and microbial community assembly during anaerobic granulation process. *Sci. Rep.* 8:15793. doi: 10.1038/s41598-018-34183-3

Marie, D., Partensky, F., Vaulot, D., and Brussaard C. (1999). Enumeration of Phytoplankton, Bacteria, and Viruses in marine samples. *Current Protocols in Cytometry 10: 11.11.1-11.11.15.* Available online at: https://doi.org/10.1002/0471142956.cy1111s10

McIntosh, M., Meyer, S., and Becker, A. (2009). Novel *Sinorhizobium meliloti* quorum sensing positive and negative regulatory feedback mechanisms respond to phosphate availability. *Mol. Microbiol.* 74, 1238–1256. doi: 10.1111/j.1365-2958.2009.06930.x

Medina-Martínez, M. S., Uyttendaele, M., Demolder, V., and Debevere, J. (2006). Effect of temperature and glucose concentration on the N-butanoyl-L-homoserine lactone production by *Aeromonas hydrophila*. *Food Microbiol.* 23, 534–540. doi: 10.1016/j.fm.2005.09.010

Miller, M. B., and Bassler, B. L. (2001). Quorum sensing in bacteria. *Annu. Rev. Microbiol.* 55, 165–199.

Mion, S., Carriot, N., Lopez, J., Plener, L., Ortalo-Magné, A., Chabrière, E., et al. (2021). Disrupting quorum sensing alters social interactions in *Chromobacterium violaceum*. *NPJ Biofilms Microbiomes* 7:40. doi: 10.1038/s41522-021-00211-w

Mukherjee, S., and Bassler, B. L. (2019). Bacterial quorum sensing in complex and dynamically changing environments. *Nat. Rev. Microbiol.* 17, 371–382.

Muras, A., López-Pérez, M., Mayer, C., Parga, A., Amaro-Blanco, J., and Otero, A. (2018). High prevalence of quorum-sensing and quorum-quenching activity among cultivable bacteria and metagenomic sequences in the Mediterranean Sea. *Genes* 9:100. doi: 10.3390/genes9020100

Nickzad, A., and Déziel, E. (2016). Adaptive significance of quorum sensing-dependent regulation of rhamnolipids by integration of growth rate in *Burkholderia glumae*: a trade-off between survival and efficiency. *Front. Microbiol.* 7:1215. doi: 10.3389/fmicb.2016.01215

Olesen, S. W., Duvallet, C., and Alm, E. J. (2017). dbOTU3: a new implementation of distribution-based OTU calling. *PLoS One* 12:e0176335. doi: 10.1371/journal.pone.0176335

Papenfort, K., and Bassler, B. L. (2016). Quorum sensing signal-response systems in Gram-negative bacteria. *Nat. Rev. Microbiol.* 14, 576–588. doi: 10.1038/nrmicro.2016.89

Payne, J. W. (ed.) (1980). *Microorganisms and Nitrogen Sources: Transport and Utilization of Amino Acids, Peptides, Proteins, and Related Substrates*. Chichester: John Wiley.

Quast, C., Pruesse, E., Yilmaz, P., Gerken, J., Schweer, T., Yarza, P., et al. (2013). The SILVA ribosomal RNA gene database project: improved data processing and web-based tools. *Nucleic Acids Res.* 41, D590–D596, doi: 10.1093/nar/gks1219

Rolland, J. L., Stien, D., Sanchez-Ferandin, S., and Lami, R. (2016). Quorum sensing and quorum quenching in the phycosphere of phytoplankton: a case of chemical interactions in ecology. *J. Chem. Ecol.* 42, 1201–1211. doi: 10.1007/s10886-016-0791-y

Romero, M., Avendaño-Herrera, R., Magariños, B., Cámara, M., and Otero, A. (2010). Acylhomoserine lactone production and degradation by the fish pathogen *Tenacibaculum maritimum*, a member of the *Cytophaga*-Flavobacterium-*Bacteroides* (CFB) group. *FEMS Microbiol. Lett.* 304, 131–139. doi: 10.1111/j.1574-6968.2009.01889.x

Schertzer, J. W., Boulette, M. L., and Whiteley, M. (2009). More than a signal: non-signaling properties of quorum sensing molecules. *Trends Microbiol.* 17, 189–195. doi: 10.1016/j.tim.2009.02.001

Schwab, M., Bergonzi, C., Sakkos, J., Staley, C., Zhang, Q., Sadowsky, M. J., et al. (2019). Signal disruption leads to changes in bacterial community population. *Front. Microbiol.* 10:611. doi: 10.3389/fmicb.2019.00611

Shrout, J. D., Chopp, D. L., Just, C. L., Hentzer, M., Givskov, M., and Parsek, M. R. (2006). The impact of quorum sensing and swarming motility on *Pseudomonas aeruginosa* biofilm formation is nutritionally conditional. *Mol. Microbiol.* 62, 1264–1277. doi: 10.1111/j.1365-2958.2006.05421.x

Smith, P., and Schuster, M. (2019). Public goods and cheating in microbes. *Curr. Biol.* 29, R442–R447.

Stock, F., Cirri, E., Nuwanthi, S. G. L. I., Stock, W., Ueberschaar, N., Mangelinckx, S., et al. (2021). Sampling, separation, and quantification of N-acyl homoserine lactones from marine intertidal sediments. *Limnol. Oceanogr. Methods* 19, 145–157.

Stocker, R. (2012). Marine microbes see a sea of gradients. *Science* 338, 628–633. doi: 10.1126/science.1208929

Su, Y., Tang, K., Liu, J., Wang, Y., Zheng, Y., and Zhang, X. H. (2019). Quorum sensing system of *Ruegeria mobilis* Rm01 controls lipase and biofilm formation. *Front. Microbiol.* 10:3304. doi: 10.3389/fmicb.2018.03304

Su, Y., Yang, Y., Zhu, X. Y., Zhang, X. H., and Yu, M. (2021). Metagenomic insights into the microbial assemblage capable of quorum sensing and quorum quenching in particulate organic matter in the Yellow Sea. *Front. Microbiol.* 11:602010. doi: 10.3389/fmicb.2020.602010

Urvoy, M., Lami, R., Dreanno, C., Daudé, D., Rodrigues, A. M. S., L'Helguen, S., et al. (2021). Quorum sensing disruption regulates hydrolytic enzyme and biofilm production in estuarine bacteria. *Environ. Microbiol.* 23, 7183−7200.

Van Mooy, B. A. S., Hmelo, L. R., Sofen, L. E., Campagna, S. R., May, A. L., Dyhrman, S. T., et al. (2012). Quorum sensing control of phosphorus acquisition in *Trichodesmium consortia*. *ISME J.* 6, 422–429. doi: 10.1038/ismej.2011.115

Waters, C. M., and Bassler, B. L. (2005). Quorum sensing: cell-to-cell communication in bacteria. *Annu. Rev. Cell Dev. Biol.* 21, 319–346.

Whalen, K. E., Becker, J. W., Schrecengost, A. M., Gao, Y., Giannetti, N., and Harvey, E. L. (2019). Bacterial alkylquinolone signaling contributes to structuring microbial communities in the ocean. *Microbiome* 7:93. doi: 10.1186/s40168-019-0711-9

Whiteley, M., Diggle, S. P., and Greenberg, E. P. (2017). Progress in and promise of bacterial quorum sensing research. *Nature* 551, 313–320. doi: 10.1038/nature24624

Zimmerman, A. E., Martiny, A. C., and Allison, S. D. (2013). Microdiversity of extracellular enzyme genes among sequenced prokaryotic genomes. *ISME J.* 7, 1187–1199. doi: 10.1038/ismej.2012.176

Conflict of Interest: The authors declare that the research was conducted in the absence of any commercial or financial relationships that could be construed as a potential conflict of interest.

Publisher's Note: All claims expressed in this article are solely those of the authors and do not necessarily represent those of their affiliated organizations, or those of the publisher, the editors and the reviewers. Any product that may be evaluated in this article, or claim that may be made by its manufacturer, is not guaranteed or endorsed by the publisher.

III. Données supplémentaires

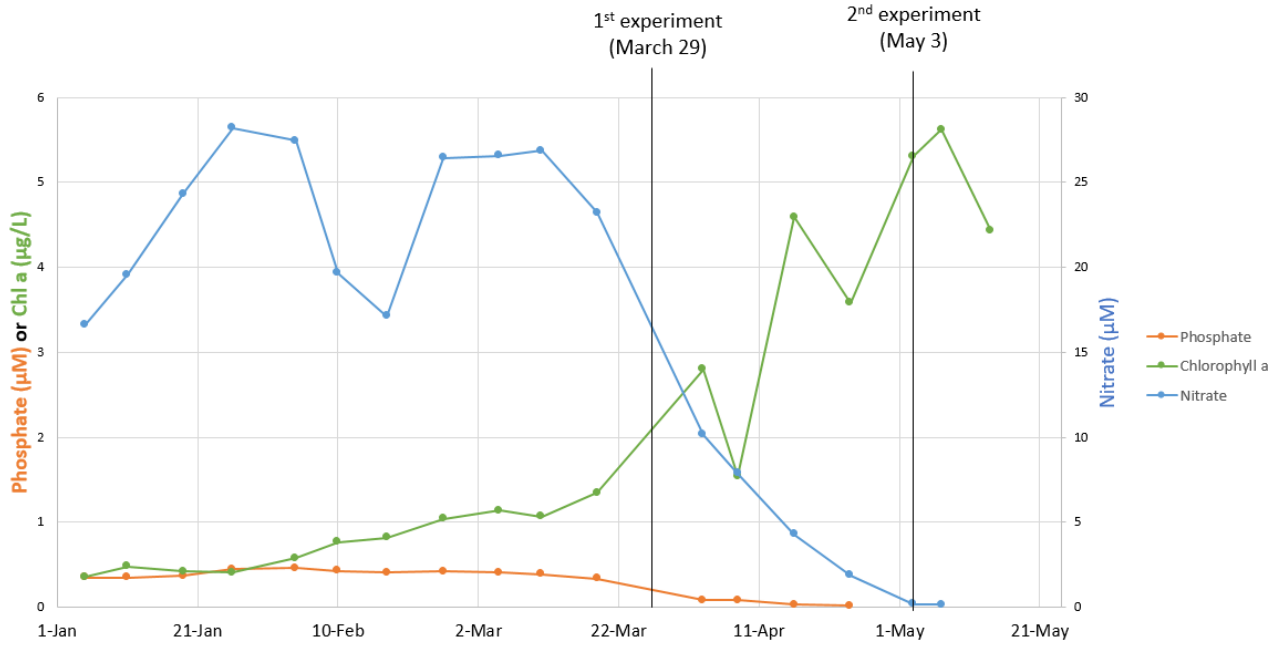

Figure S3: Environmental parameters (nitrate, phosphate and chlorophyll *a*) on the two experiment sampling dates, corresponding to the beginning (March 29) and the peak (May 3) of the phytoplankton spring growth. Data were downloaded from the SOMLIT website (https://www.somlit.fr/visualisation-des-donnees/) on September 17th 2021.

The phytoplankton communities were identified by the observation network SNO PHYTOBS (Service National d'Observation du Phytoplancton, https://www.phytobs.fr/) on dates close to the experiments (March 26 and May 2, 2021). On March 26, close to the 1st experiment (early bloom), the phytoplankton community was characterized by the presence of diatoms including *Pseudo-nitzschia* (16% of total cells), *Chaetoceros* (12.5%) and unidentified centric diatoms (12.5%). The nanophytoplankton included *Cryptophyceae* (27%). On May 2, near the 2nd experiment (peak bloom), the phytoplankton community was different and mostly dominated by the diatom *Guinardia flaccida* (10%). The nanophytoplankton community included *Cryptophyceae* (57%) and *Choanoflagellates* (15%).

Choice of AHL concentration

A preliminary experiment was performed to determine which AHLs concentration induced the most important response in three hydrolytic activities (leucine-aminopeptidases, alkaline phosphatases, β-glucosidases). To this extent, brackish water was sampled in the Aulne estuary (Bay of Brest, France) on June 9, 2019 and filtered using a 10-µm silk (Merck, Ref NY1004700). Then, C6- or C14-HSL were amended at 50, 200, 500, 1000 or 5000 nM with a constant final DMSO concentration (0.1%). Incubation were carried out at *in situ* temperature (22°C) and the resulting activity was assessed at 48 h. Hydrolytic enzymes were assayed as described in the main script, in technical duplicates.

Although no statistical test was performed given the absence of biological replicates, alkaline phosphates seemed induced with 50 nM of C14-HSL (4.4 times increase, **Fig. S2**). The C14-HSL effect seemed to lessen with increasing AHL concentration (1.6-2.2 times increase with 200 to 5000 nM, Fig. S1). The C6-HSL also seemed to induce the alkaline phosphatase, especially using 50 nM of C6-HSL but no clear trend was visible among the different concentrations (**Fig. 2**). There was no clear pattern of induction for leucine aminopeptidases and β-glucosidases (not shown). Consequently, we choose to perform the experiments using 50 nM of AHLs.

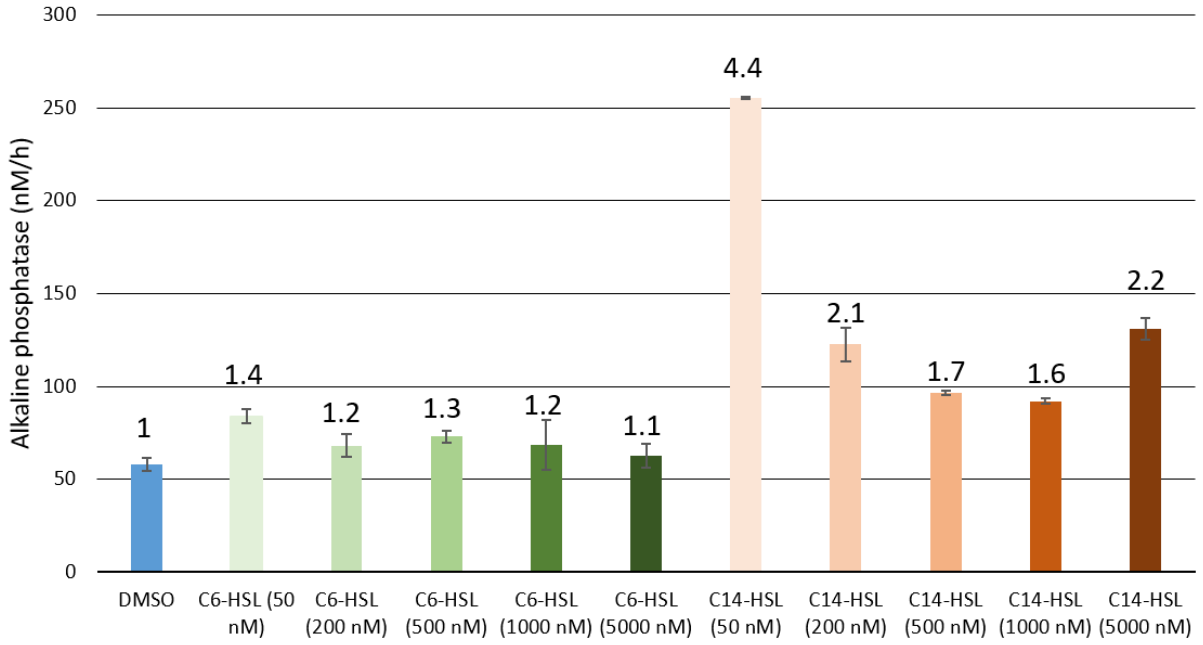

Fig. S4: Alkaline phosphatase 48 h after C6- and C14-HSL amendments. The error bars indicate standard error over technical duplicates. The ratio between the treatment and the DMSO control is annotated above the error bars.

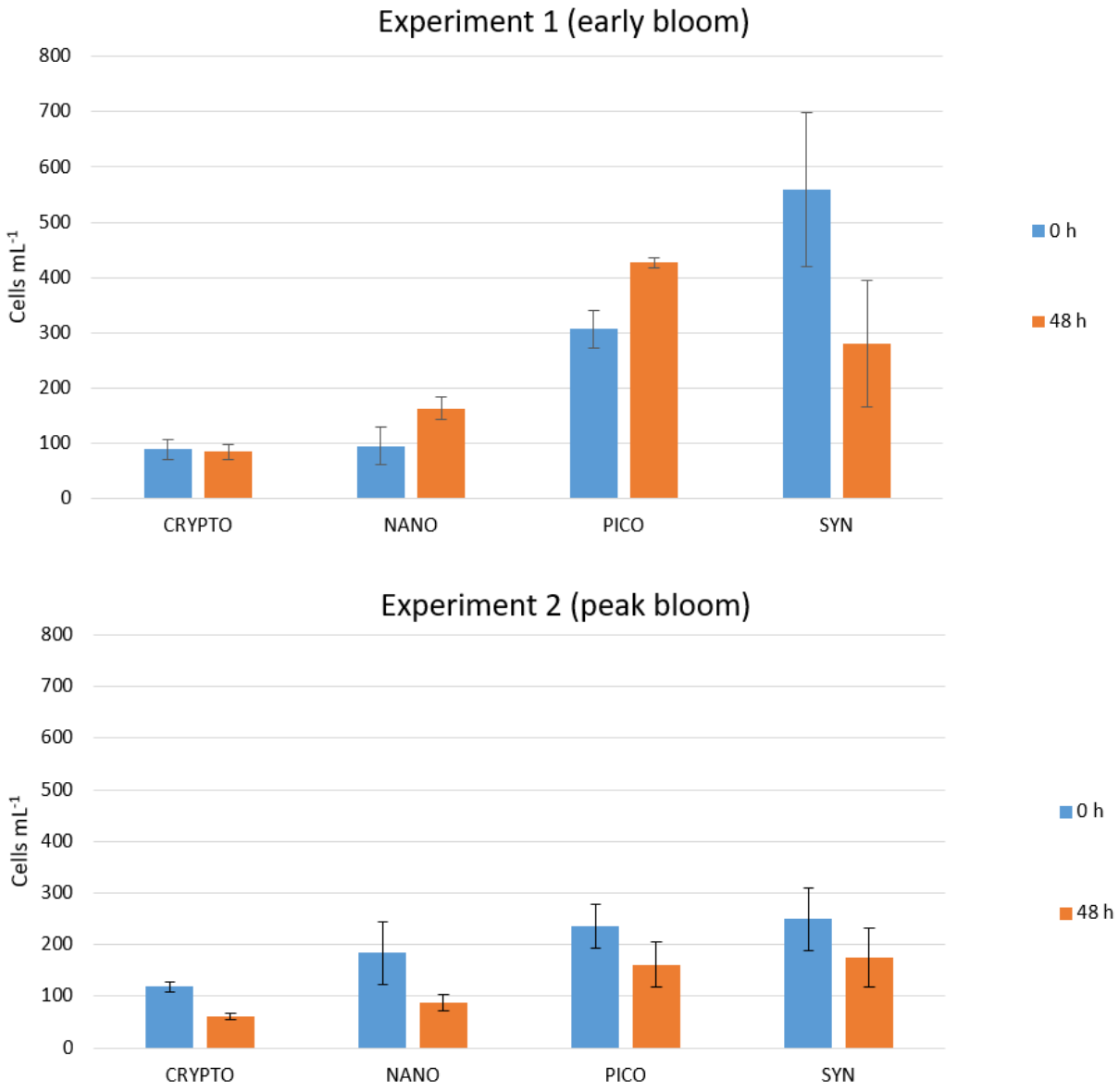

Fig. S3: Quantification of the phytoplankton cells in the 10-µm filtered seawater before dispatching (blue) and in the DMSO control at the end of the 48 h incubation (orange) for the 1st (early bloom, top) and the 2nd experiment (peak bloom, bottom). CRYPTO: cryptophytes, NANO: nanophytoplankton, PICO: picophytoplankton, SYN: *synechococcus*.

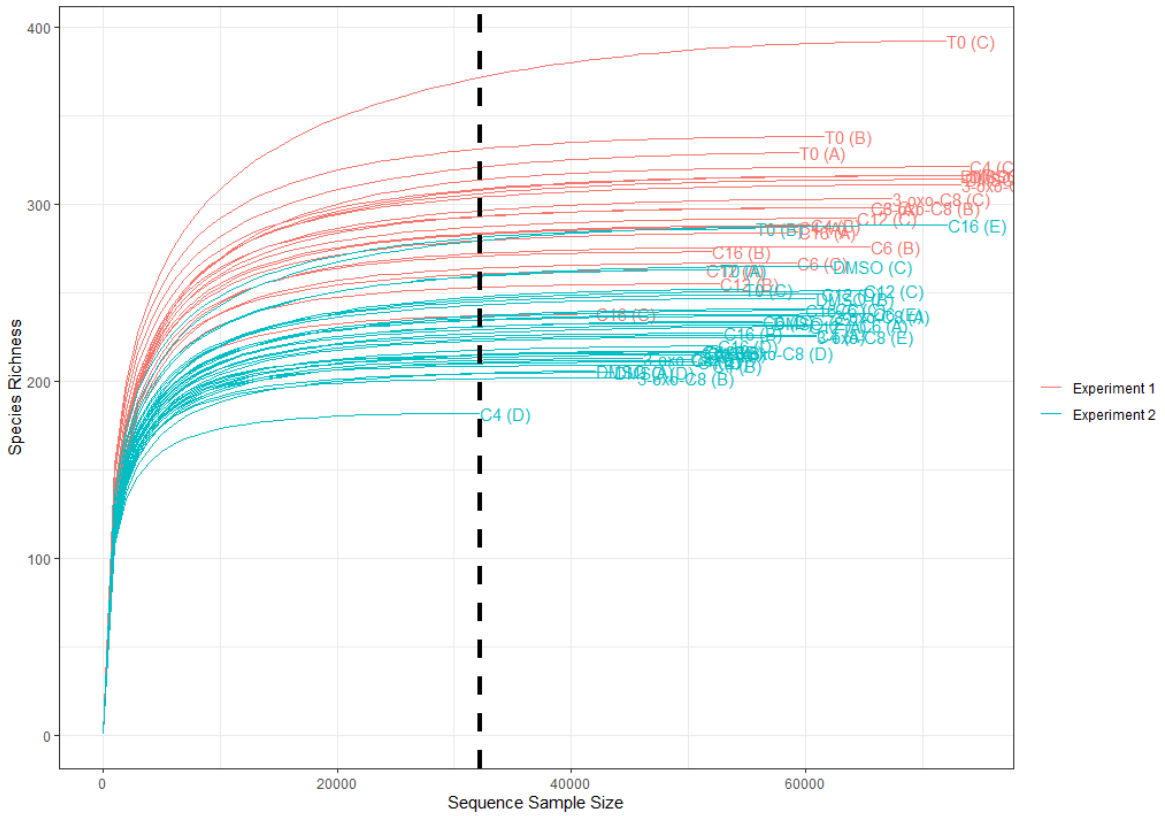

Fig. S4: Rarefaction curves for the two experiments. The vertical dashed bar represent the number of reads used for rarefaction (32 196 sequences per sample).

A)

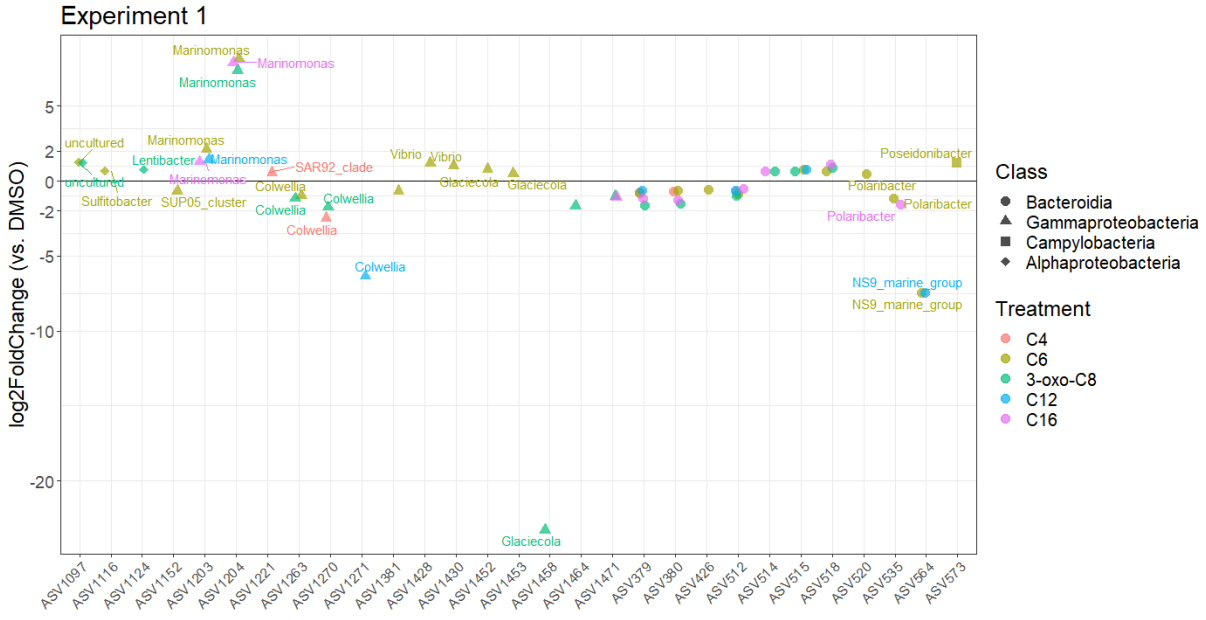

B)

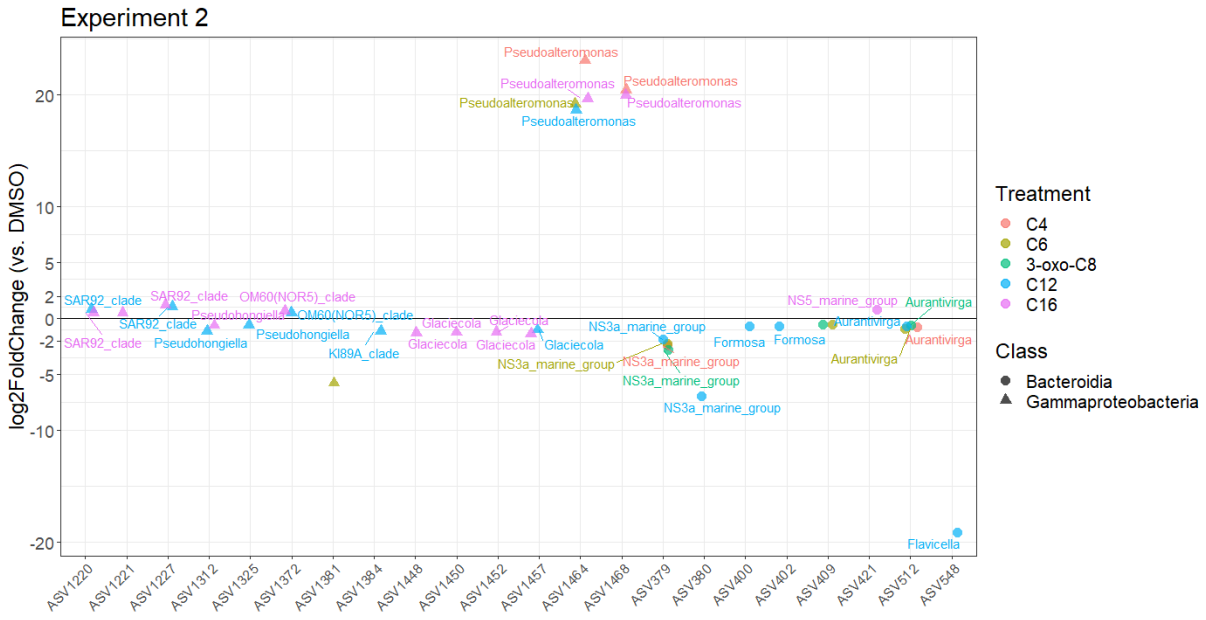

Fig. S5: Log2 fold change of the differentially abundant ASVs for each AHL-treatment compared to the DMSO control (cut-off p_{BH} = 0.05, cut-off log2FC = 0.5 or -0.5) for the 1st (early bloom, **A**) and 2nd (peak bloom) experiment (**B**).

A)

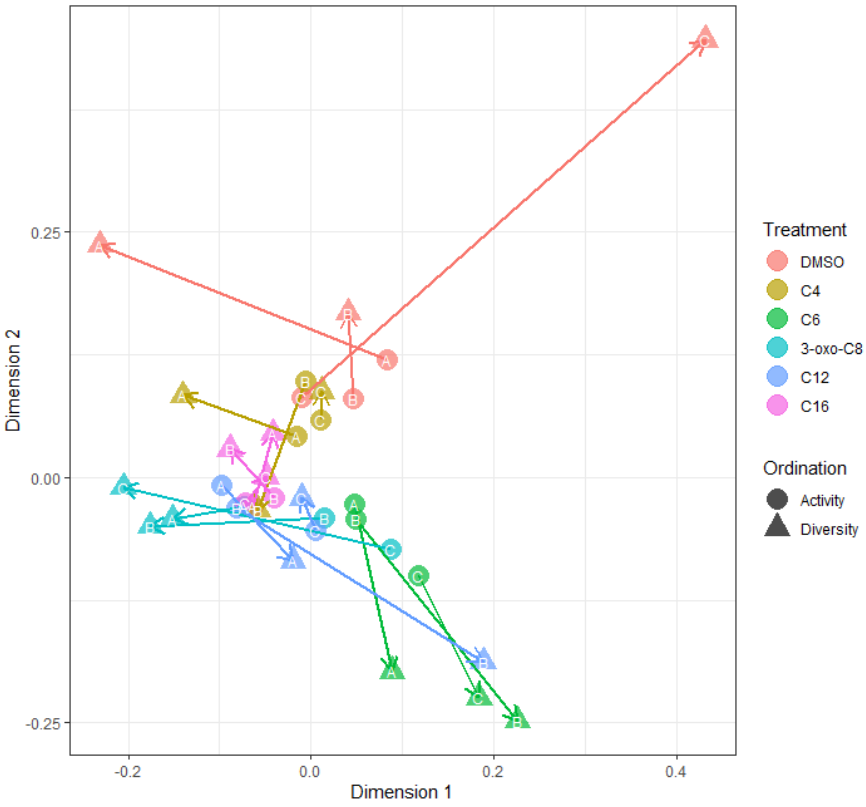

B)

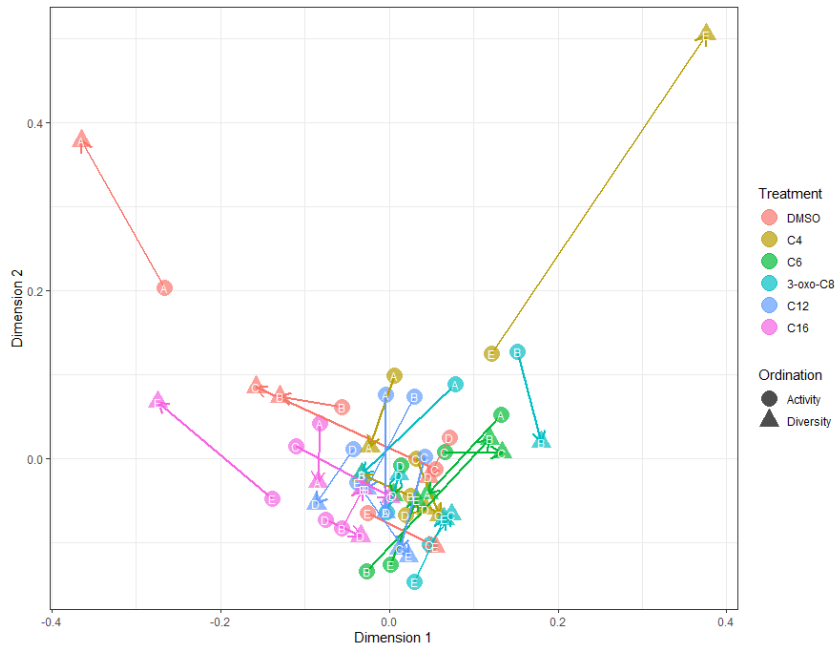

Fig. S6. Procrustes plot showing the superimposition of the specific activities and the BCC ordinations for the 1st experiment (early bloom, **A**) and the 2nd experiment (peak bloom, **B**).

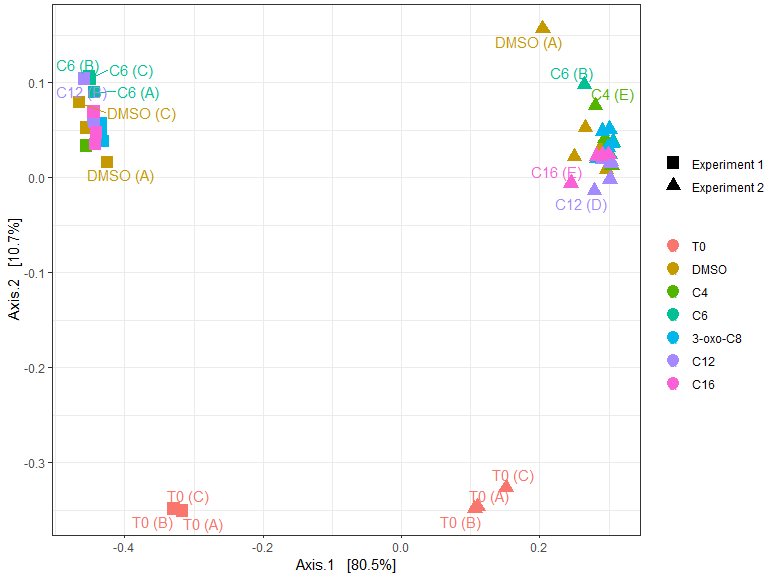

Fig. S7: Principal Coordinates analysis (PCoA) based on the Bray-Curtis dissimilarity for both experiments.

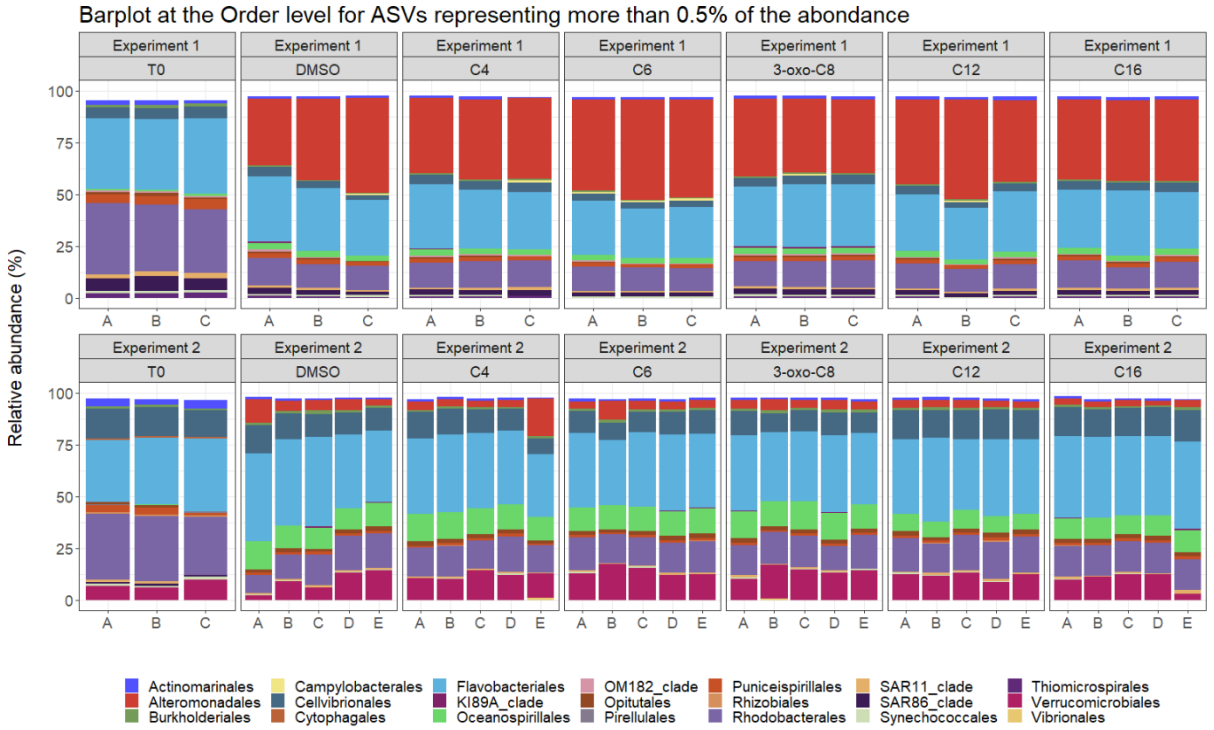

Fig. S8: Composition of the communities in the 1st (early bloom, top panels) and 2nd experiment (peak bloom, bottom panels) at the beginning (T0) and end of the 48h incubation, for the different treatments (DMSO, C4-HSL, C6-HSL, 3-oxo-C8-HSL, C12-HSL and C16-HSL). Only the ASVs representing more than 0.5% of the sample abundance are represented, agglomerated at the Order level. The different replicates are labeled A, B, C, D and E in the x-axis.

Table S3: Mean relative abundance of the 50 most abundant ASVs in the DMSO control at the end of the 48 h incubation, for the 1st (early bloom, left) and 2nd (peak bloom, right) experiment. Mean relative abundance (Ab) and standard deviation (SD) were calculated from the biological replicates. The differentially abundant ASVs were highlighted in orange (differentially abundant in one experiment) or green (differentially abundant in both experiments).

Experiment 1					Experiment 2				
ASV	Order	Genus	Ab (%)	SD	ASV	Order	Genus	Ab (%)	SD
ASV1457	Alteromonadales	Glaciecola	22.8	4.71	ASV537	Flavobacteriales	Flavicella	11.9	1.15
ASV520	Flavobacteriales	Polaribacter	7.4	2.31	ASV396	Flavobacteriales	Winogradskyella	10.7	2.78
ASV1450	Alteromonadales	Glaciecola	6.71	0.75	ASV708	Verrucomicrobiales	Persicirhabdus	8.11	4.98
ASV1073	Rhodobacterales	Amylibacter	6.45	0.91	ASV1133	Rhodobacterales	Planktomarina	7.76	3.32
ASV512	Flavobacteriales	Aurantivirga	5.66	0.81	ASV1329	Oceanospirillales	Pseudohongiella	7.48	0.89
ASV1452	Alteromonadales	Glaciecola	4.43	0.71	ASV1219	Cellvibrionales	SAR92_clade	3.66	1.03
ASV1133	Rhodobacterales	Planktomarina	4.17	1.37	ASV494	Flavobacteriales	uncultured	2.77	0.95
ASV426	Flavobacteriales	NS5_marine_group	3.81	0.66	ASV1312	Oceanospirillales	Pseudohongiella	2.75	0.42
ASV1221	Cellvibrionales	SAR92_clade	1.95	0.79	ASV512	Flavobacteriales	Aurantivirga	2.66	0.78
ASV1312	Oceanospirillales	Pseudohongiella	1.41	0.11	ASV1105	Rhodobacterales	Ascidiaceihabitans	2.36	0.33
ASV1453	Alteromonadales	Glaciecola	1.08	0.11	ASV1214	Cellvibrionales	SAR92_clade	2.12	0.31
ASV1351	SAR86_clade	SAR86_clade	1.02	0.31	ASV1073	Rhodobacterales	Amylibacter	2.11	0.16
ASV1052	Puniceispirillales	Candidatus_Puniceispirillum	1	0.14	ASV1450	Alteromonadales	Glaciecola	1.89	1.2
ASV389	Flavobacteriales	NS2b_marine_group	0.93	0.16	ASV1226	Cellvibrionales	SAR92_clade	1.6	0.06
ASV409	Flavobacteriales	NS5_marine_group	0.91	0.06	ASV1457	Alteromonadales	Glaciecola	1.59	1.09
ASV773	Actinomarinales	Candidatus_Actinomarina	0.87	0.04	ASV1220	Cellvibrionales	SAR92_clade	1.45	0.2
ASV513	Flavobacteriales	Aurantivirga	0.85	0.09	ASV383	Flavobacteriales	Ulvibacter	1.28	0.26
ASV436	Flavobacteriales	NS4_marine_group	0.81	0.23	ASV518	Flavobacteriales	Polaribacter	1.16	0.33
ASV1059	Puniceispirillales	SAR116_clade	0.79	0.02	ASV471	Flavobacteriales	Fluviicola	1	0.1
ASV518	Flavobacteriales	Polaribacter	0.74	0.33	ASV405	Flavobacteriales	Formosa	0.83	0.14
ASV496	Flavobacteriales	uncultured	0.73	0.1	ASV773	Actinomarinales	Candidatus_Actinomarina	0.8	0.16
ASV494	Flavobacteriales	uncultured	0.72	0.07	ASV409	Flavobacteriales	NS5_marine_group	0.79	0.14
ASV1372	Cellvibrionales	OM60(NOR5)_clade	0.68	0.19	ASV699	Verrucomicrobiales	Roseibacillus	0.7	0.11
ASV259	Synechococcales	Synechococcus_CC9902	0.62	0.07	ASV1448	Alteromonadales	Glaciecola	0.63	0.47
ASV379	Flavobacteriales	NS3a_marine_group	0.61	0.08	ASV1275	Alteromonadales	Colwellia	0.61	0.2
ASV515	Flavobacteriales	Polaribacter	0.6	0.26	ASV1400	Burkholderiales	OM43_clade	0.61	0.1
ASV1240	Alteromonadales	Colwellia	0.53	0.2	ASV538	Flavobacteriales	Flavicella	0.61	0.18
ASV1357	OM182_clade	OM182_clade	0.52	0.18	ASV677	Opitutales	MB11C04_marine_group	0.59	0.11
ASV1350	SAR86_clade	SAR86_clade	0.48	0.19	ASV514	Flavobacteriales	Polaribacter	0.58	0.15
ASV1325	Oceanospirillales	Pseudohongiella	0.47	0.03	ASV1124	Rhodobacterales	Lentibacter	0.54	0.12
ASV1454	Alteromonadales	Glaciecola	0.42	0.1	ASV1052	Puniceispirillales	Candidatus_Puniceispirillum	0.5	0.04
ASV1455	Alteromonadales	Glaciecola	0.42	0.1	ASV1213	Cellvibrionales	SAR92_clade	0.5	0.05
ASV1332	Oceanospirillales	Pseudohongiella	0.4	0.08	ASV400	Flavobacteriales	Formosa	0.5	0.11
ASV1105	Rhodobacterales	Ascidiaceihabitans	0.39	0.07	ASV978	SAR11_clade	Clade_Ia	0.47	0.22
ASV1152	Thiomicrospirales	SUP05_cluster	0.39	0.14	ASV1059	Puniceispirillales	SAR116_clade	0.44	0.04

ASV514	Flavobacteriales	Polaribacter	0.39	0.11	**ASV497**	Flavobacteriales	uncultured	0.43	0.06
ASV424	Flavobacteriales	NS5_marine_group	0.38	0.09	**ASV663**	Opitutales	MB11C04_marine_group	0.4	0.08
ASV386	Flavobacteriales	uncultured	0.37	0.07	**ASV416**	Flavobacteriales	NS5_marine_group	0.37	0.07
ASV975	SAR11_clade	Clade_Ia	0.36	0.09	**ASV569**	Flavobacteriales	NS9_marine_group	0.37	0.1
ASV978	SAR11_clade	Clade_Ia	0.36	0.11	**ASV259**	Synechococcales	Synechococcus_CC9902	0.33	0.08
ASV1252	Alteromonadales	Colwellia	0.35	0.29	**ASV1330**	Oceanospirillales	Pseudohongiella	0.32	0.06
ASV1124	Rhodobacterales	Lentibacter	0.34	0.11	**ASV379**	Flavobacteriales	NS3a_marine_group	0.32	0.03
ASV1382	KI89A_clade	KI89A_clade	0.33	0.16	**ASV1397**	Burkholderiales	OM43_clade	0.3	0.09
ASV410	Flavobacteriales	NS5_marine_group	0.31	0.02	**ASV669**	Opitutales	MB11C04_marine_group	0.3	0.05
ASV380	Flavobacteriales	NS3a_marine_group	0.3	0	**ASV1382**	KI89A_clade	KI89A_clade	0.29	0.12
ASV1346	SAR86_clade	SAR86_clade	0.29	0.07	**ASV1452**	Alteromonadales	Glaciecola	0.28	0.22
ASV578	Campylobacterales	uncultured	0.28	0.14	**ASV520**	Flavobacteriales	Polaribacter	0.28	0.03
ASV498	Flavobacteriales	uncultured	0.27	0.03	**ASV1325**	Oceanospirillales	Pseudohongiella	0.26	0.02
ASV1459	Alteromonadales	Glaciecola	0.26	0.23	**ASV1399**	Burkholderiales	OM43_clade	0.26	0.02
ASV771	Actinomarinales	Candidatus_Actinomarina	0.25	0.04	**ASV1221**	Cellvibrionales	SAR92_clade	0.24	0.08

Chapitre VII*. Le quorum sensing régule des processus bactériens qui ont un rôle majeur dans les cycles biogéochimiques marins*

I. Introduction

Les bactéries hétérotrophes jouent un rôle important dans les cycles biogéochimiques, en particulier de par leur production d'enzymes hydrolytiques. Le QS peut directement influencer la synthèse de ces enzymes, mais aussi indirectement, en modifiant la composition des communautés bactériennes (**chapitres V et VI**). Ce système de communication intercellulaire pourrait également réguler de nombreux autres processus microbiens, impactant l'ensemble des cycles biogéochimiques marins.

Une synthèse bibliographique a été réalisée, synthétisant les connaissances actuelles sur les processus régulés par le QS en milieu marin, principalement chez les bactéries hétérotrophes, mais aussi chez les cyanobactéries, les archées et les virus. Elle décrit d'abord les principes généraux du QS ainsi que l'intérêt renouvelé pour son étude dans les océans. Elle présente également quelques exemples de micro-niches à fortes densités cellulaires favorables au QS, ainsi que les principaux groupes bactériens les colonisant. Les études s'intéressant au rôle du QS dans le milieu marin sont par la suite synthétisées en répertoriant, d'une part, les processus impactant directement les cycles biogéochimiques (acquisition des nutriments, allocation du carbone, dégradation de la matière organique) et, d'autre part, ceux indirectement impliqués dans les cycles biogéochimiques via la structuration de la composition des communautés. Finalement, les limites actuelles et les futures perspectives concernant le lien entre QS et cycles biogéochimiques marins sont discutées.

Dans son ensemble, cette synthèse dresse un état des lieux détaillé des recherches actuelles sur les fonctions du QS en milieu marin, dévoilant à l'occasion de futures axes de recherches dans ce domaine. Elle souligne aussi l'importance de répondre à des questions d'écologie chimique afin de mieux contraindre le rôle des microorganismes dans le contrôle des cycles biogéochimiques marins. Cette synthèse bibliographique a été publiée en 2022 dans le journal *Frontiers in marine science* (section "*Aquatic microbiology*").

frontiers in Marine Science

REVIEW
published: 02 February 2022
doi: 10.3389/fmars.2022.834337

Quorum Sensing Regulates Bacterial Processes That Play a Major Role in Marine Biogeochemical Cycles

Marion Urvoy[1,2], Claire Labry[1], Stéphane L'Helguen[2] and Raphaël Lami[3]**

[1] Ifremer, DYNECO, Plouzané, France, [2] Université de Bretagne Occidentale, CNRS, IRD, Ifremer, UMR 6539, Laboratoire des Sciences de l'Environnement Marin (LEMAR), Plouzané, France, [3] Sorbonne Université, CNRS, Laboratoire de Biodiversité et Biotechnologies Microbiennes (LBBM, USR 3579), Observatoire Océanologique de Banyuls, Banyuls-sur-Mer, France

Bacteria play a crucial role in marine biogeochemistry by releasing, consuming and transforming organic matter. Far from being isolated entities, bacteria are involved in numerous cell–cell interactions. Among such interactions, quorum sensing (QS) allows bacteria to operate in unison, synchronizing their actions through chemical communication. This review aims to explore and synthesize our current knowledge of the involvement of QS in the regulation of bacterial processes that ultimately impact marine biogeochemical cycles. We first describe the principles of QS communication and the renewed interest in its study in marine environments. Second, we highlight that the microniches where QS is most likely to occur due to their high bacterial densities are also hotspots of bacterially mediated biogeochemical transformations. Many bacterial groups colonizing these microniches harbor various QS systems. Thereafter, we review relevant QS-regulated bacterial processes in marine environments, building on research performed in both complex marine assemblages and isolated marine bacteria. QS pathways have been shown to directly regulate organic matter degradation, carbon allocation and nutrient acquisition but also to structure the community composition by mediating colonization processes and microbial interactions. Finally, we discuss current limitations and future perspectives to better characterize the link between QS expression and the bacterial mediation of biogeochemical cycles. The picture drawn by this review highlights QS as one of the pivotal mechanisms impacting microbial composition and functions in the oceans, paving the way for future research to better constrain its impact on marine biogeochemical cycles.

Keywords: marine bacteria, quorum sensing, AHL (*N*-acyl-homoserine lactone), biogeochemical cycle, hydrolytic enzyme, organic matter degradation, nutrient acquisition

OPEN ACCESS

Edited by:
Gordon T. Taylor,
Stony Brook University, United States

Reviewed by:
Elena Yakubovskaya,
Stony Brook University, United States
Jürgen Tomasch,
Helmholtz Center for Infection Research, Helmholtz Association of German Research Centers (HZ), Germany
Tom Defoirdt,
Ghent University, Belgium

****Correspondence:***
Marion Urvoy
marion.urvoy@outlook.fr
Raphaël Lami
raphael.lami@obs-banyuls.fr

Specialty section:
This article was submitted to Aquatic Microbiology, a section of the journal Frontiers in Marine Science

Received: *13 December 2021*
Accepted: *11 January 2022*
Published: *02 February 2022*

Citation:
Urvoy M, Labry C, L'Helguen S and Lami R (2022) Quorum Sensing Regulates Bacterial Processes That Play a Major Role in Marine Biogeochemical Cycles. Front. Mar. Sci. 9:834337. doi: 10.3389/fmars.2022.834337

INTRODUCTION

Microorganisms dominate life in the ocean. With an estimated 10^{30} cells in the ocean (Whitman et al., 1998), prokaryotes outnumber any other life form and support the whole marine trophic web. More specifically, heterotrophic prokaryotes degrade up to 50% of the carbon (C) fixed by marine primary producers (Azam et al., 1983) and allow its reinjection to higher trophic levels through the

microbial loop (Pomeroy, 1974; Azam et al., 1983). In doing so, they also remineralize nutrients that support the growth of primary producers (Azam and Malfatti, 2007; Pomeroy, 2007). As such, microorganisms are involved in virtually all elemental cycles, including those of C, nitrogen (N), phosphorus (P), sulfur (S) or iron (Fe) (Azam and Malfatti, 2007; Pomeroy, 2007).

Organic matter (OM) is operationally defined as dissolved (DOM) or particulate organic matter (POM). DOM is essentially consumed by free-living (FL) bacteria, which constitute the bulk of the prokaryotic community (Pomeroy, 1974; Azam et al., 1983). As DOM contains compounds ranging from low to high molecular weight, bacteria implement different strategies to exploit them. Some, such as Rhodobacterales, specialize in the uptake of small compounds that can be directly incorporated into the cells (Landa et al., 2017; Ferrer-González et al., 2021). Other species, such as members of the order Flavobacteriales, target high molecular weight substrates (Elifantz et al., 2005; Fernàndez-Gómez et al., 2013; Ferrer-González et al., 2021), which must be processed before they are metabolized. The prevailing model thus far is that heterotrophic prokaryotes use extracellular hydrolytic enzymes to cleave complex molecules into freely available compounds (Arnosti, 2011). This hydrolysis step is considered a crucial rate-limiting step in bacterially mediated OM transformations (Arnosti, 2011). Scavenging bacteria can consume the released substrates without participating in hydrolytic enzyme production (Enke et al., 2019; Reintjes et al., 2019). A third widespread strategy was recently discovered: "selfish" bacteria can bind polysaccharides on their cell surface and uptake the partially degraded products into their periplasmic space, resulting in a minimal diffusive loss of the substrates to other cells (Reintjes et al., 2017, 2019).

In parallel, some bacteria use chemotaxis and motility to locate and colonize microniches, including marine particles, the microalgal phycosphere and macro- and microplastics (Azam, 1998; Pomeroy, 2007; Stocker et al., 2008; Grossart, 2010). These bacteria, referred to as particle-associated (PA) bacteria, are often phylogenetically different (Bižic-Ionescu et al., 2015; Rieck et al., 2015) and possess higher and more diversified metabolic activity than their FL counterparts (Smith et al., 1992; Grossart et al., 2007; Lyons and Dobbs, 2012; Rieck et al., 2015). Consequently, even though they represent a small proportion of the community, they disproportionately impact biogeochemical cycles by degrading and consuming POM, leading to DOM and nutrient release (Smith et al., 1992; Azam and Long, 2001; Grossart, 2010).

Bacteria were long considered unique, distinct entities whose behavior was driven by resource availability and abiotic factors (Shapiro, 1998; Strom, 2008; Schmidt et al., 2019). However, we have since realized the importance of social interactions, giving rise to the field of chemical ecology. Marine bacteria operate in unison through a complex web of social networks, which, intertwined with other environmental and abiotic cues, shape community structure and function (Atkinson and Williams, 2009; Schmidt et al., 2019). These communications occur via chemical signaling, i.e., the exchange of chemical signals between organisms, inducing an effect on the behavior and physiology of the participants (Schmidt et al., 2019). Chemical signaling includes quorum sensing (QS), a common mode of bacterial communication. One key question in environmental chemical ecology is the role of QS signals in the regulation of microbial activities, including degradation and mineralization processes. Together, these microscale interactions may ultimately impact large-scale biogeochemical processes. As such, it is essential to understand how they contribute to ecosystem functioning.

This review aims to explore and synthesize our current knowledge of how QS regulates bacterial processes that ultimately impact global biogeochemical cycles in marine environments. First, we describe QS communication principles and the renewed interest QS study in marine environments. We then review the microniches where QS most likely occurs and the main bacterial taxa colonizing them. These main groups are described, presenting their ecological importance and their various QS systems. Thereafter, we summarize how QS regulates bacterial functions that may directly or indirectly impact biogeochemical cycles. Finally, we outline current limitations and future perspectives on the subject.

AN INCREASING FOCUS ON QUORUM SENSING SIGNALS IN MARINE STUDIES

Marine bacteria constantly compete for ecological niches, C and nutrients, giving rise to many biotic interactions. These interactions can be chemically mediated by numerous bioactive metabolites, including QS molecules. QS is a density-based microbial language used to collectively regulate the expression of various genes involved in processes such as bioluminescence, biofilm formation or extracellular metabolite production (Miller and Bassler, 2001; Waters and Bassler, 2005). It depends on the production of small pheromone-like autoinducers (AIs) that are continuously produced and sensed by the cells. QS primarily relies on three components: (i) the AI synthase, which produces the signal molecule; (ii) the signal molecule itself; and (iii) the AI receptor, which initiates the transcriptional regulation of target genes when AIs reach their threshold concentration (Miller and Bassler, 2001; Waters and Bassler, 2005). AIs include *N*-acylhomoserine lactones (AHLs), furanosyl-borate diester (AI-2) and 2-heptyl-3-hydroxy-4-quinolone (*Pseudomonas* quinolone signal, PQS) (**Figure 1**), although a much greater diversity of signaling molecules exists (Miller and Bassler, 2001; Waters and Bassler, 2005). AHLs are the best-studied AIs in marine environments, as they led to the discovery of QS (Nealson et al., 1970; Eberhard, 1972) and are widely used among Gram-negative bacteria (Miller and Bassler, 2001). AHLs are produced by an AHL synthase (*luxI*, *ainS* or *hdtS* family) and released to the surrounding environment through either passive diffusion (short-chain AHLs) or active transport (long-chain AHLs) (Kaplan and Greenberg, 1985; Pearson et al., 1999). More recently, it was discovered that hydrophobic AIs (including long-chain AHLs, CAI-1 and PQS) could also be transported through outer membrane vesicles (Li et al., 2016; Toyofuku et al., 2017;

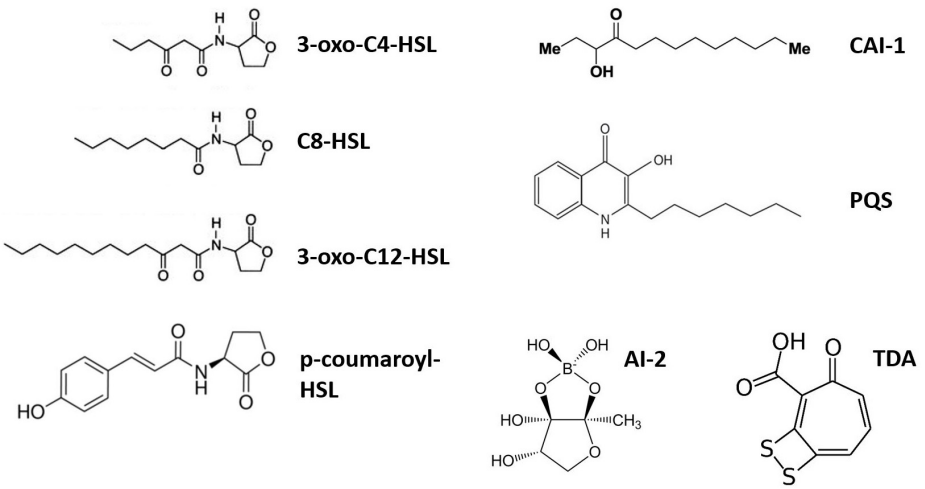

FIGURE 1 | Diversity of AI molecules produced by marine bacteria. Only three AHL (3-oxo- C4-, C8-, and 3-oxo-C12-HSL) structures are illustrated. 3-oxo-C4-HSL, *N*-3-oxo-butyryl-L-homoserine lactone; C8-HSL, *N*-octanoyl-L-homoserine lactone; 3-oxo-C12-HSL, *N*-3-oxo-dodecanoyl-L-homoserine lactone; *p*-coumaroyl-HSL, *N*-(*p*-coumaroyl)-L-homoserine lactone; CAI-1, cholera autoinducer-1 [(S)-3-hydroxytridecan-4-one]; PQS, *Pseudomonas* quinolone signal (2-heptyl-3-hydroxy-4-quinolone); AI-2, furanosyl-borate diester; TDA, tropodithietic acid.

Brameyer et al., 2018; Zhao Z. et al., 2021), facilitating their solubilization and specific delivery (Toyofuku et al., 2017; Brameyer et al., 2018). AHL receptors include cytoplasmic LuxR-type and membrane-bound LuxN-type receptors. Interestingly, both AHL synthases and receptors exist as solos, without an accompanying receptor or synthase, respectively (Fuqua, 2006; Buchan et al., 2016). As many as ∼75% of *luxR* genes are solo receptors (Hudaiberdiev et al., 2015; Subramoni et al., 2015), pointing to the existence of QS-cheaters, i.e., cells that sense AIs without producing them. In addition, QS communications can be shut down by quorum quenching (QQ), adding a layer of complexity to those cell–cell interactions (Grandclément et al., 2016). QQ encompasses different mechanisms, including the enzymatic degradation of AIs (by AHL-lactonase and acylase, for instance) or the blockage of AI reception or production through QS inhibitors (QSIs) (Grandclément et al., 2016; Saurav et al., 2017).

While the concept of QS was elaborated by studying the marine bacterium *Vibrio fischeri* (Nealson et al., 1970; Eberhard, 1972; Fuqua et al., 1994), it was subsequently studied mostly through a medical or agronomic lens (Lami, 2019). Little attention was given to QS from an ecological perspective before the 2000s, when studies from McLean et al. (1997) and Bachofen and Schenk (1998) suggested its importance in natural environments. Given the initial definition of QS (i.e., a cell-density-based system), the focus was almost immediately placed on bacteria colonizing particles living among dense biofilms. One of the first hypotheses was that bacteria colonizing marine snow used QS to synchronize the expression of extracellular hydrolytic enzymes, which are crucial for POM mineralization processes (Gram et al., 2002; Kiørboe et al., 2002). Gram et al. (2002) first reported the production of AHLs within bacterial strains isolated from marine snow, supporting this hypothesis. Since then, the advent of omics techniques has allowed us to better appreciate the importance of QS and QQ in marine genomes and metagenomes (Romero et al., 2012; Doberva et al., 2015; Su et al., 2021), more generally raising the question of the importance of QS in the regulation of marine biogeochemical processes.

MARINE QUORUM SENSING-BASED COMMUNICATIONS OCCUR IN DENSE BACTERIAL HOTSPOTS

In marine environments, QS communications are favored in specific microniches corresponding to densely colonized, biofilm-covered, biotic and abiotic surfaces (Hmelo and Van Mooy, 2009; Hmelo, 2017). Indeed, these microniches contain high OM concentrations, favoring a high cellular density. This allows AI accumulation and exacerbates the potential for bacterial interactions and communications (Moons et al., 2009; Dang and Lovell, 2016). In contrast, QS communication are thought to be limited in FL communities due to the spatial separation between the cells and the limited distance of QS signals diffusion (Hmelo and Van Mooy, 2009; Hmelo, 2017). These high cell-density microniches incidentally correspond to hotspots of bacterially mediated OM transformation and include, among others, marine aggregates, microbial mats, various microbiomes, and anthropogenic contaminants.

Marine aggregates, including marine snow particles, are rich in organic substrates, and are a well-known hotspot of bacterial mineralization mediated by extracellular hydrolytic enzymes (Smith et al., 1992; Dang and Lovell, 2016). These degradation processes are key in the ocean's biogeochemistry, as they solubilize aggregates and thereby modify the flux of sinking POM and its subsequent storage in deep ocean sediments (Smith et al., 1992; Azam and Long, 2001). The

marine communities colonizing aggregates can reach densities of 10^8–10^9 cells mL^{-1} (Azam and Long, 2001; Simon et al., 2002). They are especially enriched in Gammaproteobacteria (e.g., Oceanospirillales, Alteromonadales, Pseudomonadales) and Bacteroidetes (e.g., Flavobacteriales, Sphingobacteriales) but also in Alphaproteobacteria (e.g., Rhodobacterales, Rhizobiales, Rickettsiales), Betaproteobacteria (e.g., Burkholderiales) and Planctomycetes (e.g., Planctomycetales) (Rink et al., 2008; Bižic-Ionescu et al., 2015; Mestre et al., 2017, 2020; Li et al., 2021).

Microbial mats develop at liquid–solid interfaces, such as the water-sediment interface. They are thick, vertically layered biofilm structures experiencing sharp physicochemical gradients driving niche differentiation (van Gemerden, 1993; Visscher and Stolz, 2005). Microbial mats are characterized by some of the highest metabolic rates on earth and usually exhibit tight coupling between autotrophic and heterotrophic processes, resulting in the rapid cycling of elements (Visscher and Stolz, 2005). They are composed of dense microbial communities, whose densities may reach 10^9 cells g^{-1} (Carreira et al., 2015). Coastal microbial mats have been found to mainly host Alphaproteobacteria (e.g., Rhodobacterales and Sphingomonadales), Gammaproteobacteria (e.g., Chromatiales), Deltaproteobacteria (e.g., Desulfobacteriales and Desulfovibrionales), Bacteroidetes (e.g., Flavobacteriales and Sphingobacteriales), Actinobacteria but also Cyanobacteria and Archaea (Bolhuis and Stal, 2011).

The phycosphere is the diffusive boundary layer immediately surrounding phytoplankton cells. It is enriched in DOM and nutrients due to phytoplankton metabolic activity (Seymour et al., 2017). It also contains compounds such as dimethylsulfoniopropionate that act as chemoattractants for chemotactic bacteria (Stocker, 2012; Seymour et al., 2017). Dimethylsulfoniopropionate is an ecologically relevant S-containing metabolite produced by various marine algae and is an important C and S source for microorganisms (Yoch, 2002). Consequently, the phycosphere fosters a dense community of heterotrophic bacteria that process and transform this phytoplankton-derived OM, reaching densities of 10^8–10^{11} cells mL^{-1} (Sheridan et al., 2002). This coupling increases the rate and efficiency of OM transformation (Stocker, 2012; Seymour et al., 2017) and exerts an ecosystem-scale influence on biogeochemistry processes (Seymour et al., 2017). The typical bacteria often found in association with the phycosphere are dominated by Alphaproteobacteria (e.g., Rhodobacterales), Gammaproteobacteria (e.g., Vibrionales and Oceanospiralles) and Bacteroidetes (e.g., Flavobacteriales) (Goecke et al., 2013; Buchan et al., 2014).

Other relevant microbiomes include coral-, macroalga- or vertebrate-associated communities, among others. Macroalgae are especially important in coastal ecosystems, where they account for a large fraction of C burial (Duarte et al., 2005). Macroalgal biomass recycling is mainly mediated by colonizing epiphytic bacteria that form dense biofilms comprising 10^3–10^9 cells cm^{-2} (Martin et al., 2014; Lage and Graça, 2016). Alphaproteobacteria (e.g., Rhodobacterales and Sphingomonadales), Gammaproteobacteria (e.g., Alteromonadales, Pseudomonadales, Vibrionales), Bacteroidetes (e.g., Cytophagales and Flavobacteriales), Firmicutes (e.g., Bacillales), Actinobacteria (e.g., Actinomycetales) or Planctomycetes (e.g., Planctomycetales) are the major components of these communities (Hollants et al., 2013; Martin et al., 2014; Lage and Graça, 2016; Oh et al., 2021).

Finally, anthropogenic contaminants such as hydrocarbons or plastics are emerging microniches with biogeochemical implications. Hydrocarbons, such as alkanes or polycyclic aromatic compounds (PAHs), are solely composed of C and hydrogen. They represent one of the main sources of marine pollution and can persist for years in the environment, where bacteria play a key role in their biodegradation (Duran and Cravo-laureau, 2016). Hydrocarbonoclastic bacteria mostly belong to Gammaproteobacteria-affiliated genera, including specialized genera such as *Cycloclasticus* and *Alcanivorax* (Harayama et al., 2004; Chernikova et al., 2020), but also several other non-specialist bacterial genera such as *Pseudomonas*, *Vibrio* and *Marinobacter* (Dashti et al., 2015; Chernikova et al., 2020; Kumari et al., 2020). The plastisphere (the microbial community colonizing macro- and microplastics) is another niche of emerging relevance in marine biogeochemistry. Every year, tons of plastic waste enter the ocean, and an estimated five trillion plastic particles are currently floating in the seas (Eriksen et al., 2014). Immerged plastics are rapidly colonized by biofilm-forming bacteria, which can reach densities of 10^8 cells cm^{-2} (Schlundt et al., 2020), offering new hotspots for bacterial colonization and activity (Zettler et al., 2013). The plastisphere communities are enriched in bacteria belonging to Bacteroidetes (e.g., Flavobacteriales and Sphingobacteriales), Alphaproteobacteria (e.g., Rhodobacterales and Sphingomonadales), Betaproteobacteria (e.g., Burkholderiales) or Gammaproteobacteria (e.g., Oceanospirillales, Alteromonadales, Vibrionales) (Zettler et al., 2013; Schlundt et al., 2020; Wright et al., 2021).

MAJOR BACTERIAL TAXA COLONIZING MARINE BACTERIAL HOTSPOTS HARBOR QUORUM SENSING COMMUNICATION SYSTEMS

The bacterial hotspots highlighted above are colonized by highly diverse bacteria, dominated by a few reoccurring groups, belonging to the Alphaproteobacteria (e.g., Rhodobacterales and Sphingomonadales), Gammaproteobacteria (e.g., Alteromonadales, Pseudomonadales, and Vibrionales) or Bacteroidetes (e.g., Flavobacteriales). They are ecologically relevant given their abundance and their involvement in all major biogeochemical cycles (**Figure 2**). These groups are notably largely involved in the consumption and transformation of algal-derived organic substrates that constitute the bulk of DOM (Buchan et al., 2016; Teeling et al., 2016). Interestingly, there is overlap between the taxa colonizing the highlighted biogeochemical hotspots and the taxa known to harbor QS systems. Indeed, the AHL-based QS and QQ genes found in marine metagenomics

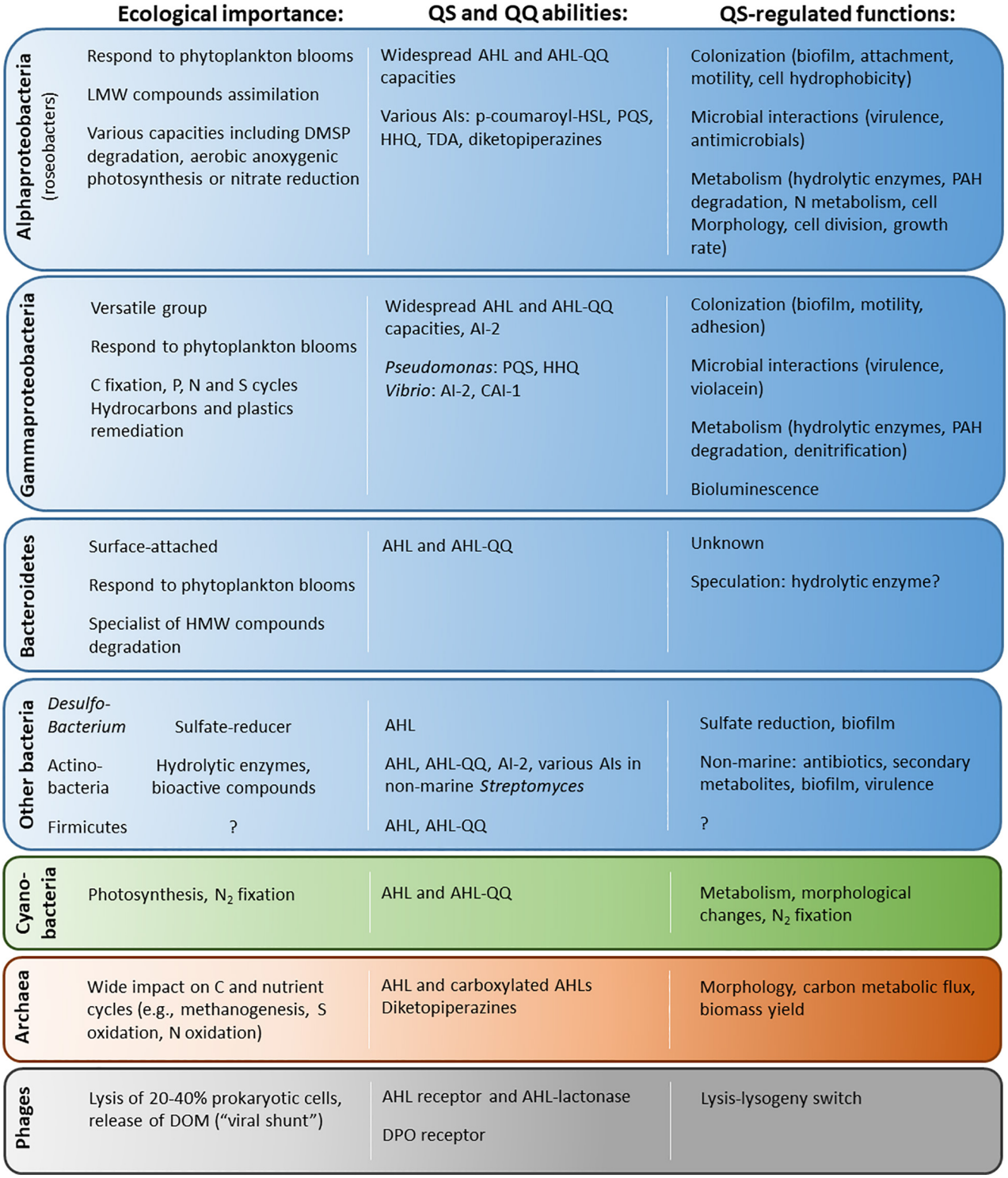

FIGURE 2 | Ecological importance, QS pathways and QS-regulated functions in the main prokaryotic groups (as well as phages) presented in this review. The relevant references can be found in the main text as well as in **Supplementary Table 4** concerning QS circuits.

studies (Romero et al., 2012; Doberva et al., 2015; Huang et al., 2018; Muras et al., 2018; Su et al., 2021) are mostly affiliated with the roseobacter group (Rhodobacterales and Alphaproteobacteria), Gammaproteobacteria genera (such as Pseudomonadales, Alteromonadales or Vibrionales) and Flavobacteriales (Bacteroidetes) (**Supplementary Table 1**). In

addition, several strains affiliated with these groups have been shown to produce AHLs and AI-2 during cultivation (**Figure 2** and **Supplementary Tables 2, 3**). They also encode a variety of other communication systems, although they are much less investigated.

Alphaproteobacteria

Ecological and Biogeochemical Importance

The Alphaproteobacteria class comprises numerous, diverse orders, including Rhodobacterales, Pelagibacterales, and Sphingomonadales. Within the Rhodobacterales order, the roseobacter group is of particular interest (Buchan et al., 2005; Geng and Belas, 2010a). Indeed, it is one of the most readily cultivated and extensively studied marine lineages (Wagner-Döbler and Biebl, 2006; Buchan et al., 2014). In addition, roseobacter members (hereinafter roseobacters) are present in all major marine habitats, including living freely in bulk seawater, in association with phytoplankton, marine snow, and plastics or within sediments and microbial mats (Buchan et al., 2005; Wagner-Döbler and Biebl, 2006; Luo and Moran, 2014). They can constitute up to 25% of the bacterial communities at the ocean surface (Buchan et al., 2005; Luo and Moran, 2014) and have been reported to be major primary colonizers in coastal waters (Dang et al., 2008).

Alphaproteobacteria are thought to primarily consume small organic molecules such as sugar monomers, amino acids, dimethylsulfoniopropionate or phosphonates (Buchan et al., 2005; Wagner-Döbler and Biebl, 2006; Luo and Moran, 2014). They possess versatile metabolic capacities with important implications for the C, N and S cycles: they are able to perform aerobic anoxygenic photosynthesis, degrade sulfur compounds (including dimethylsulfoniopropionate) and aromatics, perform assimilatory and dissimilatory nitrate reduction, and produce multiple bioactive secondary metabolites (Buchan et al., 2005; Wagner-Döbler and Biebl, 2006; Luo and Moran, 2014). They play an especially important role in the microalgal phycosphere, where they are well adapted to form symbioses (Geng and Belas, 2010a).

Quorum Sensing and Quorum Quenching Pathways

Alphaproteobacteria, particularly roseobacters, are widely involved in AHL-based QS communication in marine environments. They constitute the majority of the AHL-producing bacteria isolated from various environments, including marine snow, coastal biofilms, or marine seagrasses (Gram et al., 2002; Wagner-Döbler et al., 2005; Huang et al., 2008; Blanchet et al., 2017; Su et al., 2019; **Supplementary Table 2**). In addition, Rhodobacterales are among the main contributors to AHL-related genes in marine metagenomics studies (Doberva et al., 2015; Huang et al., 2018; Su et al., 2021; **Supplementary Table 1**). The roseobacter group is perhaps the most frequently investigated group in AHL-based QS studies, and this communication system is widespread among its members (Wagner-Döbler and Biebl, 2006; Buchan et al., 2016). It has been shown that 82% of roseobacters possess at least one *luxRI* gene cassette and that 28% possess two (Buchan et al., 2016). Additionally, roseobacters often possess solo *luxI* genes (i.e., genes that are not located near a tandem *luxR* receptor gene), although their ecological role is unclear thus far (Cude and Buchan, 2013; Buchan et al., 2016). Solo *luxI* are especially common among the *Sulfitobacter*, *Ruegeria* and *Phaeobacter* genera (Buchan et al., 2016). Among roseobacters, AHL-based QS seems to be involved in the production of antimicrobials (e.g., indigoidine and tropodiethietic acid), polysaccharide production, gene transfer, biofilm formation and motility, among others (Wagner-Döbler and Biebl, 2006; Buchan et al., 2016).

The marine members of the Alphaproteobacteria also use other QS systems (**Figure 2** and **Supplementary Table 3**), including systems based on tropodiethietic acid, *p*-coumaroyl-homoserine lactone (*p*-coumaroyl-HSL) or AI-2. Tropodiethietic acid is a sulfur-containing molecule whose production is common among roseobacters (Buchan et al., 2016). It plays dual roles, serving both as an antibiotic and an AI signal at subinhibitory concentrations (Geng and Belas, 2010b; Beyersmann et al., 2017). Similar to AHLs, tropodiethietic acid modulates motility, biofilm and antibiotic production in the marine bacterium *Phaeobacter inhibens*, which are important traits during algal colonization (Beyersmann et al., 2017).

In addition, p-coumaroyl-HSL production has been demonstrated in the marine strains *Silicibacter pomeroyi* DSS-3 (Schaefer et al., 2008) and *Ruegeria* sp. KLH11 (Zan et al., 2015). Schaefer et al. (2008) illustrated that an AHL synthase could use a non-fatty acyl substrate to synthesize aryl-HSL derivatives such as p-coumaroyl-HSL, suggesting that a large pool of fatty acids could be used to generate a number of as-yet-undiscovered AI signals. This could be beneficial to organisms using QS to control functions that are useful only under a particular set of conditions (Schaefer et al., 2008), including during algal/bacterial interactions (Schaefer et al., 2008).

Finally, Alphaproteobacteria also seem to use QS systems based on AI-2. This boron-containing molecule is often considered a universal AI mediating interspecies communication (Xavier and Bassler, 2003). However, the function of AI-2 as a QS signal has been debated, since it may also represent a metabolic side-product in a number of bacteria (Diggle et al., 2007; Rezzonico and Duffy, 2008). In any case, AI-2-producing (Blanchet et al., 2017; Tourneroche et al., 2019) and AI-2-sensing (Pereira et al., 2008; Su et al., 2019) marine and soil Alphaproteobacteria have been reported.

Alphaproteobacteria also encode AHL-QQ mechanisms. They represent a large number of marine bacterial isolates with QQ capacities (Romero et al., 2011a; Blanchet et al., 2017; Rehman and Leiknes, 2018; Su et al., 2019; **Supplementary Tables 2, 3**). Zhao et al. (2019) reported that marine Alphaproteobacteria constituted 21% of marine isolates with potential AHL-QQ capacities (across 19 reviewed studies). Quite interestingly, Alphaproteobacteria are not the main contributors of enzymatic QQ-related sequences (AHL lactonases and acylases) according to metagenomics studies (Huang et al., 2018; Su et al., 2021). This could suggest that they mainly employ QSI-based QQ, although this could also result from a cultivation bias.

Gammaproteobacteria

Ecological and Biogeochemical Importance

Gammaproteobacteria is one of the most genus-rich prokaryotic taxa. This class includes the well-studied Vibrionales order as well as other easily culturable bacterial genera, such as *Alteromonas*, *Pseudoalteromonas*, *Marinomas*, or *Oceanospirillum* (Fuhrman and Hagström, 2008). Consequently, the Gammaproteobacteria is a diverse group and its members can thrive under various conditions. They can constitute up to 40% of the bacterial community in different oceans (Sunagawa et al., 2015), sediments (Zinger et al., 2011; Dyksma et al., 2016), or marine snow (Mestre et al., 2017).

This phylogenetic diversity translates into a variety of metabolic functions and an important contribution to biogeochemical-related processes. Gammaproteobacteria generally have high potential growth rates and have been shown to respond rapidly to OM concentration increases (Fuhrman and Hagström, 2008). As such, they participate in C mineralization by processing phytoplankton-derived compounds during blooms with a lifestyle that overlaps with those of Bacteroidetes and Alphaproteobacteria, consuming both high and low molecular weight molecules (Ferrer-González et al., 2021; Francis et al., 2021). Gammaproteobacteria also play a major role in dark C fixation in coastal sediments, representing an important C sink (Dyksma et al., 2016). In addition, they widely participate in P, N, and S nutrient cycles in different habitats (Villarreal-Chiu et al., 2012; Baker et al., 2015; Zhou et al., 2020). Finally, Gammaproteobacteria play an important role in the bioremediation of anthropogenic pollutants such as hydrocarbons or plastic particles. For instance, bacteria of the *Alcanivorax* genus (Oceanospirillales) are able to degrade petroleum hydrocarbons and are among the first responders to oil spills (Harayama et al., 2004). Several other Gammaproteobacteria genera have been shown to degrade hydrocarbons such as *Marinobacter*, *Oleiphilus*, and *Oleispira* but also the more generalists *Vibrio*, *Pseudoalteromonas,* or *Marinomonas* (Harayama et al., 2004; Zhou et al., 2020). Likewise, plastics are hydrocarbon-derived polymers that can be biodegraded by marine Gammaproteobacteria, notably *Pseudomonas*- or *Vibrio*-affiliated strains (Jacquin et al., 2019; Roager and Sonnenschein, 2019).

Quorum Sensing and Quorum Quenching Pathways

The Gammaproteobacteria class probably contains bacteria with the best-characterized AHL-based QS systems, such as members of the *Vibrio*, *Pseudomonas,* and *Acinetobacter* genera. They are also among the most common AHL producers isolated from various marine habitats (Cuadrado-Silva et al., 2013; Jatt et al., 2015; Freckelton et al., 2018; Charlesworth et al., 2019; Reen et al., 2019; Su et al., 2019; Urvoy et al., 2021a; **Supplementary Table 2**). In addition, they constitute the main class contributing to AHL production and sensing genes in marine metagenomics surveys, especially members of Vibrionales, Pseudomonadales, or Alteromonadales (Doberva et al., 2015; Huang et al., 2018; Su et al., 2021; **Supplementary Table 1**). Gammaproteobacteria AHL pathways have been shown to control various phenotypes with potential biogeochemical relevance, such as biofilm formation, hydrolytic enzyme (including metalloproteases, chitinase, caseinase, amylase, alkaline phosphatase, and DNAse) production, siderophore production and motility (reviewed in Torres et al., 2019).

In addition to AHL signals, marine Gammaproteobacteria possess a range of diverse, interconnected QS pathways involved in inter- and intraspecies communication, and based on AI-2, PQS or CAI-1 signals, among others (**Figure 2** and **Supplementary Table 3**). As noted previously, the function of AI-2 as a QS signal has been debated but has been demonstrated in several *Vibrio* and *Shewanella* strains (Sun et al., 2004; Bodor et al., 2008; Rezzonico and Duffy, 2008). AI-2 can be sensed by the periplasmic binding receptors *luxPQ* (In *Vibrionaceae*), LsrB and probably other uncharacterized receptors (Chen et al., 2002; Zhang et al., 2020). The AI-2 system has notably been demonstrated to regulate bioluminescence, biofilm formation, motility, chemotaxis, proteases and virulence factor production in various strains, such as the marine *V. harveyi* (reviewed in Pereira et al., 2013).

Pseudomonas quinolone signal, as suggested by its name, is a QS signal that is considered to be specific to the *Pseudomonas* genus. The production of PQS is encoded by the *pqsABCDE* operon, and its immediate precursor is HHQ (4-hydroxy-2-heptylquinoline), which also acts as an AI. The PQS system has mostly been studied in clinical *Pseudomonas* strains, where it regulates virulence factors (such as biofilm, elastase, rhamnolipid or pyocyanin) production and promotes infection (as reviewed in García-Reyes et al., 2020). However, the synthesis of PQS and HHQ has been discovered in other genera, such as *Burkholderia* and a marine *Pseudoalteromonas* bacterium (Vial et al., 2008; Paulsen et al., 2020). In addition, it has been shown that PQS acts as a signal molecule in several Gram-negative and Gram-positive strains (including marine isolates) (Reen et al., 2011) as well as in multispecies marine communities (Wang et al., 2020), highlighting its role as a possible interspecies signal.

Finally, the CAI-1 signaling molecule is an example of an intraspecies-specific AI that is used among the *Vibrio* genus and synthesized by the CqsA protein (Henke and Bassler, 2004). This AI could regulate virulence factors operating through the CqsS receptor (Henke and Bassler, 2004). Its relevance in the ocean still has to be studied, especially in niches where *Vibrio* are dominant, such as on certain plastic particles (Zettler et al., 2013) or macroalgae (Hollants et al., 2013).

Marine Gammaproteobacteria are also actively engaged in AHL-QQ mechanisms involving both QQ enzymes and QSIs. Several studies have reported that isolated marine Gammaproteobacteria strains possess QQ capacities, in which they were often the most represented taxon (Torres et al., 2016; Freckelton et al., 2018; Su et al., 2019; Urvoy et al., 2021a; **Supplementary Table 2**). In their review, Zhao et al. (2019) reported that 27% of marine bacterial isolates with QQ capacities were Gammaproteobacteria. In addition to the common AHL acylase and lactonase, marine strains have been reported to produce QSIs such as cyclic peptides (*Marinobacter* sp., *Photobacterium halotolerans*) or phenol derivatives (*Vibrio*

alginolyticus) (as reviewed in Saurav et al., 2017 or Zhao et al., 2019). In marine metagenomics, Gammaproteobacteria often constitute the majority of AHL-QQ enzyme sequences (Huang et al., 2018; Su et al., 2021; **Supplementary Table 1**).

Bacteroidetes

Ecological and Biogeochemical Importance

Bacteroidetes are thought to be among the most abundant groups of marine bacteria with the Proteobacteria and Cyanobacteria (Kirchman, 2002), contributing up to 50% of the total bacteria in some marine ecosystems (Cottrell and Kirchman, 2000; Acinas et al., 2015). The Bacteroidetes phylum comprises the Bacteroidia, Flavobacteria, Sphingobacteria, and Cytophagia classes. Bacteroidetes mostly live attached to surfaces such as aggregates and micro- or macroalgae (Kirchman, 2002). They can constitute one of the most abundant phyla detected on marine and estuarine particles (Delong et al., 1993; Ploug and Grossart, 1999), which was linked to their capacities to colonize surfaces and degrade complex, recalcitrant polymers (Kirchman, 2002). Indeed, Bacteroidetes (particularly Flavobacteriales) are largely considered specialists in polymers degradation and comparative genomics has demonstrated that they contain many peptidases and carbohydrate-active enzymes (Cottrell and Kirchman, 2000; Thomas et al., 2011; Fernàndez-Gómez et al., 2013). Bacteroidetes have evolved a unique degradation system known as polysaccharide utilization loci, in which all relevant genes involved in the cleavage of a particular carbohydrate are grouped together (Grondin et al., 2017). They often include energy-dependent TonB-dependent transporters that allow the sequestration of large molecules in the periplasmic space prior to further degradation, protecting them from scavenging bacteria (Grondin et al., 2017).

Quorum Sensing and Quorum Quenching Pathways

Despite their importance in colonization and OM degradation, Bacteroidetes are not well studied in terms of QS pathways. However, several marine Bacteroidetes strains have been shown to produce AHLs during cultivation, such as *Flammeovirga* sp., *Muricauda* sp., *Tenacibaculum* spp., *Maribacter* sp. and *Aquimarina* sp. (Huang et al., 2008; Romero et al., 2010; Abdul Malik et al., 2020; **Figure 2** and **Supplementary Tables 2, 3**). In addition, genes related to AHL sensing (Su et al., 2021) and AI-2 synthesis (Huang et al., 2018) have been affiliated with Bacteroidetes during metagenomic surveys (**Supplementary Table 1**). It seems that marine Bacteroidetes show widespread QQ capacities, as highlighted by several studies (Romero et al., 2010, 2011a, 2012; Su et al., 2019; **Supplementary Table 2**). Zhao et al. (2019) found that Bacteroidetes represented 9% of QQ-capable marine bacterial isolates across 19 studies. Su et al. (2021) also reported that Flavobacteriales contributed to the lactonase and acylase AHL-QQ gene pool during a marine metagenomic study. An interesting finding has been made by Barriuso and Martínez (2018) concerning QS pathways in environmental Bacteroidetes. They examined the QS-related genes (AHLs and AI-2 synthases and receptors) present in 22 metagenomes from natural and artificial biofilm habitats and found that all sequences related to Bacteroidetes corresponded to LuxR-encoding genes. The imbalanced ratio between AHL receptors and synthases points toward the existence of AHL-QS cheaters in this group. This also seems to be reflected by marine metagenomics studies, as Su et al. (2021) showed that Flavobacteriales contributes to AHL-sensing and AHL-QQ genes, although they do not contribute to the AHL-synthase gene pool. Given the lack of data on this phylum, the physiological processes under QS control in Bacteroidetes are far from elucidated, especially concerning the potential role of QS in OM degradation.

Other Groups

Alphaproteobacteria, Gammaproteobacteria and Bacteroidetes represent the majority of isolated bacteria with QS or QQ capacities and are the main contributors of QS genes in marine metagenomic datasets. However, some data show that other ecologically relevant microorganisms may use QS communications, notably members of Actinobacteria, Firmicutes, Cyanobacteria, Archaea and even bacteriophages.

Actinobacteria

Actinobacteria (Gram-positive) are ubiquitous in the ocean realm (Giovannoni and Stingl, 2005) and can reach high abundance in deep-sea sediments (Zinger et al., 2011; Chen et al., 2016), marine aggregates (Grossart et al., 2004) and macroalgae (Oh et al., 2021). Although their metabolism and roles are largely unknown, these bacteria possess various extracellular hydrolytic enzymes that are able to degrade recalcitrant OM (Lam, 2006; Chen et al., 2016). They are also recognized for their production of diverse bioactive compounds (Lam, 2006; Chen et al., 2016). In terms of QS, several marine AHL-producing strains have been isolated from marine snow (Su et al., 2019), microbial mats (Charlesworth et al., 2019) or marine sponges (Bose et al., 2017; **Supplementary Tables 2, 3**). In addition, AHL-quenching strains affiliated with Actinobacteria have been isolated from various coastal communities (Romero et al., 2011a), the Mediterranean Sea (Muras et al., 2018), the Colombian Caribbean Sea (Betancur et al., 2017) and marine snow (Su et al., 2019; **Supplementary Table 2**). These bacteria are mostly affiliated with genera such as *Streptomyces*, *Salinispora* or *Microbacterium*. Actinobacteria also use other QS systems based on AIs such as gamma-butyrolactone or AI-2 (reviewed in Polkade et al., 2016), although this has not been well explored in marine bacteria.

Firmicutes

Firmicutes members are mostly Gram-positive bacteria. Their role and prevalence in the oceans are poorly characterized, but they can constitute an important fraction of the epiphytic macroalgal community (Hollants et al., 2013; Oh et al., 2021), microbial mats (Bolhuis and Stal, 2011) and sediments (Zinger et al., 2011). A few studies have reported Firmicutes-affiliated strains isolated from marine environments with AHL-based QS or QQ capacities (**Supplementary Table 2**). AHL production has been reported in genera such as *Bacillus* spp. (Freckelton et al., 2018; Charlesworth et al., 2019), *Exiguobacterium* sp. (Biswa and Doble, 2013), *Virgibacillus* sp. (Charlesworth et al., 2019) and *Halobacillus*

sp. (Charlesworth et al., 2019). In addition, strains such as *Bacillus* spp. (Kanagasabhapathy et al., 2009; Romero et al., 2011a; Teasdale et al., 2011), *Planomicrobium chinense* (Muras et al., 2018) and *Oceanobacillus* sp. (Romero et al., 2011a) have showed QQ capacities.

Cyanobacteria

As obligate phototrophs, Cyanobacteria are commonly found in the photic zone of all oceans and can account for up to 90% of primary production in oligotrophic waters (Stockner, 1988). Cyanobacteria play a crucial role in N_2 fixation, which significantly contributes to global N budgets (Fuhrman and Hagström, 2008). Although QS is not well studied in cyanobacteria, at least two reports have demonstrated AHL production in non-marine axenic cultures of cyanobacteria. Sharif et al. (2008) demonstrated that the epilithic colonial cyanobacterium *Gloeothece* PCC6909 (and its sheathless mutant PCC6909/1) produced C8-HSL, which seemed involved in carbohydrate and amino acid metabolism. Zhai et al. (2012) reported that a lacustrine *Microcystis aeruginosa* PCC7820 produced three putative AHLs, although their structure was not fully determined. The authors suggested that QS might regulate morphological changes. In addition, several marine cyanobacteria have been shown to produce AHL-QSIs (as reviewed in Saurav et al., 2017) and AHL-QQ enzymes (Romero et al., 2008). For example, the marine nitrogen-fixing bacterium *Anabaena* sp. PCC7120 produces the AHL-lactonase AiiC which has a wide range of AHL degradation capacities (Romero et al., 2008).

Archaea

Although archaea were initially considered extremophiles, they have since been shown to be present in nearly every marine environment, representing an estimated number of $\sim 10^{28}$ cells in the oceans (Karner et al., 2001). They are particularly abundant in the deep ocean, where they can constitute up to 39% of the total picoplanktonic community (Karner et al., 2001). Archaea perform important functions such as methanogenesis, S oxidation and ammonia oxidation (Jarrell et al., 2011; Santoro et al., 2019). Few papers have addressed QS communications in archaea thus far, especially in marine environments. To our knowledge, only Charlesworth et al. (2020) identified marine archaeal strains that induce an AHL biosensor. In addition, Su et al. (2021) highlighted AHL-lactonase sequences affiliated with archaea during a marine metagenomics survey. Additional studies were performed in non-marine environments, suggesting that QS could be an overlooked mechanism in marine archaea. For instance, several archaeal strains isolated from various lakes activated AHL biosensors (Paggi et al., 2003; Liao et al., 2016; Charlesworth et al., 2020), although the underlying compounds were not analytically determined. The *Methanosaeta harundinacea* 6Ac strain, isolated from an anaerobic digester, produces carboxylated AHLs that modulates cell morphology and C metabolic fluxes (Zhang et al., 2012). In addition, the authors identified the first putative archaeal AHL synthase, which was different from any known bacterial synthase (Zhang et al., 2012). Rajput and Kumar (2017) identified numerous solo *luxR* genes by mining the Interpro archaeal genomes. Finally, outside of the AHL system, the lacustrine halophilic *Haloterrigena hispanica* was shown to use diketopiperazines as a QS signal, although their role remains unclear (Tommonaro et al., 2012). Archaeal enzymes and overall metabolism vastly differ from bacteria. As such, the presence of bacterial QS systems in Archaea could point to a punctual adaptation (e.g., lateral gene transfer) to their environment, although this should be further investigated.

Bacteriophages

Viruses are by far the most abundant entities in the oceans: although they represent only 5% of the marine bacterial biomass, they constitute up to 94% of marine microorganisms (Suttle, 2007). By lysing 20–40% of prokaryotes in surface waters each day, bacteriophages shape the bacterial community composition (BCC) and release copious amounts of labile DOM ("viral shunt"), thus playing a major role in marine biogeochemistry (Suttle, 2005, 2007). Recent studies highlighted that phages could harbor genes related to bacterial QS. Silpe et al. (2020) reported that the *vibriophage* VP882, infecting *Vibrio cholera,* carries a gene encoding a DPO-binding (3,5-dimethylpyrazin-2-ol, an AI used by *V. cholera*) protein driving the lysis-lysogeny decision. In addition, several phages seem to encode AHL-receptor *luxR* genes, including two phages infecting *Aeromonas* spp. (Silpe and Bassler, 2019) and marine flavobacterial phages (Bartlau et al., 2021). Finally, Su et al. (2021) reported phage-affiliated AHL lactonases during a metagenomics study.

QUORUM SENSING-REGULATED PHENOTYPES ARE BIOGEOCHEMICALLY RELEVANT IN MARINE ENVIRONMENTS

The numerous QS circuits present among marine bacteria could directly impact biogeochemical cycles through the transcriptional regulation of genes involved in degradation, C allocation and nutrient acquisition, among others. QS may also indirectly modulate those phenotypes by altering bacterial community structure and functions, which has been highlighted in both marine bacterial strains and complex bacterial communities (**Figure 3** and **Supplementary Tables 3, 4**).

Quorum Sensing Directly Impacts Organic Matter Degradation, Carbon Allocation and Nutrient Acquisition

(i) Organic Matter and Pollutant Degradation

One of the best-studied functions of QS expression in the marine environment is the regulation of extracellular hydrolytic enzyme production, including cell-bound and dissolved (i.e., cell-free) enzymes. The bacterial degradation of OM by hydrolytic enzymes is essential to marine life, as it allows heterotrophic bacteria to grow and initiates the microbial loop (Arnosti, 2011). The possible role of QS in synchronizing hydrolase expression in bacteria would impact C, P, and N cycles through the degradation of various polymers. Several studies have examined

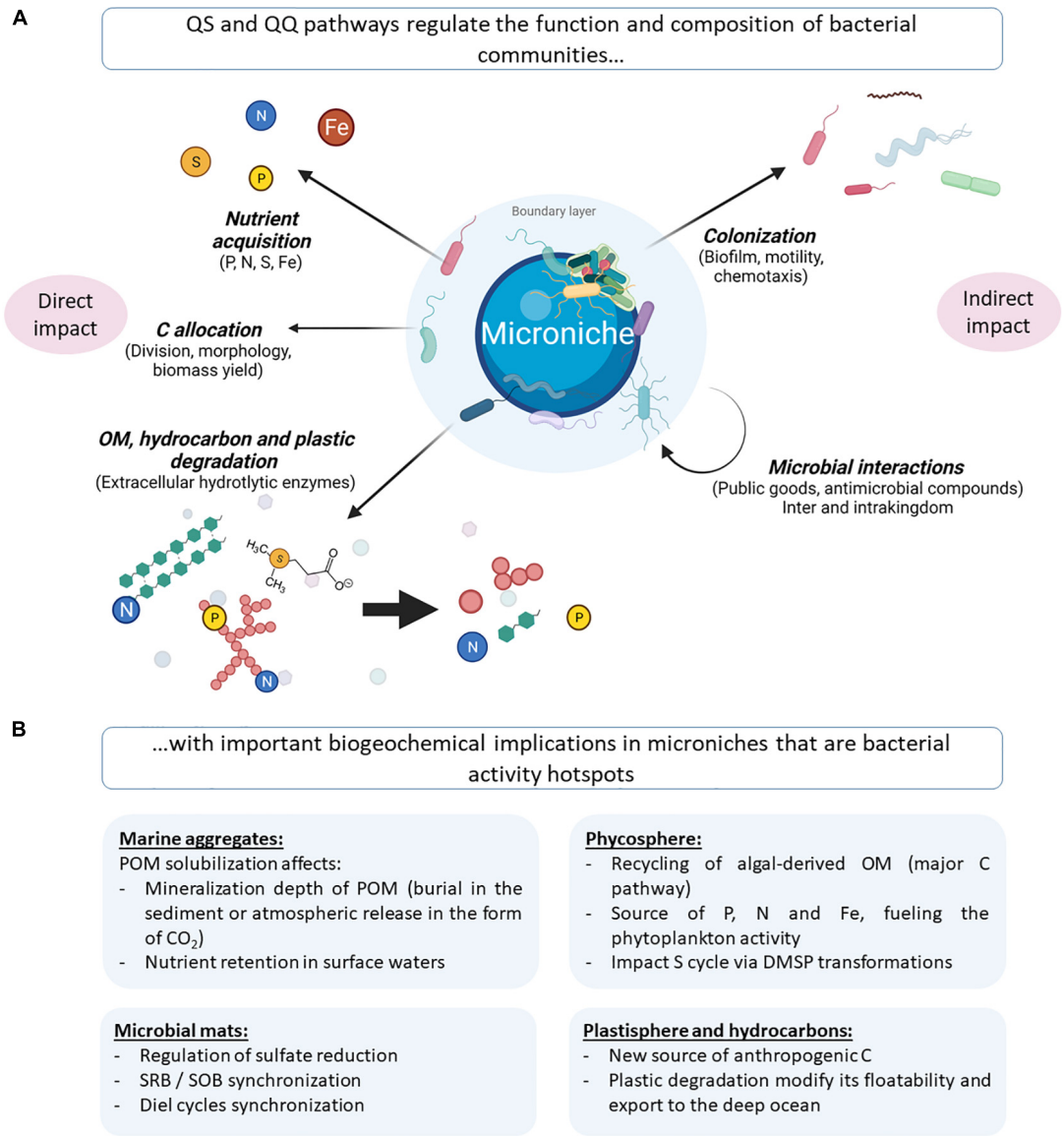

FIGURE 3 | (A) Illustration of QS-regulated processes that potentially impact biogeochemical cycles, either directly through the modulation of OM degradation and nutrient acquisition (left) or indirectly through the modulation of the microbial composition (right). **(B)** Illustration of the repercussions of the highlighted QS-regulated processes in microniches that are bacterial activity hotspots. OM, organic matter; POM, particulate organic matter; DMSP, dimethylsulfoniopropionate; SRB, sulfate-reducing bacteria; SOB, sulfide-oxidizing bacteria. Created with BioRender.com.

the implications of QS in hydrolase expression in either isolated strains (Jatt et al., 2015; Su et al., 2019; Urvoy et al., 2021a) or natural bacterial communities from various environments (Hmelo et al., 2011; Van Mooy et al., 2012; Krupke et al., 2016; Su et al., 2019; Urvoy et al., 2021b; **Supplementary Table 4**). These studies, mainly performed in the context of AHL-based QS, have largely demonstrated the complexity of QS regulation, as no clear pattern has emerged.

Hmelo et al. (2011) were the first to demonstrate that the addition of AHL signals (3-oxo-C6-HSL or 3-oxo-C8-HSL) to bacterial communities colonizing marine snow particles increased their extracellular aminopeptidase, lipase and phosphatase activities (total activity, including cell-bound and cell-free activities). These findings were later reinforced by Krupke et al. (2016) and Su et al. (2019). Krupke et al. (2016) found that AHL amendment (3-oxo-C8-HSL or a cocktail of C10-, C12- and C14-HSL) caused as much inhibition as stimulation of extracellular aminopeptidase, lipase and phosphatase (total activity) across five locations in the Atlantic and Pacific oceans. They particularly highlighted the complexity of these cell–cell mechanisms, as the responses varied depending on the sampling location, AHL concentration, and time scale. Su et al. (2019) demonstrated that the addition of 3-oxo-C8-HSL to marine snow collected in the Yellow

Sea upregulated galactosaminidase and β-xylosidase but downregulated β-glucosidase and mannosidase (cell-free activity) extending QS involvement to glucosidases. Van Mooy et al. (2012) made similar observations in epibiontic bacteria colonizing *Trichodesmium* colonies, demonstrating that the addition of C8-, 3-oxo-C8-HSL and long-chain AHLs (a cocktail of C10-, C12- and C14-HSL) induced a doubling of extracellular alkaline phosphatase activity (total activity). Finally, Urvoy et al. (2021b) showed that the addition of low concentrations of C4-, C6-, 3-oxo- C8-, C12- or C16-HSL to coastal bacterioplankton communities sampled in two contrasting stages of the spring phytoplankton bloom differently modified their extracellular leucine aminopeptidase, *N*-acetyl glucosaminidase, lipase and β-glucuronidase activities (total activity), further highlighting the complexity of QS regulation.

A few studies on isolated strains have illustrated the implications of AHL-based QS in hydrolytic enzyme regulation. Jatt et al. (2015) showed that in *Pantoea ananatis B9* (Enterobacteriales, Gammaproteobacteria) isolated from marine snow, extracellular (cell-free) phosphatase activity was increased by C10-HSL amendment and decreased by the AHL-lactonase AiiA. Su et al. (2019) highlighted that lipase (cell-free) production was increased by several AHLs and decreased by the AHL-lactonase MomL in *Ruegeria mobilis Rm01* (Rhodobacterales, Alphaproteobacteria) isolated from marine snow. Finally, Urvoy et al. (2021a) tested the effect of endogenous AHL disruption on both cell-free and cell-bound β-glucosidase and leucine aminopeptidase in 28 estuarine strains affiliated with Gammaproteobacteria (Pseudomonadales, Vibrionales and Enterobacterales) and Bacteroidetes (Sphingobacteriales) using a lactonase preparation. AHL disruption affected the activity of at least one enzyme in 23 strains, resulting in both increased and decreased activities. Interestingly, AHL disruption could differentially regulate cell-bound and cell-free activities in some strains, highlighting the need to study the two pools of extracellular enzymes separately. In addition to these widespread hydrolases, QS was shown to regulate more specific enzymes degrading anthropogenic compounds in several marine strains. For instance, Mangwani et al. (2015) showed that the marine bacterium *Pseudomonas aeruginosa* N6P6 (Gammaproteobacteria) used AHL-based QS to regulate PAH (phenanthrene and pyrene) degradation, which was reduced in the presence of an AHL QSI. Kumari et al. (2020) later showed that the same strain mediated naphthalene degradation through QS-regulated naphthalene dioxygenase gene expression. In addition, Yu et al. (2020) used deletion mutants to highlight that the strain *Croceicoccus naphthovorans* PQ-2 (Sphingomonadales, Alphaproteobacteria), isolated from a marine biofilm, could degrade various PAHs and that AHL-based QS regulated several of its PAH-degrading genes. Finally, Huang et al. (2013) highlighted the evident overlap between PAH degradation and AHL-related genes in bacteria and supported this hypothesis by mining the NCBI genome database, suggesting that AHL-based regulation could play a pivotal role in the bioremediation of hydrocarbons and PAHs.

Much less is known about the impact of non-AHL QS signals on hydrolytic enzymes, which could either exacerbate or mitigate AHL-based regulation. Indeed, Van Mooy et al. (2012) showed that the addition of (S)-4,5-dihydroxy-2,3-pentanedione (DPD, which spontaneously transforms into AI-2 in seawater) decreased extracellular phosphatase production by the epibiont of *Trichodesmium* colonies, while AHL addition increased phosphatase activity. In contrast, Su et al. (2019) demonstrated that AI-2 addition increased lipase production in *R. mobilis* Rm01 (Alphaproteobacteria), similar to the effect of AHL amendment.

It is clear that QS is an important mechanism involved in hydrolytic enzyme regulation with potentially strong ecological implications in all the mentioned microniches. In aggregates and marine snow, the QS-based regulation of hydrolases could impact the solubilization of sinking POM, retaining particles and nutrients in surface waters (Hmelo et al., 2011). In the phycosphere, the degradation of organic P by QS-regulated-alkaline phosphatase may impact the productivity of the broader phytoplanktonic community and P cycling at the ocean surface (Van Mooy et al., 2012). The regulation of enzymes degrading hydrocarbons could play a pivotal role in their bioremediation, generating new C sources for marine bacteria and affecting the transport of those compounds to the deep ocean. However, these regulation mechanisms seem to be extremely complex, as no clear trend has emerged: QS-based regulation impact different sets of activities in both isolated strains and natural communities, and AI amendment or disruption can provoke both an increase or decrease in activity, respectively. In addition, these studies highlight the need to investigate both cell-bound and cell-free activities separately.

(ii) Carbon Allocation

As the main component of life, it is of utmost importance to understand the mechanisms driving the marine C cycle. In addition to regulating the degradation of C-containing substrates, QS could influence the marine C cycle in more subtle ways by altering phenotypes involved in cell morphology and biomass yield. Using transcriptomic and mutant construction techniques, Patzelt et al. (2013) demonstrated that QS induced morphological heterogeneity and controlled cell division in the marine bacterium *Dinoroseobacter shibae* (roseobacter, Alphaproteobacteria). Indeed, the wild-type (AHL-producing) strain exhibited a heterogeneous cell morphology, with the coexistence of ovoid and rod-shaped cells reaching up to 10 μm. The elongated cells divided by forming one smaller daughter cell (polar growth), while small ovoid cells divided by binary fission, yielding two equally sized cells. In contrast, the *luxI* knockout mutant (non-AHL-producing) grew faster, was homogeneous in terms of size and morphology (small ovoid rods) and replicated only via binary fission. As such, by controlling morphology, cell division and growth rates, QS ultimately impacts the utilization and cellular allocation of C. This induced morphological heterogeneity could be beneficial under changing conditions, such as in the phycosphere during a bloom. Other reports in non-marine bacteria further suggest QS involvement in such processes. For instance, in *Escherichia coli*, AI-2-based QS was reported to modify cell division, cell shape and morphology (DeLisa et al., 2001; Sperandio et al., 2001). Zhang et al. (2012) reported that in the archaeon

Methanosaeta harundinacea 6Ac (isolated from an anaerobic digester), carboxylated AHLs facilitated the transition from a short cell morphology to filamentous growth. This change in morphology was accompanied by important changes in metabolism, with an altered carbon metabolic flux that reduced the cellular biomass yield.

(iii) Phosphorus Acquisition

Phosphorus is an important element involved in energy storage, cell structure, signal relay and genetic material (White and Dyhrman, 2013). In the ocean, P is essentially available to microorganisms in its phosphate form, which can be released from dissolved and particulate organic P using alkaline phosphatases (Chróst, 1990). As outlined above, AHLs and AI-2 were shown to impact alkaline phosphatase activities (Hmelo et al., 2011; Van Mooy et al., 2012; Krupke et al., 2016). However, QS could be involved in many more mechanisms impacting the fate of this nutrient, as recently demonstrated by Xu et al. (2021) in a lacustrine community. AHL addition to a limnic epiphytic biofilm showed that QS mediated both intra- and extracellular P entrapment, i.e., P storage in polyphosphate-accumulating bacteria or extracellular polymeric substances (EPS) (Xu et al., 2021). QS promoted intracellular P entrapment via the upregulation of 43% of the genes identified as being involved in inorganic and organic P accumulation (e.g., alkaline phosphatases *phoA*, *phoX*, and *phoD*), P uptake and transport (e.g., phosphate-specific transport operon *pst*), and P regulation (e.g., *phoB*, *phoR*, and *phoU*), as determined via metatranscriptomics. In addition, it promoted extracellular P entrapment via the upregulation of EPS production and the modification of their composition. EPS impact P entrapment by complexing with phosphate through the amine groups present in their polysaccharidic and proteic fractions (Xu et al., 2020). Although performed in a lacustrine biofilm, we hypothesize that similar mechanisms occur in marine environments. QS-regulated P acquisition could be important in the phycosphere, especially in P-limited environments where bacteria could supply (or compete for) available P to phytoplankton cells.

(iv) Nitrogen Acquisition

Nitrogen is an important macronutrient and one of the main factors limiting primary production in the oceans (Pajares and Ramos, 2019). It mainly occurs as dinitrogen (N_2), only available to nitrogen-fixing microorganisms (mostly cyanobacteria) that convert it into more available forms, such as ammonium, thereby playing a critical role in the N cycle (Voss et al., 2013; Pajares and Ramos, 2019). In addition, processes such as nitrification and denitrification play a crucial role in the maintenance of the global N cycle in the ocean (Pajares and Ramos, 2019). A very limited number of studies have investigated whether QS mediates N transformation in marine (and, more widely, aquatic) environments. For instance, there is strong evidence that QS pathways and denitrification are interconnected in the marine strain *D. shibae*, as illustrated by Koppenhöfer and Lang (2020). These authors re-analyzed several transcriptomic datasets and showed that the redox regulators controlling denitrification (among others) also interacts with the strain QS pathways. One *luxI*-knockout mutant also had significantly overexpressed denitrification genes. In addition, Romero et al. (2011b) showed that AHL amendment to the cyanobacterium *Anabaena* sp. PCCC7120 strongly inhibited its N_2 fixation ability, possibly via the post-transcriptional regulation of nitrogenase activity. The regulation of the bacterially mediated transformation of N compounds by QS pathways has also been suggested in several non-marine studies. QS was notably shown to impact processes such as anaerobic ammonium oxidation, ammonia oxidation and N_2 fixation in soil and wastewater treatment systems (reviewed in Wang et al., 2021; Zhao Z. C. et al., 2021). In addition, AHLs and PQS were shown to regulate denitrification in the clinical isolate *Pseudomonas aeruginosa* PAO1 (Gammaproteobacteria) (Toyofuku et al., 2008). The implications of QS-regulated N transformations in marine environments need to be further investigated. They could have strong implications for the phycosphere, where the phytoplankton cells may benefit from the bacterially mediated fixation of N_2 into available forms.

(v) Sulfur Acquisition

Sulfur is a key element for life and primarily occurs in proteins, coenzymes and ligands binding to proteins. It goes through a complex biogeochemical cycle driven by microbial transformation (Sievert et al., 2007; Muyzer and Stams, 2008). Indeed, marine bacteria can use S-containing compounds as electron acceptors or donors to generate energy (Sievert et al., 2007; Muyzer and Stams, 2008). Sulfate-reducing bacteria (SRB) use sulfate as an electron acceptor for OM degradation, playing an important role in anoxic environments such as sediments and bacterial mats (Muyzer and Stams, 2008). Sivakumar et al. (2019) highlighted the link between QS and sulfate reduction in two SRB: the soil bacterium *Desulfovibrio vulgaris* Hildenborough (Deltaproteobacteria) and the marine bacterium *Desulfobacterium corrodens* (Deltaproteobacteria). The authors measured the effect of three QSIs on sulfate reduction, specific growth rates and biofilm formation. QSI addition significantly decreased the specific growth rates, the biofilm formation and sulfate reduction abilities of the two strains, even at subinhibitory concentrations. In addition, SRB can work in concert with sulfide-oxidizing bacteria (SOB) that use reduced S as an electron donor (Baumgartner et al., 2006). As such, it has been hypothesized that QS could contribute to this synergy by coordinating their metabolism (Decho et al., 2009, 2010; Montgomery et al., 2013), although experimental data are currently lacking. Consequently, QS-mediated S transformations could be especially important in sediments and microbial mats.

(vi) Iron Acquisition

Iron is a vital micronutrient for all living organisms, (co)limiting the growth of microorganisms in nearly all open-ocean waters (Morel et al., 1991). It is involved in numerous metabolic processes, including photosynthesis, respiration and N cycling (Butler, 2005). In addition, Fe is a necessary cofactor for certain alkaline phosphatases, used to access organic P pools (Browning et al., 2017). Bacterial Fe uptake is achieved using siderophores, i.e., Fe-scavenging molecules (Butler, 2005). AHL- and PQS-based QS-regulated siderophore production

has been well documented in a few clinical *Pseudomonas* (Gammaproteobacteria) strains (Ren et al., 2005; Popat et al., 2017) and in several marine *Vibrio* strains (Wang et al., 2007; Wen et al., 2012; McRose et al., 2018). McRose et al. (2018) notably showed that depending on its cell density, the marine bacterium *V. harveyi* could produce either cell-associated or soluble siderophores, which likely serve different purposes depending on the environment and growth contexts. Interestingly, several AIs have been shown to possess siderophore activity (Schertzer et al., 2009), suggesting dual roles of these molecules.

Quorum Sensing Indirectly Impacts Biogeochemical-Related Processes by Modulating the Bacterial Composition

Quorum sensing and QQ can also indirectly impact bacterial processes involved in biogeochemistry by altering the BCC and, consequently, its associated functions. Indeed, different bacterial communities may possess different gene contents related to OM degradation and nutrient cycling, depending on the presence of different functional groups (Zimmerman et al., 2013; Arnosti, 2014). QS pathways could play a pivotal role in the structuration of bacterial communities, although few studies have experimentally demonstrated their impact on marine communities thus far (**Supplementary Table 4**). The mechanisms driving changes in the BCC are unclear and probably multiple. We hypothesize that QS- and QQ-induced changes in the BCC could result from (i) their impact on colonization processes and (ii) their regulation of microbial interactions.

(i) Colonization Processes

Autoinducer diffusing away from AI-producing cells in microniches (e.g., in the marine snow plume or the phycosphere) could mediate the surface colonization of nearby FL bacteria. In this sense, Dobretsov et al. (2007) demonstrated that different QSIs induced changes in the marine bacterial community colonizing polystyrene Petri dishes. The most affected groups were Alphaproteobacteria, Gammaproteobacteria, and Cytophagales (Bacteroidetes). More recently, Huang et al. (2019) demonstrated that AHL disruption in marine communities colonizing immersed steel coupons coated with the QQ AHL-lactonase *Sso*Pox W263I significantly altered their composition. The lactonase-based degradation of AHLs greatly reduced the abundances of Burkholderiales (Betaproteobacteria), Pseudomonadales (Gammaproteobacteria), and Rhodospirillales (Alphaproteobacteria), among others. The authors simultaneously demonstrated that lactonase coating resulted in a change in the metabolism of colonizing bacteria, reducing steel coupons biocorrosion.

Quorum sensing could impact the composition of colonizing bacterial communities by regulating various phenotypes, such as motility (e.g., swimming, gliding, swarming, and chemotaxis) and adhesion (e.g., biofilm production and cell hydrophobicity), which are known to drive colonization (Dang and Lovell, 2016; Raina et al., 2019). Numerous examples of QS involvement in these phenotypes in marine strains have been reported. For instance, Fei et al. (2020) demonstrated that QS regulates motility and attachment in two Rhodobacterales-affiliated strains (*Sulfitobacter pseudonitzschiae* F5 and *Phaeobacter* sp. F10). Gardiner et al. (2015) showed that a *luxR* knockout of marine *Nautella italica* R11 (roseobacter) could not form biofilms or attach to the red alga *Delisea pulchra*. Yu et al. (2020) showed that QS regulated cell hydrophobicity in marine *C. naphthovorans* PQ-2, driving its adhesion to PAHs. QS widely regulates motility in marine strains affiliated with *Vibrio* (Lupp and Ruby, 2005; Tian et al., 2008) and *Pseudoalteromonas* (Ayé et al., 2015). Finally, several studies have implicated QS in biofilm formation among marine and estuarine strains, including *Vibrio* sp. (Liu et al., 2017; Urvoy et al., 2021a), Rhodobacterales (Su et al., 2019; Fei et al., 2020), Pseudomonadales (Mangwani et al., 2015; Urvoy et al., 2021a) and *Pseudoalteromonas* sp. (Ayé et al., 2015). As such, QS mediation of colonization through motility, chemotaxis and biofilm formation could impact the colonization of microbial communities (thus, their composition) in all the highlighted microniches.

(ii) Microbial Interactions

Once bacterial cells settle into relevant microniches, QS regulates a myriad of phenotypes that could further alter the BCC. Thus far, four studies have demonstrated a direct influence of AI amendment on the composition of marine planktonic communities (Whalen et al., 2019; Urvoy et al., 2021b) and established marine and lacustrine biofilm communities (Wang et al., 2020; Xu et al., 2021). Whalen et al. (2019) showed that HHQ addition to microbial communities sampled along a simulated phytoplanktonic bloom altered the BCC of both PA and FL heterotrophic bacteria, with highly variable effects depending on the bloom stage. Overall, HHQ exposure favored Gammaproteobacteria (including the HHQ producers *Pseudoalteromas* spp.) and Alphaproteobacteria, while the relative abundance of Bacteroidetes decreased. Whalen et al. (2019) also found that HHQ exposure reduced the growth of eukaryotes (especially nanoeukaryotes) without altering their composition. Urvoy et al. (2021b) showed that amendment with low concentrations of different AHLs (50 nM, C4- to C16-HSL) altered the composition of planktonic bacterial communities sampled at two stages of coastal phytoplanktonic spring bloom as well as their hydrolytic activities. Similar to Whalen et al. (2019), the AHL effect widely differed depending on the bloom stage. The AHL treatment mostly affected Bacteroidetes (only Flavobacteriales), Gammaproteobacteria (mainly Vibrionales, Alteromonadales, and Oceanospirillales) and Alphaproteobacteria (only Rhodobacterales). Wang et al. (2020) tested the effect of AHLs (C6- and C12-HSL), PQS and cyclic di-guanosine monophosphate (c-di-GMP) on the taxonomic structure and functional profiles of 9-day-old biofilms developed on Petri dishes in the coastal subtidal zone of Hong Kong Port. They showed that AI amendments altered the taxonomy and structure of the biofilm communities, especially the C12-HSL and PQS treatments. The PQS treatment specifically increased the relative abundance of groups belonging to Alphaproteobacteria (e.g., *Sulfitobacter*, *Thalassospira*, *Ruegeria*, *Erythrobacter*) and Gammaproteobacteria (e.g.,

Alteromonas). The PQS and C12-HSL treatments also increased the relative abundance of genes involved in membrane transport, motility, chemotaxis and cell signaling. Finally, Xu et al. (2021) performed AHL amendments to limnic biofilms (as described above) and showed that it induced a shift in the community composition by increasing the abundance of polyphosphate-accumulating organisms.

The mechanisms driving changes in BCC in these experiments are largely unclear. We can speculate that, in addition to regulating colonization processes, QS further drives these changes by mediating both intra- and interkingdom microbial interactions, for instance, through the regulation of public goods production and prophage lysis. Public goods are compounds providing a collective benefit, including hydrolytic enzymes, siderophores, exopolysaccharides, antibiotics and algaecides (Smith and Schuster, 2019). QS is known to regulate the production of a number of public goods (Whiteley et al., 2017; Mukherjee and Bassler, 2019). In the highlighted articles, QS altered hydrolytic enzymes (Urvoy et al., 2021b) and polysaccharide production (Xu et al., 2021), which could drive changes in the BCC. In the study by Urvoy et al. (2021b), the changes in hydrolytic enzymes and bacterial diversity were correlated, supporting this hypothesis. Additionally, Whalen et al. (2019) indicated that the alteration of phytoplankton growth rates following HHQ exposure suggested that HHQ could mediate interkingdom microbial interactions. Finally, QS could also modulate BCC by triggering the induction of prophages, leading to cell lysis and the release of phage particles. As highlighted above, several phages, including marine phages, have been shown to carry bacterial QS receptors. One of them was shown to regulate the lysis-lysogeny decision in the vibriophage VP882 infecting *V. cholerae* (Silpe et al., 2020). In addition, AHL amendments induced phage lysis in natural soil and groundwater communities (Ghosh et al., 2009; Liang et al., 2020), resulting in the alteration of the BCC in one study (Liang et al., 2020). To our knowledge, the direct link between QS and prophage induction has yet to be demonstrated in marine communities.

CURRENT LIMITATIONS TO INVESTIGATE THE ROLE OF QUORUM SENSING IN MARINE BACTERIAL COMMUNITIES

Quorum sensing regulates several microbial processes, ultimately impacting marine biogeochemistry. However, most of the studies to date were performed on isolated bacteria in dense liquid monocultures, and few of them have investigated the role of QS under environmentally relevant conditions. This can be explained by the complexity of studying cell–cell communication in natural environments, requiring multidisciplinary skills to overcome technical limitations, and by the inherent complexity of QS communications (Whiteley et al., 2017; Schmidt et al., 2019; **Figure 4**).

Technical limitations are a major constraint restricting our capacity to study QS roles and functions in natural environments, whether it concerns the dosage of AIs or the monitoring of the presence and expression of QS genes. The dosing of AI in natural environments presents a challenge because of their low concentrations, their wide range of polarities and the inner complexity of their environmental matrices (Stock et al., 2021). A few studies have achieved AHL dosing in dense environments such as marine snow particles (Hmelo et al., 2011; Jatt et al., 2015), the phycosphere (Van Mooy et al., 2012), microbial mats (Decho et al., 2009), biofilms (Huang et al., 2009; Xu et al., 2021) and sediments (Stock et al., 2021). These reports remain limited, and no study has yet achieved AHL dosing directly in the water column. There is also a lack of quantitative measurements of other AIs in marine environments. Only Wang et al. (2018) reported AI-2 dosing, with a quantification method that required large sample amounts and a concentration step for both seawater and marine biofilms. Pollara et al. (2021) reported the dosing of HHQ in marine waters via a method involving an adsorption step on polystyrene resin, but it required the integration of 400–600 L of seawater. Although AI dosing is necessary, it does not allow the identification of the AI-producing organisms. Metagenomic (or metatranscriptomic) techniques offer the possibility of surveying the presence (or expression) of genes involved in QS and QQ. However, the diversity of the genetic machinery encoding these systems remains under characterized and those genes can be difficult to detect in such datasets. This is especially true for AHL synthase and receptor genes, which are highly variable: known *luxR* and *luxI* genes only share 18–25% and 28–35% similarity, respectively, despite the relatively conserved structure of AHLs (Fuqua et al., 1996). As such, there are most likely new AHL-related gene families to discover. The use of bacterial genes to query archaeal (Zhang et al., 2012) and viral (Silpe and Bassler, 2019) genomes probably contributes to the limited success in the identification of their QS genes thus far.

To circumvent the limitations associated with natural environments, a common method is the isolation and cultivation of bacteria, followed by the screening of their production of QS or QQ compounds using biosensor reporter strains (**Supplementary Table 2**). Biosensor strains are bacteria that have been engineered to produce a detectable response upon AI sensing (production of bioluminescence, fluorescence or pigments). They are often used as a screening tool due to their sensitivity, easy implementation and low cost. Various biosensors have been developed to sense different AIs, including AHLs (Riedel et al., 2001; Steidle et al., 2001), AI-2 (Miller et al., 2004) and PQS and HHQ (Fletcher et al., 2007). However, this workflow also has some disadvantages. First, only a minor fraction of marine bacteria are cultivable. This limits our study capacity to a few bacterial groups whose representativeness may be debatable. Second, biosensors are prone to produce both false-negative and false-positive results. Indeed, AI receptors can bind non-native ligands that acts as agonists (false-positive) or antagonists (false-negative). Such effects have been demonstrated for various receptors with natural and synthetic molecules (Holden et al., 1999; Geske et al., 2008; Swem et al., 2008). Given these drawbacks, biosensors should be used in concert

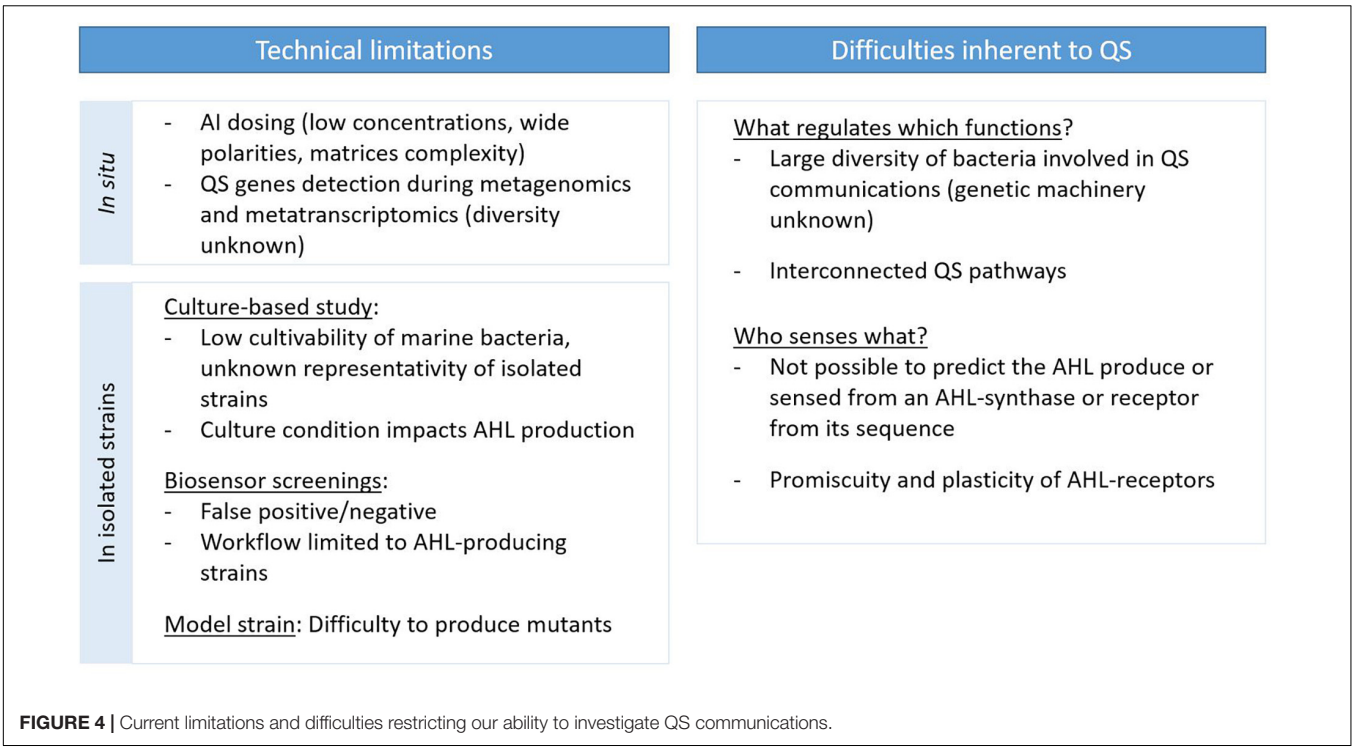

FIGURE 4 | Current limitations and difficulties restricting our ability to investigate QS communications.

with analytical methods to confirm the presence of AIs and to identify and quantify them. These analytical methods often include liquid (LC) or gas chromatography (GC) coupled to mass spectrometry (MS) or tandem MS (MS/MS) (**Supplementary Table 2**). Another limit of this workflow is the dependence upon culture conditions, as factors such as temperature, medium composition (C sources and nutrients) and shaking can influence AI production (Medina-Martínez et al., 2006; Shrout et al., 2006; Boyle et al., 2015). In addition, the use of pure cultures could limit the expression of QS genes (Albataineh et al., 2021). As such, QS systems may be more prevalent than what has been reported to date. The workflow based on bacterial isolation and the detection of AI production *de facto* restricts QS studies to strains that produce AIs. Consequently, marine QS cheaters are not as actively studied as AHL-producing strains despite their well-established prevalence.

Finally, the lack of marine model strains with adequate molecular tools also limits our ability to study the role of QS in ecologically relevant strains. The construction of deletion or recombinant mutants is crucial to identify QS circuits and their regulated functions. However, our capacity to adapt genetic tools to produce mutants is limited, as this process is time-consuming and expensive, and can be especially difficult outside of a few well-managed groups such as in the *Vibrio* genus and in roseobacters (Lami et al., 2021). Consequently, only a few marine bacterial QS models currently exist (Lami et al., 2021), including the marine bacteria *Vibrio fischeri* (in which QS was discovered), *Ruegeria* sp. KLH11 (a model for studying QS in marine sponge symbionts) (Zan et al., 2015) and *Dinoroseobacter shibae* (an algal symbiont characterized by a pronounced pleomorphism) (Patzelt et al., 2013; Koppenhöfer et al., 2019).

Several difficulties in the study of QS pathways are linked to their inherent complexity. QS systems occur in a large diversity of bacteria, and the diversity of the genetic machinery encoding these systems is not well known. A single bacterium can produce a multitude of AIs, and single strains producing more than 20 AHLs have been reported (Ortori et al., 2007; Doberva et al., 2017). In addition, QS pathways based on different AI systems are often interconnected, with different hierarchies between them (Long et al., 2009; Lee and Zhang, 2015). Another difficulty concerning AHL-based QS is the impossibility of predicting the AHL synthesized by an AHL synthase or fixed by an AHL receptor from their genetic sequence, due to their low identity (Fuqua et al., 1996; Wellington Miranda et al., 2021). AHL receptors may exhibit some degree of promiscuity; that is to say that they can fix non-AHL ligands, expanding the range of QS crosstalk and responses (Wellington and Greenberg, 2019; Prescott and Decho, 2020). Very little is known about the factors driving QS system selectivity (Wellington Miranda et al., 2021). They also seem highly plastic and can rapidly evolve to adapt their ligand preference (as reviewed in Prescott and Decho, 2020). Consequently, it is difficult to determine the diversity of bacteria producing or targeted by a given AHL.

FUTURE PERSPECTIVES AND NEW TOOLS TO ADDRESS THE CURRENT CHALLENGES

Several techniques and improvements may alleviate the current constraints and provide new perspectives in environmental QS studies. More specifically, these techniques could help

characterize the diversity of QS systems in marine environments as well as their roles and effective ranges. This would allow us to better appreciate the role of QS as a regulatory mechanism involved in bacterial processes that ultimately affect marine biogeochemistry, especially outside of the few well-characterized bacterial groups, such as *Vibrio* and roseobacters. QS studies can be performed at three scales: (i) in isolated strains, (ii) in simplified bacterial communities, and (iii) in complex natural communities (**Figure 5**).

A first step would be to move from the initial understanding of QS, based on dense, homogeneous liquid monocultures, to a more environmentally relevant perspective. Indeed, the principles of QS were originally formulated using dense monocultures (Nealson et al., 1970; Eberhard, 1972). However, QS regulation most likely results from the integration of various factors that are not accounted for in such models. Consequently, several attempts have been made to redefine QS as a means of sensing: (i) the mass transfer properties of the surrounding medium ("diffusion sensing," Redfield, 2002); (ii) the combination of cell density, mass transfer properties and the spatial distribution of cells, indistinguishably ("efficiency sensing," Hense et al., 2007); and (iii) a combination of social (cell density) and physical (mass transfer) properties, which can be distinguished by the integration of several QS pathways ("combinatorial sensing," Cornforth et al., 2014). These studies highlighted the crucial importance of considering the spatial and physical heterogeneity faced by microorganisms in their environment at the microscale. Environmental conditions could be better simulated through the use of microfluidics (Aleklett et al., 2018). Microfluidics refers to the manipulation of fluids at the microscale, allowing the fine control of various parameters, including flows, chemical gradients and bacterial density (Whitesides, 2006). Microfluidics has already been successfully used to explore the effect of cell-density (down to a few cells) on QS induction (Boedicker et al., 2009), the effect of spatial heterogeneity on QS dynamics (reviewed in Mukherjee and Bassler, 2019) and the effect of AI molecules as chemoattractants (Nagy et al., 2015). However, many unanswered questions remain, such as questions concerning the effective range of AIs *in situ* (calling distance and quorum size) and the role of outer membrane vesicles-packed AIs. To our knowledge, calling distances (i.e., the distance over which bacteria can communicate) have not been characterized in marine environments, although they have been estimated to 1–100 μm in the tomato rhizosphere (Gantner et al., 2006) and up to 176 μm for clinical *P. aeruginosa* aggregates (Darch et al., 2018), suggesting the possibility of interaggregates signaling. A few reports have yielded questions regarding the bacterial quorum size (the number of cells required for QS induction), which could be reduced to a few cell clusters under appropriate conditions (Dulla and Lindow, 2008). In addition, the recent discovery of AIs packed in outer membrane vesicles could allow the targeted delivery of hydrophobic AIs over long distances in marine environments and induce single cells (Li et al., 2016; Toyofuku et al., 2017). These discoveries reshuffle the cards concerning the mode and range of action of QS in the environment and need to be addressed to better constrain its impact on bacterial processes and marine biogeochemistry.

Second, as QS is a social trait, the total implications of this mechanism can only be addressed when studied in mixed bacterial communities comprising several bacterial types. Synthetic communities are artificial communities created by coculturing two or more species (Großkopf and Soyer, 2014). They exhibit some of the key features of the mimicked communities with reduced complexity. Such cocultures have mostly been used to study clinically relevant strains thus far (reviewed in Abisado et al., 2018). The more widespread use of synthetic communities coupled with other techniques would allow to study QS in communities more similar to natural assemblages. This could particularly help

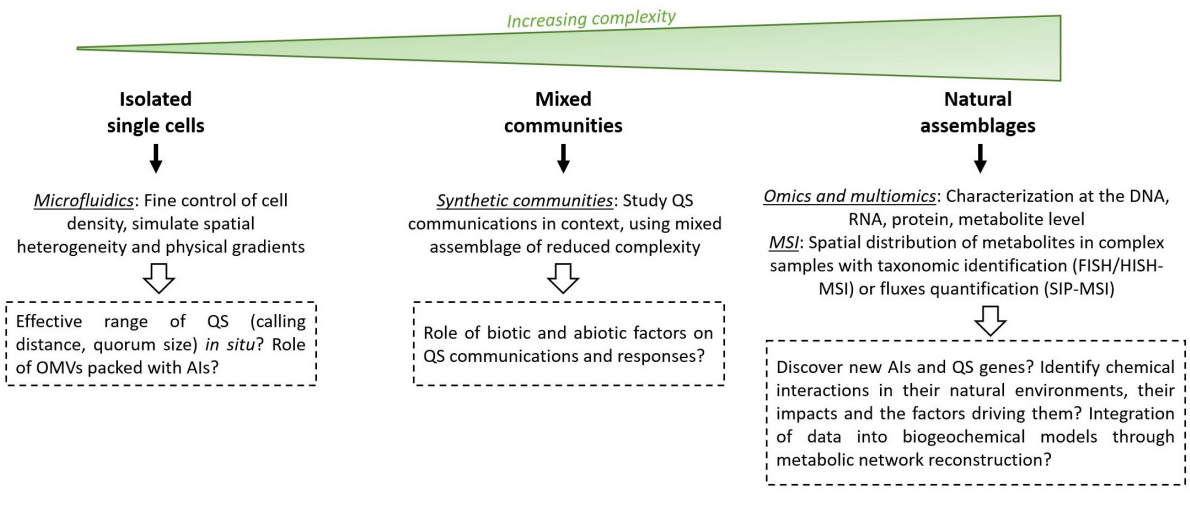

FIGURE 5 | Future perspectives and new tools in QS studies. AI, autoinducer; OMVs, outer membrane vesicles; MSI, mass spectrometry imaging; FISH, fluorescence *in situ* hybridization; HISH, halogen *in situ* hybridization; SIP, stable isotope probing.

us assess the roles of biotic and abiotic factors in shaping QS interactions and responses, for instance, in the case of symbiotic associations between a microalga and different synthetic microalgal microbiomes.

Finally, when working on complex natural assemblages, several techniques can be implemented. The use of omics (metagenomics, metatranscriptomics, metabolomics or metaproteomics) and multiomics (the integrated use of several omics approaches) would allow a better depiction of the diversity of QS systems, the functions they regulate and their impact on natural communities. Although omics techniques are increasingly being used, few studies implementing them in the context of marine QS studies have been published thus far. They could notably aid in the discovery of new AIs and their encoding genes, especially in understudied microbial groups. For instance, functional metagenomics (i.e., the construction and screening of libraries containing DNA cloned from environmental metagenomes) is an excellent tool for revealing new QS and QQ genes (Williamson et al., 2005; Weiland-Bräuer et al., 2016), while comparative proteomics or metabolomics could help to discover new AIs (Prado et al., 2016). Multiomics could also allow the identification of chemical communications in their natural environments and a better understanding of the impact of QS-regulated functions in key processes, such as the colonization of marine aggregates by mixed communities. These approaches could help unravel the genetic and molecular bases of chemical communications (e.g., their biosynthesis and transportation pathways) and how biotic and abiotic factors trigger and modulate them. Studies carried out at several levels (i.e., DNA > RNA > metabolites, proteins) would offer a more holistic view of bacterial interactions *in situ*. Multiomics integrations can lead to metabolic network reconstructions (at the genome or community level) (Prado et al., 2016), allowing the prediction of QS communication impacts on cellular metabolism under changing conditions, ultimately integrating such networks within global biogeochemical flux models.

Another promising emergent tool is the use of mass spectrometry imaging (MSI). MSI is an untargeted approach used to visualize the spatial distribution of molecules. In MSI, the sample surface is swept by a focused ionizing beam. The resulting ions released to the gas phase are analyzed by MS. Several ionization techniques can be used, including matrix-assisted laser desorption/ionization, desorption electrospray ionization and secondary ion mass spectrometry, each offering different advantages (as reviewed in several articles, such as Dunham et al., 2016). MSI provides new opportunities to study QS in its ecological context, as it enables the spatial resolution of metabolites without the need for extraction steps, making it possible to track minute quantities of AIs in complex environments. In addition, MSI can be coupled with other techniques to further expand its abilities, for instance, to allow the identification of the studied bacteria (using fluorescence or halogen *in situ* hybridization) and to trace the uptake and incorporation of labeled substrates (using stable isotope probing). This could allow the study of the impact of QS on microbial metabolism and organic matter incorporation at the cellular level in a mixed population.

PENDING QUESTIONS

Future research will need to address several questions concerning the prevalence and diversity of QS systems, as well as their role and effective range in marine environments:

- What is the global diversity of AHL-related QS genes, and do unknown families remain to be discovered? What is the prevalence of solo *luxI* genes and promiscuous AHL receptors? How widespread are non-AHL-based QS systems in the ocean?
- Which other traits are QS-regulated in marine bacteria, and how do they affect biogeochemical cycles? By which mechanisms does QS shape the composition of microbial groups? To what extent does QS contribute to the selection of initial colonizers? How do these interactions drive the evolution of QS systems? What are the role and ecological implications of QQ? What is the role of QS in terms of interkingdom crosstalk and especially in the induction of prophage lysis?
- What is the effective range (calling distance, quorum size) of QS communications in marine environments? Does QS occur outside of biofilms? What are the effective range and the function of outer membrane vesicles-packed AIs in the environment?

CONCLUSION

Cell–cell communication systems are increasingly being studied in marine environments, where they allow prokaryotes to cooperate with or compete against each other, especially in dense microniches such as marine aggregates, microbial mats and the microalgal phycosphere. Together, these microscale interactions have global, large-scale repercussions. Indeed, QS-based regulations may be important for marine biogeochemical cycles, as they are involved in many ecologically relevant bacterial processes. In addition, this communication system is prevalent among groups such as Alphaproteobacteria, Gammaproteobacteria and Bacteroidetes, which are abundant in marine bacterial hotspots and are involved in all major cycles. QS may directly regulate phenotypes involved in OM degradation, C allocation and nutrient acquisition and may indirectly structure marine communities. However, much remains to be revealed about QS prevalence and function in marine environments. Although an increasing number of studies have described the production of AHLs and QQ compounds in marine strains, other QS systems have been much less described. Beyond the depiction of QS system prevalence and diversity, there are still many unknowns concerning their ranges and roles in marine environments. In the future, we will need to simultaneously (i) improve culture-based studies through the development of new marine model strains, the use of synthetic communities and the better simulation of microenvironment heterogeneity; and (ii) improve studies on natural communities, with better integration of omics and MSI techniques, and the quantification of QS impacts on the fluxes of C and nutrients. Overall, the real

extent of bacterial diversity involved in QS and its ecological and biogeochemical consequences remain to be characterized in marine environments.

AUTHOR CONTRIBUTIONS

All authors participated in the manuscript design. MU wrote the first draft. All authors substantially edited, proofread, and approved the final manuscript.

FUNDING

This work was supported by the French National program EC2CO (Ecosphère Continentale et Côtière) and by an ISblue (Interdisciplinary graduate school for the blue planet) project (ANR-17-EURE-0015), co-funded by a grant from the French government under the program 'Investissements d'Avenir.' This work was also carried out in conjunction with the European Marine Biological Resource Centre (EMBRC-ERIC) and EMBRC-France. French state funds are managed by the ANR within the Investments of the Future program under the grant number ANR-10-INSB-02.

SUPPLEMENTARY MATERIAL

The Supplementary Material for this article can be found online at: https://www.frontiersin.org/articles/10.3389/fmars.2022.834337/full#supplementary-material

REFERENCES

Abdul Malik, S. A., Bazire, A., Gamboa-Muñoz, A., Bedoux, G., Robledo, D., García-Maldonado, J. Q., et al. (2020). Screening of surface-associated bacteria from the mexican red alga *Halymenia floresii* for quorum sensing activity. *Microbiology* 89, 778–788. doi: 10.1134/S0026261720060132

Abisado, R. G., Benomar, S., Klaus, J. R., Dandekar, A. A., and Chandler, J. R. (2018). Bacterial quorum sensing and microbial community interactions. *mBio* 9:e02331-17.

Acinas, S. G., Ferrera, I., Sarmento, H., Díez-Vives, C., Forn, I., Ruiz-González, C., et al. (2015). Validation of a new catalysed reporter deposition- fluorescence in situ hybridization probe for the accurate quantification of marine Bacteroidetes populations. *Environ. Microbiol.* 17, 3557–3569. doi: 10.1111/1462-2920.12517

Albataineh, H., Duke, M., Misra, S. K., Sharp, J. S., and Stevens, D. C. (2021). Identification of a solo acylhomoserine lactone synthase from the myxobacterium *Archangium gephyra*. *Sci. Rep.* 11:3018. doi: 10.1038/s41598-021-82480-1

Aleklett, K., Kiers, E. T., Ohlsson, P., Shimizu, T. S., Caldas, V. E., and Hammer, E. C. (2018). Build your own soil: exploring microfluidics to create microbial habitat structures. *ISME J.* 12, 312–319. doi: 10.1038/ismej.2017.184

Arnosti, C. (2011). Microbial extracellular enzymes and the marine carbon cycle. *Annu. Rev. Mar. Sci.* 3, 401–425. doi: 10.1146/annurev-marine-120709-142731

Arnosti, C. (2014). Patterns of microbially driven carbon cycling in the ocean: links between extracellular enzymes and microbial communities. *Adv. Oceanogr.* 2014:706082. doi: 10.1155/2014/706082

Atkinson, S., and Williams, P. (2009). Quorum sensing and social networking in the microbial world. *J. R. Soc. Interface* 6, 959–978. doi: 10.1098/rsif.2009.0203

Ayé, A. M., Bonnin-Jusserand, M., Brian-Jaisson, F., Ortalo-Magné, A., Culioli, G., Koffi, Nevry R, et al. (2015). Modulation of violacein production and phenotypes associated with biofilm by exogenous quorum sensing N-acylhomoserine lactones in the marine bacterium *Pseudoalteromonas ulvae* TC14. *Microbiology* 161, 2039–2052. doi: 10.1099/mic.0.000147

Azam, F. (1998). Microbial control of oceanic carbon flux: the plot thickens. *Science* 280, 694–696. doi: 10.1126/science.280.5364.694

Azam, F., Fenchel, T., Field, J., Gray, J., Meyer-Reil, L., and Thingstad, F. (1983). The ecological role of water-column microbes in the Sea. *Mar. Ecol. Prog. Ser.* 10, 257–263. doi: 10.3354/meps010257

Azam, F., and Long, R. A. (2001). Sea snow microcosms. *Nature* 414, 495–498.

Azam, F., and Malfatti, F. (2007). Microbial structuring of marine ecosystems. *Nat. Rev. Microbiol.* 5, 782–791. doi: 10.1038/nrmicro1747

Bachofen, R., and Schenk, A. (1998). Quorum sensing autoinducers: do they play a role in natural microbial habitats? *Microbiol. Res.* 153, 61–63. doi: 10.1016/S0944-5013(98)80022-0

Baker, B. J., Lazar, C. S., Teske, A. P., and Dick, G. J. (2015). Genomic resolution of linkages in carbon, nitrogen, and sulfur cycling among widespread estuary sediment bacteria. *Microbiome* 3:14. doi: 10.1186/s40168-015-0077-6

Barriuso, J., and Martínez, M. J. (2018). In Silico analysis of the Quorum Sensing metagenome in environmental biofilm samples. *Front. Microbiol.* 9:1243. doi: 10.3389/fmicb.2018.01243

Bartlau, N., Wichels, A., Krohne, G., and Adriaenssens, E. M. (2021). Highly diverse flavobacterial phages isolated from North Sea spring blooms. *ISME J.* [Epub ahead of print]. doi: 10.1038/s41396-021-01097-4

Baumgartner, L. K., Reid, R. P., Dupraz, C., Decho, A. W., Buckley, D. H., Spear, J. R., et al. (2006). Sulfate reducing bacteria in microbial mats: changing paradigms, new discoveries. *Sediment. Geol.* 185, 131–145. doi: 10.1016/j.sedgeo.2005.12.008

Betancur, L. A., Naranjo-Gaybor, S. J., Vinchira-Villarraga, D. M., Moreno-Sarmiento, N. C., Maldonado, L. A., Suarez-Moreno, Z. R., et al. (2017). Marine Actinobacteria as a source of compounds for phytopathogen control: an integrative metabolic-profiling/bioactivity and taxonomical approach. *PLoS One* 12:e0170148. doi: 10.1371/journal.pone.0170148

Beyersmann, P. G., Tomasch, J., Son, K., Stocker, R., Göker, M., Wagner-Döbler, I., et al. (2017). Dual function of tropodithietic acid as antibiotic and signaling molecule in global gene regulation of the probiotic bacterium Phaeobacter inhibens. *Sci. Rep.* 7:730. doi: 10.1038/s41598-017-00784-7

Biswa, P., and Doble, M. (2013). Production of acylated homoserine lactone by Gram-positive bacteria isolated from marine water. *FEMS Microbiol. Lett.* 343, 34–41. doi: 10.1111/1574-6968.12123

Bižic-Ionescu, M., Zeder, M., Ionescu, D., Orlic, S., Fuchs, B. M., Grossart, H., et al. (2015). Comparison of bacterial communities on limnic versus coastal marine particles reveals profound differences in colonization. *Environ. Microbiol.* 17, 3500–3514. doi: 10.1111/1462-2920.12466

Blanchet, E., Prado, S., Stien, D., Oliveira da Silva, J., Ferandin, Y., Batailler, N., et al. (2017). Quorum sensing and quorum quenching in the Mediterranean Seagrass Posidonia *Oceanica microbiota*. *Front. Mar. Sci.* 4:218. doi: 10.3389/fmars.2017.00218

Bodor, A., Elxnat, B., Thiel, V., Schulz, S., and Wagner-Döbler, I. (2008). Potential for luxS related signalling in marine bacteria and production of autoinducer-2 in the genus Shewanella. *BMC Microbiol.* 8:13. doi: 10.1186/1471-2180-8-13

Boedicker, J. Q., Vincent, M. E., and Ismagilov, R. F. (2009). Microfluidic confinement of single cells of bacteria in small volumes initiates high-density behavior of quorum sensing and growth and reveals its variability. *Angew. Chemie Int. Ed.* 48, 5908–5911. doi: 10.1002/anie.200901550

Bolhuis, H., and Stal, L. J. (2011). Analysis of bacterial and archaeal diversity in coastal microbial mats using massive parallel 16S rRNA gene tag sequencing. *ISME J.* 5, 1701–1712. doi: 10.1038/ismej.2011.52

Bose, U., Ortori, C. A., Sarmad, S., Barrett, D. A., Hewavitharana, A. K., Hodson, M. P., et al. (2017). Production of N-acyl homoserine lactones by the sponge-associated marine actinobacteria *Salinispora arenicola* and *Salinispora pacifica*. *FEMS Microbiol. Lett.* 364, 1–7. doi: 10.1093/femsle/fnx002

Boyle, K. E., Monaco, H., van Ditmarsch, D., Deforet, M., and Xavier, J. B. (2015). Integration of metabolic and quorum sensing signals governing the decision to cooperate in a bacterial social trait. *PLoS Comput. Biol.* 11:e1004279. doi: 10.1371/journal.pcbi.1004279

Brameyer, S., Plener, L., Müller, A., Klingl, A., Wanner, G., and Jung, K. (2018). Outer membrane vesicles facilitate trafficking of the hydrophobic signaling molecule CAI-1 between Vibrio harveyi cells. *J. Bacteriol.* 200: e000740-17.

Browning, T. J., Achterberg, E. P., Yong, J. C., Rapp, I., Utermann, C., Engel, A., et al. (2017). Iron limitation of microbial phosphorus acquisition in the tropical North Atlantic. *Nat. Commun.* 8:15465. doi: 10.1038/ncomms15465

Buchan, A., Gonzalez, J. M., and Moran, M. A. (2005). Overview of the marine roseobacter lineage. *Appl. Environ. Microbiol.* 71, 5665–5677. doi: 10.1128/AEM.71.10.5665

Buchan, A., Lecleir, G. R., Gulvik, C. A., and González, J. M. (2014). Master recyclers: features and functions of bacteria associated with phytoplankton blooms. *Nat. Rev. Microbiol.* 12, 686–698. doi: 10.1038/nrmicro3326

Buchan, A., Mitchell, A., Cude, W. N., and Campagna, S. (2016). "Acyl-homoserine lactone-based quorum sensing in members of the marine bacterial Roseobacter clade: complex cell-to-cell communication controls multiple physiologies," in *Stress and Environmental Regulation of Gene Expression and Adaptation in Bacteria*, ed. F. J. De Bruijn (Hoboken, NJ: John Wiley & Sons), 225–233.

Butler, A. (2005). Marine siderophores and microbial iron mobilization. *BioMetals* 18, 369–374. doi: 10.1007/s10534-005-3711-0

Carreira, C., Staal, M., Middelboe, M., and Brussaard, C. P. D. (2015). Counting viruses and bacteria in photosynthetic microbial mats. *Appl. Environ. Microbiol.* 81, 2149–2155. doi: 10.1128/AEM.02863-14

Charlesworth, J., Kimyon, O., Manefield, M., Beloe, C. J., and Burns, B. P. (2020). Archaea join the conversation: detection of AHL-like activity across a range of archaeal isolates. *FEMS Microbiol. Lett.* 367, 1–9. doi: 10.1093/femsle/fnaa123

Charlesworth, J. C., Watters, C., Wong, H. L., Visscher, P. T., and Burns, B. P. (2019). Isolation of novel quorum-sensing active bacteria from microbial mats in Shark Bay Australia. *FEMS Microbiol. Ecol.* 95, 1–14. doi: 10.1093/femsec/fiz035

Chen, P., Zhang, L., Guo, X., Dai, X., Liu, L., Xi, L., et al. (2016). Diversity, biogeography, and biodegradation potential of actinobacteria in the deep-sea sediments along the southwest Indian ridge. *Front. Microbiol.* 7:1340. doi: 10.3389/fmicb.2016.01340

Chen, X., Schauder, S., Potier, N., Van Dorsselaer, A., Pelczer, I., Bassler, B. L., et al. (2002). Structural identification of a bacterial quorum-sensing signal containing boron. *Nature* 415, 545–549. doi: 10.1038/415545a

Chernikova, T. N., Bargiela, R., Toshchakov, S. V., Shivaraman, V., Lunev, E. A., Yakimov, M. M., et al. (2020). Hydrocarbon-degrading bacteria alcanivorax and marinobacter associated with microalgae *Pavlova lutheri* and *Nannochloropsis oculata*. *Front. Microbiol.* 11:572931. doi: 10.3389/fmicb.2020.572931

Chróst, R. J. (1990). "Microbial ectoenzymes in aquatic environments," in *Aquatic Microbial Ecology: Biochemical and Molecular Approaches*, eds J. Overbeck and R. J. Chróst (Berlin: Springer), 47–77.

Cornforth, D. M., Popat, R., McNally, L., Gurney, J., Scott-Phillips, T. C., Ivens, A., et al. (2014). Combinatorial quorum sensing allows bacteria to resolve their social and physical environment. *Proc. Natl. Acad. Sci. U.S.A.* 111, 4280–4284. doi: 10.1073/pnas.1319175111

Cottrell, M. T., and Kirchman, D. L. (2000). Natural assemblages of marine *Proteobacteria* and members of the *Cytophaga*-flavobacter cluster consuming low- and high-molecular-weight dissolved organic matter. *Appl. Environ. Microbiol.* 66, 1692–1697. doi: 10.1128/AEM.66.4.1692-1697.2000

Cuadrado-Silva, C. T., Castellanos, L., Arévalo-Ferro, C., and Osorno, O. E. (2013). Detection of quorum sensing systems of bacteria isolated from fouled marine organisms. *Biochem. Syst. Ecol.* 46, 101–107. doi: 10.1016/j.bse.2012.09.010

Cude, W. N., and Buchan, A. (2013). Acyl-homoserine lactone-based quorum sensing in the *Roseobacter clade*: complex cell-to-cell communication controls multiple physiologies. *Front. Microbiol.* 4:336. doi: 10.3389/fmicb.2013.00336

Dang, H., Li, T., Chen, M., and Huang, G. (2008). Cross-ocean distribution of rhodobacterales bacteria as primary surface colonizers in temperate coastal marine waters. *Appl. Environ. Microbiol.* 74, 52–60. doi: 10.1128/AEM.01400-07

Dang, H., and Lovell, C. R. (2016). Microbial surface colonization and biofilm development in marine environments. *Microbiol. Mol. Biol. Rev.* 80, 91–138. doi: 10.1128/MMBR.00037-15.Address

Darch, S. E., Simoska, O., Fitzpatrick, M., Barraza, J. P., Stevenson, K. J., Bonnecaze, R. T., et al. (2018). Spatial determinants of quorum signaling in a *Pseudomonas aeruginosa* infection model. *Proc. Natl. Acad. Sci. U.S.A.* 115, 4779–4784. doi: 10.1073/pnas.1719317115

Dashti, N., Ali, N., Eliyas, M., Khanafer, M., Sorkhoh, N. A., and Radwan, S. S. (2015). Most hydrocarbonoclastic bacteria in the total environment are diazotrophic, which highlights their value in the bioremediation of hydrocarbon contaminants. *Microbes Environ.* 30, 70–75. doi: 10.1264/jsme2.ME14090

Decho, A. W., Norman, R. S., and Visscher, P. T. (2010). Quorum sensing in natural environments: emerging views from microbial mats. *Trends Microbiol.* 18, 73–80. doi: 10.1016/j.tim.2009.12.008

Decho, A. W., Visscher, P. T., Ferry, J., Kawaguchi, T., He, L., Przekop, K. M., et al. (2009). Autoinducers extracted from microbial mats reveal a surprising diversity of N-acylhomoserine lactones (AHLs) and abundance changes that may relate to diel pH. *Environ. Microbiol.* 11, 409–420. doi: 10.1111/j.1462-2920.2008.01780.x

DeLisa, M. P., Wu, C., Wang, L., Valdes, J. J., and Bentley, W. E. (2001). DNA microarray-based identification of genes controlled by autoinducer 2-stimulated quorum sensing in *Escherichia coli*. *J. Bacteriol.* 183, 5239–5247. doi: 10.1128/JB.183.18.5239

Delong, E. F., Franks, D. G., and Alldredge, A. L. (1993). Phylogenetic diversity of aggregate-attached vs free-living marine bacterial assemblages. *Limnol. Oceanogr.* 38, 924–934.

Diggle, S. P., Gardner, A., West, S. A., and Griffin, A. S. (2007). Evolutionary theory of bacterial quorum sensing: when is a signal not a signal? *Philos. Trans. R. Soc. B Biol. Sci.* 362, 1241–1249. doi: 10.1098/rstb.2007.2049

Doberva, M., Sanchez-Ferandin, S., Toulza, E., Lebaron, P., and Lami, R. (2015). Diversity of quorum sensing autoinducer synthases in the Global Ocean Sampling metagenomic database. *Aquat. Microb. Ecol.* 74, 107–119. doi: 10.3354/ame01734

Doberva, M., Stien, D., Sorres, J., Hue, N., Sanchez-Ferandin, S., Eparvier, V., et al. (2017). Large diversity and original structures of acyl-homoserine lactones in strain MOLA 401, a marine rhodobacteraceae bacterium. *Front. Microbiol.* 8:1152. doi: 10.3389/fmicb.2017.01152

Dobretsov, S., Dahms, H. U., Yili, H., Wahl, M., and Qian, P. Y. (2007). The effect of quorum-sensing blockers on the formation of marine microbial communities and larval attachment. *FEMS Microbiol. Ecol.* 60, 177–188. doi: 10.1111/j.1574-6941.2007.00285.x

Duarte, C. M., Middelburg, J. J., and Caraco, N. (2005). Major role of marine vegetation on the oceanic carbon cycle. *Biogeosciences* 2, 1–8.

Dulla, G., and Lindow, S. E. (2008). Quorum size of *Pseudomonas* syringae is small and dictated by water availability on the leaf surface. *Proc. Natl. Acad. Sci. U.S.A.* 105, 3082–3087. doi: 10.1073/pnas.0711723105

Dunham, S. J. B., Ellis, J. F., Li, B., and Sweedler, J. V. (2016). Mass spectrometry imaging of complex microbial communities. *Acc. Chem. Res.* 50, 96–104. doi: 10.1021/acs.accounts.6b00503

Duran, R., and Cravo-laureau, C. (2016). Role of environmental factors and microorganisms in determining the fate of polycyclic aromatic hydrocarbons in the marine environment. *FEMS Microbiol. Rev.* 40, 814–830. doi: 10.1093/femsre/fuw031

Dyksma, S., Bischof, K., Fuchs, B. M., Hoffmann, K., Meier, D., Meyerdierks, A., et al. (2016). Ubiquitous Gamma*proteobacteria* dominate dark carbon fixation in coastal sediments. *ISME J.* 10, 1939–1953. doi: 10.1038/ismej.2015.257

Eberhard, A. (1972). Inhibition and activation of bacterial luciferase synthesis. *J. Bacteriol.* 109, 1101–1105.

Elifantz, H., Malmstrom, R. R., Cottrell, M. T., and Kirchman, D. L. (2005). Assimilation of polysaccharides and glucose by major bacterial groups in the delaware estuary. *Appl. Environ. Microbiol.* 71, 7799–7805. doi: 10.1128/AEM.71.12.7799

Enke, T. N., Datta, M. S., Schwartzman, J., Cermak, N., Schmitz, D., Barrere, J., et al. (2019). Modular assembly of polysaccharide-degrading marine microbial communities. *Curr. Biol. Rep.* 29, 1528–1535. doi: 10.1016/j.cub.2019.03.047

Eriksen, M., Lebreton, L. C. M., Carson, H. S., Thiel, M., Moore, C. J., Borerro, J. C., et al. (2014). Plastic pollution in the world's oceans: more than 5 trillion plastic pieces weighing over 250,000 tons afloat at sea. *PLoS One* 9:e111913. doi: 10.1371/journal.pone.0111913

Fei, C., Ochsenkühn, M. A., Shibl, A. A., Isaac, A., Wang, C., and Amin, S. A. (2020). Quorum sensing regulates 'swim-or-stick' lifestyle in the phycosphere. *Environ. Microbiol.* 22, 4761–4778. doi: 10.1111/1462-2920.15228

Fernàndez-Gómez, B., Richter, M., Schüler, M., Pinhassi, J., Acinas, S. G., Gonzàles, J. M., et al. (2013). Ecology of marine Bacteroidetes: a comparative genomics approach. *ISME J.* 7, 1026–1037. doi: 10.1038/ismej.2012.169

Ferrer-González, F. X., Widner, B., Holderman, N. R., Glushka, J., Edison, A. S., Kujawinski, E. B., et al. (2021). Resource partitioning of phytoplankton metabolites that support bacterial heterotrophy. *ISME J.* 15, 762–773. doi: 10.1038/s41396-020-00811-y

Fletcher, M. P., Diggle, S. P., Cámara, M., and Williams, P. (2007). Biosensor-based assays for PQS, HHQ and related 2-alkyl-4-quinolone quorum sensing signal molecules. *Nat. Protoc.* 2, 1254–1262. doi: 10.1038/nprot.2007.158

Francis, B., Urich, T., Mikolasch, A., Teeling, H., and Amann, R. (2021). North Sea spring bloom-associated Gamma*proteobacteria* fill diverse heterotrophic niches. *Environ. Microbiomes* 16:15. doi: 10.1186/s40793-021-00385-y

Freckelton, M. L., Høj, L., and Bowden, B. F. (2018). Quorum sensing interference and structural variation of Quorum Sensing mimics in Australian soft coral. *Front. Mar. Sci.* 5:198. doi: 10.3389/fmars.2018.00198

Fuhrman, J. A., and Hagström, Å (2008). "Bacterial and archaeal community structure and its patterns," in *Microbial Ecology of the Oceans*, ed. D. L. Kirchman (Hoboken, NJ: Wiley).

Fuqua, C. (2006). The QscR quorum-sensing regulon of *Pseudomonas aeruginosa*: an orphan claims its identity. *J. Bacteriol.* 188, 3161–3171. doi: 10.1128/JB.188.9.3169-3171.2006

Fuqua, C., Winans, S. C., and Greenberg, P. E. (1996). Census and consensus in bacterial ecosystems: the LuxR-LuxI family of quorum-sensing transcriptional regulators. *Annu. Rev. Microbiol.* 50, 727–751.

Fuqua, W. C., Winans, S. C., and Greenberg, E. P. (1994). Quorum sensing in bacteria: the LuxR-LuxI family of cell density- responsive transcriptional regulators. *J. Bacteriol.* 176, 269–275. doi: 10.1128/jb.176.2.269-275.1994

Gantner, S., Schmid, M., Christine, D., Schuhegger, R., Steidle, A., Hutzler, P., et al. (2006). In situ quantitation of the spatial scale of calling distances and population density-independent N-acylhomoserine lactone-mediated communication by rhizobacteria colonized on plant roots. *FEMS Microbiol. Ecol.* 56, 188–194. doi: 10.1111/j.1574-6941.2005.00037.x

García-Reyes, S., Soberón-Chávez, G., and Cocotl-Yanez, M. (2020). The third quorum-sensing system of *Pseudomonas aeruginosa*: *Pseudomonas* quinolone signal and the enigmatic PqsE protein. *J. Med. Microbiol.* 69, 25–34. doi: 10.1099/jmm.0.001116

Gardiner, M., Fernandes, N. D., Nowakowski, D., Raftery, M., Kjelleberg, S., Zhong, L., et al. (2015). VarR controls colonization and virulence in the marine macroalgal pathogen *Nautella italica* R11. *Front. Microbiol.* 6:1130. doi: 10.3389/fmicb.2015.01130

Geng, H., and Belas, R. (2010a). Molecular mechanisms underlying roseobacter–phytoplankton symbioses. *Curr. Opin. Biotechnol.* 21, 332–338. doi: 10.1016/j.copbio.2010.03.013

Geng, H., and Belas, R. (2010b). Expression of tropodithietic acid biosynthesis is controlled by a novel autoinducer. *J. Bacteriol.* 192, 4377–4387. doi: 10.1128/JB.00410-10

Geske, G. D., O'Neill, J. C., Miller, D. M., Wezeman, R. J., Mattmann, M. E., Lin, Q., et al. (2008). Comparative analyses of N-acylated homoserine lactones reveal unique structural features that dictate their ability to activate or inhibit quorum sensing. *ChemBioChem* 9, 389–400. doi: 10.1002/cbic.200700551.Comparative

Ghosh, D., Roy, K., Williamson, K. E., Srinivasiah, S., Wommack, K. E., and Radosevich, M. (2009). Acyl-homoserine lactones can induce virus production in lysogenic bacteria: an alternative paradigm for prophage induction. *Appl. Environ. Microbiol.* 75, 7142–7152. doi: 10.1128/AEM.00950-09

Giovannoni, S. J., and Stingl, U. (2005). Molecular diversity and ecology of microbial plankton. *Nature* 437, 343–348.

Goecke, F., Thiel, V., Wiese, J., Labes, A., and Imhoff, J. F. (2013). Algae as an important environment for bacteria - Phylogenetic relationships among new bacterial species isolated from algae. *Phycologia* 52, 14–24. doi: 10.2216/12-24.1

Gram, L., Grossart, H. P., Schlingloff, A., and Kiørboe, T. (2002). Possible quorum sensing in marine snow bacteria: production of acylated homoserine lactones by Roseobacter strains isolated from marine snow. *Appl. Environ. Microbiol.* 68, 4111–4116. doi: 10.1128/AEM.68.8.4111-4116.2002

Grandclément, C., Tannières, M., Moréra, S., Dessaux, Y., and Faure, D. (2016). Quorum quenching: role in nature and applied developments. *FEMS Microbiol. Rev.* 40, 86–116. doi: 10.1093/femsre/fuv038

Grondin, J. M., Tamura, K., Déjean, G., Abbott, D. W., and Brumer, H. (2017). Polysaccharide utilization loci: fuelling microbial communities. *J. Bacteriol.* 199:e00860-16. doi: 10.1128/JB.00860-16

Grossart, H. P. (2010). Ecological consequences of bacterioplankton lifestyles: changes in concepts are needed. *Environ. Microbiol. Rep.* 2, 706–714. doi: 10.1111/j.1758-2229.2010.00179.x

Grossart, H. P., Schlingloff, A., Bernhard, M., Simon, M., and Brinkhoff, T. (2004). Antagonistic activity of bacteria isolated from organic aggregates of the German Wadden Sea. *FEMS Microbiol. Ecol.* 47, 387–396. doi: 10.1016/S0168-6496(03)00305-2

Grossart, H. P., Tang, K. W., Kiørboe, T., and Ploug, H. (2007). Comparison of cell-specific activity between free-living and attached bacteria using isolates and natural assemblages. *FEMS Microbiol. Lett.* 266, 194–200. doi: 10.1111/j.1574-6968.2006.00520.x

Großkopf, T., and Soyer, O. S. (2014). Synthetic microbial communities. *Curr. Opin. Microbiol.* 18, 72–77. doi: 10.1016/j.mib.2014.02.002

Harayama, S., Kasai, Y., and Hara, A. (2004). Microbial communities in oil-contaminated seawater. *Curr. Opin. Biotechnol.* 15, 205–214. doi: 10.1016/j.copbio.2004.04.002

Henke, J. M., and Bassler, B. L. (2004). Three parallel quorum-sensing systems regulate gene expression in *Vibrio harveyi*. *J. Bacteriol.* 186, 6902–6914. doi: 10.1128/JB.186.20.6902-6914.2004

Hense, B. A., Kuttler, C., Müller, J., Rothballer, M., Hartmann, A., and Kreft, J. U. (2007). Does efficiency sensing unify diffusion and quorum sensing? *Nat. Rev. Microbiol.* 5, 230–239. doi: 10.1038/nrmicro1600

Hmelo, L., and Van Mooy, B. A. S. (2009). Kinetic constraints on acylated homoserine lactone-based quorum sensing in marine environments. *Aquat. Microb. Ecol.* 54, 127–133. doi: 10.3354/ame01261

Hmelo, L. R. (2017). Quorum sensing in marine microbial environments. *Ann. Rev. Mar. Sci.* 9, 257–281. doi: 10.1146/annurev-marine-010816-060656

Hmelo, L. R., Mincer, T. J., and Van Mooy, B. A. S. (2011). Possible influence of bacterial quorum sensing on the hydrolysis of sinking particulate organic carbon in marine environments. *Environ. Microbiol. Rep.* 3, 682–688. doi: 10.1111/j.1758-2229.2011.00281.x

Holden, M. T. G., Chhabra, S. R., De Nys, R., Stead, P., Bainton, N. J., Hill, P. J., et al. (1999). Quorum-sensing cross talk: isolation and chemical characterization of cyclic dipeptides from *Pseudomonas aeruginosa* and other Gram-negative bacteria. *Mol. Microbiol.* 33, 1254–1266. doi: 10.1046/j.1365-2958.1999.01577.x

Hollants, J., Leliaert, F., De Clerck, O., and Willems, A. (2013). What we can learn from sushi: a review on seaweed-bacterial associations. *FEMS Microbiol. Ecol.* 83, 1–16. doi: 10.1111/j.1574-6941.2012.01446.x

Huang, S., Bergonzi, C., Schwab, M., Elias, M., and Hicks, R. E. (2019). Evaluation of biological and enzymatic quorum quencher coating additives to reduce biocorrosion of steel. *PLoS One* 14:0217059. doi: 10.1371/journal.pone.0217059

Huang, X., Zhu, J., Cai, Z., Lao, Y., Jin, H., Yu, K., et al. (2018). Profiles of quorum sensing (QS)-related sequences in phycospheric microorganisms during a marine dinoflagellate bloom, as determined by a metagenomic approach. *Microbiol. Res.* 217, 1–13. doi: 10.1016/j.micres.2018.08.015

Huang, Y., Ki, J., Lee, O. O., and Qian, P. (2009). Evidence for the dynamics of Acyl homoserine lactone and AHL-producing bacteria during subtidal biofilm formation. *ISME J.* 3, 296–304. doi: 10.1038/ismej.2008.105

Huang, Y., Zeng, Y., Yu, Z., Zhang, J., Feng, H., and Lin, X. (2013). In silico and experimental methods revealed highly diverse bacteria with quorum sensing and aromatics biodegradation systems - A potential broad application on bioremediation. *Bioresour. Technol.* 148, 311–316. doi: 10.1016/j.biortech.2013.08.155

Huang, Y. L., Ki, J. S., Case, R. J., and Qian, P. Y. (2008). Diversity and acyl-homoserine lactone production among subtidal biofilm-forming bacteria. *Aquat. Microb. Ecol.* 52, 185–193. doi: 10.3354/ame01215

Hudaiberdiev, S., Choudhary, K. S., Alvarez, R. V., Ligeti, B., Lamba, D., and Pongor, S. (2015). Census of solo LuxR genes in prokaryotic genomes. *Front. Cell. Infect. Microbiol.* 5:20. doi: 10.3389/fcimb.2015.00020

Jacquin, J., Cheng, J., Odobel, C., Pandin, C., Conan, P., Pujo-Pay, M., et al. (2019). Microbial ecotoxicology of marine plastic debris: a review on colonization and biodegradation by the "plastisphere.". *Front. Microbiol.* 10:856. doi: 10.3389/fmicb.2019.00865

Jarrell, K. F., Walters, A. D., Bochiwal, C., Borgia, J. M., Dickinson, T., and Chong, J. P. J. (2011). Major players on the microbial stage: why Archaea are important. *Microbiology* 157, 919–936. doi: 10.1099/mic.0.047837-0

Jatt, A. N., Tang, K., Liu, J., Zhang, Z., and Zhang, X. H. (2015). Quorum sensing in marine snow and its possible influence on production of extracellular hydrolytic enzymes in marine snow bacterium *Pantoea ananatis* B9. *FEMS Microbiol. Ecol.* 91, 1–13. doi: 10.1093/femsec/fiu030

Kanagasabhapathy, M., Yamazaki, G., Ishida, A., Sasaki, H., and Nagata, S. (2009). Presence of quorum-sensing inhibitor-like compounds from bacteria isolated from the brown alga *Colpomenia sinuosa*. *Lett. Appl. Microbiol.* 49, 573–579. doi: 10.1111/j.1472-765X.2009.02712.x

Kaplan, H. B., and Greenberg, E. P. (1985). Diffusion of autoinducer is involved in regulation of the *Vibrio fischeri* luminescence system. *J. Bacteriol.* 163, 1210–1214. doi: 10.1128/jb.163.3.1210-1214.1985

Karner, M. B., Delong, E. F., and Karl, D. M. (2001). Archaeal dominance in the mesopelagic zone of the Pacific Ocean. *Nature* 409, 507–510. doi: 10.1038/35054051

Kiørboe, T., Grossart, H. P., Ploug, H., and Tang, K. (2002). Mechanisms and rates of colonisation of sinking aggregates. *Appl. Environ. Microbiol.* 68, 3996–4006. doi: 10.1128/AEM.68.8.3996

Kirchman, D. L. (2002). The ecology of *Cytophaga*-flavobacteria in aquatic environments. *FEMS Microbiol. Ecol.* 39, 91–100. doi: 10.1016/S0168-6496(01)00206-9

Koppenhöfer, S., and Lang, A. S. (2020). Interactions among redox regulators and the CtrA phosphorelay in *Dinoroseobacter shibae* and *Rhodobacter capsulatus*. *Microorganisms* 8:562. doi: 10.3390/microorganisms8040562

Koppenhöfer, S., Wang, H., Scharfe, M., Kaever, V., Wagner-Döbler, I., and Tomasch, J. (2019). Integrated transcriptional regulatory network of quorum sensing, replication control, and SOS response in dinoroseobacter shibae. *Front. Microbiol.* 10:803. doi: 10.3389/fmicb.2019.00803

Krupke, A., Hmelo, L. R., Ossolinski, J. E., Mincer, T. J., and Van Mooy, B. A. S. (2016). Quorum Sensing plays a complex role in regulating the enzyme hydrolysis activity of microbes associated with sinking particles in the ocean. *Front. Mar. Sci.* 3:55. doi: 10.3389/fmars.2016.00055

Kumari, S., Mangwani, N., and Das, S. (2020). Naphthalene catabolism by biofilm forming marine bacterium *Pseudomonas aeruginosa* N6P6 and the role of quorum sensing in regulation of dioxygenase gene. *J. Appl. Microbiol.* 130, 1217–1231. doi: 10.1111/jam.14867

Lage, O. M., and Graça, A. P. (2016). "Biofilms: an extra coat on macroalgae," in *Algae - Organisms for Imminent Biotechnology*, eds N. Thajuddin and D. Dhanasekaran (London: InTech).

Lam, K. S. (2006). Discovery of novel metabolites from marine actinomycetes. *Curr. Opin. Microbiol.* 9, 245–251. doi: 10.1016/j.mib.2006.03.004

Lami, R. (2019). "Quorum sensing in marine biofilms and environments," in *Quorum Sensing: Molecular Mechanism and Biotechnological Application*, ed. G. Tommonaro (Cambridge, MA: Academic Press).

Lami, R., Grimaud, R., Sanchez-brosseau, S., Six, C., Thomas, F., West, N. J., et al. (2021). "Marine bacterial models for experimental biology," in *Handbook of Marine Model Organisms in Experimental Biology*, eds A. Boutet and B. Schierwater (Boca Raton, FL: CRC Press).

Landa, M., Burns, A. S., Roth, S. J., and Moran, M. A. (2017). Bacterial transcriptome remodeling during sequential co-culture with a marine dinoflagellate and diatom. *ISME J.* 11, 2677–2690. doi: 10.1038/ismej.2017.117

Lee, J., and Zhang, L. (2015). The hierarchy quorum sensing network in *Pseudomonas aeruginosa*. *Protein Cell* 6, 26–41. doi: 10.1007/s13238-014-0100-x

Li, J., Azam, F., Zhang, S., Biology, M., Diego, S., and Jolla, L. (2016). Outer membrane vesicles containing signalling molecules and active hydrolytic enzymes released by a coral pathogen *Vibrio shilonii* AK1. *Environ. Microbiol.* 18, 3850–3866. doi: 10.1111/1462-2920.13344

Li, J., Gu, L., Bai, S., Wang, J., Su, L., Wei, B., et al. (2021). Characterization of particle-associated and free-living bacterial and archaeal communities along the water columns of the South China Sea. *Biogeosciences* 18, 113–133. doi: 10.5194/bg-2020-115

Liang, X., Wagner, R. E., Li, B., Zhang, N., Radosevich, M., and Emerson, J. B. (2020). Quorum sensing signals alter in vitro soil virus abundance and bacterial community composition. *Front. Microbiol.* 11:1287. doi: 10.3389/fmicb.2020.01287

Liao, Y., Williams, T. J., Ye, J., Charlesworth, J., Burns, B. P., Poljak, A., et al. (2016). Morphological and proteomic analysis of biofilms from the Antarctic archaeon, Halorubrum lacusprofundi. *Sci. Rep.* 6:37454. doi: 10.1038/srep37454

Liu, J., Fu, K., Wang, Y., Wu, C., Li, F., Shi, L., et al. (2017). Detection of diverse N-Acyl-homoserine lactones in *Vibrio alginolyticus* and regulation of biofilm formation by lactone in vitro. *Front. Microbiol.* 8:1097. doi: 10.3389/fmicb.2017.01097

Long, T., Tu, K. C., Wang, Y., Mehta, P., Ong, N. P., Bassler, B. L., et al. (2009). Quantifying the integration of quorum-sensing signals with single-cell resolution. *PLoS Biol.* 7:e1000068. doi: 10.1371/journal.pbio.1000068

Luo, H., and Moran, M. A. (2014). Evolutionary ecology of the marine roseobacter clade. *Microbiol. Mol. Biol. Rev.* 78, 573–587. doi: 10.1128/MMBR.00020-14

Lupp, C., and Ruby, E. G. (2005). Vibrio fischeri uses two quorum-sensing systems for the regulation of early and late colonization factors. *J. Bacteriol.* 187, 3620–3629. doi: 10.1128/JB.187.11.3620-3629.2005

Lyons, M. M., and Dobbs, F. C. (2012). Differential utilization of carbon substrates by aggregate-associated and water-associated heterotrophic bacterial communities. *Hydrobiologia* 686, 181–193. doi: 10.1007/s10750-012-1010-7

Mangwani, N., Kumari, S., and Das, S. (2015). Involvement of quorum sensing genes in biofilm development and degradation of polycyclic aromatic hydrocarbons by a marine bacterium *Pseudomonas aeruginosa* N6P6. *Appl. Microbiol. Biotechnol.* 99, 10283–10297. doi: 10.1007/s00253-015-6868-7

Martin, M., Portetelle, D., Michel, G., and Vandenbol, M. (2014). Microorganisms living on macroalgae: diversity, interactions, and biotechnological applications. *Appl. Microbiol. Biotechnol.* 98, 2917–2935. doi: 10.1007/s00253-014-5557-2

McLean, R. J. C., Whiteley, M., Stickler, D. J., and Fuqua, W. C. (1997). Evidence of autoinducer activity in naturally occurring biofilms. *FEMS Microbiol. Lett.* 154, 259–263. doi: 10.1016/S0378-1097(97)00336-4

McRose, D. L., Baars, O., Seyedsayamdost, M. R., and Morel, F. M. M. (2018). Quorum sensing and iron regulate a two-for-one siderophore gene cluster in Vibrio harveyi. *Proc. Natl. Acad. Sci. U.S.A.* 115, 7511–7586. doi: 10.1073/pnas.1805791115

Medina-Martínez, M. S., Uyttendaele, M., Demolder, V., and Debevere, J. (2006). Effect of temperature and glucose concentration on the N-butanoyl-L-homoserine lactone production by *Aeromonas hydrophila*. *Food Microbiol.* 23, 534–540. doi: 10.1016/j.fm.2005.09.010

Mestre, M., Ferrera, I., Borrull, E., Ortega-Retuerta, E., Mbedi, S., Grossart, H. P., et al. (2017). Spatial variability of marine bacterial and archaeal communities along the particulate matter continuum. *Mol. Ecol.* 26, 6827–6840. doi: 10.1111/mec.14421

Mestre, M., Höfer, J., Sala, M. M., and Gasol, J. M. (2020). Seasonal variation of bacterial diversity along the marine particulate matter continuum. *Front. Microbiol.* 11:1590. doi: 10.3389/fmicb.2020.01590

Miller, M. B., and Bassler, B. L. (2001). Quorum sensing in bacteria. *Annu. Rev. Microbiol.* 55, 165–199. doi: 10.1146/annurev.micro.55.1.165

Miller, S. T., Xavier, K. B., Campagna, S. R., Taga, M. E., Semmelhack, M. F., Bassler, B. L., et al. (2004). *Salmonella typhimurium* recognizes a chemically distinct form of the bacterial quorum-sensing signal AI-2. *Mol. Cell* 15, 677–687. doi: 10.1016/j.molcel.2004.07.020

Montgomery, K., Charlesworth, J., LeBard, R., Visscher, P. T., and Burns, B. P. (2013). Quorum sensing in extreme environments. *Life* 3, 131–148. doi: 10.3390/life3010131

Moons, P., Michiels, C. W., Aertsen, A., Moons, P., Michiels, C. W., and Aertsen, A. (2009). Bacterial interactions in biofilms. *Crit. Rev. Microbiol.* 35, 157–168. doi: 10.1080/10408410902809431

Morel, F., Rueter, J., and Price, N. (1991). Iron nutrition of phytoplankton and its possible importance in the ecology of ocean regions with high nutrient and low biomass. *Oceanography* 4, 56–61. doi: 10.5670/oceanog.1991.03

Mukherjee, S., and Bassler, B. L. (2019). Bacterial quorum sensing in complex and dynamically changing environments. *Nat. Rev. Microbiol.* 17, 371–382. doi: 10.1038/s41579-019-0186-5

Muras, A., López-Pérez, M., Mayer, C., Parga, A., Amaro-Blanco, J., and Otero, A. (2018). High prevalence of quorum-sensing and quorum-quenching activity among cultivable bacteria and metagenomic sequences in the mediterranean sea. *Genes* 9:100. doi: 10.3390/genes9020100

Muyzer, G., and Stams, A. J. M. (2008). The ecology and biotechnology of sulphate-reducing bacteria. *Nat. Rev. Microbiol.* 6, 441–454. doi: 10.1038/nrmicro1892

Nagy, K., Sipos, O., Valkai, S., Gombai, É, Hodula, O., Kerényi, Á, et al. (2015). Microfluidic study of the chemotactic response of *Escherichia coli* to amino acids, signaling molecules and secondary metabolites. *Biomicrofluidics* 9:e044105. doi: 10.1063/1.4926981

Nealson, K. H., Platt, T., and Hastings, J. W. (1970). Cellular control of the synthesis and activity of the bacterial luminescent system. *J. Bacteriol.* 104, 313–322.

Oh, R. M., Bollati, E., Maithani, P., Huang, D., and Wainwright, B. J. (2021). The microbiome of the reef macroalga sargassum ilicifolium in Singapore. *Microorganisms* 9:898. doi: 10.3390/microorganisms9050898

Ortori, C. A., Atkinson, S., Chhabra, S. R., Cámara, M., Williams, P., and Barrett, D. A. (2007). Comprehensive profiling of N-acylhomoserine lactones produced by *Yersinia pseudotuberculosis* using liquid chromatography coupled to hybrid quadrupole–linear ion trap mass spectrometry. *Anal. Bioanal. Chem.* 387, 497–511. doi: 10.1007/s00216-006-0710-0

Paggi, R. A., Martone, C. B., Fuqua, C., and De Castro, R. E. (2003). Detection of quorum sensing signals in the haloalkaliphilic archaeon *Natronococcus occultus*. *FEMS Microbiol. Lett.* 221, 49–52. doi: 10.1016/S0378-1097(03)00174-5

Pajares, S., and Ramos, R. (2019). Processes and microorganisms involved in the marine nitrogen cycle: knowledge and gaps. *Front. Mar. Sci.* 6:739. doi: 10.3389/fmars.2019.00739

Patzelt, D., Wang, H., Buchholz, I., Rohde, M., Gröbe, L., Pradella, S., et al. (2013). You are what you talk: quorum sensing induces individual morphologies and cell division modes in *Dinoroseobacter shibae*. *ISME J.* 7, 2274–2286. doi: 10.1038/ismej.2013.107

Paulsen, S. S., Isbrandt, T., Kirkegaard, M., Buijs, Y., Strube, M. L., Sonnenschein, E. C., et al. (2020). Production of the antimicrobial compound tetrabromopyrrole and the *Pseudomonas* quinolone system precursor, 2-heptyl-4-quinolone, by a novel marine species *Pseudoalteromonas galatheae* sp. nov. *Sci. Rep.* 10:21630. doi: 10.1038/s41598-020-78439-3

Pearson, J. P., Van Delden, C., and Iglewski, B. H. (1999). Active efflux and diffusion are involved in transport of *Pseudomonas aeruginosa* cell-to-cell signals. *J. Bacteriol.* 181, 1203–1210. doi: 10.1128/jb.181.4.1203-1210.1999

Pereira, C. S., Mcauley, J. R., Taga, M. E., Xavier, K. B., and Miller, S. T. (2008). Sinorhizobium meliloti, a bacterium lacking the supplied by other bacteria. *Mol. Microbiol.* 70, 1223–1235. doi: 10.1111/j.1365-2958.2008.06477.x

Pereira, C. S., Thompson, J. A., and Xavier, K. B. (2013). AI-2-mediated signalling in bacteria. *FEMS Microbiol. Rev.* 37, 156–181. doi: 10.1111/j.1574-6976.2012.00345.x

Ploug, H., and Grossart, H. P. (1999). Bacterial production and respiration in suspended aggregates - A matter of the incubation method. *Aquat. Microb. Ecol.* 20, 21–29. doi: 10.3354/ame020021

Polkade, A. V., Mantri, S. S., Patwekar, U. J., and Jangid, K. (2016). Quorum sensing: an under-explored phenomenon in the phylum Actinobacteria. *Front. Microbiol.* 7:131. doi: 10.3389/fmicb.2016.00131

Pollara, S. B., Becker, J. W., Nunn, B. L., Boiteau, R., Repeta, D., Mudge, M. C., et al. (2021). Bacterial quorum-sensing signal arrests phytoplankton cell division and impacts virus-induced mortality. *mSphere* 6:e00009-21.

Pomeroy, L. R. (1974). The ocean's food web, a changing paradigm. *Bioscience* 24, 499–504. doi: 10.2307/1296885

Pomeroy, L. R. (2007). The microbial loop. *Oceanography* 20, 28–33.

Popat, R., Harrison, F., Silva, A. C., Easton, S. A. S., Mcnally, L., Williams, P., et al. (2017). Environmental modification via a quorum sensing molecule influences the social landscape of siderophore production. *Proc. R. Soc. B Biol. Sci.* 284:20170200.

Prado, S., Leblanc, C., and Rebuffat, S. (2016). "Microbiota and chemical ecology," in *Chemical Ecology*, eds A.-G. Bagnères and M. Hossaert-Mckey (Hoboken, NJ: John Wiley & Sons, Inc).

Prescott, R. D., and Decho, A. W. (2020). Flexibility and adaptability of quorum sensing in nature. *Trends Microbiol.* 28, 436–444. doi: 10.1016/j.tim.2019.12.004

Raina, J. B., Fernandez, V., Lambert, B., Stocker, R., and Seymour, J. R. (2019). The role of microbial motility and chemotaxis in symbiosis. *Nat. Rev. Microbiol.* 17, 284–294. doi: 10.1038/s41579-019-0182-9

Rajput, A., and Kumar, M. (2017). Computational exploration of putative LuxR solos in Archaea and their functional implications in quorum sensing. *Front. Microbiol.* 8:798. doi: 10.3389/fmicb.2017.00798

Redfield, R. J. (2002). Is quorum sensing a side effect of diffusion sensing? *Trends Microbiol.* 10, 365–370. doi: 10.1016/S0966-842X(02)02400-9

Reen, F. J., Gutiérrez-Barranquero, J. A., McCarthy, R. R., Woods, D. F., Scarciglia, S., Adams, C., et al. (2019). Quorum sensing signaling alters virulence potential and population dynamics in complex microbiome-host interactomes. *Front. Microbiol.* 10:2131. doi: 10.3389/fmicb.2019.02131

Reen, F. J., Mooij, M. J., Holcombe, L. J., Mcsweeney, C. M., Mcglacken, G. P., Morrissey, J. P., et al. (2011). The *Pseudomonas* quinolone signal (PQS), and its precursor HHQ, modulate interspecies and interkingdom behaviour. *FEMS Microbiol. Ecol.* 77, 413–428. doi: 10.1111/j.1574-6941.2011.01121.x

Rehman, Z. U., and Leiknes, T. O. (2018). Quorum-quenching bacteria isolated from red sea sediments reduce biofilm formation by *Pseudomonas aeruginosa*. *Front. Microbiol.* 9:1354. doi: 10.3389/fmicb.2018.01354

Reintjes, G., Arnosti, C., Fuchs, B., and Amann, R. (2019). Selfish, sharing and scavenging bacteria in the Atlantic Ocean: a biogeographical study of bacterial substrate utilisation. *ISME J.* 13, 1119–1132. doi: 10.1038/s41396-018-0326-3

Reintjes, G., Arnosti, C., Fuchs, B. M., and Amann, R. (2017). An alternative polysaccharide uptake mechanism of marine bacteria. *ISME J.* 11, 1640–1650. doi: 10.1038/ismej.2017.26

Ren, D., Zuo, R., and Wood, T. K. (2005). Quorum-sensing antagonist influences siderophore biosynthesis in *Pseudomonas* putida and *Pseudomonas aeruginosa*. *Appl. Microbiol. Biotechnol.* 66, 689–695. doi: 10.1007/s00253-004-1691-6

Rezzonico, F., and Duffy, B. (2008). Lack of genomic evidence of AI-2 receptors suggests a non-quorum sensing role for luxS in most bacteria. *BMC Microbiol.* 8:154. doi: 10.1186/1471-2180-8-154

Rieck, A., Herlemann, D. P. R., Jürgens, K., and Grossart, H. (2015). Particle-associated differ from free-living bacteria in surface waters of the baltic sea particle-associated differ from free-living bacteria in surface waters of the baltic sea. *Front. Microbiol.* 6:1297. doi: 10.3389/fmicb.2015.01297

Riedel, K., Hentzer, M., Geisenberger, O., Huber, B., Steidle, A., Wu, H., et al. (2001). N-acylhomoserine-lactone-mediated communication between *Pseudomonas aeruginosa* and *Burkholderia cepacia* in mixed biofilms. *Microbiology* 147, 3249–3262. doi: 10.1099/00221287-147-12-3249

Rink, B., Martens, T., Fischer, D., Lemke, A., Grossart, H. P., Simon, M., et al. (2008). Short-term dynamics of bacterial communities in a tidally affected coastal ecosystem. *FEMS Microbiol. Ecol.* 66, 306–319. doi: 10.1111/j.1574-6941.2008.00573.x

Roager, L., and Sonnenschein, E. C. (2019). Bacterial candidates for colonization and degradation of marine plastic debris. *Environ. Sci. Technol.* 53, 11636–11643. doi: 10.1021/acs.est.9b02212

Romero, M., Avendaño-Herrera, R., Magariños, B., Cámara, M., and Otero, A. (2010). Acylhomoserine lactone production and degradation by the fish pathogen *Tenacibaculum maritimum*, a member of the *Cytophaga*-Flavobacterium-*Bacteroides* (CFB) group. *FEMS Microbiol. Lett.* 304, 131–139. doi: 10.1111/j.1574-6968.2009.01889.x

Romero, M., Diggle, S. P., Heeb, S., Cámara, M., and Otero, A. (2008). Quorum quenching activity in *Anabaena* sp. PCC 7120: identification of AiiC, a novel AHL-acylase. *FEMS Microbiol. Lett.* 280, 73–80. doi: 10.1111/j.1574-6968.2007.01046.x

Romero, M., Martin-Cuadrado, A. B., and Otero, A. (2012). Determination of whether quorum quenching is a common activity in marine bacteria by analysis of cultivable bacteria and metagenomic sequences. *Appl. Environ. Microbiol.* 78, 6345–6348. doi: 10.1128/AEM.01266-12

Romero, M., Martin-Cuadrado, A. B., Roca-Rivada, A., Cabello, A. M., and Otero, A. (2011a). Quorum quenching in cultivable bacteria from dense marine coastal microbial communities. *FEMS Microbiol. Ecol.* 75, 205–217. doi: 10.1111/j.1574-6941.2010.01011.x

Romero, M., Muro-Pastor, A. M., and Otero, A. (2011b). Quorum sensing N-acylhomoserine lactone signals affect nitrogen fixation in the

cyanobacterium *Anabaena* sp. PCC7120. *FEMS Microbiol. Lett.* 315, 101–108. doi: 10.1111/j.1574-6968.2010.02175.x

Santoro, A. E., Richter, R. A., and Dupont, C. L. (2019). Planktonic marine archaea. *Ann. Rev. Mar. Sci.* 11, 131–158. doi: 10.1146/annurev-marine-121916-063141

Saurav, K., Costantino, V., Venturi, V., and Steindler, L. (2017). Quorum sensing inhibitors from the sea discovered using bacterial N -acyl-homoserine lactone-based biosensors. *Mar. Drugs* 15:53. doi: 10.3390/md15030053

Schaefer, A. L., Greenberg, E. P., Oliver, C. M., Oda, Y., Huang, J. J., Bittan-Banin, G., et al. (2008). A new class of homoserine lactone quorum-sensing signals. *Nature* 454, 595–600. doi: 10.1038/nature07088

Schertzer, J. W., Boulette, M. L., and Whiteley, M. (2009). More than a signal: non-signaling properties of quorum sensing molecules. *Trends Microbiol.* 17, 189–195. doi: 10.1016/j.tim.2009.02.001

Schlundt, C., Mark, J. L., Anna, W., and Amaral-zettler, E. R. Z. L. A. (2020). Spatial structure in the "Plastisphere": molecular resources for imaging microscopic communities on plastic marine debris. *Mol. Ecol. Resour.* 20, 620–634. doi: 10.1111/1755-0998.13119

Schmidt, R., Ulanova, D., Wick, L. Y., Bode, H. B., and Garbeva, P. (2019). Microbe-driven chemical ecology: past, present and future. *ISME J.* 13, 2656–2663. doi: 10.1038/s41396-019-0469-x

Seymour, J. R., Amin, S. A., Raina, J. B., and Stocker, R. (2017). Zooming in on the phycosphere: the ecological interface for phytoplankton-bacteria relationships. *Nat. Microbiol.* 2:17065. doi: 10.1038/nmicrobiol.2017.65

Shapiro, J. A. (1998). Thinking about bacterial populations as multicellular organisms. *Annu. Rev. Microbiol.* 52, 81–104. doi: 10.1146/annurev.micro.52.1.81

Sharif, D. I., Gallon, J., Smith, C. J., and Dudley, E. (2008). Quorum sensing in Cyanobacteria: N-octanoyl-homoserine lactone release and response, by the epilithic colonial cyanobacterium Gloeothece PCC6909. *ISME J.* 2, 1171–1182. doi: 10.1038/ismej.2008.68

Sheridan, C. C., Steinberg, D. K., and Kling, G. W. (2002). The microbial and metazoan community associated with colonies of *Trichodesmium* spp.: a quantitative survey. *J. Plankton Res.* 24, 913–922. doi: 10.1093/plankt/24.9.913

Shrout, J. D., Chopp, D. L., Just, C. L., Hentzer, M., Givskov, M., and Parsek, M. R. (2006). The impact of quorum sensing and swarming motility on *Pseudomonas aeruginosa* biofilm formation is nutritionally conditional. *Mol. Microbiol.* 62, 1264–1277. doi: 10.1111/j.1365-2958.2006.05421.x

Sievert, S. M., Kiene, R. P., and Schulz-vogt, H. N. (2007). The sulfur cycle. *Oceanography* 20, 117–123.

Silpe, J. E., and Bassler, B. L. (2019). Phage-encoded LuxR-type receptors responsive to host- produced bacterial quorum-sensing autoinducers. *mBio* 10: e00638-19.

Silpe, J. E., Bridges, A. A., Huang, X., Coronado, D. R., Duddy, O. P., and Bassler, B. L. (2020). Separating functions of the phage-encoded Quorum-Sensing-activated antirepressor Qtip. *Cell Host Microbe* 27, 629.e4–641.e4. doi: 10.1016/j.chom.2020.01.024

Simon, M., Grossart, H. P., Schweitzer, B., and Ploug, H. (2002). Microbial ecology of organic aggregates in aquatic ecosystems. *Aquat. Microb. Ecol.* 28, 175–211. doi: 10.3354/ame028175

Sivakumar, K., Scarascia, G., Zaouri, N., Wang, T., Kaksonen, A. H., and Hong, P. Y. (2019). Salinity-mediated increment in sulfate reduction, biofilm formation, and quorum sensing: a potential connection between quorum sensing and sulfate reduction? *Front. Microbiol.* 10:188. doi: 10.3389/fmicb.2019.00188

Smith, D. C., Simon, M., Alldredge, A. L., and Azam, F. (1992). Intense hydrolytic enzyme activity on marine aggregates and implications for rapid particle dissolution. *Nature* 359, 139–142. doi: 10.1038/355242a0

Smith, P., and Schuster, M. (2019). Public goods and cheating in microbes. *Curr. Biol.* 29, R442–R447. doi: 10.1016/j.cub.2019.03.001

Sperandio, V., Torres, A. G., Giro, J. A., and Kaper, J. B. (2001). Quorum sensing is a global regulatory mechanism in enterohemorrhagic *Escherichia coli* O157:H7. *J. Bacteriol.* 183, 5187–5197. doi: 10.1128/JB.183.17.5187

Steidle, A., Sigl, K., Schuhegger, R., Ihring, A., Schmid, M., Gantner, S., et al. (2001). Visualization of N-acylhomoserine lactone-mediated cell-cell communication between bacteria colonizing the tomato rhizosphere. *Appl. Environ. Microbiol.* 67, 5761–5770. doi: 10.1128/AEM.67.12.5761-5770.2001

Stock, F., Cirri, E., Nuwanthi, S. G. L. I., Stock, W., Ueberschaar, N., Mangelinckx, S., et al. (2021). Sampling, separation, and quantification of N-acyl homoserine lactones from marine intertidal sediments. *Limnol. Oceanogr. Methods* 19, 145–157. doi: 10.1002/lom3.10412

Stocker, R. (2012). Marine microbes see a sea of gradients. *Science* 338, 628–633. doi: 10.1126/science.1208929

Stocker, R., Seymour, J. R., Samadani, A., Hunt, D. E., and Polz, M. F. (2008). Rapid chemotactic response enables marine bacteria to exploit ephemeral microscale nutrient patches. *Proc. Natl. Acad. Sci. U.S.A.* 105, 4209–4214. doi: 10.1073/pnas.0709765105

Stockner, J. G. (1988). Phototrophic picoplankton: an overview from marine and freshwater ecosystems. *Limnol. Oceanogr.* 33, 765–775. doi: 10.4319/lo.1988.33.4part2.0765

Strom, S. L. (2008). Microbial ecology of ocean biogeochemistry: a community perspective. *Science* 320, 1043–1045. doi: 10.1126/science.1153527

Su, Y., Tang, K., Liu, J., Wang, Y., Zheng, Y., and Zhang, X. H. (2019). Quorum sensing system of *Ruegeria mobilis* Rm01 controls lipase and biofilm formation. *Front. Microbiol.* 10:3304. doi: 10.3389/fmicb.2018.03304

Su, Y., Yang, Y., Zhu, X. Y., Zhang, X. H., and Yu, M. (2021). Metagenomic insights into the microbial assemblage capable of quorum sensing and quorum quenching in particulate organic matter in the yellow sea. *Front. Microbiol.* 11:602010. doi: 10.3389/fmicb.2020.602010

Subramoni, S., Salcedo, D. V. F., and Suarez-Moreno, Z. R. (2015). A bioinformatic survey of distribution, conservation, and probable functions of LuxR solo regulators in bacteria. *Front. Cell. Infect. Microbiol.* 5:16. doi: 10.3389/fcimb.2015.00016

Sun, J., Daniel, R., Wagner-Döbler, I., and Zeng, A. P. (2004). Is autoinducer-2 a universal signal for interspecies communication: a comparative genomic and phylogenetic analysis of the synthesis and signal transduction pathways. *BMC Evol. Biol.* 4:36. doi: 10.1186/1471-2148-4-36

Sunagawa, S., Coelho, L. P., Chaffron, S., Kultima, J. R., Labadie, K., Salazar, G., et al. (2015). Structure and function of the global ocean microbiome. *Science* 348:1261359. doi: 10.1126/science.1261359

Suttle, C. A. (2005). Viruses in the sea. *Nature* 437, 356–361.

Suttle, C. A. (2007). Marine viruses — major players in the global ecosystem. *Nat. Rev. Microbiol.* 5, 801–812. doi: 10.1038/nrmicro1750

Swem, L. R., Swem, D. L., Wingreen, N. S., and Bassler, B. L. (2008). Deducing receptor signaling parameters from in vivo analysis: LuxN/AI-1 quorum sensing in *Vibrio harveyi*. *Cell* 134, 461–473. doi: 10.1016/j.cell.2008.06.023

Teasdale, M. E., Donovan, K. A., Forschner-Dancause, S. R., and Rowley, D. C. (2011). Gram-positive marine bacteria as a potential resource for the discovery of quorum sensing inhibitors. *Mar. Biotechnol.* 13, 722–732. doi: 10.1007/s10126-010-9334-7

Teeling, H., Fuchs, B. M., Bennke, C. M., Krüger, K., Chafee, M., Kappelmann, L., et al. (2016). Recurring patterns in bacterioplankton dynamics during coastal spring algae blooms. *elife* 5:e11888. doi: 10.7554/eLife.11888

Thomas, F., Hehemann, J. H., Rebuffet, E., Czjzek, M., and Michel, G. (2011). Environmental and gut bacteroidetes: the food connection. *Front. Microbiol.* 2:93. doi: 10.3389/fmicb.2011.00093

Tian, Y., Wang, Q., Liu, Q., Ma, Y., Cao, X., Guan, L., et al. (2008). Involvement of LuxS in the regulation of motility and flagella biogenesis in *Vibrio alginolyticus*. *Biosci. Biotechnol. Biochem.* 72, 1063–1071. doi: 10.1271/bbb.70812

Tommonaro, G., Abbamondi, G. R., Iodice, C., Tait, K., and De Rosa, S. (2012). Diketopiperazines produced by the halophilic archaeon, haloterrigena hispanica, activate AHL bioreporters. *Microb. Ecol.* 63, 490–495. doi: 10.1007/s00248-011-9980-y

Torres, M., Dessaux, Y., and Llamas, I. (2019). Saline environments as a source of potential quorum sensing disruptors to control bacterial infections: a review. *Mar. Drugs* 17, 1–28. doi: 10.3390/md17030191

Torres, M., Rubio-Portillo, E., Antón, J., Ramos-Esplá, A. A., Quesada, E., and Llamas, I. (2016). Selection of the N-acylhomoserine lactone-degrading bacterium *Alteromonas stellipolaris* PQQ-42 and of its potential for biocontrol in aquaculture. *Front. Microbiol.* 7:646. doi: 10.3389/fmicb.2016.00646

Tourneroche, A., Lami, R., Hubas, C., Blanchet, E., Vallet, M., Escoubeyrou, K., et al. (2019). Bacterial-fungal interactions in the kelp endomicrobiota drive autoinducer-2 quorum sensing. *Front. Microbiol.* 10:1693. doi: 10.3389/fmicb.2019.01693

Toyofuku, M., Morinaga, K., Hashimoto , Y., Uhl, J., Shimamura, H., Inaba, H., et al. (2017). Membrane vesicle-mediated bacterial communication. *ISME J.* 11, 1504–1509. doi: 10.1038/ismej.2017.13

Toyofuku, M., Nomura, N., Kuno, E., Tashiro, Y., Nakajima, T., and Uchiyama, H. (2008). Influence of the *Pseudomonas* quinolone signal on denitrification in *Pseudomonas aeruginosa*. *J. Bacteriol.* 190, 7947–7956. doi: 10.1128/JB.00968-08

Urvoy, M., Lami, R., Dreanno, C., Daudé, D., Rodrigues, A. M. S., Gourmelon, M., et al. (2021a). Quorum sensing disruption regulates hydrolytic enzyme and biofilm production in estuarine bacteria. *Environ. Microbiol.* 23, 7183–7200. doi: 10.1111/1462-2920.15775

Urvoy, M., Lami, R., Dreanno, C., Delmas, D., L'Helguen, S., and Labry, C. (2021b). Quorum sensing regulates the hydrolytic enzyme production and community composition of heterotrophic bacteria in coastal waters. *Front. Microbiol.* 12:780759. doi: 10.3389/fmicb.2021.780759

van Gemerden, H. (1993). Microbial mats: a joint venture. *Mar. Geol.* 113, 3–25. doi: 10.1016/0025-3227(93)90146-M

Van Mooy, B. A. S., Hmelo, L. R., Sofen, L. E., Campagna, S. R., May, A. L., Dyhrman, S. T., et al. (2012). Quorum sensing control of phosphorus acquisition in *Trichodesmium consortia*. *ISME J.* 6, 422–429. doi: 10.1038/ismej.2011.115

Vial, L., Lépine, F., Milot, S., Groleau, M. C., Dekimpe, V., Woods, D. E., et al. (2008). *Burkholderia pseudomallei*, *B. thailandensis*, and *B. ambifaria* produce 4-hydroxy-2-alkylquinoline analogues with a methyl group at the 3 position that is required for quorum-sensing regulation. *J. Bacteriol.* 190, 5339–5352. doi: 10.1128/JB.00400-08

Villarreal-Chiu, J. F., Quinn, J. P., and McGrath, J. W. (2012). The genes and enzymes of phosphonate metabolism by bacteria, and their distribution in the marine environment. *Front. Microbiol.* 3:19. doi: 10.3389/fmicb.2012.00019

Visscher, P. T., and Stolz, J. F. (2005). Microbial mats as bioreactors: populations, processes, and products. *Palaeogeogr. Palaeoclimatol. Palaeoecol.* 219, 87–100. doi: 10.1016/j.palaeo.2004.10.016

Voss, M., Bange, H. W., Dippner, J. W., Middelburg, J. J., Montoya, J. P., and Ward, B. (2013). The marine nitrogen cycle: recent discoveries, uncertainties and the potential relevance of climate change. *Philos. Trans. R. Soc. Lond. B* 368:20130121.

Wagner-Döbler, I., and Biebl, H. (2006). Environmental biology of the marine roseobacter lineage. *Annu. Rev. Microbiol.* 60, 255–280. doi: 10.1146/annurev.micro.60.080805.142115

Wagner-Döbler, I., Thiel, V., Eberl, L., Allgaier, M., Bodor, A., Meyer, S., et al. (2005). Discovery of complex mixtures of novel long- chain quorum sensing signals in free-living and host-associated marine Alpha*proteobacteria*. *ChemBioChem* 6, 2195–2206. doi: 10.1002/cbic.200500189

Wang, N., Gao, J., Liu, Y., Wang, Q., Zhuang, X., and Zhuang, G. (2021). Realizing the role of N-acyl-homoserine lactone-mediated quorum sensing in nitrification and denitrification: a review. *Chemosphere* 274:129970. doi: 10.1016/j.chemosphere.2021.129970

Wang, Q., Liu, Q., Ma, Y., Rui, H., and Zhang, Y. (2007). LuxO controls extracellular protease, haemolytic activities and siderophore production in fish pathogen *Vibrio alginolyticus*. *J. Appl. Microbiol.* 103, 1525–1534. doi: 10.1111/j.1365-2672.2007.03380.x

Wang, R., Ding, W., Long, L., Lan, Y., Tong, H., Saha, S., et al. (2020). Exploring the influence of signal molecules on marine biofilms development. *Front. Microbiol.* 11:571400. doi: 10.3389/fmicb.2020.571400

Wang, T.-N., Kaksonen, A. H., and Hong, P.-Y. (2018). Evaluation of two autoinducer-2 quantification methods for application in marine environments. *J. Appl. Microbiol.* 124, 1469–1479. doi: 10.1111/jam.13725

Waters, C. M., and Bassler, B. L. (2005). Quorum sensing: cell-to-cell communication in bacteria. *Annu. Rev. Cell Dev. Biol.* 21, 319–346. doi: 10.1146/annurev.cellbio.21.012704.131001

Weiland-Bräuer, N., Kisch, M. J., Pinnow, N., Liese, A., and Schmitz, R. A. (2016). Highly effective inhibition of biofilm formation by the first metagenome-derived AI-2 quenching enzyme. *Front. Microbiol.* 7:1098. doi: 10.3389/fmicb.2016.01098

Wellington, S., and Greenberg, E. P. (2019). Quorum sensing signal selectivity and the potential for interspecies cross talk. *mBio* 10:e00146-19.

Wellington Miranda, S., Cong, Q., Schaefer, A. L., Macleod, E. K., Zimenko, A., Baker, D., et al. (2021). A covariation analysis reveals elements of selectivity in quorum sensing systems. *eLife* 10:e69169.

Wen, Y. I, Kim, H., Son, J., Lee, B., and Kim, K. (2012). Iron and quorum sensing coordinately regulate the expression of vulnibactin biosynthesis in *Vibrio vulnificus*. *J. Biol. Chem.* 287, 26727–26739. doi: 10.1074/jbc.M112.374165

Whalen, K. E., Becker, J. W., Schrecengost, A. M., Gao, Y., Giannetti, N., and Harvey, E. L. (2019). Bacterial alkylquinolone signaling contributes to structuring microbial communities in the ocean. *Microbiome* 7:93. doi: 10.1186/s40168-019-0711-9

White, A., and Dyhrman, S. (2013). The marine phosphorus cycle. *Front. Microbiol.* 4:105. doi: 10.3389/fmicb.2013.00105

Whiteley, M., Diggle, S. P., and Greenberg, E. P. (2017). Progress in and promise of bacterial quorum sensing research. *Nature* 551, 313–320. doi: 10.1038/nature24624

Whitesides, G. M. (2006). The origins and the future of microfluidics. *Nature* 442, 368–373. doi: 10.1038/nature05058

Whitman, W. B., Coleman, D. C., and Wiebe, W. J. (1998). Prokaryotes: the unseen majority. *Proc. Natl. Acad. Sci. U.S.A.* 95, 6578–6583. doi: 10.1073/pnas.95.12.6578

Williamson, L. L., Borlee, B. R., Schloss, P. D., Guan, C., Allen, H. K., and Handelsman, J. (2005). Intracellular screen to identify metagenomic clones that induce or inhibit a quorum-sensing biosensor. *Appl. Environ. Microbiol.* 71, 6335–6344. doi: 10.1128/AEM.71.10.6335

Wright, R. J., Langille, M. G. I., Walker, T. R., and Wright, R. J. (2021). Food or just a free ride? A meta-analysis reveals the global diversity of the Plastisphere. *ISME J.* 15, 789–806. doi: 10.1038/s41396-020-00814-9

Xavier, K. B., and Bassler, B. L. (2003). LuxS quorum sensing: more than just a numbers game. *Curr. Opin. Microbiol.* 6, 191–197. doi: 10.1016/S1369-5274(03)00028-6

Xu, Y., Curtis, T., Dolfing, J., Wu, Y., and Rittmann, B. E. (2021). N-acyl-homoserine-lactones signaling as a critical control point for phosphorus entrapment by multi-species microbial aggregates. *Water Res.* 204:117627. doi: 10.1016/j.watres.2021.117627

Xu, Y., Wu, Y., Esquivel-Elizondo, S., Dolfing, J., and Rittmann, B. E. (2020). Using microbial aggregates to entrap aqueous phosphorus. *Trends Biotechnol.* 38, 1292–1303. doi: 10.1016/j.tibtech.2020.03.012

Yoch, D. C. (2002). Dimethylsulfoniopropionate: its sources, role in the marine food web, and biological degradation to dimethylsulfide. *Appl. Environ. Microbiol.* 68, 5804–5815. doi: 10.1128/AEM.68.12.5804-5815.2002

Yu, Z., Hu, Z., Xu, Q., Zhang, M., Yuan, N., Liu, J., et al. (2020). The luxI/luxR-type quorum sensing system regulates degradation of polycyclic aromatic hydrocarbons via two mechanisms. *Int. J. Mol. Sci.* 21:5548. doi: 10.3390/ijms21155548

Zan, J., Choi, O., Meharena, H., Uhlson, C. L., Churchill, M. E. A., Hill, R. T., et al. (2015). A solo luxI -type gene directs acylhomoserine lactone synthesis and contributes to motility control in the marine sponge symbiont Ruegeria sp. KLH11. *Microbiology* 161, 50–56. doi: 10.1099/mic.0.083956-0

Zettler, E. R., Mincer, T. J., and Amaral-zettler, L. A. (2013). Life in the "plastisphere": microbial communities on plastic marine debris. *Environ. Sci. Technol.* 47, 7137–7146.

Zhai, C., Zhang, P., Shen, F., Zhou, C., and Liu, C. (2012). Does Microcystis aeruginosa have quorum sensing? *FEMS Microbiol. Lett.* 336, 38–44. doi: 10.1111/j.1574-6968.2012.02650.x

Zhang, G., Zhang, F., Ding, G., Li, J., Guo, X., Zhu, J., et al. (2012). Acyl homoserine lactone-based quorum sensing in a methanogenic archaeon. *ISME J.* 6, 1336–1344. doi: 10.1038/ismej.2011.203

Zhang, L., Li, S., Liu, X., Wang, Z., Jiang, M., Wang, R., et al. (2020). Sensing of autoinducer-2 by functionally distinct receptors in prokaryotes. *Nat. Commun.* 11:5371. doi: 10.1038/s41467-020-19243-5

Zhao, J., Li, X., Hou, X., Quan, C., and Chen, M. (2019). Widespread existence of quorum sensing inhibitors in marine bacteria: potential drugs to combat pathogens with novel strategies. *Mar. Drugs* 17:275. doi: 10.3390/md17050275

Zhao, Z., Wang, L., Miao, J., Zhang, Z., Ruan, J., Xu, L., et al. (2021). Regulation of the formation and structure of biofilms by quorum sensing signal molecules packaged in outer membrane vesicles. *Sci. Total Environ.* 806:151403. doi: 10.1016/j.scitotenv.2021.151403

Zhao, Z. C., Xie, G. J., Liu, B. F., Xing, D. F., Ding, J., Han, H. J., et al. (2021). A review of quorum sensing improving partial nitritation-anammox process: functions, mechanisms and prospects. *Sci. Total Environ.* 765:142703. doi: 10.1016/j.scitotenv.2020.142703

Zhou, Z., Liu, Y., Pan, J., Toner, B. M., Anantharaman, K., Breier, J. A., et al. (2020). Gamma*proteobacteria* mediating utilization of methyl-, sulfur- and petroleum organic compounds in deep ocean hydrothermal plumes. *ISME J.* 14, 3136–3148. doi: 10.1038/s41396-020-00745-5

Zimmerman, A. E., Martiny, A. C., and Allison, S. D. (2013). Microdiversity of extracellular enzyme genes among sequenced prokaryotic genomes. *ISME J.* 7, 1187–1199. doi: 10.1038/ismej.2012.176

Zinger, L., Amaral-Zettler, L. A., Fuhrman, J. A., Horner-Devine, M. C., Huse, S. M., Welch, D. B., et al. (2011). Global patterns of bacterial beta-diversity in seafloor and seawater ecosystems. *PLoS One* 6:e24570. doi: 10.1371/journal.pone.0024570

Conflict of Interest: The authors declare that the research was conducted in the absence of any commercial or financial relationships that could be construed as a potential conflict of interest.

III. Données supplémentaires

Table S1. Marine metagenomics survey of QS genes. nd.: not determined

Study	Type of data		AHL-synthase	AHL-receptor	AHL-lactonase	AHL-acylase	AI-2-synthase	Comments
Romero *et al.* (2012)	Metagenomics	GOS dataset (North Pacific subtropical gyre - 10, 70, 130, 200, 500, 770, 4000 m depth), 2 samples from whale carcasses, 2 samples from antartic community	nd.	nd.	0.01-0.13 sequences/Mpb (taxonomic affiliation nd.)	0.01- 0.34 sequences/Mpb (taxonomic affiliation nd.)	nd.	The frequency of QQ genes was higher than or comparable to the frequency of genes related to nutrient acquisition and oxidative metabolism in marine bacteria, suggesting that AHL degradation is an important process in the sea.
Doberva *et al.* (2015)	Metagenomics	GOS dataset (58 stations covering 11 habitat types)	- AinS: 1 sequence (0.02%) - exclusively *Vibrionaceae* - LuxI: 29 sequence (0.7%) - exclusively Proteobacteria - HdtS: 653 sequence (14.8%) - exclusively Alpha-, Beta- and Gammaproteobacteria	nd.	nd.	nd.	LuxS: 31 hits (0.7%) large coverage of bacterial phyla	Relative abundance calculated using rpoB gene.
Muras *et al.* (2018)	Metagenomics	One sampling site in the Mediterranean Sea, 8 depths from 90 to 2000 m	Sum of AinS, LuxI and HdtS: < 0.5 relative frequency (taxonomic affiliation nd.)	LuxR: 3-20 relative frequency (taxonomic affiliation nd.)	0.01-2.22 relative frequency (taxonomic affiliation nd.)	0.1-0.99 relative frequency (taxonomic affiliation nd.)	LuxS: no hits	Relative abundance calculated using *recA +radA* genes Low representation of AHL synthases in comparison to AHL receptors. No AI-2 synthase despite the presence of *Vibrio* in the cultivable fraction
Huang *et al.* (2018)	Metagenomics	8 samples following a dinoflagellate bloom in the YanTian Port (China)	- AinS: 0-26 sequences - exclusively *Vibrio* sp. - LuxI: 2-23 sequences - mainly Alpha-, Beta- and Gammaproteobacteria (mainly Pelagibacterales and Rhodobacterales) - HdtS: 65-739 sequences - mainly Alpha- and Gammaproteobacteria (mainly Rhodobacterales, Sphingomonadales, Pseudomonadales, Vibrionales, Rhizobiales)	nd.	Sum of lactonases and acylases: 3-26 sequences Mainly Alpha- and Gammaproteobacteria (mainly Vibrionales, Kiloniellales, Pseudomonales)		LuxS: 4-33 sequences - wide taxonomic coverage (mainly Gamma-, Beta- and Epsilonprotobacteria, Actinobacteria, Bacteroidetes)	The number of QS and QQ genes was normalized by the *rpoB* gene count. The *hdtS* -synthase dominated, mostly affiliated to Pelagibacterales (Alphaproteobacteria, representing 50%–80% of *hdtS*) and Rhodobacterales (Alphaproteobacteria, representing 25–30% of *htdS*). There was a correlation between QS and QQ signals frequency although QQ were less frequent than QS genes.
Su *et al.* (2021)	Metagenomics	2 sites in the Yellow Sea (China) with each 5 samples from surface and bottom seawater (fraction >0.2 µm and >3 µm) and surficial sediment	LuxI: 0.008-0.059 average gene copie per cell Mainly Gammaproteobacteria (Alteromonadales), Alphaproteobacteria (Rhodobacterales)	LuxR: 0.176-1.464 average gene copie per cell Mainly Gammaproteobacteria (Alteromonadales, Cellvibrionales, Chromatiales), Alphaproteobacteria (Rhodobacteria) and Bacteroidetes (Flavobacteriales)	1.126-4.419 average gene copie per cell, mainly Cellvibrionales, Pelagibacterales, Flavobacteriales, Chromatiales	0.114-1.148 average gene copie per cell, mainly Gammaproteobacteria (Cellvibrionales, Chromatiales, Alteromonadales) and Bacteroidetes (Flavobacteriales)	nd.	Average gene copie per cell were calculated normalizing by the *recA* gene counts. Shifts in abundance of QS and QQ genes as well as their contributing species were observed with depth

Doberva, M., Sanchez-Ferandin, S., Toulza, E., Lebaron, P., and Lami, R. (2015) Diversity of quorum sensing autoinducer synthases in the Global Ocean Sampling metagenomic database. Aquat Microb Ecol 74: 107–119.

Huang, X., Zhu, J., Cai, Z., Lao, Y., Jin, H., Yu, K., et al. (2018) Profiles of quorum sensing (QS)-related sequences in phycospheric microorganisms during a marine dinoflagellate bloom, as determined by a metagenomic approach. Microbiol Res 217: 1–13.

Muras, A., López-Pérez, M., Mayer, C., Parga, A., Amaro-Blanco, J., and Otero, A. (2018) High Prevalence of Quorum-Sensing and Quorum-Quenching Activity among Cultivable Bacteria and Metagenomic Sequences in the Mediterranean Sea. Genes (Basel) 9: 100.

Romero, M., Martin-Cuadrado, A.B., and Otero, A. (2012) Determination of whether quorum quenching is a common activity in marine bacteria by analysis of cultivable bacteria and metagenomic sequences. Appl Environ Microbiol 78: 6345–6348.

Su, Y., Yang, Y., Zhu, X.Y., Zhang, X.H., and Yu, M. (2021) Metagenomic Insights Into the Microbial Assemblage Capable of Quorum Sensing and Quorum Quenching in Particulate Organic Matter in the Yellow Sea. Front Microbiol 11: 602010.

Table S2. Screening of QS and QQ capacities of marine isolates. AHL names are abbreviated according to the size of the acyl chain and its possible substitution at the third C [e.g., *N*-(3-oxohexanoyl)-L-homoserine lactone is abbreviated as 3-oxo-C6-HSL]. nd.: not determined. BS: biosensor; TLC: Thin-layer chromatography; CG: Gas chromatography; LC: Liquid chromatography; HPLC: High performance LC; MS: Mass spectrometry; HRMS: High resolution MS. Rf: Retention factor. *Screening was performed with a biosensor integrating three AIs (AHL, AI-2, CAI-1) and did not exclusively represent AHL- and AI-2-quenching isolate

	Isolated from	Number of screened strains	Number of AHL-producing strains	Number of AHL-quenching strains	Number of AI-2-producing strains	Other
Gram *et al.* (2002)	Marine snow particles or axenic diatoms immerged in the surface waters of the Øresund (Denmark) and in the German Waddensea (Neuharlingersiel)	43 strains (41 Alphaproteobacteria, 10 Bacteroidetes, 9 Gammaproteobacteria, 7 Firmicutes, 3 Actinomycetes, 1 Cyanobacteria)	BS and TLC: 3 Alphaproteobacteria (*Roseobacter*), 1 Gammaprotobacteria (*Marinobacter*)	nd.	nd.	
Wagner-Dobler *et al.* (2005)	Various habitats from the North Sea (dinoflagellate, picoplancton, water column, laminaria, diatoms)	102 strains (14 Gammaproteobacteria, 65 Alphaprotobacteria, 18 Bacteroidetes, 3 Actinobacteria, 2 Firmicutes)	BS: 41 strains induced BS (38 Alphaproteobacteria, 2 Gammaproteobacteria, 1 Bacteroidetes) GC-MS: 22 Alphaproteobacteria strains (out of the 41 BS-positive strains)	nd.	nd.	
Huang *et al.* (2008)	9 d-old subtidal biofilms developed at a coastal fish farm	68 strains (51 Gammaproteobacteria, 13 Alphaproteobacteria, 4 Bacteroidetes)	BS: 21 strains (13 Gammaproteobacteria, 5 Alphaproteobacteria, 3 Bacteroidetes) GC-MS: 20 strains (13 Gammaproteobacteria, 5 Alphaproteobacteria, 2 Bacteroidetes)	nd.	nd.	
Kanagasabhapathy *et al.* (2009)	Epibiotic bacteria of *Colpomenia sinuosa*(brown algae) from the intertidal zone, Japan	96 strains (overall diversity nd.)	nd.	BS: 11 strains (12%) 6 Firmicutes (*Bacillus*), 5 Gammaproteobacteria (3 *Pseudoalteromonas*, 2 *Vibrio*)	nd.	

Tait *et al.* (2010)	Healthy and diseased corals (Australia, Hawaii, Mediterranean Sea, Red Sea, Zanzibar, England)	29 *Vibrio* strains	BS and TLC: 17 *Vibrio* strains	nd.	BS: 29 *Vibrio* strains	
Romero *et al*. (2010)	3 strains from the National Collections of Industrial, Food and Marine Bacteria Ltd (Aberdeen, UK), 6 strains from fish farm disease outbreaks (Spain and Portugal)	9 *Tenacibaculum maritimum* strains (Bacteroidetes)	BS and TLC: 9 *T. maritimum* (Bacteroidetes) strains LC-MS: 1 strain (1 tested)	In 1 strain (*T. maritimus* NCIMB2154T): QQ of C6- and C10-HSL BS and HPLC: complete degradation of C10-HSL	nd.	
Romero *et al.* (2011)	3 samples from coastal marine communities of Spain (diatom-dominated biofilm, *F. vesiculosus* surface and sedimentation tank of marine fish culture circuit)	166 strains (overall diversity unknown)	nd.	BS: 24 strains quenched C6-HSL; Among those 24 strains: 15 strains also quenched C10-HSL (6 Alphaproteobacteria, 2 Gammaproteobacteria, 4 Firmicutes, 2 Actinobacteria, 1 Bacteroidetes) (using BS and HPLC-MS); Among those 15 strains: 10 strains also quenched 3-oxo-C12-HSL (BS and HPLC-MS)	nd.	
Teasdale *et al.* (2011)	Various marine locations (New England, Bahamas, Puerto Rico) and sources (algae, invertebrates, sediments)	332 Gram-positive isolates (overal diversity nd.)	nd.	BS: 49 active isolates* Among the 49, 28 were also active when using extracts* Among the 49, 8 extracts were also strictly AHL-QQ (7 *Bacillus*, 1 *Halobacillus*)	BS: 49 active isolates* Among the 49, 28 were also active when using extracts*	
Romero *et al.* (2012)	3 samples: surface waters of an estuary, 0- an 10-m depth of the Atlantic ocean (Spain)	464 strains (overall diversity nd.)	nd.	BS: 85 strains interfered with C6- and C10-HSL Among those 85 strains: 85 also quenched C12-HSL while 4 also quenched C4-HSL (HPLC-MS) (2 Oceanospirillales, 2 Flavobacteriales)	nd.	

Cuadrado-Silva *et al.* (2013)	Biofilm coating sponges, shell of a bivalve and submerged phytagel dishes in the Colombian Caribbean Sea	8 strains: 6 Gammaproteobacteria (4 *Vibrio,* 1 *Shewanella*, 1 *Alteromonas*), 2 Alphaproteobacteria (2 *Ochrobactrum*)	BS, TCL, GC-MS, HPLC-MS: 8 strains (4 *Vibrio*, 2 *Ochrobactrum*, 1 *Shewanella*, 1 *Alteromonas*)	nd.	nd.	
Jatt *et al.* (2015)	Marine snow collected in the surface water in the Yellow Sea (China)	53 strains (31 Gammaproteobacteria, 7 Alphaproteobacteria, 5 Firmicutes, 5 Actinobacteria, 4 Betaproteobacteria, 1 Flavobacteria)	BS: 10 strains (9 Gammaproteobacteria, 1 Alphaproteobacteria) (TLC and GC-MS for *P. ananatis* B9 strain)	nd.	nd.	
Torres *et al.* (2016)	Seawater from a fish hatchery tank in Granada (Spain)	450 strains (overall diversity nd.)	nd.	BS: 112 strains degraded both C6- and C10-HSL Among those 112 strains: 12 strains (6 *Pseudoalteromonas*, 6 *Alteromonas*) degraded a wide range of AHLs (C6-, C8-, C10-, C12-, 3-oxo-C12- and 3-OH-C10-HSL) (confirmed by HPLC-MS for C6- and C10-HSL)	nd.	
Betancur *et al.* (2017)	Invertebrates, algae and sediments from the Colombian Caribbean Sea	24 Actinobacteria strains (22 *Streptomyces,* 1 *Gordonia,* 1 *Micromonospora*)	nd.	BS: 8 strains interfered with *C. violaceum* native QS system (7 *Streptomyces*, 1 *Micromonospora*)	nd.	Metabolic profiling
Blanchet *et al.* (2017)	*Posidonia oceanica* rhizomes and leaves from Banyuls-sur-mer (France)	60 strains (72% Alphaproteobacteria, 20% Gammaproteobacteria, 3% Flavobacteria, 5% Actinobacteria, Bacilli)	BS and UPHLC-HRMS/MS: 6 Alphaproteobacteria strains (3 *Pseudophaeobacter,* 2 *Cohaesibater,* 1 *Labrenzia*)	BS: 4 Alphaproteobacteria, 1 Gammaproteobacteria	BS: 15 Alphaproteobacteria, 2 Gammaproteobacteria, 2 Flavobacteria	
Bose *et al*. (2017)	Great Barrier Reef marine sponges	30 strains (15 *Salinispora arenicola* and 15 *Salinispora pacifica*)	LC-MS/MS:	nd.	nd.	

Freckelton *et al.* (2018)	Surface mucosal layer from three healthy coral colonies from the Great Barrier Reef (Australia)	62 strains (mainly Gammaproteobacteria, but also Alphaproteobacteria, Actinobacteria and Firmicutes)	BS: 18 strains (15 Gammaproteobacteria, 2 Alphaproteobacteria, 1 Firmicutes) (no analytical assay)	BS: 15 Gammaproteobacteria strains (no analytical assay)	nd.	
Rehman & Leiknes (2018)	Red Sea sediments, with and without seagrass	72 strains (overall diversity nd.)	nd.	BS (C6-HSL): 14 strains Among those 14 strains : 6 Alphaproteobacteria (2 *Erythrobacter*, 4 *Labrenzia*) and 1 Gammaproteobacteria (*Bacterioplanes*) quenched at least one of 6 AHLs (HPLC-MS)	nd.	Draft genome of *Erythrobacter* sp. VG1, *Labrenzia* sp. VG12, *Bacterioplane* sp. NV9
Muras *et al.* (2018)	90 and 2000 m depths in the Mediterranean Sea	605 bacteria: 231 from 90 m and 374 from 2000 m (35% Gammaproteobacteria, 31% Firmicutes, 17% Alphaproteobacteria, 7% Bacteroidetes, 7% Actinobacteria)	BS: 21% of the strains (diversity no precised) (no analytical assay)	BS: 2% of strains quenched C6-HSL, 38% quenched the C12-HSL (no analytical assay) Diversity of 12 wide-spectrum QQ strains: 8 Alphaproteobacteria, 1 Firmicutes, 1 Actinobacteria, 1 Gammaproteobacteria, 1 Betaproteobacteria	nd.	Comparison with metagenomic data
Su *et al.* (2019)	Marine snow particles collected in the Yellow Sea (China)	122 strains (98 Proteobacteria, 10 Bacteroidetes, 10 Actinobacteria, 4 Firmicutes)	BS: 20 strains (12 Alphaproteobacteria, 7 Gammaproteobacteria, 1 Actinobacteria) (GC-MS for *Ruegeria mobilis* Rm01)	BS: 62 strains quenched C6- or C12-HSL (32 Gammaproteobacteria, 18 Alphaproteobacteria, 10 Bacteroidetes, 2 Actinobacteria)	nd.	Draft genome of *Ruegeria mobilis* Rm01
Tourneroche *et al.* (2019)	Four brown algae (Roscoff, France and Oban, Scotland)	209 strains (96 Bacilli, 62 Gammaproteobacteria, 34 Actinobacteria, 9 Bacteroidetes, 8 Alphaproteobacteria)	nd.	nd.	BS: 180 strains (mostly *Bacillus*, *Pseudoalteromonas* and *Cobetia*) (LC-MS/MS confirmation in 3 strains)	
Reen *et al.* (2019)	Dfferent sponge genera from the west coast of Ireland	650 strains (including Proteobacteria, Actinobacteria, Bacteroidetes, Firmicutes)	BS, TLC: 10 Gammaproteobacteria (4 Pseudomonadales, 4 Alteromonadales, 1 Vibrionales, 1 Oceanospiralles) UHPLC-HRMS: 8 strains (3 Pseudomonadales, 3	nd.	nd.	Draft genome of *Psychrobacter* sp.

			Alteromonadales, 1 Vibrionales, 1 Oceanospiralles)			
Charlesworth *et al.* (2019)	Four microbial mats in Shark Bay (Australia)	165 strains (overall diversity nd.)	30 strains activated the BS, 18 had Rf value in TLC assay (9 Proteobacteria, 6 Firmicutes, 3 Actinobacteria) (BS-based and TLC)	nd.	nd.	
Abdul Malik *et al.* (2020)	*Halymenia floresii* collected from the shores in Yucutan, Mexico	31 strains (14 Gammaproteobacteria, 12 Alphaproteobacteria, 4 Bacteroidetes, 1 Firmicutes)	17 strains activated the BS (8 Gammaproteobacteria, 5 Alphaproteobacteria, 4 Bacteroidetes)	nd.	nd.	
Charlesworth *et al.* (2020)	Various marine (stromatolite, microbial mat, Dead Sea) and non-marine sources	17 Archaea (3 marine strains)	BS and TLC: 11 strains including 3 marine ones (Archaea)	nd.	nd.	
Urvoy *et al.* (2021a)	Estuarine waters from the Bay of Brest (France)	299 strains (overall diversity nd.)	BS: 75 strains UPHCL-MS/MS: 28 strains (15 Pseudomonadales, 10 Vibrionales, 2 Enterobacterales, 1 Sphingomonadales	BS: 10 strains quenched C6- or C12-HSL among the 28 AHL-producing strains (8 Pseudomonadales, 1 Vibrionales, 1 Enterobacterales)	nd.	Four draft genomes (2 *Pseudomonas*, 1 *Vibrio,* 1 *Acinetobacter)*

Abdul Malik, S.A., Bazire, A., Gamboa-Muñoz, A., Bedoux, G., Robledo, D., García-Maldonado, J.Q., and Bourgougnon, N. (2020) Screening of Surface-associated Bacteria from the Mexican Red Alga Halymenia floresii for Quorum Sensing Activity. Microbiology 89: 778–788.

Betancur, L.A., Naranjo-Gaybor, S.J., Vinchira-Villarraga, D.M., Moreno-Sarmiento, N.C., Maldonado, L.A., Suarez-Moreno, Z.R., et al. (2017) Marine Actinobacteria as a source of compounds for phytopathogen control: An integrative metabolic-profiling/bioactivity and taxonomical approach. PLoS One 12: e0170148.

Blanchet, E., Prado, S., Stien, D., da Silva, J.O., Ferandin, Y., Batailler, N., et al. (2017) Quorum sensing and quorum quenching in the Mediterranean Seagrass Posidonia Oceanica microbiota. Front Mar Sci 4: 218.

Bose, U., Ortori, C.A., Sarmad, S., Barrett, D.A., Hewavitharana, A.K., Hodson, M.P., et al. (2017) Production of N-acyl homoserine lactones by the sponge-associated marine actinobacteria Salinispora arenicola and Salinispora pacifica. FEMS Microbiol Lett 364: 1–7.

Charlesworth, J., Kimyon, O., Manefield, M., Beloe, C.J., and Burns, B.P. (2020) Archaea join the conversation: detection of AHL-like activity across a range of archaeal isolates. FEMS Microbiol Lett 367: 1–9.

Charlesworth, J.C., Watters, C., Wong, H.L., Visscher, P.T., and Burns, B.P. (2019) Isolation of novel quorum-sensing active bacteria from microbial mats in Shark Bay Australia. FEMS Microbiol Ecol 95: 1–14.

Cuadrado-Silva, C.T., Castellanos, L., Arévalo-Ferro, C., and Osorno, O.E. (2013) Detection of quorum sensing systems of bacteria isolated from fouled marine organisms. Biochem Syst Ecol 46: 101–107.

Freckelton, M.L., Høj, L., and Bowden, B.F. (2018) Quorum sensing interference and structural variation of Quorum Sensing mimics in Australian Soft Coral. Front Mar Sci 5: 198.

Gram, L., Grossart, H.P., Schlingloff, A., and Kiørboe, T. (2002) Possible quorum sensing in marine snow bacteria: production of acylated homoserine lactones by Roseobacter strains isolated from marine snow. Appl Environ Microbiol 68: 4111–4116.

Huang, Y.L., Ki, J.S., Case, R.J., and Qian, P.Y. (2008) Diversity and acyl-homoserine lactone production among subtidal biofilm-forming bacteria. Aquat Microb Ecol 52: 185–193.

Jatt, A.N., Tang, K., Liu, J., Zhang, Z., and Zhang, X.H. (2015) Quorum sensing in marine snow and its possible influence on production of extracellular hydrolytic enzymes in marine snow bacterium Pantoea ananatis B9. FEMS Microbiol Ecol 91: 1–13.

Kanagasabhapathy, M., Yamazaki, G., Ishida, A., Sasaki, H., and Nagata, S. (2009) Presence of quorum-sensing inhibitor-like compounds from bacteria isolated from the brown alga Colpomenia sinuosa. Lett Appl Microbiol 49: 573–579.

Muras, A., López-Pérez, M., Mayer, C., Parga, A., Amaro-Blanco, J., and Otero, A. (2018) High Prevalence of Quorum-Sensing and Quorum-Quenching Activity among Cultivable Bacteria and Metagenomic Sequences in the Mediterranean Sea. Genes (Basel) 9: 100.

Reen, F.J., Gutiérrez-Barranquero, J.A., McCarthy, R.R., Woods, D.F., Scarciglia, S., Adams, C., et al. (2019) Quorum Sensing Signaling Alters Virulence Potential and Population Dynamics in Complex Microbiome-Host Interactomes. Front Microbiol 10: 1–13.

Rehman, Z.U. and Leiknes, T.O. (2018) Quorum-quenching bacteria isolated from red sea sediments reduce biofilm formation by Pseudomonas aeruginosa. Front Microbiol 9: 1354.

Romero, M., Avendaño-Herrera, R., Magariños, B., Cámara, M., and Otero, A. (2010) Acylhomoserine lactone production and degradation by the fish pathogen Tenacibaculum maritimum, a member of the Cytophaga-Flavobacterium-Bacteroides (CFB) group. FEMS Microbiol Lett 304: 131–139.

Romero, M., Martin-Cuadrado, A.B., and Otero, A. (2012) Determination of whether quorum quenching is a common activity in marine bacteria by analysis of cultivable bacteria and metagenomic sequences. Appl Environ Microbiol 78: 6345–6348.

Romero, M., Martin-Cuadrado, A.B., Roca-Rivada, A., Cabello, A.M., and Otero, A. (2011) Quorum quenching in cultivable bacteria from dense marine coastal microbial communities. FEMS Microbiol Ecol 75: 205–217.

Su, Y., Tang, K., Liu, J., Wang, Y., Zheng, Y., and Zhang, X.H. (2019) Quorum sensing system of Ruegeria mobilis Rm01 controls lipase and biofilm formation. Front Microbiol 10: 3304.

Tait, K., Hutchison, Z., Thompson, F.L., and Munn, C.B. (2010) Quorum sensing signal production and inhibition by coral-associated vibrios. Environ Microbiol Rep 2: 145–150.

Teasdale, M.E., Donovan, K.A., Forschner-Dancause, S.R., and Rowley, D.C. (2011) Gram-Positive Marine Bacteria as a Potential Resource for the Discovery of Quorum Sensing Inhibitors. Mar Biotechnol 13: 722–732.

Torres, M., Rubio-Portillo, E., Antón, J., Ramos-Esplá, A.A., Quesada, E., and Llamas, I. (2016) Selection of the N-acylhomoserine lactone-degrading bacterium Alteromonas stellipolaris PQQ-42 and of its potential for biocontrol in aquaculture. Front Microbiol 7: 646.

Tourneroche, A., Lami, R., Hubas, C., Blanchet, E., Vallet, M., Escoubeyrou, K., et al. (2019) Bacterial-fungal interactions in the kelp endomicrobiota drive autoinducer-2 quorum sensing. Front Microbiol 10: 1–14.

Urvoy, M., Lami, R., Dreanno, C., Daudé, D., Rodrigues, A.M.S., Gourmelon, M., et al. (2021a) Quorum sensing disruption regulates hydrolytic enzyme and biofilm production in estuarine bacteria. Environ Microbiol.

Wagner-Döbler, I., Thiel, V., Eberl, L., Allgaier, M., Bodor, A., Meyer, S., et al. (2005) Discovery of Complex Mixtures of Novel Long-Chain Quorum Sensing Signals in Free-Living and Host-Associated Marine Alphaproteobacteria. ChemBioChem 6: 2195–2206.

Table S3. QS and QQ pathways and QS functions of the main prokaryotic groups presented in this review. The genera for which QS functions were investigated are included as well as the genera for which several AI-producing strains have been isolated (across different studies). This table was used to design Figure 1. Black print: marine study, blue print: aquatic study, green print: non-aquatic study. Anti-AHL: unknown compound (including QQ-enzymes and QSIs); Anti-QS: screening performed with a biosensor integrating three AIs; DPO: 3,5-dimethylpyrazin-2-ol. *QS gene presence or function was hinted at by omic studies but not proven.

Phylum	*Class*	*Order*	*Genus*	*Production of QS compounds*	QS-regulated function	*Production of QQ compounds*
Actinobacteria	Actinobacteria	Micronosporales	*Salinispora*	AHL (Bose *et al.*2017)		
		Micrococcales	*Kocuria*	AHL (Su *et al.* 2019)		
		Actinomycetales	*Streptomyces*	AI-2 (Tourneroche *et al.* 2019) Gamma-butyrolactone (reviewed in Polkade *et al.*2016)	Antibiotics, morphogenesis, sporulation (reviewed in Polkade *et al.*2016)	Anti-AHL (Betancur *et al.* 2017), Anti-QS (Teasdale *et al.* 2011)
			Microbacterium	AHL (Charlesworth *et al.* 2019) AI-2 (Tourneroche *et al.* 2019)		Anti-AHL (Muras *et al.*2018; Su *et al*. 2019)
Firmicutes	Bacilli	Bacillales	*Bacillus*	AHL (Freckelton *et al.* 2018; Charlesworth *et al.* 2019) AI-2 (Tourneroche *et al.* 2019)		Anti-AHL (Kanagasabhapathy *et al.* 2009; Romero *et al.* 2011a; Teasdale *et al.* 2011) including QSI and lactonase (Teasdale *et al.* 2011); Anti-QS (Teasdale *et al.* 2011)
			Oceanobacilus			AHL-acylase (Romero *et al.* 2011a); AHL-QSI (reviewed in Saurav *et al.* 2017)
			Halobacillus			Anti-QS (Teasdale *et al.* 2011); Anti-AHL (Teasdale *et al.* 2011; Charlesworth *et al.* 2019)
Bacteroidetes	Cytophagia	Cytophagales	*Flammeovirga*	AHL (Huang *et al.* 2008)		
	Flavobacteria	Flavobacteriales	*Tenacibaculum*	AHL (Romero *et al.* 2010; Abdul malik *et al.* 2020)		Anti-AHL (Romero *et al.* 2010, 2011a; Su *et al.* 2019)
			Muricauda	AHL (Huang *et al.* 2008)		Anti-AHL (Su *et al.* 2019)
			Maribacter	AHL (Abdul Malik *et al.* 2020)		Anti-AHL (Su *et al.* 2019)
	Sphingobacteria	Sphingobacteriales	*Sphingobacterium*	AHL (Urvoy *et al.* 2021a)	Extracellular proteases (Urvoy *et al.* 2021a)	

Proteobacteria	α	Rhodobacterales	*Dinoroseobacter*	AHL (Wagner-Döbler *et al.* 2005; Patzelt *et al.* 2013)	Heterogeneity in cell morphology and cell division, growth rate (Patzelt *et al.* 2013)	
			Labrenzia	AHL (Blanchet *et al.* 2017); AI-2 (Blanchet *et al.* 2017; Tourneroche *et al.* 2019)		Anti-AHL (Rehman & Leiknes, 2018; Su *et al.* 2019)
			Nautella	AHL (Su *et al.* 2019)	Biofilm, attachment, virulence (Gardinier *et al.* 2015)	
			Paracoccus	AHL (Saurav *et al.* 2016) and OMVs packed AHL (Toyofuku *et al.* 2017)		
			Phaeobacter	AHL (Fei *et al.* 2020) TDA (reviewed in Buchan *et al.* 2016)	Motility, biofilm formation, attachment (Fei *et al.* 2020) Antimicrobials (reviewed in Buchan *et al.* 2016)	Anti-AHL (Romero *et al.* 2011a)
			Ruegeria	AHL (Huang *et al.* 2008; Su *et al.* 2019; Zan *et al.* 2015; Abdul Malik *et al.* 2020) p-coumaroyl-HSL (Zan *et al.* 2015), TDA (reviewed in Buchan et al. 2016), diketopiperazines (Mitova *et al.* 2004)	Extracellular lipase and biofilm formation (Su *et al.* 2019), motility (Zan *et al.* 2013, 2015), antimicrobial (reviewed in Buchan *et al.* 2016)	AHL-lactonase (Su *et al.* 2019)
			Roseobacter	AHL (Gram *et al.* 2002; Wagner-Döbler *et al.* 2005; Abdul Malik *et al.* 2020)		
			Silicibacter	p-coumaroyl-HSL (Schaefer *et al.* 2008)		
			Sulfitobacter	AHL (Fei *et al.* 2020)	Motility, biofilm formation and attachment (Fei *et al.* 2020)	
		Hyphomicrobiales	*Nitrobacter*	AHL (Shen *et al.* 2016; Mellbye *et al.* 2016)	Nitrogen metabolism (Shen *et al.* 2016; Mellbye *et al.* 2016, 2017a, 2017b)	
		Sphingomonadales	*Croceicoccus*	AHL (Yu *et al.* 2020)	PAH degradation, cell hydrophobicity and adhesion (Yu *et al.* 2020)	
			Erythrobacter	AHL (Su *et al.* 2019; Jatt *et al.* 2015; Abdul Malik *et al.* 2020)		Anti-AHL (Muras *et al.* 2018; Su *et al.* 2019) including lactonase (Rehman & Leiknes, 2018)
	β	Burkholderiales	*Alcaligenes*	AHL (Jatt *et al.* 2015)		

Proteobacteria	γ	Aeromonadales	*Aeromonas*	AHL (Jatt *et al.* 2015)	Extracellular protease, biofilm formation (reviewed in Torres *et al.* 2019)	
		Alteromonadales	*Alteromonas*	AHL (Cuadrado-Silva *et al.* 2013; Jatt *et al.* 2015; Freckelton *et al.* 2018; Abdul Malik *et al.* 2020) AI-2 (Tourneroche *et al.* 2019)		Anti-AHL (Torres *et al.* 2016; Su *et al.* 2019) including acylase (Romero *et al.* 2011a)
			Marinomas	AI-2 (Tourneroche *et al.* 2019)		
			Marinobacter	AHL (Gram *et al.* 2002)		Anti-AHL (Su *et al.* 2019) including AHL-QSI (reviewed in Saurav *et al.* 2017)
			Pseudoalteromonas	AHL (Huang *et al.* 2008; Jatt *et al.* 2015; Freckelton *et al.* 2018; Reen *et al.* 2019; Abdul Malik *et al.* 2020) AI-2 (Tourneroche *et al.* 2019) HHQ (Paulsen *et al.* 2020)	Violaceine, motility, adhesion, biofilm formation (Ayé *et al.* 2015)	Anti-AHL (Torres *et al.* 2016; Su *et al.* 2019)
			Shewanella	AHL (Jatt *et al.* 2015; Cuadrado-Silva *et al.* 2013); AI-2 (Tourneroche *et al.* 2019)		Anti-AHL (Su *et al.* 2019)
		Oceanospiralles	*Alcanivorax*	AHL (Su *et al.* 2019)	*Attachement to alkane droplet (Sabirova *et al.* 2011)	Anti-AHL (Su *et al.* 2019)
			Halomonas			Anti-AHL (Romero *et al.* 2011a)
		Enterobacteriales	*Pantoea*	AHL (Jatt *et al.* 2015)	Extracellular phosphatase (Jatt *et al.* 2015)	Anti-AHL (Muras *et al.* 2018)
		Pseudomonadales	*Acinetobacter*	AHL (Zhang *et al.* 2020; Urvoy *et al.* 2021a; reviewed in Saipriya et al. 2019)	Algicidal activity (Zhang et al. 2020); Extracellular proteases and glucosidases (Urvoy *et al.* 2021a); Virulence and biofilm formation (reviewed in Saipriya et al. 2019)	Anti-AHL (Su *et al.* 2019)
			Pseudomonas	AHL (Jatt *et al.* 2015; Reen *et al.* 2019) PQS and HHQ (reviewed in García-Reyes et al. 2020); OMVs packed PQS (Zhao *et al.* 2021)	PAH degradation (Mangwani *et al.* 2015; Kumari *et al.* 2021); Biofilm production (Urvoy *et al.* 2021a); Extracellular proteases and glucosidases (Urvoy *et al.* 2021a); Denitrification (Toyofuku *et al.* 2008) Virulence factors (reviewed in in García-Reyes *et al.* 2020); Denitrification (Toyofuku *et al.* 2008)	Anti-AHL (Su *et al.* 2019)

		Vibrionales	*Vibrio*	AHL (Huang *et al.* 2008; Cuadrado-Silva *et al.* 2013; Liu *et al.* 2017; Su *et al.* 2019; Jatt *et al.* 2015; Urvoy *et al.* 2021a); OMVs packed AHL (Li *et al.* 2016) AI-2 (Tait *et al.* 2010; Blanchet *et al.* 2017) CAI-1 (Henke and Bassler 2004) and OMVs packed CAI-1 (Brameyer *et al.* 2018)	Bioluminescence (Fuqua *et al.* 1994); Biofilm formation (Liu *et al.* 2017; Urvoy *et al.* 2021a); Extracellular proteases and glucosidases (Urvoy *et al.* 2021a); Siderophores (McRose *et al.* 2018) Bioluminescence, morphology, biofilm formation, proteases, virulence factors, siderophores (reviewed in Pereira *et al.* 2013) Bioluminescence and virulence factors (Henke *et al.* 2004)	Anti-AHL (Torres *et al.* 2016; Blanchet *et al.* 2017; Freckelton *et al.* 2018; Su *et al.* 2019)
	δ	Desulfobacterales	*Desulfobacterium*	AHL (Sivakumar *et al.* 2019)	Biofilm formation, sulfate reduction (Sivakumar *et al.* 2019)	
Cyanobacteria	Cyanophyceae	Chroococcales	*Gloeothece*	AHL (Sharif *et al.* 2008)	Carbohydrates and amino acids metabolism (Sharif *et al.* 2008)	
			Microcystis	AHL (Zhai *et al.* 2012)	Morphological changes (Zhai *et al.* 2012)	
		Nostacales	*Anabaena*		N_2 fixation (Romero *et al.* 2011b)	AHL-acylase (AiiC) (Romero *et al.* 2008)
Euryarcheota	Halobacteria	Halobacteriales	*Natronococcus*	AHL (Paggi *et al.* 2003; Charlesworth *et al.* 2020)		
			Halorubrum	AHL (Liao *et al.* 2016, Charlesworth *et al.* 2020)		
			Halococcus	AHL (Charlesworth *et al.* 2020)		
			Haloferax	AHL (Charlesworth *et al.* 2020)		
			Haloterrigena	Diketopiperazines (Tommonaro *et al.* 2012)		
	Methanomicrobia	Methanosarcinales	*Methanosaeta*	*N*-carboxyl-C12-HSL (Zhang *et al.* 2012)	Morphology, carbon metabolic flux, biomass yield (Zhang *et al.* 2012)	

	Order	*Specie*	*Host*	*QS receptor*	QS-regulated function	*Production of QQ compounds*
Phage	Caudovirales	*Vibrio phage VP882*	*Vibrio cholerae* str. C6706	DPO-binding receptor (Silpe *et al.* 2020)	Lysis-lysogeny switch (Silpe *et al.* 2020)	
		phiARM81ld	*Aeromonas* sp. ARM81	AHL-binding receptor (Silpe and Bassler 2019)		
		Apop	*Aeromonas popoffii* CIP 105493	AHL-binding receptor (Silpe and Bassler 2019)		
		Leefvirus Leef	*Polaribacter* sp. AHE13PA	AHL-binding receptor (Bartlau *et al.* 2021)		
		Ingelinevirus Ingeline	*Cellulophaga* sp. HaHaR_3_176	AHL-binding receptor (Bartlau *et al.* 2021)		
	unspecified	*unspecified*	*unspecified*			AHL-lactonase (Su et al. 2021)

Abdul Malik, S.A., Bazire, A., Gamboa-Muñoz, A., Bedoux, G., Robledo, D., García-Maldonado, J.Q., and Bourgougnon, N. (2020) Screening of Surface-associated Bacteria from the Mexican Red Alga Halymenia floresii for Quorum Sensing Activity. Microbiology 89: 778–788.

Ayé, A.M., Bonnin-Jusserand, M., Brian-Jaisson, F., Ortalo-Magné, A., Culioli, G., Nevry, R.K., et al. (2015) Modulation of violacein production and phenotypes associated with biofilm by exogenous quorum sensing N-acylhomoserine lactones in the marine bacterium Pseudoalteromonas ulvae TC14. Microbiology 161: 2039–2052.

Bartlau, N., Wichels, A., Krohne, G., and Adriaenssens, E.M. (2021) Highly diverse flavobacterial phages isolated from North Sea spring blooms. ISME J.

Betancur, L.A., Naranjo-Gaybor, S.J., Vinchira-Villarraga, D.M., Moreno-Sarmiento, N.C., Maldonado, L.A., Suarez-Moreno, Z.R., et al. (2017) Marine Actinobacteria as a source of compounds for phytopathogen control: An integrative metabolic-profiling/bioactivity and taxonomical approach. PLoS One 12: e0170148.

Blanchet, E., Prado, S., Stien, D., da Silva, J.O., Ferandin, Y., Batailler, N., et al. (2017) Quorum sensing and quorum quenching in the Mediterranean Seagrass Posidonia Oceanica microbiota. Front Mar Sci 4: 218.

Bose, U., Ortori, C.A., Sarmad, S., Barrett, D.A., Hewavitharana, A.K., Hodson, M.P., et al. (2017) Production of N-acyl homoserine lactones by the sponge-associated marine actinobacteria Salinispora arenicola and Salinispora pacifica. FEMS Microbiol Lett 364: 1–7.

Brameyer, S., Plener, L., Müller, A., Klingl, A., Wanner, G., and Jung, K. (2018) Outer membrane vesicles facilitate trafficking of the hydrophobic signaling molecule CAI-1 between Vibrio harveyi cells. J Bacteriol 200: e00740-17.

Buchan, A., Mitchell, A., Cude, W.N., and Campagna, S. (2016) Acyl-homoserine lactone-based quorum sensing in members of the marine bacterial Roseobacter clade: complex cell-to-cell communication controls multiple physiologies. In Stress and Environmental Regulation of Gene Expression and Adaptation in Bacteria. de Bruijn, F.J. (ed). John Wiley & Sons, pp. 225–233.

Charlesworth, J., Kimyon, O., Manefield, M., Beloe, C.J., and Burns, B.P. (2020) Archaea join the conversation: detection of AHL-like activity across a range of archaeal isolates. FEMS Microbiol Lett 367: 1–9.

Charlesworth, J.C., Watters, C., Wong, H.L., Visscher, P.T., and Burns, B.P. (2019) Isolation of novel quorum-sensing active bacteria from microbial mats in Shark Bay Australia. FEMS Microbiol Ecol 95: 1–14.

Cuadrado-Silva, C.T., Castellanos, L., Arévalo-Ferro, C., and Osorno, O.E. (2013) Detection of quorum sensing systems of bacteria isolated from fouled marine organisms. Biochem Syst Ecol 46: 101–107.

Fei, C., Ochsenkühn, M.A., Shibl, A.A., Isaac, A., Wang, C., and Amin, S.A. (2020) Quorum sensing regulates 'swim-or-stick' lifestyle in the phycosphere. Environ Microbiol 22: 4761–4778.

Freckelton, M.L., Høj, L., and Bowden, B.F. (2018) Quorum sensing interference and structural variation of Quorum Sensing mimics in Australian Soft Coral. Front Mar Sci 5: 198.

Fuqua, W.C., Winans, S.C., and Greenberg, E.P. (1994) Quorum sensing in bacteria: The LuxR-LuxI family of cell density-responsive transcriptional regulators. J Bacteriol 176: 269–275.

García-Reyes, S., Soberón-Chávez, G., and Cocotl-Yanez, M. (2020) The third quorum-sensing system of Pseudomonas aeruginosa: Pseudomonas quinolone signal and the enigmatic PqsE protein. J Med Microbiol 69: 25–3

Gardiner, M., Fernandes, N.D., Nowakowski, D., Raftery, M., Kjelleberg, S., Zhong, L., et al. (2015) VarR controls colonization and virulence in the marine macroalgal pathogen Nautella italica R11. Front Microbiol 6: 1130.

Gram, L., Grossart, H.P., Schlingloff, A., and Kiørboe, T. (2002) Possible quorum sensing in marine snow bacteria: production of acylated homoserine lactones by Roseobacter strains isolated from marine snow. Appl Environ Microbiol 68: 4111–4116.

Henke, J.M. and Bassler, B.L. (2004) Three parallel quorum-sensing systems regulate gene expression in Vibrio harveyi. J Bacteriol 186: 6902–6914.

Huang, Y.L., Ki, J.S., Case, R.J., and Qian, P.Y. (2008) Diversity and acyl-homoserine lactone production among subtidal biofilm-forming bacteria. Aquat Microb Ecol 52: 185–193.

Jatt, A.N., Tang, K., Liu, J., Zhang, Z., and Zhang, X.H. (2015) Quorum sensing in marine snow and its possible influence on production of extracellular hydrolytic enzymes in marine snow bacterium Pantoea ananatis B9. FEMS Microbiol Ecol 91: 1–13.

Kanagasabhapathy, M., Yamazaki, G., Ishida, A., Sasaki, H., and Nagata, S. (2009) Presence of quorum-sensing inhibitor-like compounds from bacteria isolated from the brown alga Colpomenia sinuosa. Lett Appl Microbiol 49: 573–579.

Kumari, S., Mangwani, N., and Das, S. (2020) Naphthalene catabolism by biofilm forming marine bacterium Pseudomonas aeruginosa N6P6 and the role of quorum sensing in regulation of dioxygenase gene. J Appl Microbiol 130: 1217–1231.

Li, J., Azam, F., Zhang, S., Biology, M., Diego, S., and Jolla, L. (2016) Outer membrane vesicles containing signalling molecules and active hydrolytic enzymes released by a coral pathogen Vibrio shilonii AK1. Environ Microbiol 18: 3850–3866.

Liao, Y., Williams, T.J., Ye, J., Charlesworth, J., Burns, B.P., Poljak, A., et al. (2016) Morphological and proteomic analysis of biofilms from the Antarctic archaeon, Halorubrum lacusprofundi. Sci Rep 6: 37454.

Liu, J., Fu, K., Wang, Y., Wu, C., Li, F., Shi, L., and Ge, Y. (2017) Detection of Diverse N-Acyl-Homoserine Lactones in Vibrio alginolyticus and Regulation of Biofilm Formation by Lactone In vitro. Front Microbiol 8: 1097.

Mangwani, N., Kumari, S., and Das, S. (2015) Involvement of quorum sensing genes in biofilm development and degradation of polycyclic aromatic hydrocarbons by a marine bacterium Pseudomonas aeruginosa N6P6. Appl Microbiol Biotechnol 99: 10283–10297.

McRose, D.L., Baars, O., Seyedsayamdost, M.R., and Morel, F.M.M. (2018) Quorum sensing and iron regulate a two-for-one siderophore gene cluster in Vibrio harveyi. Proc Natl Acad Sci 115: 751–7586.

Mellbye, B.L., Giguere, A.T., Bottomley, P.J., and Sayavedra-Soto, L.A. (2016) Quorum quenching of Nitrobacter winogradskyi suggests that quorum sensing regulates fluxes of nitrogen oxide(s) during nitrification. MBio 7: e01753-16.

Mitova, M., Popov, S., and De Rosa, S. (2004) Cyclic peptides from a Ruegeria strain of bacteria associated with the sponge Suberites domuncula. J Nat Prod 67: 1178–1181.

Muras, A., López-Pérez, M., Mayer, C., Parga, A., Amaro-Blanco, J., and Otero, A. (2018) High Prevalence of Quorum-Sensing and Quorum-Quenching Activity among Cultivable Bacteria and Metagenomic Sequences in the Mediterranean Sea. Genes (Basel) 9: 100.

Paggi, R.A., Martone, C.B., Fuqua, C., and De Castro, R.E. (2003) Detection of quorum sensing signals in the haloalkaliphilic archaeon Natronococcus occultus. FEMS Microbiol Lett 221: 49–52.

Patzelt, D., Wang, H., Buchholz, I., Rohde, M., Gröbe, L., Pradella, S., et al. (2013) You are what you talk: quorum sensing induces individual morphologies and cell division modes in Dinoroseobacter shibae. ISME J 7: 2274–2286.

Paulsen, S.S., Isbrandt, T., Kirkegaard, M., Buijs, Y., Strube, M.L., Sonnenschein, E.C., et al. (2020) Production of the antimicrobial compound tetrabromopyrrole and the Pseudomonas quinolone system precursor, 2-heptyl-4-quinolone, by a novel marine species Pseudoalteromonas galatheae sp. nov. Sci Rep 10: 21630.

Pereira, C.S., Thompson, J.A., and Xavier, K.B. (2013) AI-2-mediated signalling in bacteria. FEMS Microbiol Rev 37: 156–181.

Polkade, A. V., Mantri, S.S., Patwekar, U.J., and Jangid, K. (2016) Quorum sensing: An under-explored phenomenon in the phylum Actinobacteria. Front Microbiol 7: 131.

Reen, F.J., Gutiérrez-Barranquero, J.A., McCarthy, R.R., Woods, D.F., Scarciglia, S., Adams, C., et al. (2019) Quorum Sensing Signaling Alters Virulence Potential and Population Dynamics in Complex Microbiome-Host Interactomes. Front Microbiol 10: 2131.

Rehman, Z.U. and Leiknes, T.O. (2018) Quorum-quenching bacteria isolated from red sea sediments reduce biofilm formation by Pseudomonas aeruginosa. Front Microbiol 9: 1354.

Romero, M., Avendaño-Herrera, R., Magariños, B., Cámara, M., and Otero, A. (2010) Acylhomoserine lactone production and degradation by the fish pathogen Tenacibaculum maritimum, a member of the Cytophaga-Flavobacterium-Bacteroides (CFB) group. FEMS Microbiol Lett 304: 131–139.

Romero, M., Diggle, S.P., Heeb, S., Cámara, M., and Otero, A. (2008) Quorum quenching activity in Anabaena sp. PCC 7120: Identification of AiiC, a novel AHL-acylase. FEMS Microbiol Lett 280: 73–80.

Romero, M., Martin-Cuadrado, A.B., Roca-Rivada, A., Cabello, A.M., and Otero, A. (2011a) Quorum quenching in cultivable bacteria from dense marine coastal microbial communities. FEMS Microbiol Ecol 75: 205–217.

Romero, M., Muro-Pastor, A.M., and Otero, A. (2011b) Quorum sensing N-acylhomoserine lactone signals affect nitrogen fixation in the cyanobacterium Anabaena sp. PCC7120. FEMS Microbiol Lett 315: 101–108.

Sabirova, J.S., Becker, A., Lünsdorf, H., Nicaud, J.M., Timmis, K.N., and Golyshin, P.N. (2011) Transcriptional profiling of the marine oil-degrading bacterium Alcanivorax borkumensis during growth on n-alkanes. FEMS Microbiol Lett 319: 160–168.

Saurav, K., Burgsdorf, I., Teta, R., Esposito, G., Bar-Shalom, R., Costantino, V., and Steindler, L. (2016) Isolation of Marine Paracoccus sp. Ss63 from the Sponge Sarcotragus sp. and Characterization of its Quorum-Sensing Chemical-Signaling Molecules by LC-MS/MS Analysis. Isr J Chem 56: 330–340.

Saurav, K., Costantino, V., Venturi, V., and Steindler, L. (2017) Quorum Sensing Inhibitors from the Sea Discovered Using Bacterial N-acyl-homoserine lactone-based biosensors. Mar Drugs 15: 53.

Schaefer, A.L., Greenberg, E.P., Oliver, C.M., Oda, Y., Huang, J.J., Bittan-banin, G., et al. (2008) A new class of homoserine lactone quorum-sensing signals. Nature 454: 595–600.

Sharif, D.I., Gallon, J., Smith, C.J., and Dudley, E. (2008) Quorum sensing in Cyanobacteria: N-octanoyl-homoserine lactone release and response, by the epilithic colonial cyanobacterium Gloeothece PCC6909. ISME J 2: 1171–1182.

Shen, Q., Gao, J., Liu, J., Liu, S., Liu, Z., Wang, Y., et al. (2016) A New Acyl-homoserine Lactone Molecule Generated by Nitrobacter winogradskyi. Sci Rep 6: 22903.

Silpe, J.E. and Bassler, B.L. (2019) Phage-Encoded LuxR-Type Receptors Responsive to Host- Produced Bacterial Quorum-Sensing Autoinducers. MBio 10: e00638-19.

Silpe, J.E., Bridges, A.A., Huang, X., Coronado, D.R., Duddy, O.P., and Bassler, B.L. (2020) Separating functions of the phage-encoded Quorum-Sensing-activated antirepressor Qtip. Cell Host Microbe 27: 629-641.e4.

Sivakumar, K., Scarascia, G., Zaouri, N., Wang, T., Kaksonen, A.H., and Hong, P.Y. (2019) Salinity-Mediated Increment in Sulfate Reduction, Biofilm Formation, and Quorum Sensing: A Potential Connection Between Quorum Sensing and Sulfate Reduction? Front Microbiol 10: 188.

Su, Y., Tang, K., Liu, J., Wang, Y., Zheng, Y., and Zhang, X.H. (2019) Quorum sensing system of Ruegeria mobilis Rm01 controls lipase and biofilm formation. Front Microbiol 10: 3304.

Su, Y., Yang, Y., Zhu, X.Y., Zhang, X.H., and Yu, M. (2021) Metagenomic Insights Into the Microbial Assemblage Capable of Quorum Sensing and Quorum Quenching in Particulate Organic Matter in the Yellow Sea. Front Microbiol 11: 602010.

Tait, K., Hutchison, Z., Thompson, F.L., and Munn, C.B. (2010) Quorum sensing signal production and inhibition by coral-associated vibrios. Environ Microbiol Rep 2: 145–150.

Teasdale, M.E., Donovan, K.A., Forschner-Dancause, S.R., and Rowley, D.C. (2011) Gram-Positive Marine Bacteria as a Potential Resource for the Discovery of Quorum Sensing Inhibitors. Mar Biotechnol 13: 722–732.

Tommonaro, G., Abbamondi, G.R., Iodice, C., Tait, K., and De Rosa, S. (2012) Diketopiperazines Produced by the Halophilic Archaeon, Haloterrigena hispanica, Activate AHL Bioreporters. Microb Ecol 63: 490–495.

Torres, M., Dessaux, Y., and Llamas, I. (2019) Saline environments as a source of potential quorum sensing disruptors to control bacterial infections: A review. Mar Drugs 17: 1–28.

Torres, M., Rubio-Portillo, E., Antón, J., Ramos-Esplá, A.A., Quesada, E., and Llamas, I. (2016) Selection of the N-acylhomoserine lactone-degrading bacterium Alteromonas stellipolaris PQQ-42 and of its potential for biocontrol in aquaculture. Front Microbiol 7: 646.

Tourneroche, A., Lami, R., Hubas, C., Blanchet, E., Vallet, M., Escoubeyrou, K., et al. (2019) Bacterial-fungal interactions in the kelp endomicrobiota drive autoinducer-2 quorum sensing. Front Microbiol 10: 1–14.

Toyofuku, M., Morinaga, K., Hashimoto, Y., Uhl, J., Shimamura, H., Inaba, H., et al. (2017) Membrane vesicle-mediated bacterial communication. ISME J 11: 1504–1509.

Toyofuku, M., Nomura, N., Kuno, E., Tashiro, Y., Nakajima, T., and Uchiyama, H. (2008) Influence of the Pseudomonas quinolone signal on denitrification in Pseudomonas aeruginosa. J Bacteriol 190: 7947–7956.

Urvoy, M., Lami, R., Dreanno, C., Daudé, D., Rodrigues, A.M.S., Gourmelon, M., et al. (2021a) Quorum sensing disruption regulates hydrolytic enzyme and biofilm production in estuarine bacteria. Environ Microbiol.

Wagner-Döbler, I., Thiel, V., Eberl, L., Allgaier, M., Bodor, A., Meyer, S., et al. (2005) Discovery of Complex Mixtures of Novel Long- Chain Quorum Sensing Signals in Free-Living and Host-Associated Marine Alphaproteobacteria. ChemBioChem 6: 2195–2206.

Yu, Z., Hu, Z., Xu, Q., Zhang, M., Yuan, N., Liu, J., et al. (2020) The luxI/luxR-type quorum sensing system regulates degradation of polycyclic aromatic hydrocarbons via two mechanisms. Int J Mol Sci 21: 5548.

Zan, J., Choi, O., Meharena, H., Uhlson, C.L., Churchill, M.E.A., Hill, R.T., and Fuqua, C. (2015) A solo luxI -type gene directs acylhomoserine lactone synthesis and contributes to motility control in the marine sponge symbiont Ruegeria sp. KLH11. Microbiology 50–56.

Zhai, C., Zhang, P., Shen, F., Zhou, C., and Liu, C. (2012) Does Microcystis aeruginosa have quorum sensing? FEMS Microbiol Lett 336: 38–44.

Zhang, C., Li, Y., Meng, C.X., Yang, M.J., Wang, Y.G., Cai, Z.H., et al. (2020) Complete genome sequence of Acinetobacter baumanni J1, a quorum sensing-producing algicidal bacterium, isolated from Eastern Pacific Ocean. Mar Genomics 52: 100719.

Zhang, Guishan, Zhang, F., Ding, G., Li, J., Guo, X., Zhu, J., et al. (2012) Acyl homoserine lactone-based quorum sensing in a methanogenic archaeon. ISME J 6: 1336–1344.

Zhao, Z., Wang, L., Miao, J., Zhang, Z., Ruan, J., Xu, L., et al. (2021) Regulation of the formation and structure of biofilms by quorum sensing signal molecules packaged in outer membrane vesicles. Sci Total Environ in press.

Table S4. AI amendment experiments in marine isolates or natural communities. AHL names are abbreviated according to the size of the acyl chain and its possible substitution at the third C [e.g., N-(3-oxohexanoyl)-L-homoserine lactone is abbreviated as 3-oxo-C6-HSL]. nd: not determined; exp.:experiment; BS: Biosensor; TLC: Thin-layer chromatography; CG: Gas chromatography; LC: Liquid chromatography; HPLC: High performance LC; MS: Mass spectrometry; ESI: Electrospray ionization; EEA: Extracellular enzymatic activity.

	Reference	Bacteria/community to which AIs were added	Studied phenotype/goal	AI detected	AI or QSI added	Exposure time	Main results	Keywords
AIs amendment to isolated strain	**Jatt *et al.* (2015)**	1 Bacteria isolated from marine snow particles (Chinal marginal seas) among a collection of 53 strains	- Quantification of AHLs on marine snow particles - Screening of AHLs production of 53 isolates and analytical determination for one strain (*Pantoea ananatis* B9, Gammaproteobacteria) - Effect of AHL amendment and disruption on the extracellular hydrolytic enzymes (cell-free) of *P. ananatis* B9	*Marine snow*: C6- and 3-oxo-C6-HSL (TLC) and C8-HSL (GC-MS) *P. ananatis* B9: C4-, C6-, C10-, C12- and C14-HSL (GC-MS)	3-oxo-C6-, C6-, C8-, C10- or C12-HSL (10 µM) or AiiA lactonase (enzymatic degradation of endogenous AHLs)	?	10 strains activated the biosensors (9 Gamma-, 1 Alphaproteobacteria). Among them, *P. ananatis* B9 produced several AHLs as well as amylase, protease, lipase, alkaline phosphatase and gelatinase. C10-HSL enhanced alkaline phosphatase (x1.08) while AiiA inhibited it (x0.27).	AHL, QQ enzyme (AHL), marine snow, isolates, EEA
	Mangwani *et al.* (2015)	*P. aeruginosa* N6P6 and *P. pseudoalcaligenes* NP103 (Gammaproteobacteria) (isolated from marine water sample collected from Odisha coast, India)	- Effect of AHLs amendment on: planctonic and biofilm growth, cell surface hydrophobicity, auto-aggregation, polycyclic aromatic hydrocarbons degradation	Screening with the *A. tumefacien* NTL4 and *C. violaceum* CV026 BS No analytic determination of the AHLs produced by the strains	C4-, C8-, 3-oxo-C8 and 3-oxo-C12-HSL at 1, 2 or 3 µg/mL	16 h, 48 h or 7 days depending on the phenotype	An increase in biofilm growth, auto-aggregation and swarming motility was observed in the presence of 3-oxo-C8- and 3-oxo-C12-HSL, resulting in enhanced phenanthrene and pyrene degradation	AHL, *Pseudomonas*, biofilm, aggregation, swarming, cell-surface hydrophobicity, aromatic compound degradation
	Liu *et al.* (2017)	2 marine *Vibrio*sp. (Bohai, China) among a collection of 47	- AHLs produced by 47 marine *Vibrio* strains (Gammaproteobacteria) - Effect of AHL amendment on the biofilm production of two strains with contrasting biofilm production abilities	43 strains (out of 47) activated *A. tumefaciens* KYC55 BS, all of them produced AHLs using HPLC-MS/MS (11 different AHLs detected)	3-oxo-C10-HSL (2, 5, 10, 20, 40, or 100 µmol/L)	36 h	The AHL amendment differently affected the biofilm production of the two tested strain. At 16°C, it increased the production of strain 24 (which had low initial biofilm production), but decreased the production of strain 40 (which had high initial production). The exogenous AHL amendment effect was different at 16 and 28°C.	AHL, *Vibrio*, biofilm

	Fei *et al.* (2020)	*Sulfitobacter pseudonitzschiae* F5, *Phaeobacter* sp. F10, *Alteromonas macleodii* F12 (isolated the diatom *Asterionellopsis glacialis*)	- AHL production by three strains isolated from the phycosphere - Influence of AHL and QSI amendments on their ability to colonize the phycosphere (motility and biofilm production)	3-oxo-C10-, 3-oxo-C16-, 3-oxo-C16:1-HSL (detected using HPLC-MS)	HSL: 3-oxo-C10-, 3-oxo-C16-, 3-oxo-C16:1-HSL; QSI: 2(5H)-furanone, Furanone C-30 2 µM for motility, 10 µg/mL for biofilm assay	Motility: 3 days Biofilm: 24 h	3-oxo-C16:1-HSL strongly inhibited bacterial motility and stimulated biofilm production	**AHL,** phycosphere, motility and adherence
	Kumari *et al.* (2021)	*P. aeruginosa* N6P6 (Gammaproteobacteria) (isolated from marine water sample collected from Odisha coast, India)	- Study of *P. aeruginosa* N6P6 naphthalene degradation (pathways and metabolites involved) - Effect of an AHL-QSI on planktonic and biofilm-mediated napththalene degradation, on the expression of the *ndo* gene and N12O enzyme activity (involved in napththalene metabolism)	C4- and 3-oxo-C12-HSL (determined in Kumari *et al.* 2016 using TLC and GC-MS)	Tannic acid (QSI) at 0.3 mg mL^{-1}	24 h	The AHL QSI reduced *ndo*expression (by 55-fold), the N12O enzyme activity (by 44%) and the naphthalene degradation efficacy (by 37%), demonstrating that napththalene degradation is QS-mediated in *P. aeruginosa* N6P6	**QSI (AHL)**, *Pseudomonas,* aromatic compound degradation
	Urvoy *et al.* (2021a)	28 Estuarine bacteria (Aulne estuary, France) among a collection of 299 strains	- AHL screening of 299 estuarine strains and analytic quantification in 75 strains - Effect of AHL disruption on dissolved and cell-bound leucine-aminopeptidase and beta-glucosidase activity and biofilm production among the 28-AHLs producing strains	28 strains (out of 75 preselected strains) produced AHLs using UHPLC-MS/MS (14 different AHLs)	Lactonase (enzymatic degradation of endogenous AHLs)	24 or 48 h	28 strains produced AHLs (mostly *Pseudomondales* and *Vibrionales,* Gammaproteobacteria). With the lactonase treatment, biofilm production, dissolved and cell-bound β-glucosidase and leucine-aminopeptidase activities significantly increased in 4%-68% of strains but decreased in 0%-21% of those 28 strains.	**QQ enzyme (AHL)**, estuary, isolates, biofilm, EEA (cell-free and cell-bound)

Both	**Su *et al.* (2019)**	Marine snow particles and 1 strain isolated from marine snow particles (Yellow Sea, China) among a collection of 122 strains	- Detection of AHLs production and QQ capacities of 122 bacteria isolated from marine snow particles - Impact of AHLs amendment on extracellular cell-free enzymatic activities (alpha- and beta-glucosidase, beta-xylosidase, mannosidase, cellulase, galactosaminidase, chitobiase, aminopeptidase, phosphatase, lipase) in marine snow particles - Impact of AI amendments and disruption on biofilm production and cell-free extracellular lipases in *Ruegeria mobilis* Rm01 (Alphaproteobacteria)	No analytic determination of the AHLs excepted for *R. mobilis* Rm01 (produced 3-oxo-C10-, C10- and C12-HSL)	*Marine snow:* 3-oxo-C8-HSL (50, 100, 500 or 1000 nM) *R. mobilis:* 3-oxo-C8-, 3-oxo-C10-, C10-, C12-HSL, AI-2, MomL lactonase (enzymatic degradation of the endogenous AHLs)	*Marine snow:* 6 and 24 h *R. mobilis:* 8 h (biofilm) and 24 h (EEA)	*Marine snow:* 3-oxo-C8-HSL upregulated galactosaminidase (x3-4) and beta-xylosidase but downregulated beta-glucosidase and mannosidase. *Isolates:* 20 and 62 species had AHL-producing and AHL-degrading capacities, respectively (out of 122) *R. mobilis:* biofilm production was upregulated with C10-, C12, C14-HSL and MomL but downregulated with 3-oxo-C10-, 3-oxo-C8-HSL and AI-2. Lipase production was stimulated by all used AHLs and AI-2 but inhibited with MomL.	**AHL**, **QQ enzyme (AHL)**, **AI-2**, marine snow, isolate, EEA
	Wang *et al.* (2020)	9 d-old biofilms from the coastal marine subtidal zone of the Hong Kong Port Shelter	- Effect of C6-, C12-HSL, PQS and c-di-GMP to the taxonomic structure and functional profiles of marine biofilm (metagenomics) - Efect of PQS on the planktonic growth, biofilm production and gene expression of the marine strain *Erythrobacter* sp. HKB8 (Alphaproteobacteria) isolated from the biofilm (comparative transcriptomics)	Not performed	*Biofilms:* C6-, C12-HSL, PQS (at 10 µM) and c-di-GMP (at 2.5 µM) *Erythrobacter* sp.: PQS at 10 µM	24 h	*Biofilm:* The AI amendment induced changes in taxonomy and structure, with the C12-HSL- and PQS-treated comunities being the most distant to the control group. The C12-HSL and PQS treatment increased the relative abundance of genes involved in membrane transport, motility, chemotaxis and cell signaling. *Erythrobacter* sp.: PQS exposure did not affect the planktonic growth but increased biofilm production. PQS exposure modulated the expression of 314 genes.	**AHL**, **PQS**, marine snow, isolates, biofilm, transcriptomic

AIs amendment to natural community	**Dobretsov et al. (2007)**	Resuspended biofilm-forming communities from a subtidal zone	Effect of various QSI on the development of biofilm-forming communities colonizing polystyrene Petri dishes (bacterial density, composition, percentage of metabolically active cells)	Not performed	5-hydroxy-3[(1R)-1-hydroxypropyl]-4-methylfuran-2(5H)-one (FUR1), (5R)-3,4-dihydroxy-5-[(1S)-1,2-dihydroxyethyl]furan-2(5H)-one (FUR2), triclosan (TRI) at 10^{-2}, 10^{-3} and 10^{-4} M	48 h	The QSIs affected the biofilm density and its composition, each QSI inducing different effects. The affected groups included Alphaproteobacteria, Betaproteobacteria, Gammaproteobacteria and Bacteroidetes.	**QSI (AHL)**, biofilm-forming bacteria, biofilm, diversity
	Hmelo *et al.* (2011)	Marine snow communities (Clayoquot Sound, western coast of Vancouver Island)	- AHL produced by the community colonizing the marine snow particle - Effect of AHLs amendment on the production of extracellular (cell-bound and cell-free hydrolytic activities: aminopeptidase, lipase, phosphatase, chitobiase, alpha- and beta-glucosidase	On the marine snow particles: C8- and C12-HSL (detected using HPLC/ESI-MS), 3-oxo-C6- and 3-oxo-C8-HSL (Fourier-transform ion cyclotron resonance MS)	3-oxo-C6- and 3-oxo-C8-HSL, 500 and 5000 nM	6 h and 48 h	Increase in aminopeptidase (max. x2), lipase (max. x3) and phosphatase (max. x8), glucosidases were not affected. Different marine snow traps yielded different results.	**AHL**, marine snow, EEA (cell-bound an cell-free)
	Van Mooy *et al.* (2012)	Epibiotic bacteria colonizing *Trichodesmium* consortia sampled in the subtropical North Atlantic Ocean	- AHL produced by 141 strains isolated from *Trichodesmium* epibiont - AIs produced by wild *Trichodesmium* colonies - Effect of AHL and DPD amendments on extracellular (cell-bound and cell-free) phophatases production in wild *Trichodesmium* colonies	*Strains:* 3-oxo-C8-, 3-oxo-C9, 3-oxo-C10, 3-oxo-C11, 3-oxo-C12, C12-, C13-, C14-HSL (detected using HPLC-MS/MS) *Natural communities*: C14-HSL and AI-2 (detected using HPLC-MS/MS)	C8- or 3-oxo-C8-HSL, cocktail (C10-, C12- and C14-HSL) or DPD, 500 nM	24 h	AIs were detected in both isolated strains (in 5 *Vibrio* sp. and 2 *Erythrobacter* sp.) and natural epiobiont. AHLs amendments to wild *Trichodesmium* colonies induced an increase in phophatase (x1.8-2.5) while DPD induced a decrease (x0.8)	**AHL**, **AI-2**, phycosphere, EEA

	Krupke *et al.* (2016)	Marine snow communities (5 locations in the Atlantic and Pacific Ocean)	- Effect of AHLs amendment on the production of extracellular (cell-bound and cell-free) hydrolytic activities: aminopeptidase, lipase and phosphatase - At the end of the incubation: detection of AHLs on marine snow particles	No evidence of endogenous AHLs	For all experiments: 3-oxo-C8-HSL or cocktail (C10-, C12- and C14-HSL) at 500 nM In addition: 100, 250, 750 and 1000 Nm in western tropical north atlantic	24 h Additionnal sampling at 3, 6 and 12 h in the Sargasso Sea and western tropical atlantic ocan	The AHL amendment affected the hydrolytic enzyme activity (0.4-3.7 variation range, with as much inhibition as stimulation). There were large variation accross sample locations with no obvious geographical pattern. Few concentration-dependent patterns were observed. Two AHLs rarely elicited the same response.	**AHL**, marine snow, EEA (cell-bound and cell-free)
	Huang *et al.* (2019)	Communities from the Duluth Superior Harbor (USA) colonizing immerged steel coupons	Effect of different coating or additives (including QQ agent, lactonase) on the biocorrosion and the diversity of bacteria colonizing immerged steel coupons	Not performed	*Sso*Pox W263I lactonase coated on steel coupons (enzymatic degradation of the endogenous AHLs)	8 weeks	The lactonase coating reduced the biocorrosion and modified the composition of the colonizing bacteria. Burkholderiales, Pseudomonadales adn Rhodospirillales were greatly reduced.	**QQ enzyme (AHL)**, lactonase, colozing bacteria, diversity
	Whalen *et al.* (2019)	Marine communities from coastal waters (Raune-fjord, Norway)	Effect of HHQ amendment on the growth rate and composition of bacteria (free-living and particle-attached) and eukaryotes during a mesocosm-stimulated bloom of phytoplancton (4 amendment experiments at different stage of the bloom)	Not performed	410 nM of 2-heptyl-4-quinolone (HHQ)	24 h	Exposure to HHQ caused nanoplankton and prokaryotic cell abundances to decrease without modifying their composition. It also altered the composition of particle-associated and free-living microbiota, favoring both Gamma- and Alphaproteobacteria but defavoring Bacteroidetes. This effect was highly variable depending on the bloom stage.	**HHQ**, free-living and particle-attached marine bacteria, eukaryotes, growth rate, diversity
	Urvoy *et al.* (2021b)	Marine communities from coastal waters (Bay of Brest, France)	Effect of AHLs amendment on the growth, composition and extracellular hydrolytic activities (protease, beta-glucosidase, beta-glucuronidase, *N*-actetyl-glucosaminidase, lipase, phosphatase, sum of cell-free and cell-bound) of marine bacteria (2 experiments at contrasting period of the phytoplankton growth)	Not performed	50 nM of C4-, C6-, 3-oxo-C8-, C12-, C16-HSL	6, 24 and 48 h	AHLs amendment impacted both hydrolytics activities (1st exp.: *N*-acetyl glucosaminidase and lipase, 2nd exp.: protease and beta-glucuronidase) and bacterial composition, with highly variable effects between the two experiments. The AHLs mostly affected Bacteroidetes (Flavobacteriales), Gamma- (Vibrionales, Alteromonadales and Oceanospirillales) and Alphaproteobacteria (Rhodobacterales).	**AHL**, planktonic bacteria, EEA (cell-bound + cell-free), diversity
	Xu *et al.* (2021)	Epiphytic biofilm collected from the Xuanwu Lake	- Detection of the AHLs in the periphytic biofilm - Effect of AHL amendment (11 AHLs) on P entrapment.	Mainly C12-, 3-oxo-C8- and C8-HSL, but also C6- and C10-HSL	2 µM of C4-, C6-, 3-oxo-C6-, C8-, 3-oxo-C8-, C10-, 3-oxo-C10, C12-, 3-	P speciation: sampling every day for 7 days	- Strong positive correlation between P-entrapment and concentration of total AHLs secreted by periphytic biofilms and AHL amendment enhanced P	**AHL**, periphytic biofilm, P entrapment, metatranscripto

		(China) and matured in the lab	- Effects of three AHLs (C8-, 3-oxo-C8-, C12-HSL) on EPS production, total biomass, chlorophyll *a*, alkaline phophatase, physical structure of the biofilm and metatranscriptome		oxo-C12, C14- or 3-oxo-C14-HSL (AHLs were daily replenished)	(11 AHLS); Other parameters: sampling on day 7 (3 AHLs)	entrapment by 38-156% - AHL addition: stimulated biofilm formation and induced a shift in community composition (increase of PAOs); promoted extracellular P entrapment via EPS production; promoted intracellular P entrapment via the upregulation of specific genes (inorganic P accumulation, organic P mineralization, P uptake and transport, P regulation)	mic, phosphatase, EPS production

Fei, C., Ochsenkühn, M.A., Shibl, A.A., Isaac, A., Wang, C., and Amin, S.A. (2020) Quorum sensing regulates 'swim-or-stick' lifestyle in the phycosphere. Environ Microbiol 22: 4761–4778.

Hmelo, L.R., Mincer, T.J., and Van Mooy, B.A.S. (2011) Possible influence of bacterial quorum sensing on the hydrolysis of sinking particulate organic carbon in marine environments. Environ Microbiol Rep 3: 682–688.

Huang, S., Bergonzi, C., Schwab, M., Elias, M., and Hicks, R.E. (2019) Evaluation of biological and enzymatic quorum quencher coating additives to reduce biocorrosion of steel. PLoS One 14:.

Jatt, A.N., Tang, K., Liu, J., Zhang, Z., and Zhang, X.H. (2015) Quorum sensing in marine snow and its possible influence on production of extracellular hydrolytic enzymes in marine snow bacterium Pantoea ananatis B9. FEMS Microbiol Ecol 91: 1–13.

Krupke, A., Hmelo, L.R., Ossolinski, J.E., Mincer, T.J., and Van Mooy, B.A.S. (2016) Quorum Sensing plays a complex role in regulating the enzyme hydrolysis activity of microbes associated with sinking particles in the ocean. Front Mar Sci 3: 55.

Kumari, S., Mangwani, N., and Das, S. (2020) Naphthalene catabolism by biofilm forming marine bacterium Pseudomonas aeruginosa N6P6 and the role of quorum sensing in regulation of dioxygenase gene. J Appl Microbiol 130: 1217–1231.

Liu, J., Fu, K., Wang, Y., Wu, C., Li, F., Shi, L., and Ge, Y. (2017) Detection of Diverse N-Acyl-Homoserine Lactones in Vibrio alginolyticus and Regulation of Biofilm Formation by Lactone In vitro. Front Microbiol 8: 1097.

Mangwani, N., Kumari, S., and Das, S. (2015) Involvement of quorum sensing genes in biofilm development and degradation of polycyclic aromatic hydrocarbons by a marine bacterium Pseudomonas aeruginosa N6P6. Appl Microbiol Biotechnol 99: 10283–10297.

Van Mooy, B.A.S., Hmelo, L.R., Sofen, L.E., Campagna, S.R., May, A.L., Dyhrman, S.T., et al. (2012) Quorum sensing control of phosphorus acquisition in Trichodesmium consortia. ISME J 6: 422–429.

Su, Y., Tang, K., Liu, J., Wang, Y., Zheng, Y., and Zhang, X.H. (2019) Quorum sensing system of Ruegeria mobilis Rm01 controls lipase and biofilm formation. Front Microbiol 10: 3304.

Urvoy, M., Lami, R., Dreanno, C., Daudé, D., Rodrigues, A.M.S., Gourmelon, M., et al. (2021a) Quorum sensing disruption regulates hydrolytic enzyme and biofilm production in estuarine bacteria. Environ Microbiol.

Urvoy, M., Lami, R., Dreanno, C., Delmas, D., L'Helguen, S., and Labry, C. (2021b) Quorum sensing regulates the hydrolytic enzyme production and community composition of heterotrophic bacteria in coastal waters. Front Microbiol in press.

Wang, R., Ding, W., Long, L., Lan, Y., Tong, H., Saha, S., et al. (2020) Exploring the Influence of Signal Molecules on Marine Biofilms Development. Front Microbiol 11: 571400.

Whalen, K.E., Becker, J.W., Schrecengost, A.M., Gao, Y., Giannetti, N., and Harvey, E.L. (2019) Bacterial alkylquinolone signaling contributes to structuring microbial communities in the ocean. Microbiome 7: 93.

Xu, Y., Curtis, T., Dolfing, J., Wu, Y., and Rittmann, B.E. (2021) N-acyl-homoserine-lactones signaling as a critical control point for phosphorus entrapment by multi-species microbial aggregates. Water Res 204: 117627.

Chapitre VIII. Discussion générale et perspectives

Dans son ensemble, cette thèse s'est attelée à étudier les facteurs influençant la composition des communautés bactériennes estuariennes et marines et leur synthèse d'enzymes d'hydrolyse de la matière organique. Une première partie a consisté en une étude au sein de l'estuaire de l'Aulne et des eaux côtières de la rade de Brest adjacentes. L'objectif était de déterminer les variations spatiotemporelles de la composition des communautés bactériennes libres et attachées aux particules (**chapitre III**) et de leurs activités enzymatiques hydrolytiques (**chapitre IV**), ainsi que les facteurs les contrôlant. Une deuxième partie s'est intéressée de manière plus spécifique au rôle d'un système de communication intercellulaire bactérien, le quorum sensing (QS), dans la régulation de ces paramètres. Pour cela, des expériences ont été réalisées à la fois sur des souches bactériennes isolées (**chapitre V**) et sur des communautés bactériennes naturelles (**chapitre VI**). Enfin, une revue de la littérature a permis une synthèse des connaissances actuelles sur le lien entre QS et cycles biogéochimiques (**chapitre VII**). Ce huitième chapitre résume (**Figure VIII.1**), discute et met en perspectives les principaux points développés durant ces travaux de thèse.

I. Synthèse des travaux réalisés

I.A. *Variations spatiotemporelles et déterminants de la composition des communautés bactériennes et de leurs activités hydrolytiques*

Le **chapitre III** a montré que les communautés bactériennes de l'Aulne sont très largement structurées par des processus déterministes et qu'elles suivent des variations spatiotemporelles marquées, logiquement expliquées par des variables spatiales (salinité) et temporelles (e.g., température, chlorophylle *a*). De manière intéressante, la cohésion, une variable représentant le degré de connectivité des communautés, explique également une part importante de la variation des communautés. Nous nous sommes également intéressés aux facteurs impactant la dissimilarité taxonomique et phylogénétique entre les communautés libres (< 3 µm) et attachées aux particules (> 3 µm), puisque celles-ci influent différemment sur le devenir de la matière organique. La dissimilarité entre les deux communautés varie dans l'espace et dans le temps : elle est plus importante dans les eaux douces et marines que dans les eaux estuariennes et elle diminue en été. Elle semble impactée par la labilité de la matière organique, ainsi que par le niveau de concentration en phosphate et par la cohésion des communautés.

Le **chapitre IV** s'est intéressé aux variations spatiotemporelles de trois activités enzymatiques hydrolysant les protéines (leucine aminopeptidase – LAM), les polymères de glucose (β-glucosidase – GLU) et les phosphomonoesters (phosphatase alcaline – PA) le long l'estuaire de l'Aulne, ainsi qu'aux facteurs les contrôlant. Cet estuaire abrite de très forts taux de production bactérienne, supportés par des activités hydrolytiques intenses. Ce travail a mis en lumière différentes zones dans l'estuaire : i) les eaux douces, caractérisées par une dominance des bactéries libres et par une contribution plus

importante des GLU et des PA à l'activité enzymatique totale que dans le reste de l'estuaire ; ii) la zone du bouchon vaseux, qui contient une majorité de bactéries attachées dont la proportion de LAM, GLU et PA varie selon la saison ; et iii) les stations en aval de l'estuaire, avec une dominance des bactéries libres et de leurs activités LAM. Ces différences de patrons spatiotemporels s'expliquent par l'implication de divers facteurs dans la régulation des activités hydrolytiques. Par exemple, les activités PA et GLU des communautés attachées sont plus influencées par la quantité de matière particulaire et la composition des communautés bactériennes que les LAM. Ces dernières suivent principalement une évolution saisonnière, liée à l'abondance bactérienne et à la température. Les PA et les GLU synthétisées par certains taxons bactériens des communautés attachées pourraient leur permettre d'accéder à la partie carbonée du substrat hydrolysé. Les activités hydrolytiques des communautés libres semblent, elles, principalement régulées par des facteurs saisonniers (abondance bactérienne) ainsi que par la composition de la matière organique pour les GLU et les PA.

I.B. *Rôle du quorum sensing dans la régulation de la synthèse d'enzymes hydrolytiques et la structuration des communautés*

Le **chapitre V** a montré que la production de *N*-acyle homosérine lactones (AHLs), les molécules signal les plus étudiées du QS, est relativement répandue au sein des souches bactériennes isolées de l'estuaire de l'Aulne. Cette étude a permis la caractérisation de 28 souches produisant diverses AHLs. Une approche basée sur l'utilisation de lactonases a démontré que, chez ces 28 souches, les AHLs sont largement impliquées dans la régulation de la synthèse de LAM et de GLU dissoutes et liées aux cellules, ainsi que dans la production de biofilm. Ces expériences ont aussi mis en évidence la complexité de ces mécanismes de régulation puisque l'effet de la disruption du QS peut différer largement au sein de souches appartenant à un même genre bactérien.

Grâce à une approche par microcosme, le **chapitre VI** a ensuite révélé que le QS affecte également la synthèse d'enzymes hydrolytiques et la composition de communautés bactériennes naturelles de la rade de Brest. Ces résultats se sont avérés extrêmement variables selon que les communautés ont été prélevées en début ou au pic du développement printanier du phytoplancton. De plus, l'addition d'AHLs aux communautés bactériennes modifie très rapidement le niveau d'activités hydrolytiques, dès 6 h d'incubation. Cela suggère une régulation transcriptionnelle de ces phénotypes, par opposition à un effet lié à une modification de la composition des communautés. Les mécanismes moléculaires impliqués restent peu élucidés mais il est possible que les changements de composition des communautés soient liés à la modification du niveau d'activités hydrolytiques.

Le **chapitre VII** constitue une synthèse de la littérature qui porte sur les mécanismes régulés par le QS et leur lien avec les cycles biogéochimiques marins. De nombreux mécanismes sont en effet sous l'influence de ces voies de régulation, non seulement chez les bactéries hétérotrophes marines, mais aussi chez les bactéries autotrophes, les archées et même chez certains bactériophages. Le QS

peut ainsi directement influencer les cycles biogéochimiques en modulant des phénotypes impliqués dans i) la dégradation de la matière organique et de polluants (e.g., plastiques, hydrocarbones) ; ii) l'allocation du carbone intracellulaire ; et iii) l'acquisition de nutriments (phosphore, azote, soufre et fer). Le QS peut également impacter indirectement les cycles biogéochimiques en modulant la composition des communautés bactériennes et donc, les fonctions associées. La modification de la composition des communautés peut s'effectuer en régulant des processus touchant à la colonisation (e.g., motilité, chimiotactisme, production de biofilm, hydrophobicité des cellules) ou aux interactions microbiennes (e.g., production de « *public goods* » comme les sidérophores, exopolysaccharides ou les enzymes hydrolytiques ; induction de la lyse virale).

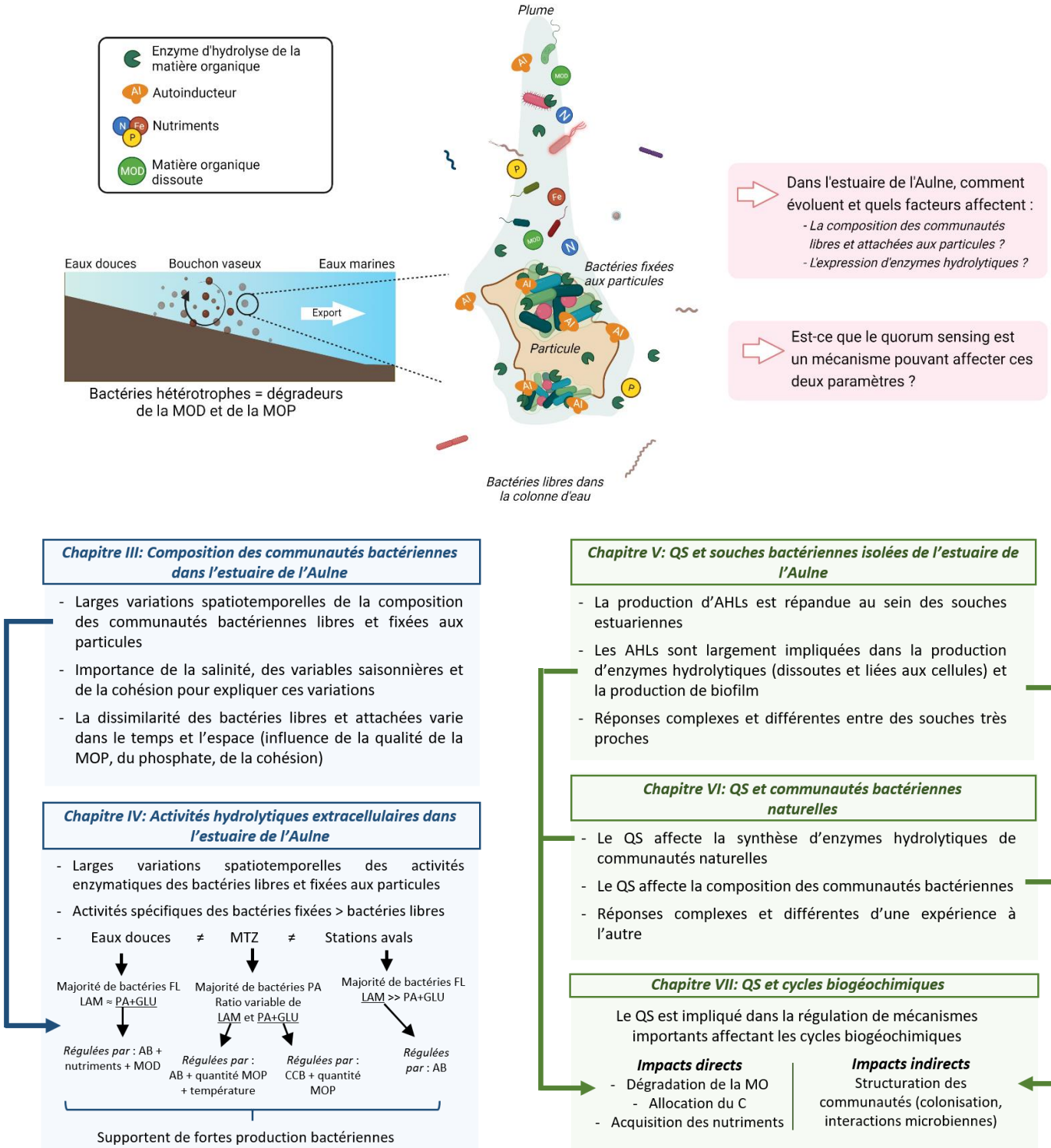

Figure VIII.1. Schéma conceptuel des problématiques développées en début du manuscrit de thèse et réponses apportées dans les différents chapitres. MOP : matière organique particulaire ; MOD : matière organique dissoute ; AB : abondance bactérienne ; MTZ : zone de turbidité maximum ; PA : phosphatase alcaline ; LAM : leucine aminopeptidase ; GLU : β-glucosidase ; CCB : composition des communautés bactériennes ; AHL : *N*-acyle homosérine lactone ; QS : quorum sensing ; C : carbone ; MO : matière organique.

II. Discussion et perspectives

II.A. *Les estuaires, de véritables bioréacteurs naturels*

Les estuaires macrotidaux, notamment celui de l'Aulne, constituent des écosystèmes modèles pour l'étude de la structuration des communautés hétérotrophes bactériennes ainsi que leur influence sur la matière organique. En effet, ces systèmes très dynamiques présentent de forts gradients physicochimiques, à la fois spatiaux et temporels. Le mélange des eaux douces et des eaux marines entraine le mélange de matières organiques de composition et de qualité très distinctes, qui favorisent des activités bactériennes hétérotrophes intenses (Bianchi, 2011). Les productions bactériennes mesurées au sein de l'estuaire de l'Aulne sont ainsi extrêmement fortes (**chapitre IV**), laissant supposer des temps de génération très faibles des communautés libres et attachées aux particules. Ces faibles temps de génération semblent avoir permis la formation d'une communauté bactérienne propre à l'estuaire, dont l'assemblage est largement déterminé par des processus déterministes (**chapitre III**). Cette observation laisse supposer que ces communautés sont bien adaptées aux conditions environnantes. Associées à des activités enzymatiques très intenses (**chapitre IV**), ces résultats sous-entendent un impact important des communautés bactériennes de l'estuaire de l'Aulne sur le devenir de la matière organique estuarienne exportée vers les eaux côtières, qu'elle soit dissoute ou particulaire.

Grâce à une collaboration avec Gabriel Dulaquais et Ricardo Riso (Université de Bretagne Occidentale, LEMAR), le jeu de données caractérisant la MOD dans l'estuaire de l'Aulne (**chapitre IV**) sera complété par une analyse plus fine, basée sur l'utilisation de la chromatographie d'exclusion stérique couplée à différents détecteurs de carbone organique, d'UV et d'azote organique (SEC-OCD-UVD-OND) (Dulaquais, Breitenstein, *et al.*, 2018). Six classes de composés viendront ainsi compléter les données déjà disponibles : les biopolymères (> 1 000 Da) ; les substances humiques (600-1 000 Da) ; les « *building blocks* » (350-600 Da) ; les molécules acides de faible poids moléculaire (< 350 Da) ; les molécules neutres de faible poids moléculaire (< 350 Da) et le carbone organique hydrophobe. Ces données nous permettront de mieux apprécier la transformation de la MOD le long du gradient de salinité de l'estuaire de l'Aulne, en prenant notamment en compte l'évolution des substances humiques qui peuvent représenter la majorité du COD dans les estuaires (Dittmar et Kattner, 2003; Dulaquais, Breitenstein, *et al.*, 2018).

Si nos études ont permis d'évaluer l'influence relative des facteurs environnementaux (e.g., température, quantité et qualité de la matière organique) et de la composition des communautés bactériennes dans le contrôle de la synthèse d'enzymes hydrolytiques, il reste de nombreuses questions quant à leurs impacts biogéochimiques sur les eaux exportées vers la rade de Brest. Notamment, la synthèse des PA ne semble pas être liée à un besoin en phosphore des bactéries mais pourrait servir à acquérir la partie carbonée des substrats hydrolysés (**chapitre IV**). Ainsi, le phosphate

libéré par les PA pourrait s'accumuler dans l'environnement estuarien et combler en partie la limitation de la production primaire par le phosphore dans les eaux côtières de la rade de Brest. Cette hypothèse est confortée par le fait que les activités PA corrèlent positivement avec les concentrations en phosphate. L'impact réel de cette activité enzymatique sur la spéciation du phosphore dans l'estuaire de l'Aulne demeure cependant inconnu. Les activités PA ne sont généralement pas mesurées dans les estuaires, des écosystèmes qui contiennent habituellement de fortes teneurs en phosphate. Or, leur quantification semble nécessaire afin de mieux caractériser les apports des différentes formes de phosphore vers les eaux côtières et d'envisager leur possible intégration dans les modèles biogéochimiques actuels.

II.B. *De la prise en compte des facteurs abiotiques vers celle des facteurs biotiques*

Historiquement, ce sont principalement des aspects abiotiques qui ont été investigués en écologie microbienne. Des questions clefs concernent, par exemple, la détermination des facteurs physicochimiques (e.g., température, salinité, composition de la matière organique) structurant la biogéographie des communautés microbiennes ou contrôlant l'expression de fonctions clefs (e.g., synthèse d'enzymes hydrolytiques, production bactérienne, assimilation de phosphate) (Fortunato *et al.*, 2012; Teeling *et al.*, 2012; Sunagawa *et al.*, 2015). Cependant, il existe un intérêt de plus en plus marqué pour l'étude de l'importance des facteurs biotiques.

i) Facteurs biotiques et structuration des communautés

Les interactions trophiques sont considérées comme cruciales dans la structuration des communautés bactériennes (Gralka *et al.*, 2020), bien qu'il existe de nombreuses interactions non trophiques (e.g., production d'antibiotique, échange de matériel génétique) tout aussi importantes. Dû à leurs complexités, ces interactions sont souvent inférées statistiquement, via des mesures de cooccurrences. Les relations de cooccurrence sont néanmoins imparfaites pour traduire l'existence d'une interaction car elles peuvent résulter d'autres facteurs (Carr *et al.*, 2019). Par exemple, une corrélation positive entre deux taxons peut traduire une interaction positive (e.g., coopération, « *cross-feeding* », symbiose), mais aussi une niche environnementale partagée. De la même manière, des corrélations négatives peuvent traduire des interactions négatives (e.g., exclusion compétitive, production de toxines, prédation) ou des niches environnementales différentes.

Dans l'étude sur les communautés de l'estuaire de l'Aulne (**chapitre III**), nous avons utilisé la métrique de cohésion, récemment développée par Herren et McMahon (2017). Celle-ci comprend la cohésion positive et négative, reflétant respectivement le degré de corrélations positives et négatives existant au sein d'une communauté. Plus spécifiquement, la valeur absolue de la cohésion augmente avec l'abondance de taxons très connectés (i.e., ayant beaucoup de corrélations positives ou négatives). Notre étude a montré que la cohésion pouvait, à elle seule, expliquer une part significative

de la variation des communautés de l'estuaire de l'Aulne (environ 10 %). D'autres études ont avancé des résultats comparables, suggérant également l'importance des relations de cooccurrence et de la cohésion dans la structuration des communautés (Herren et McMahon, 2017; 2018; Danczak *et al.*, 2018; Hernandez *et al.*, 2021; Liu *et al.*, 2022). Il conviendra dans le futur d'affiner cette analyse, par exemple en réalisant une analyse de réseaux de cooccurrence afin de mieux caractériser les différences entre les communautés libres et attachées. Une des limites de notre étude est qu'elle reste cantonnée aux interactions bactériennes, alors que les interactions interrègnes (par exemple avec les virus, le phytoplancton ou les brouteurs) ont également un rôle essentiel dans la structuration des communautés bactériennes.

Le QS est un mécanisme moléculaire qui pourrait participer à la régulation des interactions microbiennes. L'étude en microcosme (**chapitre VI**) a notamment montré que l'ajout de molécules signal du QS pouvait modifier la composition de communautés bactériennes naturelles. Les régulations derrière ces observations restent peu élucidées mais la synthèse bibliographique réalisée montre qu'une myriade de mécanismes pourraient entrer en jeu (e.g., production d'antibiotiques, de sidérophores, régulation des mécanismes de colonisation, régulation du taux de croissance) (**chapitre VII**). Ainsi, il parait important de mieux caractériser les liens entre communications chimiques et interactions, trophiques ou non, au sein de communautés microbiennes complexes pour mieux comprendre les facteurs participant à leur structuration.

ii) Facteurs biotiques et synthèse d'enzymes hydrolytiques

L'impact relatif de la composition des communautés bactériennes et des conditions environnementales sur la synthèse d'enzymes hydrolytiques et, de manière générale sur la fonction des communautés, est une question importante encore largement débattue (Gray et Head, 2001; Bertilsson *et al.*, 2007; Boucher et Debroas, 2009). Il est bien établi que certains taxons possèdent des capacités métaboliques spécifiques. Par exemple, les Flavobacteria sont souvent reconnues comme des spécialistes de la dégradation de composés complexes de haut poids moléculaire (Fernàndez-Gómez *et al.*, 2013; Ferrer-González *et al.*, 2021), tandis que les Roseobacter sont plutôt considérées comme des spécialistes de l'assimilation de petits composés (Buchan *et al.*, 2005; Wagner-Döbler et Biebl, 2006). La présence de différentes espèces est donc largement susceptible d'influer sur les capacités métaboliques d'une communauté dans son ensemble. Cependant, il reste souvent complexe d'établir un lien clair entre la fonction et la composition d'une communauté en raison des phénomènes de redondance fonctionnelle, i.e., des espèces différentes effectuant la même fonction (Louca *et al.*, 2018). Il a ainsi été avancé que les conditions environnementales étaient plus importantes que la composition des communautés dans la détermination du niveau d'activité hydrolytique (e.g., Langenheder *et al.*, 2005; Comte et Del Giorgio, 2010; Lindström *et al.*, 2010). A contrario, différentes études ont démontré un lien entre la composition des communautés bactériennes et leur capacité de

dégradation de la matière organique (Bertilsson *et al.*, 2007; Boucher et Debroas, 2009; Comte et Del Giorgio, 2010; Delgado-Baquerizo *et al.*, 2016). Dans notre étude (**chapitre IV**), nous avons pu mettre en évidence que la composition des communautés fixées aux particules influençait leur expression d'activités PA et GLU. Il est possible que ces activités soient surexprimées par des taxons spécifiques, capables de dégrader certains composés de la MOP (e.g., carbohydrates, substances humiques). Plusieurs expériences de colonisation ont avancé des résultats allant en ce sens, avec une sélection de taxons spécifiques lors de la colonisation de billes contenant des polysaccharides comme la chitine (Datta *et al.*, 2016; Enke *et al.*, 2018, 2019). Nos résultats ont par ailleurs montré que les LAM des bactéries attachées, elles, semblaient principalement suivre un cycle saisonnier, suggérant une importante redondance fonctionnelle de ces activités et soulignant leur côté indispensable pour les bactéries. Nous n'avons pas non plus trouvé de lien entre la composition des communautés bactériennes libres et l'expression de leurs activités GLU, PA et LAM. Les activités enzymatiques des bactéries libres semblent principalement modulées par leur abondance (suivant un cycle saisonnier) ainsi que par la teneur en MOD et en nutriments pour les GLU et PA. L'importance relative de la composition des communautés et des facteurs environnementaux peut donc varier selon la fonction considérée, les trois étant de toute manière intrinsèquement liés. Il serait intéressant de cibler plus spécifiquement les activités enzymatiques mesurées. Les LAM incluent par exemple l'activité de plusieurs peptidases différentes (Steen *et al.*, 2015) et les GLU, enzymes à large spectre, ne représentent qu'une fraction des enzymes de dégradation des carbohydrates. La diversification des activités enzymatiques mesurées pourrait aussi être couplée à des mesures d'assimilation des monomères libérés, afin d'estimer l'efficacité des différentes hydrolyses et le bénéfice qu'en retirent les bactéries.

Nos résultats ont également montré une large implication du QS dans la régulation des activités hydrolytiques extracellulaires (**chapitre V, VI**). Ainsi, la présence de bactéries produisant un certain type de molécule signal au sein d'une communauté pourrait influencer son expression d'enzymes hydrolytiques. De manière intéressante, l'étude réalisée sur les souches de l'estuaire de l'Aulne (**chapitre V**) a illustré que, au sein d'une même souche, le QS pouvait différemment influer sur la synthèse d'enzymes hydrolytiques dissoutes ou liées aux cellules. Par exemple, la disruption des communications basées sur les AHLs a entrainé une augmentation des LAM dissoutes et, simultanément, une diminution des LAM liées aux cellules chez certaines souches (e.g., *Vibrio* sp. EFL16, EF02-7, E15 ; *Acinetobacter* sp. DF3-8). L'effet inverse a été observé chez *Pseudomonas* sp. AF3-9. Ce résultat est original car jusqu'à maintenant, les études réalisées sur des souches isolées se sont généralement concentrées uniquement sur les enzymes dissoutes (e.g., Jatt *et al.*, 2015; Li *et al.*, 2019; Su *et al.*, 2019; Mahan *et al.*, 2020). Dans les études environnementales, ce sont au contraire les enzymes totales ou liées aux cellules qui sont le plus souvent mesurées (e.g., Hmelo *et al.*, 2011; Krupke

et al., 2016). Or, ces différences de localisation pourraient avoir des implications écologiques différentes. En effet, les enzymes dissoutes hydrolysent le substrat indépendamment de la cellule productrice d'enzymes, découplant les phénomènes d'hydrolyse et d'assimilation ; ce qui permettrait éventuellement un relargage de produits d'hydrolyse disponibles pour des cellules non productrices d'enzymes (dites « *scavengers* »). A contrario, la synthèse d'enzymes liées aux cellules pourrait permettre un couplage plus fin de ces mécanismes en hydrolysant les substrats à proximité des cellules. Le QS pourrait ainsi potentiellement moduler la mise en place d'interactions trophiques selon qu'il agisse sur les enzymes dissoutes ou liées aux cellules. De manière intéressante, ces résultats sont comparables à ceux de McRose *et al.* (2018), où la production de sidérophores dissous ou liées aux cellules au sein de *Vibrio harveyi* est sous l'influence du QS. Il est cependant peu clair si l'impact du QS sur le niveau d'enzymes dissoutes relève d'un mécanisme actif (i.e., impact direct sur la sécrétion) ou d'un mécanisme passif (e.g., changement de perméabilité des cellules, lyse).

II.C. *Le métabolisme intense des bactéries fixées aux particules*

De nombreuses études ont révélé que les communautés bactériennes établies au sein d'agrégats possédaient généralement des métabolismes (e.g., production bactérienne spécifique, activités hydrolytiques spécifiques) plus élevés que les communautés libres environnantes. Ce phénomène pourrait être dû : i) à une composition spécifique de ces communautés, qui peuvent être enrichies en taxons copiotrophes à croissance rapide et/ou à fort potentiel de dégradation (e.g., Gammaproteobacteria, Flavobacteria) ; ii) à une surexpression transcriptionnelle des gènes de dégradation. Cette surexpression pourrait notamment être liée aux fortes concentrations en substrats des agrégats, mais aussi à un effet de la seule fixation des bactéries, indépendamment du substrat colonisé. Dans ce dernier cas, le QS a été évoqué comme un mécanisme pouvant expliquer l'augmentation des métabolismes suite à la fixation à une surface solide. Si nos études ne testent pas directement ces trois hypothèses, les résultats obtenus permettent tout de même de les éclairer.

i) Influence de la composition des communautés

Nos travaux dans l'estuaire de l'Aulne ont examiné les liens entre la composition et l'expression d'activités hydrolytiques au sein des communautés libres et attachées mais ils ne permettent pas d'évaluer directement si les métabolismes intenses des bactéries fixées aux particules estuariennes résultent de ces différences de composition. Comme discuté précédemment, la surexpression de certaines activités enzymatiques (PA, GLU) chez ces communautés bactériennes pourrait être liée à leur composition. Cependant, un impact de la composition des communautés attachées aux particules ne semble pas être une explication suffisante. En effet, il existe toujours un fort différentiel entre les activités spécifiques des communautés libres et attachées en été alors que la dissimilarité entre les deux communautés diminue à cette saison. De plus, la composition des

communautés ne semble pas impliquée dans l'activité des LAM, qui est fortement surexprimée chez les communautés fixées aux particules.

ii) Induction par le substrat

Nos résultats laissent penser qu'une induction par le substrat pourrait être un mécanisme important derrière l'augmentation du métabolisme des bactéries attachées. La quantité de matière particulaire impacte en effet les trois activités hydrolytiques mesurées (PA, GLU et LAM) ainsi que la production bactérienne, qui dépend en partie de ces activités (**chapitre IV**). Il est donc possible que la présence de fortes concentrations en matière organique au sein des agrégats suffise à expliquer l'augmentation générale des métabolismes bactériens. L'expression des activités enzymatiques ne semble, par contre, pas être significativement liée à la qualité de la matière organique particulaire. Celle-ci a cependant été estimée par des mesures globales de composition élémentaire (C/N) ou biochimique (e.g., ratio de carbohydrates insolubles et solubles). Une caractérisation plus fine de la composition de ces agrégats pourrait permettre une meilleure évaluation de l'impact de la qualité de la matière organique particulaire sur l'expression des enzymes des communautés attachées.

iii) Influence du quorum sensing

S'il est probable que la quantité de matière organique présente dans les agrégats induise de plus forts métabolismes bactériens, plusieurs études ont montré que la simple fixation de bactéries à une surface inerte comme du verre (ne contenant donc pas de substrat organique) pouvait suffire pour induire ce phénomène (Taylor et Gulnick, 1996; Bonin *et al.*, 2001). Quelques auteurs ont ainsi émis l'hypothèse qu'une régulation par le QS pourrait être à l'origine de la surexpression des enzymes hydrolytiques au sein des communautés fixées aux particules (Gram *et al.*, 2002; Grossart *et al.*, 2007). Les communautés attachées s'établissent généralement sous forme de biofilm, ce qui favoriserait l'accumulation d'AIs et permettrait l'induction de la synthèse d'enzymes. Nos études, menées sur des souches isolées et sur des communautés naturelles, montrent sans aucun doute que le QS est impliqué dans la régulation de la synthèse des activités hydrolytiques bactériennes. En revanche, nos données laissent penser que cette hypothèse initiale est trop simpliste. L'effet de la disruption du QS est très contrasté d'une souche à l'autre, même au sein de souches proche d'un point de vue phylogénétique (**chapitre V**). De manière similaire, l'ajout d'AHLs à des communautés bactériennes naturelles différentes a mené à des résultats extrêmement variables (**chapitre VI**). De plus, dans ces deux études, l'inhibition des activités enzymatiques par le QS est aussi fréquente que leur induction. Cette variabilité de réponse suite à l'ajout d'AHL ou de lactonases va à l'encontre de l'hypothèse initiale, puisque celle-ci sous-entend une réponse commune et unilatérale des différentes espèces colonisant les particules. Des expériences de colonisation pourraient permettre d'élucider ces questions, en regardant en

particulier les activités enzymatiques de souches colonisant des surfaces inertes (e.g., verre), produisant ou non des AIs (création de mutant de délétion).

En revanche, nos résultats montrent que le QS influence la composition des communautés fixées aux particules. Il pourrait ainsi participer, par exemple, à la sélection de taxons à forts potentiels dégradeurs en régulant les phénomènes de colonisation (e.g., modulation de la production de biofilm, **chapitre V**) et intervenir dans le devenir de ces communautés via son impact sur les interactions microbiennes y prenant place (**chapitre VI**).

II.D. *Une vue encore parcellaire des voies de communications bactériennes*

Le QS reste largement sous exploré dans les environnements marins. Bien que ce mécanisme ait été découvert chez la bactérie marine *Vibrio fischeri*, il a ensuite été généralement étudié chez quelques souches d'intérêt médicale ou agronomique (Lami, 2019). De nouveaux modèles marins pour l'étude du QS tendent néanmoins à émerger, comme par exemple *Ruegeria* sp. KLH11, un symbionte d'éponge marine (Zan *et al.*, 2015) ou *Dinoroseobacter shibae*, un symbionte algal (Patzelt *et al.*, 2013). Cependant, nous ne possédons qu'une vue parcellaire des fonctions régulées par le QS et de la mise en œuvre de ces régulations d'un point de vue moléculaire, limitée à quelques souches cultivables. Pourtant, le QS semble impliqué dans la régulation de nombreux phénotypes clefs d'un point de vue écologique et biogéochimique, comme le montre notre synthèse bibliographique (**chapitre VII**). Cette synthèse identifie plusieurs axes de recherche pour le futur et différentes méthodologies pour y répondre. Premièrement, il reste essentiel d'identifier les organismes engagés dans les communications de QS, au-delà des groupes bien connus (Gammaprotéobactéries, Alphaprotéobactéries) et de les relier au type de molécules produites. En ce sens, une étude initiée au cours de la thèse, non présentée dans ce manuscrit, concerne le développement d'AHLs marquées à l'aide d'un fluorophore. L'objectif de ce projet, inspiré par différentes études (Gomes *et al.*, 2013; Mukherji *et al.*, 2013; Chahande *et al.*, 2021), est de pouvoir comptabiliser et identifier les bactéries utilisant une AHL donnée au sein d'une population naturelle en visualisant la fluorescence émise par les AHLs marquées. Dans ce but, plusieurs AHLs avec des longueurs de chaines acyles différentes (C6-, C12- et C18-HSL) greffées d'un groupement fluorescent ont été synthétisées par Mathieu Berchel (Université de Bretagne Occidentale, CEMCA) et testées sur différents biosenseurs. Ce projet est encore en cours de réalisation.

Un deuxième axe de recherche concerne une meilleure identification des fonctions régulées par le QS en milieu marin et de leurs impacts possibles sur les cycles biogéochimiques. En effet, si nos travaux se sont concentrés sur le lien entre QS et activités hydrolytiques extracellulaires, ce mécanisme impacte de nombreux autres processus bactériens, extrêmement variés. L'identification des fonctions QS-dépendantes nécessite des approches sur des souches isolées, permettant d'identifier et de caractériser précisément des mécanismes d'un point de vue moléculaire. En ce sens, de futurs travaux

sont prévus dans la continuité de notre collaboration avec Raphaël Lami (*Observatoire de Banyuls*) et David Daudé (Gene&Green TK) pour implémenter des approches de protéomique et de métabolomique sur les souches de l'estuaire de l'Aulne productrices d'AHLs. La mise en place d'approches intégrées sur des communautés naturelles est également nécessaire pour mieux comprendre le QS dans son ensemble, au-delà des AHLs. Par exemple, des approches de metatranscriptomique et/ou multi-omiques pourraient permettre de mieux saisir l'ensemble des processus permettant au QS de modifier la composition des communautés microbiennes.

Enfin, un troisième axe d'étude concerne la question de l'ampleur du QS dans les milieux marins. Les concentrations d'AIs sont susceptibles d'être hétérogènes dans l'environnement, avec de fortes concentrations atteintes localement (par exemple, au sein d'un biofilm formé sur une particule) et des gradients de concentrations en dehors de ces biofilms. Cela soulève une question importante : est-ce que les communications intercellulaires jouent un rôle en dehors des micro-niches à fortes densités (e.g., particules, phycosphère, microplastiques) ? Les temps de réponse courts suivant l'ajout d'AHLs (dès 6 h d'incubation, **chapitre VII**) suggèrent que le QS pourrait avoir un rôle dans l'environnement proche de ces micro-niches (e.g., la trainée entourant un agrégat) où le temps de réponse des bactéries serait plus rapide que le temps de diffusion et de dégradation de ces molécules. Cependant, il reste complexe d'émettre des hypothèses sur le sujet car certains paramètres clefs restent à évaluer. Par exemple, nous avons relativement peu de connaissances sur : i) les concentrations d'AIs suffisantes pour induire une réponse ; ii) la taille du quorum (nombre de cellules) correspondant à ces concentrations seuils ; iii) la distance maximale entre une cellule émettrice et une cellule réceptrice d'AIs (« *calling distance* »), liée notamment à la solubilité, au taux de diffusion et de dispersion des AIs (Decho *et al.*, 2011) ; iv) la prévalence de l'utilisation de vésicules membranaires pour empaqueter les AIs, qui augmentent leur solubilité et permettent leur livraison spécifique à une cellule cible (Li *et al.*, 2016; Toyofuku *et al.*, 2017).

III. Conclusion générale

Cette thèse s'est intéressée aux différents facteurs influençant la composition des communautés bactériennes estuariennes et marines, ainsi que leurs fonctions dans la dégradation de la matière organique. Pour investiguer ces problématiques, nous avons mené une étude de terrain au sein de l'estuaire de l'Aulne et de la rade de Brest et réalisé des expériences spécifiques sur le rôle des communications intercellulaires basées sur le QS.

Dans une première partie, nous avons montré que l'estuaire de l'Aulne était un véritable bioréacteur naturel qui abrite des communautés bactériennes libres et fixées aux particules exhibant de forts patrons spatiotemporels. Ces variations de composition semblent liées aux conditions environnementales (e.g., salinité, composition de la matière organique) mais également à la cohésion des communautés, qui représente le degré de cooccurrence des différentes espèces. Ces communautés bactériennes possèdent des niveaux d'activités enzymatiques intenses, supportant des taux de production bactériennes parmi les plus importants mesurés dans les environnements marins. De manière intéressante, ces activités sont régulées par différents facteurs. Les LAM, dégradant les protéines, suivent majoritairement des variations saisonnières marquées liées à l'abondance bactérienne et à la température. Les GLU (hydrolyse des polymères de glucose) et les PA (hydrolyse des phosphomonoesters) semblent plus impactées par la quantité de matière organique. La composition des communautés semble également jouer un rôle important dans l'expression des activités PA et GLU des bactéries fixées aux particules. Dans une deuxième partie, nous avons démontré que le QS était largement impliqué dans la régulation des activités enzymatiques d'hydrolyse de la matière organique au sein de souches provenant de l'estuaire de l'Aulne et de communautés naturelles de la rade de Brest. De plus, le QS semble pouvoir impacter la structuration des communautés bactériennes, soit en régulant les processus liés à la colonisation (e.g., formation de biofilm), soit en modulant les interactions microbiennes, qu'elles soient trophiques ou non (e.g., synthèse d'enzymes hydrolytiques, de sidérophores, d'antibiotiques).

Dans leur globalité, nos résultats mettent en avant l'importance d'affiner nos connaissances sur les processus de transformation de la matière organique dans les zones estuariennes, afin de mieux quantifier les apports aux zones côtières. Ils soulignent aussi l'importance des facteurs biotiques dans l'étude des communautés bactériennes naturelles. Enfin, ils mettent en relief le besoin de mieux caractériser les interactions microbiennes, de leur mise en place d'un point de vue moléculaire à leurs impacts biogéochimiques globaux au sein des écosystèmes marins.

Annexes

I. Microbial enzymatic assays in environmental water samples: Impact of inner filter effect and substrate concentrations

Une synthèse critique de la littérature sur les mesures des activités enzymatiques basées sur l'utilisation de substrats fluorogéniques a été menée dans le cadre d'un travail préliminaire à cette thèse. Ce travail a permis la rédaction d'un article de méthodologie démontrant trois écueils majeurs :

- La présence éventuelle d'un artefact intrinsèque à la fluorimétrie (l'effet de filtre interne) entrainant une sous-estimation des V_{max} mesurées. Ce phénomène est bien connu mais n'avait jamais été décrit dans les mesures d'activités enzymatiques en milieu marin ;
- L'utilisation de gammes de concentration en substrat insuffisantes lors de la réalisation de cinétique de Michaelis-Menten, qui peut mener à une estimation erronée des paramètres enzymatiques (V_{max} et K_m) ;
- La compétition entre les substrats naturellement présents dans l'eau de mer (e.g., polysaccharides, protéines, phosphomonoesters) et le substrat fluorogénique, qui peut réduire significativement la valeur de V_{max} mesurée lorsque les concentrations en substrat fluorogénique sont trop faibles.

LIMNOLOGY and OCEANOGRAPHY: METHODS

ASLO

Limnol. Oceanogr.: Methods 2020

doi: 10.1002/lom3.10398

Microbial enzymatic assays in environmental water samples: Impact of inner filter effect and substrate concentrations

Marion Urvoy,[1,2]* **Claire Labry**,[1] **Daniel Delmas**,[1] **Layla Creac'h**,[1] **Stéphane L'Helguen**[2]

[1]Ifremer, DYNECO, Plouzané, F-29280, France

[2]Université de Bretagne Occidentale, CNRS, IFREMER, IRD, UMR 6539 Laboratoire des Sciences de l'Environnement Marin (LEMAR), Institut Universitaire Européen de la Mer (IUEM), Plouzané, F-29280, France

Abstract

As microbial enzymatic activities initiate the mineralization of organic matter through the microbial loop, it is important to correctly measure those activities and be able to perform inter-study comparisons. Enzymatic activity assays are typically carried out using fluorogenic substrate analogs, such as 4-methylumbelliferone and 7-amino-4-methylcoumarin linked to sugar monomers, phosphate group, or amino acids. However, methodological divergences can be found in aquatic science literature, potentially leading to misestimated activities. To highlight some of those methodological key points, we first addressed the potential occurrence of an inner filter effect (IFE), a fluorometric artifact that affects the relationship between fluorophore concentration and fluorescence intensity, due to absorption of exciting or emitted light. It has never been considered in the context of environmental water studies before, despite significantly affecting measured activities. IFE occurred with two out of three tested spectrofluorometers when assaying proteases, although no IFE was detected for phosphatase assays. We also evaluated how substrate concentration ranges might affect kinetic parameters estimation, revealing that a many existing studies might use insufficient maximum substrate concentration. Finally, for single substrate concentration assays, we argued for the use of saturating substrate concentration, as naturally occurring substrates might compete with the fluorogenic analog at trace level. The amendment of a molecule mimicking natural substrates generated a significant inhibition of natural seawater phosphatases and proteases assayed with trace concentrations of fluorogenic substrate, while almost no inhibition occurred at higher concentrations. Those key points need to be addressed in order to assess enzymatic rates and allow inter-study comparison.

Extracellular enzymes are mostly produced by heterotrophic prokaryotes that hydrolyze polymeric organic matter into units smaller than 600 dalton, transportable across their cell membranes (Payne 1980). Although they are the only entity capable to significantly affect both dissolved and particulate organic matter (Chróst 1990), other organisms can release extracellular enzymes as well. For instance, phytoplankton, phototrophic prokaryotes, metazoa, and macroalgae are able to contribute to the pool of alkaline phosphatases (Hoppe 2003; Niell et al. 2003; Labry et al. 2005).

Microbial enzymes play a major role in the ocean: they initiate the mineralization of complex organic matter through the microbial loop, transforming both dissolved and particulate organic matter into living biomass, dissolved organic carbon or carbon dioxide. The activity and specificity of extracellular enzymes therefore affect global carbon and nutrient cycling, carbon flow through aquatic food web as well as carbon export to the deep ocean (Azam et al. 1983; Azam 1998; Bidle 2010). As hydrolysis is considered the limiting step of organic matter utilization, any factors affecting enzyme activity might affect the entire mineralization pathway. As such, enzymatic assays are widespread and degradation capacity has been investigated in relation to diverse factors, such as for instance: substrate composition and size, microbial community structure, or environmental conditions (Azam et al. 1983; Chróst 1990; Kirchman 2008).

Measurements of enzyme activity are typically carried out using fluorogenic molecules consisting of a substrate moiety covalently linked to a fluorophore (or fluorochrome). Non-hydrolyzed substrate has a low background fluorescence, while upon hydrolysis the fluorescence spectra of the released fluorophore is considerably modified, allowing its selective detection (Fig. 1). The most commonly used molecules include 4-methylumbelliferone (MUF) linked to monosaccharides (glycosidase assays) or phosphate groups (phosphatase assays) and 7-amino-4-methylcoumarin (MCA) linked to amino acids

*Correspondence: murvoy@ifremer.fr

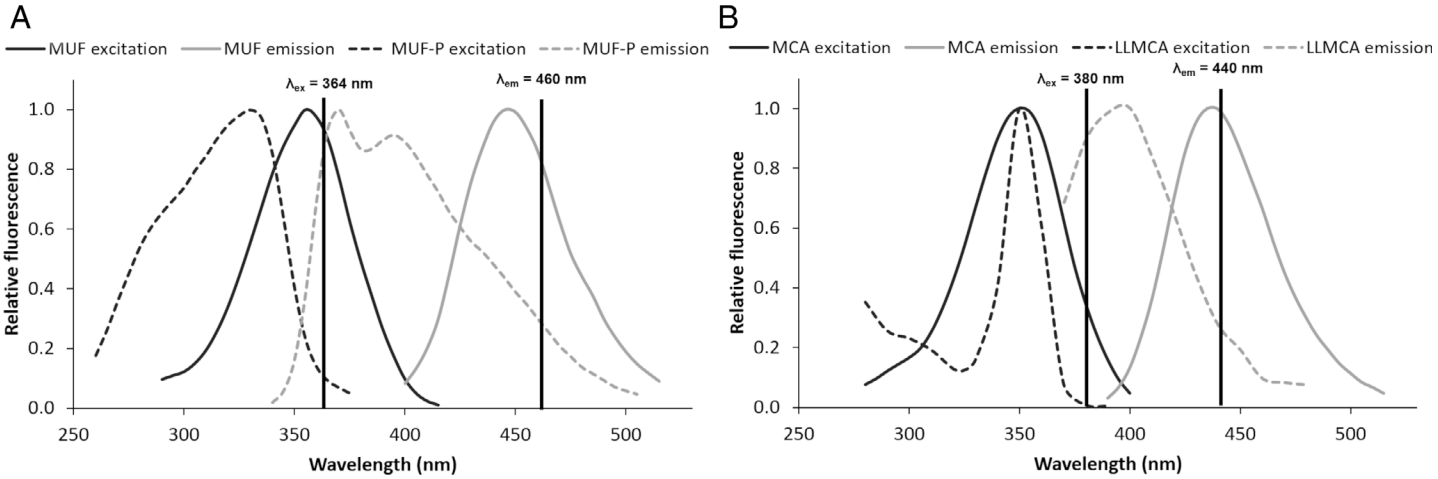

Fig 1. (**a**) Normalized fluorescence spectra of MUF-P (alkaline phosphatase substrate, dashed lines) and MUF (product, solid lines) over emission (gray lines) or excitation wavelength (black lines). Excitation spectra of MUF and MUF-P were obtained using a constant emission wavelength (460 nm) while excitation wavelength varied. Emission spectra were obtained using a constant excitation wavelength (364 nm) with variable emission wavelength. (**b**) Normalized fluorescence spectra of LLMCA (protease substrate, dashed lines) and MCA (product, solid lines) over emission (gray lines) or excitation wavelength (black lines). To obtain excitation spectra of MCA and LLMCA, emitted light was respectively collected at a wavelength of 440 and 410 nm while excitation wavelength varied. To obtain emission spectra, emitted light was collected over a range of wavelength while excitation wavelength was set to 350 and 325 nm for MCA and LLMCA, respectively. em: emission, ex: excitation. Vertical lines represent excitation and emission wavelengths used during enzymatic assays.

(protease assays) (Hoppe 1983; Arnosti 2003; Kirchman 2008). Enzymatic activity is determined by following the increase in fluorescence over time and using standards of known fluorophore concentration. Even though the use of simple substrate analogs suffers from limitations (Arnosti 2011; Steen et al. 2015), they have been widely used thanks to their sensitivity and ease of use (Chróst 1990).

However, several biases might affect result interpretation and impede inter-study comparison. The first one is a measurement artifact intrinsic to fluorimetry known as the inner filter effect (IFE), which has been completely overlooked in the literature assaying enzymatic activity in environmental water samples. With conventional spectrofluorometers, a fluorescent molecule is excited by a light source at a specific wavelength, selected by a monochromator. The emitted fluorescence is collected at right angle with respect to the incident beam and detected by a photomultiplier at the emission wavelength, also selected by a monochromator (Valeur 2001). The IFE reduces the fluorescence signal due to the absorption of exciting (excitation IFE) or emitted light (emission IFE), which affects the relationship between fluorophore concentration and fluorescence intensity (Kao et al. 1998; Valeur 2001; Eccleston et al. 2005; *see* Fig. 2 for a conceptual representation). IFE can result from the fluorophore itself or any other light-attenuating molecules naturally present in the analyzed sample.

The predominant effect, excitation or primary IFE, is caused by the absorption of the exciting light, which is attenuated as it progresses through the solution, inefficiently exciting the fluorophore. Absorption can be performed by the hydrolysis product, but also by the nonhydrolyzed substrate. For instance, in the case of phosphatase assays, both MUF-phosphate (MUF-P, alkaline phosphatase substrate) and MUF (hydrolysis product) absorb exciting light at the routinely used excitation wavelength (λ_{ex} = 364 nm; Fig. 1). Substrate absorption seems minimal and is often completely neglected by investigators, but it can be significant in enzymatic assays performed with a high substrate to product ratio. Excitation IFE is favored by the use of concentrated solutions (absorbance

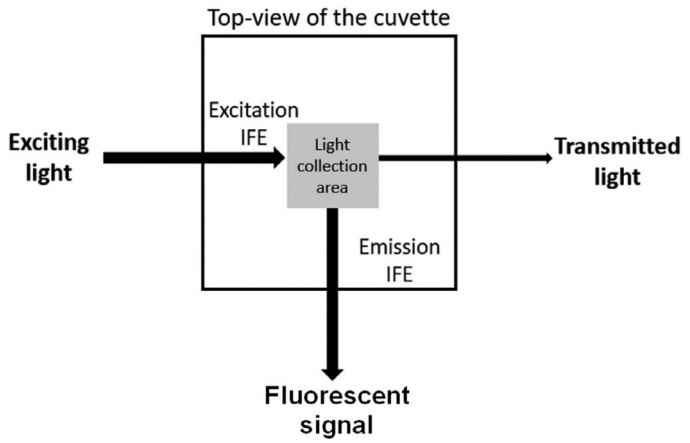

Fig 2. Conceptual illustration of excitation IFE (also termed primary IFE) and emission IFE (also termed secondary IFE) using a right angle geometry, one of the most common for cuvette system.

> 0.1), which are almost inevitable in enzymatic assays (Valeur 2001; Eccleston et al. 2005). IFE is likely to occur with the conventional right angle geometry as detection system collects light on an area restricted to the center of the cuvette: light might be absorbed before even reaching the collection area (Kao et al. 1998; Valeur 2001). Different cell configurations, such as front face illumination, were specifically developed in order to avoid this and reduce IFE. Long optic path systems (i.e., 1 cm cuvette) are especially affected by IFE, although shorter optic path systems such as microtiter plate spectrofluorometers can be impacted as well (Marathe et al. 2013, Pinto et al. 2015). The age and efficiency of the exciting lamp can also play a role in the occurrence of this effect (Valeur 2001).

A secondary IFE might also arise if the emitted light is re-absorbed by surrounding molecules. Absorption by the fluorophore itself depends on its Stokes shift, which is the difference between emission and excitation maxima (Eccleston et al. 2005). A small Stokes shift implies that absorption and emission spectra strongly overlap, so the emitted light might be absorbed by non-excited fluorophore molecules, decreasing the measured signal. For molecules with large Stokes shift, such as MUF and MCA, emission IFE is not likely to occur (Fonin et al. 2014).

The IFE has been described before in biochemical studies using substrate analogs (Puchalski et al. 1991; Liu et al. 1999; Palmier and Van Doren 2007) but, to our knowledge, has never been considered in the context of marine studies. Sebastián and Niell (2004) reported a reduction of the reaction velocity by excess of substrate when assaying high substrate concentrations. However, they did not mention a possible IFE.

The second bias is linked to the wide differences in substrate concentrations used, for both Michaelis–Menten kinetics and single point assays. Before performing a single point enzymatic assay, kinetic parameters (maximum velocity – V_{max} – and Michaelis affinity constant – K_m) should ideally be determined with a kinetic experiment using several substrate concentrations. However, there are wide differences in maximum substrate concentration used in the literature. They vary between 0.1 and 300 μM for alkaline phosphatase activities (APA) assayed with MUF-P (*see* Table 1 for references) and between 8.5 μM for exoproteolytic activities (EPA) assayed with L-leucine-MCA (LLMCA, *see* Table 2 for references). Insufficient maximum substrate concentration can affect parameters determination as the saturation of enzymatic active sites might not be reached.

As kinetics are laborious, time consuming, expensive, and require large sample volume, they are often set aside in favor of single point assays, using a single substrate concentration. A huge variability in the concentrations used is also noticed: between 0.1 and 250 μM for APA assayed with MUF-P (*see* Table 1 for references) and between 2.5 and 1000 μM for EPA assayed with LLMCA (*see* Table 2 for references). Those differences may be related to the existence of different perspectives in the current oceanographic community. Trace substrate concentration (< 1 μM) might be used in order to determine enzymatic rates and substrate turnover in conditions as close as possible to those prevailing in situ. This is opposed to a more conventional approach using a saturating substrate concentration, several times higher than the enzymes K_m which allows the determination of maximal velocity rate (Chróst 1990; Hoppe 2003). Single point assays using low substrate concentration results in several issues. (1) The substrate might not greatly exceed the enzyme concentration, which is a necessary condition to satisfy the steady-state assumption made by Michaelis–Menten. (2) Slow product formation leads to fluorometric sensitivity issue (Chróst 1990). (3) Those assays are subject to higher errors as velocities correspond to the first order part of the Michaelis–Menten equation, which is the most variable region. In consequence, small pipetting errors could result in large differences in estimated activity. (4) At low concentration, naturally occurring substrates might compete with the fluorogenic substrate analog, leading to significantly underestimated activities (Chróst 1990). Consequently, measured activities might be dependent on natural substrate concentration, potentially altering results and preventing intra and inter-study comparison.

The accumulation of these experimental biases might lead to severely misestimated enzymatic activities. The purpose of this study is to address these issues by quantifying their effect on fluorometric enzymatic assays. First, we will show how to detect the IFE occurrence, its effect on enzymatic measurements and how it can be corrected. Second, we will address the effect of the substrate concentration ranges upon the determination of kinetic parameters of pure enzymes, phytoplankton cultures and natural bacterial communities. We will finally argue in favor of using saturating substrate concentrations when performing single point assays, which allows the determination of the enzymatic equipment of the cells, rather than the in situ degradation rate.

Materials and procedures

Reagents and solutions

All chemical products were purchased from Sigma-Aldrich.

Substrate solutions

Stock solutions of 10 mM MUF-P and 40 mM LLMCA were prepared in half a volume of 2-methoxyethanol, dissolved using sonication and volume was adjusted to final concentration with Milli-Q water (Millipore purification system). Working solutions from 0.5 to 500 μM for MUF-P and from 3.9 to 1000 μM for LLMCA were obtained by successive dilutions of stock solutions in Milli-Q water and stored at –20°C.

Table 1. Literature examples showing phosphatase activity assay conditions used in different environments. All measurements were carried out using MUF-P substrate.

	Study	Environment	Substrate range for kinetic (μM)	Substrate concentration for single point assay (μM)
Oligotrophic environments	Sohm and Capone (2006)	Tropical and subtropical north Atlantic	—	0.1
	Sisma-Ventura and Rahav (2019)	Mediterranean Sea (microcosms)	—	0.1
	Duhamel et al. (2014)	North pacific subtropical gyre	0.025–1	1
	Sala et al. (2001)	Mediterranean Sea	—	200
	Van Wambeke et al. (2002)	Mediterranean Sea	0.025–1	—
	Thingstad et al. (1998)	Mediterranean Sea	0.005–0.2	—
	Yamaguchi et al. (2019)	Central north Pacific	0.100–2	—
	Bogé et al. (2012)	Northwest Mediterranean	0.03–30	—
Eutrophic environments	Rees et al. (2009)	English Channel	—	0.25
	Štrojsová et al. (2008)	Eutrophic reservoir	—	100
	Carlsson et al. (2012)	Coastal tropical Atlantic	—	250
	Koch et al. (2009)	Coastal waters Florida bay	0.05–2	—
	Davis et al. (2014)	Celtic Sea	0.8–2	—
	Chróst and Overbeck (1987)	Eutrophic Lake	10–200	—
	Labry et al. (2005)	Coastal estuarine waters	0.5–250	250
	Nausch et al. (2004)	Baltic Sea	0.1–300	—

Product solutions

Stock solutions of 2 mM MUF and 4 mM MCA were prepared as described previously and used to prepare standards, as described in the following section.

Competitors for inhibition tests

Stock solutions of 4.2 mM glucose-6-phosphate (G6P), 10 mM Leucyl-glycine (Leu-gly), 10 mM L-leucyl-glycyl-glycine (Leu-gly-gly) and 10 mM hexaglycine (Hexagly) were made in Milli-Q water, serially diluted to appropriate concentrations and stored at −20°C.

IFE detection

Standards preparation

As nonhydrolyzed substrate may affect fluorescence measurement, calibration curves of each product (MUF and MCA) were prepared in various concentration of substrate (MUF-P and LLMCA, respectively). Substrate concentrations are the ones used when determining enzymatic parameters. In practice, standards of MUF ranging from 8 nM to 2 μM were prepared in Milli-Q water or MUF-P concentration ranging from 0.5 to 500 μM, resulting in 12 calibrations for APA. Buffered formaldehyde (18%, pH 8) was added to each standard to respect assay dilution conditions (3.3% final concentration), as formaldehyde was used here to stop APA (C. Labry unpubl.). Standards of MCA ranging from 20 nM to 2 μM were prepared in Milli-Q water and in LLMCA concentration ranging from 3.9 to 500 μM resulting in nine calibrations for EPA. 10% sodium dodecyl sulfate (SDS) was added to each standard to respect assay dilution conditions (1% final) as it is used to stop EPA. This is particularly important for EPA as 1% SDS was shown to result in a 20% increase in MCA fluorescence (Delmas and Garet 1995). All standards were stored at −20°C.

Fluorometric measurements

In this study, we compared classical cuvette readings with flow injection analysis (FIA) reading (Delmas et al. 1994). Briefly, FIA is a liquid chromatography injection system (without the chromatographic column), connected to a Kontron SFM25 fluorescence spectrometer with a 1 mm optic path. This system allows a quick, sensitive, and reproducible sample processing (Delmas et al. 1994). The use of a carrier fluid (here a 0.1 M buffered borate solution adjusted to pH 10.5 and delivered at 1 mL min^{-1}) provides the possibility of setting the pH during fluorescence reading, independently from the pH of incubation. This is important as MUF fluorescence yield greatly varies with pH and is maximum at pH > 10 (Chróst and Krambeck 1986). For cuvette readings, pH was adjusted to 10 by adding 0.98 and 0.20 mL of a 0.5 M pH 12 buffered borate solution per 4 mL sample (containing preservative) for APA and EPA respectively. Measurements were carried out in a 1 cm cuvette using two spectrofluorometers, SFM25 and Perkin Elmer LS50.

All measurements were performed with a 90° angle illumination. Excitation and emission wavelength were respectively 364 and 460 nm for APA and 380 and 440 nm for EPA.

Michaelis–Menten kinetics

Michaelis–Menten kinetics were carried out on various samples to evaluate the impact of IFE and of substrate concentration ranges on kinetic parameters determination.

Table 2. Literature examples showing exoproteolytic activity assay conditions used in different environments. All measurements were carried out using LLMCA substrate.

	Study	Environment	Substrate range for kinetic (μM)	Substrate concentration for single point assay (μM)
Oligotrophic environments	Van Wambeke et al. (2009)	Mediterranean Sea	0.05–100	50
	Talbot et al. (1997)	Strait of Magellan	—	200
	Fukuda et al. (2000)	Subartic Pacific	—	200
	Misic et al. (2002)	Antartica	1–100	—
	Caruso et al. (2019)	Mediterranean Sea	20–160	—
Eutrophic environments	Gonnelli et al. (2013)	Arno river mouth (Italy)	0.05–8.5	—
	Song et al. (2019)	Brackish water microcosms	0.1–20	—
	Karner et al. (1992)	Adriatic Sea	—	2.5
	Rath et al. (1993)	Caribbean Sea	0.1–25	2.5
	Chappell and Goulder (1995)	Ouse and Derwent Rivers (UK)	0.5–100	50
	Foreman et al. (1998)	Maumee River (USA)	—	120
	Bullock et al. (2017)	Neuse and Tar-Pamlico Rivers (USA)	—	400
	Cunha et al. (2001)	Estuarine ecosystem (Portugal)	—	1000
	Patel et al. (2000)	Semi-enclosed coastal ecosystem	2.5–40	—
	Sinsabaugh et al. (1997)	Ottawa, Maumee and Hudson Rivers (USA)	5–120	—
	Shi et al. (2019)	Coastal waters, Northern South China Sea	1–350	—
	Ory et al. (2011)	Charente River (France)	2–1000	—

Sample preparation

Tested samples were either purified enzymes, phytoplankton cultures or natural microbial communities. Purified enzymes from *Escherichia coli* and shrimp (acquired from Sigma/Aldrich) were diluted to a stock concentration of 10 mU mL^{-1} in Milli-Q water and stored at 4°C. For each activity assay, stock enzyme was diluted to 250 μU mL^{-1} in 0.2 μm filtered natural seawater (Whatman Nucleopore filters).

Alexandrium minutum and *Thalassiosira weissflogii* were precultured in F/4 medium (Guillard and Ryther 1962) and inoculated in phosphate-free F/4 medium for 3 d at 18°C, under a 12 : 12 light cycle (120 μmol photons m^{-2} s^{-1}). Activities were measured on total fraction comprising algal-attached and dissolved enzymes.

Natural seawater was collected from the Brest station of the Service d'Observation en Milieu LITtoral program (SOMLIT, French marine monitoring network, http://somlit.epoc.u-bordeaux1.fr). and filtered through 0.8 μm Whatman Nucleopore filters to remove eukaryotes and larger cells.

Incubations

In order to determine kinetic parameters, 2 mL samples were incubated in the dark with 50 μL substrate solutions, with final concentrations ranging from 0.5 to 500 μM for MUF-P and from 1.95 to 1000 μM for LLMCA. Incubation time for each type of sample was previously determined so that less than 25% of the substrate was hydrolyzed, in order to measure initial linear velocity. Natural bacterial communities were incubated at in situ temperature (between 12°C and 16°C), purified enzymes and phytoplankton cultures at 20°C. At the end of the incubation, reaction was stopped by adding 18% buffered formaldehyde (pH 8, 3.3% final concentration) for APA or 10% SDS for EPA (1% final concentration). Samples were then frozen at −20°C until fluorescence measurement, which was performed as previously described. These preservatives stop enzymatic activities and allow storage at −20°C for deferred sample analysis, if necessary, without any changes on the kinetic parameters (APA: C. Labry unpubl., EPA: Delmas and Garet 1995).

Controls

As natural seawater and substrates (MUF-P and LLMCA) do produce fluorescence, a blank sample was prepared for each substrate concentration by directly mixing samples, substrate and reaction inhibitor (formaldehyde for APA, SDS for EPA) and immediately freezing them at −20°C. Blank fluorescence was then subtracted from sample fluorescence and results were converted to degradation rates using product standards diluted in Milli-Q water.

Statistical analysis

Affinity constant (K_m) and maximum velocity (V_{max}) and their standard deviations were calculated using nonlinear least squares regression of the data fitted to the Michaelis–Menten equation, using R ("nls" function in the "stats" package). Nonlinear regression seems to be the best method to estimate kinetic parameters (Chróst 1990).

Inhibition tests

To assess the effect of natural competitors on APA and EPA of natural bacterial samples, we monitored the fluorescence

emitted by 3 mL seawater sample amended with 75 μL substrate (0.125–2 μM of MUF-P, 0.125 and 2 μM of LLMCA) in a 1 cm optic path cuvette (SFM25 spectrofluorometer) during short periods of time (2–10 min). A molecule competing with the substrate analog was then added and fluorescence was monitored using the same procedure. The competitor used for APA was G6P (75 μL, final concentration from 50 nM to 1.5 μM), a natural compound involved in bacterial metabolism which is susceptible to be present in both natural environments and cultures. For EPA, three competitors were tested: Leu-gly, Leu-gly-gly and Hexagly (30 μL, final concentration of 8 and 16 μM). Fluorescence increased linearly over time and the presence of competitors visibly affected the slopes, which correspond to reaction velocities. pH was not adjusted during this measurement as slopes were not converted to actual velocities. Slopes were corrected for the dilution due to competitor's addition.

Assessment and discussion

Influence of IFE on activity assays

IFE occurs when exciting or emitted light is absorbed, decreasing the fluorescence signal and resulting in underestimated enzymatic activities. It includes all light-attenuating processes, caused by the fluorogenic substrate analog itself or by any other chromophores naturally present in samples. This study is limited to IFE caused by fluorogenic substrate as it is important during enzymatic assays using large concentration of substrate, but IFE resulting from natural organic matter may also affect fluorometric assays (Kothawala et al. 2013). IFE resulting from natural compounds should theoretically be corrected using calibration curves prepared in the same matrix as the samples (for instance 0.2 μm filtered seawater).

Detection of IFE caused by fluorogenic substrate

MUF-P/MUF and LLMCA/MCA have similar excitation and emission spectra, characterized by a large Stokes shift, meaning that emission IFE should not occur. However, both nonhydrolyzed substrates and hydrolysis products can absorb exciting light and produce an excitation IFE.

The occurrence of an excitation IFE from fluorescent products was tested by measuring calibration standards of products (MUF and MCA) diluted in Milli-Q water. If this effect occurs, the released product will absorb exciting light, with a greater impact at high product concentration. Consequently, the emitted signal will not be linear over the product range of concentration. As the curves obtained were linear (determination coefficient for linear fitting: $R^2 > 0.999$, data not shown) for the three instruments (FIA-SFM25, SFM25, and LS50), it appears that there is no IFE from the product between 0 and 2 μM, for both MUF and MCA.

Excitation IFE resulting from nonhydrolyzed substrates can be detected by measuring fluorescence of the reaction product in varying substrate concentrations. If an IFE occurs, we expect that a given substrate concentration will affect the fluorescence of all product concentrations in a similar way. The linearity of the relationship between fluorescence and product concentration would be unaffected. However, the IFE would increase with increasing substrate concentration which would result in a reduction of the calibration slope.

Figure 3 shows the results obtained for APA (no IFE detected, Fig. 3a,c,e) and EPA (IFE detected, Fig. 3b,d,f) with LS50 spectrofluorometer. Without IFE, the slope of those calibration curves is independent from MUF-P concentration (slope = -6.77×10^{-6}, correlation coefficient $r = 0.236$, df = 10, not significant, Fig. 3c) as MUF-P substrate does not affect fluorescence reading. The intercept is linearly proportional to this concentration (slope = 0.25, $r = 1.000$, df = 10, significant at 0.1%, Fig. 3e), reflecting the natural fluorescence of the substrate. These results also show the necessity of using a blank for each substrate concentration assayed. When an IFE occurred, the slope of the calibration curves decreases with increasing LLMCA concentration (slope = -4.37×10^{-5}, $r = 0.742$, df = 8, significant at 5%, Fig. 3d): as exciting light is absorbed, it becomes limiting and the fluorochrome is not fully excited. As expected, this effect is more pronounced at higher concentration of LLMCA, affecting calibration curve slopes in a greater manner. For similar reasons, the intercept does not vary linearly at high LLMCA concentrations (Fig. 3f).

Overall, no IFE was detected when assaying APA with all three tested instruments. An IFE was detected for proteases assays performed using cuvettes (SFM25 and LS50) but not using FIA-SMF25. The absence of IFE using FIA-SFM25, compared to the cuvette systems, might be due to both the sample dilution by hydraulic system (as sample is diluted about 10 times by carrier fluid) and by the 10 times shorter optic path, resulting in 100 times less substrate interfering with light flux. A greater overlap of fluorescence spectra, as well as different samples dilution (see following discussion), might favor the occurrence of IFE with the EPA assays compared to the APA assays. Those results illustrate the fact that this effect greatly depends on the type of substrate, concentrations, and equipment used and should be regularly tested for each assay protocol.

Consequences and correction of IFE

To assess the consequences of the detected IFE on natural samples, we carried out a kinetic measurement of natural bacterial communities EPA. The samples were measured using both FIA-SFM25 and cuvette operated LS50 with pH correction.

With FIA-SFM25, unweighted hyperbolic regression gave a V_{max} of 3386 ± 198 nM h^{-1} and a K_m of 275 ± 40 μM. When carried out with LS50 for which IFE occurs, V_{max} only reached 2668 ± 154 nM h^{-1} and K_m equaled 205 ± 32 μM, hence a respective difference of 21% and 26% on each parameter (Fig. 4a). The correlation between the two measurements shows that, for the tested spectrofluorometers, the IFE appears at a LLMCA concentration of 125 μM (Fig. 4a), which roughly

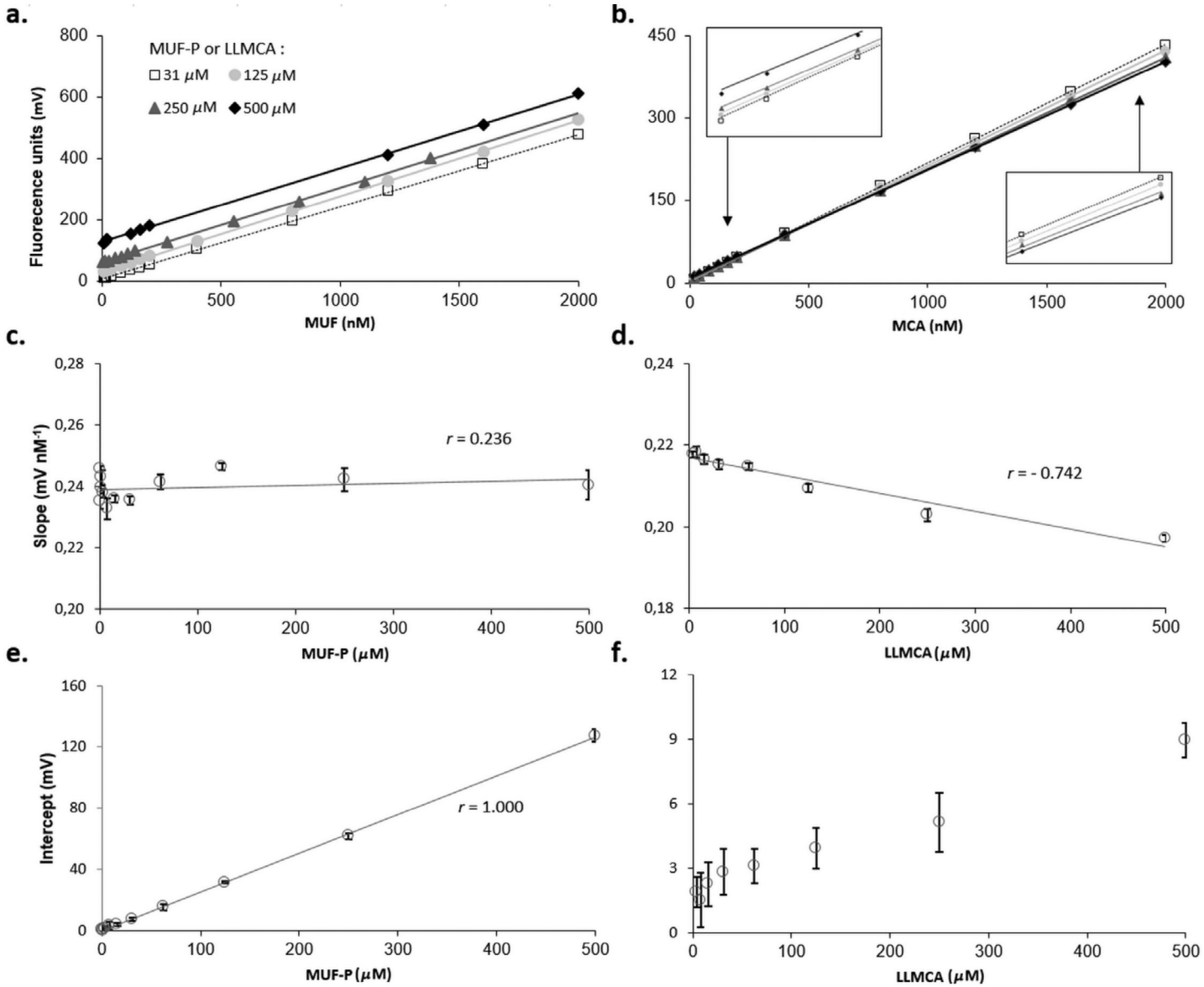

Fig 3. Detection of IFE using calibration curves of MUF (**a**, **c**, **e**) and MCA (**b**, **d**, **f**), with cuvette operated LS50 spectrofluorometer. Calibration curves (**a**, **b**) were determined from solutions prepared in varying concentration of non-hydrolysed substrate (MUF-P, LLMCA). On panel **a** and **b**, only four calibration curves are shown to facilitate readability although 12 and 9 curves were respectively measured for APA and EPA. All calibrations are displayed on other panels. Calibration of MUF shows no IFE as the slope of each calibration is not dependent on MUF-P concentration (**c**) and intercept varies linearly with MUF-P concentration (**e**). Calibration of MCA exhibits an IFE as the slope of each calibration varies significantly with LLMCA concentration (**d**) and intercept does not vary linearly above 60 μM of LLMCA (**f**). *r*: correlation coefficient. Error bars (**c**, **d**, **e**, **f**) represent 95% confidence interval of the fitted parameters.

corresponds to a rate of 1000 nM h^{-1}. Below this threshold, the two spectrofluorometers results correlate well (slope of 1.05, Fig. 4b) whereas above, cuvette measurements yield lower activities (slope of 0.70, Fig. 4b).

This threshold value is close to the 150 μM self-quenching threshold observed by Saifuku et al. (1978) in the original method of LLMCA assay. IFE can be avoided by using diluted solutions, shorter optic path, horizontal over vertical slits, a change in lamp geometry or in excitation/emission wavelengths (Valeur 2001; Eccleston et al. 2005; Fonin et al. 2014). However, it is not always possible to modify those parameters and this effect cannot always be avoided. In such cases, it should be corrected either experimentally or mathematically. If mathematic corrections are available, they can be quite complicated to implement (*see* Fonin et al. 2014 or Puchalski et al. 1991 for references). To experimentally correct the IFE in a simple way, each fluorescence value obtained with a given substrate concentration was converted into a

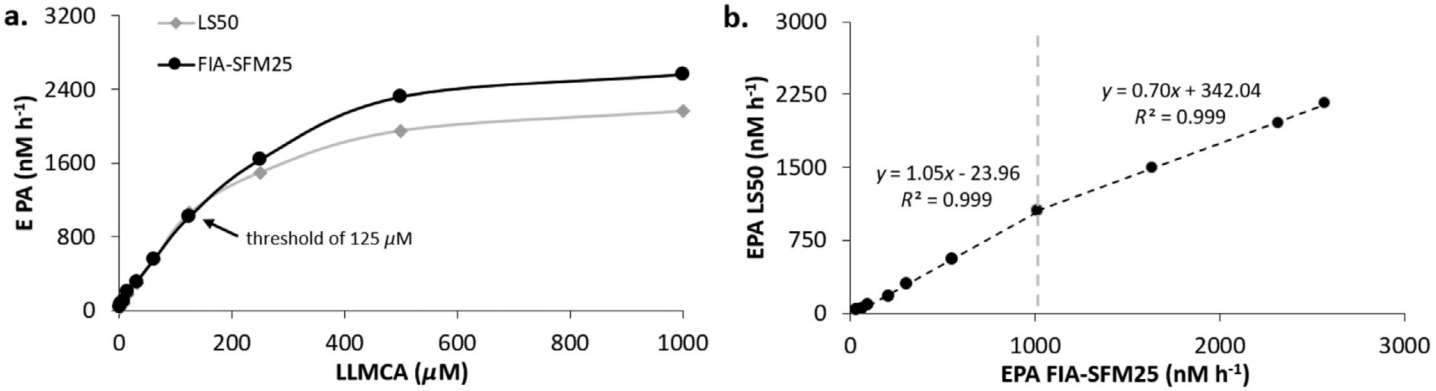

Fig 4. (**a**) Kinetics of natural bacterial communities EPA measured using FIA-SFM25 (black line) or with LS50 (using cuvette, gray line). (**b**) Correlation between EPA measured with LS50 (using cuvette) and using FIA-SFM25. Dashed line highlights the substrate concentration threshold.

concentration using the calibration curve of product prepared in the same given substrate concentration, instead of the usual calibration curve prepared in Milli-Q water. For instance, the values measured when assaying EPA with 1000 μM of LLMCA were converted using the MCA standards prepared in 1000 μM of LLMCA. The corrected values with LS50 are: V_{max} = 3267 $\pm$ 183 nM h^{-1} and K_m = 288 $\pm$ 40 μM, hence a respective difference of 4% and 5% on each parameter, which is within standard error inherent to fluorometric measurement and model fitting.

Importance of protocol and equipment used

We would like to draw specific attention to the fact that IFE greatly depends on protocol as well as equipment used.

The first methodological key point would be the preparation of calibration curves, which are necessary to correctly assess and correct IFE. As this effect is dependent on dilution, calibration solutions should be prepared in the exact same manner as the samples. In our protocol, all samples were diluted 1.2 times by the preservative (formaldehyde or SDS), which was consequently also added to the standards. Preservative is, to our knowledge, almost never amended in calibration solutions.

The second methodological key point concerns the pH adjustment when fluorescence is measured using cuvette. Our samples were further diluted by buffered borate amendment (1.24 times for APA, 1.05 times for EPA) to adjust pH to 10, which maximizes MUF and MCA fluorescence and allows the comparison between FIA and cuvette measurements. As such, IFE is minimized in our protocol. This is especially true for APA, for which larger volumes of buffer were necessary to reach pH = 10. However, in the literature, it is often unclear if pH adjustment is performed when using cuvettes or microplates. If not, IFE could be much more severe.

Another methodological key point would be the choice of excitation wavelength. For instance, Christie et al. (1978) noted that an excitation wavelength of 350 nm was necessary to overcome an IFE that was observed at 320 nm (maximum excitation wavelength) with MUF-α-D-mannopyranoside and MUF-α-D-glucopyranoside with a spectrofluorometer using cuvette. This is especially important for MCA as an excitation wavelength of 360 nm (maximum of excitation) will favor IFE due to a bigger absorbance by LLMCA (Fig. 1).

The occurrence of IFE strongly depends on the equipment used. For instance, Briciu-burghina et al. (2015) encountered a pronounced IFE in 1 cm optic path cuvette using MUF-β-D-glucuronide substrate, whose fluorescence spectra resemble MUF-P spectra, for which we found no IFE. This could be due, for example, to differences in cell geometry, slits orientation, fluorescence observation angle, lamp power and age (Valeur 2001; Eccleston et al. 2005; Fonin et al. 2014).

Microplate spectrofluorometer have been increasingly used as they allow high throughput assays and limit the substrate volume, although the small incubation volume and long incubation time may lead to bottle wall-effects (higher enzyme and substrate adsorption). IFE seems less likely to occur with those setups thanks to front-face optics and small optic path. However, studies using 96-wells microplates have shown its occurrence with MUF derivative substrates. For instance, Pinto et al. (2015) reported an IFE using MUF-galactoside, without specifying the importance of the effect. Marathe et al. (2013) found an IFE using 2′-(4-methylumbelliferyl)-α-D-N-acetylneuraminic acid, which was an important interference in their assay. Even though microplates are less prone to IFE, its occurrence should be checked in every spectrofluorometer.

Influence of substrate concentration range on kinetic parameters determination

To illustrate the effect of substrate concentration range on kinetic parameters determination, we conducted APA measurements on purified enzymes (*E. coli* and shrimp), phytoplankton cultures (*A. minutum* and *T. weissflogii*) and natural bacterial populations. Several fittings were consecutively made on each kinetics to determine V^n_{max} and K^n_m each time eliminating the highest concentration of substrate (S_{max}). This

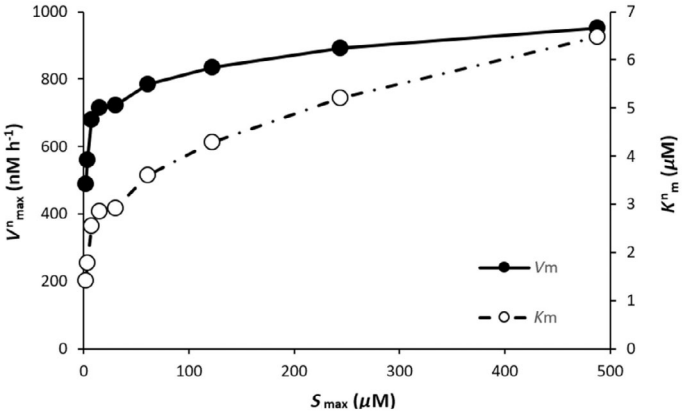

Fig 5. Evolution of kinetic parameters (V^n_{max}, K^n_m) of purified *E. coli* alkaline phosphatase over the maximum substrate concentration (S_{max}) used. Several fittings were done on the same assay data, iteratively removing the highest substrate concentration. Correlation coefficient indicated significant results for $n > 4$ (at 0.1%).

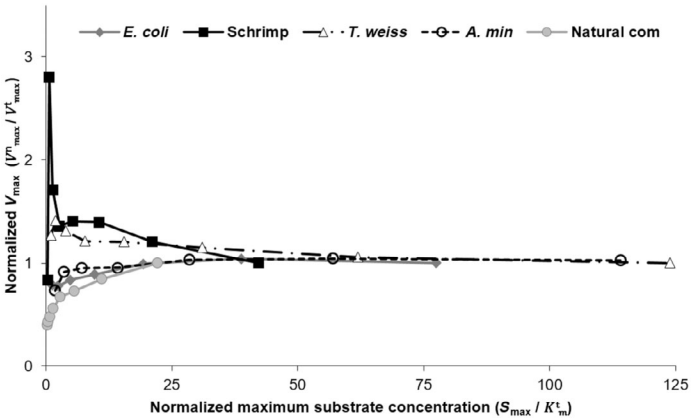

Fig 6. Normalized V_{max} (V^n_{max}/V^t_{max}) over normalized maximum substrate concentration (S_{max}/K^t_m) of APA assays conducted on various samples (purified enzymes from shrimp and *E. coli*, cultures of *T. weissflogii* and *A. minutum* and natural bacterial communities). Each dot represent a nonlinear fitting done on the same kinetic experiment data, but iteratively reducing S_{max}, which is represented normalized on the X-axis. Velocities are normalized by the "true" V^t_{max} obtained at S_{max} = 500 μM and substrate concentrations are normalized by the "true" K^t_m obtained at S_{max} = 500 μM.

process aims to illustrate the impact of substrate concentration range by decreasing the maximum concentration used from S_{max} = 500 μM (n = 11 points) to S_{max} = 2 μM (n = 3). The resulting variation of parameters is due to fitting artifact. It should be noted that only an apparent K_m can be determined, as natural substrates might be present in the medium, competing with the substrate analog.

Figure 5 shows the results obtained for the purified *E. coli* APA. Both V^n_{max} and K_m increase (respectively +61% and +157%) when S_{max} increases from 2 μM to 60 μM. Both parameters then tend to plateau at higher S_{max}, reaching what can be considered as their "true" value when S_{max} = 500 μM (V^t_{max} = 952 nM h^{-1} and K^t_m = 6.5 μM), even though K^n_m still seems to vary consequently. The threshold concentration of 60 μM roughly corresponds to 10 K^t_m. This value is generally recommended as a saturating concentration even though it deviates from true enzyme saturation since "only" 91% of active sites are occupied, as dealing with concentrated solutions can be complicated (Bisswanger 2014).

In order to compare the results of consecutive fittings performed on different enzymes, kinetic parameters (V^n_{max} and K^n_m) were normalized by the "true" kinetic parameters (V^t_{max} and K^t_m) determined using the largest substrate concentration range (S_{max} = 500 μM). Figure 6 presents the normalized velocities (V^n_{max}/V^t_{max}) plotted against the normalized maximum substrate concentration (S_{max}/K^t_m), which allows to observe the impact of S_{max} independently from the enzyme's affinity. It clearly shows the same pattern as before: V^n_{max} greatly varies with low S_{max}, then tends to stabilize around the correct parameter estimation at higher S_{max} (> 25 K^t_m). Normalized K_m follows the exact same pattern (data not shown).

This experiment illustrates the consequences of the use of insufficient S_{max} to determine kinetic parameters. Both low- and high-substrate concentrations are necessary to correctly fit all parts of the Michaelis–Menten equation (0 and 1st order; Chróst 1990). The width of the range depends on the enzyme affinity, since enzymes with low K_m are easily saturated and the curve's plateau will be reached even at low S_{max}. High-affinity enzymes (low K_m) are usually thought to occur in oligotrophic environments since they are supposed to process substrates at very low concentrations (Chróst 1991; Rath et al. 1993). However, even in those environments, S_{max} should be carefully chosen. For instance, all five studies determining enzymatic parameters in oligotrophic environments listed in Table 1 contained at least one experiment where K_m was equal or greater than S_{max}. In contrast, enzymes are considered to have lower substrate affinity (high K_m) in eutrophic environments (Chróst 1991; Rath et al. 1993), so substrate ranges should be even wider. Similar results were obtained for EPA (not shown). As the variation of kinetic parameters results from a fitting artifact, it should logically occur for all enzymatic kinetics.

Effect of natural substrates competition at trace concentration of analog substrate

Substrate concentration used for single point assays varied from 0.1 to 250 μM for APA assayed with MUF-P (*see* Table 1 for references) and from 2.5 to 1000 μM for EPA assayed with LLMCA (*see* Table 2 for references). Low substrate concentrations are usually used in oligotrophic conditions, in order to mimic mean environmental conditions. However, in such assays, naturally occurring substrates might compete with the analog substrate. To illustrate this effect, we performed APA assays on natural seawater microbial communities using trace

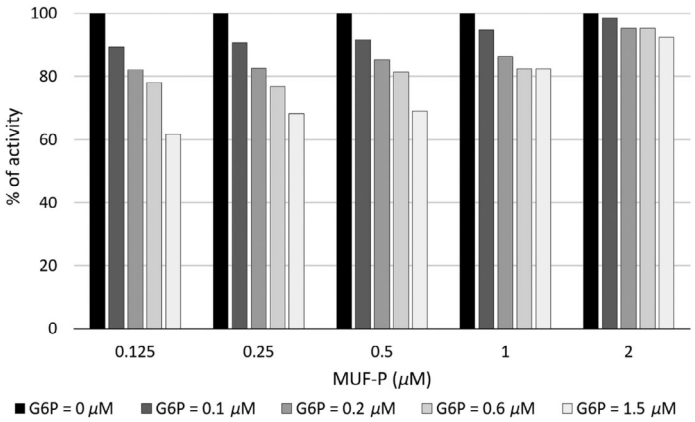

Fig 7. APA measured using trace MUF-P concentrations with various concentrations of G6P, a natural nonfluorescent competitor. Results are given in mV min^{-1} and normalized by the maximum activity obtained for each MUF-P concentration (without competitor).

substrate concentrations of MUF-P (0.125–2 μM, similar to those in studied literature) amended with different concentrations of G6P (0.1–1.5 μM). G6P was arbitrarily chosen to mimic dissolved organic phosphorus (DOP), the natural substrate of phosphatases. Concentrations were chosen to be representative of DOP concentration in natural environments: it usually ranges from 0 to 0.2 μM in open ocean surface waters (Ridal and Moore 1992; Karl and Björkman 2015) while coastal and estuarine waters often contain more than 0.25 μM DOP (Karl and Björkman 2015; Labry et al. 2016), with values sometimes exceeding 2 μM (Rinker and Powell 2006).

Activities were measured as slopes of fluorescence over time (in mV min^{-1}) and expressed as percentage of maximum activity, measured without inhibitors, for each substrate concentration (Fig. 7). With a MUF-P concentration of 0.125 μM, G6P concentrations of 0.1, 0.2, 0.6, and 1.5 μM decrease MUF-P hydrolysis by 11%, 18%, 22%, and 38%, respectively. Inhibition patterns are quite similar with 0.25, and 0.5 μM MUF-P, while those effects are lower at 1 μM and tend to disappear at 2 μM MUF-P (1–8% reduction). As measurements are carried out in seawater, naturally occurring DOP is also competing for the enzymes' active sites, so the actual effect of G6P might be underestimated. However, results clearly show that competition depends on the ratio of competitor to MUF-P and is not susceptible to happen at saturating concentration of MUF-P.

Although G6P was used as a single competitor, samples often contain a mixture of compounds with their own affinity and inhibition constant, affecting enzymatic assays in different ways. The competitor's affinity for the enzyme (hence its effect on measurement) might especially vary for polymeric substances given their huge diversity (peptides or carbohydrates for example). We conducted similar tests on EPA, amending 8 and 16 μM Leu-Gly, Leu-Gly-Gly, or Hexagly to 0.125 and 2 μM LLMCA. Although high, those competitor concentrations are representative of natural environments as combined dissolved amino acids may vary from 0.2 to 8 μM in oligotrophic to coastal waters (Keil and Kirchman 1991). As a result, 8 μM of Leu-Gly, Hexagly, and Leu-Gly-Gly generated an inhibition of 18%, 19%, and 34%, while 16 μM generated respectively 25%, 33%, and 41% of inhibition (Fig. 8a). Those results might be explained by the fact that measurements using peptidase substrates actually represent the concerted action of many distinct enzymes, as suggested by Steen et al. (2015), who performed competition experiments between 12 amino acid-p-nitroanilide compounds and 3 fluorogenic substrates (LLMCA, L-arginine-MCA, and L-proline-MCA). As expected, the use of higher concentration of LLMCA (2 μM) reduced the inhibition: 8 μM of Leu-GLy, Hexagly, and Leu-Gly-Gly generated 5%, 10%, and 8% inhibition respectively while 16 μM generated 6%, 23%, and 16% of inhibition, respectively (Fig. 8b).

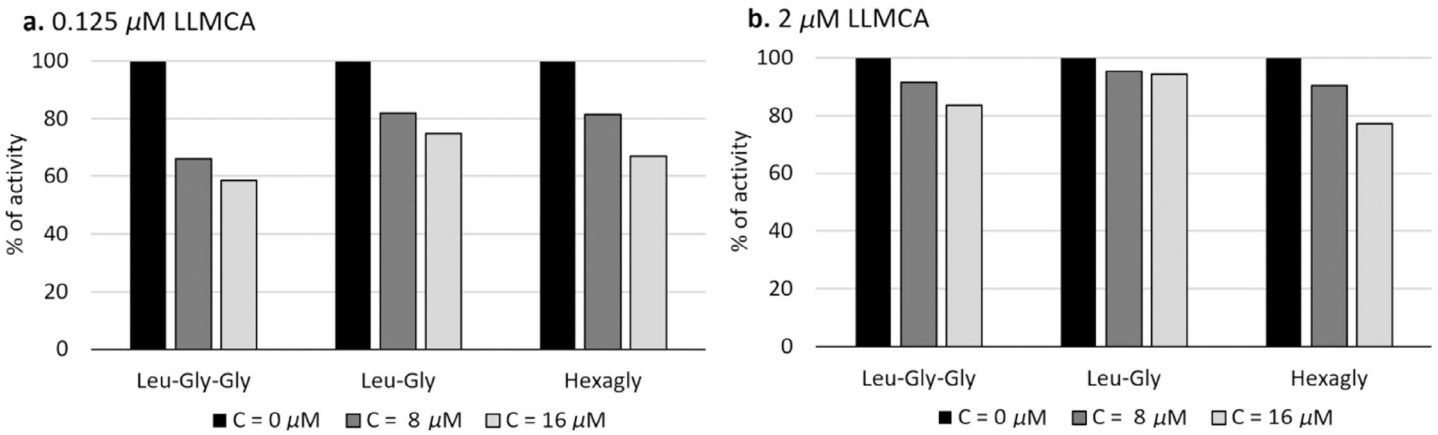

Fig 8. EPA measured using 0.125 μM LLMCA (**a**) or 2 μM LLMCA (**b**), with various concentrations of Leu-Gly-Gly, Leu-Gly, or Hexagly, acting as competitors (C). Results are measured in mV min^{-1} and normalized by the maximum activity obtained without competitor.

Several other studies have shown the competition between natural and fluorogenic substrates when assaying APA (*see* for instance Chróst 1990; Fernley and Walker 1967; Hoppe 1983), EPA (Hoppe 1983; Somville and Billen 1983; Christian and Karl 1998), or glycosidases (Hoppe 1983; Somville 1984), which confirms our results showing that natural substrates may significantly alter the measured enzymatic activities at low analog substrate concentrations.

This issue arises from the legitimate need to measure in situ degradation rates. However, as natural substrates compete with the fluorogenic analog, those measurements are unreliable and depend on sample composition, which completely impedes inter-study comparison. It raises questions regarding what we really are interested in quantifying when measuring enzyme activity rates. Single point assays using a saturating substrate concentration (> 10 K_m) allow the determination of a potential degradation rate (V_{max}). This can be considered as a determination of enzyme concentration (Billen 1991). When it is normalized by the biomass or number of cells, it reflects the enzymatic equipment of the cells. Those measurements are comparable across studies and allow, for instance, to study the regulation of enzyme synthesis in response to environmental trophic conditions. In any case, fluorogenic substrate assays should be interpreted cautiously in terms of real substrate utilization, keeping in mind that activities are measured with respect to naturally occurring substrates (Billen 1991).

Conclusion and recommendations

The starting point of this study was the comparison of the existing literature on enzymatic activity measurement in aquatic environments. We noticed substantial divergences in existing methodologies, the most notable one being the difference in substrate concentrations used for assays. Furthermore, the occurrence of IFE, a fluorometric artifact, has never been considered despite being likely to occur, especially at saturating concentrations of substrate. Those factors might alter results and therefore, investigation of past articles and inter-study comparison should be carried out cautiously. In this study, we tried to highlight several methodological key points of enzymatic assays, illustrating them with APA and EPA, although results should apply to all fluorometric enzymatic assays.

1. We would like to emphasize the possible occurrence of IFE, a fluorometric artifact that has been completely ignored in environmental water studies until now, despite having the potential to significantly affect measurements. In this study, it was not detected for APA assays but occurred for EPA assays with the two cuvette based spectrofluorometers tested, at a LLMCA threshold concentration of 125 μM. This effect can also occur with microplate readers, to a lesser extent. IFE depends on sample dilution and the equipment used and can be corrected by using appropriate calibration curves.
2. Ideally, before any single substrate assay, a kinetic analysis should be performed to determine the apparent K_m and to choose a saturating concentration. In practice, this step is laborious. However, when such experiments are carried out, a wide substrate concentration range (up to several hundred micromolar) should be used in order to reach the enzyme's active sites saturation and correctly fit both first- and zero-order part of enzyme reaction. The maximum substrate concentration should be at least 10 K_m to ensure that most enzymes are sufficiently saturated.
3. Finally, when performing a single substrate assay, saturating substrate concentrations (> 10 K_m) should be preferred, rather than trace concentrations mimicking natural conditions. Indeed, this latter approach might not fulfill Michaelis–Menten conditions (i.e., excess substrate compared to enzyme concentration) and may lead to higher uncertainties. Furthermore, it is highly dependent on both natural substrate concentrations and composition, as natural substrate might compete with the substrate analog for the enzyme active sites. Up to 41% and 38% inhibition was observed in the present study inhibition tests with natural substrates for EPA and APA, respectively.

All these methodological issues must be addressed in order to correctly measure enzymatic rates and allow inter-study comparison.

References

Arnosti, C. 2003. Microbial extracellular enzymes and their role in dissolved organic matter cycling. Aquat. Ecosyst. **342**: 315–342. doi:10.1016/B978-012256371-3/50014-7

Arnosti, C. 2011. Microbial extracellular enzymes and the marine carbon cycle. Ann. Rev. Mar. Sci. **3**: 401–425. doi:10.1146/annurev-marine-120709-142731

Azam, F., T. Fenchel, J. G. Field, J. Gray, L. Meyer-Reil, and T. F. Thingstad. 1983. The ecological role of water-column microbes in the sea. Mar. Ecol. Prog. Ser. **10**: 257–263. doi:10.3354/meps010257

Azam, F. 1998. Microbial control of oceanic carbon flux: The plot thickens. Science **280**: 694–696. doi:10.1126/science.280.5364.694

Bidle, K. D. 2010. Phytoplankton-bacteria interactions: Ectohydrolytic enzymes and their influence on biogeochemical cycling. Limnol. Oceanogr. e-Lectures **4**: 1–50. doi:10.4319/lol.2010.kbidle.4

Billen, G. 1991. Protein degradation in aquatic environments, p. 332. *In* R. J. Chróst [ed.], Microbial enzymes in aquatic environments. New York, NY: Springer-Verlag. doi:10.1007/978-1-4612-3090-8_7.

Bisswanger, H. 2014. Enzyme assays. Perspect. Sci. **1**: 41–55. doi:10.1016/j.pisc.2014.02.005

Bogé, G., M. Lespilette, D. Jamet, and J. L. Jamet. 2012. Role of sea water DIP and DOP in controlling bulk alkaline phosphatase activity in N.W. Mediterranean Sea (Toulon, France). Mar. Pollut. Bull. **64**: 1989–1996. doi:10.1016/j.marpolbul.2012.07.028

Briciu-burghina, C., B. Heery, and F. Regan. 2015. Continuous fluorometric method for measuring β-glucuronidase activity: Comparative analysis of three fluorogenic substrates. Analyst **140**: 5953–5964. doi:10.1039/c5an01021g

Bullock, A., K. Ziervogel, S. Ghobrial, S. Smith, B. McKee, and C. Arnosti. 2017. A multi-season investigation of microbial extracellular enzyme activities in two temperate coastal North Carolina rivers: Evidence of spatial but not seasonal patterns. Front. Microbiol. **8**: 2589. doi:10.3389/fmicb.2017.02589

Carlsson, P., E. Granéli, W. Granéli, E. G. Rodriguez, W. F. de Carvalho, A. Brutemark, and E. Lindehoff. 2012. Bacterial and phytoplankton nutrient limitation in tropical marine waters, and a coastal lake in Brazil. J. Exp. Mar. Bio. Ecol. **418–419**: 37–45. doi:10.1016/j.jembe.2012.03.012

Caruso, G., R. Caruso, and G. Maimone. 2019. Microbial enzymatic activity measurements by fluorogenic substrates: Evidence of inducible enzymes in oligotrophic Mediterranean areas. J. Clin. Microbiol Biochem. Technol. **5**: 19–24. doi:10.17352/jcmbt.000034

Chappell, K. R., and R. Goulder. 1995. A between-river comparison of extracellular-enzyme activity. Microb. Ecol. **29**: 1–17. doi:10.1007/BF00217419

Christian, J. R., and D. M. Karl. 1998. Ectoaminopeptidase specificity and regulation in Antarctic marine pelagic microbial communities. Aquat. Microb. Ecol. **15**: 303–310. doi:10.3354/ame015303

Christie, D. J., G. M. Alter, and J. A. Magnuson. 1978. Saccharide binding to transition metal ion free concanavalin a. Biochemistry **17**: 4425–4430. doi:10.1021/bi00614a011

Chróst, R., and H. Krambeck. 1986. Fluorescence correction for measurements of enzyme activity in natural waters using methylumbelliferyl-substrates. Arch. Hydrobiol. **106**: 79–90.

Chróst, R. J., and J. Overbeck. 1987. Kinetics of alkaline phosphatase activity and phosphorus availability for phytoplankton and bacterioplankton in Lake PluBsee (North German Eutrophic Lake). Microb. Ecol. **13**: 229–248. doi:10.1007/BF02025000

Chróst, R. J. 1990. Microbial ectoenzymes in aquatic environments, p. 47–77. *In* J. Overbeck and R. J. Chróst [eds.], Aquatic microbial ecology: Biochemical and molecular approaches. New York, NY: Springer Verlag.

Chróst, R. J. 1991. Environmental control of the synthesis and activity of aquatic microbial ectoenzymes. *In* R. J. Chróst [ed.], Microbial enzymes in aquatic environments. New York, NY: Springer.

Cunha, M. A., M. A. Almeida, and F. Alcantara. 2001. Short-term responses of the natural planktonic bacterial community to the changing water properties in an estuarine environment: Ectoenzymatic activity, glucose incorporation, and biomass production. Microb. Ecol. **42**: 69–79. doi:10.1007/s002480000098

Davis, C. E., C. Mahaffey, G. A. Wolff, and J. Sharples. 2014. A storm in a shelf sea: Variation in phosphorus distribution and organic matter stoichiometry. Geophys. Res. Lett. **41**: 8452–8459. doi:10.1002/2014GL061949

Delmas, D., C. Legrand, C. Bechemin, and C. Collinot. 1994. Exoproteolytic activity determined by flow injection analysis: Its potential importance for bacterial growth in coastal marine ponds. Aquat. Living Resour. **7**: 17–24.

Delmas, D., and M. J. Garet. 1995. SDS-preservation for deferred measurement of exoproteolytic kinetics in marine samples. J. Microbiol. Methods **22**: 243–248. doi:10.1016/0167-7012(95)00008-9

Duhamel, S., K. M. Björkman, J. K. Doggett, and D. M. Karl. 2014. Microbial response to enhanced phosphorus cycling in the North Pacific Subtropical Gyre. Mar. Ecol. Prog. Ser. **504**: 43–58. doi:10.3354/meps10757

Eccleston, J. F., J. P. Hutchinson, and D. M. Jameson. 2005. Fluorescence-based assays. Prog. Med. Chem. **43**: 19–48. doi:10.1016/S0079-6468(05)43002-7

Fernley, H. N., and P. G. Walker. 1967. Studies on alkaline phosphatase - inhibition by phosphate derivatives and the substrate specificity. Biochem. J. **104**: 1011–1018. doi:10.11405/nisshoshi1964.71.784

Fonin, A. V., A. I. Sulatskaya, I. M. Kuznetsova, and K. K. Turoverov. 2014. Fluorescence of dyes in solutions with high absorbance. Inner filter effect correction. PLoS One **9**: e103878. doi:10.1371/journal.pone.0103878

Foreman, C. M., Franchini, P., and Foreman, R. L. 1998. The trophic dynamics of riverine bacterioplankton: Relationships among substrate availability, ectoenzyme kinetics, and growth. Limnology and Oceanography. **43**: 1344–1352. doi:10.4319/lo.1998.43.6.1344.

Fukuda, R., Y. Sohrin, N. Saotome, H. Fukuda, T. Nagata, and I. Koike. 2000. East-west gradient in ectoenzyme activities in the subarctic Pacific: Possible regulation by zinc. Limnol. Oceanogr. **45**: 930–939. doi:10.4319/lo.2000.45.4.0930

Gonnelli, M., S. Vestri, and C. Santinelli. 2013. Chromophoric dissolved organic matter and microbial enzymatic activity. A biophysical approach to understand the marine carbon cycle. Biophys. Chem. **182**: 79–85. doi:10.1016/j.bpc.2013.06.016

Guillard, R. R. L., and J. H. Ryther. 1962. Studies of marine planktonic diatoms. Can. J. Microbiol. **8**: 229–239.

Hoppe, H.-G. 1983. Significance of exoenzymatic activities in the ecology of brackish water: Measurements by means of methylumbelliferyl-substrates. Mar. Ecol. Prog. Ser. **11**: 299–308. doi:10.3354/meps011299

Hoppe, H.-G. 2003. Phosphatase activity in the sea. Hydrobiologia **493**: 187–200. doi:10.1023/a:1025453918247

Kao, S., A. N. Asanov, and P. B. Oldham. 1998. A comparison of fluorescence inner-filter effects for different cell configurations. Instrum. Sci. Technol. **26**: 375–387. doi:10.1080/10739149808001906

Karl, D. M., and K. M. Björkman. 2015. Dynamics of dissolved organic phosphorus, p. 233–334. *In* D. A. Handsell and C. A. Carlson [eds.], Biogeochemistry of marine dissolved organic matter, 2nd ed. Amsterdam, The Netherlands: Academic Press.

Karner, M., D. Fuks, and G. J. Herndl. 1992. Bacterial activity along a trophic gradient. Microb. Ecol. **24**: 243–257. doi:10.1007/BF00167784

Keil, R. G., and D. L. Kirchman. 1991. Dissolved combined amino acids in marine waters as determined by a vapor-phase hydrolysis method. Mar. Chem. **33**: 243–259. doi:10.1016/0304-4203(91)90070-D

Kirchman, D. L. 2008. Microbial ecology of the oceans, 2nd Edition. Hoboken, NJ: Wiley-Blackwell, p. 477–593.

Koch, M. S., D. C. Kletou, and R. Tursi. 2009. Alkaline phosphatase activity of water column fractions and seagrass in a tropical carbonate estuary, Florida Bay. Estuar. Coast. Shelf Sci. **83**: 403–413. doi:10.1016/j.ecss.2009.04.007

Kothawala, D. N., K. R. Murphy, C. A. Stedmon, G. A. Weyhenmeyer, and L. J. Tranvik. 2013. Inner filter correction of dissolved organic matter fluorescence. Limnol. Oceanogr.: Methods **11**: 616–630. doi:10.4319/lom.2013.11.616

Labry, C., D. Delmas, and A. Herbland. 2005. Phytoplankton and bacterial alkaline phosphatase activities in relation to phosphate and DOP availability within the Gironde plume waters (Bay of Biscay). J. Exp. Mar. Bio. Ecol. **318**: 213–225. doi:10.1016/j.jembe.2004.12.017

Labry, C., D. Delmas, A. Youenou, J. Quere, A. Leynaert, S. Fraisse, M. Raimonet, and O. Ragueneau. 2016. High alkaline phosphatase activity in phosphate replete waters: The case of two macrotidal estuaries. Limnol. Oceanogr. **61**: 1513–1529. doi:10.1002/lno.10315

Liu, Y., W. Kati, C. M. Chen, R. Tripathi, A. Molla, and W. Kohlbrenner. 1999. Use of a fluorescence plate reader for measuring kinetic parameters with inner filter effect correction. Anal. Biochem. **267**: 331–335. doi:10.1006/abio.1998.3014

Marathe, B. M., V. Lévêque, K. Klumpp, R. G. Webster, and E. A. Govorkova. 2013. Determination of neuraminidase kinetic constants using whole influenza virus preparations and correction for spectroscopic interference by a fluorogenic substrate. PLoS One **8**: e71401. doi:10.1371/journal.pone.0071401

Misic, C., P. Povero, and M. Fabiano. 2002. Ectoenzymatic ratios in relation to particulate organic matter distribution (Ross Sea, Antarctica). Microb. Ecol. **44**: 224–234. doi:10.1007/s00248-002-2017-9

Nausch, M., G. Nausch, and N. Wasmund. 2004. Phosphorus dynamics during the transition from nitrogen to phosphate limitation in the central Baltic Sea. Mar. Ecol. Prog. Ser. **266**: 15–25. doi:10.3354/meps266015

Niell, F. X., B. A. Whitton, and I. Hernández. 2003. Phosphatase activity of benthic marine algae. An overview. J. Appl. Phycol. **3**: 475–487.

Ory, P., S. Palesse, D. Delmas, and H. Montanié. 2011. In situ structuring of virioplankton through bacterial exoenzymatic activity: Interaction with phytoplankton. Aquat. Microb. Ecol. **64**: 233–252. doi:10.3354/ame01524

Palmier, M. O., and S. R. Van Doren. 2007. Rapid determination of enzyme kinetics from fluorescence: Overcoming the inner filter effect. Anal. Biochem. **371**: 43–51. doi:10.1016/j.ab.2007.07.008

Patel, A. B., K. Fukami, and T. Nishijima. 2000. Regulation of seasonal variability of aminopeptidase activities in surface and bottom waters of Uranouchi Inlet, Japan. Aquat. Microb. Ecol. **21**: 139–149. doi:10.3354/ame021139

Payne, J. W. [ed.]. 1980. Microorganisms and nitrogen sources: Transport and utilization of amino acids, peptides, proteins, and related substrates. New York, NY: John Wiley, p. 870.

Pinto, M. F., B. N. Estevinho, R. Crespo, F. A. Rocha, A. M. Damas, and P. M. Martins. 2015. Enzyme kinetics: The whole picture reveals hidden meanings. FEBS J. **282**: 2309–2316. doi:10.1111/febs.13275

Puchalski, M. M., M. J. Morra, and R. von Wandruszka. 1991. Assessment of inner filter effect corrections in fluorimetry. Fresenius J. Anal. Chem. **340**: 341–344. doi:10.1007/BF00321578

Rath, J., C. Schiller, and G. J. Herndl. 1993. Ectoenzymatic activity and bacterial dynamics along a trophic gradient in the Caribbean Sea. Mar. Ecol. Prog. Ser. **102**: 89–96. doi:10.3354/meps102089

Rees, A. P., S. B. Hope, C. E. Widdicombe, J. L. Dixon, E. M. S. Woodward, and M. F. Fitzsimons. 2009. Alkaline phosphatase activity in the western English Channel: Elevations induced by high summertime rainfall. Estuar. Coast. Shelf Sci. **81**: 569–574. doi:10.1016/j.ecss.2008.12.005

Ridal, J. J., and R. M. Moore. 1992. Dissolved organic phosphorus concentrations in the northeast subarctic Pacific Ocean. Limnol. Oceanogr. **37**: 1067–1075. doi:10.4319/lo.1992.37.5.1067

Rinker, K. R., and R. T. Powell. 2006. Dissolved organic phosphorus in the Mississippi River plume during spring and fall 2002. Mar. Chem. **102**: 170–179. doi:10.1016/j.marchem.2005.09.013

Saifuku, K., T. Sekine, T. Namihisa, T. Takahashi, and Y. Kanaoka. 1978. A novel fluorometric ultramicro determination of serum leucine aminopeptidase using a coumarine derivative. Clin. Chim. Acta **84**: 85–91. doi:10.1016/0009-8981(78)90479-5

Sala, M. M., M. Karner, L. Arin, and C. Marrasé. 2001. Measurement of ectoenzyme activities as an indication of inorganic nutrient imbalance in microbial communities. Aquat. Microb. Ecol. **23**: 301–311. doi:10.3354/ame023301

Sebastián, M., and F. X. Niell. 2004. Alkaline phosphatase activity in marine oligotrophic environments: Implications of single-substrate addition assays for potential activity estimations. Mar. Ecol. Prog. Ser. **277**: 285–290. doi:10.3354/meps277285

Shi, Z., J. Xu, X. Li, R. Li, and Q. Li. 2019. Links of extracellular enzyme activities, microbial metabolism, and community composition in the river-impacted coastal waters. J. Geophys. Res. Biogeo. **124**: 3507–3520. doi:10.1029/2019JG005095

Sinsabaugh, R. L., S. Findlay, P. Franchini, and D. Fischer. 1997. Enzymatic analysis of riverine bacterioplankton production. Limnol. Oceanogr. **42**: 29–38. doi:10.4319/lo.1997.42.1.0029

Sisma-Ventura, G., and E. Rahav. 2019. DOP stimulates heterotrophic bacterial production in the oligotrophic southeastern Mediterranean coastal waters. Front. Microbiol. **10**: 1–10. doi:10.3389/fmicb.2019.01913

Sohm, J. A., and D. G. Capone. 2006. Phosphorus dynamics of the tropical and subtropical north Atlantic: Trichodesmium spp. versus bulk plankton. Mar. Ecol. Prog. Ser. **317**: 21–28. doi:10.3354/meps317021

Somville, M. 1984. Measurement and study of substrate specificity of exoglucosidase activity in eutrophic water. Appl. Environ. Microbiol. **48**: 1181–1185.

Somville, M., and G. Billen. 1983. A method for determining exoproteolytic activity in natural waters. Limnol. Oceanogr. **28**: 190–193. doi:10.4319/lo.1983.28.1.0190

Song, C., and others. 2019. Nutrient regeneration mediated by extracellular enzymes in water column and interstitial water through a microcosm experiment. Sci. Total Environ. **670**: 982–992. doi:10.1016/j.scitotenv.2019.03.297

Steen, A. D., J. P. Vazin, S. M. Hagen, K. H. Mulligan, and S. W. Wilhelm. 2015. Substrate specificity of aquatic extracellular peptidases assessed by competitive inhibition assays using synthetic substrates. Aquat. Microb. Ecol. **75**: 271–281. doi:10.3354/ame01755

Štrojsová, A., J. Nedoma, M. Štrojsová, X. Cao, and J. Vrba. 2008. The role of cell-surface-bound phosphatases in species competition within natural phytoplankton assemblage: An in situ experiment. J. Limnol. **67**: 128–138. doi:10.4081/jlimnol.2008.128

Talbot, V., L. Giuliano, V. Bruni, and M. Bianchi. 1997. Bacterial abundance, production and ectoproteolytic activity in the Strait of Magellan. Mar. Ecol. Prog. Ser. **154**: 293–302. doi:10.3354/meps154293

Thingstad, T. F., U. L. Zweifel, and F. Rassoulzadegan. 1998. P limitation of heterotrophic bacteria and phytoplankton. Limnol. Oceanogr. **4**: 88–94.

Valeur, B. 2001. Molecular fluorescence, principles and application. Weinheim< Germany: Wiley, p. 381.

Van Wambeke, F., U. Christaki, A. Giannakourou, T. Moutin, and K. Souvemerzoglou. 2002. Longitudinal and vertical trends of bacterial limitation by phosphorus and carbon in the Mediterranean Sea. Microb. Ecol. **43**: 119–133. doi:10.1007/s00248-001-0038-4

Van Wambeke, F., J.-F. Ghiglione, J. Nedoma, G. Mével, and P. Raimbault. 2009. Bottom up effects on bacterioplankton growth and composition during summer-autumn transition in the open NW Mediterranean Sea. Biogeosciences **6**: 705–720. doi:10.5194/bg-6-705-2009

Yamaguchi, T., M. Sato, F. Hashihama, M. Ehama, T. Shiozaki, K. Takahashi, and K. Furuya. 2019. Basin-scale variations in labile dissolved phosphoric monoesters and diesters in the central North Pacific Ocean. J. Geophys. Res. Ocean. **124**: 3058–3072. doi:10.1029/2018JC014763

Acknowledgments

This work was supported by the French National Program for Coastal Environment (EC2CO) and by ISblue project, Interdisciplinary graduate school for the blue planet (ANR-17-EURE-0015), cofunded by a grant from the French government under the program "Investissements d'Avenir." We wish to thank M. Latimier for the preparation of phytoplankton cultures.

Conflict of Interest

None declared.

Submitted 09 April 2020
Revised 23 September 2020
Accepted 29 September 2020

Associate editor: Gordon Taylor

II. Liste des contributions scientifiques

II.A. Articles publiés

- **Urvoy, M**., Labry, C., Delmas, D., Creac'h, L. and L'Helguen, S. (2020) Microbial enzymatic assays in environmental water samples: Impact of inner filter effect and substrate concentrations. *Limnol. Oceanogr. Methods*, 18:725-738. https://doi.org/10.1002/lom3.10398APA
- Labry, C., **Urvoy, M**. (2020) Formaldehyde preservation for deferred measurements of alkaline phosphatase activities in marine samples. *Heliyon*, 6(11):e05333. https://doi.org/10.1016/j.heliyon.2020.e05333
- **Urvoy, M**., Lami, R., Dreanno, C., Daudé, D., Rodrigues, A. M. S., L'Helguen, S., and C. Labry. (2021) Quorum sensing disruption regulates hydrolytic enzyme and biofilm production in estuarine bacteria. *Environ. Microbiol.* 23:7183−7200. https://doi.org/10.1111/1462-2920.15775
- **Urvoy, M**., Lami R., Dreanno C., Delmas D., L'Helguen S., and Labry C. (2021) Quorum sensing regulates the hydrolytic enzyme production and community composition of heterotrophic bacteria in coastal waters. *Front. Microbiol*. 12:780759. https://doi.org/10.3389/fmicb.2021.780759
- **Urvoy, M**., Labry C., Lami R., L'Helguen S., and R. Lami. (2022) Quorum sensing regulates bacterial processes that play a major role in marine biogeochemical cycles. *Front. Mar. Sci*. 9:834337. https://doi.org/10.3389/fmars.2022.834337

II.B. Articles en préparation

- **Urvoy, M**., Gourmelon M., Serghine J., L'Helguen S., and Labry C. (*en préparation*) Free-living and particle- attached bacterial community composition, assembly processes and determinants across spatiotemporal scales in a macrotidal temperate estuary.
- **Urvoy, M**., Delmas D., Lambert C., Rabiller E., L'Helguen S., Labry C. (*en préparation*) Spatiotemporal dynamics and determinants of hydrolytic enzyme activities and bacterial production in the free-living and particle-attached bacterial communities of a temperate macrotidal estuary.

II.C. Conférences et présentations

IMBeR Brest (Juin 2019) : poster ("Microbial enzymatic activities: critical methodological issues to understand organic matter cycling" - **Urvoy M.**, Creac'h L., Delmas D., Labry C., L'Helguen S.)

AFEM Bussang (Novembre 2019) : poster pitch (« Hydrolyse de la matière organique au sein des maximums turbides estuariens : rôle du Quorum sensing dans la régulation des activités enzymatiques bactériennes » - **Urvoy M.**, Labry C., Delmas D., Dreanno C., Lami R., Rabiller E., L'Helguen S.)

Présentation EMBRC (Avril 2022) : présentation dans le cadre du projet EMBRC-France QSestuaire (« Le Quorum Sensing en milieu marin et estuarien: communication bactérienne et dégradation de la matière organique » - **Urvoy M.**, Lami R., Dreanno C., Daudé D., Rodrigues A. M. S., Gourmelon M., L'Helguen S., Labry C.)

Références

Abbott, B.W., Moatar, F., Gauthier, O., Fovet, O., Antoine, V., and Ragueneau, O. (2018) Trends and seasonality of river nutrients in agricultural catchments: 18 years of weekly citizen science in France. *Sci Total Environ* **624**: 845–858.

Abril, G., Etcheber, H., Hir, P. Le, Bassoullet, P., Boutier, B., and Frankignoulle, M. (1999) Oxic / anoxic oscillations and organic carbon mineralization in an estuarine maximum turbidity zone (The Gironde, France) Pierre Le Hir and Plzilippe Bassoullet. *Limnol Oceanogr* **44**: 1304–1315.

Allen, G.P., Salomon, J.C., Bassoullet, P., Du Penhoat, Y., and De Grandpré, C. (1980) Effects of tides on mixing and suspended sediment transport in macrotidal estuaries. *Sediment Geol* **26**: 69–90.

Aller, R.C. (2004) Conceptual models of early diagenetic processes: The muddy seafloor as an unsteady, batch reactor. *J Mar Res* **62**: 815–835.

Allison, S.D. and Martiny, J.B.H. (2008) Resistance, resilience, and redundancy in microbial communities. *Proc Natl Acad Sci U S A* **105**: 11512–11519.

Alonso-Sáez, L., Díaz-Pérez, L., and Morán, X.A.G. (2015) The hidden seasonality of the rare biosphere in coastal marine bacterioplankton. *Environ Microbiol* **17**: 3766–3780.

Altschul, S.F., Gish, W., Miller, W., Myers, E.W., and Lipman, D.J. (1990) Basic local alignment search tool. *J Mol Biol* **215**: 403–410.

Aminot, A., Kérouel, R., and Coverly, S. (2009) Nutrients in seawater using segmented flow analysis. In *Practical Guidelines for the Analysis of Seawater*. Wurl, O. (ed). Boca Raton: CRC Press, pp. 143–178.

Amon, R.M.W. and Benner, R. (1996) Bacterial utilization of different size classes of dissolved organic matter. *Limnol Oceanogr* **41**: 41–51.

Andersen, J.B., Heydorn, A., Hentzer, M., Eberl, L., Geisenberger, O., Christensen, B.B., et al. (2001) GFP-based *N*-acyl homoserine-lactone sensor systems for detection of bacterial communication. *Appl Environ Microbiol* **67**: 575–585.

Anderson, D.M., Glibert, P.M., and Burkholder, J.M. (2002) Harmful Algal Blooms and Eutrophication: Nutrient Sources, Composition, and Consequences. *Estuaries* **25**: 704–726.

Arnosti, C. (1995) Measurement of depth- and site-related differences in polysaccharide hydrolysis rates in marine sediments. *Geochim Cosmochim Acta* **59**: 4247–4257.

Arnosti, C. (2011) Microbial Extracellular Enzymes and the Marine Carbon Cycle. *Ann Rev Mar Sci* **3**: 401–425.

Arnosti, C. (2014) Patterns of Microbially Driven Carbon Cycling in the Ocean: Links between Extracellular Enzymes and Microbial Communities. *Adv Oceanogr* **2014**: 1–12.

Arnosti, C., Steen, A.D., Ziervogel, K., Ghobrial, S., and Jeffrey, W.H. (2011) Latitudinal gradients in degradation of marine dissolved organic carbon. *PLoS One* **6**: e28900.

Arnosti, C., Wietz, M., Brinkhoff, T., Hehemann, J.H., Probandt, D., Zeugner, L., and Amann, R. (2021) The Biogeochemistry of Marine Polysaccharides: Sources, Inventories, and Bacterial Drivers of the Carbohydrate Cycle. *Ann Rev Mar Sci* **13**: 81–108.

Arrieta, J.M., Mayol, E., Hansman, R.L., Herndl, G.J., Dittmar, T., and Duarte, C.M. (2015) Dilution limits dissolved organic carbon utilization in the deep ocean. *Science (80)* **348**: 331–333.

Aspila, K.I., Agemian, H., and Chau, A.S.Y. (1976) A semi-automated method for the determination of inorganic, organic and total phosphate in sediments. *Analyst* **101**: 187–197.

Atkinson, S. and Williams, P. (2009) Quorum sensing and social networking in the microbial world. *J R Soc Interface* **6**: 959–978.

Auffret, G.A. (1983) Dynamique sédimentaire de la marge continentale celtique-Evolution Cénozoïque-Spécificité du Pleistocène supérieur et de l'Holocène.

Ayé, A.M., Bonnin-Jusserand, M., Brian-Jaisson, F., Ortalo-Magné, A., Culioli, G., Nevry, R.K., et al. (2015) Modulation of violacein production and phenotypes associated with biofilm by exogenous quorum sensing *N*-acylhomoserine lactones in the marine bacterium *Pseudoalteromonas ulvae* TC14. *Microbiology* **161**: 2039–2052.

Azam, F., Fenchel, T., Field, J., Gray, J., Meyer-Reil, L., and Thingstad, F. (1983) The Ecological Role of Water-Column Microbes in the Sea. *Mar Ecol Prog Ser* **10**: 257–263.

Azam, F. and Long, R.A. (2001) Sea snow microcosms. *Nature* **414**: 467–469.

Azam, F. and Malfatti, F. (2007) Microbial structuring of marine ecosystems. *Nat Rev Microbiol* **5**: 782–791.

Balmonte, J.P., Hasler-sheetal, H., Glud, R.N., Andersen, T.J., Sejr, M.K., Middelboe, M., et al. (2019) Sharp contrasts between freshwater and marine microbial enzymatic capabilities, community composition, and DOM pools in a NE Greenland fjord. *Limnol Oceanogr* **65**: 77–95.

Baltar, F. (2018) Watch out for the "living dead": Cell-free enzymes and their fate. *Front Microbiol* **8**: 2438.

Baltar, F., Arístegui, J., Gasol, J.M., Sintes, E., Van Aken, H.M., and Herndl, G.J. (2010) High dissolved extracellular enzymatic activity in the deep central Atlantic ocean. *Aquat Microb Ecol* **58**: 287–302.

Baltar, F., De Corte, D., Thomson, B., and Yokokawa, T. (2019) Teasing apart the different size pools of extracellular enzymatic activity in the ocean. *Sci Total Environ* **660**: 690–696.

Baltar, F., Morán, X.A.G., and Lønborg, C. (2017) Warming and organic matter sources impact the proportion of dissolved to total activities in marine extracellular enzymatic rates. *Biogeochemistry* **133**: 307–316.

Barberán, A., Bates, S.T., Casamayor, E.O., and Fierer, N. (2012) Using network analysis to explore co-occurrence patterns in soil microbial communities. *ISME J* **6**: 343–351.

Bassoullet, P. (1979) Etude de la dynamique des sédiments en suspension dans l'estuaire de l'Aulne (rade de Brest).

Bauer, J.E., Cai, W.J., Raymond, P.A., Bianchi, T.S., Hopkinson, C.S., and Regnier, P.A.G. (2013) The changing carbon cycle of the coastal ocean. *Nature* **504**: 61–70.

Benner, R. and Amon, R.M.W. (2015) The size-reactivity continuum of major bioelements in the Ocean. *Ann Rev Mar Sci* **7**: 185–205.

Bertilsson, S., Eiler, A., Nordqvist, A., and Jørgensen, N.O.G. (2007) Links between bacterial production, amino-acid utilization and community composition in productive lakes. *ISME J* **1**: 532–544.

Bianchi, T.S. (2011) The role of terrestrially derived organic carbon in the coastal ocean: A changing paradigm and the priming effect. *Proc Natl Acad Sci* **108**: 19473–19481.

Bianchi, T.S. and Bauer, J.E. (2012) Particulate Organic Carbon Cycling and Transformation. In *Treatise on Estuarine and Coastal Science*. Elsevier Inc., pp. 69–117.

Biggs, R.B. and Cronin, L.E. (1981) Special characteristics of estuaries. In *Estuaries and Nutrients*. Neilson, B.J. and Cronin, L.E. (eds). Humana Press, pp. 3–23.

Bižic-Ionescu, M., Zeder, M., Ionescu, D., Orlic, S., Fuchs, B.M., Grossart, H., and Amann, R. (2015) Comparison of bacterial communities on limnic versus coastal marine particles reveals profound differences in colonization. *Environ Microbiol* **17**: 3500–3514.

Bolyen, E. (2019) Reproducible, interactive, scalable and extensible microbiome data science using QIIME 2. *Nat Biotechnol* **37**: 852–857.

Bonin, P., Rontani, J.F., and Bordenave, L. (2001) Metabolic differences between attached and free-living marine bacteria: Inadequacy of liquid cultures for describing in situ bacterial activity. *FEMS Microbiol Lett* **194**: 111–119.

Borrego, C., Sabater, S., and Proia, L. (2020) Lifestyle preferences drive the structure and diversity of bacterial and archaeal communities in a small riverine reservoir. *Sci Rep* **10**: 11288.

Boucher, D. and Debroas, D. (2009) Impact of environmental factors on couplings between bacterial community composition and ectoenzymatic activities in a lacustrine ecosystem. *FEMS Microbiol Ecol* **70**: 66–78.

Boyer, M. and Wisniewski-Dyé, F. (2009) Cell-cell signalling in bacteria: Not simply a matter of quorum. *FEMS Microbiol Ecol* **70**: 1–19.

Brameyer, S., Bode, H.B., and Heermann, R. (2015) Languages and dialects: Bacterial communication beyond homoserine lactones. *Trends Microbiol* **23**: 521–523.

Bryant, J.A., Aylward, F.O., Eppley, J.M., Karl, D.M., Church, M.J., and DeLong, E.F. (2016) Wind and sunlight shape microbial diversity in surface waters of the North Pacific Subtropical Gyre. *ISME J* **10**: 1308–1322.

Buchan, A., Gonzalez, J.M., and Moran, M.A. (2005) Overview of the Marine Roseobacter Lineage. *Appl Environ Microbiol* **71**: 5665–5677.

Buchan, A., LeCleir, G.R., Gulvik, C.A., and González, J.M. (2014) Master recyclers: features and functions of bacteria associated with phytoplankton blooms. *Nat Rev Microbiol* **12**: 686–698.

Bunse, C., Bertos-Fortis, M., Sassenhagen, I., Sildever, S., Sjöqvist, C., Godhe, A., et al. (2016) Spatio-temporal interdependence of bacteria and phytoplankton during a baltic sea spring bloom. *Front Microbiol* **7**: 517.

Cai, W.J. (2011) Estuarine and coastal ocean carbon paradox: CO_2 sinks or sites of terrestrial carbon incineration? *Ann Rev Mar Sci* **3**: 123–145.

Callahan, B.J., McMurdie, P.J., Rosen, M.J., Han, A.W., Johnson, A.J.A., and Holmes, S.P. (2016) DADA2: High-resolution sample inference from Illumina amplicon data. *Nat Methods* **13**: 581–583.

Campbell, B.J. and Kirchman, D.L. (2013) Bacterial diversity , community structure and potential growth rates along an estuarine salinity gradient. *ISME J* **7**: 210–220.

Campbell, B.J., Yu, L., Heidelberg, J.F., and Kirchman, D.L. (2011) Activity of abundant and rare bacteria in a coastal ocean. *Proc Natl Acad Sci U S A* **108**: 12776–12781.

Canuel, E.A. and Hardison, A.K. (2016) Sources, Ages, and Alteration of Organic Matter in Estuaries. *Ann Rev Mar Sci* **8**: 409–434.

Carr, A., Diener, C., Baliga, N.S., and Gibbons, S.M. (2019) Use and abuse of correlation analyses in microbial ecology. *ISME J* **13**: 2647–2655.

Carreira, C., Staal, M., Middelboe, M., and Brussaard, P.D. (2015) Counting Viruses and Bacteria in Photosynthetic Microbial Mats. *Appl Environ Microbiol* **81**: 2149–2155.

Chahande, A.M., Lathigara, D., Prabhune, A.A., and Devi, R.N. (2021) Red fluorescent ultra-small gold nanoclusters functionalized with signal molecules to probe specificity in quorum sensing receptors in gram-negative bacteria. *Arch Microbiol* **203**: 4293–4301.

Chapelle, A., Le Gac, M., Labry, C., Siano, R., Quere, J., and Caradec, F. (2015) The Bay of Brest (France), a new risky site for toxic ALexandrium minutum blooms and PSP shellfish contamination. *Harmful Algae Bloom* 1–5.

Chase, J.M. and Myers, J.A. (2011) Disentangling the importance of ecological niches from stochastic processes across scales. *Philos Trans R Soc B Biol Sci* **366**: 2351–2363.

Christian, J.R. and Karl, D.M. (1995) Bacterial ectoenzymes in marine waters: Activity ratios and temperature responses in three oceanographic provinces. *Limnol Oceanogr* **40**: 1042–1049.

Chrost, R. and Krambeck, H. (1986) Fluorescence correction for measurements of enzyme activity in natural waters using methylumbelliferyl-substrates. *Arch Hydrobiol* **106**: 79–90.

Chróst, R.J. (1989) Characterization and significance of β-glucosidase activity in lake water. *Limnol Oceanogr* **34**: 660–672.

Chróst, R.J. (1990) Microbial Ectoenzymes in Aquatic Environments. In *Aquatic Microbial Ecology: Biochemical and molecular approaches*. Overbeck, J. and Chróst, R.J. (eds). New York, pp. 47–77.

Cloern, J.E. (2001) Our evolving conceptual model of the coastal eutrophication. *Mar Ecol Prog Ser* **210**: 223–253.

Cloern, J.E., Foster, S.Q., and Kleckner, A.E. (2014) Phytoplankton primary production in the world's estuarine-coastal ecosystems. *Biogeosciences* **11**: 2477–2501.

Comte, J. and Del Giorgio, P.A. (2010) Linking the patterns of change in composition and function in bacterioplankton successions along environmental gradients. *Ecology* **91**: 1466–1476.

Cooper, M.B. and Smith, A.G. (2015) Exploring mutualistic interactions between microalgae and bacteria in the omics age. *Curr Opin Plant Biol* **26**: 147–153.

Cornforth, D.M., Popat, R., McNally, L., Gurney, J., Scott-Phillips, T.C., Ivens, A., et al. (2014) Combinatorial quorum sensing allows bacteria to resolve their social and physical environment. *Proc Natl Acad Sci* **111**: 4280–4284.

Crump, B.C., Baross, J.A., and Simenstad, C.A. (1998) Dominance of particle-attached bacteria in the Columbia River estuary, USA. *Aquat Microb Ecol* **14**: 7–18.

Crump, B.C., Fine, L.M., Fortunato, C.S., Herfort, L., Needoba, J.A., Murdock, S., and Prahl, F.G. (2017) Quantity and quality of particulate organic matter controls bacterial production in the Columbia River estuary. *Limnol Oceanogr* **62**: 2713–2731.

Crump, B.C., Hopkinson, C.S., Sogin, M.L., and Hobbie, J.E. (2004) Microbial Biogeography along an Estuarine Salinity Gradient: Combined Influences of Bacterial Growth and Residence Time. *Appl Environ Microbiol* **70**: 1494–1505.

Cunha, M.A., Almeida, M.A., and Alcantara, F. (2000) Patterns of ectoenzymatic and heterotrophic bacterial activities along a salinity gradient in a shallow tidal estuary. *Mar Ecol Prog Ser* **204**: 1–12.

D'Ambrosio, L., Ziervogel, K., Macgregor, B., Teske, A., and Arnosti, C. (2014) Composition and enzymatic function of particle-associated and free-living bacteria: A coastal/offshore comparison. *ISME J* **8**: 2167–2179.

Danczak, R.E., Johnston, M.D., Kenah, C., Slattery, M., and Wilkins, M.J. (2018) Microbial Community Cohesion Mediates Community Turnover in Unperturbed Aquifers. *mSystems* **3**: e00066-18.

Dang, H. and Lovell, C.R. (2016) Microbial Surface Colonization and Biofilm Development in Marine Environments. *Microbiol Mol Biol Rev* **80**: 91–138.

Daniels, R., Reynaert, S., Hoekstra, H., Verreth, C., Janssens, J., Braeken, K., et al. (2006) Quorum signal molecules as biosurfactants affecting swarming in *Rhizobium etli*. *Proc Natl Acad Sci U S A* **103**: 14965–14970.

Datta, M.S., Sliwerska, E., Gore, J., Polz, M.F., and Cordero, O.X. (2016) Microbial interactions lead to rapid micro-scale successions on model marine particles. *Nat Commun* **7**: 11965.

David, F., Meziane, T., Marchand, C., Rolland, G., Thanh-nho, N., and Lamy, D. (2021) Estuarine, Coastal and Shelf Science Prokaryotic abundance, cell size and extracellular enzymatic activity in a human impacted and mangrove dominated tropical estuary (Can Gio, Vietnam). *Estuar Coast Shelf Sci* **251**: 107253.

Davies, J.L. (1964) A morphogenic approach to world shore-lines. *Zeitschrift für Geomorphol* **8**: 127–142.

Davis, C.E. and Mahaffey, C. (2017) Elevated alkaline phosphatase activity in a phosphate-replete environment: Influence of sinking particles. *Limnol Oceanogr* **62**: 2389–2403.

Decho, A.W., Frey, R.L., and Ferry, J.L. (2011) Chemical challenges to bacterial AHL signaling in the environment. *Chem Rev* **111**: 86–99.

Decho, A.W., Visscher, P.T., Ferry, J., Kawaguchi, T., He, L., Przekop, K.M., et al. (2009) Autoinducers extracted from microbial mats reveal a surprising diversity of *N*-acylhomoserine lactones (AHLs) and abundance changes that may relate to diel pH. *Environ Microbiol* **11**: 409–420.

Delgado-Baquerizo, M., Giaramida, L., Reich, P.B., Khachane, A.N., Hamonts, K., Edwards, C., et al. (2016) Lack of functional redundancy in the relationship between microbial diversity and ecosystem functioning. *J Ecol* **104**: 936–946.

Delmas, D. (1983) Les glucides et l'évolution de la matière organique dans les sédiments marins. *Oceanol Acta* **6**: 157–165.

Delmas, D., Frikha, M.G., and Linley, E.A.S. (1990) Dissolved primary amine measurement by flow injection analysis with o-phthaldialdehyde: Comparison with high-performance liquid chromatography. *Mar Chem* **29**: 145–154.

Delmas, D. and Garet, M.J. (1995) SDS-preservation for deferred measurement of exoproteolytic kinetics in marine samples. *J Microbiol Methods* **22**: 243–248.

Delmas, D., Legrand, C., Bechemin, C., Collinot, C., Legrand, C., Bechemin, C., and Collinot Aquat, C. (1994) Exoproteolytic activity deterrnined by flow injection analysis: its potential importance for bacterial growth in coastal marine ponds.

Delmas, R and Tréguer, P. (1983) Evolution saisonnière des nutriments dans un écosystème eutrophe d'Europe occidentale (la rade de Brest). Interactions marines et terrestres. *Oceanol acta* **6**: 345–356.

Delmas, Roger and Tréguer, P. (1983) Évolution saisonnière des nutriments dans un écosystème eutrophe d'Europe occidentale (la rade de Brest). Interactions marines et terrestres. *Oceanol Acta* **6**: 345–356.

Diggle, S.P., Gardner, A., West, S.A., and Griffin, A.S. (2007) Evolutionary theory of bacterial quorum sensing: when is a signal not a signal? *Philos Trans R Soc B Biol Sci* **362**: 1241–1249.

Dittmar, T. and Kattner, G. (2003) Recalcitrant dissolved organic matter in the ocean: Major contribution of small amphiphilics. *Mar Chem* **82**: 115–123.

Doberva, M., Sanchez-Ferandin, S., Toulza, E., Lebaron, P., and Lami, R. (2015) Diversity of quorum sensing autoinducer synthases in the Global Ocean Sampling metagenomic database. *Aquat Microb Ecol* **74**: 107–119.

Dobretsov, S., Dahms, H.U., Yili, H., Wahl, M., and Qian, P.Y. (2007) The effect of quorum-sensing blockers on the formation of marine microbial communities and larval attachment. *FEMS Microbiol Ecol* **60**: 177–188.

Duarte, C.M. (2015) Seafaring in the 21st century: The Malaspina 2010 circumnavigation expedition. *Limnol Oceanogr Bull* **24**: 11–14.

Duarte, C.M. (1995) Submerged aquatic vegetation in relation to different nutrient regimes. *Ophelia* **41**: 87–112.

Dubois, M., Gilles, K.A., Hamilton, J.K., Rebers, P.A., and Smith, F. (1956) Colorimetric Method for Determination of Sugars and Related Substances. *Anal Chem* **28**: 350–356.

Ducklow, H.W. and Carlson, C.A. (1992) Oceanic Bacterial Production. In *Advances in Microbial Ecology*. Marshall, K.C. (ed). New York: Plenum Press, pp. 113–181.

Dulaquais, G., Breitenstein, J., Waeles, M., Marsac, R., and Riso, R. (2018) Measuring dissolved organic matter in estuarine

and marine waters: Size-exclusion chromatography with various detection methods. *Environ Chem* **15**: 436–449.

Dulaquais, G., Waeles, M., Breitenstein, J., Knoery, J., and Riso, R. (2020) Links between size fractionation, chemical speciation of dissolved copper and chemical speciation of dissolved organic matter in the Loire estuary. *Environ Chem* **17**: 385–399.

Dulaquais, G., Waeles, M., Gerringa, L.J.A., Middag, R., Rijkenberg, M.J.A., and Riso, R. (2018) The Biogeochemistry of Electroactive Humic Substances and Its Connection to Iron Chemistry in the North East Atlantic and the Western Mediterranean Sea. *J Geophys Res Ocean* **123**: 5481–5499.

Eberhard, A. (1972) Inhibition and Activation of Bacterial Luciferase Synthesis. *J Bacteriol* **109**: 1101–1105.

Eberhard, A., Burlingame, A.L., Eberhard, C., Kenyon, G.L., Nealson, K.H., and Oppenheimer, N.J. (1981) Structural Identification of Autoinducer of Photobacterium fischeri Luciferase. *Biochemistry* **20**: 2444–2449.

Elifantz, H., Malmstrom, R.R., Cottrell, M.T., and Kirchman, D.L. (2005) Assimilation of Polysaccharides and Glucose by Major Bacterial Groups in the Delaware Estuary. *Appl Environ Microbiol* **71**: 7799–7805.

Engebrecht, J.A. and Silverman, M. (1984) Identification of genes and gene products necessary for bacterial bioluminescence. *Proc Natl Acad Sci U S A* **81**: 4154–4158.

Enke, T.N., Datta, M.S., Schwartzman, J., Cermak, N., Schmitz, D., Barrere, J., et al. (2019) Modular Assembly of Polysaccharide-Degrading Marine Microbial Communities. *Curr Biol* **29**: 1528-1535.e6.

Enke, T.N., Leventhal, G.E., Metzger, M., Saavedra, J.T., and Cordero, O.X. (2018) Microscale ecology regulates particulate organic matter turnover in model marine microbial communities. *Nat Commun* **9**: 2743.

Faith, D.P. (1992) Conservation evaluation and phylogenetic diversity. *Biol Conserv* **61**: 1–10.

Faust, K. and Raes, J. (2012) Microbial interactions: From networks to models. *Nat Rev Microbiol* **10**: 538–550.

Federle, M.J. and Bassler, B.L. (2003) Interspecies communication in bacteria. *J Clin Ivestigation* **112**: 1291–1299.

Fei, C., Ochsenkühn, M.A., Shibl, A.A., Isaac, A., Wang, C., and Amin, S.A. (2020) Quorum sensing regulates 'swim-or-stick' lifestyle in the phycosphere. *Environ Microbiol* **22**: 4761–4778.

Fekete, A., Kuttler, C., Rothballer, M., Hense, B.A., Fischer, D., Buddrus-Schiemann, K., et al. (2010) Dynamic regulation of *N*-acyl-homoserine lactone production and degradation in *Pseudomonas putida* IsoF. *FEMS Microbiol Ecol* **72**: 22–34.

Fernàndez-Gómez, B., Richter, M., Schüler, M., Pinhassi, J., Acinas, S.G., Gonzàles, J.M., and Pedrós-Alió, C. (2013) Ecology of marine Bacteroidetes: a comparative genomics approach. *ISME J* **7**: 1026–1037.

Ferrer-González, F.X., Widner, B., Holderman, N.R., Glushka, J., Edison, A.S., Kujawinski, E.B., and Moran, M.A. (2021) Resource partitioning of phytoplankton metabolites that support bacterial heterotrophy. *ISME J* **15**: 762–773.

Field, C.B., Behrenfeld, M.J., Randerson, J.T., and Falkowski, P.G. (1976) Primary Production of the Biosphere: integrating terrestrial and oceanic components. *Biochem Soc Trans* **281**: 237–240.

Fontaneto, D. and Hortal, J. (2012) Microbial Biogeography: Is Everything Small Everywhere? In *Microbial Ecological Theory: Current Perspectives*. Ogilvie, L.A. and Hirsch, P.R. (eds). Caister Academic Press.

Fortunato, C.S., Eiler, A., Herfort, L., Needoba, J.A., Peterson, T.D., and Crump, B.C. (2013) Determining indicator taxa across spatial and seasonal gradients in the Columbia River coastal margin. *ISME J* **7**: 1899–1911.

Fortunato, C.S., Herfort, L., Zuber, P., Baptista, A.M., and Crump, B.C. (2012) Spatial variability overwhelms seasonal patterns in bacterioplankton communities across a river to ocean gradient. *ISME J* **6**: 554–563.

Francis, B., Urich, T., Mikolasch, A., Teeling, H., and Amann, R. (2021) North Sea spring bloom-associated Gammaproteobacteria fill diverse heterotrophic niches. *Environ Microbiomes* **16**: 15.

Fuhrman, J.A. and Azam, F. (1982) Thymidine incorporation as a measure of heterotrophic bacterioplankton production in marine surface waters: Evaluation and field results. *Mar Biol* **66**: 109–120.

Fuhrman, J.A., Cram, J.A., and Needham, D.M. (2015) Marine microbial community dynamics and their ecological interpretation. *Nat Rev Microbiol* **13**: 133–146.

Fukuda, R., Sohrin, Y., Saotome, N., Fukuda, H., Nagata, T., and Koike, I. (2000) East-west gradient in ectoenzyme activities in the subarctic Pacific: Possible regulation by zinc. *Limnol Oceanogr* **45**: 930–939.

Fuqua, C. and Greenberg, E.P. (2002) Listening in on bacteria: Acyl-homoserine lactone signalling. *Nat Rev Mol Cell Biol* **3**: 685–695.

Fuqua, C., Parsek, M.R., and Greenberg, P.E. (2001) Regulation of Gene Expression by Cell-to-Cell Communication: Acyl-Homoserine Lactone Quorum Sensing Clay. *Annu Rev Genet* **35**: 439–468.

Fuqua, C., Winans, S.C., and Greenberg, P.E. (1996) CENSUS AND CONSENSUS IN BACTERIAL ECOSYSTEMS: The LuxR-LuxI Family of Quorum-Sensing Transcriptional Regulators. *Annu Rev Microbiol* **50**: 727–751.

Fuqua, W.C., Winans, S.C., and Greenberg, E.P. (1994) Quorum sensing in bacteria: The LuxR-LuxI family of cell density-responsive transcriptional regulators. *J Bacteriol* **176**: 269–275.

Galand, P.E., Casamayor, E.O., Kirchman, D.L., and Lovejoy, C. (2009) Ecology of the rare microbial biosphere of the Arctic Ocean. *Proc Natl Acad Sci U S A* **106**: 22427–22432.

Gilbert, J.A., Steele, J.A., Caporaso, J.G., Steinbrück, L., Reeder, J., Temperton, B., et al. (2012) Defining seasonal marine microbial community dynamics. *ISME J* **6**: 298–308.

Giovannoni, S.J. (2017) SAR11 Bacteria: The Most Abundant Plankton in the Oceans. *Ann Rev Mar Sci* **9**: 231–255.

Gomes, J., Huber, N., Grunau, A., Eberl, L., and Gademann, K. (2013) Fluorescent labeling agents for quorum-sensing receptors (FLAQS) in live cells. *Chem - A Eur J* **19**: 9766–9770.

Gould, T.A., Herman, J., Krank, J., Murphy, R.C., and Churchill, M.E.A. (2006) Specificity of acyl-homoserine lactone synthases examined by mass spectrometry. *J Bacteriol* **188**: 773–783.

Graham, E.B. and Stegen, J.C. (2017) Dispersal-based microbial community assembly decreases biogeochemical function. *Processes* **5**: 65.

Gralka, M., Szabo, R., Stocker, R., and Cordero, O.X. (2020) Trophic Interactions and the Drivers of Microbial Community Assembly. *Curr Biol* **30**: R1176–R1188.

Gram, L., Grossart, H.P., Schlingloff, A., and Kiørboe, T. (2002) Possible quorum sensing in marine snow bacteria: production of acylated homoserine lactones by Roseobacter strains isolated from marine snow. *Appl Environ Microbiol* **68**: 4111–4116.

Grandclément, C., Tannières, M., Moréra, S., Dessaux, Y., and Faure, D. (2015) Quorum quenching: Role in nature and applied developments. *FEMS Microbiol Rev* **40**: 86–116.

Gravel, D., Canham, C.D., Beaudet, M., and Messier, C. (2006) Reconciling niche and neutrality: The continuum hypothesis. *Ecol Lett* **9**: 399–409.

Gray, N.D. and Head, I.M. (2001) Linking genetic identity and function in communities of uncultured bacteria. *Environ Microbiol* **3**: 481–492.

Grizzetti, B., Bouraoui, F., and Aloe, A. (2012) Changes of nitrogen and phosphorus loads to European seas. *Glob Chang Biol* **18**: 769–782.

Grossart, H.P. (2010) Ecological consequences of bacterioplankton lifestyles: Changes in concepts are needed. *Environ Microbiol Rep* **2**: 706–714.

Grossart, H.P. and Tang, K.W. (2010) Communicative & Integrative Biology. *Commun Integr Biol* **3**: 491–494.

Grossart, H.P., Tang, K.W., Kiørboe, T., and Ploug, H. (2007) Comparison of cell-specific activity between free-living and attached bacteria using isolates and natural assemblages. *FEMS Microbiol Lett* **206**: 194–200.

Guendouze, A., Plener, L., Bzdrenga, J., Jacquet, P., Rémy, B., Elias, M., et al. (2017) Effect of quorum quenching lactonase in clinical isolates of Pseudomonas aeruginosa and comparison with Quorum sensing inhibitors. *Front Microbiol* **8**: 227.

Hansell, D.A. (2013) Recalcitrant dissolved organic carbon fractions. *Ann Rev Mar Sci* **5**: 421–445.

Hanson, C.A., Fuhrman, J.A., Horner-Devine, M.C., and Martiny, J.B.H. (2012) Beyond biogeographic patterns: Processes shaping the microbial landscape. *Nat Rev Microbiol* **10**: 497–506.

Harvey, H.R. (2006) Sources and Cycling of Organic Matter in the Marine Water Column. In *The Handbook of Environmental Chemistry (Volume 2)*. Hutzinger, O. (ed). Berlin: Springer-Verlag, pp. 1–25.

Hausmann, B., Pelikan, C., Rattei, T., Loy, A., and Pester, M. (2019) Long-Term Transcriptional Activity at Zero Growth of a cosmopolitan rare biosphere member. *MBio* **10**: e02189-18.

Hawver, L.A., Jung, S.A., and Ng, W.L. (2016) Specificity and complexity in bacterial quorum-sensing systems. *FEMS Microbiol Rev* **40**: 738–752.

Hayes, M.O. (1975) Morphology of sand accumulations in estuaries. In *Estuarine Research. Geology and Engineering*. Cronin, L.E. (ed). New Yo: Academic Press, pp. 3–22.

He, W., Chen, M., Schlautman, M.A., and Hur, J. (2016) Dynamic exchanges between DOM and POM pools in coastal and inland aquatic ecosystems: A review. *Sci Total Environ* **551–552**: 415–428.

Hedges, J.I., Baldock, J.A., Gelinas, Y., Lee, C., Peterson, M., and Wakeham, S.G. (2001) Evidence for non-selective preservation of organic matter in sinking marine particles. *Nature* **409**: 801–804.

Hedges, J.I., Eglinton, G., Hatcher, P.G., Kirchman, D.L., Arnosti, C., Derenne, S., et al. (2000) The molecularly-uncharacterized component of nonliving organic matter in natural environments. *Org Geochem* **31**: 945–958.

Heip, C. (1995) Eutrophication and zoobenthos dynamics. *Ophelia* **41**: 113–136.

Henrichs, S.M. and Williams, P.M. (1985) Dissolved and particulate amino acids and carbohydrates in the sea surface microlayer. *Mar Chem* **17**: 141–163.

Hense, B.A., Kuttler, C., Müller, J., Rothballer, M., Hartmann, A., and Kreft, J.U. (2007) Does efficiency sensing unify diffusion and quorum sensing? *Nat Rev Microbiol* **5**: 230–239.

Herman, P.M.J. and Heip, C.H.R. (1999) Biogeochemistry of the MAximum TURbidity Zone of Estuaries (MATURE): Some conclusions. *J Mar Syst* **22**: 89–104.

Hernandez, D.J., David, A.S., Menges, E.S., Searcy, C.A., and Afkhami, M.E. (2021) Environmental stress destabilizes microbial networks. *ISME J* **15**: 1722–1734.

Herren, C.M. and McMahon, K.D. (2017) Cohesion: A method for quantifying the connectivity of microbial communities. *ISME J* **11**: 2426–2438.

Herren, Cristina M. and McMahon, K.D. (2018) Keystone taxa predict compositional change in microbial communities. *Environ Microbiol* **20**: 2207–2217.

Hiblot, J., Gotthard, G., Elias, M., and Chabriere, E. (2013) Differential Active Site Loop Conformations Mediate Promiscuous Activities in the Lactonase SsoPox. *PLoS One* **8**: e75272.

Hmelo, L. and Van Mooy, B.A.S. (2009) Kinetic constraints on acylated homoserine lactone-based quorum sensing in marine environments. *Aquat Microb Ecol* **54**: 127–133.

Hmelo, L.R. (2017) Quorum Sensing in Marine Microbial Environments. *Ann Rev Mar Sci* **9**: 257–281.

Hmelo, L.R., Mincer, T.J., and Van Mooy, B.A.S. (2011) Possible influence of bacterial quorum sensing on the hydrolysis of sinking particulate organic carbon in marine environments. *Environ Microbiol Rep* **3**: 682–688.

Hollibaugh, J.T., Wong, P.S., and Murrell, M.C. (2000) Similarity of particle-associated and free-living bacterial communities in northern San Francisco Bay, California. *Aquat Microb Ecol* **21**: 103–114.

Holm-Hansen, O., Lorenzen, C.J., Holmes, R.W., and Strickland, J.D.H. (1965) Fluorometric determination of chlorophyll. *ICES J Mar Sci* **30**: 3–15.

Hoppe, H.G. (2003) Phosphatase activity in the sea. *Hydrobiologia* **493**: 187–200.

Hoppe, H.G. and Ullrich, S. (1999) Profiles of ectoenzymes in the Indian Ocean: Phenomena of phosphatase activity in the mesopelagic zone. *Aquat Microb Ecol* **19**: 139–148.

Hu, Y., Xie, G., Jiang, X., Shao, K., Tang, X., and Gao, G. (2020) The Relationships Between the Free-Living and Particle-Attached Bacterial Communities in Response to Elevated Eutrophication. *Front Microbiol* **11**: 423.

Huang, S., Bergonzi, C., Schwab, M., Elias, M., and Hicks, R.E. (2019) Evaluation of biological and enzymatic quorum quencher coating additives to reduce biocorrosion of steel. *PLoS One* **14**:.

Huang, Y., Ki, J., Lee, O.O., and Qian, P. (2009) Evidence for the dynamics of Acyl homoserine lactone and AHL-producing bacteria during subtidal biofilm formation. *ISME J* **3**: 296–304.

Hubbell, S.P. (2005) Neutral theory in community ecology and the hypothesis of functional equivalence. *Funct Ecol* **19**: 166–172.

Hubbell, S.P. (2001) The Unified Neutral Theory of Biodiversity and Biogeography, Princeton: Princeton University Press.

Husson, B., Hernández-Fariñas, T., Le Gendre, R., Schapira, M., and Chapelle, A. (2016) Two decades of *Pseudo-nitzschia* spp. blooms and king scallop (*Pecten maximus*) contamination by domoic acid along the French Atlantic and English Channel coasts: Seasonal dynamics, spatial heterogeneity and interannual variability. *Harmful Algae* **51**: 26–39.

Hutchinson, E.G. (1957) Population studies: animal ecology and demography—Concluding Remarks. *Cold Spring Harb Symp Quant Biol* **22**: 415(427.

Jain, A., Balmonte, J.P., Singh, R., Bhaskar, P.V., and Krishnan, K.P. (2021) Spatially resolved assembly, connectivity and structure of particle-associated and free-living bacterial communities in a high Arctic fjord. *FEMS Microbiol Ecol* **97**: 1–12.

Jatt, A.N., Tang, K., Liu, J., Zhang, Z., and Zhang, X.H. (2015) Quorum sensing in marine snow and its possible influence on production of extracellular hydrolytic enzymes in marine snow bacterium *Pantoea ananatis* B9. *FEMS Microbiol Ecol* **91**: 1–13.

Jiao, N., Herndl, G.J., Hansell, D.A., Benner, R., Kattner, G., Wilhelm, S.W., et al. (2010) Microbial production of recalcitrant dissolved organic matter: Long-term carbon storage in the global ocean. *Nat Rev Microbiol* **8**: 593–599.

Kalia, V.C. (2013) Quorum sensing inhibitors: An overview. *Biotechnol Adv* **31**: 224–245.

Kaplan, H.B. and Greenberg, E.P. (1985) Diffusion of autoinducer is involved in regulation of the Vibrio fischeri luminescence system. *J Bacteriol* **163**: 1210–1214.

Karner, M. and Herndl, G.J. (1992) Marine Biology in free-living and marine-snow-associated bacteria. *Mar Biol* **347**: 341–347.

Karner, M.B., Delong, E.F., and Karl, D.M. (2001) Archaeal dominance in the mesopelagic zone of the Pacific Ocean. *Nature* **409**: 507–510.

Kellogg, C.T.E. and Deming, J.W. (2014) Particle-associated extracellular enzyme activity and bacterial community composition across the Canadian Arctic Ocean. *FEMS Microbiol Ecol* **89**: 360–375.

Kharbush, J.J., Close, H.G., Van Mooy, B.A.S., Arnosti, C., Smittenberg, R.H., Le Moigne, F.A.C., et al. (2020) Particulate Organic Carbon Deconstructed: Molecular and Chemical Composition of Particulate Organic Carbon in the Ocean. *Front Mar Sci* **7**: 518.

Kim, O.S., Cho, Y.J., Lee, K., Yoon, S.H., Kim, M., Na, H., et al. (2012) Introducing EzTaxon-e: A prokaryotic 16s rRNA gene sequence database with phylotypes that represent uncultured species. *Int J Syst Evol Microbiol* **62**: 716–721.

Kiørboe, T., Grossart, H.P., Ploug, H., and Tang, K. (2002) Mechanisms and rates of colonisation of sinking aggregates. *Appl Environ Microbiol* **68**: 3996–4006.

Kiørboe, T. and Jackson, G.A. (2001) Marine snow, organic solute plumes, and optimal chemosensory behavior of bacteria. *Limnol Oceanogr* **46**: 1309–1318.

Kirchman, D.L. (2002) The ecology of *Cytophaga-Flavobacteria* in aquatic environments. *FEMS Microbiol Ecol* **39**: 91–100.

Kirchman, D.L. and White, J. (1999) Hydrolysis and mineralization of chitin in the Delaware Estuary. *Aquat Microb Ecol* **18**: 187–196.

Klindworth, A., Pruesse, E., Schweer, T., Peplies, J., Quast, C., Horn, M., and Glöckner, F.O. (2013) Evaluation of general 16S ribosomal RNA gene PCR primers for classical and next-generation sequencing-based diversity studies. *Nucleic Acids Res* **41**: e1.

Koike, I. and Nagata, T. (1997) High potential activity of extracellular alkaline phosphatase in deep waters of the central Pacific. *Deep Res Part II Top Stud Oceanogr* **44**: 2283–2294.

Kopf, A., Bicak, M., Kottmann, R., Schnetzer, J., Kostadinov, I., Lehmann, K., et al. (2015) The ocean sampling day consortium. *Gigascience* **4**: 27.

Koroleff, F. (1983) Determination of phosphorus. In *Methods of Seawater analysis*. Grasshoff, K., Ehrhardt, M., and Kremling, K. (eds). Weinheim: Verlag Chemie, pp. 125–139.

Krupke, A., Hmelo, L.R., Ossolinski, J.E., Mincer, T.J., and Van Mooy, B.A.S. (2016) Quorum Sensing plays a complex role in regulating the enzyme hydrolysis activity of microbes associated with sinking particles in the ocean. *Front Mar Sci* **3**: 55.

Labry, C., Delmas, D., and Herbland, A. (2005) Phytoplankton and bacterial alkaline phosphatase activities in relation to phosphate and DOP availability within the Gironde plume waters (Bay of Biscay). *J Exp Mar Bio Ecol* **318**: 213–225.

Labry, C., Delmas, D., Moriceau, B., Gallinari, M., Quere, J., and Youenou, A. (2020) Effect of P depletion on the functional pools of diatom carbohydrates, and their utilization by bacterial communities. *Mar Ecol Prog Ser* **641**: 49–62.

Labry, C., Delmas, D., Youenou, A., Quere, J., Leynaert, A., Fraisse, S., et al. (2016) High alkaline phosphatase activity in phosphate replete waters: The case of two macrotidal estuaries. *Limnol Oceanogr* **61**: 1513–1529.

Labry, C., Herbland, A., and Delmas, D. (2002) The role of phosphorus on planktonic production of the Gironde plume waters in the Bay of Biscay. *J Plankton Res* **24**: 97–117.

Labry, C. and Urvoy, M. (2020) Formaldehyde preservation for deferred measurements of alkaline phosphatase activities in marine samples. *Heliyon* **6**: e05333.

Labry, C., Youenou, A., Delmas, D., and Michelon, P. (2013) Addressing the measurement of particulate organic and inorganic phosphorus in estuarine and coastal waters. *Cont Shelf Res* **60**: 28–37.

Lami, R. (2019) Quorum Sensing in Marine Biofilms and Environments. In *Quorum Sensing: Molecular Mechanism and Biotechnological Application*.

Lamy, D., Obernosterer, I., Laghdass, M., Artigas, L.F., Breton, E., Grattepanche, J.D., et al. (2009) Temporal changes of major bacterial groups and bacterial heterotrophic activity during a *Phaeocystis globosa* bloom in the eastern English Channel. *Aquat Microb Ecol* **58**: 95–107.

Landa, M., Blain, S., Christaki, U., Monchy, S., and Obernosterer, I. (2016) Shifts in bacterial community composition associated with increased carbon cycling in a mosaic of phytoplankton blooms. *ISME J* **10**: 39–50.

Langenheder, S., Lindström, E.S., and Tranvik, L.J. (2005) Weak coupling between community composition and functioning of aquatic bacteria. *Limnol Oceanogr* **50**: 957–967.

Langille, M.G.I., Zaneveld, J., Caporaso, J.G., McDonald, D., Knights, D., Reyes, J.A., et al. (2013) Predictive functional profiling of microbial communities using 16S rRNA marker gene sequences. *Nat Biotechnol* **31**: 814–821.

Langmead, B. and Salzberg, S.L. (2012) Fast gapped-read alignment with Bowtie2. *Nat Methods* **9**: 357–359.

Lebo, M.E., Sharp, J.H., and Cifuentes, L.A. (1994) Contribution of River phosphate variation to apparrent reactivity estimated from phosphate-salinity diagrams. *Estuar Coast Shelf Sci* **39**: 583–594.

Lee, C., Wakeham, S., and Arnosti, C. (2004) Particulate organic matter in the sea: The composition conundrum. *Ambio* **33**: 565–575.

Leenheer, J.A. and Croué, J.-P. (2003) Characterizing dissolved aquatic organic matter. *Environ Sci Technol* 19–26.

Legendre, P. and Legendre, L. (2012) Numerical Ecology (third english edition), Amsterdam: Elsevier.

Lemonnier, C. (2019) Effet des changements environnementaux sur la dynamique des communautés microbiennes : évolution et adaptation des bactéries dans le cadre du développement de l'Observatoire Microbien en Rade de Brest et Mer d'Iroise.

Li, J., Azam, F., Zhang, S., Biology, M., Diego, S., and Jolla, L. (2016) Outer membrane vesicles containing signalling molecules and active hydrolytic enzymes released by a coral pathogen Vibrio shilonii AK1. *Environ Microbiol* **18**: 3850–3866.

Li, J., Gu, L., Bai, S., Wang, J., Su, L., Wei, B., et al. (2021) Characterization of particle-associated and free-living bacterial and archaeal communities along the water columns of the South China Sea. *Biogeosciences* **18**: 113–133.

Li, T., Wang, D., Ren, L., Mei, Y., Ding, T., Li, Q., et al. (2019) Involvement of Exogenous *N*-Acyl-Homoserine Lactones in Spoilage Potential of *Pseudomonas fluorescens* Isolated From Refrigerated Turbot. *Front Microbiol* **10**: 2716.

Li, Y., Jing, H., Xia, X., Cheung, S., Suzuki, K., and Liu, H. (2018) Metagenomic insights into the microbial community and nutrient cycling in the western subarctic Pacific Ocean. *Front Microbiol* **9**: 623.

Liénart, C., Savoye, N., Bozec, Y., Breton, E., Conan, P., David, V., et al. (2017) Dynamics of particulate organic matter composition in coastal systems: A spatio-temporal study at multi-systems scale. *Prog Oceanogr* **156**: 221–239.

Lima-Mendez, G., Faust, K., Henry, N., Decelle, J., Colin, S., Carcillo, F., et al. (2015) Determinants of community structure in the grobal plankton interactome. *Science (80-)* **348**: 1262073-1–10.

Lindström, E.S., Feng, X.M., Granéli, W., and Kritzberg, E.S. (2010) The interplay between bacterial community composition and the environment determining function of inland water bacteria. *Limnol Oceanogr* **55**: 2052–2060.

Liu, B., Zheng, D., Jin, Q., Chen, L., and Yang, J. (2019) VFDB 2019: A comparative pathogenomic platform with an interactive web interface. *Nucleic Acids Res* **47**: D687–D692.

Liu, J., Fu, K., Wang, Y., Wu, C., Li, F., Shi, L., and Ge, Y. (2017) Detection of Diverse *N*-Acyl-Homoserine Lactones in *Vibrio alginolyticus* and Regulation of Biofilm Formation by Lactone In vitro. *Front Microbiol* **8**: 1097.

Liu, J., Meng, Z., Liu, X., and Zhang, X.H. (2019) Microbial assembly, interaction, functioning, activity and diversification: a review derived from community compositional data. *Mar Life Sci Technol* **1**: 112–128.

Liu, S., Yu, H., Yu, Y., Huang, J., Zhou, Z., Zeng, J., et al. (2022) Ecological stability of microbial communities in Lake Donghu regulated by keystone taxa. *Ecol Indic* **136**: 108695.

Logue, J.B., Stedmon, C.A., Kellerman, A.M., Nielsen, N.J., Andersson, A.F., Laudon, H., et al. (2016) Experimental insights into

the importance of aquatic bacterial community composition to the degradation of dissolved organic matter. *ISME J* **10**: 533–545.

Lombard, V., Golaconda Ramulu, H., Drula, E., Coutinho, P.M., and Henrissat, B. (2014) The carbohydrate-active enzymes database (CAZy) in 2013. *Nucleic Acids Res* **42**: 490–495.

Louca, S., Polz, M.F., Mazel, F., Albright, M.B.N., Huber, J.A., O'Connor, M.I., et al. (2018) Function and functional redundancy in microbial systems. *Nat Ecol Evol* **2**: 936–943.

Lupp, C. and Ruby, E.G. (2005) *Vibrio fischeri* uses two quorum-sensing systems for the regulation of early and late colonization factors. *J Bacteriol* **187**: 3620–3629.

Lyons, M.M. and Dobbs, F.C. (2012) Differential utilization of carbon substrates by aggregate-associated and water-associated heterotrophic bacterial communities. *Hydrobiologia* **686**: 181–193.

Mahan, K., Martinmaki, R., Larus, I., Sikdar, R., Dunitz, J., and Elias, M. (2020) Effects of Signal Disruption Depends on the Substrate Preference of the Lactonase. *Front Microbiol* **10**: 3003.

Mangwani, N., Kumari, S., and Das, S. (2015) Involvement of quorum sensing genes in biofilm development and degradation of polycyclic aromatic hydrocarbons by a marine bacterium *Pseudomonas aeruginosa* N6P6. *Appl Microbiol Biotechnol* **99**: 10283–10297.

Marie, D., Partensky, F., Vaulot, D., and Brussaard, C. (1999) Enumeration of Phytoplankton, Bacteria, and Viruses in Marine Samples. *Curr Protoc Cytom* 11.11.1-11.11.15.

Martinez, J., Smith, D.C., Steward, G.F., and Azam, F. (1996) Variability in ectohydrolytic enzyme activities of pelagic marine bacteria and its significance for substrate processing in the sea. *Aquat Microb Ecol* **10**: 223–230.

Martiny, J.B.H., Bohannan, B.J.M., Brown, J.H., Colwell, R.K., Fuhrman, J.A., Green, J.L., et al. (2006) Microbial biogeography: Putting microorganisms on the map. *Nat Rev Microbiol* **4**: 102–112.

McKnight, D.T., Huerlimann, R., Bower, D.S., Schwarzkopf, L., Alford, R.A., and Zenger, K.R. (2019) Methods for normalizing microbiome data: An ecological perspective. *Methods Ecol Evol* **10**: 389–400.

McLean, R.J.C., Whiteley, M., Stickler, D.J., and Fuqua, W.C. (1997) Evidence of autoinducer activity in naturally occurring biofilms. *FEMS Microbiol Lett* **154**: 259–263.

McRose, D.L., Baars, O., Seyedsayamdost, M.R., and Morel, F.M.M. (2018) Quorum sensing and iron regulate a two-for-one siderophore gene cluster in Vibrio harveyi. *Proc Natl Acad Sci U S A* **115**: 7581–7586.

Mestre, M., Ferrera, I., Borrull, E., Ortega-Retuerta, E., Mbedi, S., Grossart, H.P., et al. (2017) Spatial variability of marine bacterial and archaeal communities along the particulate matter continuum. *Mol Ecol* **26**: 6827–6840.

Mestre, M., Höfer, J., Sala, M.M., and Gasol, J.M. (2020) Seasonal Variation of Bacterial Diversity Along the Marine Particulate Matter Continuum. *Front Microbiol* **11**: 1590.

Middelboe, M., Sondergaard, M., Letarte, Y., and Borch, N.H. (1995) Attached and Free-Living Bacteria: Production and Polymer Hydrolysis During a Diatom Bloom. *Microb Ecol* **29**: 231–248.

Middelburg, J.J. and Herman, P.M.J. (2007) Organic matter processing in tidal estuaries. *Mar Chem* **106**: 127–147.

Milici, M., Deng, Z.L., Tomasch, J., Decelle, J., Wos-Oxley, M.L., Wang, H., et al. (2016) Co-occurrence analysis of microbial taxa in the Atlantic ocean reveals high connectivity in the free-living bacterioplankton. *Front Microbiol* **7**: 649.

Miller, M.B. and Bassler, B.L. (2001) Quorum Sensing in Bacteria. *Annu Rev Microbiol* **55**: 165–199.

Van Mooy, B.A.S., Hmelo, L.R., Sofen, L.E., Campagna, S.R., May, A.L., Dyhrman, S.T., et al. (2012) Quorum sensing control of phosphorus acquisition in Trichodesmium consortia. *ISME J* **6**: 422–429.

Mopper, K. and Zika, R.G. (1987) Free amino acids in marine rains: evidence for oxidation and potential role in nitrogen cycling. *Nature* **325**: 246–249.

Morin, J. and Morse, J.W. (1999) Ammonium release from resuspended sediments in the Laguna Madre estuary. *Mar Chem* **65**: 97–110.

Morris, R.M., Rappé, M.S., Connon, S.A., Vergin, K.L., Siebold, W.A., Carlson, C.A., and Giovannoni, S.J. (2002) SAR11 clade dominates ocean surface bacterioplankton communities. *Nature* **420**: 806–810.

Mukherji, R., Samanta, A., Illathvalappil, R., Chowdhury, S., Prabhune, A., and Devi, R.N. (2013) Selective imaging of quorum sensing receptors in bacteria using fluorescent au nanocluster probes surface functionalized with signal molecules. *ACS Appl Mater Interfaces* **5**: 13076–13081.

Muras, A., López-Pérez, M., Mayer, C., Parga, A., Amaro-Blanco, J., and Otero, A. (2018) High Prevalence of Quorum-Sensing and Quorum-Quenching Activity among Cultivable Bacteria and Metagenomic Sequences in the Mediterranean Sea. *Genes (Basel)* **9**: 100.

Murphy, J. and Riley, J.P. (1962) A modified single solution method for the determination of phosphate in natural waters. *Anal Chim Acta* **27**: 31–36.

Murrell, M.C., Hollibaugh, J.T., Silver, M.W., and Wong, P.S. (1999) Bacterioplankton dynamics in northern San Francisco Bay: Role of particle association and seasonal freshwater flow. *Limnol Oceanogr* **44**: 295–308.

Myklestad, S.M. (1995) Release of extracellular products by phytoplankton with special emphasis on polysaccharides. *Sci Total Environ* **165**: 155–164.

Myklestad, S.M., Skånøy, E., and Hestmann, S. (1997) A sensitive and rapid method for analysis of dissolved mono- and polysaccharides in seawater. *Mar Chem* **56**: 279–286.

Nagata, T. (2008) Organic matter-bacteria interactions in seawater. In *Microbial Ecology of the Oceans, Second Edition*. Kirchman, D.L. (ed). John Wiley & Sons, pp. 207–241.

Nausch, M. (1998) Alkaline phosphatase activities and the relationship to inorganic phosphate in the Pomeranian Bight (southern Baltic Sea). *Aquat Microb Ecol* **16**: 87–94.

Nealson, K.H., Platt, T., and Hastings, J.W. (1970) Cellular Control of the Synthesis and Activity of the Bacterial Luminescent System. *J Bacteriol* **104**: 313–322.

Newton, A., Icely, J., Cristina, S., Perillo, G.M.E., Turner, R.E., Ashan, D., et al. (2020) Anthropogenic, Direct Pressures on Coastal Wetlands. *Front Ecol Evol* **8**: 144.

Newton, R.J. and McMahon, K.D. (2011) Seasonal differences in bacterial community composition following nutrient additions in a eutrophic lake. *Environ Microbiol* **13**: 887–899.

Nicholson, D., Dyhrman, S., Chavez, F., and Paytan, A. (2006) Alkaline phosphatase activity in the phytoplankton communities of Monterey Bay and San Francisco Bay. *Limnol Oceanogr* **51**: 874–883.

Noble, P.A., Bidle, K.D., and Fletcher, M. (1997) Natural microbial community compositions compared by a back-propagating neural network and cluster analysis of 5S rRNA. *Appl Environ Microbiol* **63**: 1762–1770.

Olesen, S.W., Duvallet, C., and Alm, E.J. (2017) dbOTU3: A new implementation of distribution-based OTU calling. *PLoS One* **12**: 1–13.

Ortega-Retuerta, E., Joux, F., Jeffrey, W.H., and Ghiglione, J.F. (2013) Spatial variability of particle-attached and free-living bacterial diversity in surface waters from the Mackenzie River to the Beaufort Sea (Canadian Arctic). *Biogeosciences* **10**: 2747–2759.

Pages, J. and Gadel, F. (1990) Dissolved organic matter and UV absorption in a tropical hyperhaline estuary. *Sci Total Environ* **99**: 173–204.

Panagiotopoulos, C. and Sempéré, R. (2005) Analytical methods for the determination of sugars in marine samples: A historical perspective and future directions. *Limnol Oceanogr* **3**: 419–454.

Pantoja, S., Lee, C., and Marecek, J.F. (1997) Hydrolysis of peptides in seawater and sediment. *Mar Chem* **57**: 25–40.

Patel, A.B., Fukami, K., and Nishijima, T. (2000) Regulation of seasonal variability of aminopeptidase activities in surface and bottom waters of Uranouchi Inlet, Japan. *Aquat Microb Ecol* **21**: 139–149.

Patzelt, D., Wang, H., Buchholz, I., Rohde, M., Gröbe, L., Pradella, S., et al. (2013) You are what you talk: quorum sensing induces individual morphologies and cell division modes in Dinoroseobacter shibae. *ISME J* **7**: 2274–2286.

Payne, J.W. ed. (1980) Microorganisms and nitrogen sources : transport and utilization of amino acids, peptides, proteins, and related substrates, John Wiley.

Pearson, J.P., Van Delden, C., and Iglewski, B.H. (1999) Active efflux and diffusion are involved in transport of Pseudomonas aeruginosa cell-to-cell signals. *J Bacteriol* **181**: 1203–1210.

Pedersen, B.S. and Quinlan, A.R. (2018) Mosdepth: Quick coverage calculation for genomes and exomes. *Bioinformatics* **34**: 867–868.

Peñuelas, J., Poulter, B., Sardans, J., Ciais, P., Van Der Velde, M., Bopp, L., et al. (2013) Human-induced nitrogen-phosphorus imbalances alter natural and managed ecosystems across the globe. *Nat Commun* **4**: 2934.

Pinhassi, J., Gómez-consarnau, L., Alonso-sáez, L., Pedrós-alió, C., and Gasol, J.M. (2006) Seasonal changes in bacterioplankton

nutrient limitation and their effects on bacterial community composition in the NW Mediterranean Sea. *Aquat Microb Ecol* **44**: 241–252.

Piontek, J., Sperling, M., Nöthig, E., and Engel, A. (2014) Regulation of bacterioplankton activity in Fram Strait (Arctic Ocean) during early summer: The role of organic matter supply and temperature. *J Mar Syst* **132**: 83–94.

Pollard, P.C. and Ducklow, H. (2011) Ultrahigh bacterial production in a eutrophic subtropical Australian river: Does viral lysis short-circuit the microbial loop? *Limnol Oceanogr* **56**: 1115–1129.

Pomeroy, L.R. (2007) The Microbial Loop. *Oceanography* **20**: 28–33.

Pommier, T., Canbäck, B., Riemann, L., Boström, K.H., Simu, K., Lundberg, P., et al. (2007) Global patterns of diversity and community structure in marine bacterioplankton. *Mol Ecol* **16**: 867–880.

Quast, C., Pruesse, E., Yilmaz, P., Gerken, J., Schweer, T., Yarza, P., et al. (2013) The SILVA ribosomal RNA gene database project: Improved data processing and web-based tools. *Nucleic Acids Res* **41**: 590–596.

Ragueneau, O., Quéguiner, B., and Tréguer, P. (1996) Contrast in biological responses to tidally-induced vertical mixing for two macrotidal ecosystems of Western Europe. *Estuar Coast Shelf Sci* **42**: 645–665.

Rappé, M.S., Vergin, K., and Giovannoni, S.J. (2000) Phylogenetic comparisons of a coastal bacterioplankton community with its counterparts in open ocean and freshwater systems. *FEMS Microbiol Ecol* **33**: 219–232.

Rath, J., Schiller, C., and Herndl, G.J. (1993) Ectoenzymatic activity and bacterial dynamics along a trophic gradient in the Caribbean Sea. *Mar Ecol Prog Ser* **102**: 89–96.

Rawlings, N.D., Barrett, A.J., Thomas, P.D., Huang, X., Bateman, A., and Finn, R.D. (2018) The MEROPS database of proteolytic enzymes, their substrates and inhibitors in 2017 and a comparison with peptidases in the PANTHER database. *Nucleic Acids Res* **46**: D624–D632.

Raymond, P.A. and Bauer, J.E. (2001) Riverine export of aged terrestrial organic matter to the North Atlantic Ocean. *Nature* **409**: 497–500.

Redfield, R.J. (2002) Is quorum sensing a side effect of diffusion sensing? *Trends Microbiol* **10**: 365–370.

Reintjes, G., Arnosti, C., Fuchs, B., and Amann, R. (2019) Selfish, sharing and scavenging bacteria in the Atlantic Ocean: a biogeographical study of bacterial substrate utilisation. *ISME J* **13**: 1119–1132.

Reintjes, G., Arnosti, C., Fuchs, B.M., and Amann, R. (2017) An alternative polysaccharide uptake mechanism of marine bacteria. *ISME J* **11**: 1640–1650.

Rémy, B., Plener, L., Decloquement, P., Armstrong, N., Elias, M., Daudé, D., and Chabrière, É. (2020) Lactonase Specificity Is Key to Quorum Quenching in Pseudomonas aeruginosa. *Front Microbiol* **11**: 762.

Rezzonico, F. and Duffy, B. (2008) Lack of genomic evidence of AI-2 receptors suggests a non-quorum sensing role for luxS in most bacteria. *BMC Microbiol* **8**: 154.

Rieck, A., Herlemann, D.P.R., Jürgens, K., and Grossart, H. (2015) Particle-Associated Differ from Free-Living Bacteria in Surface Waters of the Baltic Sea. *Front Microbiol* **6**: 1297.

Riedel, K., Hentzer, M., Geisenberger, O., Huber, B., Steidle, A., Wu, H., et al. (2001) *N*-acylhomoserine-lactone-mediated communication between *Pseudomonas aeruginosa* and *Burkholderia cepacia* in mixed biofilms. *Microbiology* **147**: 3249–3262.

Riemann, L., Leitet, C., Pommier, T., Simu, K., Holmfeldt, K., Larsson, U., and Hagström, Å. (2008) The native bacterioplankton community in the central Baltic Sea is influenced by freshwater bacterial species. *Appl Environ Microbiol* **74**: 503–515.

Rink, B., Martens, T., Fischer, D., Lemke, A., Grossart, H.P., Simon, M., and Brinkhoff, T. (2008) Short-term dynamics of bacterial communities in a tidally affected coastal ecosystem. *FEMS Microbiol Ecol* **66**: 306–319.

Riso, R., Mastin, M., Aschehoug, A., Davy, R., Devesa, J., Laës-Huon, A., et al. (2021) Distribution, speciation and composition of humic substances in a macro-tidal temperate estuary. *Estuar Coast Shelf Sci* **255**: 107360.

Robertson, K.J., Williams, P.M., and Bada, J.L. (1987) Acid hydrolysis of dissolved combined amino acids in seawater: A precautionary note. *Limnol Oceanogr* **32**: 996–997.

Rocker, D., Kisand, V., Scholz-Böttcher, B., Kneib, T., Lemke, A., Rullkötter, J., and Simon, M. (2012) Differential decomposition of humic acids by marine and estuarine bacterial communities at varying salinities. *Biogeochemistry* **111**: 331–346.

Rosenstock, B. and Simon, M. (2003) Consumption of dissolved amino acids and carbohydrates by limnetic bacterioplankton according to molecular weight fractions and proportions bound to humic matter. *Microb Ecol* **45**: 433–443.

Roth Rosenberg, D., Haber, M., Goldford, J., Lalzar, M., Aharonovich, D., Al-Ashhab, A., et al. (2021) Particle-associated and free-living bacterial communities in an oligotrophic sea are affected by different environmental factors. *Environ Microbiol* **23**: 4295–4308.

Sala, M.M., Karner, M., Arin, L., and Marrasé, C. (2001) Measurement of ectoenzyme activities as an indication of inorganic nutrient imbalance in microbial communities. *Aquat Microb Ecol* **23**: 301–311.

Sanchez, G. (2013) PLS Path Modeling with R. *Berkeley Trowchez Ed* 235.

Savoye, N., Aminot, A., Tréguer, P., Fontugne, M., Naulet, N., and Kérouel, R. (2003) Dynamics of particulate organic matter δ15N and δ13C during spring phytoplankton blooms in a macrotidal ecosystem (Bay of Seine, France). *Mar Ecol Prog Ser* **255**: 27–41.

Schultz, G.E., White, E.D., and Ducklow, H.W. (2003) Bacterioplankton dynamics in the York River estuary: Primary influence of temperature and freshwater inputs. *Aquat Microb Ecol* **30**: 135–148.

Schuster, M., Lostroh, C.P., Ogi, T., and Greenberg, E.P. (2003) Identification, timing, and signal Specicity of *Pseudomonas aeruginosa* Quorum-controlled genes: a transcriptome analysis. *J Bacteriol* **185**: 2066–2079.

Seemann, T. (2014) Prokka: Rapid prokaryotic genome annotation. *Bioinformatics* **30**: 2068–2069.

Servais, P. and Garnier, J. (2006) Organic carbon and bacterial heterotrophic activity in the maximum turbidity zone of the Seine estuary (France). *Aquat Sci* **68**: 78–85.

Shen, Y. and Benner, R. (2020) Molecular properties are a primary control on the microbial utilization of dissolved organic matter in the ocean. *Limnol Oceanogr* **65**: 1061–1071.

Simão, F.A., Waterhouse, R.M., Ioannidis, P., Kriventseva, E. V., and Zdobnov, E.M. (2015) BUSCO: Assessing genome assembly and annotation completeness with single-copy orthologs. *Bioinformatics* **31**: 3210–3212.

Simon, H.M., Smith, M.W., and Herfort, L. (2014) Metagenomic insights into particles and their associated microbiota in a coastal margin ecosystem. *Front Microbiol* **5**: 466.

Simon, M., Grossart, H.P., Schweitzer, B., and Ploug, H. (2002) Microbial ecology of organic aggregates in aquatic ecosystems. *Aquat Microb Ecol* **28**: 175–211.

Smith, D.C., Simon, M., Alldredge, A.L., and Azam, F. (1992) Intense hydrolytic enzyme activity on marine aggregates and implication for rapid particle dissolution. *Nature* **359**: 139–141.

Sogin, M.L., Morrison, H.G., Huber, J.A., Welch, D.M., Huse, S.M., Neal, P.R., et al. (2006) Microbial diversity in the deep sea and the underexplored "rare biosphere." *Proc Natl Acad Sci U S A* **103**: 12115–12120.

Solano, C., Echeverz, M., and Lasa, I. (2014) Biofilm dispersion and quorum sensing. *Curr Opin Microbiol* **18**: 96–104.

Solorzano, L. and Sharp, J.H. (1980) Determination of total dissolved phosphorus and particulate phosphorus in natural waters. *Limnol Oceanogr* **25**: 758–760.

Staley, J.T. and Konopka, A. (1985) Microorganisms in Aquatic and Terrestrial Habitats. *Annu Rev Microbiol* **39**: 321–346.

Steen, A.D. and Arnosti, C. (2011) Long lifetimes of β-glucosidase, leucine aminopeptidase, and phosphatase in Arctic seawater. *Mar Chem* **123**: 127–132.

Steen, A.D., Vazin, J.P., Hagen, S.M., Mulligan, K.H., and Wilhelm, S.W. (2015) Substrate specificity of aquatic extracellular peptidases assessed by competitive inhibition assays using synthetic substrates. *Aquat Microb Ecol* **75**: 271–281.

Stegen, J.C., Lin, X., Fredrickson, J.K., and Konopka, A.E. (2015) Estimating and mapping ecological processes influencing microbial community assembly. *Front Microbiol* **6**: 370.

Stegen, J.C., Lin, X., Konopka, A.E., and Fredrickson, J.K. (2012) Stochastic and deterministic assembly processes in subsurface microbial communities. *ISME J* **6**: 1653–1664.

Stocker, R. (2012) Marine microbes see a sea of gradients. *Science (80-)* **338**: 628–633.

Strom, S.L. (2008) Microbial ecology of ocean biogeochemistry: A community perspective. *Science (80-)* **320**: 1043–1045.

Su, Y., Tang, K., Liu, J., Wang, Y., Zheng, Y., and Zhang, X.H. (2019) Quorum sensing system of *Ruegeria mobilis* Rm01 controls lipase and biofilm formation. *Front Microbiol* **10**: 3304.

Sunagawa, S., Coelho, L.P., Chaffron, S., Kultima, J.R., Labadie, K., Salazar, G., et al. (2015) Structure and function of the global ocean microbiome. *Science (80-)* **348**: 1261359.

Suttle, C.A. (2007) Marine viruses — major players in the global ecosystem. *Nat Rev Microbiol* **5**: 801–812.

Takamura, N. and Nojiri, Y. (1994) Picophytoplankton biomass in relation to lake trophic state and the TN:TP ratio of lake water in Japan. *J Phycol* **30**: 439–444.

Taylor, G.T. and Gulnick, J.D. (1996) Enhancement of marine bacterial growth by mineral surfaces. *Can J Microbiol* **42**: 911–918.

Teeling, H., Fuchs, B.M., Becher, D., Klockow, C., Gardebrecht, A., Bennke, C.M., et al. (2012) Substrate-controlled succession of marine bacterioplankton populations induced by a phytoplankton bloom. *Science (80-)* **336**: 608–611.

Thomas, F., Hehemann, J.H., Rebuffet, E., Czjzek, M., and Michel, G. (2011) Environmental and gut Bacteroidetes: The food connection. *Front Microbiol* **2**: 93.

Thomson, B., Wenley, J., Currie, K., Hepburn, C., Herndl, G.J., and Baltar, F. (2019) Resolving the paradox: Continuous cell-free alkaline phosphatase activity despite high phosphate concentrations. *Mar Chem* **214**: 103671.

Thornton, D.C.O. (2014) Dissolved organic matter (DOM) release by phytoplankton in the contemporary and future ocean. *Eur J Phycol* **49**: 20–46.

Tian, Y., Wang, Q., Liu, Q., Ma, Y., Cao, X., Guan, L., and Zhang, Y. (2008) Involvement of LuxS in the regulation of motility and flagella biogenesis in *Vibrio alginolyticus*. *Biosci Biotechnol Biochem* **72**: 1063–1071.

Tietjen, T. and Wetzel, R.G. (2003) Extracellular enzyme-clay mineral complexes: Enzyme adsorption, alteration of enzyme activity, and protection from photodegradation. *Aquat Ecol* **37**: 331–339.

Toyofuku, M., Morinaga, K., Hashimoto, Y., Uhl, J., Shimamura, H., Inaba, H., et al. (2017) Membrane vesicle-mediated bacterial communication. *ISME J* **11**: 1504–1509.

Traving, S.J., Thygesen, U.H., Riemann, L., and Stedmon, C.A. (2015) A Model of Extracellular Enzymes in Free-Living Microbes: Which Strategy Pays Off? *Appl Environ Microbiol* **81**: 7385–7393.

Uncles, R.J., Stephens, J.A., and Smith, R.E. (2002) The dependence of estuarine turbidity on tidal intrusion length, tidal range and residence time. *Cont Shelf Res* **22**: 1835–1856.

Urvoy, M., Labry, C., Delmas, D., Creac'h, L., and L'Helguen, S. (2020) Microbial enzymatic assays in environmental water samples: Impact of inner filter effect and substrate concentrations. *Limnol Oceanogr Methods* **18**: 725–738.

Urvoy, M., Labry, C., L'Helguen, S., and Lami, R. (2022) Quorum Sensing Regulates Bacterial Processes That Play a Major Role in Marine Biogeochemical Cycles. *Front Mar Sci* **9**: 834337.

Venturi, V. and Ahmer, B.M.M. (2015) LuxR Solos are becoming major players in cell-cell communication in bacteria. *Front Cell Infect Microbiol* **5**: 89.

Vidal, M., Duarte, C.M., Agustí, S., Gasol, J.M., and Vaqué, D. (2003) Alkaline phosphatase activities in the central Atlantic Ocean indicate large areas with phosphorus deficiency. *Mar Ecol Prog Ser* **262**: 43–53.

Vives Rego, J., Billen, G., Fontigny, A., and Somville, M. (1985) Free and attached proteolytic activity in water environments. *Mar Ecol Prog Ser* **21**: 245–249.

Volkman, J.K. and Tanoue, E. (2002) Chemical and Biological Studies of Particulate Organic Matter in the Ocean. *J Oceanogr* **58**: 265–279.

Waeles, M., Riso, R., Pernet-Coudrier, B., Quentel, F., Durrieu, G., and Tissot, C. (2013) Annual cycle of humic substances in a temperate estuarine system affected by agricultural practices. *Geochim Cosmochim Acta* **106**: 231–246.

Wagner-Döbler, I. and Biebl, H. (2006) Environmental Biology of the Marine Roseobacter Lineage. *Annu Rev Microbiol* **60**: 255–280.

Wagner-Döbler, I., Thiel, V., Eberl, L., Allgaier, M., Bodor, A., Meyer, S., et al. (2005) Discovery of Complex Mixtures of Novel Long- Chain Quorum Sensing Signals in Free-Living and Host-Associated Marine Alphaproteobacteria. *ChemBioChem* **6**: 2195–2206.

Wang, Jianing, Wang, L., Hu, W., Pan, Z., Zhang, P., Wang, C., et al. (2021) Assembly processes and source tracking of planktonic and benthic bacterial communities in the Yellow River estuary. *Environ Microbiol* **23**: 2578–2591.

Wang, R., Ding, W., Long, L., Lan, Y., Tong, H., Saha, S., et al. (2020) Exploring the Influence of Signal Molecules on Marine Biofilms Development. *Front Microbiol* **11**: 571400.

Wang, Y., Pan, J., Yang, J., Zhou, Z., Pan, Y., and Li, M. (2020) Patterns and processes of free-living and particle-associated bacterioplankton and archaeaplankton communities in a subtropical river-bay system in South China. *Limnol Oceanogr* **65**: 161–179.

Waters, C.M. and Bassler, B.L. (2005) Quorum sensing: Cell-to-cell communication in bacteria. *Annu Rev Cell Dev Biol* **21**: 319–346.

Wellington, S. and Greenberg, E.P. (2019) Quorum Sensing Signal Selectivity and the Potential for Interspecies Cross Talk. *MBio* **10**: e00146-19.

Whalen, K.E., Becker, J.W., Schrecengost, A.M., Gao, Y., Giannetti, N., and Harvey, E.L. (2019) Bacterial alkylquinolone signaling contributes to structuring microbial communities in the ocean. *Microbiome* **7**: 93.

Whitman, W.B., Coleman, D.C., and Wiebe, W.J. (1998) Prokaryotes: The unseen majority. *Proc Natl Acad Sci U S A* **95**: 6578–6583.

Wick, R.R., Judd, L.M., Gorrie, C.L., and Holt, K.E. (2017) Unicycler: Resolving bacterial genome assemblies from short and long sequencing reads. *PLoS Comput Biol* **13**: e1005595.

Williams, C.J. and Jochem, F.J. (2015) Ectoenzyme kinetics in Florida Bay: Implications for bacterial carbon source and nutrient status. *Hydrobiologia* **569**: 113–127.

Wu, W., Xu, Z., Dai, M., Gan, J., and Liu, H. (2020) Homogeneous selection shapes free-living and particle- associated bacterial communities in subtropical coastal waters. *Divers Distrib* **00**: 1–14.

Xu, Y., Curtis, T., Dolfing, J., Wu, Y., and Rittmann, B.E. (2021) *N*-acyl-homoserine-lactones signaling as a critical control point for phosphorus entrapment by multi-species microbial aggregates. *Water Res* **204**: 117627.

Yao, Z., Du, S., Liang, C., Zhao, Y., Dini-andreote, F., Wang, K., and Zhang, D. (2019) Bacterial Community Assembly in a Typical Estuarine Marsh. *Appl Environ Microbiol* **85**: e02602-18.

Yates, E.A., Philipp, B., Buckley, C., Atkinson, S., Chhabra, S.R., Sockett, R.E., et al. (2002) *N*-acylhomoserine lactones undergo lactonolysis in a pH-, temperature-, and acyl chain length-dependent manner during growth of *Yersinia pseudotuberculosis* and *Pseudomonas aeruginosa*. *Infect Immun* **70**: 5635–5646.

Yawata, Y., Carrara, F., Menolascina, F., and Stocker, R. (2020) Constrained optimal foraging by marine bacterioplankton on particulate organic matter. *Proc Natl Acad Sci U S A* **117**: 25571–25579.

Yilmaz, P., Yarza, P., Rapp, J.Z., and Glöckner, F.O. (2016) Expanding the world of marine bacterial and archaeal clades. *Front Microbiol* **6**: 1524.

Yu, Z., Hu, Z., Xu, Q., Zhang, M., Yuan, N., Liu, J., et al. (2020) The luxI/luxR-type quorum sensing system regulates degradation of polycyclic aromatic hydrocarbons via two mechanisms. *Int J Mol Sci* **21**: 5548.

Zan, J., Choi, O., Meharena, H., Uhlson, C.L., Churchill, M.E.A., Hill, R.T., and Fuqua, C. (2015) A solo luxI-type gene directs acylhomoserine lactone synthesis and contributes to motility control in the marine sponge symbiont *Ruegeria* sp. KLH11. *Microbiology* 50–56.

Zhang, H., Yohe, T., Huang, L., Entwistle, S., Wu, P., Yang, Z., et al. (2018) DbCAN2: A meta server for automated carbohydrate-active enzyme annotation. *Nucleic Acids Res* **46**: W95–W101.

Zhou, J. and Ning, D. (2017) Stochastic Community Assembly: Does It Matter in Microbial Ecology? *Microbiol Mol Biol Rev* **81**: e00002-17.

Zhu, J. and Winans, S.C. (1999) Autoinducer binding by the quorum-sensing regulator TraR increases affinity for target promoters in vitro and decreases TraR turnover rates in whole cells. *Proc Natl Acad Sci U S A* **96**: 4832–4837.

Ziervogel, K. and Arnosti, C. (2008) Polysaccharide hydrolysis in aggregates and free enzyme activity in aggregate-free seawater from the north-eastern Gulf of Mexico. *Environ Microbiol* **10**: 289–299.

Ziervogel, K., Steen, A.D., and Arnosti, C. (2010) Changes in the spectrum and rates of extracellular enzyme activities in seawater following aggregate formation. *Biogeosciences* **7**: 1007–1015.

Zimmerman, A.E., Martiny, A.C., and Allison, S.D. (2013) Microdiversity of extracellular enzyme genes among sequenced prokaryotic genomes. *ISME J* **7**: 1187–1199.

Zinger, L., Amaral-Zettler, L.A., Fuhrman, J.A., Horner-Devine, M.C., Huse, S.M., Welch, D.B.M., et al. (2011) Global patterns of bacterial beta-diversity in seafloor and seawater ecosystems. *PLoS One* **6**: e24570.

DOCTORAT SCIENCES BRETAGNE DE LA MER LOIRE ET DU LITTORAL

UBO Université de Bretagne Occidentale

Activités enzymatiques extracellulaires et composition des communautés bactériennes dans l'estuaire de l'Aulne et la rade de Brest : facteurs de régulation et rôle du quorum sensing

Mots clés : Activités hydrolytiques extracellulaires, composition des communautés bactériennes, quorum sensing, estuaire

Résumé : Les bactéries hétérotrophes jouent un rôle primordial dans le fonctionnement des écosystèmes marins. Cette thèse s'est intéressée aux facteurs influençant la composition des communautés bactériennes estuariennes et marines ainsi que leurs fonctions dans la dégradation de la matière organique. Pour cela, une étude a été réalisée au sein de l'estuaire de l'Aulne et des eaux côtières adjacentes de la rade de Brest. Des expériences en laboratoire ont permis d'appréhender le rôle spécifique des communications bactériennes basées sur le quorum sensing (QS).

Les résultats obtenus ont montré que l'estuaire de l'Aulne était un véritable bioréacteur naturel. Il abrite des communautés bactériennes dont la composition et le niveau d'activité enzymatique suivent de fortes variations spatiotemporelles, liées aux conditions physicochimiques mais également à des facteurs biotiques comme leur degré de cooccurrence.

Ils ont également démontré la forte implication du QS dans la régulation de la synthèse d'enzymes hydrolytiques au sein de souches isolées et de communautés bactériennes naturelles. Ce mécanisme de régulation peut aussi impacter la composition des communautés bactériennes en régulant les processus liés à la colonisation et aux interactions microbiennes, qu'elles soient trophiques ou non.

Dans son ensemble, ce travail de thèse met en avant l'importance de considérer les facteurs biotiques dans l'étude des communautés bactériennes naturelles. Il souligne aussi la nécessité de mieux caractériser les interactions microbiennes, de leur mise en place d'un point de vue moléculaire à leurs impacts biogéochimiques globaux au sein des écosystèmes marins.

Extracellular hydrolytic activities and bacterial community composition in the Aulne estuary and the Bay of Brest: controlling factors and involvement of quorum sensing

Keywords : Extracellular hydrolytic activities, bacterial community composition, quorum sensing, estuary

Abstract: Heterotrophic bacterial communities play a crucial role in marine ecosystems. This thesis addressed the factors influencing marine and estuarine bacterial community composition and function in organic matter degradation. To this end, we performed both *in situ* monitoring of the Aulne estuary and the adjacent coastal waters of the Bay of Brest, as well as laboratory experiments investigating the specific role of quorum sensing (QS), a bacterial communication system.

Our results showed that the Aulne estuary acted as a natural bioreactor, fostering bacterial communities whose composition and intense hydrolytic enzymatic levels exhibited sharp spatiotemporal variations. These patterns were linked to variations in physicochemical conditions within the estuary, but also in biotic factors such as community composition or co-occurrence level.

In addition, our results demonstrated that QS was greatly involved in the regulation of hydrolytic enzymes synthesis among isolated bacterial strains and natural bacterial communities. This mechanism also impacted bacterial community composition, likely by regulating processes involved in colonization or bacterial interactions.

Altogether, this thesis highlighted the importance of considering biotic factors in the study of estuarine and marine bacterial communities. It also revealed the need to better characterize bacterial interactions, from their molecular implementation to their global biogeochemical impacts in marine ecosystems.